Photoreception in Ambulacraria: A Comprehensive Approach

Thesis

PHOTORECEPTION IN AMBULACRARIA

A Comprehensive Approach

ALBERTO VALERO-GRACIA

OPEN UNIVERSITY OF LONDON · STAZIONE ZOOLOGICA ANTON DOHRN

PHOTORECEPTION IN AMBULACRARIA
A COMPREHENSIVE APPROACH

Alberto Valero-Gracia

DISSERTATION

Open University of London, UK

–

November 2017

Director of Studies

Dr. Maria Ina Arnone, Stazione Zoologica Anton Dohrn, Italy

External Supervisor

Prof. Dan-Eric Nilsson, Lund University, Sweden

PHOTORECEPTION IN AMBULACRARIA
A COMPREHENSIVE APPROACH

Alberto Valero-Gracia

BSc and MSc in Biology

Universidad Autónoma de Madrid, Spain

DISSERTATION

By due permission of the Faculty of Biology, Open University of London, UK

To be defended in the Stazione Zoologica Anton Dohrn

Villa Comunale s/n, Naples, on 2017-11-10

Examiners

Prof. Claus Nielsen, University of Copenhagen, Denmark

Dr. Nicholas Roberts, University of Bristol, England

Stazione Zoologica Anton Dohrn, Italy
Open University of London, UK

SCIENTIFIC ENVIRONMENT

This thesis work has been carried out in the laboratory of Dr. Maria Ina Arnone (Stazione Zoologica Anton Dohrn, Italy) and Prof. Dan-Eric Nilsson (Vision group, Dept. of Biology, Lund University, Sweden)

This research work has been funded by the European Commission ('Neptune' Initial Training Network, Marie Curie Actions 7FP, grant no. 317172) as well as the The Swedish Research Council (grant no. 2011-4768)

To my parents

CONTENTS

List of Figures XIII
List of Tables XV
Acknowledgements XVII
Published Papers XIX

SUMMARY 1

GENERAL INTRODUCTION 3
The 'Cambrian Information Revolution' 5
Evolution of larvae, the state of the art knowledge 8
Hypotheses supporting that Urbilateria derived from a pelagic larva-like animal: Terminal addition hypotheses 9
Hypotheses that proposed that Urbilateria derived from a benthic organism: Intercalation theories 11
Light in the Ocean 13
Basic principles in sensory organs 17
The origin of visual systems: A problem of homology across levels of organization 18
Photoreceptor classes 19
The use of light for hunting and camouflage 24
Photoreceptor cells 27
Opsins 29
Non-visual opsins and their expression domains 32
Phototransduction 36
The Ambulacraria clade 38
Echinodermata 38
Hemichordata 42
References 45

OBJECTIVES OF THIS THESIS 61

1. OPSIN PHYLOGENY IN THE AMBULACRARIA 65
1.1 Abstract 67
1.2 Introduction 68
1.3 Results 70

1.3.1 Phylogeny and opsin distribution within Ambulacraria 70
1.3.2 Opsin fingerprint 73
1.4 Discussion 74
1.5 Material and methods 76
1.5.1 Data mining 76
1.5.2 Alignment and phylogenetic analyses 77
1.5.3 Consensus fingerprint of ambulacrarian opsin groups 77
1.5.4 Sequences used for this study 82
1.6 References 103

2. NON-DIRECTIONAL PHOTORECEPTORS IN THE PLUTEUS OF *STRONGYLOCENTROTUS PURPURATUS* 107
2.1 Abstract 109
2.2 Introduction 110
2.3 Results 113
2.3.1 The Go opsin *Sp-opsin3.2* is detected in two cells that flank the apical organ of the larva 113
2.3.2 TEM analysis reveals absence of shading pigments in the larva apical region 115
2.3.3 Sp-opsin4, the rhabdomeric opsin, was detected in the adult rudiment at pentagonal disc stages and thereafter 118
2.4 Discussion 121
2.4.1 Ancientness of Go-opsins 121
2.4.2 Non-directional photoreceptors 122
2.4.3 Bilateral disposition and lack of shading pigments 123
2.4.4 Putative role of Go-opsin positive cells in sea urchin larvae 125
2.5 Methods 126
2.5.1 *Strongylocentrotus purpuratus*, adult care and larval culture 126
2.5.2 Gene cloning and RNA probe preparation 126
2.5.3 Fluorescent in situ hybridization coupled with immunohistochemistry 127
2.5.4 Immunohistochemistry 127
2.5.5 Transmission electron microscopy 128
2.5.6 Imaging 128
2.6 References 129

3. THE EFFECT OF LIGHT ON THE VERTICAL MIGRATION OF ECHINOPLUTEUS 135

3.1 Abstract 137
3.2 Introduction 138
3.2.1 Putative driving cues I: The metabolic advantage hypotheses 138
3.2.2 Putative driving cues II: The light related hypotheses 140
3.2.3 Vertical distribution of plutei: Previous studies 141
3.3 Results 142
3.3.1 Experimental protocol I: Pilot experiments for testing the light-driven gravitaxis capability of *P. lividus* plutei 143
3.3.2 Experimental protocol II: Preliminary observations of the larval sinking speed 143
3.3.3 Experimental protocol III: First experiments with the vertical migration (VM) set up II, calculating the effect size to inform the experimental design 144
3.3.4 Experimental protocol IV: Main data collection, testing the vertical migration of four armed plutei under illumination of seven different wavelengths 149
A) The behaviour of plutei under UV (340 nm) light 150
B) The behaviour of plutei under violet (420 nm) light 152
C) The behaviour of plutei under blue (490 nm) light 153
D) The behaviour of plutei under turquoise (505 nm) light 154
E) The behaviour of plutei under green (535 nm) light 155
F) The behaviour of plutei under amber (590 nm) light 157
G) The behaviour of plutei under orange (617 nm) light 158
3.4 Discussion and future directions 159
3.4.1 Correlations found between the genomic and transcriptomic data of this species and its behavioural pattern 160
3.4.2 An energetically trade-off: Having various opsins expressed during early development could 'compensate' the lack of cell specializations founded in the class I photoreceptor cells of the echinopluteus 162

3.4.3 Echinoplutei exhibit a variety of light-driven behavioural gravitaxis patterns depending on the light stimuli provided 163
3.4.4 A mechanistic model for understanding simple photodetection 166
3.4.5 Future directions 169
3.5 Material and methods 172
3.5.1 Vertical migration (VM) set up I: A prototype for doing the pilot experiments 172
3.5.2 Vertical migration (VM) set up II: Hardware design and optical principles 173
3.5.3 VM set up II: Available light stimuli 176
3.5.4 VM set up II: Programing and data recording 179
3.5.5 Animals 180
3.5.6 Experimental design: Generalities 182
3.5.7 Experimental protocol I: Pilot experiments for testing the light-driven gravitaxis capability of *P. lividus* plutei 182
3.5.8 Experimental protocol II: Preliminary observations of the larval sinking speed 183
3.5.9 Experimental protocol III: First experiments with the VM set up II, calculating the effect size to inform the experimental design 184
3.5.10 Experimental protocol IV: Main data collection, testing the vertical migration of four armed plutei under illumination of seven different wavelengths 184
3.6 References 187

CONCLUSIONS AND FUTURE DIRECTIONS 191

Appendix I: Main programs developed to run the VM set up II 209

Appendix II: Publications 233

LIST OF FIGURES*

Fig 1. The Cambrian world 6

Fig 2. Putative triggers of the Cambrian radiation 7

Fig 3. Light absorbed by the sea 14

Fig 4. Light is not only coming from the water surface 16

Fig 5. Light in coastal waters and open ocean 16

Fig 6. Photoreceptor classes 21

Fig 7. Minimum light intensities needed for each photoreceptor class 22

Fig 8. The echinopluteus larva at four, six and eight armed stages 23, 24

Fig 9. Some adaptations to light perception exhibited in the ocean 27

Fig 10. Rhabdomeric and ciliary photoreceptor cells 28

Fig 11. Protein structure of an opsin 30

Fig 12. A general opsin phylogeny 32

Fig 13. The phototransduction cascade 37

Fig 14. Echinoderm phylogenetic relationships 41

Fig 15. The anatomy of the tornaria larva at Krohn stage 43

Fig 16. Hemichordate phylogenetic relationships 44

Fig 17. Ambulacraria phylogenetic relationships 69

Fig 18. The Ambulacraria opsin toolkit 71

Fig 19. Opsins in Ambulacraria, a phylogenetic reconstruction 72

Fig 20. Consensus sequences of the Ambulacraria opsin groups 73

Fig 21. Sequence alignment ..... 94 - 97

Fig 22. Gene expression profile of *Sp-opsins 2* and *3.2*. 113

Fig 23. Expression of the Go-opsin *Sp-opsin 3.2* in early plutei 114

Fig 24. Localisation of *Sp-opsin 3.2* positive cells in the early pluteus of *S. purpuratus*..... 115

Fig 25. Transmission electron micrographs of four armed plutei 117

Fig 26. Localisation of the rhabdomeric opsin Sp-opsin4 in the developing tube feet of the presumptive juvenile 120

Fig 27. Pilot experiments carried out about the effect size to inform the experimental design of the main data collection..... 147, 148

Fig 28. Heat maps showing the relative animal density along the height of the water column under different light stimuli..... 151-158

Fig 29. Gene expression profile of the opsins found in *P. lividus*..... 161

Fig 30. Larval distribution over the water column while applying different light stimuli 164

Fig 31. A depth-gauge model that explains the vertical migration movement of plutei in the water column in response to light cues 168

Fig 32. The 'Plankton cube' set up..... 171

Fig 33. Vertical migration set up I 173

Fig 34. Vertical migration set up II 175

Fig 35. Disposition of the IR LEDs with respect to the plankton column 175

Fig 36. Optical drawing of the IR light pathway and beam splitter functioning 176

Fig 37. Light stimuli available in the VM set up II 178

Fig 38. Light stimuli distribution over the spectrum 179

***** All figures contained in this thesis were used without commercial aim, recognizing use licenses and referencing original authorship.

LIST OF TABLES

Table 1. Opsins and transduction cascades in animal photoreceptors 36

Table 2. List of sequences used to build the phylogenetic reconstruction ..... 78 - 81

Table 3. List of specimens surveyed in this study ..... 98 - 102

Table 4. Opsin expression in *P. lividus* during early development 161

Table 5. *S. purpuratus* transcription factors involved in photoreceptor cell differentiation 197

Table 6. *S. purpuratus* ciliary and rhabdomeric phototransduction cascade components..... 199

ACKNOWLEDGEMENTS

This four-year study has been made possible by the contribution of many friends and colleagues. I would like to express my gratitude to all of them.

First, I want to thank my Director of Studies, Dr. Maria Ina Arnone, for giving me the opportunity to work in her lab, as well as to believe in my capacity to develop this project from the outset. I am also very grateful to my External Supervisor, Prof. Dan-Eric Nilsson, for giving me the chance to conduct part of my research in the Vision Group, as well as for our inspiring discussions related to the function and evolution of photoreceptor systems. I would also like to specially thank my Marie Curie Mentor, Dr. Detlev Arendt, for his guidance, help and valuable advice during this project.

I would like to thank the personnel of the Stazione Zoologica Anton Dohrn for their support, especially to Dr. Rita Marino. Rita, without your help I would have never mastered the molecular techniques that I learned at the Stazione Zoologica. Thanks also for your patience and advice, nobody could expect any more from a friend.

I am indebted to my colleagues at the Biology department of Lund University. With you, I found the critical mass needed to develop my scientific reasoning. It is impossible to speak about Lund without mentioning the support that my colleague John Kirwan has provided during our investigations. John, thanks for answering my questions regarding Matlab, as well as for all the kind help and comments given to improve my manuscripts. I am also grateful to Dr. Ahmad Darudi for his assistance during the construction of the vertical migration set-up, as well as to Dr. Ola Gustafsson and Carina Rasmussen for their assistance during the electron microscope work.

At this point, I would like to acknowledge all of my Marie Curie Neptune colleagues, both PIs and fellows. In this network I believe that we have been able to create a great collaborative atmosphere,

and an environment that has been valuable for learning about different aspects of a great discipline: Evolutionary Developmental Biology. Special thanks goes to Prof. Graham Budd, for his continuous support, sense of humour and outstanding discussions about the origin of primary larvae and complex life cycle evolution; and to Dr. Cristina Piñeiro-López for all the good time shared during the EMBO courses.

Teachers and professors of all academic levels lead in many respects the future of our society, most of the time silently, and plant and foster intellectual curiosity in all of us in our formative years. Therefore, I would like to look back and mention some of the people that have encouraged me to became involved in the adventure that Science represents; in chronological order: Dr. Esther Esteban-Salcedo and Prof. Ricardo Peris-Nieto (Colegio Internacional Nuevo Centro), Prof. Alessandro Minelli (University of Padova), Prof. Mauro Cristaldi (University of Rome La Sapienza), and Prof. Maria José Luciañez-Sánchez and Prof. Maria del Carmen López-Fernández (Universidad Autónoma de Madrid). Most of all I have to highlight the special encouragement provided by you, Carmen, during the last stage of this thesis.

I am especially grateful to my great friends that include, in alphabetical order: Mattia Aversa, David Gómez-Coronado Paredes, Inma Hormigo-González, and Irene Muñóz-Carmona. Few words are needed here, you all know that warmest gratitude goes to all of you. Your support, in one way or another, have made possible the completion of this dissertation.

Finally, but most importantly, I would like to thank my family for their support. Special thanks goes to my cousin Eva, for always being available to revise my English all over the manuscript in the best of the moods possible; and to my parents, Isabel and Santiago, for supporting me throughout all my studies and helping in the preparation of many of the drawings that illustrate this work respectively. This dissertation is dedicated to you.

PUBLISHED PAPERS

Paper I – D'Aniello, S. *, Delroisse, J. *, **Valero-Gracia, A.,** Lowe, E. K., Byrne, M., Cannon, J. T., Halanych, K. M., Elphick, M. R., Mallefet, J., Kaul-Strehlow, S., Lowe, C. J., Flammang, P., Ullrich-Lüter, E., Wanninger, A., Arnone, M. I. (2015). Opsin evolution in the Ambulacraria. *Marine Genomics*, 1–7. doi:10.1016/j.margen.2015.10.001. * Co-first authorship.

(Paper I reprinted with permission from the publisher in Appendix II)

Paper II – **Valero-Gracia, A.,** Petrone, L., Oliveri, P., Nilsson, D-E., Arnone, M. I. (2016). Non directional photoreceptors in the pluteus of *Strongylocentrotus purpuratus*. *Frontiers in Ecology and Evolution*, 1-12. doi: 10.3389/fevo.2016.00127.

(Paper II reprinted with permission from the publisher in Appendix II)

Paper III – **Valero-Gracia, A.*,** Marino, R.*, Crocetta, F., Nittoli, V., Tiozzo, S., Sordino, P. (2016). Comparative localization of serotonin-like immunoreactive cells in Thaliacea informs tunicate phylogeny. *Frontiers in Zoology,* 1-12. doi: 10.1186/s12983-016-0177-6. *Co-first authorship.

(Paper III reprinted with permission from the publisher in Appendix II)

Author contributions

Paper I: AVG had the initial idea of the work, developed the experimental design, contacted other authors to have access to their transcriptomic datasets, and contributed both with the data analysis and writing of the manuscript. SA and JD carried on the main part of the data analysis and manual alignment of the sequences. Rest of authors contributed with sequence data and gave feedback on the manuscript.

Paper II: AVG and MIA conceptualized and designed the study. AVG grew the larvae, did the fluorescence *in situ* hybridization of *Sp-opsin3.2* coupled with immunohistochemistry, performed the immunohistochemistry assays of Sp-opsin4, supervised the transmission electron microscopy assays done with the assistance of the EM personnel from the Microscopy Facility (Department of Biology, Lund University), and wrote the manuscript with the assistance of DEN, MIA and PO. LP did the molecular cloning and chromogenic *in situ* hybridization of *Sp-opsin3.2*. All authors approved the final text.

Paper III: AVG and PS conceived the paper and drafted a first version. AVG, FC, ST, VN, and PS participated in the collection of specimens. AVG, RM, and ST carried out immunocytochemical experiments and confocal laser scanning microscopy. All other authors assisted in drafting the manuscript. All authors read and approved the final manuscript.

"All men by nature desire to know.
An indication of this is the delight we take in our senses;
for even apart from their usefulness they are loved for themselves;
and above all others, the sense of sight"

Metaphysics I, 1, 1a; Aristotle

SUMMARY

Non-directional photoreceptors are the evolutionary precursors of all animal eyes; they enable the monitoring of ambient light intensity and regulate feeding, movement and reproduction. While the first animals were most likely benthic, they evolved larval stages very early on, thus conquering a new ecological niche: the pelagic. In this realm, the evolutionary pressure to prey but not be preyed upon became stronger. This implied strong selection for better sensory systems, including photoreception. How were the photoreceptor systems of the earliest primary larvae arranged? Did this system mediate vertical migration, the largest movement of biomass on Earth? To try to answer these questions, I chose the pluteus larva of the sea urchin as a model. A comprehensive array of techniques was applied, covering levels of organization from genes to behaviour. The diversity of opsins in Ambulacraria (echinoderms plus hemichordates) has been surveyed to have the first phylogenetic context on this matter (Chapter 1). A non-directional photoreceptor based on Go-opsins has been first described in an invertebrate larva of the deuterostome lineage (Chapter 2). A novel custom built behavioural set up was created to investigate the vertical migration of these pluteus larvae under different light conditions (Chapter 3). Based on these findings, a mechanistic model for understanding simple photodetection is proposed.

Keywords: eye evolution; non-directional photoreception; vertical migration; neuroethology; zooplankton; marine invertebrate larvae; dipleurula; echinopluteus; *Strongylocentrotus purpuratus*; *Paracentrotus lividus*; opsin phylogeny; Go-opsin; in situ hybridization; immunohistochemistry; transmission electron microscopy.

GENERAL INTRODUCTION

GENERAL INTRODUCTION

Here I explain the basic concepts needed to follow this doctoral dissertation. When possible, the organization of the epigraphs goes from the systemic to the molecular level.

The 'Cambrian Information Revolution'

Although life had existed for several billion years, the first animals with true resolving eyes date back to the early Cambrian (530 Ma). Twenty million years earlier, towards the end of the Precambrian, living organisms were much simpler. What could have happened in the intervening between the Precambrian and the Cambrian? Why animals evolved such a variety of body plans in during that period? Whatever happened still remains a mystery, but what we can see from the fossil record is that a rich fauna of macroscopic animals evolved, some of them with large eyes (Budd, 2008; Budd and Jensen, 2015; Land and Nilsson, 2012).

In the Ediacaran (635-542 Ma), animals were most likely confined to an essentially two-dimensional landscape (Peterson et al., 2008). At that time, the fauna was most likely benthic, but larval stages arose very early on to facilitate dispersion (Jagersten 1972; Hu et al., 2007; Vannier et al., 2007). During this process, metazoans conquered a new ecological niche: the pelagic. This represents a completely new evolutionary scenario, the three-dimensional Cambrian word (Fig. 1). There, the tremendous selective pressures to prey but not be preyed upon became stronger (Bengtson, 2002). This implied further selection for better motor systems, body armours, camouflage strategies and sensory apparatus including photoreception. Such an increasement in the available information has been referred as the 'Cambrian Information Revolution' (Plotnick

et al., 2010). Another event that implies such a number of changes in visual systems just happened once more, during the conquest of land (Land and Nilsson, 2012).

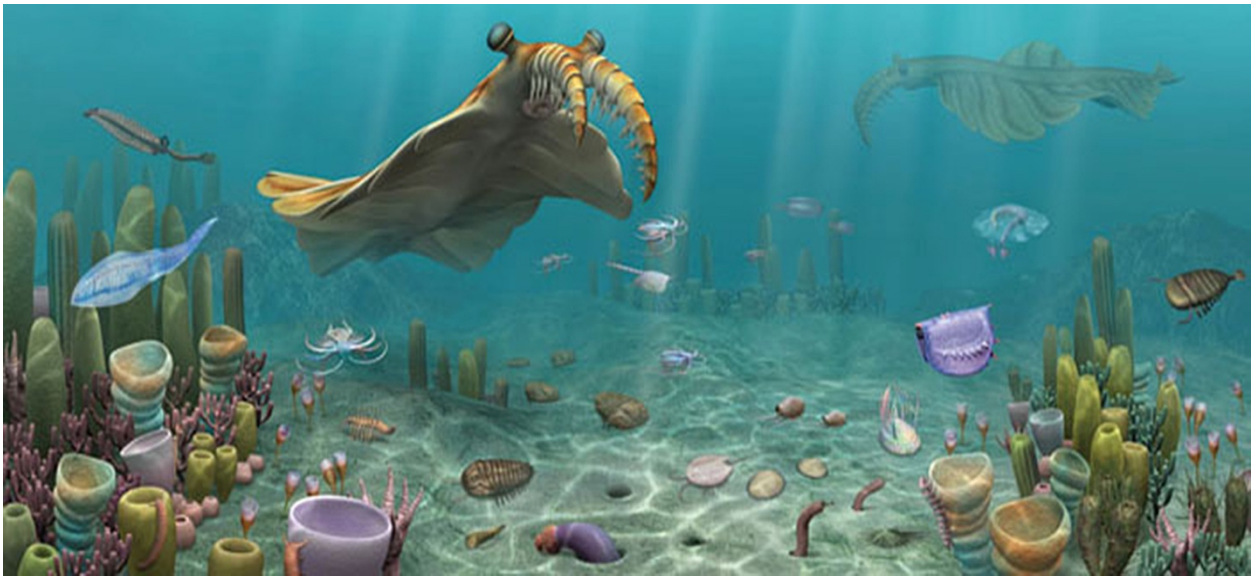

Fig 1. A representation of the Cambrian (543 to 490 Ma) world. The first faunas with large mobile animals seem to have originated at the onset of the Cambrian, during the Cambrian radiation. During a few million years, bilaterally symmetric, macroscopic, and mobile animals evolved from ancestors with soft bodies that were much smaller. The invention of visually-guided predation may have been one of the triggers for this unsurpassed evolutionary event. Drawing courtesy of Kayomi Tukimoto.

The expansion from a benthic to a pelagobenthic ecosystem leads to a great sensory revolution but, what if we go back in the past even more? An abrupt appearance of major bilaterian clades in the fossil record during early Cambrian has puzzled the scientific world since the 1830s (Zhang et al., 2014). Even so, the triggers that may had conducted to such diversification of life forms can be organized in three main categories: environmental, molecular, and ecological.

Starting with the environmental changes, we can highlight the importance of the rising of oxygen level (a process related to the 'Snowball Earth', i.e. a period situated 650 million years ago in which the Earth's surface became almost entirely frozen), the changes in seawater composition (circa 740 Ma onwards), and the subsequent increase of nutrient availability (Kirschvink, 1992;

Hoffan and Schrag, 2002). On the molecular side, the appearance and duplication of certain homeobox genes (e.g. NK, Hox and ParaHox), as well as the expression and diversification of some key metabolic proteins (e.g. Heat Shock Protein 90 and oxygen transport enzymes) acted as catalysts thus permitting an amazing increase of body plans (Zhang et al., 2014; Holland, 2015). In ecological terms, new behavioural strategies such as the development of altruistic behaviours between conspecifics or the increment of predation, may have stimulated the diversification of multicellular organisms (Conway Morris, 2000; 2006; Zhang and Shu, 2014). Albeit the organization of these evolutionary triggers in a timeline remains problematic, a good attempt to set them in chronological order can be seen in Fig. 2.

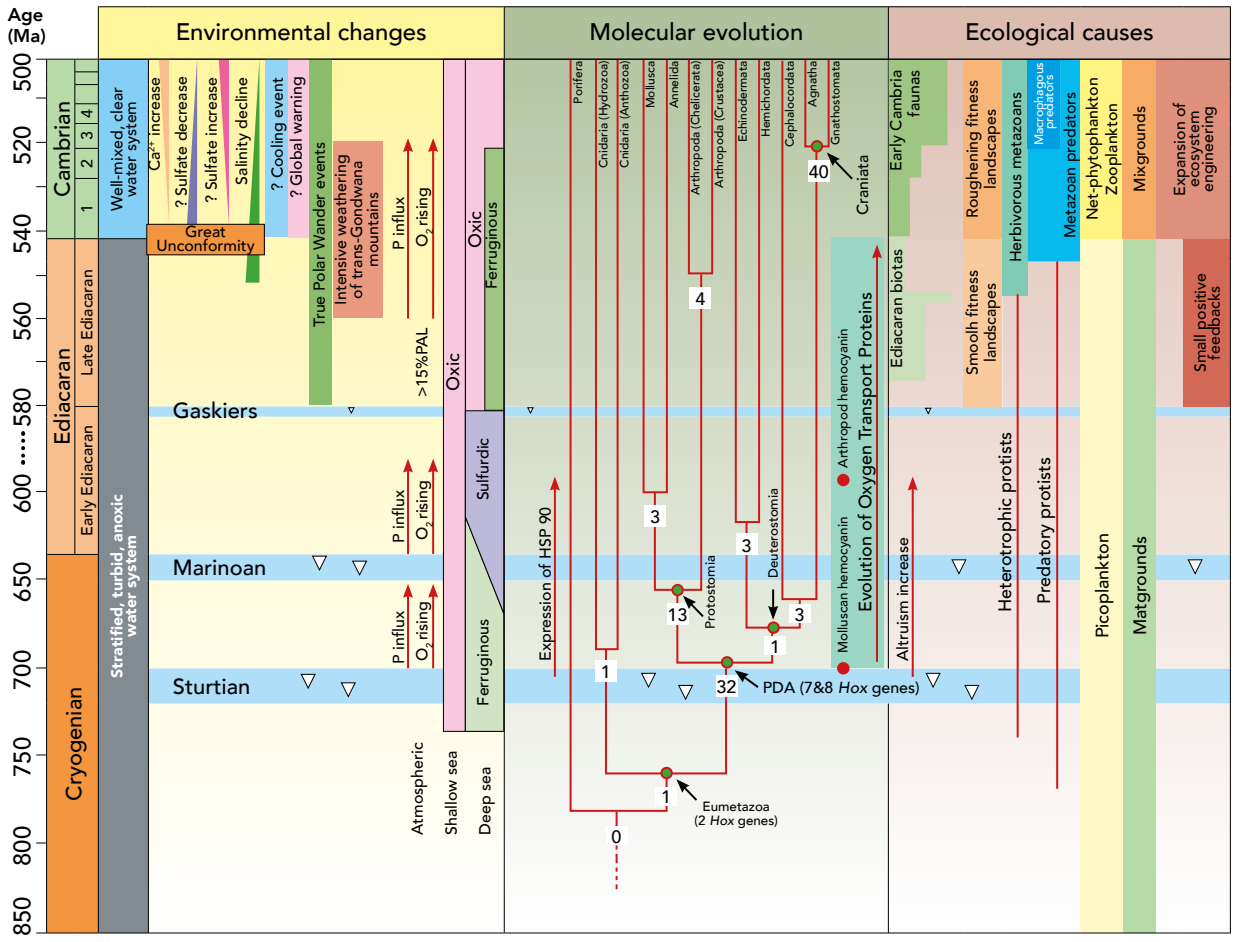

Fig 2. Timeline of environmental, molecular and ecological events that were proposed as triggers of the Cambrian radiation. The phylogenetic tree for metazoan scaled against the molecular dates of lineage splitting (Erwin et al., 2011). Note that each node is characterized by the addition of at least one new microRNA gene family, indicated

in numbers (Peterson et al., 2009). Three instances of high rate of microRNA acquisition are recognized, once at the base of protostomes and deuterostomes, once at the base of craniates, and once at the base of primates (not indicated). Numbers 1 to 4 in the age column representing the first four stages of the Cambrian. Abbreviations: HSP, heat shock protein; PDA, protostome-deuterostome ancestor. Figure modified from Zhang et al. (2014).

Palaeontologists have reviewed the distribution and morphology of complex sense organs in the fossil record (Clarkson et al., 2006; Schoenemann, 2006). However, the poor conservation of soft tissues is limiting when studying the early evolution of sense organs in the pelagic realm. This lead us to a clear conclusion: although fossils can tell us much about the evolution of how the most primitive eyes were in some benthic animals, for deciphering the origin of the earliest photoreceptors in pelagic larvae we need evidence other than the fossil record. Thus, the eco-evo-devo study of extant marine invertebrate larvae is key.

Evolution of larvae, the state of the art knowledge

The antiquity of metazoan primary larvae seems to be evident from extensive developmental, structural, functional, and molecular characters. Further, a number of apomorphies are shared among the extant trocophore larva of some protostomes and the extant dipleurula larva of deuterostomes, clades that had diverged before the Cambrian (e.g., Jägersten, 1972; Strathmann, 1978a; Nielsen, 1987; Wray, 1995; Byrne et al., 2007; Marlow et al., 2014). Phylogenetic evidence of this kind must be interpreted with caution since convergent evolution may occur (Strathmann 1978a, b). However, direct evidences in support of this idea can be extracted from the fossil record too (Jablonski and Lutz 1983; Müller and Walossek, 1988; Zhang and Pratt, 1993; Dzik, 1978; Runnegar and Bentley, 1983). Thus, there is a wide array of evidences in support of the hypothesis that both protostomes and deuterostomes already had a larva in their life cycles by the Cambrian. Other distinctive larvae have evolved within the metazoa, including cnidarian planulae, nemertean pilidia, platyhelminth Müller's, bryozoan cyphonautes and ascidian tadpoles. The clades to which

these larvae belong to are undoubtedly ancient, but the lower number of molecular and paleontological data available for these clades makes it difficult to say when each distinct larval form arose (Wray, 1995). Several authors have argued that most larvae that feed using cilia share a common origin very deep in the metazoan radiation (Jägersten, 1972; Strathmann, 1978a; Nielsen and Nørrevang, 1985; Nielsen 1987, 2004, 2005, 2008). If this is true, the peak moment of larval evolution coincided with the Cambrian explosion (Valentine et al, 1991; Valentine, 2004). Alternative explanations are possible but less well supported by the available data.

A classical topic that arises while discussing larval evolution is its relationship with the origin of the earliest animals. Since it seems clear that (at least some of) the first primary larvae arise before the Cambrian; was the common ancestor of extant bilaterians descent from a pelagic larva-like animal, or from a benthic adult?

Hypotheses supporting that Urbilateria derived from a pelagic larva-like animal: Terminal addition hypotheses

One evolutionary scenario is to derive bilaterians from adult planktonic forms, an idea already proposed by Haeckel ('Gastraea' hypothesis), that has been further developed by Jägersten ('Bilatero-gastraea' hyphotesis) and Nielsen ('Trochaea' hypothesis) (Haeckel, 1874; Jägersten,1972; Nielsen 1979, 1987, 2004, 2005, 2008; Nielsen and Nørrevang, 1985). For giving some words about the most recent hypothesis in this gastraea line of though, Nielsen proposed that the ancestral eumetazoan did not evolve directly from a blastea, but from a sexually mature larva of a homoscleromorph like sponge with a pelagobenthic life. The overall Trochaea hypothesis is quite attractive, however some authors consider that there are no paleontological evidences that support that these putative holopelagic forms ever existed as independent organisms, and that the

reconstruction of the Trochaea relies broadly upon assuming a recapitulatory scenario reminiscent of Haeckel (1866) (Wolper, 1999; Valentine, 2004).

Another hypothesis that invokes larval style body plans as ancestral to complex metazoans was presented by Davidson and co-workers (Davidson et al. 1995; see also Peterson et al., 1997, Peterson and Davidson, 2000; Arenas-Mena et al., 1998; Erwin and Davidson, 2002). In some metazoans, many adult organs are not derived from cells within larval organs, but rather from pluripotent cells sequestered during larval life that are set aside. An example of this can be seen during the development of the sea urchin rudiment studied in this work (Chapter 2). Based on these findings, Davidson and others suggest that such a 'set aside' system was an adaptation to the growing complexity of adult body plans. As more complex body plans are evolved, the cells that were used for adult body plans were not employed in the early developmental stages but were set aside then, and their fates specified during or after metamorphosis. In this scheme, the ancestral bilaterian would have possessed representatives from all of the major families of transcription factors and signalling molecules; however, it would not use these proteins for regional specialization that we see in extant bilaterian adults yet. Even if it is very plausible that a biphasic life cycle with partial dedifferentiation of intermediate juvenile or larval stages represent the mainstream developmental mode of metazoans (Arenas-Mena, 2010), the set aside hypothesis has been considered as highly recapitulatory too (Valentine, 2004).

A last terminal addition hypothesis considered that the earliest bilaterians were large animals metamorphosing from a small, free-living larva (Rieger 1986; 1994). As Budd and Jensen emphasize, it is strange that these large animals have ever existed since no trace fossils of them have been found (Budd and Jensen, 2000). Thus, this hypothesis it is not overly plausible.

A number of authors have questioned the terminal hypotheses (Knoll and Carroll, 1999; Wolpert, 1999; Jenner, 2000; Rouse, 2000; Bishop and Brandhorst, 2003). Of the issues raised, three kinds of objection carry the most weight. These are arguments on: (i) the distribution of developmental character states in bilaterians phylogeny; (ii) the lack of paleontological data in support of them; and (iii) improbabilities in the selection of set aside cells before evolution of a bilateral body plan (Sly et al., 2003; Valentine, 2004).

Hypotheses that proposed that Urbilateria derived from a benthic organism: Intercalation theories

The main bulk of available evidence favours the hypothesis that the origin and radiation of bilaterians body plans occurred almost entirely in the benthos, most probably in shallow waters rich in nutrients, and that once Metazoa had appeared, evolution proceeded among individuals rather than involving the individuation of colonies (see, for example, Sly et al., 2003; Raff, 2008; Budd and Jensen, 2017 and bibliography therein).

Two evolutionary model based on the assumption of a first benthic animal are the 'Parenchimella' hypothesis (Metschnikoff, 1886) and the 'Planuloid' hypothesis (Graff, 1882; Hyman, 1951; Salvini-Plawen, 1978; Willmer, 1990; Baguñà et al., 2008). On these theories, Urbilateria (i.e. the ancestor of all extant bilaterians; de Robertis and Sasai, 1996) is represented by small, compact organisms with direct development like the planula of some cnidarians. This planuloid model is not inconsistent with some aspects of the Trochaea and Set aside hypotheses, but contrasts sharply with other aspects. As Nielsen indicates, the main problem of this theory is related to the feeding mechanism of such a compact free living adult ancestor (Nielsen, 2008). However, extracellular digestion can be considered as the feeding mechanism of the small Urbilateria proposed by these intercalation hypotheses. Even if the Parenchymella and Planuloid

hypotheses are not perfect, a benthic Urbilateria is not only feasible, but also quite parsimonious in the general sense.

Another intercalation hypothesis that partially resolves the feeding mechanisms problem pinpointed by Nielsen is the 'Plakula' hypothesis. The Plakula proposed the existence of a benthic Urbilateria that had two layers of cells and bilateral symmetry (Bütschli, 1884; Grell, 1971; Schierwater, 2005). In this case, the separation of these two layers of cells would have permitted the invagination of the ventral cells arriving to the Gastraea proposed by Haeckel (1874), thus allowing the presence of a digestive tube. This modification of Haeckel's original hypothesis gained more strength when the clade Placozoa was discovered (Grell, 1971).

I am prone to consider the intercalation hypotheses as more plausible for the following reasons: (i) the secondary emergence of larval forms in benthic adults as a dispersal agent represents a highly adaptive advantage thus, the 'presence of larva' apomorphy may have been rapidly fixed very early during animal evolution, as the fossil record indicates ; (ii) the inclusion of a larval stage can be explained by the addition of random mutations that have led to the conservation of adult characters by the swimming gastrula during time in a heterochronic manner (it is difficult to justify the evolution from a larval stage by metamorphosis); and (iii) the intercalation hypotheses are more parsimonious while using all current metazoan phylogenies most broadly accepted (phylogenies in which the early diverging branches are represented by metazoans predominantly benthic; e.g. Dunn et al., 2014) (Olive, 1985; Jablonski, 1986; Strathmann, 2000, Sly et al., 2003). This line of reasoning is in agreement with the visions of several authors such as Garstang (1922), Ivanov (1937), de Beer (1954), Hadži (1955), Steinböck (1963), Conway Morris (1998), Valentine and Collins (2000), Hadfield and Paul (2001), and Minelli (2009) among others.

Light in the Ocean

There are two main natural sources of light in the sea: downwelling light from the sun, moon and stars, and bioluminescence produced by aquatic organisms (Warrant and Locket, 2004). Due to the optical properties of water, the prominence and intensity of both sources change with depth, transforming the visual scene from an extended field of features in the ocean's surface to a scene dominated by point source bioluminescent flashes in the vast darkness of the deep (Sosik and Johnsen, 2004; Warrant and Locket, 2004). In this thesis, I will summarize how these light changes occur while going down in the water column. This information will be relevant when discussing about the behavioural results presented in Chapter 3.

When light is incident upon a substance it can do one of four things: (i) it can be scattered (i.e. light can change in the direction of motion because of a collision with other particles); (ii) it can be transmitted through the substance; (iii) it can be absorbed (when the energy of an incoming photon is absorbed by an electron, the electron is then exited to a higher energy state); or (iv) it can be reflected, thus abruptly changing the direction of propagation when striking the boundary between different mediums (for a further description of how light interacts with matter the reader can refer to Born and Wolf, 2003; or Hecht, 2016). Circa 31% of the sunlight is reflected by the atmosphere or the ocean surface, but much also is strongly absorbed by the sea (Fig. 3). Depending on how clear the water is, the penetration rate of light changes. These differences in light penetration distance had led to the classification of oceanic waters into two basic cases: 'case 1', and 'case 2' (Morel and Prieur, 1977). Case 1 is that of a concentration of phytoplankton high compared to other particles (in other words, waters highly charged of organic compounds, generally related to coastal areas), and case 2 is the one in which the inorganic particles are dominant, as occurs in the open sea. While Morel and Prieur (1977) recognized that these ideal cases are not encountered in nature, the practise of most investigators in the following years assumed a discrete dichotomy. This led to the

establishment of more complex cases of classification based on the quantity and type of dissolved organic matter in the surface layers (Jerlov, 1976).

So, how much light reaches different depths of the water column? Which is the 'colour' of the sunlight that is absorbed? Numerous studies have shown that, under average conditions, circa 50% of the sunlight incident on the sea surface consists of infrared (IR) bands (radiations located in the band from about 700 nm to 1 mm), some 45% of visible radiation (390 to 700 nm) and only around 5% of ultraviolet (UV) (10 to 390 nm). IR radiation entering the sea is rapidly absorbed in the very thin surface layer, and is the main cause of oceanic warming. Later, the visible light spectrum narrows down with depth: greenish-yellow light is the most penetrative in sea waters containing large amounts of organic substances (case 1 waters, Fig. 5A); whereas bluish-green light penetrates the farthest in optically clear oceanic waters (case 2 waters, Fig. 5B).

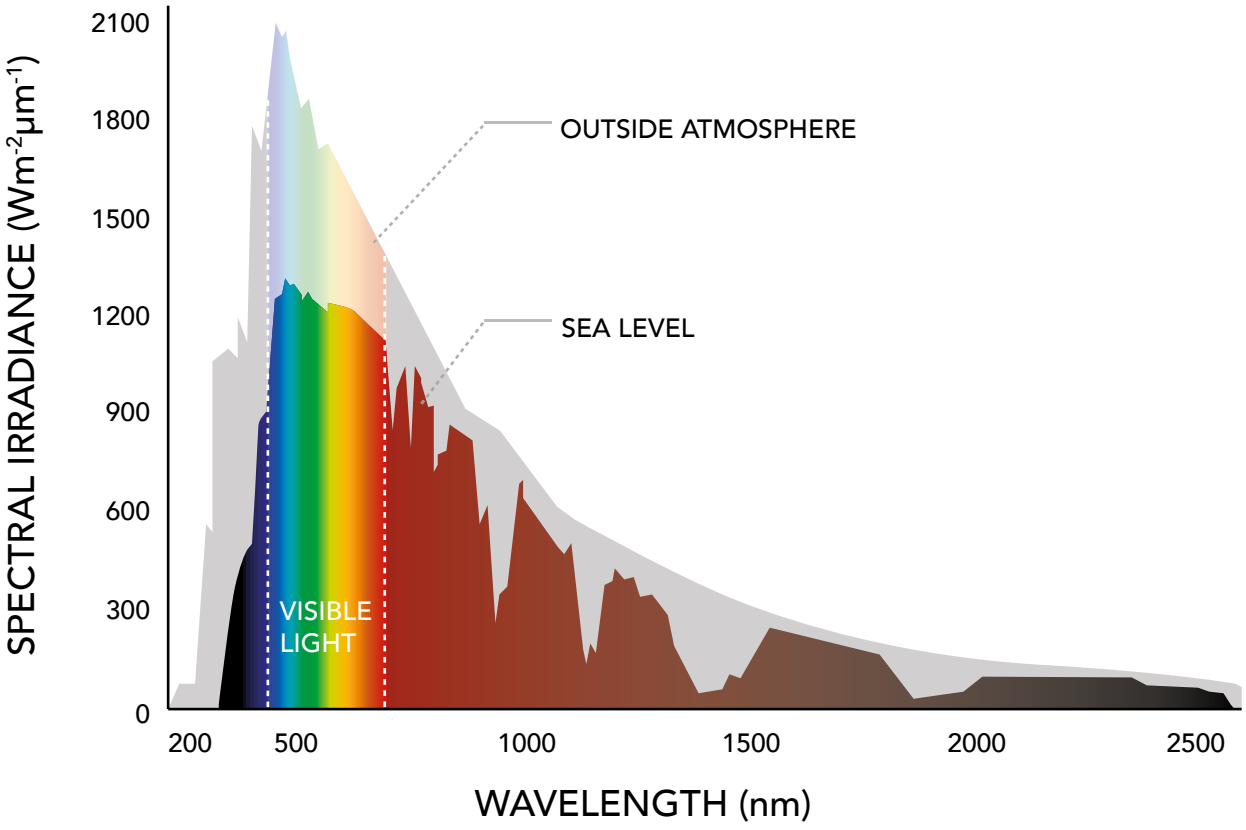

Fig 3. Much sunlight is reflected by the atmosphere or the ocean surface, but the main part is strongly absorbed by the sea. Most the solar radiation that reaches the Earth is made up of visible and infrared light. Only a small amount of ultraviolet radiation reaches the surface. Image reproduced with permission from Nate Christopher (Solar Radiation and Photosynethically Active Radiation, Fundamentals of Environmental Measurements; Fondriest Environmental, 2014.).

Marine photosynthesis is confined to the tiny fraction of the ocean where visible sunlight penetrates (at most, the upper 200 m). UV light also penetrates this region, which can cause damage to the zooplankton in this part of the water column. To solve this problem, marine organisms have evolved ways to protect themselves from this UV radiation including UV absorbing pigments, the ability to repair DNA damaged by UV, and developing behaviours to avoid UV by staying in deeper water (reviewed in Holm-Hansen et al., 1993).

In the open ocean, descending in the water column, the IR, UV, green and violet wavelengths disappear, and the light becomes blue. At 200 m depth, the boundary between the epipelagic (the surface realm), and the mesopelagic (twilight realm) zones is found. In the mesopelagic, the energy provided by sunlight is sufficient for photoreception but not for photosynthesis (Sosik and Johnsen, 2004). In this area, an array of bioluminescent organisms can be found (Fig. 4). Below 850 m our eyes are not sensitive enough to perceive the minute amounts of sunlight that haven't been absorbed by the upper water area. Still, some of the most light sensitive deep-sea animals can perceive part of the sunlight at 1,000 m, in the bathypelagic zone (Sosik and Johnsen, 2004).

The region situated below is known as the aphotic zone, an area divided into the abyssopelagic (below 4,000 m) and hadalpelagic (below 6,000 m) areas, but this is only true for sunlight, as bioluminescence is quite common (Robison, 2004).

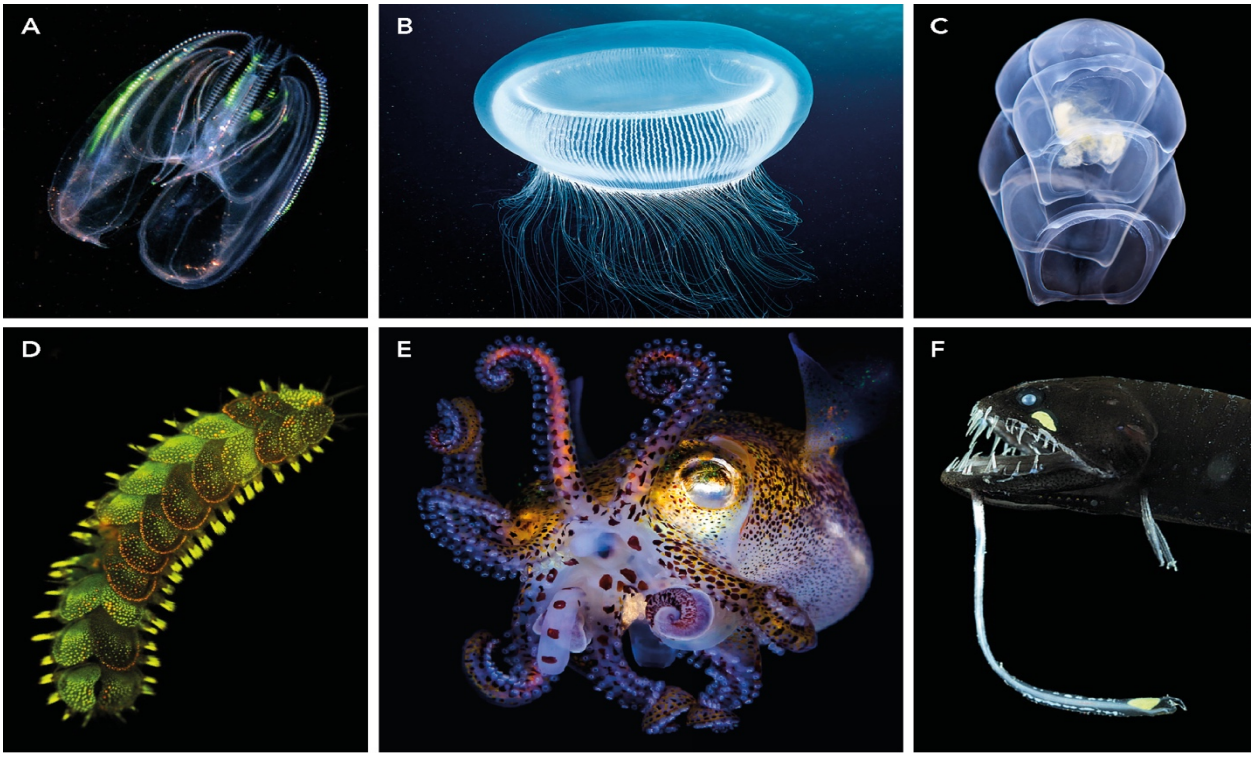

Fig 4. Light is not only coming from the water surface, but also from the oceanic chasms. Few examples on bioluminescence can be found in: A) some ctenophores, like in *Mnemiopsins leidyi* (picture: Lyubomir Klissurov); B) the hydrozoa Aeuquorea sp. (picture courtesy of Alexander Semenov); C) the siphonophore Hippopodius sp., (picture courtesy of Alexander Semenov); D) the polychaete *Lepidonotus squamatus* (picture courtesy of Alexander Semenov); E) the glowing bacteria *Vibrio fischeri* present in the light organ of the hawaiian squid *Euprymna scolopes* (in exchange for a home and a diet of sugars and amino acids provided by the squid, the bacterium helps protect *E. scolopes* from predators by illuminating it with a blue glow) (picture: Todd Bretl), or F) the scaless black dragonfish *Melanostomias biseriatus* (picture: Solvin Zankl).

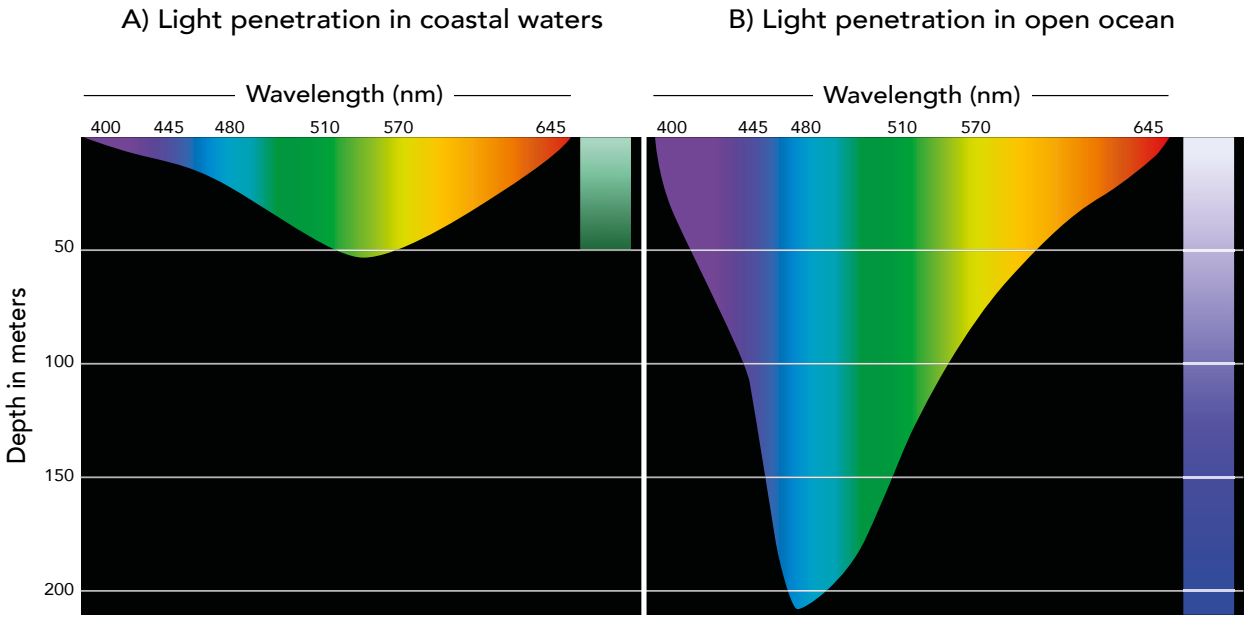

Fig 5. The depth that light penetrates depends on the quality of the water: A) light penetration in coastal waters; B) light penetration in open ocean. Long wavelengths (570 to 650 nm) are absorbed faster than short wavelengths (400 to 510 nm). Image courtesy of Kyle Carothers, NOAA OE.

Basic principles in sensory organs

Metazoan sensory organs are those that receive information (stimuli) and translate it into a signal recognizable to the nervous system. The received signal or cue can be very variable, with mechanical stimuli, taste, odour, sound, and light being the most familiar to us, but many more are possible (e.g. electric fields, temperature or pressure). In general, a ciliated sensory cell that contains receptor molecules is present as the basic unit in the sensory structure of Opisthokonta (Mitchell, 2007). Although the function of the first sensory cell cannot be reconstructed, probably the earliest receivers had chemoreceptive or mechanoreceptive functions (Emde and Warrant, 2015).

While there are several stimuli and therefore a wide range of sensory structures, the basic principles of signal transduction are similar (Fain, 2003). The recipients for a stimulus are membranous proteins that change their conformation in response to environmental changes. The effective answer is the opening or closing of ion channels that change the intracellular and extracellular ion concentration and thereby create action potentials. The sensory receptor proteins can themselves be ion channels and therefore directly receive information and transform it (e.g. mechanoreceptors); although in most cases signal transduction is more complicated, with further effector molecules and second messengers being incorporated into a signal transduction cascade. Phototransduction is an example. The exceptions to this generalized mechanism are electroreceptors, which do not need signal translation (Schmidt-Rhaesa, 2007).

The origin of visual systems, a problem of homology across levels of organization

Salvini-Plawen and Mayr (1977) noted a remarkable diversity of photoreceptor cell morphology across the animal world, thus suggested that photoreceptors evolved independently numerous times. This idea has been wearisomely discussed and contested (Gehring, 1996). Probably it is not possible to answer if the origin of eyes was monophyletic or not with a simple yes or no. Nonetheless, if we distinguish between different levels of organization, the answer would be easier to provide.

On the one hand, although the photoreceptors of different animal clades can differ in their morphology and development, and their similarities can be ascribed as the result of convergent evolution, they share deep homologies in the molecular components that they are composed of. This implies that ancient molecular modules devoted to gene expression or physiological function have been repeatedly recruited and co-opted for similar purposes in parallel metazoan lineages (Arendt, 2003; Land and Nilsson, 2012).

On the other hand, information on the evolution of eyes can be obtained also from the proteins that make up animal lenses, the crystallins. To make efficient and clear lenses, these proteins must be suitable for mass expression and dense packing, but they should not aggregate into lumps (Land and Nilsson, 2012). Different metazoans, such as cnidarians, cephalopods and vertebrates, have used different proteins for this purpose. Interestingly, the crystallins generally appear to have been recruited from proteins with other functions involved in protein assembly such as chaperones (Piatigorsky, 2009).

These explanations, in addition to the phylogenetic information commented in a subsequent chapter, suggest that an opsin based photoreception may have evolved once during early

animal evolution. With equal certainty we could say that visual dioptric systems may have evolve independently many times (Land and Nilsson, 2012). The key question that still awaits a response is what happened in between these early and late stages of photoreceptor evolution. Further, although some important ideas of how the evolution of photoreception functions will be addressed in the consecutive headings, the events that placed opsin into the first primitive photoreceptors are unknown.

Photoreceptor classes

Without an understanding of how selection guided evolution any evolutionary scenario is incomplete (Nilsson, 2009). Gene or protein phylogenies can tell us what is likely to have happened at the molecular level, morphological features can inform us about the putative function of a structure, and other approaches, such as expression studies and knockout experiments, can relate molecules to developmental trends. But to understand why features or functions have evolved we need plausible models of how they increase the fitness of the studied animal system.

In this dissertation, I refer to the four 'photoreceptor classes' established by Nilsson (2013). These categories correlate innovative features of the photoreceptor systems with the tasks that they mediate. Such innovations allow animals to adapt themselves to particular ecological problems, and its functional classification will permit a better analysis of eye evolution. Thanks to this explanation it will be easier to realise the significance of the present study, a project in which I aim to better understand the simplest and more ancient class of photoreception, the class I.

The first step in photoreceptor cell evolution must have been the appearance of a light-dependent chemical reaction coupled to a signalling system. All eumetazoans employ opsins for this purpose (Plachetzki and Oakley, 2007; Porter et al., 2011; Feuda et al., 2012; Ramirez et al., 2016). The

photoreceptors that contain opsins but nothing else are classified as non-directional (class I) photoreceptors (Nilsson, 2013). They are the most ancient in evolutionary terms and allow to monitor ambient light intensity. This light information results essential for many important behaviours such as to provide input into the circadian clocks (Bennett, 1979), to establish the vertical position in the water column (Lythgoe, 1979), or to inform about harmful levels of UV radiation (Paul and Gwynn-Jones, 2003; Leech et al., 2005). Examples of these photoreceptors can be found in the adult earthworm, as well as in pluteus and auricularia larvae of echinoderms (Röhlich et al., 1970; herein).

The second class (class II) is represented by simple directional photoreceptors. These receptors are composed of an opsin positive cell plus a screening pigment. This screening pigment, that can be both in the same cell or in the surroundings, project a shadow in part of the photoreceptor, thus informing where the light is coming from. Animals that possess these photoreceptor systems can move towards or away from light to orient their bodies, and trigger alarm responses to predators (Nilsson, 2013; Bok et al., 2016). Examples of these photoreceptors can be found in adult rotifers and kinorhynchs, as well as in the larva planula of some cnidarians, the pilidium of nemertines, or the tornaria of hemichordates (Brandenburger et al., 1973; Nordstrom et al., 2003; Mason and Cohen, 2012; Braun et al., 2015).

Although knowing from where light is coming from represents a great adaptive advantage, the loss in sensitivity caused by the addition of screening pigments is a major obstacle in the evolution of spatial vison. The problem is compounded by the fact that the integration time will have to be reduced along with the receptors field of view to keep motion blur at tolerable levels. In addition, the contrasts of interest are smaller for spatial vision than for phototaxis, which calls for larger photon samples per integration time. A consequence of this rapidly increasing need for

photons is that stacking of the photoreceptor membrane becomes an absolute prerequisite for the evolution of spatial vision (Nilsson, 2013). The third class (class III), named low resolution vision, is that in which rhabdoms and ciliary specializations occur. Even with very crude resolution, animals provided with this visual system can mediate a large number of important tasks such as detecting their own motion, avoid objects, and find preferred habitats. Some of the animals that have this photoreceptor system are flatworms, adult box jellyfishes, or sea stars (Marriott, 1958; Martin, 2004). This category introduces imaging and spatial resolution, which would require a minimum of two resolved pixels thus, representing the first true eyes (Nilsson, 2013).

Finally, class IV (high-resolution vision) is equal to the preceding class III system plus focusing lenses for increasing the image resolution. This increment in the spatial resolution allows to detect and pursuit prey and predators, as well as to recognise the mate or have more complex visual communication as happens in octopus and mantis shrimp (Wolken, 1958; Bok et al., 2014). For a small number of species this system allows them to make and use tools, as well as to read texts such as this thesis.

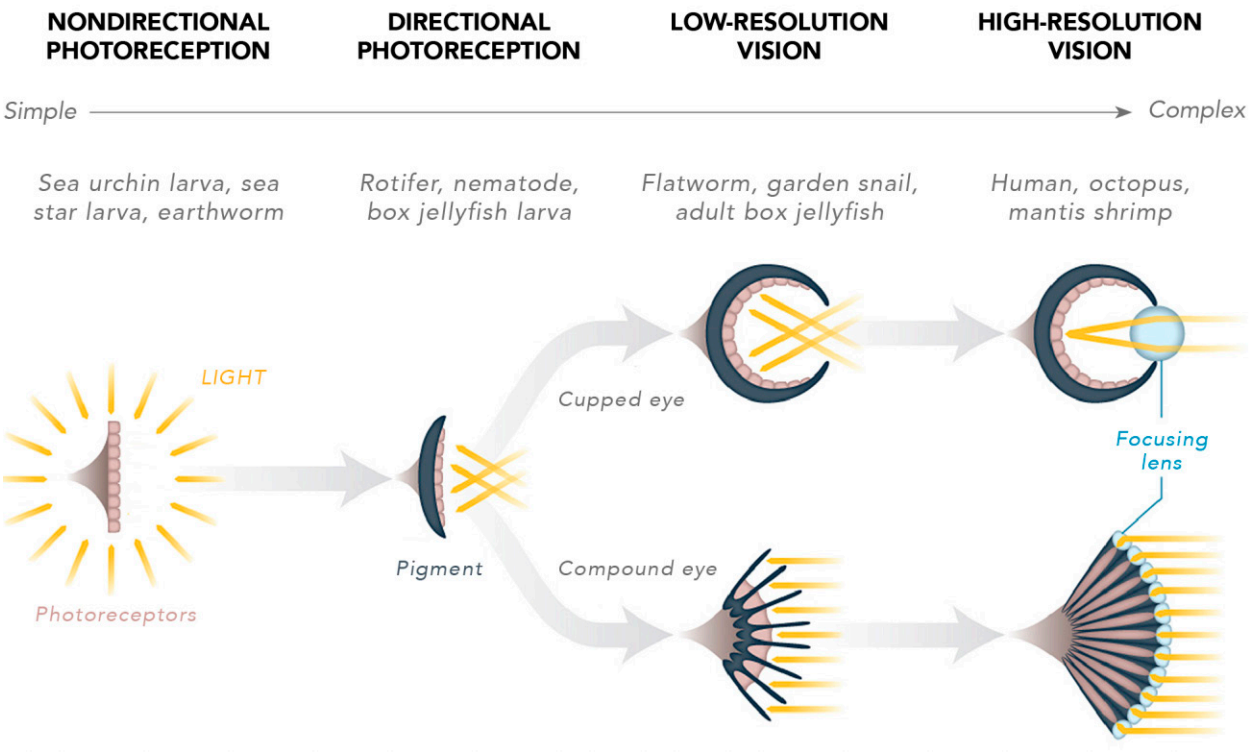

Fig 6. The diversity of photoreceptors in the animal world illustrates how natural selection can transform simple structures that respond to light (non directional photoreceptors) into camera like eyes composed of multiple parts working in tandem (high resolution vision). Drawings by Jason Treat, Ryan Williams and Chiqui Esteban taken from an article of Ed Young in National Geographic, 2016. Source: Dan-Eric Nilsson.

It is evident that these classes are organized from simpler to more complex, and that this organization follows the different stages on visual system evolution (Fig. 6). However, once evolution has reached a class, it is possible for the process to go either way, such that simpler behaviours evolved from more complex ones. In any case, the assumption that the behavioural classes originally evolved in ascending order is offered by the fact that the amount and rate of information fed to the nervous system increases steeply for each higher class of behaviours (for data on the fundamental performance requirements needed for the four classes see Nilsson, 2013). Still, complexity does not always mean better photoreceptive performance. High resolution vision (class IV) can, in principle, need more light than non-directional photoreception (class I), thus, this depends on the needs that each animal has (Fig. 7).

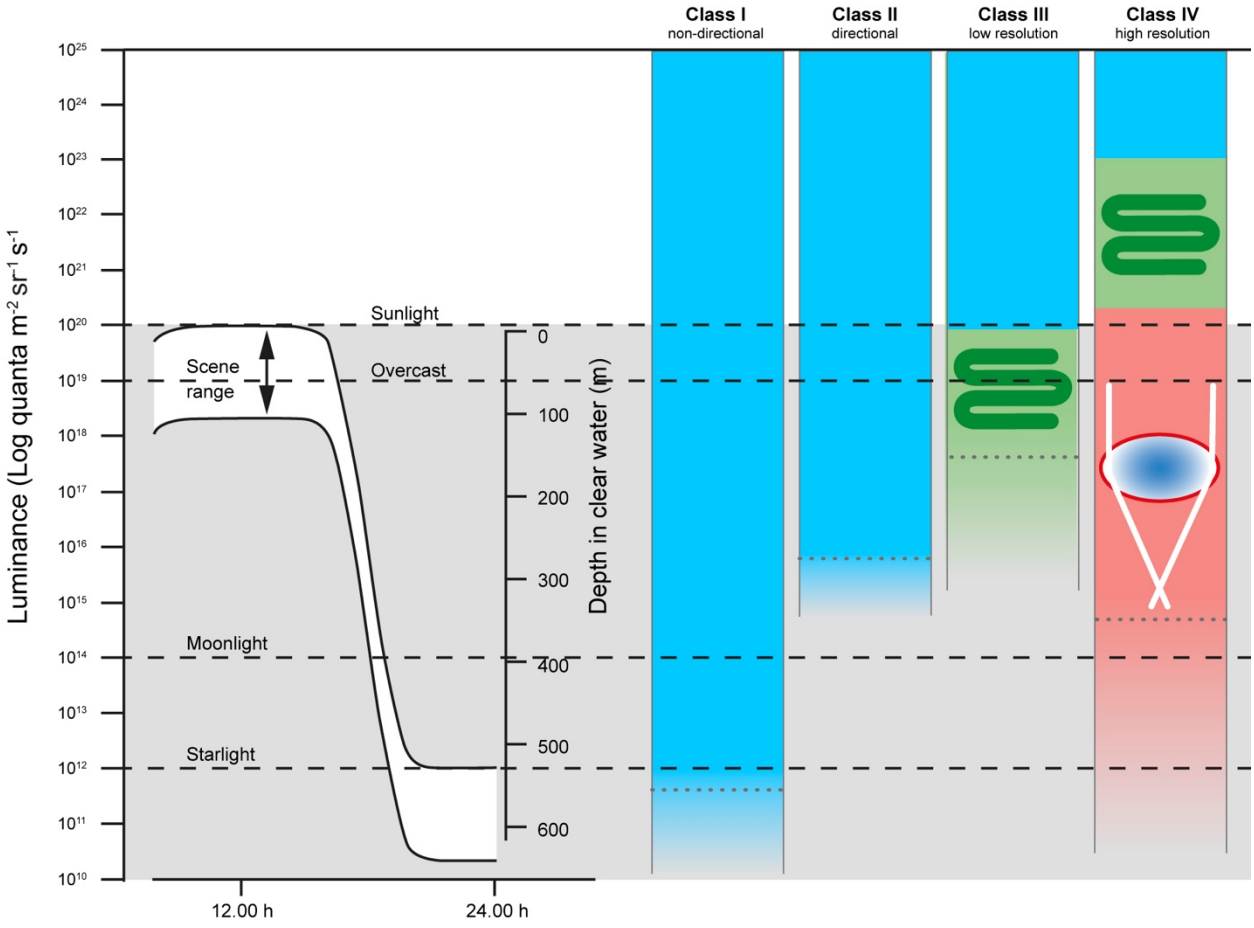

Fig 7. Minimum intensities from the four classes of sensory tasks, plotted together with the daily variation of natural luminance and daylight intensities at different depths in clear water. Blue indicates calculations for a 10 µm diameter cell with no membrane stacking and no focusing optics. Calculations for membrane stacking are indicated by green and for focusing optics by red. Figure reproduced from Nilsson (2013). The calculations of minimum intensity for the four classes of photoreceptive tasks can be found in the same publication.

Before this classification into four different classes it was traditionally laid that the starting point of the evolution of photoreceptors consisted of an epidermal ciliated cell with opsin molecules embedded in the membrane (Arendt et al., 2009). Although this view is widely accepted, numerous transparent planktonic animals lack ocelli but exhibit phototaxis. This brings us to the question 'is the photoreaction without associated shading pigments possible?' If so, the larvae of echinoderm clades seem to be a suitable material to study the depth origin of this sense. The small transparent larvae of the sea urchin (Fig. 8) have a rare example of a minimal photoreceptor system. This system is based on a Go opsin-positive cells without screening pigments in the cell itself or its surroundings. Apart from the presence of these opsin positive cells (a discovery that will be addressed in Chapter 2), these zooplanktonic larva also have motile cilia and a nervous system that may coordinate the sensory and motor cells.

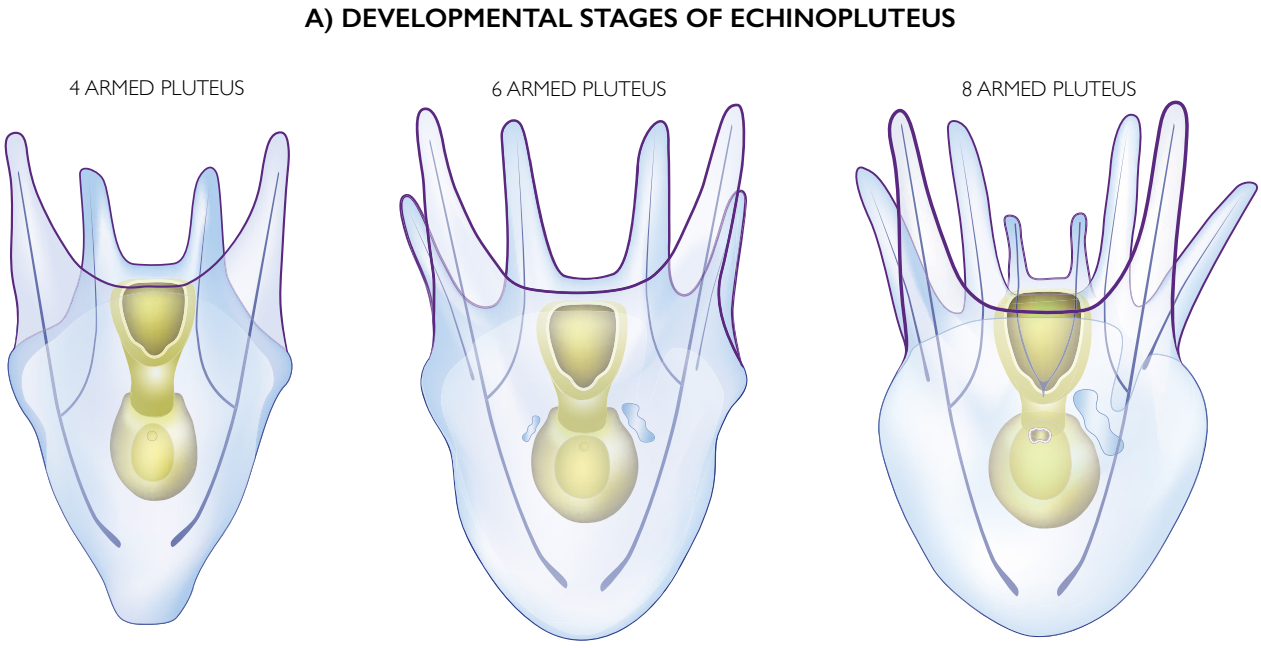

Fig 8. The sea urchin *Strongylocentrotus purpuratus*. A) The transparent pluteus larva of the sea urchin *S. purpuratus*, an ideal candidate to study the evolutionary ancient class I of photoreception, represented at 4, 6 and 8 armed stages (images not to scale). Illustrations made by Santiago Valero-Medranda.

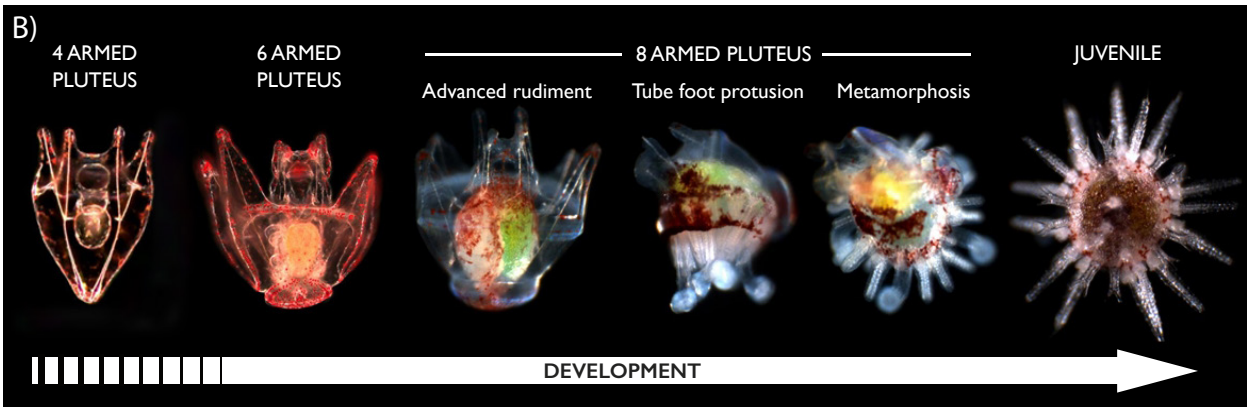

Fig 8. The sea urchin *Strongylocentrotus purpuratus*. B) Development of a sea urchin, from four armed pluteus till juvenile stage. Photographs courtesy of Yi-Jyun Luo, Su and Yu laboratory, Research Group of Development and Evolution, Academia Sinica (Taiwan).

The use of light for hunting and camouflage

The different uses of light by marine animals are not the main part of this study. It is, nonetheless, relevant to briefly mention the potential uses that these have for predating and avoiding predators in the pelagic environment. Perhaps some of these uses, most probably camouflage, explain the transparency and apparent lack of shading pigments of many dipleurula larvae, including the echinopluteus here studied.

Not surprisingly aquatic organisms possess visual systems that are specially adapted to the nature and properties of light underwater. Animals living near well-lit surface regions have colour vision, and many also develop UV photoreception, a character which advantageously extends their sensitivity range of light (Fig. 9A). Since several animals contain compounds that protect them against UV radiation by scattering, reflecting, or absorbing UV light, it results very useful to have UV receptors to detect them (Robison, 2004). In deeper oceanic environments, since both residual sunlight and bioluminescence are spectrally very restricted with most radiation being in the 450 to 500 nm region, many animals shift their spectral sensitivity to indigo ($\lambda \approx 445$ nm) and blue ($\lambda \approx 475$ nm) lights (Douglas et al., 2000; Frank et al., 2012). Further, some animals (such as

shrimps and some cephalopods), have develop polarized visual systems by means of a special geometrical arranged of their retinas (Warrant and Locket, 2004; How et al., 2015; Daly et al., 2016; Feller and Cronin, 2016) (Fig. 9A). With this ability they can navigate by the skylight polarization pattern, or detect otherwise transparent or silvery scaled preys by seeing its effect on the polarization of light (Jordan et al., 2016).

In deeper regions with less light, such as the mesopelagic, the animals have developed amazing adaptations to increase their photosensitivity (Fig. 9B). They perceive light in extremely low light levels, though decreasing its resolution and lengthening their integration times. On the one hand, very complex long, tubular, telescope eyes can be seen (e.g. in fishes or crustaceans) (Nilsson, 1996). On the other hand, very simplified photoreceptors, like the non-directional ones herein described, maximize the light capture by reducing or eliminating their screening pigments for a better photon catch. A relationship between depth and photoreceptor design is particularly evident in many animals from the dysphotic areas: the deeper the habitat, the more the eye is dedicated to upward vision (Nilsson, 1996).

Once we arrive to the aphotic region, an area in which sunlight cannot arrive, the main light sources come from bioluminescent organisms in all directions (Fig. 4). Very striking is the ability of some animals to produce their own light in a region of the spectra that is invisible for most deep-sea animals to 'see but avoid to be seen'. An example of this strategy can be found in three groups of mesopelagic dragon fishes (Malacosteus, Pachystomias and Aristostomias) that possess, in addition to blue emitting light organs, suborbital photophores that produce far-red light (Douglas et al., 1995; 2000). This photophores can be used both for private, intraspecific communication, and to cover illumination of prey at distances about ten times greater than the range of lateral line senses (Douglas et al, 1995).

But seeing is only part of the equation. Ocean organisms do have visual adaptations that matched very clever strategies to avoid being seen in an open ocean where it is difficult to hide (reviewed in Johnsen, 2014). Some organisms colour themselves in a dynamic way to match the background water (Hanlon et al., 2009). Others have mirrored teguments (a mirror in the ocean only reflects more of the ocean, and so is invisible) (Fig. 9C). Still, others camouflage themselves with light, thus hiding their silhouettes with light producing organs on their downward facing surfaces that mimic the surrounding illumination. Many are simply transparent, as several ctenophores, salps, or invertebrate larvae; thus match their background in all situations (Fig. 9D). Finally, some use light and dark for disguise. They hide in the depths during the day and rising to feed at night (the vertical movements in the water column that depend on the day-night cycle are referred as the 'diel vertical migration' phenomena, a concept that will be key in the discussion of Chapter 3). Others stay near the surface, hiding in the glittering background of the lensing waves (Sosik and Johnsen, 2004). All these adaptations are driven by selective pressures and sensory organs are costly. What we can see in the natural word are systems just good enough to do their job in the context of fitness consequences.

As commented, camouflage is the primary defence of many animals (e.g. octopus, squid, and cuttlefish) and their body patterning system must change not only accurate, but also fast. However, some studies demonstrate that some of these animals that can adapt themselves to a high number of subtle background variables such as brightness, contrast, edge, and size of objects, lack colour perception. In these cases, the vexing question of how they achieve colour blind camouflage remains (Brown and Brown, 1958; Marshall and Messenger, 1996; Mätger et al., 2006; Chiao et al., 2011).

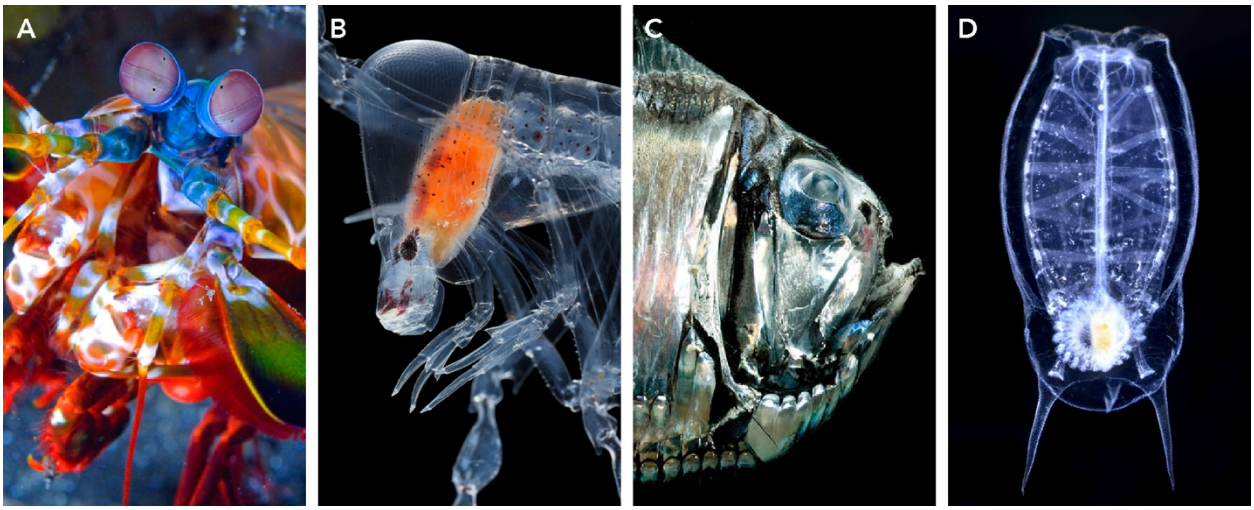

Fig 9. Some examples on the adaptations related to light perception exhibited in the ocean: A) the mantis shrimp *Odontodactylus scyllarus*, an animal with one of the most elaborate visual systems ever discovered, possesses an amazing number of 16 types of colour receptive cells (humans have three), picture: Marty Snyderman; B) the hyperiid amphipod Phronima sp., an animal equipped with two pairs of eyes especially adapted to low light conditions in which it hunts, picture: Solvin Zankl; C) a wide number of fishes, such as this Argyropelecus sp., have opted for wearing silver scales to reflect its marine surroundings, picture: Danté Fenolio; D) probably the most common strategy used by ocean fauna that want not to be seen is to develop transparency, an example of this is observed in the tunicate *Thalia democratica*, picture: Bigelow Laboratory of Ocean Sciences, USA.

The diversity of adaptations to see but avoid being seen is incredibly rich. Nevertheless, humans have had limited ability to explore the dimension of light in the ocean, and not many economical efforts are devoted to solving the mysteries of the sea depths. However, today's new technologies are allowing us to make promising steps forward to reveal how light operates in the ocean and how ocean life is adapted to different light conditions. An experimental set up to investigate the relationship between animal behaviour and downwelling light is presented in Chapter 3.

Photoreceptor cells

A remarkable clue for understanding photoreceptor cell evolution is the distinction between photoreceptor cell types (Land and Nilsson, 2012). Morphologically, most photoreceptors contain extensions of the cell membrane in the form of cilia or microvilli to maximize the accumulation of opsin proteins in a reduced space. Historically, this morphological feature has

allowed to divide photoreceptor cells in two major types: ciliary (with cilia in the apical region plus an axoneme of microtubules and a basal body, the centriole) and rhabdomeric (with microvilli or lamellae in the upper cell membrane of the plasmalemma unassociated developmentally with cilia) (Eakin, 1965) (Fig. 10). Apart from these two basic types, a third one is formed by simple coiling of the membrane to form a lamellate body (Horridge, 1964), and much more particular kinds can be found in the animal word. Moreover, there are cases in which the photoreceptor cell does not need to accumulate such a quantity of opsin protein for one or another reason, therefore these cell types lack of such membrane extensions.

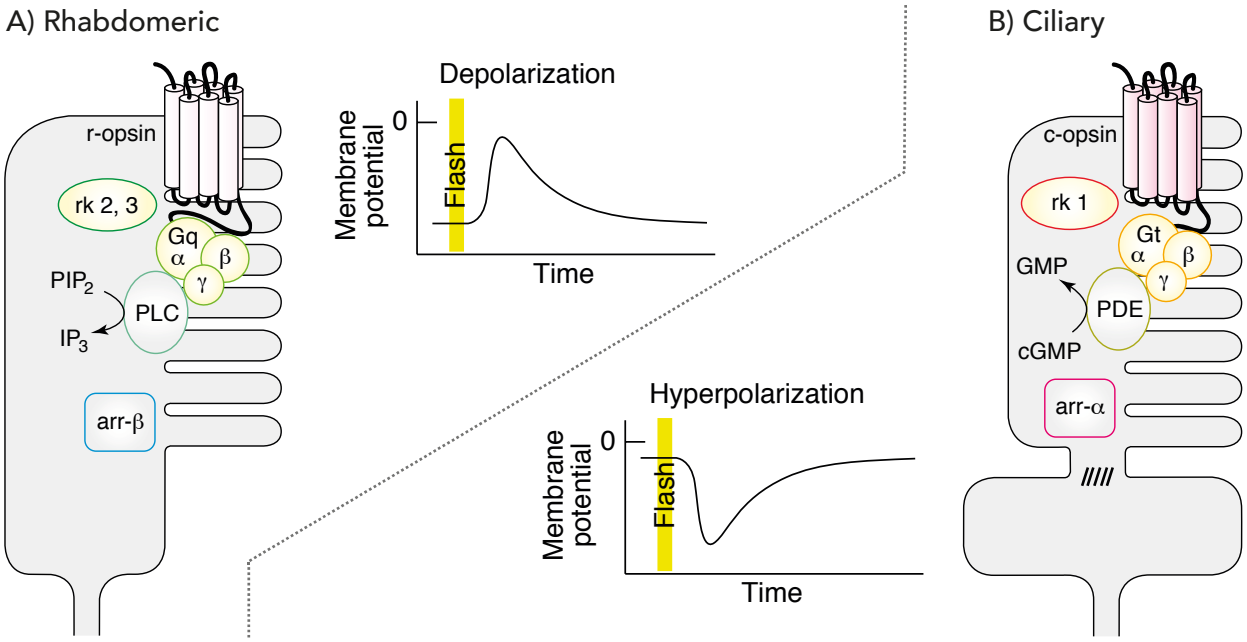

Fig 10. Two main photoreceptor cell types: A) rhabdomeric, and B) ciliary. The opsin and proteins of the transduction cascade are consistently paralogous between the two receptor types. In rhabdomeric photoreceptors, the G-protein leads to a depolarization of the membrane potential. R-opsins keep both the 11-*cis* and the *all*-trans isoforms firmly bound; they are known from the photoreceptors of invertebrate eyes and also represented by melanopsins in vertebrates. In the r-opsins, the chromophore can be converted back to the 11-*cis* form by the absorption of yet another photon, and this photoregeneration serves to replenish sensitive photo pigment. The ciliary receptor instead contains a phosphodiesterase which finally leads to hyperpolarization of the cell. C-opsins release the chromophore after it has been converted to the *all*-trans isoform; these opsins are originally known from vertebrate rods and cones. The c-opsins cannot themselves regenerate the chromophore, and a separate enzymatic system is required for this purpose. A functionally aberrant class of opsins acts not as receptor proteins but as photoisomerases that use light to convert chromophore from the *all*-trans to the 11-*cis* form, which is then

released and ready to be incorporated in a conventional opsin. Data compiled from Hamdorf (1977), Arendt and Wittbrodt (2001), Lamb and Pugh (2004) and Nilsson (2004). Figure modified from Nilsson (2004).

Even if in the past it was thought that the rhabdomeric photoreceptors were characteristic of invertebrates and the ciliary of vertebrates (Eakin, 1965; 1979), both kinds of photoreceptor cells have been found in either animal lineages, sometimes even in combination in the same photoreceptor organ (Brandenburger et al., 1973; Arendt et al., 2004; Peirson et al., 2009; Passamaneck, 2011; Braun et al., 2015). And although the structural differences between these two basic types are not entirely consistent throughout all animal groups, actual findings suggest that ciliary and rhabdomeric photoreceptors can be distinguishable at the molecular level (Arendt, 2003; Nilsson, 2004; Land and Nilsson, 2012) (Fig. 10).

With respect to opsin class and transduction cascade, there is a third type of photoreceptor primarily known from the peculiar mantle eyes of bivalves (Gomez and Nasi, 2000). The opsins of this class, Go, are closely related to photo-isomerase enzymes: proteins that are involved in regeneration of visual pigments in the 'visual cycle' described below (Land and Nilsson, 2012). A Go photoreceptor is investigated in the present work (Chapter 2).

Opsins

Taking all living organisms into consideration, there are several molecules that are photosensitive, most of which are used in photosynthesis. Since the principal molecules involved in animal photoreception are opsins, the characterization of that protein coupled receptors is useful to elucidate the origin of this sense (Wald, 1968; Dartnall, 1968; Arendt, 2003).

The study of opsins began in the late nineteenth century, with their discovery by Franz Boll and first characterization by Willy Kuhne (Marmor and Martin, 1978). Bovine rhodopsin was the first

sequenced and crystalized (Ovchinnikov, 1982; Hargrave et al., 1983; Nathans and Hogness, 1983; Palczewski et al., 2000). Since them, more than 2,000 opsins have been identified. The phylogenetic origin of these proteins seems to be related to melatonin precursors (Feuda et al., 2012), and the appearance of these receptor molecules must be very ancient, even more than planulozoans sensu Wallberg et al. (2004), given that some opsin sequences have been found in ctenophores and cnidarians (Suga et al., 2008; Ryan et al., 2010; Dunn et al., 2014; Feuda et al., 2014).

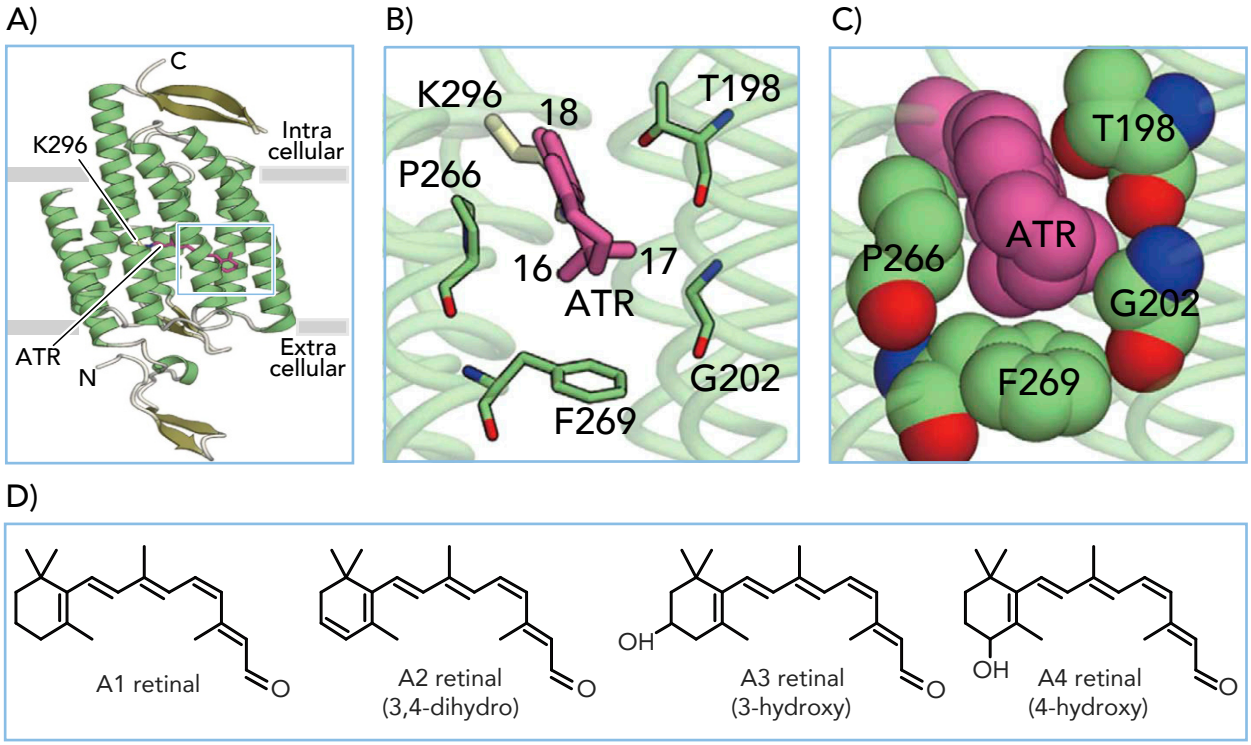

Fig 11. Protein structure of an opsin (A to C) and different chromophores that can be used for detecting light (D). A) Overall structure. Close-up views of the chromophore binding pocket around the β-ionone ring of the all-*trans* retinal (ATR) in liquorice B) and van der Waals C) representations. D) The chromophore moiety is a vitamin A-based retinaldehyde, either retinal (A1), 3,4-dehydroretinal (A2), 3-hydroxyretinal (A3) or 4-hydroxyretinal (A4). A1 retinal is the most common animal chromophore. A2 is commonly encountered in vertebrates such as fish, amphibian and reptiles. The A2 retinal generally causes a red shift in the absorbance maxima of the retinal/opsin complex, which is sometimes called porphylopsin (derived from purple) as opposed to the A1 retinal/opsin complex, which is generally called rhodopsin (derived from rose). Fresh water fishes often switch from A1 to A2 retinal to adapt to their light environment. A3 retinal is commonly observed in many insects, and the A3 retinal/opsin complex is sometimes called xanthopsin (derived from yellow). A4 retinal has been observed in the firefly squid, which seems to use A1, A2 and A4 retinals to create photoreceptor molecules of different absorbance maxima and achieve colour vision (Seidou et al., 1990). Although there are several names for a retinal-based photoreceptor molecule based on its chromophore and

its absorbance maxima, rhodopsin is used as a generic term to describe all the visual pigments (Shichida and Matsuyama, 2009). Figure modified from Kato et al. (2015); and Shichida and Matsuyama (2009).

The complex rhodopsin consists of a protein called opsin plus a 11-*cis* retinal which prevents the protein from signalling (Wald, 1968). The opsin protein has a molecular mass of 30-50 kDa, and the residue K296 (in the single letter amino acid code, taking as reference the bovine rhodopsin) in helix VII binds the retinal via a Schiff base linkage. More in detail, the nitrogen atom of the K296 amino group forms a double bond with the terminal carbon of the retinal. The key residue K296 is important for light absorption, and its presence or absence can be used as molecular fingerprint to judge whether or not a newly found rhodopsin type GPCR is a bona fide opsin. The counterion is another important residue: it is a negatively charged amino acid that helps to stabilize the protonated Schiff base (Terakita, 2005) (Fig. 12).

Although we lack a consensus about the nomenclature and phylogeny of opsins as a whole, the majority of the molecular phylogenetic hypotheses identify three large clusters: ciliary, rhabdomeric, and Go/RGR opsins (Terakita, 2005; Porter et al., 2011; Feuda et al., 2012). These three opsin clusters have been further subdivided into seven subfamilies: (i) the 'vertebrate' visual (transducing coupled) and non-visual opsin subfamily; (ii) the encephalopsin/tmt-opsin subfamily; (iii) the Gq-coupled opsin/melanopsin subfamily; (iv) the Go-coupled opsin subfamily; (v) the peropsin subfamily; (vi) the retinal photo isomerase subfamily; and (vii) the neuropsin subfamily (Terakita, 2005).

Even though this classification in three main clusters is the classical one, a more recent phylogeny on this issue reports a classification in four opsin groups: tetraopsin, xenopsin, Gq-opsin, and c-opsin (Ramirez et al., 2016) (Fig. 12). This study has been benefited of a more comprehensive opsin sequence dataset that includes the previously poorly sampled molluscs plus the Ambulacraria sequences reported in the Chapter 1 of this thesis (for publication, see Appendix II).

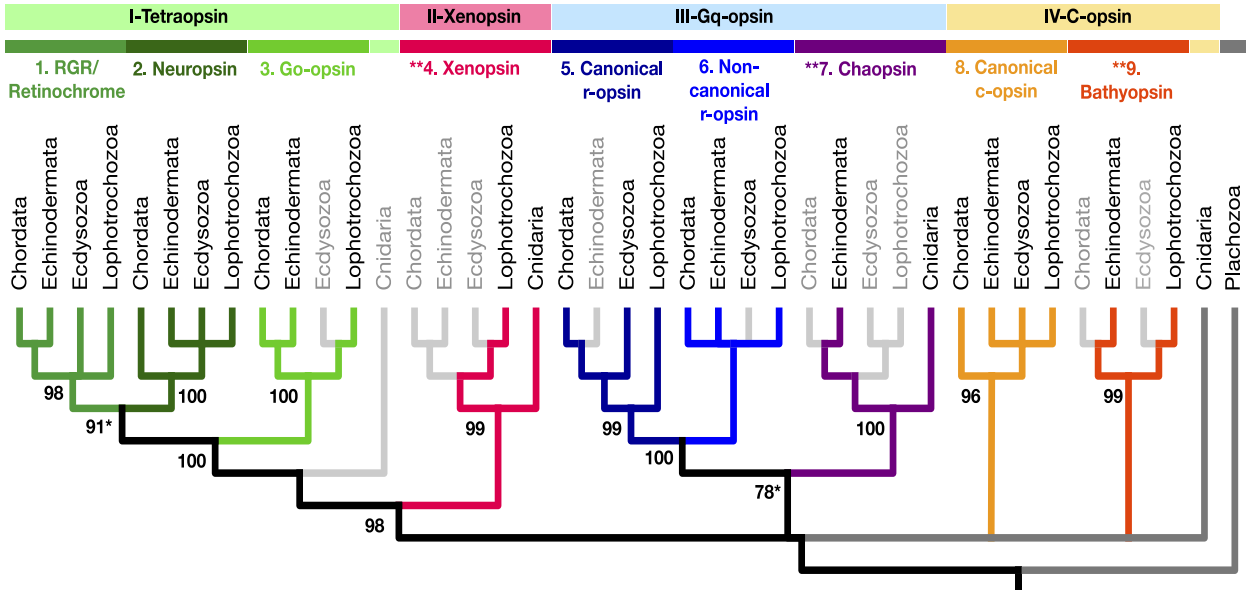

Fig 12. There are nine bilaterian opsin paralogs spread among four major eumetazoan opsin paralogs. The four major eumetazoan opsin paralogs are indicated at the top with Roman numerals. The nine bilaterian opsin paralogs are indicated with Arabic numerals and are colour coded to match the corresponding branches. Coloured branches indicate the presence of an opsin in at least one species within the major taxonomic group. Light grey branches indicate the absence of an opsin paralog from the taxa indicated at the tips. Ultrafast bootstrap (UFBoot) supports from IQ-TREE are given next to the branch they support. Bootstraps with asterisks were added from the gene tree after reconciliation analysis. Figure reproduced from Ramirez et al. (2016).

Nonetheless, the division into different subgroups in any of the classifications does not correspond well to a functional classification, but the one presented in Terakita (2005) is partly based on the type of G protein coupled to each of these GPCRs. In any case, members of the tetraopsin, xenopsin, Gq-opsin, and c-opsin groups are found in both deuterostomes and protostomes, thus suggesting that the opsin diversification occurred before the deuterostome-protostome split (Fig. 12).

Non-visual opsins and their expression domains

Even if visual systems are more studied that any other sensory system by far, we do still lack of many details about how extra-ocular photoreceptors work due to the difficulties encountered for localizing and identifying them. However, extra-ocular photoreception must be a quite common ability in the animal world. One indication of that is the number of behavioural studies in which it is described

how specimens without eyes can respond to light changes (Wapstra and van Soest, 1987; Taddei-Ferretti and Musio, 2000; Musio et al., 2001; Purschke et al., 2006; Ramirez et al., 2011).

In some cases, photoreception is regulated by dermal cells that induce colour changes or that trigger locomotory activity (Wolken and Mogus, 1979; Shand and Foster, 1999; Peirson et al., 2009). In other instances, it is assumed that nerves are photosensitive, which means that such nerve cells are likely to contain opsins in their membrane (Hankins et al., 2014). Further modifications of these neural structures have led to the development of complex organs that detect light in a non-directional manner. Of these systems two are especially remarkable: the 'pineal complex' and the 'deep-brain photoreceptors', both present in the vertebrate lineage (Shand and Foster, 1999).

The pineal complex, composed by the pineal organ and third eye, is the primary source of the neurohormone melatonin (melatonin is synthesized in the dark phase of the light/dark cycle, and acts as a signal of darkness to regulate circadian rhythms and photoperiodic responses) (Arendt, 1998; Korf et al., 1998). The term pineal complex can be used to refer to the intracranial pineal proper, as well as to speak about the parapineal and the extracranial 'third' eyes found in tuatara (Rhynchocephalia), some lizards (Squamata), and frogs (Anura) (Vollrath, 1981; Shand and Foster, 1999; Peirson et al., 2009).

In the case of the deep-brain photoreceptors, they were first described by Karl von Frisch in 1911 on European minnows (*Phoxinus phoxinus*). These fishes, when blinded and pinealectomized, still demonstrated colour changes in response to light leading to the suggestion of 'deep-diencephalic photoreceptors' (von Frisch, 1911). In similar experiments carried out with European eels (*Anguilla anguilla*), van Veen and co-workers demonstrated that

deep-brain photoreceptors mediate photo-entrainment as well as negative phototaxis (van Veen et al., 1976). The photoperiodic response in birds, whereby gonadal growth is regulated by day length, is mediated by deep-brain photoreceptors too (Benoit, 1964).

Arrived at this point, the reader will have noticed that most information on non-directional photoreceptors come from studies in vertebrates, where a complete subfamily of opsins has been named 'non-visual' opsins (Terakita, 2005). These non-visual opsins possess important characteristics of a typical opsin-based photo pigment including the lysine retinal attachment site (Lys296), the presence of a glutamate counterion at site 113 (Glu113) or 181 (Glu181) and two conserved cysteine residues (Cys110 and Cys187) that form a disulphide bridge. Despite these commonalities, each non-directional opsin is unique at both gene and protein levels. The diversity of non-visual opsins in the vertebrate lineage has its origins in at least two rounds of whole genome duplications; one early in the evolution of the whole stem group, and a second around the divergence of the teleosts (Nakatani and Morishita, 2008). Interestingly, the evolutionary retention rate of opsin and other GPCR genes during these duplications is significantly higher than for other genes by a factor from two to three (Semyonov et al., 2008). This highlights the evolutionary advantage conferred by signalling proteins and opsins in particular.

The main sensu stricto non-visual opsins studied in vertebrates are: (i) the exorhodopsin, reported for the first time in the teleost pineal gland (Vigh-Teichmann et al., 1982, 1983; Mano et al., 1999; Philp et al., 2000); (ii) the pinopsin (also called p-opsin), first extraretinal opsin to be cloned that was isolated from the pineal gland of the chicken also identified in amphibians and reptiles (Max et al., 1995; Yoshikawa et al., 1998; Kawamura and Yokoyama, 1997; Taniguchi et al., 2001; Frigato et al., 2006); (iii) the 'vertebrate ancient opsin', called in this way because the first phylogenetic analysis suggested that they diverged at the very beginning of the craniate

evolution, an idea today in disuse (Soni and Foster, 1997); (iv) the 'parietopsin', found in the parietal eye of lizards (Su et al., 2006); and (v) the 'parapinopsin', first identified in the catfish pineal and parapineal organs (Blackshaw and Snyder, 1997; Koyanagi et al, 2004).

To this list we can add other 'non-directional' opsins that are both expressed in ocular and extra-ocular photoreceptors. Examples of them are: (vi) the 'encephalopsin' (sometimes called panopsin), mainly expressed in mouse brain and testis with lower levels in the heart, liver, kidney, and retina whose function is still unknown (Blackshaw and Snyder, 1999; Halford et al., 2001); (vii) the TMT opsin, an opsin related to the circadian oscillator of zebrafish (Whitmore et al., 2000; Moutsaki et al., 2003); (viii) the 'melanopsin', a molecule originally isolated from the melanophores of Xenopus and mammals also related to the master circadian pacemaker (Provencio et al., 1998; 2000); and (ix) the 'neuropsin', first identified by means of bioinformatic approaches (Tarttelling et al., 2003). Further information on the molecular fingerprints on each of these nine non-visual opsins can be found in Peirson et al. (2009).

Despite the relatively good quantity of information about non-visual opsin in craniates, non-visual opsins have been less studied in invertebrates. Examples of these are the rhodopsin found in the parolfactory vesicles of the squid *Todarodes pacificus* (Hara and Hara, 1980); the 'cnidarian opsin' and 'Clytia opsin9' found in the gonad ectoderm of Hydra and Clytia (Musio et al., 2001; Artigas et al., 2017); the UV, blue, and long-wavelength sensitive opsins found in the extraretinal photoreceptors of the hakmoths *Manduca sexta*, *Archerontia atropos*, *Agrius convolvuli*, and *Hippotion celerio* (Lampel et al., 2005); the *c-opsin* located in the developing median brain of the annelid *Platynereis dumerilii* larva (Arendt et al., 2004); the *Go-opsin* found in the gastrula of the brachiopod *Terebratalia transversa* (Passamaneck and Martindale, 2013); or the pteropsin expressed in the honey bee brain (Velarde et al., 2005). In a humble effort to further gain insights onto the

evolutionary origin of these non-visual opsins, herein I report about the presence of a *Go-opsin* expressed in the apical organ of the sea urchin larva (Chapter 2 and Valero-Gracia et al., 2016).

Phototransduction

Phototransduction can be defined as the conversion of a light signal into a nervous impulse. The general process occurs in the following way: first, the activation of the photoreceptor cell pigment rhodopsin by light occurs through the isomerization of 11-*cis* retinal (Fig. 13A) to all-*trans* retinal (Fig. 13B); then, active rhodopsin binds and activates the α-subunit of an intracellular G-protein that in turn activates intracellular messengers to finally hyperpolarize or depolarize the photoreceptor cell (Fig. 10) (Arendt and Wittbrodt, 2001; Wright et al., 2010). Opsins from different classes coupled to distinct G-proteins are associated with different transduction cascades (Fig. 10; Table 1) (Nilsson, 2009).

Table 1 – OPSINS AND TRASDUCTION CASCADES IN ANIMAL PHOTORECEPTORS

OPSIN	G-PROTEIN	CONTROLLED ENZYME	SECOND MESSENGER	RESPONSE POLARITY
c-opsin	G_t	PDE	cGMP	hyperpolarization
r-opsin	G_q	PLC	IP_3, DAG	depolarization
G_o-opsin	G_o	GC	cGMP	hyperpolarization/ depolarization
cnidops class	G_s	AC	cAMP	depolarization

Table 1. Opsins and transduction cascades in animal photoreceptors. PDE, phosphodiesterase; PLC, phospholipase C; GC, guanylate cyclase; AC, adenylate cyclase; cGMP, cyclic guanosine phosphate; cAMP, cyclic adenosine phosphate; IP_3, inositol triphosphate; DAG, diacylglycerol. Table reproduced from Nilsson (2009).

The majority of photoreceptors use a Gα protein belonging to either of two evolutionary distinct classes: Gα-q and Gα-t (Oakley and Pankey, 2008). The G-proteins responsible for relaying the light signal consist of three subunits: α, β and γ. The α subunit binds opsin only after the opsin chromophore has accepted a photon and induced a conformational change. Upon binding, Gα hydrolyses a bound GDP for GTP, and dissociates from Gβ-γ. At this

point, Gα-GTP can activate specific targets such as phosphodiesterase (PDE) or phospholipase C (PLC) (Oakley and Pankey, 2008).

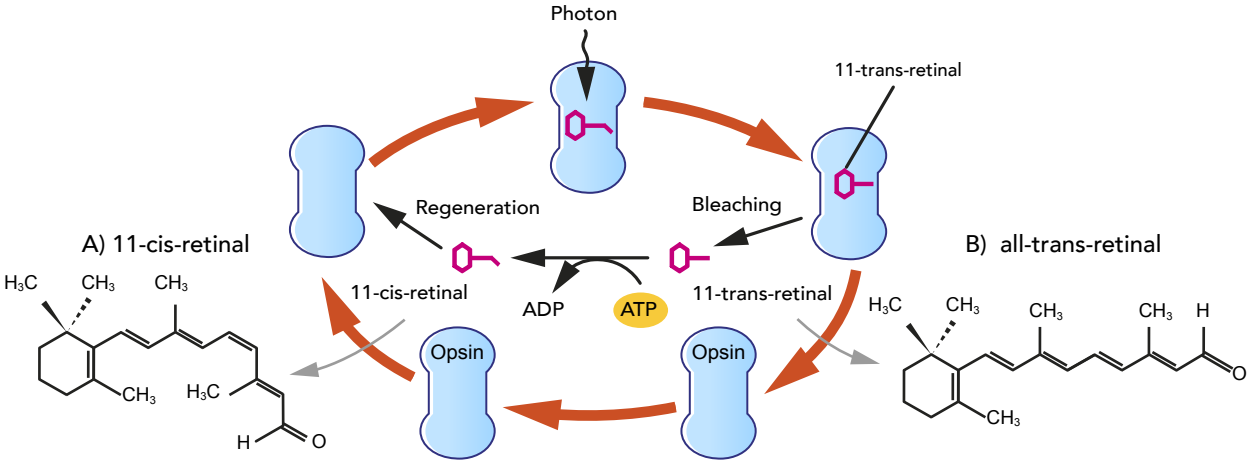

Fig 13. The retinoid cycle and photoadaptation. 11-*cis*-retinal and opsin are reassembled to form rhodopsin. The absorption of light leads to an isomeric change in the retinal molecule. Illustration from Anatomy and Physiology (2013).

Photoreceptors expressing Gα-q respond to activation by Gα-q-GTP releasing calcium from the endoplasmic reticulum. Usually, the subsequent opening of transient receptor potential (TRP) ion channels depolarize the cell (Hardie, 2001). In cells bearing opsins that target Gα-t, PDE becomes activated by Gα-t-GTP to hydrolyse cellular cGMP into 5' GMP. These cells rely on cyclic nucleotide-gated (CNG) ion channels, which only remain open in the presence of cGMP. Following photo excitation and subsequent decrease in cellular cGMP, these channels close and hyperpolarise the cell (Yau and Baylor, 1989). More details on the different components that intervene in the phototransduction cascade can be found in Pierce et al. (2002) and Terakita (2005).

In some instances (e.g. in photoreceptors based on c-opsins), the photoreceptor systems require a pathway of enzymatic reactions to recycle the retinoid employed during light detection. This group of reactions is called the 'visual cycle'. All-*trans* retinal is released from the rhodopsin complex and transported to the cytoplasm by an ATP binding cassette. The molecule, after modification to all-*trans* retinol, is sent to the photoreceptor cell were it is esterified to a fatty acyl group to form all-*trans*

retinyl ester. All-*trans* retinyl ester is subject to trans-isomerization to 11-*cis* retinal through the actions of two further enzymes. After transporting back to the photoreceptor cell, 11-*cis* retinal binds rhodopsin rendering it sensitive to light again (Wright et al., 2010). In some cases, a functional aberrant class of opsins have been co-opted to act as photo-isomerases that used light to change the retinyl conformation (Sperling and Hubbard, 1975; Gonzalez-Fernandez, 2003).

The Ambulacraria clade

Ambulacraria is a group of deuterostomes comprising the Echinodermata and Hemichordata clades. Both groups have been placed together since Metschnikoff (1881) emphasized the similarities between their coelomic systems and larvae. Also, molecular studies strongly support the monophyly of the group (Cannon et al., 2009; 2014; Dunn et al., 2014). The Ambulacraria show archimery (i.e. a division of the body into three regions: prosome, mesosome, and metasome) which cannot always be recognized externally, but that can be observed during development because of the formation of three well defined coelomic compartments: protocoel, mesocoel and metacoel (Nielsen, 2012).

Echinodermata

Echinoderms, from ancient greek 'echinos' (hedgehog) and 'derma' (skin), are a phylum that include sea lilies and feather stars (Crinoidea), sea stars (Asteroidea), brittle stars (Ophiuroidea), sea cucumbers (Holoturoidea) and sea urchins (Echinoidea) (Fig. 14). While the number of species is not great in comparison to other clades (circa 7,000 extant nominal species) (Appeltans et al., 2012), they are extremely numerous as individuals in unpolluted seas and deep water (Moore, 2006). All echinoderms are marine. Morphological and molecular studies demonstrate the existence of two clades: Pelmatozoa (Crinoidea) and Eleutherozoa (the remaining classes) (Chia and Harrison, 1994; Janies et al., 2011; Telford et al., 2014) (Fig. 14).

Crinoidea

The crinoids (sea lilies and feather stars; Fig. 14A) are the oldest surviving group of echinoderms, and resemble their ancestors in being essentially sedentary suspension feeders (Smith and Zamora, 2013; Zamora and Rahman, 2014). Comatulids (feather stars) are secondary motile, being able to swim by waving the arms up and down. In free spawning species the larva is called a doliolaria (Hyman, 1955).

Asteroidea

Asteroids (Fig. 14B) constitute a large clade with circa 2,000 species which are generally predators or scavengers (Appeltans et al., 2012). Active predators not only have to move, they must displace in a directed way from place to place. How can the radially symmetrical starfish move in one direction and, without a single cerebral ganglion, how can it coordinate the stepping of the tube feet in different arms? Observations show that any arm can become the leading arm with the other four cooperating and that the site of coordination is in the radial nerve cord (Moore, 2006). Curiously, these arms are provided with eyes at the distal end of each arm tip in many sea star species (Garm and Nilsson, 2014). Patterns of activity in any one arm can be conducted round the ring and direct the stepping of tube feet in the whole animal. In this way, a starfish can make a temporary 'brain' without having a permanently defined brain structure. Pelagic planktotrophy, pelagic lecithotrophy, and benthic lecithotrophy are widespread among asteroids. Bipinnaria and brachiolaria are the main larval types present in this animal group (Young, et al., 2012).

Ophiuroidea

The ophiuroids (Fig. 14C), commonly named brittle stars, constitute another large clade (circa 2,000 spp.) (Appeltans et al., 2012). They have harder skeleton than asteroids and, although they are stellate in form, the arms are clearly marked off from the disc.

Most ophiuroids resemble asteroids in being actively carnivores, but their methods of feeding and locomotion are very different. Interestingly, some species have marked sensitivity to light intensity enabling them to detect shadows of predators, change in colour, and escape rapidly (Moore, 2006). Light sensitive ophiuroids species incorporate calcite crystals into the skeleton and arrange them into microstructures acting as double lenses, each of them especially sensitive to light from a particular direction (Aizenberg et al., 2001; Delroisse et al., 2014). This is a nice example not only for the more elaborate photoreceptor structures required by faster moving animals, but also for a structure combining mechanical and sensory functions. Species with planktotrophic development have ophioplutei larvae. Ophioplutei are superficially similar to echinoplutei because they both have their larval arms supported by skeletal rods, but the longest pair of larval arms in ophioplutei (the posterolaterals) extend laterally from the larval anterior-posterior axis in a much significant way in comparison with the echinopluteus (Young, et al., 2002).

Holoturoidea

Sea cucumbers (Fig. 14D) comprise about 900 species which are very unlike other echinoderms (Appeltans et al., 2012). They are bilaterally symmetrical, lying on one side with an elongated body axis between the mouth and the anus. The endoskeleton is very reduced, leaving a muscular body wall with a few embedded ossicles but without spines or pedicellariae. Typically, holothuroids are deposit feeders. When pursued by predators, holoturoids may immobilise them by extruding a mass of sticky blind ending tubules (the cuvierian tubules), or may evert internal organs and leave them in the part of the predator. The rest of the holothuroid escapes, and regenerates its viscera (Moore, 2006). Two larval forms are characteristic of the clade: the auricularia and the doliolaria. Regardless of the developmental route (indirect or direct), the end of larval life is generally considered to be the pentactula, when the five primary tentacles emerge from the doliolaria (Semon, 1888).

Echinoidea

Unlike asteroids and ophiuroids, sea urchins (circa 950 spp.; Fig. 14F) are slow moving animals that feed themselves by scraping seaweed from rocks (regular forms) or that bulk feed on the sediment to extract nutrients (irregular forms). On the irregular forms, the mouth located in anterior position collects food and the anus situated posteriorly leaves the waste behind. The irregular forms derived from the regular ones. Echinoids have their body covered by spines and pedicellariae. Locomotion is mainly by spines that articulate with the main skeleton through 'ball and socket' joints, and are controlled partly by muscle and partly by mutable connective tissue (Moore, 2006). The tube feet assist locomotion and keep the urchins close to the substratum on which they are grazing or anchor them in crevices. The feeding larva of echinoids is called echinopluteus, and like feeding larvae of other echinoderms has clear bilateral symmetry. The larvae do not resemble like the adults into which they metamorphose. The name pluteus was given to feeding larvae of ophiuroids and echinoids by Müller, who thought the larva resemble an easel (Müller, 1846).

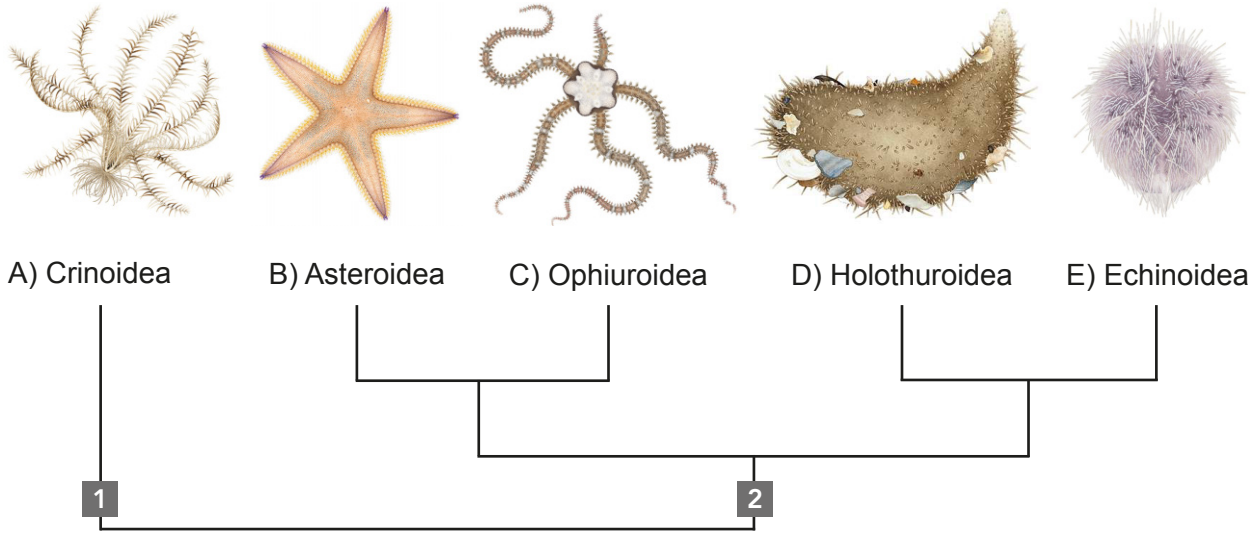

Fig 14. General view on echinoderm interrelationships according to the Asterozoa hypothesis. 1) Pelmatozoa; 2) Eleutherozoa. A) Crinoidea: *Hathrometra sarsii*; B) Asteroidea: *Astropecten irregularis*; C) Ophiuroidea: *Ophiopholis aculeata*; D) Holoturoidea: *Thyone fusus*; E) Echinoidea: *Spantangus purpureus*. Drawings from Nationalnyckeln till Sveriges Flora och Fauna. Illustrator: Helena Samuelsson (2013).

Hemichordata

Hemichordates, the sister group of echinoderms, consist of two main groups dissimilar in appeareance: enteropneusts and pterobranchs (Fig. 16). As adults, all hemichordates are benthic marine animals (except, perhaps, for *Planctosphaera pelagica*, an organism viewed as a hemichordate larva that has not been linked to a specific adult yet) (van der Horst, 1936) . These worms generally live buried in soft sediments, among algal holdfasts or under rocks. Interest in this group of animals has been largely based on their proposed morphological affinities and close phylogenetic relationship to chordates (Bateson, 1886; Berrill, 1955; Bone, 1979; Garstang, 1894; Gerhart et al., 2005; Lacalli, 2005; Nielsen, 2009; Rottinger and Lowe, 2012).

Enteropneusta

The enteropneusts (circa 70 species, 600 microns to 200 centimetres in length) are large solitary animals, burrowing in the mud or sand of the shallow seas (Worsaae et al., 2012). They are divided into four groups: Harrimaniidae, Spengelidae, Ptycoderidae, and Torquaratoridae (Cameron et al., 2000; Cannon et al., 2009; 2014; Osborn et al., 2011) (Fig. 16). The ciliated proboscis collects food into the mouth, which opens from the collar. The lobe, in front of the mouth, has a complex 'heart glomerulus' system supported by a rod like stomochord. The nervous system is not centralised, there is a nerve net resembling that of echinoderms, epidermal in origin and position. The main concentration of neural tissue in the collar is hollow, and develops much as in chordates.

The larva is a tornaria (Fig. 15), remarkably similar to the auricularia and bipinnaria larvae of echinoderms. In both, the tornaria and the bipinnaria, there is a short pore canal leading from the most anterior cavity to a 'hydropore' functioning as an excretory outlet. The tornaria also resembles most echinoderm larvae in having a gel-filled earliest body cavity, permitting development of a large larva with little cellular material (Moore, 2006).

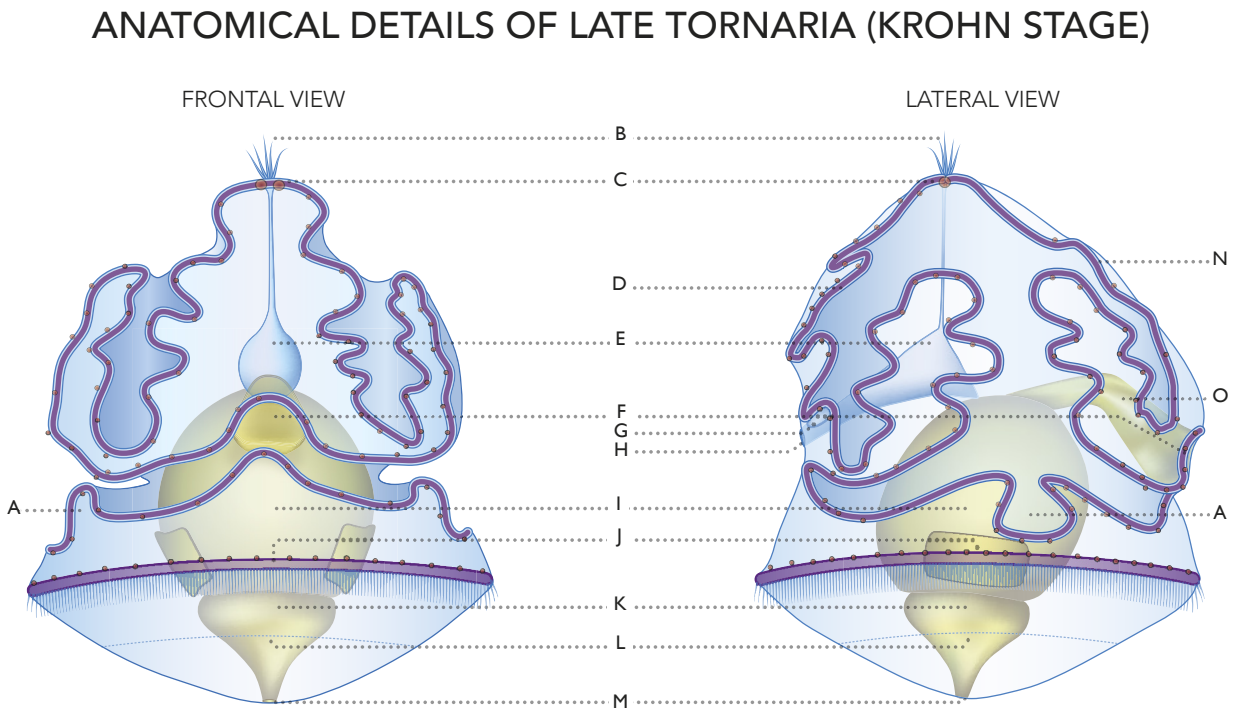

Fig 15. General view on the tornaria larva (Hemichordata) at Krohn stage, frontal and lateral views. A) Dorsal aboral field; B) apical ciliary tuft; C) ocelli; D) postoral part of neotroch; E) hydrocoele; F) buccal cavity; G) heart-kidney complex; H) hydropore; I) stomach; J) opisthotroch; K) intestine; L) perianal ciliary ring; M) anus; N) preoral part of neotroch; O) pharynx. Nomenclature in agreement with Nielsen and Hay-Schmidt, 2007. Illustration redraw from Spengel, 1893 by Santiago Valero-Medranda.

Pterobranchia

The pterobranchs (21 species divided in two groups, Cephalodiscidae and Rhabdopleuridae) are minute (circa one to five milimiters long), sessile and colonial animals, covered in cilia and with lophophores bearing tentacles that collect their food (Cannon et al., 2014). *Cephalodiscus* has a single pair of gill slits, *Rhabdopleura* has none. The simple nervous system seems to be entirely epidermal. Pterobranchs reproduce asexually by budding or sexually by releasing gametes. The larva, unlike the enteropneust tornaria, is uniformly ciliated and short lived. It has a store of yolk and does not feed itself, serving solely for dispersal (Hyman, 1959).

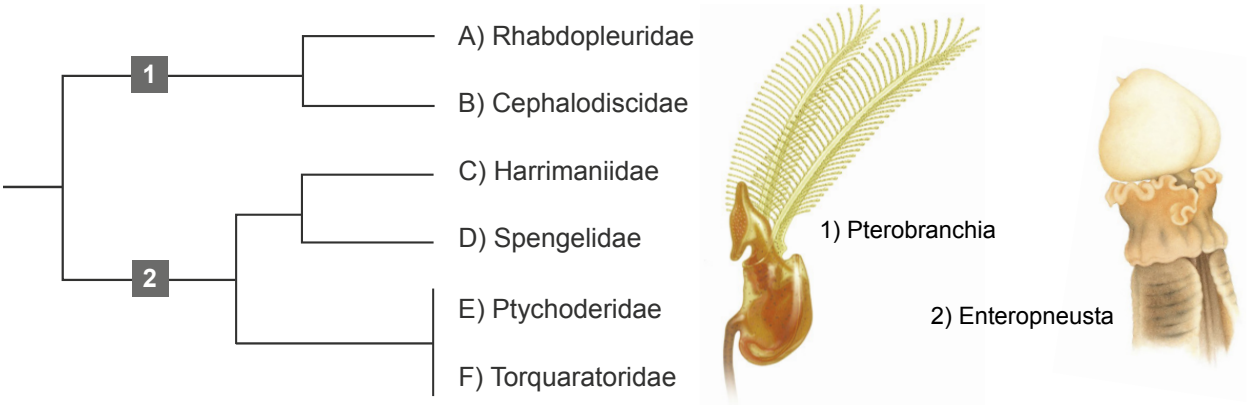

Fig 16. General view on hemichordate interrelationships, a clade subdivided in two: 1) Perobranchia, here represented by Rhabdopleura sp. (drawing from Erik Nasibov), that contains A) Rhabdopleuridae, and B) Cephalodiscidae; and 2) Enteropneusta, here represented by *Glossobalanus marginatus* (drawing from Helena Samuelsson), that contains C) Harrimaniidae, D) Spengelidae, E) Ptychoderidae, and F) Torquatoridae. Illustrations from Nationalnyckeln till Sveriges Flora och Fauna (2013).

References

Aizenberg, J., Tkachenko, A., Weiner, S., Addadi, L., & Hendler, G. (2001). Calcitic microlenses as part of the photoreceptor system in brittlestars. *Nature*, *412*(6849), 819-822.

Appeltans, W., Ahyong, S. T., Anderson, G., Angel, M. V., Artois, T., Bailly, N., ... & Błażewicz-Paszkowycz, M. (2012). The magnitude of global marine species diversity. *Current Biology*, *22*(23), 2189-2202.

Arenas-Mena, C., Martinez, P., Cameron, R. A., & Davidson, E. H. (1998). Expression of the Hox gene complex in the indirect development of a sea urchin. *Proceedings of the National Academy of Sciences*, *95*(22), 13062-13067.

Arenas-Mena, C. (2010). Indirect development, transdifferentiation and the macroregulatory evolution of metazoans. *Philosophical Transactions of the Royal Society of London B: Biological Sciences*, *365*(1540), 653-669.

Arendt, D. (2003). Evolution of eyes and photoreceptor cell types. *International Journal of Developmental Biology*, *47*(7-8), 563-571.

Arendt, D., Hausen, H., & Purschke, G. (2009). The 'division of labour'model of eye evolution. *Philosophical Transactions of the Royal Society of London B: Biological Sciences*, *364*(1531), 2809-2817.

Arendt, D., & Wittbrodt, J. (2001). Reconstructing the eyes of Urbilateria. *Philosophical Transactions of the Royal Society of London B: Biological Sciences*, *356*(1414), 1545-1563.

Arendt, D., Tessmar-Raible, K., Snyman, H., Dorresteijn, A. W., & Wittbrodt, J. (2004). Ciliary photoreceptors with a vertebrate-type opsin in an invertebrate brain. *Science*, *306*(5697), 869-871.

Arendt, J. (1998). Melatonin and the pineal gland: influence on mammalian seasonal and circadian physiology. *Reviews of Reproduction*, *3*(1), 13-22.

Artigas, G. Q., Lapébie, P., Leclère, L., Takeda, N., Deguchi, R., Jékely, G., ... & Houliston, E. (2017). CRISPR/Cas9 mutation of a gonad-expressed opsin prevents jellyfish light-induced spawning. *BioRxiv*, 140210.

Baguñà, J., Martinez, P., Paps, J., & Riutort, M. (2008). Back in time: a new systematic proposal for the Bilateria. *Philosophical Transactions of the Royal Society of London B: Biological Sciences*, *363*(1496), 1481-1491.

Bateson, W. (1886). Memoirs: the ancestry of the Chordata. *Journal of Cell Science*, *2*(104), 535-572.

de Beer, G. R. (1954). The evolution of the Metazoa, in *Evolution as a Process* (Eds J. Huxley et al.), pp. 24-33. Allen and Unwin, London.

Bengtson, S. (2002). Origins and early evolution of predation. *Paleontological Society Papers*, *8*, 289-318.

Bennett, M. F. (1979). Extraocular light receptors and circadian rhythms. In *Comparative Physiology and Evolution of Vision in Invertebrates* (pp. 641-663). Springer Berlin, Heidelberg.

Benoit, J. (1964). The role of the eye and of the hypothalamus in the photostimulation of gonads in the duck. *Annals of the New York Academy of Sciences*, *117*(1), 204-215.

Berrill, N. J. (1955). *The origin of Vertebrates*. Clarendon Press, Oxford.

Bishop, C. D., & Brandhorst, B. P. (2003). On nitric oxide signaling, metamorphosis, and the evolution of biphasic life cycles. *Evolution & Development*, *5*(5), 542-550.

Blackshaw, S., & Snyder, S. H. (1997). Parapinopsin, a novel catfish opsin localized to the parapineal organ, defines a new gene family. *Journal of Neuroscience*, *17*(21), 8083-8092.

Blackshaw, S., & Snyder, S. H. (1999). Encephalopsin: a novel mammalian extraretinal opsin discretely localized in the brain. *Journal of Neuroscience*, *19*(10), 3681-3690.

Bok, M. J., Capa, M., & Nilsson, D. E. (2016). Here, there and everywhere: The radiolar eyes of fan worms (Annelida, Sabellidae). *Integrative and Comparative Biology*, icw089.

Bok, M. J., Porter, M. L., Place, A. R., & Cronin, T. W. (2014). Biological sunscreens tune polychromatic ultraviolet vision in mantis shrimp. *Current Biology*, *24*(14), 1636-1642.

Bone, Q. (1979) *The Origin of Chordates*, 2nd ed. Carolina Biol Supply Co., Burlington.

Born, M., & Wolf, E. (2003). *Principles of Optics* (revised). Cambridge University Press, Cambridge.

Brandenburger, J. L., Woolacott, R. M., & Eakin, R. M. (1973). Fine structure of eyespots in tornarian larvae (Phylum: Hemichordata). *Cell and Tissue Research*, *142*(1), 89-102.

Braun, K., Kaul-Strehlow, S., Ullrich-Lüter, E., & Stach, T. (2015). Structure and ultrastructure of eyes of tornaria larvae of Glossobalanus marginatus. *Organisms Diversity & Evolution*, *15*(2), 423-428.

Brown, P. K., & Brown, P. S. (1958). Visual pigments of the octopus and cuttlefish. *Nature*, *182*(4645), 1288-1290.

Budd, G. E. (2008). The earliest fossil record of the animals and its significance. *Philosophical Transactions of the Royal Society B: Biological Sciences*, *363*(1496), 1425-1434.

Budd, G. E., & Jensen, S. (2000). A critical reappraisal of the fossil record of the bilaterian phyla. *Biological Reviews*, *75*(2), 253-295.

Budd, G. E., & Jensen, S. (2015). The origin of the animals and a 'Savannah' hypothesis for early bilaterian evolution. *Biological Reviews*, *92*(1), 446-473.

Bütschli, O. (1884). Bemerkungen zur Gastraea-Theorie. *Morphololog*i*sche Jahrbücher*, 9, 415-427.

Byrne, M., Nakajima, Y., Chee, F. C., & Burke, R. D. (2007). Apical organs in echinoderm larvae: insights into larval evolution in the Ambulacraria. *Evolution & Development*, *9*(5), 432-445.

Cameron, C. B., Garey, J. R., & Swalla, B. J. (2000). Evolution of the chordate body plan: new insights from phylogenetic analyses of deuterostome phyla. *Proceedings of the National Academy of Sciences*, *97*(9), 4469-4474.

Cannon, J. T., Kocot, K. M., Waits, D. S., Weese, D. A., Swalla, B. J., Santos, S. R., & Halanych, K. M. (2014). Phylogenomic resolution of the hemichordate and echinoderm clade. *Current Biology*, *24*(23), 2827-2832.

Cannon, J. T., Rychel, A. L., Eccleston, H., Halanych, K. M., & Swalla, B. J. (2009). Molecular phylogeny of hemichordata, with updated status of deep-sea enteropneusts. *Molecular Phylogenetics and Evolution*, *52*(1), 17-24.

Chia, F. S. H., & Harrison, F. W. (1994). Introduction to the Echinodermata. *Microscopic Anatomy of Invertebrates, 14,* 1-9. Wiley-Liss, New York.

Chiao, C. C., Wickiser, J. K., Allen, J. J., Genter, B., & Hanlon, R. T. (2011). Hyperspectral imaging of cuttlefish camouflage indicates good color match in the eyes of fish predators. *Proceedings of the National Academy of Sciences*, *108*(22), 9148-9153.

Clarkson, E., Levi-Setti, R., & Horváth, G. (2006). The eyes of trilobites: the oldest preserved visual system. *Arthropod Structure & Development*, *35*(4), 247-259.

Conway Morris, S. (1998). Eggs and embryos from the Cambrian. *BioEssays*, *20*(8), 676-682.

Conway Morris, S. (2000). The Cambrian "explosion": slow-fuse or megatonnage? *Proceedings of the National Academy of Sciences*, *97*(9), 4426-4429.

Conway Morris, S. (2006). Darwin's dilemma: the realities of the Cambrian 'explosion'. *Philosophical Transactions of the Royal Society of London B: Biological Sciences*, *361*(1470), 1069-1083.

Daly, I. M., How, M. J., Partridge, J. C., Temple, S. E., Marshall, N. J., Cronin, T. W., & Roberts, N. W. (2016). Dynamic polarization vision in mantis shrimps. *Nature Communications*, *7, 12140*.

Dartnall, H. J. A. (1968). The photosensitivities of visual pigments in the presence of hydroxylamine. *Vision Research*, *8*(4), 339-358.

Davidson, E. H., Peterson, K. J., & Cameron, R. A. (1995). Origin of bilaterian body plans: evolution of developmental regulatory mechanisms. *Science*, 270, 1319-1325.

Delroisse, J., Ullrich-Lüter, E., Ortega-Martinez, O., Dupont, S., Arnone, M. I., Mallefet, J., & Flammang, P. (2014). High opsin diversity in a non-visual infaunal brittle star. *BMC Genomics*, *15*(1), 1035.

Douglas, R. H., Partridge, J. C., & Hope, A. J. (1995). Visual and lenticular pigments in the eyes of demersal deep-sea fishes. *Journal of Comparative Physiology A: Neuroethology, Sensory, Neural, and Behavioral Physiology*, *177*(1), 111-122.

Douglas, R. H., Mullineaux, C. W., & Partridge, J. C. (2000). Long wave sensitivity in deep sea stomiid dragonfish with far red bioluminescence: evidence for a dietary origin of the chlorophyll derived retinal photosensitizer of Malacosteus niger. *Philosophical Transactions of the Royal Society B: Biological Sciences*, *355*(1401), 1269-1272.

Dunn, C. W., Giribet, G., Edgecombe, G. D., & Hejnol, A. (2014). Animal phylogeny and its evolutionary implications. *Annual Review of Ecology, Evolution, and Systematics*, *45*, 371-395.

Dzik, J. (1978). Larval development of hyolithids. *Lethaia*, *11*(4), 293-299.

Eakin, R. M. (1965). Evolution of photoreceptors. In *Cold Spring Harbor Symposia on Quantitative Biology* (Vol. 30, pp. 363-370). Cold Spring Harbor Laboratory Press, New York.

Eakin, R. M. (1979). Evolutionary significance of photoreceptors: in retrospect. *American Zoologist*, *19*(2), 647-653.

von der Emde, G., & Warrant, E. (Eds.). (2015). *The Ecology of Animal Senses: Matched Filters for Economical Sensing*. Springer, Berlin.

Erwin, D. H., & Davidson, E. H. (2002). The last common bilaterian ancestor. *Development*, *129*(13), 3021-3032.

Erwin, D. H., Laflamme, M., Tweedt, S. M., Sperling, E. A., Pisani, D., & Peterson, K. J. (2011). The Cambrian conundrum: Early divergence and later ecological success in the early history of animals. *Science*, *334*(6059), 1091-1097.

Fain, G. L. (2003). *Sensory Transduction*. Sinauer, Sunderland, MA.

Feller, K. D., & Cronin, T. W. (2016). Spectral absorption of visual pigments in stomatopod larval photoreceptors. *Journal of Comparative Physiology A*, *202*(3), 215-223.

Feuda, R., Hamilton, S. C., McInerney, J. O., & Pisani, D. (2012). Metazoan opsin evolution reveals a simple route to animal vision. *Proceedings of the National Academy of Sciences*, *109*(46), 18868-18872.

Feuda, R., Rota-Stabelli, O., Oakley, T. H., & Pisani, D. (2014). The comb jelly opsins and the origins of animal phototransduction. *Genome Biology and Evolution*, *6*(8), 1964-1971.

von Frisch, K. (1911). Das Parietalorgan der Fische als funktionierendes Organ. *Sitzber. Ges. Morphol. Physiol. Munich*, *27*, 16-18.

Frank, T. M., Johnsen, S., & Cronin, T. W. (2012). Light and vision in the deep-sea benthos: II. Vision in deep-sea crustaceans. *Journal of Experimental Biology*, *215*(19), 3344-3353.

Frigato, E., Vallone, D., Bertolucci, C., & Foulkes, N. S. (2006). Isolation and characterization of melanopsin and pinopsin expression within photoreceptive sites of reptiles. *Naturwissenschaften*, *93*(8), 379-385.

Garm, A., & Nilsson, D. E. (2014). Visual navigation in starfish: first evidence for the use of vision and eyes in starfish. *Proceedings of the Royal Society B,* 281(1777), 20133011.

Garstang, W. (1922). The Theory of Recapitulation: A critical re-statement of the Biogenetic Law. *Zoological Journal of the Linnean Society*, *35*(232), 81-101.

Garstang, W. (1894). Preliminary note on a new theory of the phylogeny of the Chordata. *Zoologischer Anzeiger - A Journal of Comparative Zoology*, *17*(1).

Gehring, W. J. (1996). The master control gene for morphogenesis and evolution of the eye. *Genes to Cells*, *1*(1), 11-15.

Gerhart, J., Lowe, C., & Kirschner, M. (2005). Hemichordates and the origin of chordates. *Current Opinion in Genetics & Development*, *15*(4), 461-467.

del Pilar Gomez, M., & Nasi, E. (2000). Light transduction in invertebrate hyperpolarizing photoreceptors: possible involvement of a Go-regulated guanylate cyclase. *Journal of Neuroscience*, *20*(14), 5254-5263.

Gonzalez-Fernandez, F. (2003). Interphotoreceptor retinoid-binding protein, an old gene for new eyes. *Vision Research*, *43*(28), 3021-3036.

Graff, L. V. (1882). *Monographie der Turbellarien*. Leipzig: I. Rhabdocoelida.

Grell. K. G. (1971). Trichoplax adhaerens und die Entstehung der Metazoen. *Naturwissenschaftliche Rundschau*, 24, 160-161.

Hadfield, M. G., & Paul, V. J. (2001). Natural chemical cues for settlement and metamorphosis of marine invertebrate larvae. *Marine Chemical Ecology*, 431-461.

Hadži, J. (1955). *The Evolution of the Metazoa: International Series of Monographs on Pure and Applied Biology: Zoology* (Vol. 16). Elsevier.

Haeckel, E. (1866). *Generelle Morphologie der Organismen. Allgemeine Grunzüge der organischen Formen-Wissenschaft, mechanisch begründet durch die von Charles Darwin reformirte Descendenz-Theorie. Band 1: Akkgemeine Anatomie der Organismen*, Georg Reimer, Berlin.

Haeckel, E. (1874). Memoirs: The Gastraea-Theory, the phylogenetic classification of the animal kingdom and the homology of the germ-lamellae. *Journal of Cell Science*, *2*(54), 142-165.

Halford, S., Bellingham, J., Ocaka, L., Fox, M., Johnson, S., Foster, R. G., & Hunt, D. M. (2001). Assignment1 of panopsin (OPN3) to human chromosome band 1q43 by in situ hybridization and somatic cell hybrids. *Cytogenetic and Genome Research*, *95*(3-4), 234-235.

Hamdorf, K., & Razmjoo, S. (1977). The prolonged depolarizing afterpotential and its contribution to the understanding of photoreceptor function. *European Biophysics Journal*, *3*(2), 163-170.

Hankins, M. W., Davies, W. I., & Foster, R. G. (2014). The evolution of non-visual photopigments in the central nervous system of vertebrates. In *Evolution of Visual and Non-visual Pigments* (pp. 65-103). Springer US.

Hanlon, R. T., Chiao, C. C., Mäthger, L. M., Barbosa, A., Buresch, K. C., & Chubb, C. (2009). Cephalopod dynamic camouflage: Bridging the continuum between background matching and disruptive coloration. *Philosophical Transactions of the Royal Society of London B: Biological Sciences*, *364*(1516), 429-437.

Hara, T., & Hara, R. (1980). Retinochrome and rhodopsin in the extraocular photoreceptor of the squid Todarodes. *The Journal of General Physiology*, *75*(1), 1-19.

Hardie, R. C. (2001). Phototransduction in Drosophila melanogaster. *Journal of Experimental Biology*, *204*(20), 3403-3409.

Hargrave, P. A., McDowell, J. H., Curtis, D. R., Wang, J. K., Juszczak, E., Fong, S. L., ... & Argos, P. (1983). The structure of bovine rhodopsin. *Biophysics of Structure and Mechanism*, *9*(4), 235-244.

Hecht, E. (2016). The propagation of light. *Optics, 5th ed.*, Addison-Wesley Longman, Inc., Adelphi University.

Hoffman, P. F., & Schrag, D. P. (2002). The snowball Earth hypothesis: testing the limits of global change. *Terra Nova*, *14*(3), 129-155.

Holland, P. W. (2015). Did homeobox gene duplications contribute to the Cambrian explosion? *Zoological Letters*, *1*(1), 1.

Holm-Hansen, O., Lubin, D., & Helbling, E. W. (1993). Ultraviolet radiation and its effects on organisms in aquatic environments. In *Environmental UV photobiology* (pp. 379-425). Springer US.

Horridge, G. A. (1964). Presumed photoreceptive cilia in a ctenophore. *Journal of Cell Science*, *3*(71), 311-317.

How, M. J., Christy, J. H., Temple, S. E., Hemmi, J. M., Marshall, N. J., & Roberts, N. W. (2015). Target detection is enhanced by polarization vision in a fiddler crab. *Current Biology*, *25*(23), 3069-3073.

Hu, S., Steiner, M., Zhu, M., Erdtmann, B. D., Luo, H., Chen, L., & Weber, B. (2007). Diverse pelagic predators from the Chengjiang Lagerstätte and the establishment of modern-style pelagic ecosystems in the early Cambrian. *Palaeogeography, Palaeoclimatology, Palaeoecology*, *254*(1), 307-316.

Hyman, L. H. (1951). *The Invertebrates: Platyhelminthes and Rhynchocoela, the acoelomate Bilateria* (Vol. 2). McGraw-Hill, New York.

Hyman, L. H. (1955). *The Invertebrates: Echinodermata* (Vol. 4). McGraw-Hill, New York.

Hyman, L. H. (1959). *The Invertebrates: Smaller coelomate groups* (Vol. 5). McGraw-Hill, New York, 121-244.

van der Horst, C. J. (1936). Memoirs: Planctosphaera and Tornaria. *Journal of Cell Science*, *2*(312), 605-613.

Ivanov, P. P. (1937). General and Comparative Embryology. *Ogiz-Biomedgiz*, Moscow (in Russian).

Jablonski, D. (1986). Larval ecology and macroevolution in marine invertebrates. *Bulletin of Marine Science*, *39*(2), 565-587.

Jablonski, D., & Lutz, R. A. (1983). Larval ecology of marine benthic invertebrates: paleobiological implications. *Biological Reviews*, *58*(1), 21-89.

Jägersten, G., (1972). *Evolution of the Metazoan Life Cycle*. London Academic Press, London.

Janies, D. A., Voight, J. R., & Daly, M. (2011). Echinoderm phylogeny including Xyloplax, a progenetic asteroid. *Systematic Biology*, syr044.

Jenner, R. A. (2000). Evolution of animal body plans: The role of metazoan phylogeny at the interface between pattern and process. *Evolution & Development*, *2*(4), 208-221.

Jerlov, N. G. (1976). *Marine Optics* (Vol. 14). Elsevier, Amsterdam.

Johnsen, S. (2014). Hide and seek in the open sea: pelagic camouflage and visual countermeasures. *Annual Review of Marine Science 6*, 369-392.

Jordan, T. M., Wilby, D., Chiou, T. H., Feller, K. D., Caldwell, R. L., Cronin, T. W., & Roberts, N. W. (2016). A shape-anisotropic reflective polarizer in a stomatopod crustacean. *Scientific Reports*, *6*, 21744.

Kato, H. E., Kamiya, M., Sugo, S., Ito, J., Taniguchi, R., Orito, A., ... & Ishitani, R. (2015). Atomistic design of microbial opsin-based blue-shifted optogenetics tools. *Nature Communications*, *6*.

Kawamura, S., & Yokoyama, S. (1997). Expression of visual and nonvisual opsins in American chameleon. *Vision Research*, *37*(14), 1867-1871.

Kirschvink, J.L., 1992. Late Proterozoic low-latitude global glaciation: the snowball earth. In: *The Proterozoic Biosphere* (J. W. Schopf and C. Klein, eds), pp. 51-52. Cambridge University Press, Cambridge.

Knoll, A. H., & Carroll, S. B. (1999). Early animal evolution: Emerging views from comparative biology and geology. *Science*, *284*(5423), 2129-2137.

Korf, H. W., Schomerus, C., & Stehle, J. H. (1998). Introduction. In *The Pineal Organ, Its Hormone Melatonin, and the Photoneuroendocrine System* (pp. 1-8). Springer Berlin Heidelberg.

Koyanagi, M., Kawano, E., Kinugawa, Y., Oishi, T., Shichida, Y., Tamotsu, S., & Terakita, A. (2004). Bistable UV pigment in the lamprey pineal. *Proceedings of the National Academy of Sciences of the United States of America*, *101*(17), 6687-6691.

Lacalli, T. C. (2005). Protochordate body plan and the evolutionary role of larvae: old controversies resolved? *Canadian Journal of Zoology*, *83*(1), 216-224.

Lamb, T. D., & Pugh, E. N. (2004). Dark adaptation and the retinoid cycle of vision. *Progress in Retinal and Eye Research*, *23*(3), 307-380.

Lampel, J., Briscoe, A. D., & Wasserthal, L. T. (2005). Expression of UV-, blue-, long-wavelength-sensitive opsins and melatonin in extraretinal photoreceptors of the optic lobes of hawkmoths. *Cell and tissue research*, *321*(3), 443-458.

Land, M. F., & Nilsson, D. E. (2012). *Animal Eyes*. Oxford University Press, Oxford.

Leech, D. M., Padeletti, A., & Williamson, C. E. (2005). Zooplankton behavioral responses to solar UV radiation vary within and among lakes. *Journal of Plankton Research*, *27*(5), 461-471.

Lythgoe, J. N. (1979). *The Ecology of Vision: Oxford Science Publications*. Oxford University Press, Oxford.

Mano, H., Kojima, D., & Fukada, Y. (1999). Exo-rhodopsin: a novel rhodopsin expressed in the zebrafish pineal gland. *Molecular Brain Research*, *73*(1), 110-118.

Marlow, H., Tosches, M. A., Tomer, R., Steinmetz, P. R., Lauri, A., Larsson, T., & Arendt, D. (2014). Larval body patterning and apical organs are conserved in animal evolution. *BMC Biology*, 12(1), 7.

Marmor, M. F., & Martin, L. J. (1978). 100 years of the visual cycle. *Survey of Ophthalmology*, *22*(4), 279-285.

Marriott, F. H. C. (1958). The absolute light-sensitivity and spectral threshold curve of the aquatic flatworm Dendrocoelum lacteum. *The Journal of Physiology*, *143*(2), 369-379.

Marshall, N. J., & Messenger, J. B. (1996). Colour-blind camouflage. *Nature*, *382*(6590), 408.

Martin, V. J. (2004). Photoreceptors of cubozoan jellyfish. *Hydrobiologia*, *530*(1), 135-144.

Mason, B. M., & Cohen, J. H. (2012). Long-wavelength photosensitivity in coral planula larvae. *The Biological Bulletin*, *222*(2), 88-92.

Max, M., McKinnon, P. J., Seidenman, K. J., & Barrett, R. K. (1995). Pineal opsin: a nonvisual opsin expressed in chick pineal. *Science*, *267*(5203), 1502.

Mäthger, L. M., Barbosa, A., Miner, S., & Hanlon, R. T. (2006). Color blindness and contrast perception in cuttlefish (Sepia officinalis) determined by a visual sensorimotor assay. *Vision Research*, *46*(11), 1746-1753.

Metschnikoff, V. E. (1881). Über die systematische Stellung von Balanoglossus. *Zoologischer Anzeiger - A Journal of Comparative Zoology*, *4*, 139-157.

Metschnikoff, V. E. (1886). *Embryologische Studien an Medusen: Ein Beitrag zur Genealogie der primitiven Organe*. Hölder, Wien.

Minelli, A. (2009). *Perspectives in Animal Phylogeny and Evolution*. Oxford University Press, Oxford.

Mitchell, D. R. (2007). The evolution of eukaryotic cilia and flagella as motile and sensory organelles. In *Eukaryotic Membranes and Cytoskeleton* (pp. 130-140). Springer New York.

Moore, J. (2006). *An Introduction to the Invertebrates*. Cambridge University Press, Cambridge.

Morel, A., & Prieur, L. (1977). Analysis of variations in ocean color. *Limnology and Oceanography*, *22*(4), 709-722.

Moutsaki, P., Whitmore, D., Bellingham, J., Sakamoto, K., David-Gray, Z. K., & Foster, R. G. (2003). Teleost multiple tissue (tmt) opsin: a candidate photopigment regulating the peripheral clocks of zebrafish? *Molecular Brain Research*, *112*(1), 135-145.

Musio, C., Santillo, S., Taddei-Ferretti, C., Robles, L. J., Vismara, R., Barsanti, L., & Gualtieri, P. (2001). First identification and localization of a visual pigment in Hydra (Cnidaria, Hydrozoa). *Journal of Comparative Physiology A: Neuroethology, Sensory, Neural, and Behavioral Physiology*, *187*(1), 79-81.

Müller, J. (1846). *Über den Bau und die Grenzen der Ganoiden und über das natürliche System der Fische*. Gedruckt in der Druckerei der Königlichen Akademie der Wissenschaften.

Müller, K. J., & Walossek, D. (1988). *External morphology and larval development of the Upper Cambrian maxillopod Bredocaris admirabilis*. Universitetsforlaget.

Nakatani, Y., Qu, W., & Morishita, S. (2008). Comparing the Human and Fish Genomes. *eLS*.

Nathans, J., & Hogness, D. S. (1983). Isolation, sequence analysis, and intron-exon arrangement of the gene encoding bovine rhodopsin. *Cell*, *34*(3), 807-814.

Nielsen, C. (1979). Larval ciliary bands and metazoan phylogeny. *Fortschr. Zool. Syst. Evol-Forsch*, 1, 178-184.

Nielsen, C., & Nørrevang, A. (1985). The trochaea theory: an example of life cycle phylogeny. In *Systematics Association Special Volume* (pp. 28-41). Oxford University Press.

Nielsen, C. (1987). Structure and function of metazoan ciliary bands and their phylogenetic significance. *Acta Zoologica*, *68*(4), 205-262.

Nielsen, C. (2004). Trochophora larvae: Cell-lineages, ciliary bands, and body regions 1. Annelida and Mollusca. *Journal of Experimental Zoology Part B: Molecular and Developmental Evolution*, *302*(1), 35-68.

Nielsen, C. (2005). Trochophora larvae: cell-lineages, ciliary bands and body regions 2. Other groups and general discussion. *Journal of Experimental Zoology Part B: Molecular and Developmental Evolution*, *304*(5), 401-447.

Nielsen, C., & Hay-Schmidt, A. (2007). Development of the enteropneust Ptychodera flava: ciliary bands and nervous system. *Journal of Morphology*, *268*(7), 551-570.

Nielsen, C. (2008). Six major steps in animal evolution: are we derived sponge larvae? *Evolution & Development*, *10*(2), 241-257.

Nielsen, C. (2009). How did indirect development with planktotrophic larvae evolve?. *The Biological Bulletin*, *216*(3), 203-215.

Nielsen, C. (2012). *Animal Evolution: Interrelationships of the Living Phyla*. Oxford University Press, Oxford.

Nilsson, D. E. (1996). Eye ancestry: old genes for new eyes. *Current Biology*, *6*(1), 39-42.

Nilsson, D. E. (2004). Eye evolution: a question of genetic promiscuity. *Current Opinion in Neurobiology*, *14*(4), 407-414.

Nilsson, D. E. (2009). The evolution of eyes and visually guided behaviour. *Philosophical Transactions of the Royal Society of London B: Biological Sciences*, *364*(1531), 2833-2847.

Nilsson, D. E. (2013). Eye evolution and its functional basis. *Visual Neuroscience*, *30* (1-2), 5-20.

Nordström, K., Seymour, J., & Nilsson, D. (2003). A simple visual system without neurons in jellyfish larvae. *Proceedings of the Royal Society of London B: Biological Sciences*, *270*(1531), 2349-2354.

Oakley, T. H., & Pankey, M. S. (2008). Opening the "black box": the genetic and biochemical basis of eye evolution. *Evolution: Education and Outreach*, *1*(4), 390-402.

Olive, P. J. W. (1985). Environmental control of reproduction in Polychaeta. *Fortschritte der Zoologie Neue Folge*, 29, 17-38.

Osborn, K. J., Kuhnz, L. A., Priede, I. G., Urata, M., Gebruk, A. V., & Holland, N. D. (2011). Diversification of acorn worms (Hemichordata, Enteropneusta) revealed in the deep sea. *Proceedings of the Royal Society of London B: Biological Sciences*, rspb20111916.

Ovchinnikov, Y. A. (1982). Rhodopsin and bacteriorhodopsin: structure, function and relationships. *FEBS letters*, *148*(2), 179-191.

Palczewski, K., Kumasaka, T., Hori, T., Behnke, C. A., Motoshima, H., Fox, B. A., ... & Yamamoto, M. (2000). Crystal structure of rhodopsin: AG protein-coupled receptor. *Science*, *289*(5480), 739-745.

Passamaneck, Y. J., Furchheim, N., Hejnol, A., Martindale, M. Q., & Lüter, C. (2011). Ciliary photoreceptors in the cerebral eyes of a protostome larva. *EvoDevo*, *2*(1), 6.

Passamaneck, Y. J., & Martindale, M. Q. (2013). Evidence for a phototransduction cascade in an early brachiopod embryo. *Integrative and Comparative Biology*, 53 (1): 17-26.

Paul, N. D., & Gwynn-Jones, D. (2003). Ecological roles of solar UV radiation: towards an integrated approach. *Trends in Ecology & Evolution*, *18*(1), 48-55.

Peirson, S. N., Halford, S., & Foster, R. G. (2009). The evolution of irradiance detection: melanopsin and the non-visual opsins. *Philosophical Transactions of the Royal Society B: Biological Sciences*, *364*(1531), 2849-2865.

Peterson, K. J., Cameron, R. A., & Davidson, E. H. (1997). Set-aside cells in maximal indirect development: Evolutionary and developmental significance. *BioEssays*, *19*(7), 623-631.

Peterson, K. J., & Davidson, E. H. (2000). Regulatory evolution and the origin of the bilaterians. *Proceedings of the National Academy of Sciences*, *97*(9), 4430-4433.

Peterson, K. J., Cameron, R. A., & Davidson, E. H. (2000). Bilaterian origins: significance of new experimental observations. *Developmental biology*, *219*(1), 1-17.

Peterson, K. J., Cotton, J. A., Gehling, J. G., & Pisani, D. (2008). The Ediacaran emergence of bilaterians: congruence between the genetic and the geological fossil records. *Philosophical Transactions of the Royal Society of London B: Biological Sciences*, *363*(1496), 1435-1443.

Peterson, K. J., Dietrich, M. R., & McPeek, M. A. (2009). MicroRNAs and metazoan macroevolution: insights into canalization, complexity, and the Cambrian explosion. *Bioessays*, *31*(7), 736-747.

Philp, A. R., Garcia-Fernandez, J. M., Soni, B. G., Lucas, R. J., Bellingham, J. A. M. E. S., & Foster, R. G. (2000). Vertebrate ancient (VA) opsin and extraretinal photoreception in the Atlantic salmon (Salmo salar). *Journal of Experimental Biology*, *203*(12), 1925-1936.

Piatigorsky, J., (2009). *Gene Sharing and Evolution: The diversity of protein functions*. Harvard University Press, Harvard.

Pierce, K. L., Premont, R. T., & Lefkowitz, R. J. (2002). Seven-transmembrane receptors. *Nature Reviews Molecular Cell Biology*, *3*(9), 639-650.

Plachetzki, D. C., & Oakley, T. H. (2007). Key transitions during the evolution of animal phototransduction: novelty, "tree-thinking," co-option, and co-duplication. *Integrative and Comparative Biology*, *47*(5), 759-769.

Plotnick, R. E., Dornbos, S. Q., & Chen, J. (2010). Information landscapes and sensory ecology of the Cambrian Radiation. *Paleobiology*, *36*(2), 303-317.

Porter, M. L., Blasic, J. R., Bok, M. J., Cameron, E. G., Pringle, T., Cronin, T. W., & Robinson, P. R. (2011). Shedding new light on opsin evolution. *Proceedings of the Royal Society B: Biological Sciences* 279, 3-14.

Provencio, I., Jiang, G., Willem, J., Hayes, W. P., & Rollag, M. D. (1998). Melanopsin: An opsin in melanophores, brain, and eye. *Proceedings of the National Academy of Sciences*, *95*(1), 340-345.

Provencio, I., Rodriguez, I. R., Jiang, G., Hayes, W. P., Moreira, E. F., & Rollag, M. D. (2000). A novel human opsin in the inner retina. *Journal of Neuroscience*, *20*(2), 600-605.

Purschke, G., Arendt, D., Hausen, H., & Müller, M. C. (2006). Photoreceptor cells and eyes in Annelida. *Arthropod Structure & Development*, *35*(4), 211-230.

Raff, R. A. (2008). Origins of the other metazoan body plans: the evolution of larval forms. *Philosophical Transactions of the Royal Society of London B: Biological Sciences*, *363*(1496), 1473-1479.

Ramirez, M. D., Pairett, A. N., Pankey, M. S., Serb, J. M., Speiser, D. I., Swafford, A. J., & Oakley, T. H. (2016). The last common ancestor of bilaterian animals possessed at least 7 opsins. *bioRxiv*, 052902.

Ramirez, M. D., Speiser, D. I., Pankey, M. S., & Oakley, T. H. (2011). Understanding the dermal light sense in the context of integrative photoreceptor cell biology. *Visual Neuroscience*, *28*(4), 265-279.

Rieger, R. M. (1986). Über den Urspring der Bilateria: Die Bedeutung der Ultrastrukturforschung für ein neues Verstehen der Metazoenevolution. *Verhandlungen der Deutschen Zoologischen Gesellschaft* 79, 31-50

Rieger, R. M. (1994). Evolution of the 'lower Metazoa'. In *Early Life on Earth.* (S. Bengton Ed.) Nobel Symposium No. 84, pp. 475-488, Columbia University Press, New York.

de Robertis, E. M., & Sasai, Y. (1996). A common plan for dorsoventral patterning in Bilateria. *Nature*, *380*(6569), 37-40.

Robison, B. H. (2004). Deep pelagic biology. *Journal of Experimental Marine Biology and Ecology*, *300*(1), 253-272.

Rouse, G. W. (2000). Bias? What bias? The evolution of downstream larval-feeding in animals. *Zoologica Scripta*, *29*(3), 213-236.

Röttinger, E., & Lowe, C. J. (2012). Evolutionary crossroads in developmental biology: hemichordates. *Development*, *139*(14), 2463-2475.

Röhlich, P., Aros, B., & Virágh, S. (1970). Fine structure of photoreceptor cells in the earthworm, Lumbricus terrestris. *Cell and Tissue Research*, *104*(3), 345-357.

Runnegar, B., & Bentley, C. (1983). Anatomy, ecology and affinities of the Australian Early Cambrian bivalve Pojetaia runnegari Jell. *Journal of Paleontology*, 73-92.

Ryan, J. F., Pang, K., Mullikin, J. C., Martindale, M. Q., & Baxevanis, A. D. (2010). The homeodomain complement of the ctenophore Mnemiopsis leidyi suggests that Ctenophora and Porifera diverged prior to the ParaHoxozoa. *EvoDevo*, *1*(1), 9.

Salvini-Plawen, L. V. (1978). On the origin and evolution of the lower Metazoa. *Journal of Zoological Systematics and Evolutionary Research*, *16*(1), 40-87.

Salvini-Plawen, L. V., & Mayr (1977). On the evolution of photoreceptors and eyes. *Evolutionary Biology*, 10, 207-263.

Schierwater, B. (2005). My favorite animal, Trichoplax adhaerens. *Bioessays*, *27*(12), 1294-1302.

Schmidt-Rhaesa, A. (2007). *The Evolution of Organ Systems*. Oxford University Press, USA.

Schoenemann, B. (2006). Cambrian view. *Palaeoworld*, *15*(3), 307-314.

Seidou, M., Sugahara, M., Uchiyama, H., Hiraki, K., Hamanaka, T., Michinomae, M., ... & Kito, Y. (1990). On the three visual pigments in the retina of the firefly squid, Watasenia scintillans. *Journal of Comparative Physiology A: Neuroethology, Sensory, Neural, and Behavioral Physiology*, *166*(6), 769-773.

Semyonov, J., Park, J. I., Chang, C. L., & Hsu, S. Y. T. (2008). GPCR genes are preferentially retained after whole genome duplication. *PLoS One*, *3*(4), e1903.

Semon, R. W. (1888). *Die Entwickelung der Synapata digitata und die Stammesgeschichte der Echinodermen* (Vol. 22). Gustav Fischer, Berlin.

Shand, J., & Foster, R. G. (1999). The extraretinal photoreceptors of non-mammalian vertebrates. In *Adaptive Mechanisms in the Ecology of Vision* (pp. 197-222). Springer Netherlands.

Shichida, Y., & Matsuyama, T. (2009). Evolution of opsins and phototransduction. *Philosophical Transactions of the Royal Society of London B: Biological Sciences*, *364*(1531), 2881-2895.

Sly, B. J., Snoke, M. S., & Raff, R. A. (2003). Who came first, larvae or adults? Origins of bilaterian metazoan larvae. *International Journal of Developmental Biology*, *47*(7-8), 623-632.

Smith, A. B., & Zamora, S. (2013). Cambrian spiral-plated echinoderms from Gondwana reveal the earliest pentaradial body plan. *Proceedings of the Royal Society of London B: Biological Sciences*, *280*(1765), 20131197.

Soni, B. G., & Foster, R. G. (1997). A novel and ancient vertebrate opsin. *FEBS Letters*, *406*(3), 279-283.

Sosik, H. & Johnsen, S. (2004). Shedding light on light in the ocean. *Oceanus*, *43*(2), 24.

Spengel, J. W. (1893). Die Enteropneusten des Golfes von Neapel und der angrenzenden Meeres-Abschnitte. *Fauna und Flora des Golfes von Neapel*, vol. 18.

Sperling, L., & Hubbard, R. (1975). Squid retinochrome. *The Journal of General Physiology*, *65*(2), 235-251.

Steinböck, O. (1963). Origin and affinities of the Lower Metazoa: The 'aceloid'ancestry of the Eumetazoa. *The Lower Metazoa*, 40-54.

Strathmann, R. R. (1978a). The evolution and loss of feeding larval stages of marine invertebrates. *Evolution*, *32*(4), 894-906.

Strathmann, R. R. (1978b). Progressive vacating of adaptive types during the Phanerozoic. *Evolution*, *32*(4), 907-914.

Strathmann, R. R. (2000). Functional design in the evolution of embryos and larvae. In *Seminars in Cell & Developmental Biology* (Vol. 11, No. 6, pp. 395-402). Academic Press, Cambridge.

Su, C. Y., Luo, D. G., Terakita, A., Shichida, Y., Liao, H. W., Kazmi, M. A., ... & Yau, K. W. (2006). Parietal-eye phototransduction components and their potential evolutionary implications. *Science*, *311*(5767), 1617-1621.

Suga, H., Schmid, V., & Gehring, W. J. (2008). Evolution and functional diversity of jellyfish opsins. *Current Biology*, *18*(1), 51-55.

Taddei-Ferretti, C., & Musio, C. (2000). Photobehaviour of Hydra (Cnidaria, Hydrozoa) and correlated mechanisms: a case of extraocular photosensitivity. *Journal of Photochemistry and Photobiology B: Biology*, *55*(2), 88-101.

Taniguchi, Y., Hisatomi, O., Yoshida, M., & Tokunaga, F. (2001). Pinopsin expressed in the retinal photoreceptors of a diurnal gecko. *FEBS Letters*, *496*(2-3), 69-74.

Tarttelin, E. E., Bellingham, J., Hankins, M. W., Foster, R. G., & Lucas, R. J. (2003). Neuropsin (Opn5): a novel opsin identified in mammalian neural tissue. *FEBS Letters*, *554*(3), 410-416.

Telford, M. J., Lowe, C. J., Cameron, C. B., Ortega-Martinez, O., Aronowicz, J., Oliveri, P., & Copley, R. R. (2014). Phylogenomic analysis of echinoderm class relationships supports Asterozoa. *Proceedings of the Royal Society of London B: Biological Sciences*, *281*(1786), 20140479.

Terakita, A. (2005). The opsins. *Genome Biology* 6, 213.

Valentine, J. W. (2004). *On the Origin of Phyla*. University of Chicago Press, Chicago.

Valentine, J. W., Awramik, S. M., Signor, P. W., & Sadler, P. M. (1991). The biological explosion at the Precambrian-Cambrian boundary. *Evolutionary Biology*, *25*, 279-356.

Valentine, J. W., & Collins, A. G. (2000). The significance of moulting in Ecdysozoan evolution. *Evolution & Development*, *2*(3), 152-156.

Valero-Gracia, A., Petrone, L., Oliveri, P., Nilsson, D. E., & Arnone, M. I. (2016). Non-directional Photoreceptors in the Pluteus of Strongylocentrotus purpuratus. *Frontiers in Ecology and Evolution*, *4*, 127.

Vannier, J., Steiner, M., Renvoisé, E., Hu, S. X., & Casanova, J. P. (2007). Early Cambrian origin of modern food webs: evidence from predator arrow worms. *Proceedings of the Royal Society of London B: Biological Sciences*, *274*(1610), 627-633.

van Veen, T., Hartwig, H. G., & Müller, K. (1976). Light-dependent motor activity and photonegative behavior in the eel (Anguilla anguilla L.). *Journal of Comparative Physiology*, *111*(2), 209-219.

Velarde, R. A., Sauer, C. D., Walden, K. K., Fahrbach, S. E., & Robertson, H. M. (2005). Pteropsin: a vertebrate-like non-visual opsin expressed in the honey bee brain. *Insect Biochemistry and Molecular Biology*, *35*(12), 1367-1377.

Vigh-Teichmann, I., Korf, H. W., Oksche, A., & Vigh, B. (1982). Opsin-immunoreactive outer segments and acetylcholinesterase-positive neurons in the pineal complex of Phoxinus phoxinus (Teleostei, Cyprinidae). *Cell and Tissue Research*, *227*(2), 351-369.

Vigh-Teichmann, I., Korf, H. W., Nürnberger, F., Oksche, A., Vigh, B., & Olsson, R. (1983). Opsin-immunoreactive outer segments in the pineal and parapineal organs of the lamprey (Lampetra fluviatilis), the eel (Anguilla anguilla), and the rainbow trout (Salmo gairdneri). *Cell and Tissue Research*, *230*(2), 289-307.

Vollrath, L. (1981). The pineal organ. *Hanbduch der mikroskopischen Anatomie des Menschen, VI/7*, 177-180.

Wald, G. (1968). The molecular basis of visual excitation. *Nature*, *219*, 800-807.

Wallberg, A., Thollesson, M., Farris, J. S., & Jondelius, U. (2004). The phylogenetic position of the comb jellies (Ctenophora) and the importance of taxonomic sampling. *Cladistics*, *20*(6), 558-578.

Wapstra, M., & Van Soest, R. W. M. (1987). Sexual reproduction, larval morphology and behaviour in demosponges from the southwest of the Netherlands. In *Taxonomy of Porifera* (pp. 281-307). Springer, Berlin, Heidelberg.

Warrant, E. J., & Locket, N. A. (2004). Vision in the deep sea. *Biological Reviews*, *79*(3), 671-712.

Willmer, P. (1990). *Invertebrate Relationships: Patterns in animal evolution*. Cambridge University Press, Cambridge.

Whitmore, D., Foulkes, N. S., & Sassone-Corsi, P. (2000). Light acts directly on organs and cells in culture to set the vertebrate circadian clock. *Nature*, *404*(6773), 87.

Wolpert, L. (1999). From egg to adult to larva. *Evolution & Development*, *1*(1), 3-4.

Wolken, J. J. (1958). Retinal structure. Mollusc cephalopods: octopus, sepia. *The Journal of Biophysical and Biochemical Cytology*, *4*(6), 835.

Wolken, J. J., & Mogus, M. A. (1979). Extra-ocular photosensitivity. *Photochemistry and Photobiology*, *29*(1), 189-196.

Worsaae K, Sterrer W, Kaul-Strehlow S, Hay-Schmidt A, Giribet G (2012) An Anatomical Description of a Miniaturized Acorn Worm (Hemichordata, Enteropneusta) with Asexual Reproduction by Paratomy. *PLoS ONE* 7(11): e48529.

Wray, G. A. (1995). Evolution of larvae and developmental modes. *Ecology of Marine Invertebrate Larvae*, 413-447. Larry McEdward (Ed.). CRC press, USA.

Wright, A. F., Chakarova, C. F., El-Aziz, M. M. A., & Bhattacharya, S. S. (2010). Photoreceptor degeneration: genetic and mechanistic dissection of a complex trait. *Nature Reviews Genetics*, *11*(4), 273-284.

Yau, K. W., & Baylor, D. A. (1989). Cyclic GMP-activated conductance of retinal photoreceptor cells. *Annual Review of Neuroscience*, *12*(1), 289-327.

Yoshikawa, S., Shinzawa-Itoh, K., Nakashima, R., Yaono, R., Yamashita, E., Inoue, N., ... & Yamaguchi, H. (1998). Redox-coupled crystal structural changes in bovine heart cytochrome c oxidase. *Science*, *280*(5370), 1723-1729.

Young, C. M., Sewell, M. A., & Rice, M. E. (Eds.). (2002). *Atlas of Marine Invertebrate Larvae*. John Wiley and Sons Academic press, USA.

Zamora, S., & Rahman, I. A. (2014). Deciphering the early evolution of echinoderms with Cambrian fossils. *Palaeontology*, *57*(6), 1105-1119.

Zhang, X., & Pratt, B. (1993). Early Cambrian ostracode larvae with a univalved carapace. *Science*, 266, 93-94.

Zhang, X., & Shu, D. (2014). Causes and consequences of the Cambrian explosion. *Science China. Earth Sciences*, *57*(5), 930.

Zhang, X., Shu, D., Han, J., Zhang, Z., Liu, J., & Fu, D. (2014). Triggers for the Cambrian explosion: hypotheses and problems. *Gondwana Research*, *25*(3), 896-909.

OBJECTIVES OF THIS THESIS

OBJECTIVES OF THIS THESIS

This study aims to better understand the photoreceptor mechanisms of the Ambulacraria clade. The objectives addressed are:

1) To create a comprehensive phylogeny of ambulacrarian opsins to assess orthologies and identify gene novelties and modifications (Chapter 1).

2) To localize and characterize, both molecularly (analysing the fingerprint mRNA and protein opsin expression) and morphologically (by means of transmission electron microscopy), the putative photoreceptor cells of the pluteus larva of *Strongylocentrotus purpuratus* (Chapter 2).

3) To utilise a novel quantitative methodology to investigate if echinopluteus larvae equipped with non-directional photoreceptors can undergo vertical migration as well as of comparing differences in their behaviour depending on the light conditions provided (Chapter 3).

With the data collected I aim to contribute to the understanding of the onset and evolution of non-directional photoreception in the echinopluteus larva, as well as to provide new insight into the photoreception mechanisms of Ambulacraria: a group of deuterostomes exhibiting varied photoreceptor classes between different clades and life stages.

1. OPSIN PHYLOGENY IN THE AMBULACRARIA

1. OPSIN PHYLOGENY IN THE AMBULACRARIA

1.1 Abstract

Opsins, G protein coupled receptors involved in photoreception, have been extensively surveyed in chordates. However, little is known about the evolution and functions of these proteins within the Ambulacraria, a clade form by echinoderms and hemichordates. This chapter aims to start to fill that gap by providing insights into the opsin toolkit of this deuterostome group. Such a phylogenetic background will help future investigations focused on the understanding of the photoreception mechanisms of these animals, a clade adapted to a variety of ecological niches and, therefore, light conditions. For doing so, a methodical data analysis that includes for first time hemichordate opsin sequences plus an expanded echinoderm dataset, was carried out. This survey, that has involved over a hundred of sequences coming from laboratories from all over the world, has resulted in the first opsin phylogeny dedicated to this cornerstone clade. In total, 119 ambulacrarian opsin sequences were collected: 22 belonging to hemichordates and 97 to echinoderms. This opsin repertoire was framed by using human opsins as reference. As a result, the presence of all major opsin groups has been verified in Ambulacraria thus, supporting the hypotheses in which 'Urbilateria' (i.e. the hypothetical last common ancestor to all bilaterians) already possessed r-opsin, c-opsin, and Go-opsin in his genetic toolkit. Further, two opsin groups have been ascribed as specific to echinoderms. All together, these data represent a promising step for future investigation of light perception in non-chordate deuterostomes.

1.2 Introduction

The prototypical proteins involved in animal photoreception are opsins. Opsins are GPCR that consist of an apoprotein covalently bound to a chromophore (11-retinal). The nitrogen atom of the amino group of residues K296, situated in helix VII, binds to the retinal molecule through a Schiff-base linkage, forming a double bond with the carbon atom at the end of this molecule (Hargrave et al., 1983; Terakita, 2005). Residue K296 is, therefore, crucial for light absorption, and its presence or absence can be potentially used as a fingerprint to judge whether a newly found GPCR is a bona fide opsin.

Classical opsin classifications show three large clusters: ciliary, rhabdomeric, and Go/RGR opsins (e.g. Terakita, 2005; Porter et al., 2011; Feuda et al., 2012). Moreover, the most recent investigation on opsin phylogeny resolved four distinct groups: tetraopsin, xenopsin, Gq-opsin, and c-opsin (Ramirez et al., 2016). Within deuterostomes, genomic and transcriptomic data derived from a number of chordates have been used to identify the opsins of this clade (e.g. Lamb et al 2007; Holland et al., 2008). However, less attention has been paid to Ambulacraria, the sister group to all extant chordates (Fig. 17). This study results essential to gain insights into the opsin toolkit present in Urbilateria, as well as to identify opsin duplications among ambulacrarian lineages.

Although photoreceptor systems have been described in some adult echinoderm species (e.g. Blevins and Johnsen, 2004; Ullrich-Lüter et al., 2011; Garm and Nilsson, 2014; Sigl et al., 2016), their opsin toolkit has remained largely unexplored on the whole. Further, almost nothing is known about the photoreceptor mechanisms of hemichordates; the only available data being provided is the ultrastructural studies on the ocelli of the tornaria larvae of *Ptychodera flava* and *Glossobalanus marginatus* (Brandenburger et al., 1973; Braun et al., 2015).

In terms of genetic data, few opsin sequences were surveyed in ambulacrarians before this study. The first survey was carried out in the genome of the echinoid *Strongylocentrotus purpuratus* (Raible et al., 2006; Burke et al., 2006). On it, authors predicted six opsin genes, four of which were reported independently by Burke et al. (2006). Subsequently, Ooka et al. (2010) cloned an 'encephalopsin' orthologue in the sea urchin *Hemicentrotus pulcherrimus*. More recently, other opsin sequences have been found in asteroids (*Asterias rubens*) and ophiuroids (*Ophiocomina nigra*, *Amphiura filiformis*) species (Delroisse et al., 2013; 2014).

To describe the diversity of opsins in Ambulacraria, a detailed analysis of 6 genomic and 24 transcriptomic databases was carried out. Here, opsin sequences from echinoderms (Crinoidea, Asteroidea, Ophiuroidea, Holoturoidea, and Echinoidea), and enteropneust hemichordates (Harrimaniidae, Spengelidae, Ptychoderidae, and Torquaratoridae) have been collected. This is the first and, to date, more complete survey of the Ambulacraria opsin toolkit.

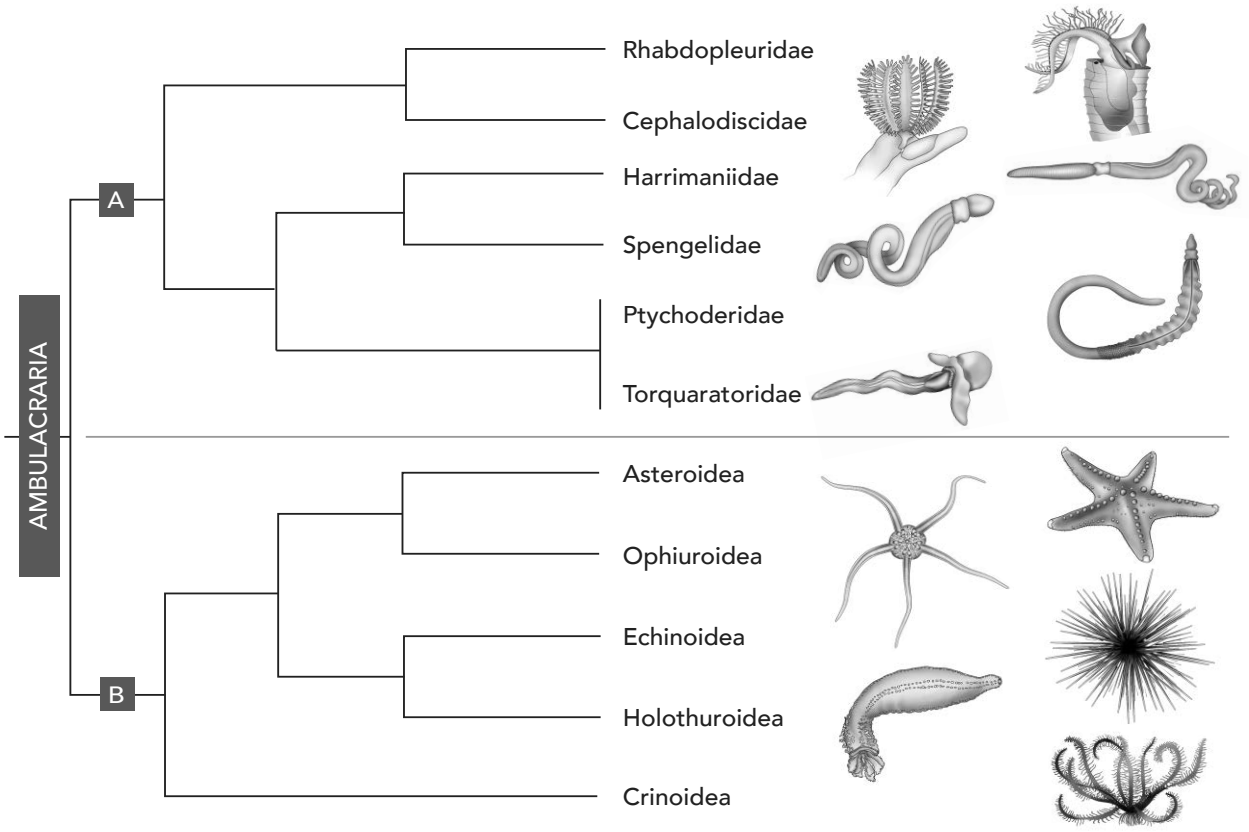

Fig 17. Ambulacrarian phylogenetic relationships and their adult forms. The Ambulacraria consist of two clades: A) Hemichordata (Cephalodiscidae, Rhabdopleuridae, Harrimaniidae, Spengelidae, Ptychoderidae, and Torquaratoridae), and B) Echinodermata (Crinoidea, Ophiuroidea, Asteroidea, Holoturoidea, and Echinoidea). Drawings: Santiago Valero-Medranda.

1.3 Results

1.3.1 Phylogeny and opsin distribution within Ambulacraria

All the main opsin clusters (i.e. ciliary, rhabdomeric, and Go/RGR opsins; for having an overlook to the different opsin groups see General Introduction, Fig. 12) are well supported in this analysis, thus confirming that Ambulacraria have a complete opsin toolkit (Fig. 19). Interestingly, two non-canonical opsin groups were also found. Since these groups do not contain any hemichordates or chordate sequence, they might be considered as echinoderm specific. Therefore, we decided to name them echinopsin '1' and '2'. Still, these groupings must be taken cautiously; such non-canonical clades could be an artefact related to a reduce data sampling.

A complete opsin profile (i.e. a toolkit that includes at least one representative of each prototypical opsin family) was detected in the sea urchin *Strongylocentrotus purpuratus*, but not in other echinoid genomes surveyed. The genomes of *L. variegatus* and *P. lividus* are not fully assembled yet, therefore some sequences may be missing here due to an incomplete sequence coverage. The genome of the asteroid *Patiria miniata* have all opsins groups except for the echinopsin '2'. Remarkably, no rhabdomeric or Go-opsins have been found in any of the hemichordate species here explored. Still, various lineage-specific opsin duplications have been here detected in some Ambulacraria species: two RGR-opsins in *Amphipholis* sp., *A. rubens* and *P. miniata*; two peropsins in *H. glaberrima*, *P. flava*, and *S. kowalevskii*; four r-opsins in *L. annulatus*; and two Go-opsins in *A. rubens*, *L. variegatus*, *S. purpuratus*, and *Heliocidaris erythrogramma*. A chart in which each studied species can be easily associated with its opsin repertoire can be found in Fig. 18.

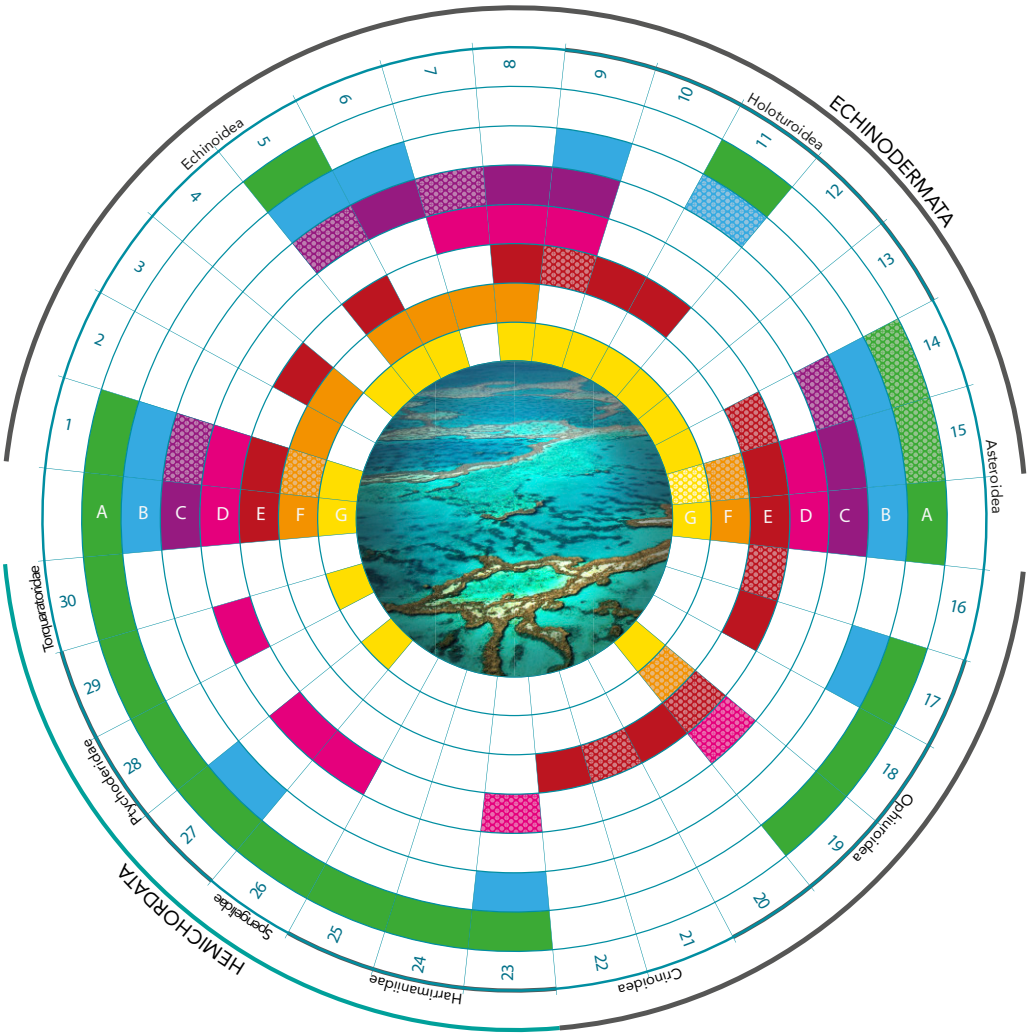

ECHINODERMATA

Echinoidea
1. *Strongylocentrotus purpuratus* (Stimpson, 1857)
2. *Strongylocentrotus droebachiensis* (O.F. Müller, 1776)
3. *Strongylocentrotus intermedius* (A. Agassiz, 1864)
4. *Hemicentrotus pulcherrimus* (A. Agassiz, 1864)
5. *Paracentrotus lividus* (Lamarck, 1816)
6. *Lytechinus variegatus* (Lamarck, 1816)
7. *Heliocidaris sp.* (L. Agassiz & Desor, 1846)
8. *Eucidaris tribuloides* (Lamarck, 1816)

Holoturoidea
9. *Parastichopus parvimensis* (Clark, 1922)
10. *Holothuria forskali* (Delle Chiaje, 1823)
11. *Holothuria glaberrima* (Selenka, 1867)
12. *Leptosynapta clarki* (Heding, 1928)
13. *Apostichopus californicus* (Stimpson, 1857)

Asteroidea
14. *Asterias rubens* (Linnaeus, 1758)
15. *Patiria miniata* (Brandt, 1835)
16. *Labidiaster annulatus* (Sladen, 1889)

Ophiuroidea
17. *Ophiopsila aranea* (Forbes, 1843)
18. *Amphipholis sp.* (Ljungman, 1866)
19. *Amphiura filiformis* (O.F. Müller, 1776)
20. *Astrotomma agassizii* (Lyman, 1875)

Crinoidea
21. *Antedon mediterranea* (Lamarck, 1816)
22. *Florometra serratissima* (A.H. Clark, 1907)

HEMICHORDATA

Harrimaniidae
23. *Saccoglossus kowalevskii* (Agassiz, 1873)
24. *Saccoglossus mereschkowskii* (Wagner, 1885)
25. Harrimaniidae sp. (Iceland) (van der Horst, 1935)

Spengelidae
26. Schizocardium sp. (Spengel, 1893)

Ptychoderidae
27. *Ptychodera flava* (Eschscholtz, 1825)
28. *Ptychodera bahamensis* (Spengel, 1893)
29. Balanoglossus sp. (Delle Chiaje, 1829)
30. Torquaratorid sp. (Iceland) (Holland, Clague, Gordon, Gebruk, Pawson & Vecchione, 2005)

Fig 18. Chart representing the opsin toolkit of the surveyed Ambulacrarian species. On it, each letter corresponds to an opsin subgroup: A) RGR opsins; B) peropsins; C) Go opsins; D) neuropsins; E) Rhabdomeric opsins; F) echinopsins 1 and 2; G) ciliary opsins; while each number refers to the species studied. For reference on the studied species, see the numbers in the faunal list situated below the chart. Stippled areas indicate duplications on the opsin family. Further details and references of where the genetic information used for each species is derived can be found in Table 2. Figure: Santiago Valero-Medranda.

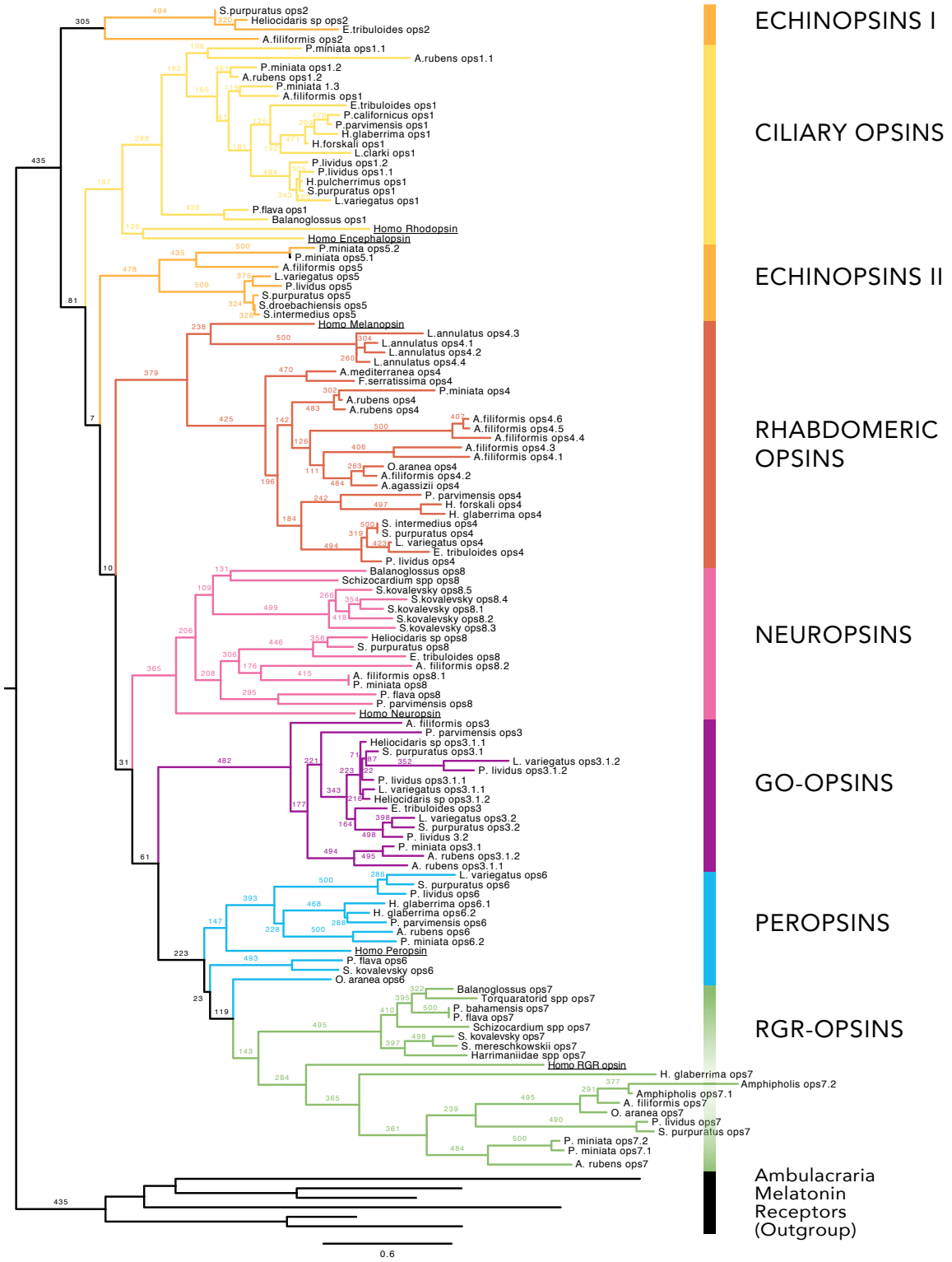

Fig 19. Maximum likelihood phylogenetic reconstruction of ambulacrarian opsins. 119 opsins from 31 different Ambulacraria species cluster in eight groups. RGR-opsins in green, peropsins in blue; Go-opsins in purple, neuropsins in pink, rhabdomeric-opsins in red, echinopsins 1 and 2 in orange, and ciliary opsins in yellow. Visualization generated with Figtree. Figure reproduced from D'Aniello et al. (2015) with permission of the publisher.

1.3.2 Opsin fingerprint

To build a consensus fingerprint for each ambulacrarian opsins group (ciliary, rhabdomeric, Go-opsin, RGR-opsin, neuropsin, peropsin, echinopsin '1', and echinopsin '2') the 7th transmembrane domain and C-terminal tail regions of the sequence dataset were aligned and a graphical representation was generated (Fig. 20).

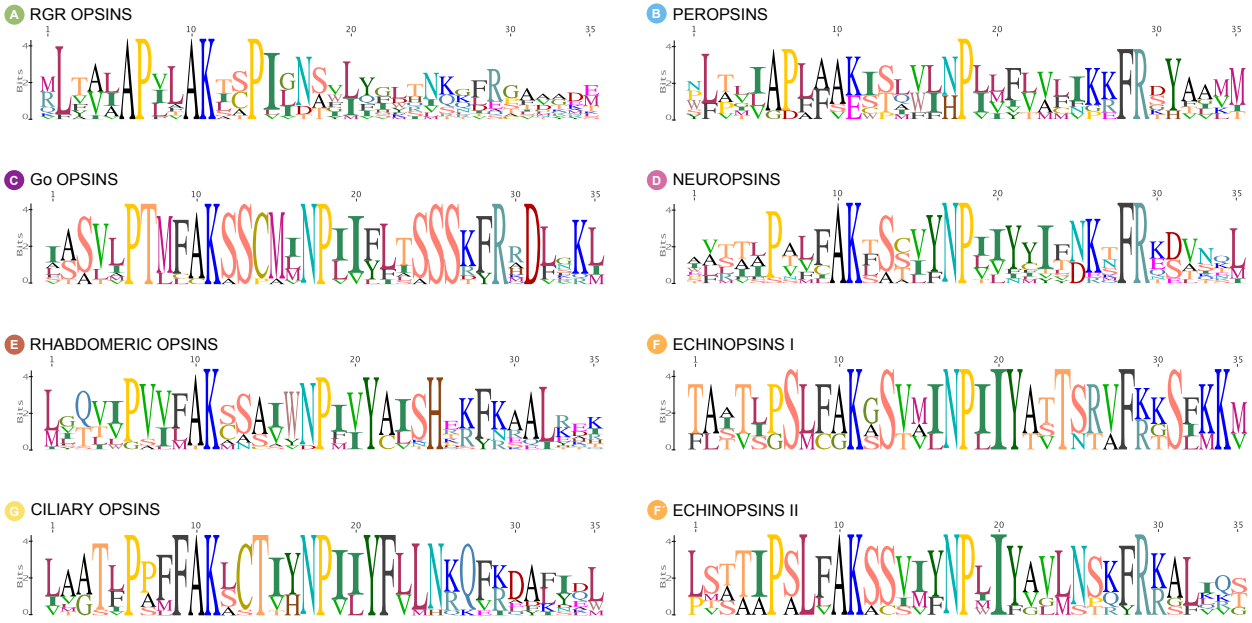

Fig 20. Consensus sequences of different opsin groups. Graphical representations of opsin amino acid patterns within the multiple alignments of the 7th transmembrane domain and the protein G linkage site. These consensus motives show the highly-conserved regions including the opsin-specific lysine residue and the 'NPxxY(x)6F' pattern. The lysine residue involved in the Schiff base formation (equivalent to K296 of the bovine rhodopsin) is present in position 10. The pattern 'NPxxY(x)6F' (position 302-313 of the *R. norvegicus* rhodopsin sequence) is present in position 17-28. The relative size of each amino acid letter indicates the probability to find this specific amino acid for the considered position. Figure reproduced from D'Aniello et al. (2015) with permission of the publisher.

Observing these motives, we can draw some points. Almost all analysed opsins contained the highly-conserved lysine residue in a location equivalent to K296 of the bovine rhodopsin. In very few cases from the peropsin group, though, this lysine has been substituted by glutamic acid (E). Still, due to the great similarity of the flanking sequence regions, these particular peropsin

sequences were included in our survey. The dipeptide NP (position 302-303 of the reference protein) is also highly conserved among all the subfamilies except in peropsins (N/HP) and RGR-opsins. Ambulacrarian c-opsins, r-opsins and echinopsins 'A' displayed a highly-conserved tyrosine (Y306). Conversely, the histidine (H310) appears distinctive of the r-opsins here represented. In this dataset, the tripeptide SSS, positioned at residues 309-402 of the reference protein, is a distinctive feature of ambulacrarian Go-opsins.

1.4 Discussion

This phylogenetic analysis confirms the presence of the prototypical bilaterian opsin clusters in Ambulacraria, thus giving support to the scenario in which Urbilateria had ciliary, rhabdomeric and Go-opsins. Further, this data suggests the presence of the two novel opsin groups echinopsin '1' and echinopsin '2'. Echinopsin sequences were found only in Echinoidea, Ophiuroidea and Asteroidea. A wider taxonomic sampling is needed to better determine if these echinopsin groups represent an echinoderm novelty or not. The graphical representations here shown will be particularly useful in future analysis to assign novel, unknown sequences to lineage-specific opsin groups.

The absence of rhabdomeric opsin in enteropneusts in remarkable, as the tornaria larva (planktotrophic) possesses eyespots that bear photoreceptors with clear microvillar surface enlargements (Brandenburger et al., 1973; Braun et al., 2015); however, this analysis does not reveal r-opsins in any of the examined enteropneust species (Table 3). It should be noted that genomic information is only available from *S. kovalewskii*, a species with a lecithotrophic larva. Moreover, as most of hemichordate transcriptomic data here considered were generated using adult tissues, is therefore likely that the absence of r-opsin in this group of animals is biased due to the limitation of the data availability from this animal clade. If the absence of r-opsin in

enteropneusts is confirmed, it would be of great interest to investigate which is the opsin that mediate the photoreception of the microvilli-based ocelli present in the tornaria.

The fragmentary information about putative duplicates in different lineages makes it difficult to predict the exact number of functional opsin proteins. Whether or not these duplicated genes have sub-functionalized roles should be experimentally investigated by gene expression plus knock out or silencing experiments. In a few cases, the locus of duplication prompted a large expansion of the gene family, as is the case of the five neuropsins found in *S. kowalevskii* and the six rhabdomeric opsins in *A. filiformis*. The presence of opsin in the nervous system from *Asterias rubens* is in accordance with the electrophysiological experiments showing that the echinoid radial nerve reacts to illumination and shading by creating action potentials (Millott, 1975). These findings also corroborate the immunochemical observations done by Ullrich-Lüter et al. (2013).

As all living animals diversified from a common ancestor, exploring the same function in several species can help to understand general principles. Conversely, an ancestral gene that performed a particular function could also have diversified and co-opted over the course of evolution. Given that, the diversity of opsins among living organisms provides a window to extract information about the evolution of photoreception throughout geological time.

Until recently, the under representation of comparative studies in photoreceptor cell evolution has hidden the real extent of opsin diversity (Porter et al., 2011; Feuda et al., 2014). As more opsins have been characterized, these sequences have been classified into narrow pre-defined groups, implying theoretical function similarities that might not always be correct (Shichida and Matsuyama, 2009). At present, the rapidly increasing availability of entire genomes and transcriptomes provides a great opportunity for investigating the evolution and functional

diversity of the opsin family in a detailed way. Although currently available molecular data have already uncovered an unexpected diversity of opsins, the cumulative addition of this sort of information will provide a more comprehensive picture of the origin and diversification of opsins over evolutionary time. Naturally, such a diversification and categorization must be correlated with the necessity to conquer new ecological niches that provided a new variety of light stimuli to be integrated.

1.5 Material and methods

1.5.1 Data mining

Strongylocentrotus purpuratus opsins were used as starting query for tBLASTx against NCBI, JGI, Ensemble, Echinobase, BioInformatique CNRS-UPMC, and Genoscope databases. Additionally, the dataset was enriched using unpublished genomic and transcriptomic sequences obtained from independent research projects (see Table 2 for details on data source). This includes transcriptomes from adult tissues, such as cuverian tubules and integument from *Holothuria forskali*, muscle of *Parastichopus californicus,* radial nerve from *Asterias rubens*, arms from *Labidiaster annulatus*, *Ophiopsila aranea*, *Astrotomma agassizii, Antedon mediterranea,* proboscis from *Saccoglossus mereschkowskii* and a Torquaratorid sp., whole adult body of *Leptosynapta clarki,* and anterior part of the body from Harrimaniidae sp., and *Schizocardium braziliense*. Several other transcriptomes were prepared from embryos or larvae from *Paracentrotus lividus*, *Heliocidaris erythrogramma*, *Eucidaris tribuloides*, *Parasticopus parvimensis*, *Saccoglossus kowalevskii*, *and Ptychodera flava* (Table 3). A final dataset of 119 protein sequences coming from 31 ambulacrarian species was used for the phylogenetic reconstruction (all the sequences can be found at the end of the chapter, pp 82-93, in FASTA format). Further, 6 human opsin sequences were used as reference of the main canonical opsin groups, and 6 melatonin receptor sequences were considered as out-group.

1.5.2 Alignment and phylogenetic analyses

Protein alignments were performed with SeaView v4.2.12 (Galtier et al., 1996; Gouy et al., 2009) using the MUSCLE algorithm (Edgar, 2004). To improve the phylogenetic reconstruction, the alignment was manually corrected, and the N- and C-terminal ends were trimmed (Fig. 21). The sequences used for this study can be consulted in page 82 and followings. Sequences shorter than 60 amino acids were removed to avoid bias.

Maximum likelihood analyses were conducted using PhyML v3.0 (Guindon and Gascuel, 2003). Nodal support was obtained following analysis with 10,000 bootstrapping replicates. A best-fit model analysis was performed using Mega v5.2.1 following the AIC criteria (Tamura et al. 2007, Kumar et al. 2008), and 'Wheland and Goldman model of protein evolution' was found to be the best suited (Whelan and Goldman, 2001). Three melatonin receptor sequences from *S. purpuratus* (Echinodermata) and three from *Saccoglossus kowalevskii* (Hemichordata) were chosen as out-group.

1.5.3 Consensus fingerprint of ambulacrarian opsin groups

Ambulacraria opsins were clustered according to their estimated position within opsin subfamilies, and a multiple alignment of 35 amino acid long peptide region (including the 7th transmembrane domain with the opsin-specific lysine K296), was performed with SeaView v4.2.12 for each opsin group. The selected region spanned from the residues 286 to 320 of the *Rattus norvegicus* rhodopsin sequence, which was used as reference (Palczewski et al., 2000). The consensus sequence was generated on base of the alignment for each class of ambulacrarian opsin using Geneious® 8.1.5.

Table 2 – LIST OF SEQUENCES USED TO BUILT THE PHYLOGENETIC RECONSTRUCTION

A) HEMICHORDATA

CLADE	SPECIES	SEQUENCING WORKFLOW	# READS	# UNIGENES	ACCESSION #S	TISSUE	LITERATURE
Ptychoderidae	*Ptychodera flava*	Roche GS FLX Titanium	879681	125601	BioProject PRJNA227405	embryos (mixed stages)	Chen et al., 2014
	Ptychodera bahamensis	HudsonAlpha (Illumina)	41174126	115310	SAMN03012539	proboscis	Cannon et al., 2014
	Glossobalanus marginatus	Engercore (454 Titanium)	230141	101125	SAMN03012540	proboscis	Cannon et al., 2015
	Balanoglossus aurantiacus	HudsonAlpha (Illumina)	52013666	143815	SAMN03012541	whole anterior	Cannon et al., 2014
Harrimaniidae	*Saccoglossus mereschkowskii*	HudsonAlpha (Illumina)	50630972	145937	SAMN03012542	proboscis	Cannon et al., 2014
	Saccoglossus kowalevskii	Sanger sequencing	Genome	182607	FF418995-534157 FF602128-677500	embryos (mixed stages)	Freeman et al., 2008
	Harrimaniidae spp. (Iceland)	HudsonAlpha (Illumina)	66151572	230054	SAMN03012550	whole anterior	Cannon et al., 2014
	Harrimaniidae spp. (Norway)	HudsonAlpha (Illumina)	69266416	274434	SAMN03012543	whole anterior	Cannon et al., 2015
	Stereobalanus canadiensis	HudsonAlpha (Illumina)	19290646 50206164	18843	SAMN03012552 SAMN03012551	proboscis; gonad	Cannon et al., 2014
Spengelidae	*Schizocardium braziliense*	HudsonAlpha (Illumina) Engencore (454 GS-FLX)	40083244 98989	101457	SAMN03012605 SAMN03012582	whole anterior	Cannon et al., 2014
Torquaratoridae	*Torquaratorid spp.* (Iceland)	HudsonAlpha (Illumina)	73725698	102971	SAMN03012583	proboscis	Cannon et al., 2014

Torquaratoridae	*Torquaratorid spp.* (Antartica)	HudsonAlpha (Illumina)	45751208	145544	SAMN03012584	proboscis	Cannon et al., 2015
Cephalodiscida	*Cephalodiscus hodgsoni*	HudsonAlpha (Illumina) Engencore(454 GS-FLX)	17183978 85028	14441	SAMN03012607 SAMN03012606	multiple zooids	Cannon et al., 2014
	Cephalodiscus nigrescens	HudsonAlpha (Illumina)	23413166	23130	SAMN03012608	multiple zooids	Cannon et al., 2014
	Cephalodiscus gracilis	HudsonAlpha (Illumina)	47746306	57139	SAMN03012629	multiple zooids	Cannon et al., 2014
Rhabdopleurida	*Rhabdopleura normani*	Engencore (454 GS-FLX, Titanium)	82283 104634	66988	SAMN03012742	multiple zooids	Cannon et al., 2014
	Rhabdopleura sp. Iceland	HudsonAlpha (Illumina)	13703832	4790	SAMN03012743	multiple zooids	Cannon et al., 2014

B) ECHINODERMATA

CLADE	SPECIES	SEQUENCING WORKFLOW	# READS	# UNIGENES	ACCESSION #S	TISSUE	LITERATURE
Echinoidea	*Strongylocentrotus purpuratus*	Whole-genome shotgun + BAC	Genome	259778	SPU005569 XP_783302.2	sperm	Sodergen et al., 2006
	Strongylocentrotus droebachiensis	HudsonAlpha (Ilumina)	–	under annotation	ABB89040	tube foot	unpublished
	Strongylocentrotus intermedius	HudsonAlpha (Ilumina)	–	under annotation	AHH29342	tube foot	unpublished
	Lytechinus variegatus	Roche 454	–	under annotation	Bioproject62465	gastrula	Echinobase
	Paracentrotus lividus	Roche 454	–	under annotation	AIU94629	integument	unpublished
	Hemicentrotus pulcherrimus	Ilumina HiSeq2000	–	under annotation	BAH28806	Embryos (mixed stages)	unpublished

Table 2. A) List of hemichordate sequences used to build the phylogenetic reconstruction. B) The ambulacrarian opsin sequences used in this analysis are reported with reference to the sequence workflow used as well as the number of reads, accession and unigenes number, stage, and/or tissue used for the extraction of the genetic material, and accompanying literature.

Table 2 – LIST OF SEQUENCES USED TO BUILT THE PHYLOGENETIC RECONSTRUCTION

B) ECHINODERMATA (Continuation)

CLADE	SPECIES	SEQUENCING WORKFLOW	# READS	# UNIGENES	ACCESSION #S	TISSUE	LITERATURE
Echinoidea	*Heliocidaris erythrogramma*	HudsonAlpha (Illumina)	416000000 223000000	under annotation	PRJNA243078	six embryos stages	Wygoda et al., 2014 Byrne et al., 2015
	Eucidaris tribuloides	Roche 454	56717282	under annotation	BioPoject 62465	gastrula	Echinobase
Holothuroidea	*Parastichopus californicus*	HudsonAlpha (Illumina)	52003372	134640	SAMN03012744	muscle tissue	Cannon et al., 2014
	Parastichopus parvimensis	Illumina HiSeq2000	290617210	125524	unpublished	embryos (blastula to juvenile)	unpublished
	Leptosynapta clarki	HudsonAlpha (Illumina)	56022502	242126	SAMN03012745	muscle tissue	Cannon et al., 2014
	Holoturia forskali (a)	Illumina HiSeq 2000	4936120650	156918	unpublished	cuverian tubules	unpublished
	Holoturia forskali (b)	Illumina HiSeq 2001	4376870800	111194	unpublished	integument (dorsal)	unpublished
	Holoturia forskali (c)	Illumina HiSeq 2002	4232124600	111194	unpublished	integument (ventral)	unpublished
	Holoturia glaberrima	455 + Illumina	2428740 331931211	under annotation	SRA051991	regenerating radial nerve cord	unpublished
Ophiuroidea	*Astrotoma agssizii*	HudsonAlpha (Illumina)	54375996	156062	SAMN03012756	arm	Cannon et al., 2014
	Ophiopsila aranea	Illumina HiSeq2000	45158822	127324	unpublished	arm	Delroisse et al., 2016

Ophiuroidea	*Ophiocomina wendtii*	Roche 454	354586	14261	unpublished	gastrula	Vaughn et al., 2012
	Ophionotus victoriae	Roche 454	183721	18000	SRP013357.1	arms	Burns et al., 2013 (SRS334699)
	Ophionotus victoriae	IlluminaHiSeq2500	155931609	669744	unpublished	adult	Elphick et al., 2015
	Ophionotus victoriae	Engencore (454 Titanium)	157023	34062	SAMN03012751	arm	Cannon et al., 2014
Asteroidea	*Labidiaster annulatus*	HudsonAlpha (Illumina)	71361592, 53268480	210764	SAMN03012748 SAMN03012747	arm	Cannon et al., 2014
	Odontaster validus	Engencore (454 Titanium)	171417	39461	SAMN03012746	arm	Cannon et al., 2014
	Asterias rubens	Illumina HiSeq	-	326816	unpublished	radial nerve	Semmens et al., 2016
Crinoidea	*Florometra serratissima*	Illumina HiSeq2000	100764755	89664	unpublished	embryos 24 hpf; larvae 5 dpf	unpublished
	Promachocrinus kerguelensis	Engencore (454 Titanium)	190565	35867	SAMN03012749	arm	Cannon et al., 2014
	Dumetocrinus sp. Antarctica	HudsonAlpha (Illumina)	49481384	127039	SAMN03012750	arm; stalk	Cannon et al., 2014
	Antedon mediterranea	IlluminaHiSeq2500	116089417	675534	unpublished	arms	Elphick et al., 2015
	Promachocrinus kerguelensis	Engencore (454 Titanium)	190565	35867	SAMN03012749	arm	Cannon et al., 2014

Table 2. B) List of echinoderm sequences used to build the phylogenetic reconstruction. The ambulacrarian opsin sequences used in this analysis are reported with reference to the sequence workflow used as well as the number of reads, accession and unigenes number, stage, and/or tissue used for the extraction of the genetic material, and accompanying literature.

1.5.4 Sequences used for this study (FASTA format)

>Plividus_ops1.A

MNSSTPVMTSTDYAPSSWSSSLQSSTISSLMTDIVSTVNVLSGLSNETSSTVGPSSLVVPVSRTTYNYLTVYTGFLTIFGILNNGIVMVLFARFPSL
RHPINSFLFNVSLSDLIISCLASPFTFASNFAGRWLFGDIGCTLYAFLVFVAAGDR

>Plividus_ops1.B

CSVAWNSRIPGSFGYIIFIFVMVLIIPFGIIVFAYALLVYAVKKISRTQAALSSEAKADRKVTKMIFIMILGFLVAWMPYTVFSLYVAFGKDVVLTP
LAATFPPFFAKLCTIHNPIIYFLLNKQFKDALIQLFCCGENPFDRDESEHERQGTRRQPVGGRTAASGSMNPGTRGRASSLPTATSVLDIPQAVATA
SSSPGHDHEQGPSTSAPNERVFELSSKIQKFQISEKNSGSMSEKPGTSSSGTLKPPRRAMKNQ

>Plividus_ops3.1.A

MATSAGEHSVTEALSKLQPEYMTPLTRTGYLLTAIYLTIIGTIATVGNVSVICVLCRYGTFRKRSINLLLINMAASDLGVSVTGYPLTTASGYWGRW
LFGDVGCQFYAFCVYTLSCSTISTHAIIAIYRYIYIVKTDL

>Plividus_ops3.1.B

IDPIRAEEKDAGVIIFGKLRKREAKIDTHVTKMCFMMMISFIIVWAPYAVECLMAAHVERLSPLTSVLPTMFAKSSCMINPIIFLTSSSKFRKDLNK
LLSRPLSSEAQRVQEDRNKTQRSFYVRQSEIATTQGNSTAAVFYDKERIYIGEMRASSLQKEAELMQRDPELFSIASSTSSDVQFVVRDRPRPEDRR
ASRPQGPRGPEMFTASGYANQGSSTTDSGAQSTSSGTTSSKQRRTGFGSRKASRHYSLKSQSEETGTSGEIFTLDGSSLEMMSLRKL

>Plividus_3.2

MASLSENSYVTEPTSQVPSEGPPSYLTPLSRTGYLFTALYLTLVGSIATIGNITVLCVLCRYGTFRRRCVNILLMNMAFSDLGVSIAGYPLTTISGY
RGKWLFADIGCQFYAFCVYTLSCSTIGSHVVISFYRFIYVVKPNFRWSSYTYEPFGTSCSINWTGKSFSDTSYMIACNVFVFILPISIMLYCYIRVG
KKIKGIDPLRAEGRDMGVVVFGKLRKHETKIDTHVTKICFMMMAGFIICWTPYAVGSIWASQVGKVSTIASVLPTMFAKSSCMINPIIFLTSSSKFR
HDLNKLFNRPGPEHTIRVEERSREERSFYVRQSALSDAMGSHSASVYYNKERIYIGEMHASNIQKESDLLERDPEAISIGSSTSSSLKFVLKDRLNR
HKKRAGKSSKKMLDVVHSPFDGAASDDSEENTTENNMTRARSISIPSENVSRIFVPSAKMPTMKRSLSQPDLPGTSADSFSKNPSEY

>Plividus_ops4

VTHHAHHMMCYTGMRVHKKRQKGSAFSISACYDRKKKISLRTDADRTEVRIPVTSFGWTKSLRTPPNMLIVNLAISDFGMVITNFPLMFASTLYNRW
LFGDLGCQIYAFCGALFGIMSIANMTAIALDRYYVICWSLEAVRSVTKRRSMIIILIVWAYAIFWSIPPFIGFGSYVLEGYGLGCTFDFMTHDTNHY
LHVSLLFVSSFIVPVAIIVACFTRIAITVRKHRHELNKMRTRLTDDKDKKHKSSIRRADKAKTEFQIAKVGFQVTIFYICSWMPYSIVAVIGQYFDP
GLLSPLGTVVPVIFAKCSAIWNPIIYCLSHEKFNAALKERIMVLCGIEVPSKHRSMGSQESSVTGRRGMHRQNSSTLSESSVSSTVEQGDMELKDRK
QGPATVRVQQEKGEAGTYRRNPGDVSFSKDVGVEIEEKSPRGDQGGRDDRVTSQGEGQMDQWSQPPPATAPAPGVNDKEYLTKM

>Plividus_ops5

MANLTSGRMTDFDEIEQMNDDDPAFRLIAGYLLMVVVIGTLGNLTVISTFLRCKKLHSPINILIVNLSASDLLVATTGTPLSMVSNFYGRWLFGTNA
CAFYGFVNYYCGCISLNSLAAISVFRYMIVVRGNVQNKKLSLRSSIYAVLIIHMYTLIFSTPPLYGWNRFVLAGYRTGCDIDFYTKTPLFISYICYM
FIFLFFIPLGLISWSYFKIYQRISRHSRSMRTSLCSVTKEPHSEAWLKKVKNSQILQKPVSLLPLKTRFEPRFRNRRTVSTILITIIVFLIAWLPYC
VVSLWILIDNTNSISKLTATIPSLFAKSSVMYNPMIYVLLNTKFRRGLVQSLQPLNCFSSHRLGDSSS

>Plividus_ops6

VFLLSWLPYNVLLLFAITNDPEDMPSNLTVIAPLFVEITLWIHPILFLVLFKKFRGYAALMICCRTEVEAMIDVNASDSSNPRTSDVRRFADHFV

>Plividus_ops7

MSPVAAVSSFSEEWAYGSSGCQTYSFVANFFGLVSIWSLVAMVLHHYQSSRIGAKKDDINSQYSMIIALIWGGALFWSATPLPFIGWGRYVVEPFGT
GCLLDFADRSPSYFLYLVGFTTLGLAFPIALLITRGLNYEKVPIESVIACWKAVLVLCFYWGCYGLVAVATALSGPGRVSVRLYAVAPLFAKTCPVI
NAFLFGDSLTTDEAVATKEQKKH

>Lvariegatus_ops1

MSNLMTEVLTTVNAFSGIGNATPSTLRPRSLVVPVSRSTYNYLTVYTGFLTIFGILNNGLVMVLFARFPSLRHPINSFLFNVSLSDLIISCLASPFT
FASNFAGRWLFGDLGCTLYAFLVFHLGTEQIVILAALSIQRCMLVVRPFTAQKMTHNWAVFFLFALTWLYSLIICLPPLFGWNSYTYEGPGTACSIA
WNSNLPGDSSYIIFIFVMVLVIPFTIIIFSYGLLVYAVKKVISQTQAAMSSEAKADRKVTKMIFIMIIFFLITWAPYSGFSLYVAFGKNVVITPLAG
TFPPFFAKLCTIHNPIIYFLLNKQVRQFKDALIQFLCCGENPFDRDESDQGGRRHRPLGGRTGASGTIPQGGRGRASSLPTATSMLDIPQAASPSAL
SGSTQNKHNLEQGGASTSTTKDDRLFEISSKIQKFEISEKMNASCSQEASGAPSSSGVMKPTRRAMKNQVGCLPPVDN

>Lvariegatus_ops3.1.A

MATTTESYHSGTEALSNLQPEYMTPLSKTGYLLTGIYLTIVGTIATIGNITVICVLFRYGTFRKRSINLLLINMAASDLGVSVTGYPLTTLSGYWGR
WLFGDVGCKFYAFCVYTLSCSTITTHAVIAFYRYIYIVKTDLSEYHHS

>Lvariegatus_ops3.1.B

MTEIQKSWSRDEDAGRIRGIDPERTQGKDSGVNVFRKLRRREAKIDTHVTKMCFMMMISFIIVWTPYAVESLRVAHVHRISAFSAVIPTMFAKSSCM
LNPIIFLSSSSKFRRDLRKMWSSPPSHESLRQEERNKTQPSLYVRHSDISSVYRNNTASVYYDKERIYIGEMRATSIQKEAELMRRDPEVLSIASST
SSDVHFVVRDSKRPKRALGPRGPEMFTASGYTNHASSTSDSAGQSTSSGTKRTGFGSRKASRQYSVKSQSEETANSGEIFTLDGSGLEMMSLRRL

>Lvariegatus_ops3.2

MLCHKVITHKSPTYLFDIISSYVPIRNLRVVASIGNITVLCVLCRYGTFRKRSVNILLMNMAISDLGVSIAGYPLTTISGYRGKWLFADIGCQFSGF
CVYTLSCSTISSHAVVAIYRYIYIVKPNLRPKLSTWNSCLCLFGIWAFSLFWTVAPFFGWSSYTYEPFGTSCSINWFGNTLGDKSYMIACTVFVFIL
PIAIMLYCYIKICFMMMASFIIVWTPYAVGSIWASQVDKVSAAASVVPTMFAKSSCMINPIIFLTSSSKFRHDLGKLWNRPSPEHTIRFEERSREQR
SFYVRQSALSDAMGSHSASVYYDKERIYIGEMHAASIQKESDLLQRDPEAISIGSSTNSSLQFVLKDRQKRYKKKAGEPSKKGVDTPHFPYDDSERG
VIGKWMRPRSHSVVSDNINRDVIQSVKRPTKKRSVSQPDIHGASAELFIVSPTRSTNFQK

>Lvariegatus_ops4

TKSLRTPPNMLIVNLAISDFGMVITNFPLMFASTIYNRWLFGDIGFEFTGCQFYAFCGALFGIMSIANMTAIALDRRYYVICWSLEAVRSVTHRRSM
IIILIVWAYAIFWSIPPFFGVGSYVLEGYGLGCTFDFMTQDLNHYLHVSFLFASSFVVPVTIIVACFTRIAVTVRKHRHELNKMRTRLTEDKDKKHK
SSIRRADKAKTEFQIAKVGFQVTIFYILSWLPYAVVAVIGQYFDPDLLTPLGTVVPVIFAKCSAIWNPIIYCLSHEKFNAALKEKLMEMCGVELPSK
HRSMGSQESSVTGRRGMHRQNSSTLSESSVSSTVEQDAMELKDRKQGPGPATVRVQQEKGEAAGTYRRNPEEVTFSKDTGAEIEEKGRGDQGQRDDR
VKQHGEGQMDQWSQPPPAAPGVNDKEYLTKMEGQMDQWSQPPPAAPGVNDKEYLTKM

>Lvariegatus_ops5

MLLTDNHTHDQMPDDQGEGEDNAFLLIGGYLLVVVVLGTMGNVTVIYTFLRVKKLHSPTNLLIVNLSASDLLVATTGTPLSMISNFYGRWIFGSHTC
AFYGFVNYYCGCISLNSLAAISVFRYIIVVRGNVQNQRLTLRSSVYAIGIIHLYTMIFSTPPLYGWNRFVLAGFHTGCDIDFHTKTPLFISYICYMF
FFLFFLPLGLISWSYFKIYQRVSQHSDSMRRTFPHVAKETSSDEKRIWLEQMKNTKLLHQPVKLLRLKPKFKPRFHQRRTASTILITIAVFLISWLP
YCIVSLWILIGDENSISQLSATIPSLFAKSSVMYNPLIYAVMNSRFRKALLKSLSSLKCLGRHELNQSN

>Lvariegatus_ops6

MGSSGPSCPYLAGAVTTSKAPLQTTCFVDWQRTDLSYVSYIISWFVVNFVLPLSLMVFAYVSAFLMRQEGQFADPIRNNEPLPSNVDWASQPEAHWV
GIATVVVFVLSWLPYSVVFLHAIAENIGDMPPNLPIIAPLFAEITLWIHPILFLVFIKKFRSYAAMMICCRTEVEEIEINPQADNSHRTSETRRFAD
HFV

>Heliocidaris_Ops2

IQELDIFIIIALFIVFQMANLTLIFMDGTYGENSDGETWPDYAYLLSGIYLTVVFIIALIGNSLVIFLFGWDHQLRTPTNMFLLSITVSDWLITVAG
IPFVTSSIYAHRWLFAHAGCISYAFIMTFLGLNSLMSHAVIAVDRYLVITKPHFGIVVTYPKAFLMISVPWLFSFAWAVFPLAGWGEFTYEGPGAWC
SVRWDSDEPEIMAYVLGMMFLTFVTSILVMMYCYICIFLTMRSMPRWATSNSIKTHERNRRKRELKLMKTLVAIAIAYLVAWSPYAVTSMIAIFGHS
ELLSVTASTLPSLFAKGSVMINPIIYATTSTVFKKSFMKMVNSFCPRHRAWMKSGKSTPSSSKRTVPFSSDGKHKKSQDDQTSSVLVPGSTEICAAP
IPVSSPSRFFPDMKVKPGGKRLSAAIEMDRFNKLLPGKHKKGPAPHSGGRRPSDIPIPET

>Heliocidaris_ops3.1.A

GVYLVQIIIMLYCYVRVAKKIRGIDPERTEEKDAGVVVFGKLRKRDAKIDTHVTKMCFMMMISFIVVWTPYAVESLRAAHVHRISAISSVLPTMFAK
SSCMINPIIYLTSSSKFRRDLSKLWSRPSSQQALRLEERNKTQRSFYVRHSEISSAHGNNTASVYYDKERIYIGEMRATSIQKEAELMQRDPELLSI
ASSTSSDVQFVVRDRPKLYAKKPAKAQGPRGPDMFIASGYTNQGSSTGDSGGQSTSSGTTGSKHRRTGFGSRKASRQYSLKSQSEETGNSGEIFTLD
GSALEMMSLRKL

>Heliocidaris_ops3.1.B

LTTVSGYWGRWLFGDVGCQFYAFCVYTLSCVTITTHAVIAIYRYIYIVKTDLRPKLSANFTSVVILLIWLYAFFWTVTPFIGWSSYIYE

>Heliocidaris_sp_ops8

INSLIFSVSYLFHAALTAFIGNISVIVISLRKREKLKPLDLLTINLAISDFLISIVSYPLPMISAFRHGWSFGRIGCIWYGFTGFLFAVGSMATLTV
IALFRYAKLCRENVDHYQSRQFVIKVIVAIWAFSIFITVPPLFGWSRFVATPLAPKLLIRVFGVVY

>Etribuloides_ops1

NSLWQISSTQAAQSSTNKADRRVTKMVALMVFAFLFAWTPYAVFSLYVAFGENVQVGPVAATLPAFFAKLCTVYNPIIYFLMNKQVRLYLSL

>Etribuloides_ops2

IHSMLRSPFIYLCRELKMLKTVMLIAFGFLVAWTPYAVTSLIAMFGGPDMLSVTAAVIPSLFAKGSVVINPIIYATTSRVFKTSFKKVCYSPRVPRP
LQKLGRTLGTI

>Etribuloides_ops3

MCFMMMVSFIIVWTPYAVESLWASQHEVGPIAAVIPTMFAKSSCMLNPVIFLASSSKFRRDLSKLWSRPSTDQTAAAAKAQQPPTFYMRQSAVSSAVG

>Etribuloides_ops4

RYYVICWSLEAVKTVTHRRSAIIIVIVWIYAIFWSVPPFFGIGSYVLEGYGLGCTFDFMTQDMNHYIHVSFLFVSSFIVPLVVIIFCYSQIAWTVRK
HRKELNKVRARLSEDKDKKHKASIRRADRAKTEFQIAKVGIMVTVMYILSWLPYSIVAIIGQYFSPDLLTPLGTVVPVIFAKCSAIWNPLVYAISHE
KFKAALKERFLALCGIEVPQKSRSTIGSQESSITGRRGMSRQYSSTLSDTSVSSTLEHEAMEMTDKKPGPKPGAGAPSAERPPKVRVQEKSEGGTYR
REHPVEQADYDQDVEVKVDEGVEVKKKRKGSKSGRDDRVKKTPEASSHPQEEGGKQDSGGLDQWSQPPAHLESGRNDDEYLTKM

>Etribuloides_ops8

PQSLNCFYFLQTACALTIAYIVSWSPYAIVCMWATFDEVTAIPDSFRIIPVFFAKTAAIYNPIIYCIFNKNFRQEVQTLLCWCACQCYSVSINMKLN
TLAQEQLLVVETRRLKSPSSPHRAQIVWINPFQRKLGHRSSLVRHPRLRLSLRTLHAKAQLATKPGNMRVTFSPTADCVQFDERVSADALRPGICTR
GSVNSPGKPDLDWELPSGDNISIVSPSKSQVSVPDTVIRHQSMADLHAEFLDPQAASKNVRVIFVQPNVDQELSSDA

>Pparvimensis_ops1

HLGFSQSRTAMANITAAGGITSTVSTTTIPELPVILPAELSRSAYNFLAVYTGFLTVVGIFNNGLVIFLFIKFPNLRQPVNIFLLNLSISDMTVSLF
GSPLTFASNIAGYWLFGQIGCSIYAFIVMIGGTEQIVALAAVSVHRCFLVVRPFTAKKMTTSWAVFFVFLTWLYSFILSIPPAFGWNEFVREGAGTA
CAINWTDSKPGNTSYVIFLFLTVLLVPLLVIIFSYGLLIFAVKKISASEAAQSTENKAEGRVTKMVMIMIFFFLFAWTPYSAFALYVVFGRTHTVSP
IVATLPPFFAKSCTIYNPVLYFVLNRQFRDAIYELIGYEPPDPLDSSGGANQSGNANQQQQQQGASNTRKSMQRSASVATVMSELPSVRHDTFKTPG
QFLAGGRVDPTGRALSKSYKKTSGGEGSERLGIPPSLPGQSVEMTDSMRALHDSEETNLACEKDKGSSSEDKSNEGKVIRTRHLGPSTLNDTGEHAN
DGYEAGQEGDELKTVYVQRVNVKSANNDEEQTSMRHRKEPTGMPDVNM

>Pparvimensis_ops3.1

TQCPKLTAAVTRRVIIALWFHAFFWAVTPLIGWSKYDYEPFGTSCSIDWISRTVNNYSFMLLTTITNYVIPVIIMVICYTKIIRRSRKVDPLRVEER
DRSMRVINKLDQLEIKIDTHVTKMCIVMTCSFIIAWTPYAVESLWMSQSSEFVGPISSTLPTMLAKSSCMMNPLIYLTSSSTFRMDVVKLLRRASRR
PILDDNIQAPPEQGDGNGPQTSGRFYLRNTKNAHGKTSCAIYFDKKQIFIGDVSPESIERDSSLAQRDPDKISVRFSSFDGPPTGKEHQLNLPANQN
LDKPEVDLPKYFEMNDNPGTSSDSKQQSRMTTSPIFN

>Pparvimensis_ops4

AMIICNCPIILLSIHYGYWHLGESFCNIYAFLGSICSFVSIGSMAAIALDRYYVICHCFHALMNVSRSRTMVIIFLVWLYACLWSLPPFVGIGAYIE
EGFGIGCTFDYITRNLTTQIHIALLYVGGFALPILTIIICYVKIVLTVRKHRKEIESYSAKPALSKDQKGSTQSKKNKHGHSKKRRYYEILATHGSL
STLSGRNHSDGHFHIIMGSIRNNSSLQSISTE

>Pparvimensis_ops6

TLKGTETCRICFLSKPSRIFKMVTEINEATYEIERPEHVVVAVFLILCAIIGLIANGLIIAMFARFRQLNNPSNLLILSLALVDIGMIILCFPLTIW
ASLVGKWTFGSKGCNYYGFFSMLSGISVIGILTLMAIDRYVVICRKTIASNLNVKHYGAALIVVVVNASFWAIMPNLGWSRYDIEPSGISCSVDYHN
NDIYYVTYIVALFAVCFVVPLTVMVTCYWMAQSVMSKRVEVQNAITEGASAPINVEWCNQKEVTQMGAMLVFLFLLSWSLIAVVCLWAVFGEPSNVP
YPLVLIAPLAAKSSMVLNPLVVTAMIGKFRTHVAMMFKYQPEVTSLSGNASQLISDVEKEL

>Pparvimensis_ops8

PTVQKFWQIFFKCEFPQMATTMWHVGQEGSNILSLQTNLELNGLKLNSSSYSTDEFRSQLTRTGDILAGIHLVLVCILTTVGNLLIIILSKQDWRSF
KPIDKLIVNIAVSDLLTGLFGYPLPMLSSFRHRWDFGLAGCTWYSFLAFTGGTVSMVSISFVAIFRYIKISQSTSEYQRSFNRNISFAIAFSWIYAV
AWSAFPLIGWGRYTLEPFHTSCTVDWTSVLPGDRIYIVTIMIAVFGLPLGLIITCYVAIARKLYRHQLQFRQRGNRNYSTFIQFRNENRLIVTALVV
TSCCLITWTPYAIASMILIAIGDNANLSAPVSFFPAMFAKTSTIYNPIIYFILNKNFRKDAIKMLCRCGCKLFHFNVNIREEWCENHSGGIKIIISG
RRVNYRVVCGHPLCRQVRRAESSEGDAIPLRDLQKVSIKHCQVCEDNPEVSTPNSHLKRPVRTVSAHVASCSKEREPRGHEEAHASGTYSSSLISPN
DLPGQPSRTLENRTSFRRLPRSTIPRQCPV

>Hforskali_ops1

MVVVMVFFFLFAWTPYAAFALYVTFGESHTVSPLAATLPPFFAKSCTIYNPILYFVLNRQ

>Hforskali_ops4

LNVSRGRTLIIIFLVWFYAFIWSVLPFFGLGVYIEEGYGIGCTFDYVSQDMNTKVHVALLVVGGFLTPVTVIVVCYSKIVSKVRKHTREMERHSRRG
PQGTKRTSVDSANKPNRGFKIISRTMAHYRLARVGFITTVVFCLSWGPYALIALYSEYLSPKSTLKPLVQVIPAVFAKMSAIWNPFVYAVSHTRFKE
ALYHTLRTRFSCESKGIHKESNSHEINVDFSKTPPDGSKSTSSIKQSAAMQTLPDTVTTDKQNGIPLLPITNKTFK

>Hglaberrima_ops1

DADHASSVNIFCLNLSISDMSVSLLASPLTFASNIAGHWLFGQIGCSIYAFVVMIGGFEQIVALTAVSIHRCFLVVRPFTAKKMTMSWAVFFVSLTW
LYSFILTIPPAFGWNEFVPEGAGTACSVNWTETKPGNTSYVVFIFVMVLVVPLTVLVFSYGLLIFAVKKISASEAAQSTENKAEGRVTKMVVVMVFF
FLFAWTPYAVFALFVVFGNTHMSPLLATLPAFFAKSCTIYNPILYFVLNRQFRDAFYDLIGYQPPEEPDNSGQQQNRNVDSQLPGANQRQTMQRTAS
VATVMSELPSVRHDAFRTSGQFLAGGKVDPTGRALSKTYKKSAEEDPSRLAPPLPGQSVEMSDSLKGLNGSDEADKEKHASEPPRYSEVEKGAHVNE
GYQTGAESGKTVFVHRVKVKSANGDDDDDDSHRKDVKGMPDVEM

>Hglaberrima_ops4

SMGTEKKPKGRFKKISRVMAQYQLARVGIIATVVFCLSWGPYALIALYSEFLSPKSTLNPLVQVVPVIFAKMSSIWNPFVYAVSHTRYKKALYHTLR
KGLKCLGTGLDDDTESQELNFDLSRSPRDGSGSVSSTKRSANKSTLPDTLVTDKEKHIPLPPMKKKPLNKIKSDPGISKPAEKSIPIA

>Hglaberrima_ops6.1

MMNGTSNEESRPEHTIIGVFLIICAIVALVGNGSIVAMFAKYRQLRNPSNLLIATLALIDIGMAVLCFPVSAWASIAGSWTFGDRGCHYYGFISMFS
GISVIGIL

>Hglaberrima_ops6.2

IMPNLGWSSYAIEPSLTSCAIDYQTNDMYYITYLVALFIVCFVMPLCVMVFCYWRAHSVMSKREEIQNAITEESAAPINAEWCNQKEVTQMGAVLVF
LFLLAWSTEAVVCLWAAFGEPSNIPYPLTLLGPLAAKSSIVLNPLVI

>Hglaberrima_ops7

MAENNNYTRSNGALSSSEKRAFAVAFSVEGIVGMVCALYSLRCSFKYRQTNDKPLRFYTSLAIADIGIAALCPITAYGFMSTGGWPFGDGACDTYGF
VAMLFGSACIWSLLMTAFESLMVFTRKYNETLINMLLMLTWLNALFWSSAPLLGWGRYVPESYEAGCLFDMNAADRGGLTYLLGYPTAVLILPMGIL
LCALTFSGLGESFRSFSVKACSLVTLAISICWGTYCLEEIWVLVTGRKDTFPIKLAVLAPFTAKLSPILDTFIIQKIVSGLAPSNQYTVKGKKE

>Lclarki_ops1

GIFNNSIVIYLFVKYSSLRQPINYFLLNICVCDFLISTIASPMTFASNIAGHWLFGDLACRIYAFFVTVGG

>Pcalifornicus_ops1

ITAGEGRVTKMVMVMIFFFLFAWTPYSAFALYVVFGRTHTVSPIVATLPPFFAKSCTIYNPVLYFVLNRQFRDAFYELIGYEPPDPLDTSGGANQSG
NANQQQQQQGASNTRQSMQRSASVATVMS

>Arubens_ops1.1

WYAFLSSLCGCEQIASIAAIALQRYFFVVKYNLSARTNVYVIACICFTWLYSLAAVIPPAIGWSEFTVEGGGTSCSVNWESGDPSYIIFIFTLVLVI
PSSIIIYSYGSILSTVKKTEKVSTLHRCRLRRADKQVTTMAIILVLAFMITWGPYAVYSMY

>Arubens_ops1.2

SATVYNATAVYLGLLTFFGIFNNGLVLFLYARYRNLRNPINMFLVNISVGDLSVSIFGSPFTFASNVARRWLFGPGGCTWYAFIVTVCGTEQIVALA
AVSIHRCCLVVRPFTAQKMNTRW

>Arubens_Opsin3.1.B

MDPQPLIGDFYVNTTRNAEIFIAVYVSTVGFVATIGNICVLFILLRFNTFRKKSINYLLVNIAASDLGVSFSGYPMTSSSAFAGYWLFGDGGCHYYA
FCVYTCSCSAIGSHVAVAVYRYIYVCKPAHKHKLTAKLTFTVIASIWAFAL

>Arubens_Ops3.1.A

MIYCYYEVGKRSNQINPDRRDERDKGMAVFLQIQKKEKKIDIHVTKMCFLSTMSFVIAWTPYTILCIWVVSINSDVQLSLAASLLPTLFAKSSCAMN
PLVYFLSSSRYRRDFFKIFRRPRRAREFNGTDPYRQTERDANAGGPSNRADDNPLYLRRTVSPTGDISASVYFNKERIYIGDIKPAGISQEATLMQK
DAEVLSLTSSNSSVFQVVVKEPKKKFEMTTVQIEI

>Arubens_ops4

RASMETFIDLNTTEGFPTEAPIRMPPFLDYGLAFFLFIAFIFGVTGNGVTIWIFLRTKSLRTPPNMLIVNLAFSDVAMVLTNFPLMFASTLQGRWTF
GQMTCDIYAFCGALFGFMSITTMTAIALDRHYVICHSMEAMRTVTKRRSLYKIILVWIYSSIWSLLPFFGLGAYVLEGYGVNCTFDYIDQSLKNRIY
VGTIFIFGFFLPLTIIIGCYAHIATLRVHRLQLLSVQNDLRGSGNDKAQAAAIRKVKNDKMEWQIAKIGIMLTVLFCASWMPYASVAFVGEFIDVKL
VTPMIQVIPVVLAKSS

>Arubens_ops6

MADDGSTDTVKILVGGFMIFQTIAGLFGNSVIIKMFWTFKQLRTPSNNLLLVLSIANIGMCLCMPFSTASTFAGHWVFDTSGCKFYGFASMFFGLSV
IGILTCLSIDRYLVVCRRSLASMLTHVHYNYMSLAAYVNALFWAIMPVFGWARYEEDPGSGCALDWNRGGASYISYLFTLFVINFLVPLIVMVTCFG
RAHAVMVKREQVHAASSDNDLTPINSDWANQKQVTMLGVALIVVFLFTWSPFAIICIWGAIGDPHNVPHWFAVIAPFAAKWSQVLNPLMFVMFIKRF
RDYTLVILCCKTHVETIELTQQTTSDQQAVERAL

>Arubens_ops7_RadialNerve

MEVAALGPLEYYIMGLILTVEAILGTICCVRLLLVYLKNPTLHQPQSLLGITLCIGDLGIALMCPFAAFASFSETWPFGDEYCQLYAFAGMLFGTLS
ISAMACLALDKYYSSSNDAKGGSSQPYILITSIIWLNALFWSLTPLSPIGWGRYAIEPPKSTCMLDFANREPSYMMYLFLMTSTVYALPVGAILWCL
VKLRKGKDPNNGKSKVCLLVLFSLIVYWGAYGIVALWAALDDIHNVPLRLVAAAPILAKICPIGNTVMQVLTNRNIRCLMYRKETVASNKRE

>Arubens_ops7_tubefeet

FTGMLFGTLSISAMACLALDKCYSSSNDAKGGSSQPYILITSIIWLNALFWSLTPLSPIGWGRYAIEPPKSTCMLDFANREPSYMMYLFLMASTVYA
LPVGAILWCLVKLRKGKDPNNGKSKVCLLVLFSLIVYWGAYGIVALWAALDDIHNVPLRLVAAAPILAKICPIGNTVMQVLTNRNIRCLMYRKETVA
SNKRE

>Pminiata_ops1.1

SGYTGFAVYLAVVIFFSVSGNVTVILLYASNRSLHNVVNILLLNVSVADLSVAVLGTPVSFAASAAGHWLLGPIGCTWYGFICTLSGCAQIVGIAAV
SLHRYFLVVKPFVAKRLTTGGALVCVGFTWVYSLAVALPPVLGWSEFTREGAGISCSVSWHSGSRSYTFFIFTMILAIPMAIILFSYSQILFTVKKS
CPFVLFLFHLKMAKCQVSNQRSREAEKKVTIMIIVMVLTFLVAWTPYAALSLYMALGGDSVSITPLTATLPSMFAKASTTYNPVIYFLLHKKEIADK
NKWRLLHQSLSRRDRAMVVLY

>Pminiata_ops1.2

MNATLDGPTGSTPASPEGFYGRIPGAVYDVTAVYLGLLTFFGIFNNGLVLVLYARYKTLQNPVNLFLINICLGDLSVSLFGSPFTFAANVARRWLFG
AGGCTWYAFIVTVCGTEQIVSLAAVSVHRCCLVVRPFTAQKMTTRLALLFIALTWAYSLMVSLPPAIGWNSYVLEGTGTGW

>Pminiata_ops1.3

PYSVFSLYVAASKNNTVSPVAASIPAMFAKACTVYNPIIYFLLNQQFKDAFIDMMCCGRNPFSNDDVIDDTARTRALRQAT

>Pminiata_ops3.1

MDDTLVGDIYINMTRQAQIFVAVYVTTVGTIATVGNISVLIILLRFNTFRKKSINFLLINMAASDLGVSISGYPMTSSSAYAGHWLFGDSGCRYLAF
CVYTFSCSTIGSHVALAVYRYIYVCKPASKHKLTPKVTFIVLVVIWAKALFWTVTPFIGWSSYTYEPFGLSCSLDWTARTFSHLSYNVACVLGVFVA
PLAVMLACYYRVAKRSNQVDPTRMEERDLGVAMFLQMHRKDVKVDFHVTKMCVLMTLSFMIAWTPYTVVCVWVVFNKLELNIVASLAPTLFAKSSCM
MNPLIYFIASSRYRRDFLRMFRASGSGAPTGQSGDRTEGGRSSKPGTSAAGDGSGAVYLRRTTSPSGDISASMYFNKERIYIGDIKPSGIDKEAKLI
GKDPDVLSMSSSNTSDEYRVYVKEMKKVEEPIVQLEIDIH

>Pminiata_ops4

MENTSWNLDPLTGTTPLPAGPPPMPPFLDYGLAFFLFIAFIFGIAGNGITIWIFVRTKSLRTAPNMLIVNLAFICEIYGFLGGLFGFMSII
TMTAIALDRHAILFNRHYVICHSMEAMRTVTKRKAVYKILLVWIYSMIWALLPFFGFGAYVLEGYGVNCTFEYLDLSLKNRLYVGVIFMFG
FLIPLGVIIACYAHIAYTLRQHRLQLMRVQNDLRSPGNDKAQASAIRKVKADNVEWQIAKVGIMLTVLFCASWMPYASIAFIGEYIDSALV
TPMGQVIPVLFAKSSASWNPLVYAISHQRFKEALRDRFFVYCCGEAESRRQHRSTTRSMSSDNRNTDSRATSVRSVISEVDKRDRTGTVMS
TVSTKTDEIEMDSGALHYKPAKSSLKGGRERANKNTNNNDQEPVSEQRRRSLPDTSTVDSGNVNLVMKSRDGAKIQGQYVAYDNPAASLSD
RDELTKL

>Pminiata_ops5

MAAYVAIGVYLCAVIIVGFVGNVLVIVAFCKFKKLRTANNCLIMNLSVSDLAMAVVGTPMSCSSSFAGRWLYGQGGCTYYGFINYYCGCISLNTFAA
ISVYRYIVIMRHGPNRRFTGTMILKVIAAVHVITLIFTTPPLYGWNEFILEGFKTQCDINYRDKSPLFVSYIAFMFIALFFAPLGIIVNCYWRIFTF
LHRRTQEHISQSVSLQLRNSARTMEKRTTIMMLVCLSFFLLAWTPYCFVSLWSLFGDHRDITPPVSAAPALVAKSCIVFNPIIYGVMSPQYRRSFQR
GASSDRPTWYPAPAIVYNLKCKFERL

>Pminiata_ops6

MSSQQFLQKIVHSDGIMGDGSSPSYGESLTSGSKAGLGGLMFIQFLVGIFGNSVILYMFWKFKQLQTPSNIIFIFLLIANLGMCFCIPFSAASMLAG
SWLFDSAGCKFYGFASMFFGLAVIGLLACLSIDRYIVICRPSLASSLTHSHYTYMSMAAYLNAIFWAIMPIFGWAHYDEVGTSGCSVDWTRADAPYI
SYLFSLFMVCFVLPIVTMVFCFGRTHTVLVMRQQVQNIGSRDNLSPVNSDWANQKQVTQLGVVLIVIFILTWSPFAIVCLWGALGDPQSIPLWLATL
APFAAKCSQFLNPLMFVVLIKRFRDYAVVMLCCRTHVETIELTPSAAQDDRNEGEL

>Pminiata_ops7.1

GKAYQIVASAIWLNAVFWAVTPLPFVGWGRYAIEPQKTTCMLDFAAHGAPYVSYLVAMMGVVYVLPMGAVTWCLMKLREGGGAEDTKKIAAKKEAAM
TCVLVLLSLMVYWGAYGVVALWAAADDIDNVPIQLVAAAPLLAKICPIGNAVLQGLTNQGLRSFDREESRAADKKK

>Pminiata_ops7.2

LQLFFIRNYCVAGFIVYRQPFSPSYTTRIMESESPSVENLNMPLSSYEYYIMGLVLTAEGILGILFNGMLLVVFLTKTSLRRPQSVLAISLCIGDLG
IGLMCPFAAMASFKENWLYGDQGCQLYASAGMLFGTVSITSLVSIAVDKYYSAIGNTGGGKAYPIIASAIWLNAVFWAVTPLPFVGWGRYAIEPQKT
TCMLDFAAHGAPYVSYLVAMMGVVYVLPMGVVTWCLMKLREGGGAEDTKKIAAKKEAAMTCVLVLLSLMVYWGAYGVVALWAAADDIDNVPIQLVAA
APLLAKICPIGNAVLQGLTNQGLRSFDGEESRAADKKK

>Pminiata_ops8

VSPVSEDLVSLMSTMEEDAFASELPNVAAILSGVWILMIILISCVGNGAVLVTSLRKRRNLKALDLLTINLAVSDLTVCLIGYPLPAVSGFADRWMF
GESGCIWYGFCGFFFPMNAMMTLVAIAVCRYLKLCKKNFDDTLLAKHMPKIIAAVWMYALVWTVPPLMGWSRYVPERFRTSCTVDWASRLPSDQAYI
ICIFIFCYLFPLMCLIGCYGAITKAIFAHRRMILQQHTTHFTHFWTEVRLIKSSF

>Lannulatus_ops4.1

MSYWNDPANMASNALPSTNPFGNYTVVDTVPKELLHMVDPHWYQFPPMNPLWYGLVGFFMVVMGILSVVGNFVVIWVFMNTKSLRTPANLLVVNLAF
SDFFMMLTMFPPMVVSCYWQTWTLGAFFCEIYAFLGSLFGCVSIWTMVWITLDRYNVIVKGVSGEPLTSGGAMARIGGTWATALAWCLPPFFGWNRY
VPEGNMTACGTDYLSGESFSNSYLYIYSAWVYFTPLFLNIYLYSFIIKAVANHEKQMREQAKKMG

>Lannulatus_ops4.2

MSWNSPAYAEATSLPSTNPFGNFTVVDLAPKEILHMVDPHWYQFPPLNPLWYGLLMLWMIIMGTMSLAGNFIVIWVFMNTKSLRTPANLLVVNLAVS
DFFMMFTMFPPMLVTCYWQTWTLGAFFCEMYGFLGSLFGCVSIWSMVWITLDRYNVIVKGVSGEPLTSSGAMARIGGTWATALAWCLPPFFGWNRYV
PEGNMTACGTDYLTDTQLSKSYLYIYSIWVYIFPLFLNIYLYSHIISAVASHEKQMREQAKKMGVKSLRSEESQKTSAECRLAKVALMTVSLWFIAW
TPYFVTNYAGMFAKHTVSPLYTIWGSVFAKANAVYNPIVYAISHPKYRAALEKKLPCLSCQTEGHDNISSETSATAPEKSESS

>Lannulatus_ops4.3

AAVASQEKRRREQAKKMGVKARRSEESQKTSAECRLAKVALMTVSLWFMAWTPYFIINYTGMLNKSSVTPLFSIWGSVFAKANAVYNPIIYAISHPK
YRAALEKKLPCLACATDGRDNISNDTTQVAEKSESA

>Lannulatus_ops4.4

MVWNTPTIPRDYSLPSTNPFGNYTVVDTAPNEILHMVDSHWYQFPPMNPLWYSLVGFFVVITGLLSLIGNFVVIWVFLNTKSLRTPTNLLVVNLAFS
DFLMMFTMFPPMVFSCYWQTWTLGAFFCELYGFFGSLFGCVSIWTMVWITLDRYNVIVKGISGKPLTSGGAMARIMGTWVVCLAWCLPPFFGWNRYV
PEGNLTACGTDYLTEGLFSQSYLYIYSVWVYIFPLFLNIYLYTFIIKAVANHEKQMREQAKKMGVKSLRSEENQKTSAECRLAKVALMTVSLWFVAW
TPYFIINYT

>Amphipholis_ops7

MSPARSSLAVSLALSDMRIAIMCPFAASASFTESWPFGDAGCQTYAFFGMVFGIASVTNLAAMTVDIYRESQGQPAKSNSVLIMAIWVNALFWGWHR

>Aagassizii_ops4

AITAGGKIGCDVYAWGGAMFGVLSISTLTAIAFDRQYAICSSLDKLSNITYARAFRMIVCVWIYSLLWAILPLFGIGAYVLEGYGVSCTFEYLDQSR
ANQIFVGFLFFGDFLVPLTAIILCYTNIVNTVRKNRKNLQDISKDDSIKKDSKKKKVP

>Amediterranea_ops4

MSITSMATIALDRYYVICNAMRATRTVTKKRSRYIILFVWLYSLTWSVPPLFGFGRYTSEGYDLSCTFDYQDQATNNMIFVGLIFVTDFFLPLIVII
CCYTKIVISVRKHRIGMKKIVDSKRDSTKSKQIAEEKKEFKIAKIGMIITALFCIAWLPYATVAFIGQFIDEEIPTPLLQTLPVVFAKSSCVVNPIV
YAITHDKFKAALTQKYIKMCCSQYEKDSRASQHKGGRSMAKRESSIASTVNSMEFNLEDDPPKVDTKQPNVVEKGNTDVVQQPSSNTDKPVVVAAIS
GGIDNPPLQLDNTDL

>Fserratissima_ops4

MVITQYPAMFFTTVSGKWLYGDIGCQVYAFFGSMFGIMSIASMSAISVDRYYAICKPMKSTRTMTKRRSRRIVLVVWLYSLAWTVPPFFGFGRYTRE
GYGLSCTFDYEDQDIINLSVVG

>Skowalevskii_ops6

MDDKTSTDEPSALTTFSESGNIVMGIFLLVTAVLSVIGNSVVLEMFRRYKELLSPSAILLISLALADLGLTIFGMSLSCVSSFAGRWLFGKFGCYFH
GFAGMLFGLGSIGNLTVISIDRYIITCKRSLQWSYRHYYALLAVAWSNALFWSMMPLFGWSSYALEPEGTSCTIDWMNNDNQYISYVSCVTVTCFIL
PCAVMTYDYLAAYMKMVKAGYTLSEETEKPNNDGENIENIETGTRVKGVSIRVNSFIRPDWKQTKYATKMCIALVAAFLLSWFPSATVFLWAAFGNP
GNIPLSFTGVADAFSKIPAVFNPVIYVALNPEFRKYFGKTIGCRRKRKKPIAVRLNGKWVSKLYQLYGGVISMIGRDYINDVVGEAFGAISMVGREH
LNEGGALKRWGETISTTGWNHINDG

>Skowalevskii_ops7

MVTTDSLANSTDEPVPSILTLQQHYAASVTLLALAVIGTVLSSVNFRMLLSNPDYCSKAGNFFLSLAVTDLCVCIFETPFSAFSHHAGFWIFGDTAC
QLYAFFGIFFGLVNIFMVTFISLDRYWATCSPVEVELKSKYYTRMTALGWMVALFWAAAPVFGWSRYAMEPSMASCSIDYMTNDFSYVTYITCLTLT
CYVVPIVVMVYCYVKASKNIKYTGKVTEWAHENNATKISRLCVLQLVFCWSLYGFNCMWTVVADDVETLPKMLTVLAPILAKTTPILNSGLYFLHNK
KFRGAAVDMFKAKEE

>Skowalevskii_ops8.5

MFMISSNIIKLPPCAVSDLLSLFGNTIVLVVKVKNRKQLKTHDYLIANIAIADIGAVTTGYTLTAVSALTHKLYFGAIGCSVAGFSGWFFNCVSMIT
LSVIAIVRYLIVVHNHGSYFKGKTIIVIIVIIWLYSAFWATAPLIGWNRYAPEPHMTSCTLDWTSTQPADIAYIACIYTCCFALPLISIIYCYGGII
LHVRRVQRNSNGQIRVIKKEGKTTKVFAIITICFLCSWTPYAVVSLITVVKGGSADISKTVTTLPTLFAKLSCVYNPLLYYITDKTFRKSVNQLFFS
SCSSCCVYQTTSNVQLQELSIQVNTAHTSVQN

>Skowalevskii_ops8.1

MTLNNPSGLSSTADIAVCTYLVVMCILSLFGNVTVLAVKVKNRKQLKTHDYFIINIAVADIGAVTTGYVLAAVSARNHMWYFGSTGCSLVGFSGWFF
NCVSMITLSVIAIVRYSIVVGNQGTSIKKNTILIIIAMIWLYSAFWSVAPLVGWDRYALEPHLTSCTIDWTSTQKADIAYIVCIFVWCFAFCLVSIV
YSYGGIILTVRQIQQNLFSDSRKSEMNKQRKTTKMFAITTICYLVSWTPYAVMSLISVIQGSAAGIPIALTTLPTLFAKFSCVYNPVVYYITDETFR
KSTSQMFGGIRSLFCGNRVTPDVVV

>Skowalevskii_ops8.2

MTSPETMAWNNTSGLGHIAEVGVGTYVTIMCTLSLFGNVTVLAVKIKNRKQLKSHDYFIINIAIADIGAVTTGYLLMVVSASNHMLYFVSSECTLVG
FSGWFFNCVSMTTLSVIAIMRYLIVVRSQGSFFEKKKRIIGIIVFIWLYSAFWATAPLVGWDRYVPEPYLSSCSLDWTSTQPADIAYIVCIFVWCFL
LCVIAIIFSYGSIILKVRQIQRNLNPNKSAMKKHGKITKMFAITTICFLVSWTPYAIVSFVSVIKGSSADIPLIVLTSPNLFAKFSCVYNPIVYYTT
DKMFRKSVNQLFWSICLPCCEYHITSDVQPQDLTLHADAAHTSMQGRCQDKVEQPCNRLPLPNDSEVVIVQESRFQHDNTIHAS

>Skowalevskii_opsin8.3

MAIGTYLTSICLLSLFGNVIYLASKFKQRKQLKIPDYLLANIAIADIGAVTTSYMLAAISSFSTKWRFGSIGCTLTGFSGWFFNCVSMITLAVVAIVRRL
LVVNNHEYFQKKKTIFVIITSIWLYSAFWAIAPLIGWNRYAPEPHLTSCTLDWTSNLPADIIYVICIFVFCFGFTLISLIYNYYDITSKVRRIRPQIDAD
QSEPQNIAKSRNITQVFVIITTCFFVSWTPYAVLSLFSAIQGSSAGIPIIVTALPTLFAKLSCVYNPLVNYYSDRTFRNSVKNLFPIRSSDSDVCSVGGS

>Skowalevskii_ops8.4

MEYPNCKNQAQLRTGIVADYVYTMSTEETIASGLGSIADIAVCTYLVVMCIMSLFGNIIVLVVKIKNRKQLKTHDYFIANIAIADIGAVTTGYLLAA
VSACKHMWYFGSIGCSLVGFSGWFFNCVSMVTLSVIAIIRYLIVVGNHGTAITQKTTTIIIAMIWLYSAFWATAPLIGWDRYAPEPHLTSCTLDWTS
TQPADIAYIVCIFVLCFAFCLVSIIYSYGGIIAKIKQTQRNLYPESQQCEMNKEGRTTKVECDNLKQVTVYATPVGVIRCLMEKDEKY

>Smereschkowskii_ops7

EVPVPSLLTVEQHYAASVTLLALVVVGTVLSSVNFRMLLSNPDYCSKSGVFFLSLAVTDLCMCVCTTPFAALSHHIGFWVFGDTLCQLYAFICMFFG
INAIFMACFISLDRYWATCSLVEVELKSKYYPRMAALGWVMALFWAAAPLLGWSQYAMEPSMTSCAIDYMTNDANYVTYIAGVTVTCYVVPIVVIVY
CYVKASKNIKSTGKVTEWADETNVTMISGLCVFQLLLCWGLYGFNCMWRVVTDDVETFPKMLTVLAPILAKTSPILNSGLYFLHNKKFRGAAANMFK
AKEE

>Harrimaniidae_ops7

MATTEIPPDMDNEEVFNLPDLLTREQHAAASVTLFALALVGTIVCTMNFRMLLSNSDCRNKAGPFFFVLVLTDLCICVFETPFAAFSHHIGFWFFGD
TICQTYAFGGMFLAIINVFMVTLISLDRCWTTCSPLEAEMKFKNYPWMIVIGSLIGLFWAAAPLPLFGWSRYSIEPSGVSCHIDYMTNDRSYATYMA
AMIIVCFFIPIGIMVYSYRKASANIKINSKVTGWADEFNVTQISAMCLFQVLFCWGLYVFIWTWTALAEDAETLPKMLTILAPILAKSSPLLNSWIY
FFQNKQFRGAVADMFKAKEE

>Schizocardium_spp_ops7

MIGTVLGTMNILMFLSNPEYRLKGGIFYFHLVITNCCMVMFGTPFTAVSHFVGRWVFGDLFCQMYAFMGMWFGITHIFMLALISWDRYRTLSSPKEA
DGGSRIYPLLTAASWLIGLIAASAPLQPFGWSRYTYEPSGAACAVDYMSVDADYVKYILTVFAVCFTLPIGLMAYSYAMATMDIKHTGKVCDWADET
NVAWQSALCLFQLVFCWGLYGVVCLWTVVATPSSLPKVLTVIAPVAAKASPILTSWIYIMQIKRFRGAVADLFKPKEE

>Schizocardium_spp_ops8

CTDLSPNMTTTTEDISIELTTASPFTEGIGDLYPSKLPSNVDRLVGIYLTITGILATVGNGLVLVLLFKKRGNLKPLDVLVLNLALSDLGLAV
LGYPFAAAASYRHKWYLGKGGCDWYGFAGSFFSYVSMYTMTILAFLRYVKICIHNKVYWINKRNVNIGITISWIFAMVWSIFPLIGWNRYQPE
PFGISCTVHWDSRKVSDIMYIVSIFLFCYILPLTVTVFSYASIMRRIRVNRRNQAARRVRRDHPLEHEITKIGVLISLFFVIAWTPYAVVSIW
GSVTESQNIPLAAMTAPALFAKFASVYNPVIFYIFNKTFRTDVNKLVCRCGCKCFNVAINVSENGDLDTTRNTELSKTKVLFCVNNTRVDVLT
SAGLTQSTTRPANMAAQSIYDDTAVPSTSQLMQANAAVKHPQFSAKPEVDDYANDLTSNNTDDSVLFSPAPTAPVVSSYITRVITPKPSHTVN
GSAVTLDPCRVQSIDSCDSV

>Pflava_ops1

STTHRHRRAGTTPRTTPLRVTIFSRAGYTNVAIILGVIGLFGFLNNLLVIMAWVKNKSLRTPVNMFLINLCIGDFTVSVFGTPFAFAANVAGKWLYG
EVGCSWYAFIN

>Pflava_ops6

VISVDRYLVICRRDLLWSYRQYGGLIAVAWFNALFWALVPIFGWSSYSLDPNGTACTINWMDNDGGYISFVCCVFVVCFVLPIGVMCFDYYAVYRKM
RKAGYSHNTSGISNIAAANEDDAGDLKDGNAYPVLIGQKQNTSQGCA

>Pflava_ops7

MMATAAADEMPVSPGVLTAQQHYALSVTLFALATIGTVMGSMNIRMFLSNPEFIARGGLFYLNMVISDMCMAMLESPFTAISHFHGKWMFGDVACRL
YGFAGMFFGISNIFMLAFISLDRCWTTCSPTEVEQKAKFYPLMVAIGWFVGLVSAGAPLFGWSSYEYEPSGTS

>Pflava_ops8

MWVAVSGTDIIPTGLSAASAVLAKTSSIYNPLIYYIVNKKFREDANRLVCCCGCMVLQLRFNYGPDVMGDMVQNLPSRREVA

>Pbahamensis_ops7

MMATAAADEMPVSPGVLTAQQHYALSVTLFALATIGTVMGSMNIRMFLSNPEFIARGGLFYLNMVISDMCMAMLESPFTAISHFHGKWMFGDVACRL
YGFAGMFFGISNIFMLAFISLDRCWTTCSPTEVEQKAKFYPLMVAIGWFVGLVSAGAPLFGWSSYEYEPSGTSCALDYMKNDATYIRYIICVFVTCF
AVPILIMVYSYGKASRVVKATGKVTDWANESNVTLQSALCVMQLVFCWGMYGVNCLWTVFAPSSTLPPMLTVIAPVLAKTSPIINSWLYIYRVKKFR
GAVGDMFKPKEE

>Baurantiacus_ops1

DVNYPLALGNTSADGNSFSRTGYTNVAIILGVIGTFGFLNNLLVILVWLKNKSLRRPMNIFLINLSIGDITVSIFGTPFTFAANVVGKWPFGATGCA
WYAFITTTAGIGAIITLTVVSLERYYMLV

>Baurantiacus_ops7

PTLLTVQQHSAISVTVFAFAIIGTVMGSLNIRLFMTNPDLISKGGIFYLNMVITDLCMAMFESPFTAISHFYGSWVFGDAACQVYSFAGMFFGIAGI
FMLTFISLDRYWTTCSPVVEQKKVRYYPYMVVVGWLSALVWAAAPLPPFGWSSYAIEPSGASCSIDYMTNDATYVRYIISVTVCCFILPIAVMLYSY
GKMISMIKSTGKVTDWADESNVTLQSCLCLFQLFFCWGLYGVNCLWTAFAHSNTLPKMFTVIAPVLAKSSPIINSYLYIYRIKNFR

>Baurantiacus_ops8

TILSILGNGLVILVYYKNRRSLNSFDLLAVNIALSDLLYPVLGHGLHIYSSFSHKWMFGTIGCQIYGFLSSFLNYVSMVTLAALSFSRYIKVCSVPY
GRYIDKRNTVFALVFIWIYSLLWALPPLIGWNRYVLEPCGVFCTLDWIDRDSHGFSYTICLFVLVFFIPLMVIVASYSAIIHTTREQRKEVGVSSKK
SSAVRLKLQKRLTKVAIAMTAAFLLSWSPYAAVSLWAVAIGGQPPISVELLTAPSVFAKLSTLYNPILIIIFNKNFRE

>Torquaratorid_ops7

MVVPDADQMSEYPTLLTEQQHYAISVTLFAFAIIGTVMSSLNIRMFLSNPKLMSKGGIFYLNMVISDMCVCMLQTPFSAISHFYGNWLFGDDVCKLY
GFTGMLCVITNIFMLAFISLDRFWTTCSPVEAQKNVKYYPYMVAMGWLVGLVCAATPLQPFGWSSYAVEPSGASCTLPAVMA

Figure 21 – SEQUENCE ALIGNMENT (1A)

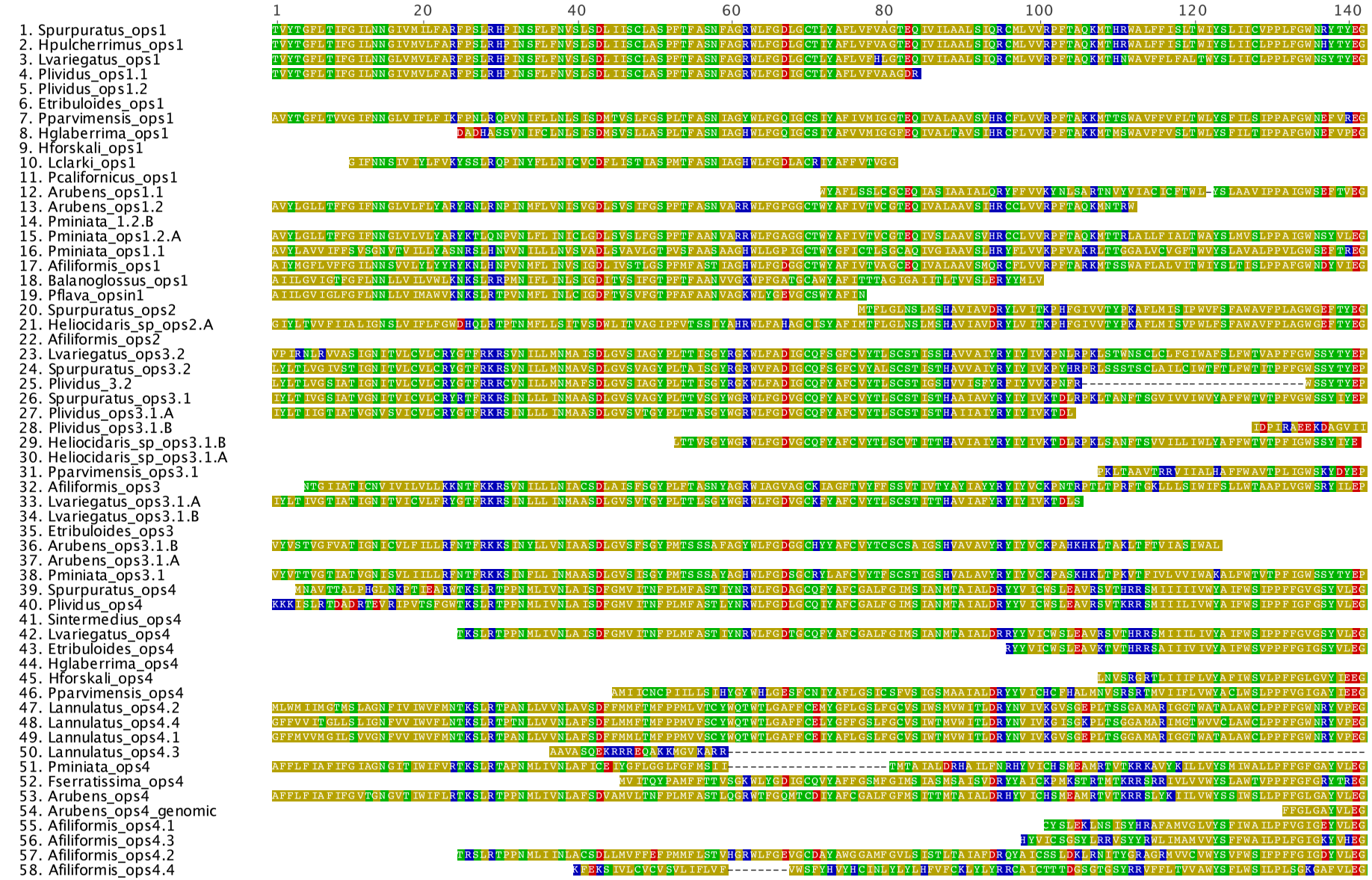

Figure 21 – SEQUENCE ALIGNMENT (1B)

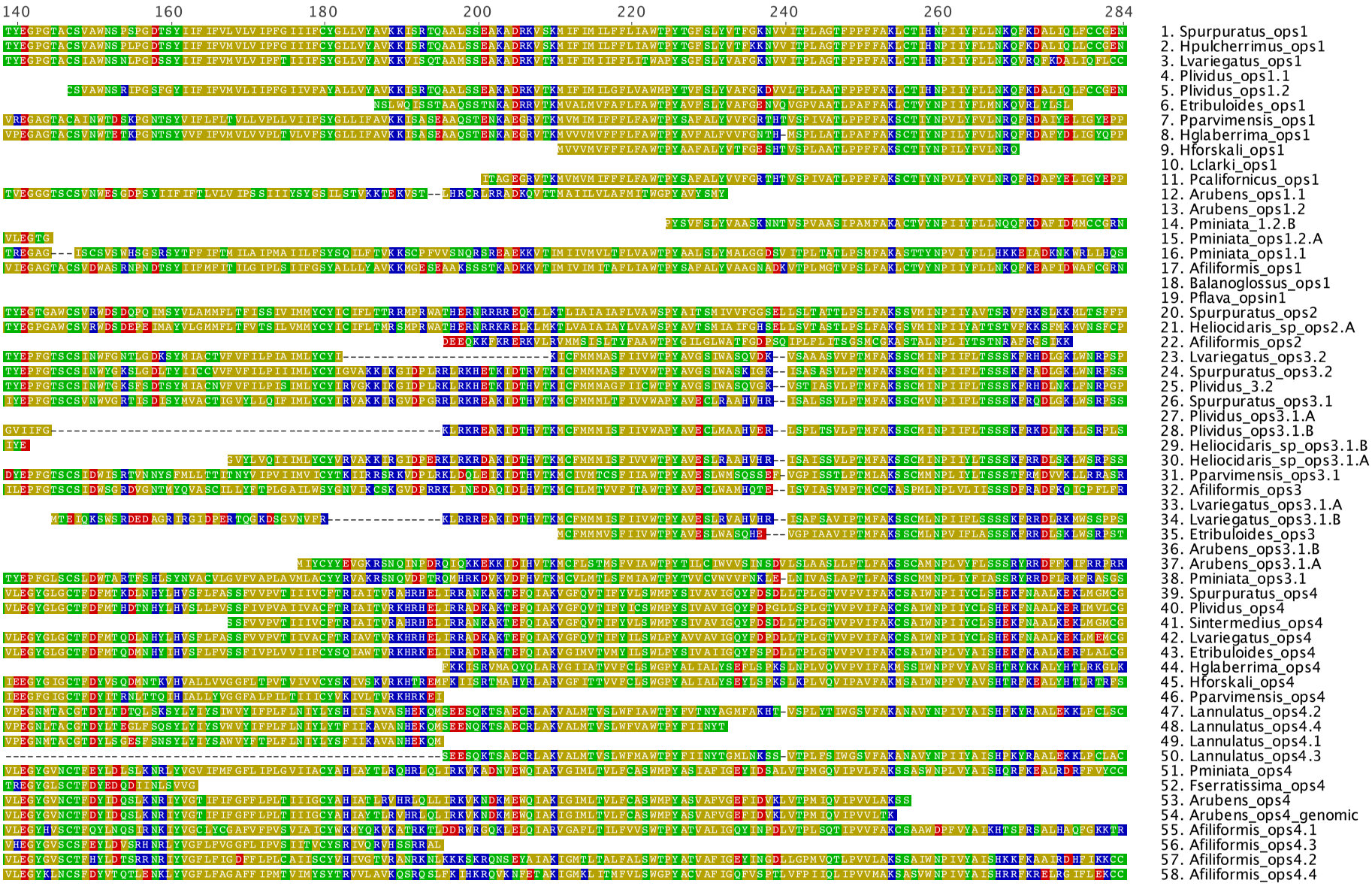

Figure 21 – SEQUENCE ALIGNMENT (2A)

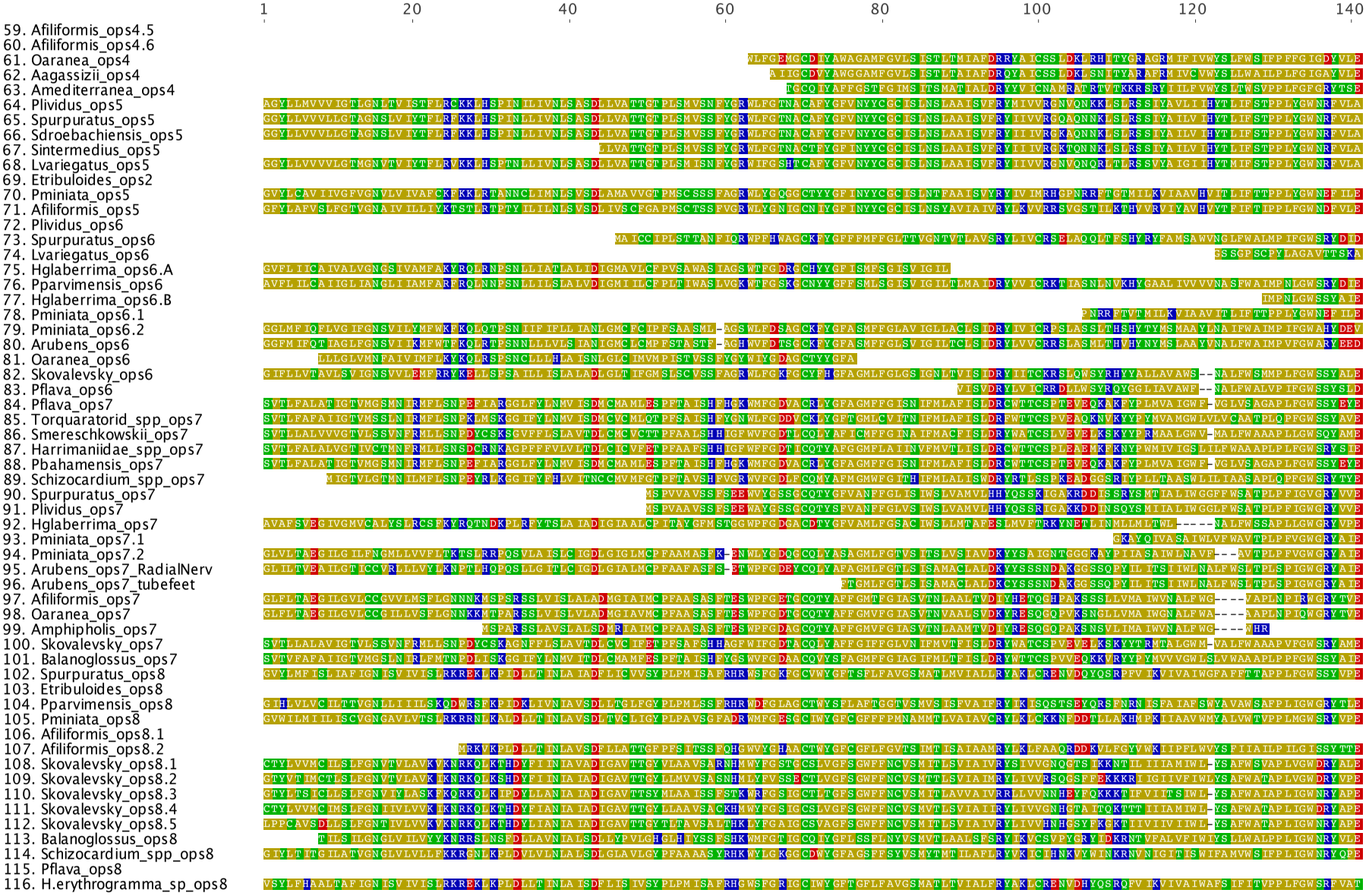

Figure 21 – SEQUENCE ALIGNMENT (2B)

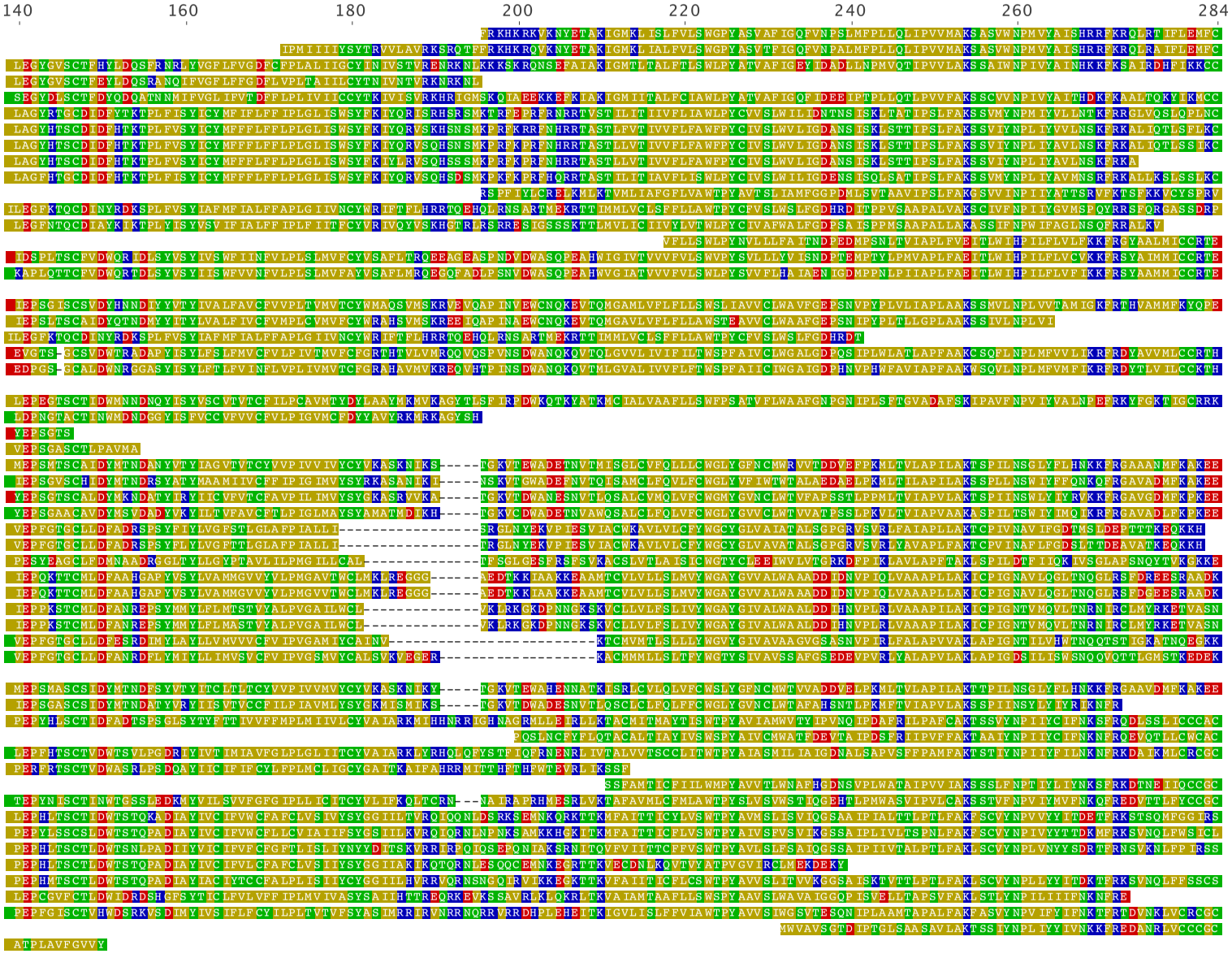

59. Afiliformis_ops4.5
60. Afiliformis_ops4.6
61. Oaranea_ops4
62. Aagassizii_ops4
63. Amediterranea_ops4
64. Plividus_ops5
65. Spurpuratus_ops5
66. Sdroebachiensis_ops5
67. Sintermedius_ops5
68. Lvariegatus_ops5
69. Etribuloides_ops2
70. Pminiata_ops5
71. Afiliformis_ops5
72. Plividus_ops6
73. Spurpuratus_ops6
74. Lvariegatus_ops6
75. Hglaberrima_ops6.A
76. Pparvimensis_ops6
77. Hglaberrima_ops6.B
78. Pminiata_ops6.1
79. Pminiata_ops6.2
80. Arubens_ops6
81. Oaranea_ops6
82. Skovalevsky_ops6
83. Pflava_ops6
84. Pflava_ops7
85. Torquaratorid_spp_ops7
86. Smereschkowskii_ops7
87. Harrimaniidae_spp_ops7
88. Pbahamensis_ops7
89. Schizocardium_spp_ops7
90. Spurpuratus_ops7
91. Plividus_ops7
92. Hglaberrima_ops7
93. Pminiata_ops7.1
94. Pminiata_ops7.2
95. Arubens_ops7_RadialNerv
96. Arubens_ops7_tubefeet
97. Afiliformis_ops7
98. Oaranea_ops7
99. Amphipholis_ops7
100. Skovalevsky_ops7
101. Balanoglossus_ops7
102. Spurpuratus_ops8
103. Etribuloides_ops8
104. Pparvimensis_ops8
105. Pminiata_ops8
106. Afiliformis_ops8.1
107. Afiliformis_ops8.2
108. Skovalevsky_ops8.1
109. Skovalevsky_ops8.2
110. Skovalevsky_ops8.3
111. Skovalevsky_ops8.4
112. Skovalevsky_ops8.5
113. Balanoglossus_ops8
114. Schizocardium_spp_ops8
115. Pflava_ops8
116. H.erythrogramma_sp_ops8

Table 3 – LIST OF SPECIMENS SURVEYED IN THIS STUDY

NAME (SPECIES & OPSIN)	METHOD/TISSUE	SOURCE
A) AMBULACRARIA OPSINS		
ECHINODERMATA/ECHINOIDEA		
Strongylocentrotus purpuratus		
Sp-opsin 1	Genome	NCBI
Sp-opsin 2	Genome	NCBI
Sp-opsin 3.1	Genome	NCBI
Sp-opsin 3.2	Genome	NCBI
Sp-opsin 4	Genome	NCBI
Sp-opsin 5	Genome	NCBI
Sp-opsin 6	Genome	NCBI
Sp-opsin 7	Genome	NCBI
Sp-opsin 8	Genome	NCBI
Strongylocentrotus droebachiensis		
Sd-opsin 5	Isolated sequence/Tube foot	NCBI, Lesser et al. 2011
Strongylocentrotus intermedius		
Si-opsin 4	Isolated sequence/Tube foot	NCBI, Zhao et al. 2015
Si-opsin 5	Isolated sequence/Tube foot	NCBI, Zhao et al. 2015
Hemicentrotus pulcherrimus		
Hp-opsin 1 (encephalopsin)	RNA-seq/Embryos-Larvae	NCBI, Ooka et al. 2010
Paracentrotus lividus		
Pl-opsin 1.A	Genome	Genoscope
Pl-opsin 1.B	Genome	Genoscope
Pl-opsin 3.1.A	Genome	Genoscope
Pl-opsin 3.1.B	Genome	Genoscope
Pl-opsin 3.2	Genome	Genoscope
Pl-opsin 4	Genome	Delroisse et al. 2013, Genoscope
Pl-opsin 5	Genome	Genoscope
Pl-opsin 6	Genome	Genoscope
Pl-opsin 7	Genome	Genoscope
Lytechinus variegatus		
Lv-opsin 1	Genome	Echinobase
Lv-opsin 3.1.A	Genome	Echinobase
Lv-opsin 3.1.B	Genome	Echinobase
Lv-opsin 3.2	Genome	Echinobase
Lv-opsin 4	Genome	Echinobase
Lv-opsin 5	Genome	Echinobase
Lv-opsin 6	Genome	Echinobase
Heliocidaris erythrogramma		
He-opsin 2	RNA-seq/Larvae	Cannon et al. 2014
He-opsin 3.1.A	RNA-seq/Larvae	Cannon et al. 2014
He-opsin 3.1.B	RNA-seq/Larvae	Cannon et al. 2014
He-opsin 8	RNA-seq/Larvae	Cannon et al. 2014
Eucidaris tribuloides		
Et-opsin 1	RNA-seq/Embryos	Echinobase
Et-opsin 2	RNA-seq/Embryos	Echinobase
Et-opsin 3	RNA-seq/Embryos	Echinobase
Et-opsin 4	RNA-seq/Embryos	Echinobase
Et-opsin 8	RNA-seq/Embryos	Echinobase

Table 3 – LIST OF SPECIMENS SURVEYED IN THIS STUDY

NAME (SPECIES & OPSIN)	METHOD/TISSUE	SOURCE
A) AMBULACRARIA OPSINS (Continuation)		
ECHINODERMATA/HOLOTHUROIDEA		
Parastichopus parvimensis		
Pp-opsin 1	RNA-seq/Larvae	Unpublished data
Pp-opsin 3.1	RNA-seq/Larvae	Unpublished data
Pp-opsin 4	RNA-seq/Larvae	Unpublished data
Pp-opsin 6	RNA-seq/Larvae	Unpublished data
Pp-opsin 8	RNA-seq/Larvae	Unpublished data
Holothuria forskali		
Hf-opsin 1	RNA-seq/Cuverian Tubules	Unpublished data
Hf-opsin 4	RNA-seq/Integument	Unpublished data
Holothuria glaberrima		
Hg-opsin 1	RNA-seq/Radial Nerve	Mashanov et al., 2014
Hg-opsin 4	RNA-seq/Radial Nerve	Mashanov et al., 2014
Hg-opsin 6.1	RNA-seq/Radial Nerve	Mashanov et al., 2014
Hg-opsin 6.2	RNA-seq/Radial Nerve	Mashanov et al., 2014
Hg-opsin 7	RNA-seq/Radial Nerve	Mashanov et al., 2014
L*eptosynapta clarki*		
Lc-opsin 1	RNA-seq/Adult	Cannon et al., 2014
Parastichopus californicus		
Pc-opsin 1	RNA-seq/Muscle	Cannon et al., 2014
Apostichopus japonicus		
No opsin found	RNA-seq/Multiple tissues	Zhou et al., 2014; Du et al., 2012
ECHINODERMATA/ASTEROIDEA		
Asteria rubens		
Ar-opsin 1.1	RNA-seq/Radial Nerve	Semmens et al., 2015
Ar-opsin 1.2	RNA-seq/Radial Nerve	Semmens et al., 2015
Ar-opsin 3.1.A	RNA-seq/Radial Nerve	Semmens et al., 2015
Ar-opsin 3.1.B	RNA-seq/Radial Nerve	Semmens et al., 2015
Ar-opsin 4	Isolated sequence - RNA-seq/Radial Nerve	Delroisse et al., 2013; Semmens et al., 2015
Ar-opsin 6	RNA-seq/Radial Nerve	Semmens et al., 2015
Ar-opsin 7	RNA-seq/Tube Foot-Radial Nerve	Hennebert et al., 2015; Semmens et al., 2015
Patiria miniata		
Pm-opsin 1.1	Genome	Echinobase
Pm-opsin 1.2.A	Genome	Echinobase
Pm-opsin 1.2.B	Genome	Echinobase
Pm-opsin 3.1	Genome	Echinobase
Pm-opsin 4	Genome	Echinobase
Pm-opsin 5	Genome	Echinobase
Pm-opsin 6.1	Genome	Echinobase
Pm-opsin 6.2	Genome	Echinobase
Pm-opsin 7.1	Genome	Echinobase
Pm-opsin 7.2	Genome	Echinobase
Pm-opsin 8	Genome	Echinobase
Labidiaster annulatus		
La-opsin 4.1	RNA-seq/Arms	Cannon et al., 2014
La-opsin 4.2	RNA-seq/Arms	Cannon et al., 2014

Table 3 – LIST OF SPECIMENS SURVEYED IN THIS STUDY

NAME (SPECIES & OPSIN)	METHOD/TISSUE	SOURCE
A) AMBULACRARIA OPSINS (Continuation)		
ECHINODERMATA/ASTEROIDEA		
Labidiaster annulatus		
La-opsin 4.3	RNA-seq/Arms	Cannon et al., 2014
La-opsin 4.4	RNA-seq/Arms	Cannon et al., 2014
Odontaster validus		
No opsin found	RNA-seq/Arms	Cannon et al., 2014
ECHINODERMATA/OPHIUROIDEA		
Ophiopsila aranea		
Oa-opsin 4	RNA-seq/Arms	Delroisse et al., 2015
Oa-opsin 6	RNA-seq/Arms	Delroisse et al., 2015
Oa-opsin 7	RNA-seq/Arms	Delroisse et al., 2015
Amphipholis sp		
A-Opsin 7		Unpublished data
Amphiura filiformis		
Af-opsin 1	Genome	Delroisse et al., 2014
Af-opsin 2	Genome	Delroisse et al., 2014
Af-opsin 3	Genome	Delroisse et al., 2014
Af-opsin 4.1	Genome	Delroisse et al., 2014
Af-opsin 4.2	Genome	Delroisse et al., 2014
Af-opsin 4.3	Genome	Delroisse et al., 2014
Af-opsin 4.4	Genome	Delroisse et al., 2014
Af-opsin 4.5	Genome	Delroisse et al., 2014
Af-opsin 4.6	Genome	Delroisse et al., 2014
Af-opsin 5	Genome	Delroisse et al., 2014
Af-opsin 7	Genome	Delroisse et al., 2014
Af-opsin 8.1	Genome	Delroisse et al., 2014
Af-opsin 8.2	Genome	Delroisse et al., 2014
Astrotomma agassizii		
Aa-opsin 4	RNA-seq/Arms	Cannon et al., 2014
Ophionotus victoriae		
No opsin found	RNA-seq/Arms	Burns et al. 2013; Cannon et al. 2014; Elphick et al. 2015
Ophiocomina wendtii		
No opsin found	RNA-seq/Embryos	Vaughn et al., 2012
ECHINODERMATA/CRINOIDEA		
Antedon mediterranea		
Am-opsin 4	RNA-seq/Arms	Elphick et al., 2015
Florometra serratissima		
Fs-opsin	RNA-seq/Arms	Unpublished data
Promachocrinus kerguelensis		
No opsin found	RNA-seq/Arms	Cannon et al., 2014
Dumetocrinus sp.		
No opsin found	RNA-seq/Arms	Cannon et al., 2014
Oxycomanthus japonicus		
No opsin found	RNA-seq/Embryos	Unpublished data (Akihito Omori)

Table 3 – LIST OF SPECIMENS SURVEYED IN THIS STUDY

NAME (SPECIES & OPSIN)	METHOD/TISSUE	SOURCE
A) AMBULACRARIA OPSINS (Continuation)		
HEMICHORDATA/RHABDOPLEURIDAE		
Rhabdopleura normani		
No opsin found	RNA-seq/multiple zooids	Cannon et al., 2014
Rhabdopleura sp. (Iceland)		
No opsin found	RNA-seq/multiple zooids	Cannon et al., 2014
HEMICHORDATA/CEPHALODISCIDAE		
Cephalodiscus gracilis		
No opsin found	RNA-seq/multiple zooids	Cannon et al., 2014
Cephalodiscus hodgsoni		
No opsin found	RNA-seq/multiple zooids	Cannon et al., 2014
Cephalodiscus nigrescens		
No opsin found	RNA-seq/multiple zooids	Cannon et al., 2014
HEMICHORDATA/HARRIMANIIDAE		
Saccoglossus kowalevskii		
Sk-opsin 6	Genome - RNA-seq/Embryos	NBCI - Freeman et al., 2008
Sk-opsin 7	Genome - RNA-seq/Embryos	NCBI - Freeman et al., 2008
Sk-opsin 8.1	Genome - RNA-seq/Embryos	NCBI - Freeman et al., 2008
Sk-opsin 8.2	Genome	NCBI
Sk-opsin 8.3	RNA-seq/Embryos	Freeman et al., 2008
Sk-opsin 8.4	RNA-seq/Embryos	Freeman et al., 2008
Sk-opsin 8.5	RNA-seq/Embryos	Freeman et al., 2008
Saccoglossus mereschkowskii		
Sm-opsin 7	RNA-seq/Proboscis	Cannon et al., 2014
Harrimaniidae sp (Iceland)		
H-opsin 7	RNA-seq/Whole Anterior	Cannon et al., 2014
Harrimaniidae sp (Norway)		
No opsin found	RNA-seq/Whole Anterior	Cannon et al., 2014
Stereobalanus canadensis		
No opsin found	RNA-seq/Proboscis, gonad	Cannon et al., 2014
HEMICHORDATA/SPENGELIDAE		
Schizocardium cf. brazilienze		
Sb-opsin 7	RNA-seq/Whole Anterior	Cannon et al., 2014
Sb-opsin 8	RNA-seq/Whole Anterior	Cannon et al., 2014
HEMICHORDATA/PTYCHODERIDAE		
Ptychodera flava		
Pf-opsin 6	RNA-seq/Embryos	Cannon et al., 2014
Pf-opsin 7	RNA-seq/Embryos	Cannon et al., 2014
Pf-opsin 8	RNA-seq/Embryos	Cannon et al., 2014
Ptychodera bahamensis		
Pb-opsin 7	RNA-seq/Proboscis	Cannon et al., 2014
Balanoglossus aurantiacus		
Ba-opsin 1	RNA-seq/Whole Anterior	Cannon et al., 2014
Ba-opsin 7	RNA-seq/Whole Anterior	Cannon et al., 2014
Ba-opsin 8	RNA-seq/Whole Anterior	Cannon et al., 2014
Glossobalanus marginatus		
No opsin found	RNA-seq/Proboscis	Cannon et al., 2014

Table 3 – LIST OF SPECIMENS SURVEYED IN THIS STUDY

NAME (SPECIES & OPSIN)	METHOD/TISSUE	SOURCE
A) AMBULACRARIA OPSINS (Continuation)		
HEMICHORDATA/TORQUARATORIDAE		
Torquaratorid sp (Iceland)		
T-opsin 7	RNA-seq/Proboscis	Cannon et al., 2014
Torquaratorid sp (Antartica)		
No opsin found	RNA-seq/Proboscis	Cannon et al., 2014
B) HOMO SAPIENS OPSINS		
Homo sapiens		
Encephalopsin	Genome	NCBI
Rhodopsin	Genome	NCBI
Peropsin	Genome	NCBI
Melanopsin	Genome	NCBI
RGR	Genome	NCBI
Neuropsin	Genome	NCBI
C) MELATONIN RECEPTORS (OUTGROUP)		
Strongylocentrotus purpuratus		
Melatonin R1A	Genome	NCBI
Melatonin R1B	Genome	NCBI
Melatonin R1C	Genome	NCBI
Saccoglossus kowalevskii		
Melatonin R1A	Genome	NCBI
Melatonin R1B	Genome	NCBI
Melatonin R1C	Genome	NCBI

1.6 References

Arendt, D. (2008). The evolution of cell types in animals: Emerging principles from molecular studies. *Nature Reviews Genetics*, *9*(11), 868-882.

Blevins, E., & Johnsen, S. (2004). Spatial vision in the echinoid genus Echinometra. *Journal of Experimental Biology*, *207*(24), 4249-4253.

Brandenburger, J. L., Woolacott, R. M., & Eakin, R. M. (1973). Fine structure of eyespots in tornarian larvae (Phylum: Hemichordata). *Cell and Tissue Research*, *142*(1), 89-102.

Braun, K., Kaul-Strehlow, S., Ullrich-Lüter, E., & Stach, T. (2015). Structure and ultrastructure of eyes of tornaria larvae of Glossobalanus marginatus. *Organisms Diversity & Evolution*, *15*(2), 423-428.

Burke, R. D., Angerer, L. M., Elphick, M. R., Humphrey, G. W., Yaguchi, S., Kiyama, T., ... & Brandhorst, B. P. (2006). A genomic view of the sea urchin nervous system. *Developmental Biology*, *300*(1), 434-460.

Burns, G., Thorndyke, M. C., Peck, L. S., & Clark, M. S. (2013). Transcriptome pyrosequencing of the Antarctic brittle star Ophionotus victoriae. *Marine Genomics*, *9*, 9-15.

Byrne, M., Koop, D., Cisternas, P., Strbenac, D., Yang, J. Y. H., & Wray, G. A. (2015). Transcriptomic analysis of Nodal-and BMP-associated genes during juvenile development of the sea urchin Heliocidaris erythrogramma. *Marine genomics*, *24*, 41-45.

Cannon, J. T., Kocot, K. M., Waits, D. S., Weese, D. A., Swalla, B. J., Santos, S. R., & Halanych, K. M. (2014). Phylogenomic resolution of the hemichordate and echinoderm clade. *Current Biology*, *24*(23), 2827-2832.

Cannon, J. T., Kocot, K. M., Waits, D. S., Weese, D. A., Swalla, B. J., Santos, S. R., & Halanych, K. M. (2014). Phylogenomic resolution of the hemichordate and echinoderm clade. *Current Biology*, *24*(23), 2827-2832. CAMBIAR AÑO DE 2015 A 2014 EN Pág.78

Chen, S. H., Li, K. L., Lu, I. H., Wang, Y. B., Tung, C. H., Ting, H. C., ... & Yu, J. K. (2014). Sequencing and analysis of the transcriptome of the acorn worm Ptychodera flava, an indirect developing hemichordate. *Marine genomics*, *15*, 35-43.

D'Aniello, S., Delroisse, J., Valero-Gracia, A., Lowe, E. K., Byrne, M., Cannon, J. T., ... & Lowe, C. J. (2015). Opsin evolution in the Ambulacraria. *Marine Genomics*, *24*, 177-183.

Delroisse, J., Lanterbecq, D., Eeckhaut, I., Mallefet, J., & Flammang, P. (2013). Opsin detection in the sea urchin Paracentrotus lividus and the sea star Asterias rubens. *Cahiers de Biologie Marine*, *54*, 721-727.

Delroisse, J., Ullrich-Lüter, E., Ortega-Martinez, O., Dupont, S., Arnone, M. I., Mallefet, J., & Flammang, P. (2014). High opsin diversity in a non-visual infaunal brittle star. *BMC Genomics*, *15*(1), 1035.

Delroisse, J., Ortega-Martinez, O., Dupont, S., Mallefet, J., & Flammang, P. (2015). De novo transcriptome of the European brittle star Amphiura filiformis pluteus larvae. *Marine genomics*, *23*, 109-121.

Delroisse, J., Mallefet, J., & Flammang, P. (2016). De novo adult transcriptomes of two European brittle stars: Spotlight on opsin-based photoreception. *PloS One*, *11*(4), e0152988.

Du, H., Bao, Z., Hou, R., Wang, S., Su, H., Yan, J., ... & Hu, X. (2012). Transcriptome sequencing and characterization for the sea cucumber Apostichopus japonicus (Selenka, 1867). *PloS One*, *7*(3), e33311.

Edgar, R. C. (2004). MUSCLE: multiple sequence alignment with high accuracy and high throughput. *Nucleic Acids Research*, *32*(5), 1792-1797.

Elphick, M. R., Semmens, D. C., Blowes, L. M., Levine, J., Lowe, C. J., Arnone, M. I., & Clark, M. S. (2015). Reconstructing SALMFamide neuropeptide precursor evolution in the phylum Echinodermata: ophiuroid and crinoid sequence data provide new insights. *Frontiers in Endocrinology*, *6*, 2.

Feuda, R., Hamilton, S. C., McInerney, J. O., & Pisani, D. (2012). Metazoan opsin evolution reveals a simple route to animal vision. *Proceedings of the National Academy of Sciences*, *109*(46), 18868-18872.

Feuda, R., Rota-Stabelli, O., Oakley, T. H., & Pisani, D. (2014). The comb jelly opsins and the origins of animal phototransduction. *Genome Biology and Evolution*, *6*(8), 1964-1971.

Freeman Jr, R. M., Wu, M., Cordonnier-Pratt, M. M., Pratt, L. H., Gruber, C. E., Smith, M., ... & Kirschner, M. (2008). cDNA sequences for transcription factors and signaling proteins of the hemichordate Saccoglossus kowalevskii: efficacy of the expressed sequence tag (EST) approach for evolutionary and developmental studies of a new organism. *The Biological Bulletin*, *214*(3), 284-302.

Galtier, N., Gouy, M., & Gautier, C. (1996). SEAVIEW and PHYLO_WIN: Two graphic tools for sequence alignment and molecular phylogeny. *Computer Applications in the Biosciences*, *12*(6), 543-548.

Garm, A., & Nilsson, D. E. (2014). Visual navigation in starfish: first evidence for the use of vision and eyes in starfish. *Proceedings of the Royal Society B,* 281(1777), 20133011.

Gouy, M., Guindon, S., & Gascuel, O. (2009). SeaView version 4: A multiplatform graphical user interface for sequence alignment and phylogenetic tree building. *Molecular Biology and Evolution*, *27*(2), 221-224.

Guindon, S., & Gascuel, O. (2003). A simple, fast, and accurate algorithm to estimate large phylogenies by maximum likelihood. *Systematic Biology*, *52*(5), 696-704.

Hargrave, P. A., McDowell, J. H., Curtis, D. R., Wang, J. K., Juszczak, E., Fong, S. L., ... & Argos, P. (1983). The structure of bovine rhodopsin. *Biophysics of Structure and Mechanism*, *9*(4), 235-244.

Hennebert, E., Leroy, B., Wattiez, R., & Ladurner, P. (2015). An integrated transcriptomic and proteomic analysis of sea star epidermal secretions identifies proteins involved in defense and adhesion. *Journal of proteomics*, *128*, 83-91.

Holland, L. Z., Albalat, R., Azumi, K., Benito-Gutiérrez, È., Blow, M. J., Bronner-Fraser, M., ... & Ferrier, D. E. (2008). The amphioxus genome illuminates vertebrate origins and cephalochordate biology. *Genome Research*, *18*(7), 1100-1111.

Kumar, S., Nei, M., Dudley, J., & Tamura, K. (2008). MEGA: a biologist-centric software for evolutionary analysis of DNA and protein sequences. *Briefings in Bioinformatics*, *9*(4), 299-306.

Lamb, T. D., Collin, S. P., & Pugh, E. N. (2007). Evolution of the vertebrate eye: Opsins, photoreceptors, retina and eye cup. *Nature Reviews Neuroscience*, *8*(12), 960-976.

Lesser, M. P., Carleton, K. L., Böttger, S. A., Barry, T. M., & Walker, C. W. (2011). Sea urchin tube feet are photosensory organs that express a rhabdomeric-like opsin and PAX6. *Proceedings of the Royal Society of London B: Biological Sciences*, *278*(1723), 3371-3379.

Millott, N. (1975). The photosensitivity of echinoids. *Advances in Marine Biology*, 13, 1-52.

Mashanov, V. S., Zueva, O. R., & García-Arrarás, J. E. (2014). Transcriptomic changes during regeneration of the central nervous system in an echinoderm. *BMC genomics*, *15*(1), 357. sobra

Ooka, S., Katow, T., Yaguchi, S., Yaguchi, J., & Katow, H. (2010). Spatiotemporal expression pattern of an encephalopsin orthologue of the sea urchin Hemicentrotus pulcherrimus during early development, and its potential role in larval vertical migration. *Development, Growth & Differentiation*, *52*(2), 195-207.

Palczewski, K., Kumasaka, T., Hori, T., Behnke, C. A., Motoshima, H., Fox, B. A., ... & Yamamoto, M. (2000). Crystal structure of rhodopsin: AG protein-coupled receptor. *Science*, *289*(5480), 739-745.

Porter, M. L., Blasic, J. R., Bok, M. J., Cameron, E. G., Pringle, T., Cronin, T. W., & Robinson, P. R. (2011). Shedding new light on opsin evolution. *Proceedings of the Royal Society B: Biological Sciences, 279(1726), 3-14*.

Raible, F., Tessmar-Raible, K., Arboleda, E., Kaller, T., Bork, P., Arendt, D., & Arnone, M. I. (2006). Opsins and clusters of sensory G-protein-coupled receptors in the sea urchin genome. *Developmental Biology*, *300*(1), 461-475.

Ramirez, M. D., Pairett, A. N., Pankey, M. S., Serb, J. M., Speiser, D. I., Swafford, A. J., & Oakley, T. H. (2016). The last common ancestor of bilaterian animals possessed at least 7 opsins. *bioRxiv*, 052902.

Semmens, D. C., Mirabeau, O., Moghul, I., Pancholi, M. R., Wurm, Y., & Elphick, M. R. (2016). Transcriptomic identification of starfish neuropeptide precursors yields new insights into neuropeptide evolution. *Open Biology*, *6*(2), 150224.

Semmens, D. C., Beets, I., Rowe, M. L., Blowes, L. M., Oliveri, P., & Elphick, M. R. (2015). Discovery of sea urchin NGFFFamide receptor unites a bilaterian neuropeptide family. *Open biology*, *5*(4), 150030.

Shichida, Y., & Matsuyama, T. (2009). Evolution of opsins and phototransduction. *Philosophical Transactions of the Royal Society B: Biological Sciences*, *364*(1531), 2881-2895.

Sigl, R., Steibl, S., & Laforsch, C. (2016). The role of vision for navigation in the crown-of-thorns seastar, Acanthaster planci. *Scientific reports*, *6*, 30834.

Sodergren, E., Weinstock, G. M., Davidson, E. H., Cameron, R.A., Gibbs, R. A., Angerer,R. C., … & Coffrman, J. A. (2006). The genome of the sea urchin Strongylocentrotus purpuratus. *Science, 314*(5801), 941-952.

Tamura, K., Dudley, J., Nei, M., & Kumar, S. (2007). MEGA4: molecular evolutionary genetics analysis (MEGA) software version 4.0. *Molecular Biology and Evolution*, *24*(8), 1596-1599.

Terakita, A. (2005). The opsins. *Genome Biology*, *6*(3), 213.

Ullrich-Lüter, E. M., Dupont, S., Arboleda, E., Hausen, H., & Arnone, M. I. (2011). Unique system of photoreceptors in sea urchin tube feet. *Proceedings of the National Academy of Sciences*, *108*(20), 8367-8372.

Ullrich-Lüter, E. M., D'Aniello, S., & Arnone, M. I. (2013). C-opsin expressing photoreceptors in echinoderms. *Integrative and Comparative Biology*, *53*(1), 27-38.

Vaughn, R., Garnhart, N., Garey, J. R., Thomas, W. K., & Livingston, B. T. (2012). Sequencing and analysis of the gastrula transcriptome of the brittle star Ophiocoma wendtii. *EvoDevo*, *3*(1), 19.

Whelan, S., Goldman, N. (2001). A general empirical model of protein evolution derived from multiple protein families using a maximum-likelihood approach. *Molecular Biology and Evolution, 18(5), 691-699.*

Wygoda, J. A., Yang, Y., Byrne, M., & Wray, G. A. (2014). Transcriptomic analysis of the highly derived radial body plan of a sea urchin. *Genome biology and evolution*, *6*(4), 964-973.

Zhao, C., Ji, N., Tian, X., Feng, W., Sun, P., Wei, J., & Chang, Y. (2015). Opsin4, Opsin5, and Pax6 significantly increase their expression in recently settled juveniles of the sea urchin Strongylocentrotus intermedius (Echinodermata: Echinoidea). *Invertebrate Reproduction & Development*, *59*(3), 119-123.

Zhou, Z. C., Dong, Y., Sun, H. J., Yang, A. F., Chen, Z., Gao, S., ... & Wang, B. (2014). Transcriptome sequencing of sea cucumber (Apostichopus japonicus) and the identification of gene-associated markers. *Molecular Ecology Resources*, *14*(1), 127-138.

2. NON-DIRECTIONAL PHOTORECEPTORS IN THE PLUTEUS OF *STRONGYLOCENTROTUS PURPURATUS*

2. NON-DIRECTIONAL PHOTORECEPTORS IN THE PLUTEUS OF *STRONGYLOCENTROTUS PURPURATUS*

2.1 Abstract

In comparison to complex visual systems, non-directional photoreception (the most primitive form of biological photodetection) has been poorly investigated, although it is essential to many biological processes such as circadian and seasonal rhythms. Here we describe the spatiotemporal expression pattern of the major molecular actors mediating light reception, opsins, localized in the *Strongylocentrotus purpuratus* larva. In contrast to other zooplanktonic larvae, the echinopluteus lacks photoreceptor cells with observable shading pigments involved in directional visual tasks. Nonetheless, the echinopluteus expresses two distinct classes of opsins: a Go-opsin and a rhabdomeric opsin. The Go-opsin, *Sp-opsin3.2,* is detectable at early (three days' post fertilization) and four armed pluteus stages (four days' post fertilization) in two cells that flank the apical organ. To rule out the presence of shading pigments involved in directional photoreception, we used electron microscopy to explore the expression domain of Go-opsin *Sp-opsin3.2* positive cells. The rhabdomeric opsin Sp-opsin4 expression is detectable in clusters of cells located around the primary podia at the five-fold ectoderm pentagonal disc stage (day 18-21) and thereafter, thus indicating that Sp-opsin4 may not be involved in the photoreception mechanism of the larva, but only of the juvenile. We discuss the putative function of the relevant cells in their neural context, and propose a model for understanding simple photodetection in marine larvae.

2.2 Introduction

While the vast majority of studies on animal photoreception have so far focused on directional photoreceptors, systems comprising at least one cell with a photosensitive opsin together with shading pigments that enable it to discriminate the directionality of light, less is known about non-directional photoreception, the simplest and earliest evolving type of photoreception. Non-directional photoreceptors, which can be difficult to detect due to a lack of visible screening pigments, allow the monitoring of absolute light intensities of the environment. Consequently, they are widely used as an input to the circadian clock system and for a wide variety of other tasks (Turner and Mainster, 2008). For instance, non-directional photoreceptors can be used as a depth gauge, as a warning for harmful levels of UV radiation, for shadow detection, or be involved in the regulation of feeding, movement and reproduction rhythms (Bennett, 1979; Paul and Gwynn-Jones, 2003; Leech et al., 2005; Nilsson, 2009; 2013).

Opsins are G-protein coupled receptors involved in light-perception. Based on their amino acid sequence they can be divided into four groups: tetraopsin, xenopsin, Gq-opsin, and c-opsin (Ramirez et al., 2016; for other classifications see: Palczewski et al., 2007; Arendt, 2008; Koyanagi et al., 2008; Porter et al., 2011; Feuda et al., 2012). The presence of opsins provides a clear landmark for localizing putative photoreceptor cells even in the absence of shading pigments and, therefore, the localization of opsin-expressing cells is important for finding directional and non-directional photoreceptors.

In echinoderms, efforts to describe photoreceptors have primarily focused on adult specimens. The phototactic behaviour commonly observed in adult sea urchins, in addition to their photosensitive ectoderm associated with an endoskeleton (which could act as shading structure, lens or filter) make them a useful model for studying diffuse photoreception (Raup, 1966; Hendler and Byrne, 1987;

Johnsen, 1997; Johnsen and Kier, 1999; Aizenberg et al., 2001). Before the advent of molecular genetics, studies of photoreception in echinoids concentrated on cell morphology and physiology, as well as understanding behavioural responses such as spine movements, tube foot reaction, covering, colour change and, more recently, visual navigation (Holmes, 1912; Millot, 1953; 1954; 1976; Millot and Manly, 1961; Millot and Yoshida, 1958; Thornton, 1956; Yoshida, 1966; Yoshida et al., 1984; Johnsen, 1994; Blevins and Johnsen, 2004; Yeramilli and Johnsen, 2010). Later, the publication of the sea urchin *Strongylocentrotus purpuratus* genome lead to the discovery of nine opsins, a number of transcription factors involved in photoreceptor cell differentiation (e.g. *irx5*, *irx6*, *dlx1/dlx2*, *rx*, *ath*; see Table 4 for further details) and several orthologous genes putatively involved in the phototransduction cascade (e.g. visual G-beta subunit, rhodopsin kinase, arrestin, retinal-binding protein, G-alpha-s subunit, transducin G-gamma-t1, recoverin, G-alpha-q subunit; see Table 5 for further details) in this species (Sodergren et al., 2006; D'Aniello et al., 2015). This information has made it possible to use molecular tools to investigate photoreception in echinoids (Burke et al., 2006; Raible et al., 2006).

The first biochemical efforts to investigate the mechanisms of photoreception in *S. purpuratus* have resulted in the localization of the rhabdomeric opsin Sp-opsin4 in basal (i.e. in the stalk area proximal to the compound plates) and disk (i.e. in the tube feet most apical part) microvillar cells of the adult tube feet (Ullrich-Lüter et al., 2011). Furthermore, a ciliary opsin, Sp-opsin1 has been immunodetected in cells located in locomotory and buccal tube feet, as well as in the proximal stalk region of tridentate pedicellaria (Ullrich-Lüter et al., 2013), the latter being jawed appendages used against parasites (Coppard et al., 2012). These findings have allowed Ullrich-Lüter and co-authors to describe a unique system of photoreception in which the entire sea urchin, using its skeleton as photoreceptor screening device, functions as a 'giant eye' (Ullrich-Lüter et al., 2011). This is also in agreement with previous

observations on the photo-behaviour of a *Diadema* species that lead to the suggestion that the shadow produced by the spines on the animal body surface is used for inferring the visual landscape (Woodley, 1982). However, in comparison with the light detection systems of adult echinoids, the photoreception mechanisms of their planktonic larvae have been so far poorly investigated.

While ancestral adult metazoans were likely benthic, it is probable that a pelagic larval stage evolved very early in animal evolution (Jägersten, 1972; Nielsen, 2008). This idea has led many scientists to investigate the directional simple eyespots of marine larvae in search of something resembling a 'proto-eye' (Smith, 1935; Thorson, 1964; Brandenburger et al., 1973; Marsden, 1984; Pires and Woollacott, 1997; Leys and Degnan, 2001; Nordström et al., 2003; Jékely et al., 2008; Gühmann et al., 2015). Such simple eyespots or ocelli constitute class II photoreceptors (photoreceptor cells associated with shading pigments) in accordance with the classification of Nilsson (2013). To our knowledge, only few cases of non-directional (class I) photoreceptors have been documented in marine zooplanktonic larvae (Arendt et al., 2004; Passamaneck et al., 2011; Vöcking et al., 2015). In these cases, and in contrast to what we can observe in the echinopluteus, the larvae studied possess eyespots, thus making it more difficult to study class I photoreception in an independent way.

To better elucidate the origins of animal vision, an event that most probably happened in the Precambrian marine environment, the study of larvae with class I photoreception is essential. In this work we identify a Go based photoreceptor system in a zooplanktonic larva of the deuterostome lineage that potentially lacks directional photoreceptors. To localize the putative photoreceptor cells of the larva at early and late developmental stages, we analysed the expression of the opsins *Sp-opsin3.2* (Go) and Sp-opsin4 (rhabdomeric) using whole mount in situ hybridization and immunohistochemistry, respectively. Further, the presence of shading pigments near the encountered Go-opsin based photoreceptor cells was ruled out by

exploring both the apical organ as well as the basal area of the anterolateral arms by using a transmission electron microscopy (TEM) approach. The putative role of these photoreceptor cells in non-directional photoreception of the pluteus is discussed.

2.3 Results

2.3.1 The Go opsin *Sp-opsin3.2* is detected in two cells that flank the apical organ

To characterize the presence of putative photoreceptor cells in the sea urchin larva we first consulted the transcriptomic expression of *S. purpuratus* opsins. After analysing the publicly available RNAseq data coming from a survey of ten embryonic stages (Tu et al., 2014) we concluded that, of the nine genes encoding opsins found in the genome, the Go opsin *Sp-opsin3.2* (SPU027633) and the echinopsin *Sp-opsin2* (SPU003451) are the only opsin genes expressed at significant levels. Starting from the late gastrula stage (48 hours post fertilization), these two genes show expression levels reaching the value of about 100 transcripts per embryo at the early pluteus stage (72 hours post fertilization), when neurons start to differentiate (for gene expression profiling, see Fig. 22). Next, successful amplification of the Go opsin *Sp-opsin3.2* was carried out, and the corresponding antisense riboprobe was used to localize the cells of interest. Unfortunately, various attempts in the amplification with different set of primers of the 'echinopsin' *Sp-opsin2* did not give any result.

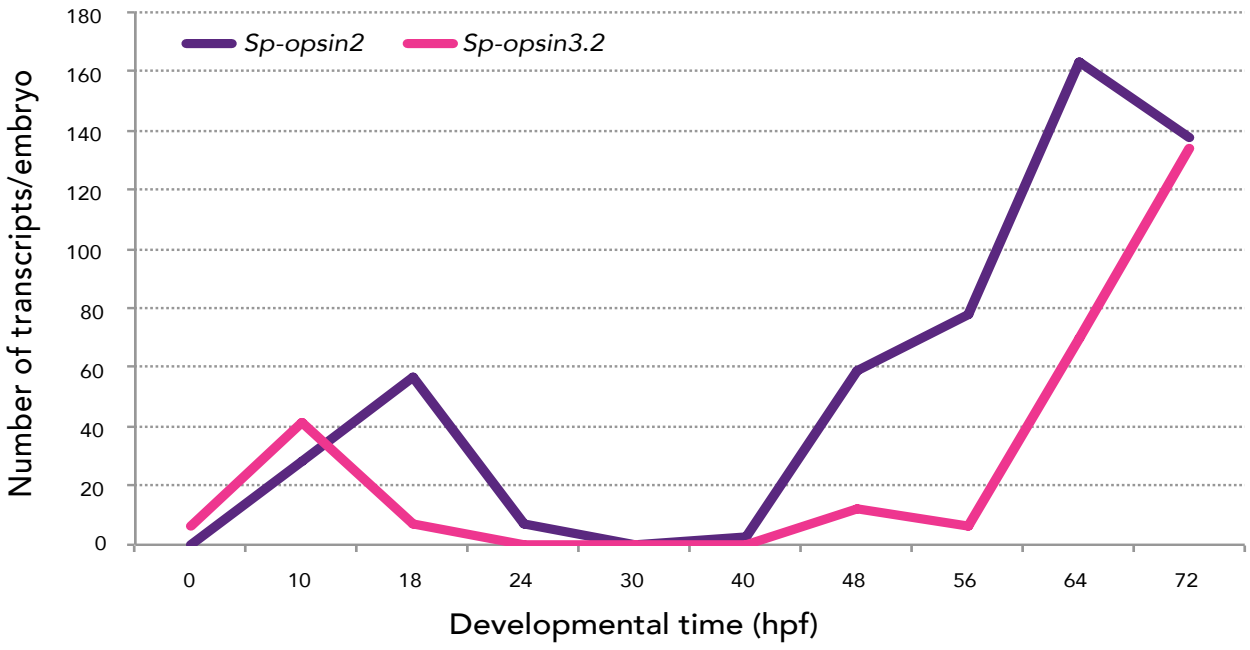

Fig 22. Gene expression profile of *Sp-opsins 2* (purple) and *3.2* (magenta). During the first 72 hours of development, two maximum peaks of *Sp-opsin2* expression are found: one at 64 hours (163 transcripts per individual) and another one at 18 hours post fertilization (58 transcripts per individual). During the same time lapse, maximum peaks of *Sp-opsin 3.2* expression are found at 72 hours (139 transcripts per individual) and at 10 hours (42 transcripts per individual). Please, note that these numbers represent an overall estimation. Data from Tu et al. (2014) (echinobase.org:3838/quantdev).

Here, RNA fluorescence (Fig. 23; 3 days post fertilization: dpf larvae, early four armed larvae) whole mount in situ hybridization (WMISH) revealed that the Go opsin *Sp-opsin3.2* is expressed in two cells arranged bilaterally adjacent the apical organ, i.e. a portion of the epithelium that form the oral hood that is considered to act as central nervous system of the larva (Byrne et al., 2007), and at the base of the left and right anterolateral arms (for a schematic view of the four-armed pluteus in which we included the terminology used in this work, see Fig. 24).

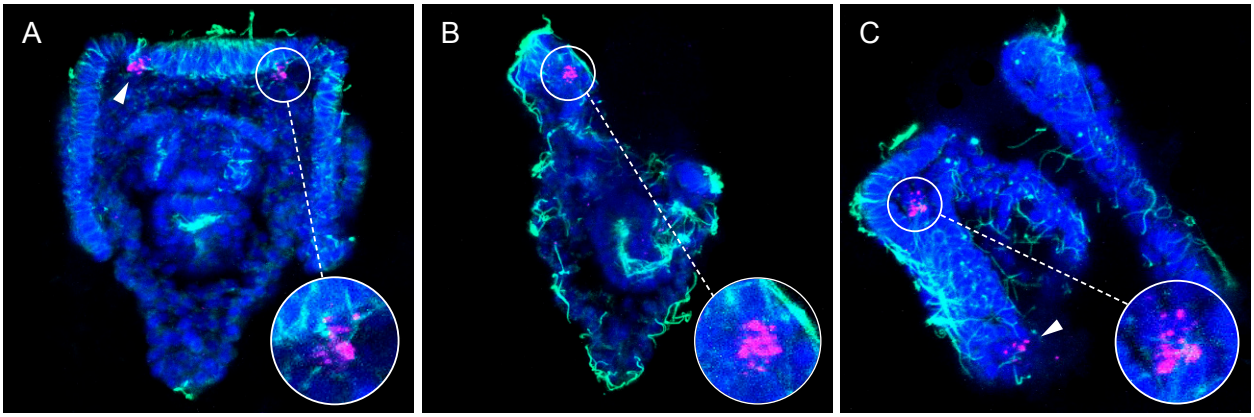

Fig 23. Expression of the Go-opsin *Sp-opsin3.2* in early plutei. A couple of *Sp-opsin3.2* bilateral symmetrical cells were detected at cellular resolution between the base of the anterolateral arms and the apical organ of echinopluteus (3dpf) by means of fluorescent *in situ* hybridization. A-C) Confocal-micrographs; *Sp-opsin3.2 in situ* hybridization (magenta) was coupled with acetylated α-tubulin immunohistochemistry (green); nuclei were counterstained with DAPI (blue). A) Abanal view; B) right-lateral view; C) mouth view. Arrowheads indicate *Sp-opsin3.2* positive cells.

The expression of this gene in such a small number of cells is consistent with the above mentioned low levels of expression observed from the transcriptomic data. To identify the position of these *Sp-opsin3.2* positive cells with respect to the ciliary band (the distinct thickening of ciliated epidermis that outlines the oral field and traces the edges of the four

larval arms), cilia were labelled by immunohistochemistry with anti-acetylated α-tubulin after *Sp-opsin3.2* WMISH.

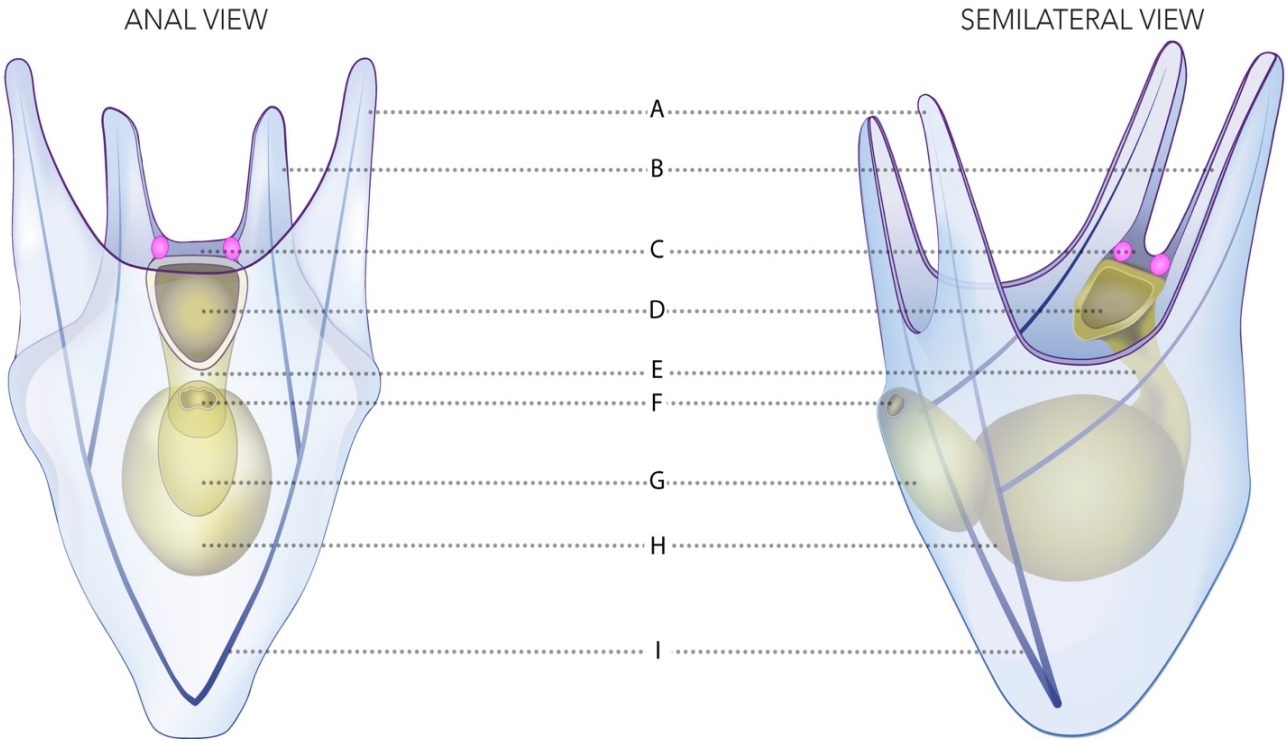

Fig 24. Drawing of the four armed pluteus of *S. purpuratus*; the Go *Sp-opsin3.2* opsin positive cells are represented in pink. A) Post oral arms. B) Anterolateral arms. C) Apical organ. D) Mouth. E) Oesophagus. F) Anus. G) Intestine. H) Stomach. I) Skeletal rods. Illustration made by Santiago Valero-Medranda.

As shown by fluorescence in situ hybridization (Fig. 23), the main body of these cells appear to be located just orally to the thick epidermal band of the ciliated cells (see Fig. 24 for schematic representation). The *Sp-opsin3.2* positive cells are suggestive of the presence of a photoreception system in the sea urchin larvae.

2.3.2 TEM analysis reveals absence of shading pigments in the larva apical region

A key difference between visual and non-visual photoreception system is the presence of shading structures, generally in the form of pigment cells, in proximity of light perceiving

cells. Therefore, *S. purpuratus* larvae were observed under the light microscope at 4, 6 and 8 armed stages to detect for the presence of observable pigments that can be organized to act as shading for the described *Sp-opsin3.2* positive cells. The only pigmented cells found near these cells were the granulated pigment cells, a population of red coloured cells of dendritic morphology and immune role that are distributed all over the body (Ho et al., 2016). We therefore decided to explore the presence of screening pigments in the vicinities of the Go *Sp-opsin3.2* opsin-positive cells by means of TEM.

Shading pigments involved in directional photoreception, which can be located both in the opsin positive cells or adjacently, are easily recognized in TEM as a group of black-solid dots in the cytoplasm (e.g. Marshall and Hodgson, 1990; Leys and Degnan, 2001). For our TEM analysis, three larvae were fixed, and transversal sections of 50 to 70 nm were made in the apical region in search of shading pigments (Fig. 25A). Of them, micrographs corresponding to different sections of the apical organ (Fig. 25D, E) and the bases of the left (Fig. 25B, C) and right (Fig. 25F, G) anterolateral arms were selected. Interestingly, none of the cells embedded in the apical organ nor in the area of the ciliary band exhibited observable shading pigments.

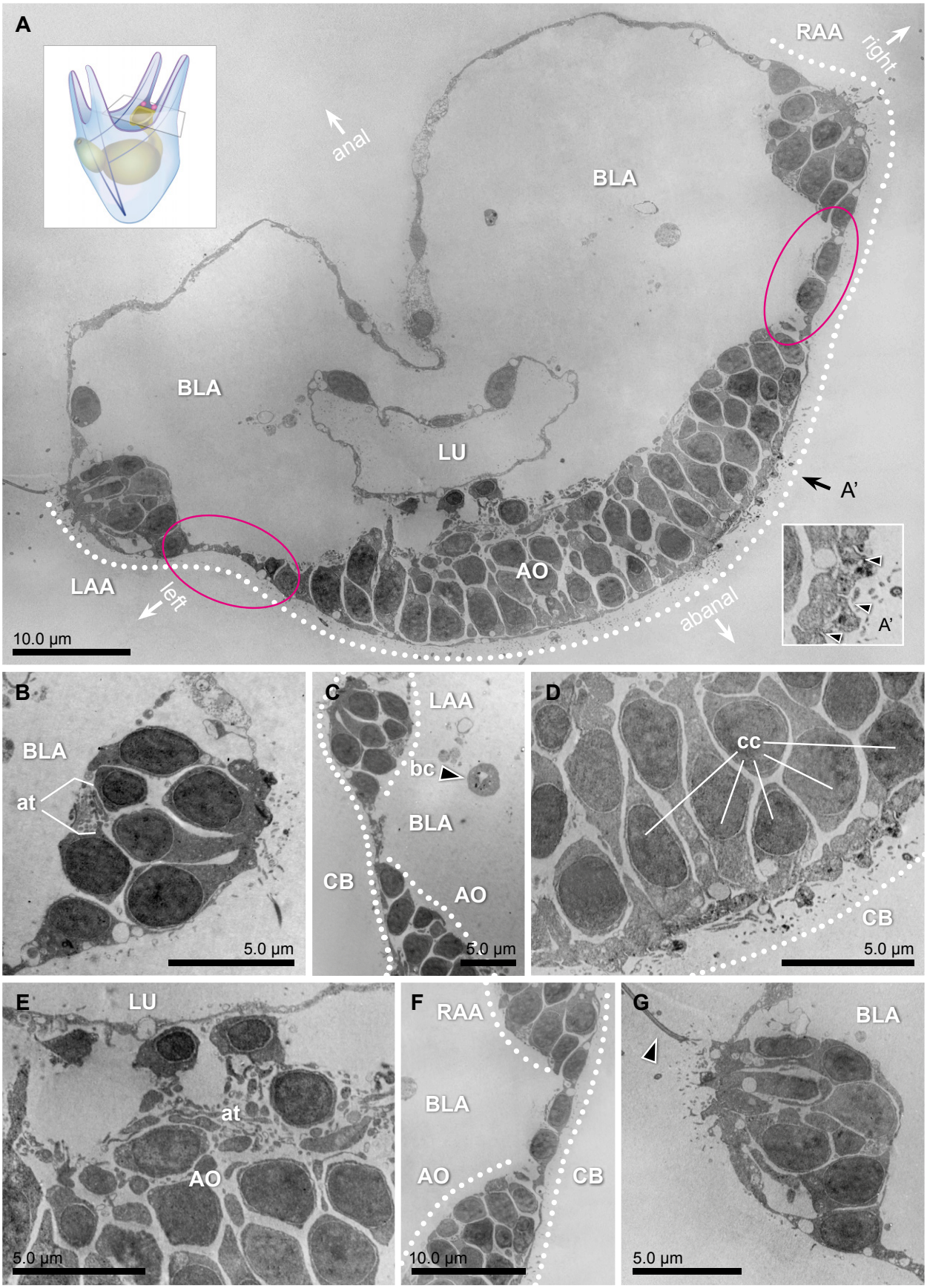
A
RAA
right
anal
BLA
BLA
LU
A'
AO
LAA
left
abanal
10.0 µm
A'
B
BLA
at
5.0 µm
C
LAA
bc
BLA
CB
AO
5.0 µm
D
cc
CB
5.0 µm
E
LU
at
AO
5.0 µm
F
RAA
BLA
AO
CB
10.0 µm
G
BLA
5.0 µm

Fig 25. Transmission electron micrographs of a 3dpf (early 4 armed) pluteus, different sections of three specimens at the level of the apical region. A) Collage of 324 transversal micrographs showing a panoramic view of the abanal half of the larvae (apical region). On it, the bases of the left and right anterolateral arms (LAA and RAA, respectively), as well as the lumen (LU) of the gut, surrounded by the blastocoel (BLA), and the apical organ (AO) are shown. The stippled line corresponds to the ectodermal region in which the ciliary band is located. A representation of the whole 4 armed pluteus larva and cutting area can be seen in the upper left corner. A') Detail of the cross-sectional profile of the motile cilia (arrows) that compose the ciliary band. The orientation of the animal is defined by the axes: anal, abanal, left and right. B) Transversal section of the base of the anterolateral arm, right side. On it, the axon tract (at) that connects this area with the nervous system can be distinguished. C) Transversal section of the region that connects the right anterolateral arm (LAA) with the apical organ (AO). Pigmented cells cannot be detected in any of the cells flanking the apical organ, where the Go-opsin *Sp-opsin3.2* was detected. The black arrowed points to a blastocoelar cell (bc). D, E) Detail micrographs of the apical organ, an area considered as the central system of the animal, rich on ciliated cells (cc) and axon tracts (at). F) Transversal section of the region that connects the left anterolateral arm (RAA), with the apical organ (AO). G) Transversal section of the base of the anterolateral arm, left side. Illustration made by Santiago Valero-Medranda.

The regions of the ectoderm in between the apical organ and either left or right anterolateral arms (encircled in Fig. 25A; Fig. 25C, F) where the *Sp-opsin3.2* positive cells are located (see also schematics of Fig. 24) are void of shading pigment granules. These findings suggest that the *Sp-opsin3.2* positive cells are not involved in directional photoreception. Although it would be interesting to have higher magnification images of the discovered opsin-positive cells, the current state of the art 'does not allow to distinguish between the different sensory cell types located in the ciliary band or in the apical organ of the sea urchin larva' (Thurston Lacalli, University of Saskatchewan, Canada; and Robert Burke, University of Victoria, Canada, personal communication). Thus, serial multiplex immunogold labelling experiments are needed to better characterize the morphology of the encountered *Sp-opsin3.2* positive cells.

2.3.3 Sp-opsin4, the rhabdomeric opsin, was detected in the adult rudiment at pentagonal disc stages and thereafter

Due to limitations of WMISH efficiency on late developmental stages and the availability of a specific antibody against the sea urchin rhabdomeric opsin Sp-opsin4, we decided to use an

immunohistochemical approach to explore the opsin toolkit of the premetamorphic larva. During late larval development (second week of development and thereafter), a portion of the coelom and the overlying ectoderm gets in contact and forms the imaginal adult rudiment (Smith et al., 2008; Heyland and Hodin, 2014; for a schematic view see drawings in Fig. 26). This rudiment represents the developing juvenile that grows from the left side of the larva (for a schematic, see Fig. 26A). In order to analyse the spatiotemporal expression of the rhabdomeric opsin Sp-opsin4, we tested its presence in time series of 3, 4, 5, 6 and 7 days (four armed pluteus), 16d (six armed pluteus, contact flattened stage), 17d (six armed pluteus, five-fold mesoderm stage), 18d (eight armed pluteus, five-fold ectoderm stage), 19d (eight armed pluteus, primary podia stage), 21d (eight armed pluteus, primary podia-folded stage), and 23d (eight armed pluteus, primary podia-touching stage) post fertilization (for staging of the echinopluteus see also Smith et al., 2008; Heyland and Hodin, 2014). These experiments suggested the absence of expression of the rhabdomeric opsin Sp-opsin4 prior to the tube feet formation in any part of the larva. No protein expression was found either in sensu stricto larval structures until the five-fold mesoderm stages (17dpf; Figs. 26B, B') with our method. Larvae started to exhibit Sp-opsin4 positivity in conspicuous clusters of cells on the vestibular floor at pentagonal disc stage that would give rise to the tube feet disc during five-fold ectoderm stage, a stage in which the ectoderm and the primordia of the five podia begin to push through the floor of the vestibular ectoderm (day 18; Figs. 26C, C'). At this point, the interior of the five incipient podia are spherical in shape or shorter than wide. We also detected Sp-opsin4 positive cells later on, in the tube feet disc during advanced rudiment stage, when the primary podia are taller than they are wide, but the podia are not yet folding in towards one another (day 20-21; Figs. 26D and D'). At tube-foot protrusion stage (day 21-45), Sp-opsin4 positive cells were detected both in disc (Fig. 26E) and basal (Fig. 26F) photoreceptors of the tube feet. These data indicate that the rhabdomeric opsin Sp-opsin4 may not regulate the photoreception mechanism of the larva, but only of the juvenile, where it appears to be involved in negative phototaxis (Ullrich-Lüter et al., 2011). For a schematic view on the different rudimental stages, see Figs. 26B'- F'.

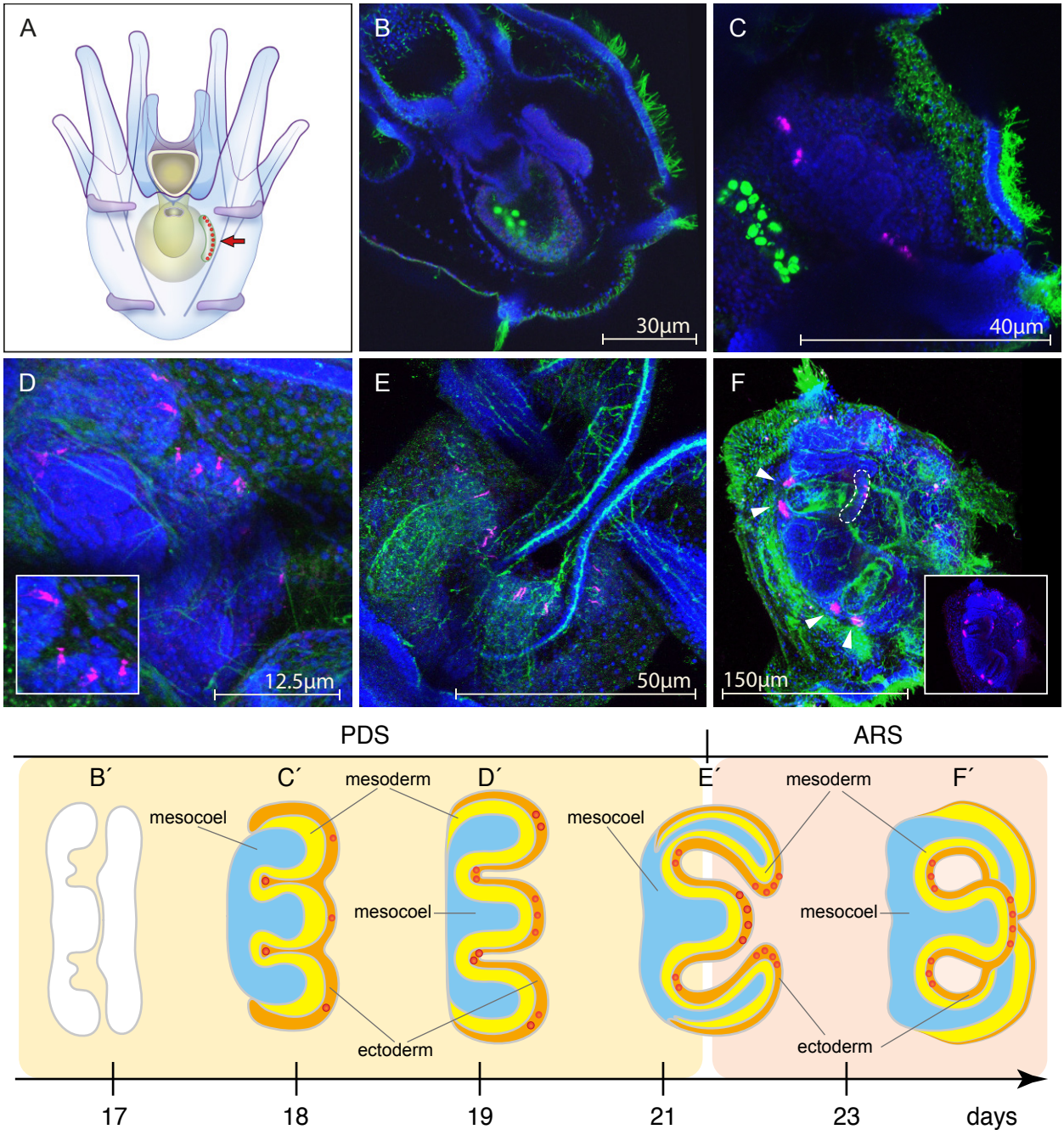

Fig 26. Localisation of the rhabdomeric opsin Sp-opsin4 in the developing tube feet of the juvenile. A) Schematic of the 8 armed pluteus stage, anal view, in which the area of growing of the rudiment (arrow) is shown. B, B') Sp-opsin4 was not detected in adult plate at fivefold ectoderm stage (day 17; pentagonal disc stage, PDS). C, C') During the five folding of the ectoderm (day 18, PDS), the rudiment of the larva starts to exhibit Sp-opsin4 positivity in clusters of conspicuous cells at the developing basal tube feet. D, D') At primary podia stage (day 19, PDS), the developing disc tube feet of the vestibular floor are positive for Sp-opsin4. E, E') Sp-opsin4 photoreceptor cells are visible in the tube feet disc of the folded primary podia (day 21; transition between the PDS and the advanced rudiment stage, ARS), both in disc and basal photoreceptor cells of the tube feet. F, F') Sp-opsin4 positive cells were detected at tube-foot protrusion stage (day 23-45, ARS). Stages redrawn from Heyland and Hodin, 2014. Colouring of figures C' to F' was done following guidelines given by Prof. Claus Nielsen. PDS

and ARS stages are named following the nomenclature proposed by Smith *et al.*, 2008. Confocal micrographs colour code: Sp-opsin4 in magenta; acetylated α-tubulin (B-E) and 1E11 (F) in green; DAPI in blue. The bright green staining in the stomach of the larvae shown in A and B is due to autofluorescence of the ingested microalgae. Illustrations made by Santiago Valero-Medranda.

2.4 Discussion

Our findings show that, at least, two opsin classes are expressed in *Strongylocentrotus purpuratus* prior to metamorphosis: first the Go opsin *Sp-opsin3.2* in the apical region of the larva at 3 and 4 dpf (four armed pluteus), and then the rhabdomeric opsin Sp-opsin4 in the tube feet of the developing juvenile (day 29 and thereafter, eight armed pluteus). The different opsin classes in the sea urchin may serve different needs to integrate light information depending on the life stage, where the pelagic larva and the benthic adult face very different challenges.

Of the opsin-positive cells encountered, just the two *Sp-opsin3.2* positive-cells localized in the flanks of the apical organ can be considered part of the sensu stricto larval tissues. In our study, no rhabdomeric opsins have been found in larval structures. Because the aim of this study is to improve our understanding of photoreception in marine larvae, the rhabdomeric opsin Sp-opsin4, which is expressed in juvenile tissues, will not be further discussed (for an account on the possible role of Sp-opsin4 in adult sea urchins, see Ullrich-Lüter et al., 2011).

2.4.1 Ancientness of Go-opsins

Phylogenetic analyses indicate the presence of at least seven opsins in the last common ancestor of Bilateria (Ramirez et al., 2016), thus suggesting that light reception had many roles very early in animal evolution. These opsins, together with present-day animal opsins, have been classified into four groups: (i) tetraopsins (Go-opsins, RGR/retinochrome opsins and neuropsins), (ii) xenopsins, (iii) Gq-opsins (including canonical and non-canonical r-opsins as well as 'chaopsins'), and (iv)

c-opsins, i.e. canonical c-opsins and bathyopsins (Ramirez et al., 2016). While the canonical c- and r-opsin groups have been extensively studied, little is known about the Go opsin group included in the tetraopsin clade (Gühmann et al., 2015).

In support of the ancient origin of Go opsins, cells expressing this class of opsins have been localised in diverse animal clades, thereby suggesting the presence of this opsin group before the protostome-deuterostome split. Examples of Go-opsins are found in the ciliary cells of the eyes of the adult scallop *Patinopecten yesooensis* (Kojima et al., 1997), in the gastrula of the brachiopod *Terebratalia transversa* (Passamaneck and Martindale, 2013), in the rhabdomeric adult eye of the polychaete *Platynereis dumerilii* (Gühmann et al., 2015) as well as in the photoreceptor system here described. In the amphioxus *Branchiostoma belcheri,* a Go-opsin has been demonstrated by an in vitro analysis (Koyanagi et al., 2002) but, to our best knowledge, this is the first report in which the spatial expression of a Go-opsin has been described in a deuterostome larva.

2.4.2 Non-directional photoreceptors

In marine invertebrates, the expression of opsins in non-visual photoreceptors has been documented in the apical organ of planktonic larvae of protostome and deuterostome lineages (e.g. Arendt et al., 2004; Valero-Gracia et al., 2016; and herein). A shared feature of these apical organs, regions specified by conserved developmental patterning mechanisms (Marlow et al., 2014), is the presence of multiple sensory cells connected to the nervous system, which regulate ciliary beating and the vertical position of the animal in the water column (Tosches et al., 2014). In vertebrates, a population of non-directional retinal ganglion cells (the intrinsically photosensitive photoreceptive retinal ganglion cells: ipRGCs), are critical in relaying light information to the brain to control circadian photo-entrainment, pupillary light reflex, and sleep (Provencio et al., 1998; Schimdt et al., 2011).

Our discovery of non-directional photoreceptors in the pluteus of *S. purpuratus* suggests that these cells may also have a role in controlling the vertical position of the larva in the water column, which may be used for monitoring the time of day or the depth (Nilsson, 2013). This adjustment is likely to be achieved by modulating the length and frequency of ciliary arrests, as proposed for this and other marine larvae (e.g. Wada et al., 1997; Maldonado et al., 2003; Braubach et al., 2006; Jekely et al., 2008; and herein). The use of non-directional photoreceptors in vertebrates for tasks such as the regulation of nocturnal-diurnal behaviours (Provencio et al., 1998; Schimdt et al., 2011) could represent the retention of such chronobiological role.

2.4.3 Bilateral disposition and lack of shading pigments

The absence of shading pigments in the region where the *Sp-opsin3.2* is expressed strongly suggests that these opsin-positive cells lack directional sensitivity, but whether this represents a plesiomorphic character or a secondary loss is not immediately clear. Directional photoreception for phototaxis, with shading pigment near the site of opsin expression, is believed to have evolved from non-directional photoreception where screening pigment is not needed (Nilsson 2009; 2013). Directional photoreceptors are typically bilaterally paired organs (Brandenburger et al., 1973; Arendt and Wittbrodt, 2001; Braun et al., 2015), whereas non-directional photoreceptors are often unpaired median structures (Mano and Fukada, 2007; van Gelder, 2008). Our finding of paired non-directional photoreceptors represents an interesting intermediate.

The bilateral arrangement of photoreceptor cells is typically associated with helical swimming behaviours in the pluteus and other marine invertebrate larvae (Lacalli et al., 1990; reviewed in Jékely, 2009). Bilaterally paired photoreceptors may seem redundant for non-directional photoreception, and without shading pigment they do not have the directionality required for phototaxis.

It is possible that the shading pigment associated with these opsin-positive cells might have been lost during evolution to increase transparency or to reduce energy expenditure. The lack of shading pigments may have been favoured by selection to allow a better camouflage against predators (Nilsson, 1996). Consequently, the bilateral arrangement of these opsin positive cells may be primitive, and the lack of screening pigment a consequence of an adaptive transition from a directional to a non-directional role. Alternatively, it is possible that the pluteus have retained the non-directional photoreceptors of 'Urbilateria', an ancestor that may have had both directional and non-directional photoreceptors (Arendt and Wittbrodt, 2001). The bilateral arrangement of these non-directional photoreceptors would have been the result of developmental constrains associated with the bilateral symmetry, or may be profitable for increasing the robustness and sensitivity of the photoreceptor system.

To better understand when a possible switch occurred (i.e. whether Go-opsins originally mediated a non-directional task in the dipleurula larvae of the Ambulacraria stem group, or if an association with screening pigments was lost secondarily in the Echinodermata crown group) a further comparison between the photoreceptor systems of different dipleurula-type larvae is required.

The fact that the bilaterally paired photoreceptors use a Go-opsin in the sea urchin larva, while r-opsins are present in similar structures of nearly all other larvae, results remarkable. One possible explanation to why putative homologous paired photoreceptors express distinct opsins in different Bilateria clades could be that Urbilateria had bilaterally paired photoreceptors with r-opsin, c-opsins and Go-opsins serving different functions (Feuda et al., 2012; Ramirez et al., 2016). This variety of functions can be ascribed to the need of different spectral or temporal properties, as well as to different roles in the chromophore isomerization cycle. Losses would then account for the fact that echinoid larvae seem to have only a Go-opsin, most other

protostomes only a r-opsin, and vertebrates c- and r-opsins. Cell duplication and subsequent specialization must also be assumed for vertebrates.

2.4.4 Putative role of Go-opsin positive cells in sea urchin larvae

The most plausible role of the Go photoreceptors described in this study is the regulation of vertical movement of the larva during photoperiodic transitions (Jekely et al., 2008; Mason and Cohen, 2012). Such a unimodal system could resemble the earliest photoreceptor mechanism in the first marine larvae. If this is the case, study of this system could provide clues as how the first planktonic animals perceived light cues (see Chapter 3 for further details). It remains possible that other opsins are present at the same larval stage that have not been identified.

Because the main locomotory organ of the pluteus is the ciliary band, it would be informative to know whether the *Sp-opsin3.2* positive cells are connected to the ciliary band via the nervous system, which has been described as "a network of cells that span the blastocoel and connect nearly all parts of the larva" (Ryberg, 1977). Previous studies of the nervous system of the pluteus of *Strongylocentrotus droebrachiensis* (Burke, 1978), a closely related species, report the presence of serotonergic neurons in the area of the apical organ, located between the cells homologous to the Go-opsin expressing cells of *S. purpuratus*. This serotonergic system is suggested to be involved in the regulation of the ciliary band activity in the pluteus (Gustafson et al., 1972; Burke, 1978; Yaguchi and Katow, 2003) and in many other marine larvae (e.g. Mackie et al., 1969; Beiras and Widdows, 1995; Pires and Woollacott, 1997; Kuang and Goldberg, 2001). The topology of the *Sp-opsin3.2* expressing cells in the proximity of serotonergic neurons lead us to hypothesize that Go expressing cells may be involved in locomotory control, probably in the activation or excitation of the ciliary band to position the animal in the upper photic zone. Knock out experiments of this opsin coupled with behavioural experiments could be used to test this hypothesis.

2.5 Methods

2.5.1 *Strongylocentrotus purpuratus*, adult care and larval culture

Adult *S. purpuratus* were obtained from San Diego Bay at 25-30 m in depth (San Diego, CA, USA) and housed in 12°C circulating seawater aquaria at the Stazione Zoologica Anton Dohrn, Italy. Spawning was induced by intracoelomic injection of 0.5M KCl. Embryos/larvae were cultured in Mediterranean filtered seawater (mesh pore size: 0.2 mm) diluted in de-ionized water (final salinity: 32.5‰) and kept at 15°C on a 12/12h light/dark cycle. From three days onwards, larvae were fed with a mixed diet of *Isochrysis galbana* [~2,000 cells mL^{-1}] and Rhodomonas sp. [~2,000 cells mL^{-1}]. All larval cultures were maintained at a decreasing concentration of 5 to 1 pluteus mL^{-1} depending on larval stage, mixed by gentle rotary stirring and washed every other day. Larval washes were made by inverted filtration (mesh size: 100 µM).

2.5.2 Gene cloning and RNA probe preparation

Contig sequence for *Sp-opsin3.2* was identified in the genome (ref. code: SPU027633) and transcriptome (ref. code: WHL22.338995) data sets. A 1,175 bp transcript was amplified by PCR with the cloning primers *Sp-opsin3.2*-F (5'-CCACTCATTTCGTGCGGATT-3') and *Sp-opsin3.2*-R (5'-CTCTAGTGATGACGGGCGAT-3') from cDNA prepared with a Bio-Rad iScript synthesis kit, ligated into pGEMT-easy vector (Promega), and transformed into Top10 chemically competent *Escherichia coli* (Invitrogen). Clone fragments were verified by Sanger sequencing prior to riboprobe generation. DIG-labelled antisense and sense (negative control) RNA probes were generated from plasmid DNA with T7- and SP6-RNA polymerases (Roche) respectively, and purify with mini Quick Spim Columns (Roche).

2.5.3 Fluorescent *in situ* hybridization coupled with immunohistochemistry

S. purpuratus larvae were collected at early pluteus stage (3dpf), fixed overnight at 4°C in 4% paraformaldehyde/0.1M MOPS pH 7, 0.5M NaCl, washed thoroughly in MOPS buffer, and stored in 70% ethanol until use. Whole mount fluorescent in situ hybridization (FISH) was performed as described in Andrikou et al., (2013). Immunohistochemistry coupled to WMISH was performed by incubating the larvae with anti-acetylated α-tubulin antibody (Sigma-Aldrich T6793, St Louis, MO, USA) in a dilution 1:250 together with the anti-DIG antibody; the secondary antibody was a goat anti-mouse IgG-Alexa 488 (Invitrogen, CA, USA) diluted 1: 1,000.

2.5.4 Immunohistochemistry

Larvae were fixed in 4% paraformaldehyde/0.1M PBS pH 7.4 containing 0.5M NaCl for 30 minutes at room temperature. Late six and eight armed larvae (days 14-23) were post-treated 2 minutes with pure cold MetOH to partially remove membrane lipids and facilitate antibody penetration. After five 5 minute rinses in phosphate buffered saline (PBS), samples were washed thoroughly in PBS/0.1% Tween-20 (PBST). Following incubations were carried out on an orbital shaker. The first blocking step was performed with 4% heat-inactivated Normal Goat Serum (NGS) in PBST for 1 hour, prior to incubating specimens with primary antibodies anti-Sp-opsin4 1:50 [1.21mg mL^{-1}] (Ullrich-Lüter et al., 2011), anti-1E11 an antibody against Synaptotagmin B considered as 'pan-neural' marker of *Strongylocentrotus purpuratus* nervous system) 1:100 [~10.00 mg mL^{-1}] (Nakajima et al., 2004), and anti-acetylated α-tubulin (Sigma T6793) 1:250 in PBST overnight at 4°C. After five washes in PBST, a second blocking step was performed as described above prior to incubating specimens with secondary antibodies (goat anti-rabbit IgG-Alexa 488 and goat anti-mouse IgG-Alexa 647) diluted 1: 1,000 in blocking buffer (4% NGS in PBST) at 4°C overnight. All specimens were washed thoroughly in PBS and

then counterstained with DAPI (1µg/mL in PBS) for nuclear labelling. For Sp-opsin4 antibodies, controls were carried out using their respective rabbit pre-immune sera. For commercial antibodies, control experiments were run in parallel by omitting primary antibodies.

2.5.5 Transmission Electron Microscopy

S. purpuratus plutei were first fixed in modified Karnovsky solution (2.5% glutaraldehyde, 2% paraformaldehyde, and 3% sucrose in 0.1 M phosphate buffer pH 7.4 containing 0.5M NaCl) for 1 hour at room temperature. After several rinses in PBS, samples were post fixed in 1% osmium tetraoxide in distilled water 1 hour at 7°C, and dehydrated in a series of ethanol (30/50/70/96/100) and infiltrated and embedded in EPON (Agar 100). Samples were kept at 60°C for 48 hours to allow polymerization. Thin sections (50-70 nm) were cut with a diamond knife with a Leica EM UC7 ultramicrotome and mounted on pioloform coated copper grids.

2.5.6 Imaging

Light microscopic images were taken using a Zeiss M1 Axio Imager microscope. Confocal acquisition was performed on a Zeiss LSM 510 Meta confocal microscope. TEM acquisitions were performed on a 120 kV JEOL 1400 plus microscope with a bottom mounted CMOS camera. Figure plates were made with Illustrator CS6 (Adobe). Brightness, contrast, and colour balance adjustments were always applied to the whole image and not to parts.

2.7 References

Aizenberg, J., Tkachenko, A., Weiner, S., Addadi, L., & Hendler, G. (2001). Calcitic microlenses as part of the photoreceptor system in brittlestars. *Nature*, *412*(6849), 819-822.

Andrikou, C., Iovene, E., Rizzo, F., Oliveri, P., & Arnone, M. I. (2013). Myogenesis in the sea urchin embryo: The molecular fingerprint of the myoblast precursors. *EvoDevo*, *4*(1), 33.

Arendt, D. (2008). The evolution of cell types in animals: Emerging principles from molecular studies. *Nature Reviews Genetics*, *9*(11), 868-882.

Arendt, D., Tessmar-Raible, K., Snyman, H., Dorresteijn, A. W., & Wittbrodt, J. (2004). Ciliary photoreceptors with a vertebrate-type opsin in an invertebrate brain. *Science*, *306*(5697), 869-871.

Arendt, D., & Wittbrodt, J. (2001). Reconstructing the eyes of Urbilateria. *Philosophical Transactions of the Royal Society of London B: Biological Sciences*, *356*(1414), 1545-1563.

Beiras, R., & Widdows, J. (1995). Effect of the neurotransmitters dopamine, serotonin and norepinephrine on the ciliary activity of mussel (Mytilus edulis) larvae. *Marine Biology*, *122*(4), 597-603.

Bennett, M. F. (1979). Extraocular light receptors and circadian rhythms. In *Comparative Physiology and Evolution of Vision in Invertebrates* (pp. 641-663). Springer Berlin, Heidelberg.

Blevins, E., & Johnsen, S. (2004). Spatial vision in the echinoid genus Echinometra. *Journal of Experimental Biology*, *207*(24), 4249-4253.

Brandenburger, J. L., Woolacott, R. M., & Eakin, R. M. (1973). Fine structure of eyespots in tornarian larvae (Phylum: Hemichordata). *Cell and Tissue Research*, *142*(1), 89-102.

Braubach, O. R., Dickinson, A. J., Evans, C. C., & Croll, R. P. (2006). Neural control of the velum in larvae of the gastropod, Ilyanassa obsoleta. *Journal of Experimental Biology*, *209*(23), 4676-4689.

Braun, K., Kaul-Strehlow, S., Ullrich-Lüter, E., & Stach, T. (2015). Structure and ultrastructure of eyes of tornaria larvae of Glossobalanus marginatus. *Organisms Diversity & Evolution*, *15*(2), 423-428.

Burke, R. D. (1978). The structure of the nervous system of the pluteus larva of Strongylocentrotus purpuratus. *Cell and Tissue Research*, *191*(2), 233-247.

Burke, R. D., Angerer, L. M., Elphick, M. R., Humphrey, G. W., Yaguchi, S., Kiyama, T., ... & Brandhorst, B. P. (2006). A genomic view of the sea urchin nervous system. *Developmental Biology*, *300*(1), 434-460.

Byrne, M., Nakajima, Y., Chee, F. C., & Burke, R. D. (2007). Apical organs in echinoderm larvae: insights into larval evolution in the Ambulacraria. *Evolution & Development*, *9*(5), 432-445.

Coppard, S. E., Kroh, A., & Smith, A. B. (2012). The evolution of pedicellariae in echinoids: an arms race against pests and parasites. *Acta Zoologica*, *93*(2), 125-148.

D'Aniello, S., Delroisse, J., Valero-Gracia, A., Lowe, E. K., Byrne, M., Cannon, J. T., ... & Lowe, C. J. (2015). Opsin evolution in the Ambulacraria. *Marine Genomics*, *24*, 177-183.

Feuda, R., Hamilton, S. C., McInerney, J. O., & Pisani, D. (2012). Metazoan opsin evolution reveals a simple route to animal vision. *Proceedings of the National Academy of Sciences*, *109*(46), 18868-18872.

Gühmann, M., Jia, H., Randel, N., Verasztó, C., Bezares-Calderón, L. A., Michiels, N. K., ... & Jékely, G. (2015). Spectral tuning of phototaxis by a go-opsin in the rhabdomeric eyes of Platynereis. *Current Biology*, *25*(17), 2265-2271.

Gustafson, T., Lundgren, B., & Treufeldt, R. (1972). Serotonin and contractile activity in the echinopluteus: a study of the cellular basis of larval behaviour. *Experimental Cell Research*, *72*(1), 115-139.

Hendler, G., & Byrne, M. (1987). Fine structure of the dorsal arm plate of Ophiocoma wendti: evidence for a photoreceptor system (Echinodermata, Ophiuroidea). *Zoomorphology*, *107*(5), 261-272.

Heyland, A., & Hodin, J. (2014). A detailed staging scheme for late larval development in Strongylocentrotus purpuratus focused on readily-visible juvenile structures within the rudiment. *BMC Developmental Biology*, *14*(1), 22.

Ho, E. C., Buckley, K. M., Schrankel, C. S., Schuh, N. W., Hibino, T., Solek, C. M., ... & Rast, J. P. (2016). Perturbation of gut bacteria induces a coordinated cellular immune response in the purple sea urchin larva. *Immunology and Cell Biology*, *94(9)*, *861-874*.

Holmes, S. J. (1912). Phototaxis in the sea urchin, Arbacia punctulata. *Journal of Animal Behavior*, *2*(2), 126-136.

Jagersten, G., (1972). *Evolution of the Metazoan life cycle*. London Academic Press, London.

Jékely, G. (2009). Evolution of phototaxis. *Philosophical Transactions of the Royal Society of London B: Biological Sciences*, *364*(1531), 2795-2808.

Jékely, G., Colombelli, J., Hausen, H., Guy, K., Stelzer, E., Nédélec, F., & Arendt, D. (2008). Mechanism of phototaxis in marine zooplankton. *Nature*, *456*(7220), 395-399.

Johnsen, S. Ö. N. K. E. (1994). Extraocular sensitivity to polarized light in an echinoderm. *Journal of Experimental Biology*, *195*(1), 281-291.

Johnsen, S. (1997). Identification and localization of a possible rhodopsin in the echinoderms Asterias forbesi (Asteroidea) and Ophioderma brevispinum (Ophiuroidea). *The Biological Bulletin*, *193*(1), 97-105.

Johnsen, S., & Kier, W. M. (1999). Shade-seeking behaviour under polarized light by the brittlestar Ophioderma brevispinum (Echinodermata: Ophiuroidea). *Journal of the Marine Biological Association of the UK*, *79*(04), 761-763.

Kojima, D., Terakita, A., Ishikawa, T., Tsukahara, Y., Maeda, A., & Shichida, Y. (1997). A novel Go-mediated phototransduction cascade in scallop visual cells. *Journal of Biological Chemistry*, *272*(37), 22979-22982.

Koyanagi, M., Terakita, A., Kubokawa, K., & Shichida, Y. (2002). Amphioxus homologs of Go-coupled rhodopsin and peropsin having 11-cis-and all-trans-retinals as their chromophores. *FEBS letters*, *531*(3), 525-528.

Koyanagi, M., Takano, K., Tsukamoto, H., Ohtsu, K., Tokunaga, F., & Terakita, A. (2008). Jellyfish vision starts with cAMP signaling mediated by opsin-Gs cascade. *Proceedings of the National Academy of Sciences*, *105*(40), 15576-15580.

Kuang, S., & Goldberg, J. I. (2001). Laser ablation reveals regulation of ciliary activity by serotonergic neurons in molluscan embryos. *Journal of Neurobiology*, *47*(1), 1-15.

Lacalli, T. C., Gilmour, T. H. J., & West, J. E. (1990). Ciliary band innervation in the bipinnaria larva of Piaster ochraceus. *Philosophical Transactions of the Royal Society of London B: Biological Sciences*, *330*(1258), 371-390.

Leech, D. M., Padeletti, A., & Williamson, C. E. (2005). Zooplankton behavioral responses to solar UV radiation vary within and among lakes. *Journal of Plankton Research*, *27*(5), 461-471.

Leys, S. P., & Degnan, B. M. (2001). Cytological basis of photoresponsive behavior in a sponge larva. *The Biological Bulletin*, *201*(3), 323-338.

Mackie, G. O., Spencer, A. N., & Strathmann, R. (1969). Electrical activity associated with ciliary reversal in an echinoderm larva. *Nature*, *223*(5213), 1384-1385.

Maldonado, M., Durfort, M., McCarthy, D. A., & Young, C. M. (2003). The cellular basis of photobehavior in the tufted parenchymella larva of demosponges. *Marine Biology*, *143*(3), 427-441.

Mano, H., & Fukada, Y. (2007). A median third eye: pineal gland retraces evolution of vertebrate photoreceptive organs. *Photochemistry and Photobiology*, *83*(1), 11-18.

Marlow, H., Tosches, M. A., Tomer, R., Steinmetz, P. R., Lauri, A., Larsson, T., & Arendt, D. (2014). Larval body patterning and apical organs are conserved in animal evolution. *BMC Biology*, *12*(1), 1-17.

Marsden, J. R. (1984). Swimming in response to light by larvae of the tropical serpulid Spirobranchus giganteus. *Marine Biology*, *83*(1), 13-16.

Marshall, D. J., & Hodgson, A. N. (1990). Structure of the cephalic tentacles of some species of prosobranch limpet (Patellidae and Fissurellidae). *Journal of Molluscan Studies*, *56*(3), 415-424.

Mason, B. M., & Cohen, J. H. (2012). Long-wavelength photosensitivity in coral planula larvae. *The Biological Bulletin*, *222*(2), 88-92.

Millot, N., & Yoshida, M. (1958). The Photosensitivity of the sea echinoid Diadema antillarum Phillipi: responses to increases in light intensity. *Proceedings of The Zoological Society of London, 133*, 67-71.

Millott, N. (1976). The photosensitivity of echinoids. *Advances in Marine Biology, 13*, 1-52, Elsevier, London.

Millott, N. (1953). Light emission and light perception in species of Diadema. *Nature*, *171*(4361), 973-974.

Millott, N. (1954). Sensitivity to light and the reactions to changes in light intensity of the echinoid Diadema antillarum Philippi. *Philosophical Transactions of the Royal Society of London B: Biological Sciences*, *238*(655), 187-220.

Millott, N., & Manly, B. M. (1961). The iridophores of the echinoid Diadema antillarum. *Journal of Cell Science*, *3*(58), 181-194.

Nakajima, Y., Kaneko, H., Murray, G., & Burke, R. D. (2004). Divergent patterns of neural development in larval echinoids and asteroids. *Evolution & Development*, *6*(2), 95-104.

Nielsen, C. (2008). Six major steps in animal evolution: are we derived sponge larvae? *Evolution & Development*, *10*(2), 241-257.

Nilsson, D. E. (2009). The evolution of eyes and visually guided behavior. *Philosophical Transactions of the Royal Society of London B: Biological Sciences*, *364*(1531), 2833-2847.

Nilsson, D. E. (1996). Eye ancestry: Old genes for new eyes. *Current Biology*, *6*(1), 39-42.

Nilsson, D. E. (2013). Eye evolution and its functional basis. *Visual Neuroscience*, *30*(1-2), 5-20.

Nordström, K., Seymour, J., & Nilsson, D. (2003). A simple visual system without neurons in jellyfish larvae. *Proceedings of the Royal Society of London B: Biological Sciences*, *270*(1531), 2349-2354.

Passamaneck, Y. J., Furchheim, N., Hejnol, A., Martindale, M. Q., & Lüter, C. (2011). Ciliary photoreceptors in the cerebral eyes of a protostome larva. *EvoDevo*, *2*(1), 6.

Passamaneck, Y. J., & Martindale, M. Q. (2013). Evidence for a phototransduction cascade in an early brachiopod embryo. *Integrative and Comparative Biology*, *53*(1), 17-26.

Paul, N. D., & Gwynn-Jones, D. (2003). Ecological roles of solar UV radiation: Towards an integrated approach. *Trends in Ecology & Evolution*, *18*(1), 48-55.

Pires, A., & Woollacott, R. M. (1997). Serotonin and dopamine have opposite effects on phototaxis in larvae of the bryozoan Bugula neritina. *The Biological Bulletin*, *192*(3), 399-409.

Plachetzki, D. C., Degnan, B. M., & Oakley, T. H. (2007). The origins of novel protein interactions during animal opsin evolution. *PloS One*, *2*(10), e1054.

Porter, M. L., Blasic, J. R., Bok, M. J., Cameron, E. G., Pringle, T., Cronin, T. W., & Robinson, P. R. (2011). Shedding new light on opsin evolution. *Proceedings of the Royal Society of London B: Biological Sciences*, *279*(1726), 3-14.

Provencio, I., Jiang, G., Willem, J., Hayes, W. P., & Rollag, M. D. (1998). Melanopsin: An opsin in melanophores, brain, and eye. *Proceedings of the National Academy of Sciences*, *95*(1), 340-345.

Raible, F., Tessmar-Raible, K., Arboleda, E., Kaller, T., Bork, P., Arendt, D., & Arnone, M. I. (2006). Opsins and clusters of sensory G-protein-coupled receptors in the sea urchin genome. *Developmental Biology*, *300*(1), 461-475.

Ramirez, M. D., Pairett, A. N., Pankey, M. S., Serb, J. M., Speiser, D. I., Swafford, A. J., & Oakley, T. H. (2016). The last common ancestor of bilaterian animals possessed at least 7 opsins. *BioRxiv*, 052902.

Raup, D. M., (1966) *The Endoskeleton*. In: Boolootian R. A. (ed) Physiology of Echinodermata, 379-395, Interscience, New York.

Ryberg, E. (1977). The nervous system of the early echinopluteus. *Cell and tissue research*, *179*(2), 157-167.

Schmidt, T. M., Chen, S. K., & Hattar, S. (2011). Intrinsically photosensitive retinal ganglion cells: Many subtypes, diverse functions. *Trends in Neurosciences*, *34*(11), 572-580.

Smith, F. G. W. (1935). The development of Patella vulgata. *Philosophical Transactions of the Royal Society of London. Series B, Biological Sciences*, *225*(520), 95-125.

Smith, M. M., Cruz Smith, L., Cameron, R. A., & Urry, L. A. (2008). The larval stages of the sea urchin, Strongylocentrotus purpuratus. *Journal of Morphology*, *269*(6), 713-733.

Sodergren, E., Weinstock, G. M., Davidson, E. H., Cameron, R. A., Gibbs, R. A., Angerer, R. C., ... & Coffman, J. A. (2006). The genome of the sea urchin Strongylocentrotus purpuratus. *Science*, *314*(5801), 941-952.

Thornton, I. W. B. (1956). Diurnal migrations of the echinoid Diadema setosum (Leske). *The British Journal of Animal Behavior*, *4*(4), 143-146.

Thorson, G. (1964). Light as an ecological factor in the dispersal and settlement of larvae of marine bottom invertebrates. *Ophelia*, *1*(1), 167-208.

Tosches, M. A., Bucher, D., Vopalensky, P., & Arendt, D. (2014). Melatonin signaling controls circadian swimming behavior in marine zooplankton. *Cell*, *159*(1), 46-57.

Tu, Q., Cameron, R. A., & Davidson, E. H. (2014). Quantitative developmental transcriptomes of the sea urchin Strongylocentrotus purpuratus. *Developmental Biology*, *385*(2), 160-167.

Turner, P. L., & Mainster, M. A. (2008). Circadian photoreception: Ageing and the eye's important role in systemic health. *British Journal of Ophthalmology*, *92*(11), 1439-1444.

Ullrich-Lüter, E. M., D'Aniello, S., & Arnone, M. I. (2013). C-opsin expressing photoreceptors in echinoderms. *Integrative and Comparative Biology*, *53*(1), 27-38.

Ullrich-Lüter, E. M., Dupont, S., Arboleda, E., Hausen, H., & Arnone, M. I. (2011). Unique system of photoreceptors in sea urchin tube feet. *Proceedings of the National Academy of Sciences*, *108*(20), 8367-8372.

Valero-Gracia, A., Petrone, L., Oliveri, P., Nilsson, D. E., & Arnone, M. I. (2016). Non-directional Photoreceptors in the Pluteus of Strongylocentrotus purpuratus. *Frontiers in Ecology and Evolution*, *4*, 127.

Van Gelder, R. N. (2008). Non-visual photoreception: Sensing light without sight. *Current Biology*, *18*(1), R38-R39.

Vöcking, O., Kourtesis, I., & Hausen, H. (2015). Posterior eyespots in larval chitons have a molecular identity similar to anterior cerebral eyes in other bilaterians. *EvoDevo*, *6*(1), 40.

Wada, Y., Mogami, Y., and Baba, S. (1997). Modification of ciliary beating in sea urchin larvae induced by neurotransmitters: beat-plane rotation and control of frequency fluctuation. *Journal of Experimental Biology*, *200*(1), 9-18.

Woodley, J. D. (1982) Photosensitivity in Diadema antillarum: Does it show scototaxis? In *The International Echinoderm Conference*, 61, Ed Lawrence, J. M., Rotterdam.

Yaguchi, S., & Katow, H. (2003). Expression of tryptophan 5-hydroxylase gene during sea urchin neurogenesis and role of serotonergic nervous system in larval behavior. *Journal of Comparative Neurology*, *466*(2), 219-229.

Yerramilli, D., & Johnsen, S. (2010). Spatial vision in the purple sea urchin Strongylocentrotus purpuratus (Echinoidea). *Journal of Experimental Biology*, *213*(2), 249-255.

Yoshida, M. (1966). Photosensitivity in *Physiology of Echinodermata,* 435-464, John Whiley & Sons, New York.

Yoshida, M., Takasu, N., and Tamotsu, S. (1984). Photoreception in echinoderms in *Photoreception and Vision in Invertebrates*, 743-771, Springer, US.

3. THE EFFECT OF LIGHT ON THE VERTICAL MIGRATION OF ECHINOPLUTEUS

3. THE EFFECT OF LIGHT ON THE VERTICAL MIGRATION OF ECHINOPLUTEUS

3.1 Abstract

Diel vertical migration is the synchronised vertical movement of plankton in the water column over the daily cycle. Typically, animals migrate upwards towards the surface at dusk, and descend back to deeper water before dawn, though this may also occur in reverse. Although this vertical movement is of great ecological importance, the cues that drive this migration in several invertebrate clades are not clearly identified. Furthermore, very few tools devoted to studying the potential drivers of vertical migration in a controlled environment have been created. In Chapter 3 we investigate this problem by applying a novel set up that mimics the different light conditions available in the oceanic water column at different depths. This environment can be calibrated with respect to the photic conditions and it quantifies the animals' movements in real time. Therefore, this device can help to demonstrate or discard the hypothesis that a dipleurula larva only equipped with non-directional photoreceptors can control its position in the water column depending on light cues. This research has been successful in demonstrating that echinopluteus is clearly able to swim or sink in response to light. Such capability to undergo a light-driven gravitaxis prone me to propose a hypothetical photoreceptor system composed by more than one photosensible protein. This photoreceptor apparatus must be finely coordinated with the ciliary band by means of the nervous net, thus allowing the larva to activate or stop the ciliary beating for actively swimming up or sinking down in the water column. The functional data here supported

the aforementioned light-related hypotheses, therefore informing the importance of light acting as a driving force that controls the vertical migration of this zooplankton in absence of predators. Future efforts in which to create response/intensity curves at different wavelengths are needed to separate the effect of spectral sensitivity and spectral discrimination by these animals.

3.2 Introduction

Daily, zooplankton moves to deeper water in the morning and rises at dusk, or vice versa. This process, known as diurnal or diel vertical migration, is carried out all over the world by marine and freshwater plankton alike, thus representing the biggest biomass movement on Earth (Brierley, 2014). The presence of vertical migration in so many organisms, in spite of the energetic cost involved, suggests that this phenomenon must have an important adaptive value (Lampert, 1989). Indeed, this phenomenon must be even more important in life forms that possess planktonic larvae in their life cycles, a stage crucial for conquering new ecological niches. However, very few tools are devoted to the study of these small transparent organisms. Environmental cues are required to guide the vertical migration, and which cues are involved has been the subject of research. As a result, a variety of hypotheses attempting to identify this driving signal have been proposed. Many of those can be grouped into two big categories: metabolic advantage hypotheses, and light dependent hypotheses.

3.2.1. Putative driving cues I: The metabolic advantage hypotheses

The idea that zooplankton migration could provide a metabolic advantage was originally proposed by McLaren during the 1960s (McLaren, 1963; 1974). McLaren estimated an energetic gain for animals (in his study case, copepods), feeding at night in the warm, food-

rich waters, and resting in colder areas during the day. However, in spite of this, experimental data on various species both in the field and in laboratory conditions indicate a retardation of development at low temperatures, therefore decreasing the population growth (Lock and McLaren, 1970; Swift, 1976; Orcutt and Porter, 1983; Stich and Lampert, 1984). These and further findings refuted the demographic advantage hypothesis as well as related models (e.g. the starvation avoidance hypothesis; Geller, 1986) and suggested that, at least in some species, vertical migration per se may be energetically disadvantageous (Kerfoot, 1985).

After the McLaren model, a second hypothesis was proposed by Enright, which incorporates feedbacks between filter feeding zooplankton and their algal prey into a metabolic model (Enright, 1977). His model differed from McLarens' (1963) in two main assumptions: (i) since photosynthesis takes place during the day, but only losses (respiration and grazing) occur at night, algal biomass must be greater in the evening than in the morning. Furthermore, (ii) algal quality must also differ as the cells will be filled with reserves at dusk. Contrary to McLarens' metabolic advantage hypothesis, Enright's model incorporates the timing of migration. Hence, vertical migrations may arise from the need to accumulate rather than conserve energy. This model has been tested by a series of detailed sampling of the marine copepod *Calanus*, but the predicted pattern was only found in some experiments (Enright and Honegger, 1977). Therefore, authors conclude that other factors may also influence the behaviour (Lampert, 1989). Moreover, this behavioural model raised the question of how planktonic animals can establish the appropriate timing to ascend before the sunset to feed themselves (Kremer and Kremer, 1988; Pearre, 1979). To date, there is little evidence to support the metabolic advantage hypotheses as unique driving cause of diel vertical migration.

3.2.2 Putative driving cues II: The light related hypotheses

The second main group of hypotheses is based on the influence of light. On this category, the first hypothesis is mainly based upon the assumption that animals should avoid the the shallowest area of the epilimnion because of the deleterious effect caused by short wavelength light (Siebeck, 1978). Protection from UV light damage would not require deep migrations, as UV is absorbed in the uppermost region of the water column (for further details, see General Introduction). Effects of blue light may be important too as it penetrates much deeper. Nevertheless, sometimes it is difficult to separate the harmful effects of short wave radiation from visual predation effects (the second light related hypothesis), especially in the open ocean (Byron, 1982; Zaret and Suffern, 1976).

As just mentioned, the second light related hypothesis is focused on the interactions between prey and predators. The concept of vertical migration as a predator evasion is the most straightforward of the light dependent hypotheses in most of the cases. The pelagic environment is relatively homogeneous, zooplankton has no shelter to hide from visual predators and therefore they have developed strategies to become less visible and hide in the darker regions of the water column. However, as not all animals have resolving vision, their ability to avoid predators may be limited. An example of it is the pluteus larvae used here.

In combination, the light related hypotheses make two main predictions: (i) zooplankton must ascend in the evening and descend at dawn (reverse migrations can be explained as predator avoidance; predators tend to follow their prey, and by migrating opposite to most prey, the risk of predation can be reduced), and (ii) vertical migration should predominate in more conspicuous animals that can be better detected (Lampert, 1989).

Some of the problems that these light dependent hypotheses encountered are related to the relative abundance of predators in some environments. Since both groups of hypotheses (metabolic advantage and light related) are still debated, the use of laboratory custom built set ups like the one here presented gaves a great opportunity to better explore these ideas by providing a controlled environment free of predators. Moreover, for our study we have chosen the pluteus of *Paracentrotus lividus* to test if animals putatively equipped with class I photoreceptors are capable to control its vertical migration based on light cues.

3.2.3 Vertical distribution of plutei: Previous studies

The depth regulatory behaviour of marine invertebrate larvae has received considerable attention (reviewed in Thorson, 1964). However, models of depth regulation are based largely on the study of coloured larvae of fouling animals, estuarine bivalves and crustaceans. Conversely, small transparent larvae such as echinopluteus, which do not show obvious responses to environmental stimuli, have been neglected (Reese, 1966). Nevertheless, some mutually-exclusive theories about the possible photobehaviour of pluteus larvae have been proposed. In chronological order, Théel did not state if *Echinocyamus pusillus* plutei are photosensitive or not, but that they swam to the surface (Théel, 1892). Mortensen did not study the phototaxis of the plutei of *Laganum diplopora* in detail, but he reported that the larvae tend to swim towards the bottom of the culture dishes (Mortensen, 1921). Fox (1924) reported that the blastulae, gastrulae and larvae of *Diadema setosum* migrate towards the bottom of a plankton column after half an hour of 'illumination'. Neya (1965), described the horizontal movements of plutei of *Hemicentrotus pulcherrimus* in response to both horizontally and vertically oriented beams of artificial 'white' light; and Eastwood described horizontal and vertical movements of *Lytechinus*

variegaus plutei in response to downwelling light (Eastwood, 1972). To the best of my knowledge, prior to this study, the more recent and detailed examination of depth regulation of an echinoderm larva is the one described by Pennington and Emlet (1986). Pennington and Emlet examined the depth regulation of the pluteus larvae of *Dendraster excentricus* both in the field (by collecting samples at different depths), in an enclosure situated at Friday Harbour bay (Washington, USA), and in an aquarium. These experiments established that the plutei of this species rise towards the surface at night, and descend during daytime, as commonly occurs in many other planktonic larvae (Pennington and Emlet, 1986).

In this work, I present my data on the vertical migration photobehaviour of echinopluteus under seven light sources of different wavelength (340, 420, 490, 505, 535, 590, and 617 nm) at a given radiance. Up to my knowledge, these insights represent the most systematic and widest light-driven gravitaxis study made in a larva of the Ambulacraria clade. Thanks to it, we demonstrated that the pluteus larva, a larva equipped with class I photoreceptors, is able to undergo vertical migrations. The occurrence of a light-driven gravitaxis prone me to propose a hypothetical light dependent deep-gauge mechanism for controlling the larval position in the water column.

3.3 Results

Results section has been located after the Introduction to keep the organisation followed all through this thesis. However, since the methodology employed for obtaining these data involved two novel set ups designed for this project, I suggest to the reader to first consult the heading 'Material and methods' of this chapter to help with an overview of the technology and protocols used.

3.3.1 Experimental protocol I: Pilot experiments for testing the light-driven gravitaxis capability of *P. lividus* plutei

For the experiments described here and in the following section, the set up used was the vertical migration set up I (Fig. 33). Once this set of experiments was settled following the protocol described below (see section 3.5, Material and methods), de visu observations about changes in vertical distribution of plutei were done and annotated at different times of the day. Thanks to these assays I observed that pluteus larvae exhibit a light-driven gravitaxis behaviour to 380-700 nm 'white' light, and that animals tend to distribute themselves homogeneously all over the water column in absence of light.

3.3.2 Experimental protocol II: Preliminary observations of the larval sinking speed

As result of these experiments, cylinder I (10 minutes of 380-700 nm 'white' light exposure) did not show almost any sign of light-driven gravitaxis behaviour in any of the experiments done independently of the time of the day, thus the larval population was randomly distributed all over the water column. Cylinder II (30 minutes of 'white' light exposure) showed a similar situation but larvae started to form clusters and to line up themselves in the centre of the cylinder all over its length; however, this lineal organization was not observed in all cases though. After 60 minutes of 'white' light exposure (cylinder III) the vertical distribution of plutei was qualitatively noted, thus showing the main part of the animal population is located in the third section of the cylinder which is located towards the base. Cylinder IV (90 minutes of 'white' light exposure) brought an identical behavioural pattern to the one found in cylinder III; such a pattern was more pronounced in some cases. In all experiments done, the control cylinder (cylinder V) showed the larvae homogeneously distributed themselves independently all over the water column of when the time had come for the results to be collected from the culture beakers: 12 am of day 1, 12 pm of day 1, or 12 am of day 2.

After comparing the differences in the migration movements on cylinders I to IV, it was considered that four armed plutei have an average sinking speed of 0.6 cm per minute. This observation is in agreement with previous experiments carried out at the Stazione Zoologica Anton Dohrn (Dr. Giuseppe Bianco, personal communication). Taking this into account, the duration of each stimulus for the main data collection was set as 60 minutes. Since at this stage of the experiments there was no clue on which light source (if any) was going to attract the animals towards the surface, it was not possible to establish an average swimming up speed. To compare if the average swimming speed up and speed of sinking are similar, another set up in which it is possible to change the light source direction must be used. An example of such a set up design is being provided in the section 'Discussion and future directions' (Fig. 32).

3.3.3 Experimental protocol III: First experiments with the vertical migration (VM) set up II, calculating the effect size to inform the experimental design

From this point onwards, the experimental set up used was the VM set up II (Fig. 34) and the experiments were performed at the Vision Group laboratories (Lund University, Sweden). This sophisticate set up was useful not only to better control the properties of the light used as stimulus, but also to have an unbiased graphical record of the experiments done.

As a result of these experiments, a graphical image record that shows the vertical migration movements of the larval population was obtained (Fig. 27). In these images it is possible to see the movement of the larvae through a density profile in function of time. This type of analysis was developed by Jochen Smolka (Lund University,

Sweden). More in detail, for each experiment a set of two images is shown, one graph showing the average movement of the masscentre of the population in the water column over the duration (Fig. 27A, B, C, D), and another graph in which it is shown the density profile of the larval population in relationship with the distance from the water surface (Fig. 27A', B', C', and D'). In Fig. 27A, B, C, and D; *y* axis represents the mean position of the animal population in centimetres, and *x* axis represents the time in minutes. Further, a graphical representation of the stimulus provided to the animals is shown as a bar under the horizontal axis.

The different colour that fills the horizontal bar (in the case of these experiments, purple or black) indicates if animals are being treated with 'light' or 'no light' stimuli, respectively. When possible, the colours chosen for filling the bar correspond to the 'colour' of the light stimulus used. In total, each experiment is composed by six phases of stimuli indicated as S, I, II, III, IV, and V; and lasted a total time of 360 minutes. The separation of such phases are being highlighted as a vertical bar when the light stimulus changes. Animals were recorded in a time series of circa 1 second per frame.

In Fig. 27A', B', C', and D'; the *x* axis represents the relative quantity of animal units (a.u.) for each phase of the experiment depending on depth, and the *y* axis indicates the position of the larval population in the water column. In a similar manner to what it was done for Fig. 27A, B, C, and D; the different phases of the experiment are being highlighted in different colours and have been indicated by Roman numerals. For these figures just four phases, the central ones (I, II, III, IV), are being represented.

On the one hand, while comparing the mean position of the larval population when using 250 individuals (Fig. 27A, B), there is not a clear and consistent temporary pattern of larval movement independently of the light stimulus provided. In fact, the larval mean position is roughly maintained in the middle of the column at 20 cm from the water surface, just in the middle of the plankton cell. Still, there is a smoothly clearer pattern of migration in the experiment recorded with animals collected during night time (Fig. 27B) compared to the one recorded with animals collected during day time (Fig. 27A). Such oscillation in the animal mean position consists of a slightly upper location of the animals during 'no light' phases in comparison with the 340 nm UV illuminated ones. Furthermore, when comparing the relative distribution of the animal population in the water column (Fig. 27A', B'), the main part of the larvae seems to have a tendency to stay more closely positioned towards the surface when the animals were collected in the dark half of the day (Fig. 27A') in respect of the condition observed in animals collected in the light half (Fig. 27B').

On the other hand, while comparing the mean position of the larval population when using 2,500 individuals (Figs. 27C, D), there is a much clearer net pattern of movement of the mean position of larvae during time. Indeed, in both cases, the average mean position all over the time is also at 20 cm from the water surface, but oscillations of about 5.5 cm can be seen depending on the stimulus provided. These vertical oscillations indicate that the larvae undergo light-driven gravitaxis while stimulated with 340 nm UV at $6{,}2 \times 10^{7}$ photons d^{-1} sr^{-1} cm^{-2}.

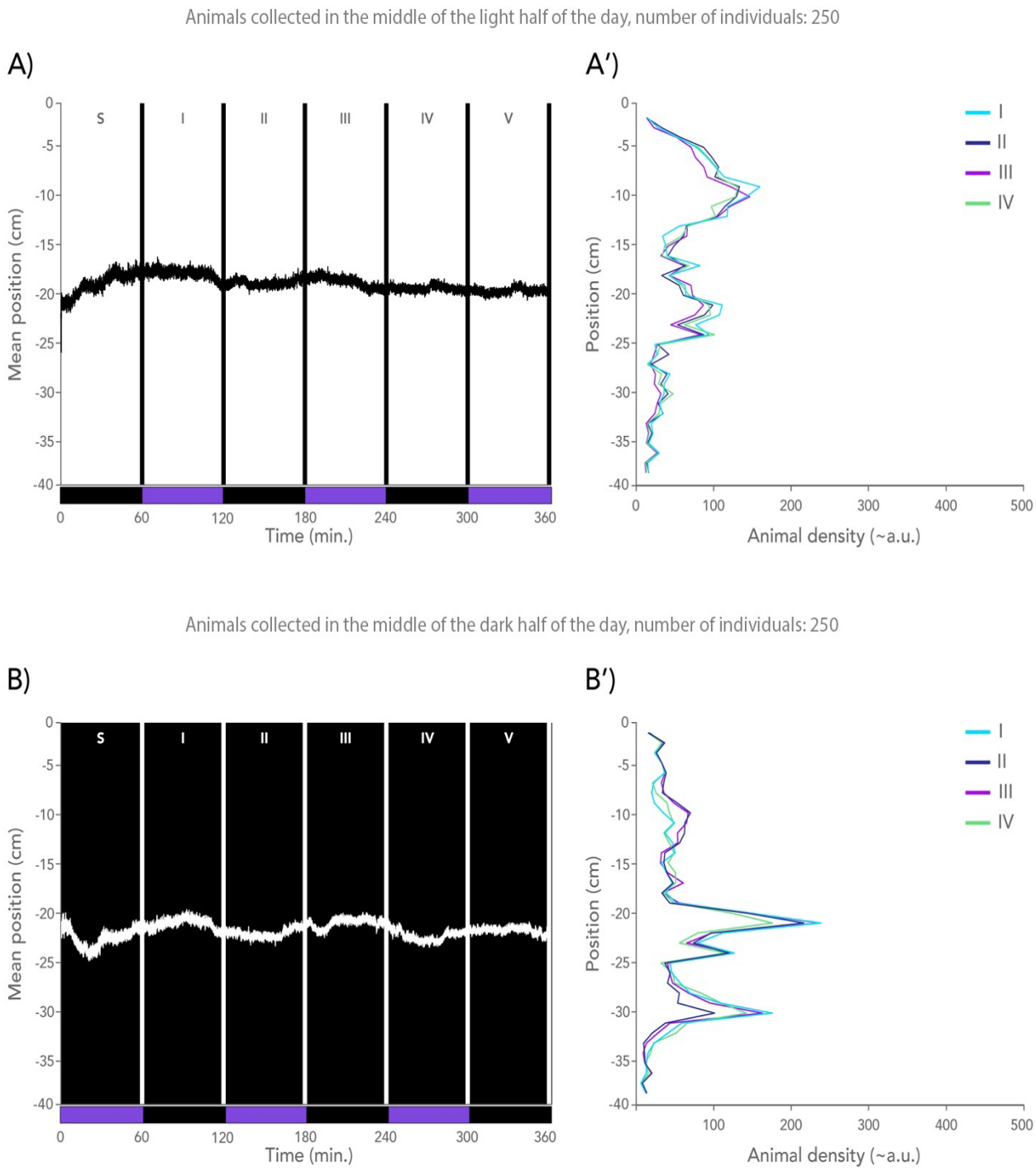

Fig 27. Graphical results of the pilot experiments carried out about the effect size to inform the experimental design of the main data collection. A) Mean position of the larval population while using 250 individuals collected in the middle of the light half of the day. A') Relative position of the animal population in the water column over time while using 250 individuals collected in the middle of the light half of the day. B) Mean position of the larval population while using 250 individuals collected in the middle of the dark half of the day. B') Relative position of the animal population in the water column over time while using 250 individuals collected in the middle of the dark half of the day.

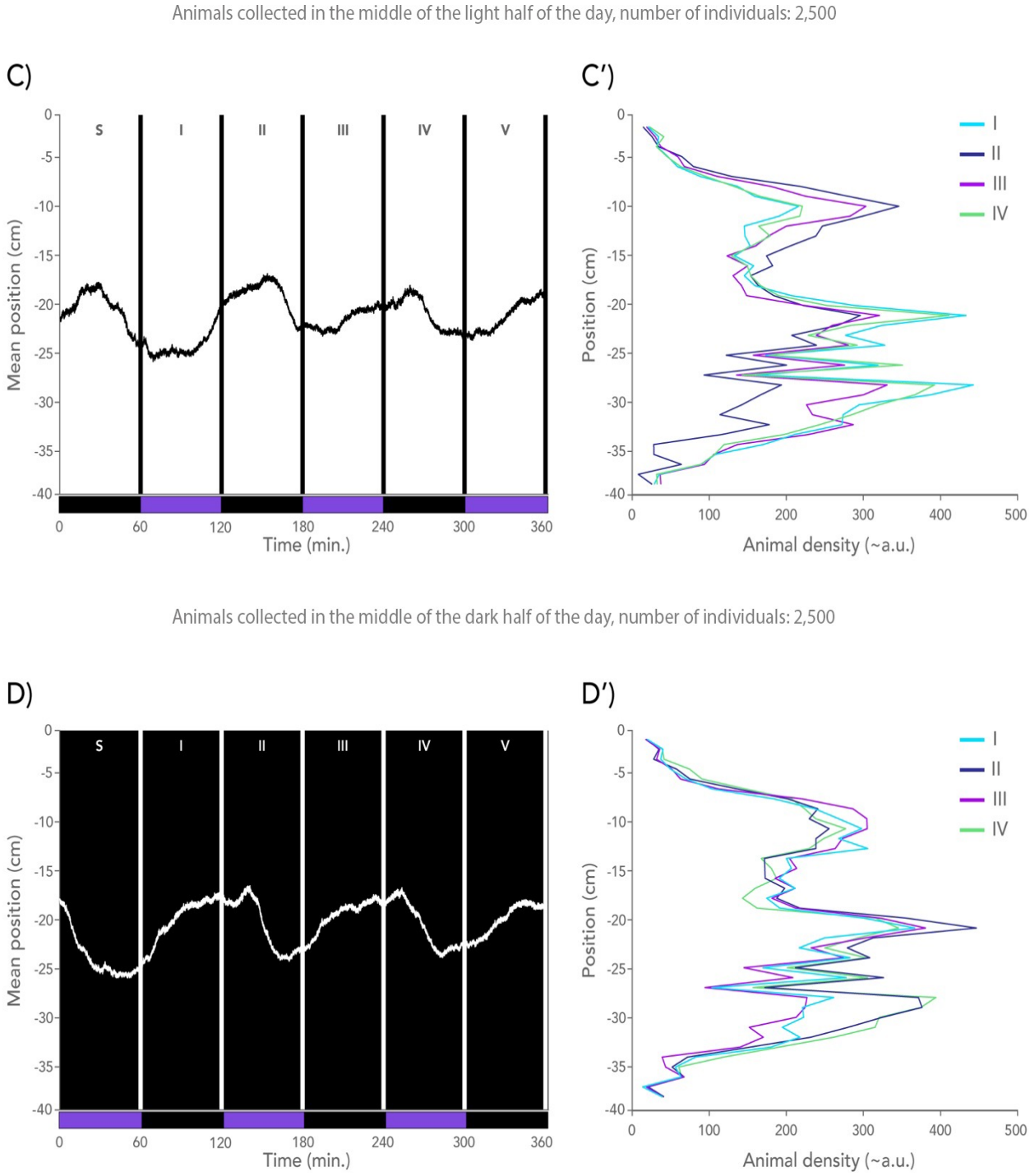

Fig 27. Graphical results of the pilot experiments carried out about the effect size to inform the experimental design of the main data collection. C) Mean position of the larval population while using 2,500 individuals collected in the middle of the light half of the day. C') Relative position of the animal population in the water column over time while using 2,500 individuals collected in the middle of the light half of the day. D) Mean position of the larval population while using 2,500 individuals collected in the middle of the dark half of the day. D') Relative position of the animal population in the water column over time while using 2,500 individuals collected in the middle of the dark half of the day.

Light-driven gravitaxis behavioural data collected by using 2,500 individuals are in agreement with the observations made in pilot experiments, and are maintained constant independently of whether animals where collected in the light or dark half of the day. Thus, experiments done with a higher density of larvae seem to be more stable independently on when the animals were collected. Taking the data into account, it is possible to conclude that an optimal quantity of 2,500 animals must be used in each assay to observe more clear patterns of movement of the larval population. Such a concentration is well balanced not only for avoiding an overcrowding of the plankton column, but also for maintaining a statistically meaningful number of specimens. Since the movement of using 250 larvae seems to be more accused while starting the experiment with larvae collected in the dark phase, following experiments were done collecting the animals at the end of the dark phase of the day. Even if this data set gave a similar pattern of larval behaviour, age, nutritional stage, and circadian clock must be carefully controlled during experimentation.

3.3.4 Experimental protocol IV: Main data collection, testing the vertical migration of four armed plutei under illumination of seven different wavelengths

For the experiments of this section, two graphical representations are provided. The left one is a heat map that shows the distribution of bright pixels (corresponding to a planktonic organism) as a function of density per unit of space per time, and the right one is a graph that shows the animal vertical distribution over the water column in each phase.

In the heat map (left side) we can observe two bars: the horizontal one under the heat map indicating the stimulus applied, and the vertical one at the right of the heat map informing about

the correspondence between the animal units (a.u.) and the colours represented in the graph (note that even if colours in the vertical bar are always the same ones, the relationship between colours and animal units' changes depending on how animals are grouped). Coinciding with the lower bar, five vertical parallel lines have been drawn to facilitate the reader to identify when a phase starts and ends, as well as when the stimulus is applied.

In the graph that shows the animal vertical distribution over the water column in each phase (right side), the mean vertical distribution of the animal density over the water column is represented. In this graph, there are two 'types' of phases represented: (i) the curves highlighted in colours correspond to phases I and III, thus being the ones recorded under light stimulus; and (ii) the ones highlighted in black that correspond to phases II and IV, therefore summarizing the two central phases recorded under no-light conditions. In each of these curves, the maximum density peak of animals has been indicated with a red dot. These red dots are connected to the phase number to which they correspond by a dotted line. Thanks to such levels it is easier to compare main differences in the centre of animal mass distribution for each phase. When there is a proximity correspondence within the picks of each kind of phase (i.e., when two light phase peaks are closer together than they would be to a dark phase peak; or vice versa) the experimental result is considered as solid and a photobehavioural conclusion can be made.

A) The behaviour of plutei under UV (340 nm) light

After determining an optimal quantity of animals of 2,500 specimens for each experiment, first main data were collected by using 340 nm UV as light stimulus in an intensity of $6{,}2x10^{7}$ photons d^{-1} sr^{-1} cm^{-2}. In Fig. 28A it is possible to distinguish a homogeneous distribution of animals during the phase 'S'. Such a distribution indicates that the rotations applied of the water

column prior to starting the experiment were successful in distributing the larvae homogeneously all over the water column. This step is important to 'disorient' the animals too. Similar starting conditions can be seen also in the phase 'S' of all other main experiments (Fig. 28B, C, D, E, F, and G), thus indicating that all experiments done started in similar conditions not just in terms of when animals were collected (end of the dark phase of the day), but also in their distribution over the cell. Following, in phase I the 340 nm UV stimulus was applied, and a net movement towards the base of the water column can be observed. In phase II, when the light stimulus was turned off, animals came back to the initial condition in which they were distributed relatively homogeneously all over the column.

These two phases (I and II) regime were repeated. While comparing this regime with the second round of repetition (phases III and IV), similar behavioural patterns can be observed. In phase V, animals were distributed mainly in the second half more closely located to the bottom of the cell, just as in phases I and III.

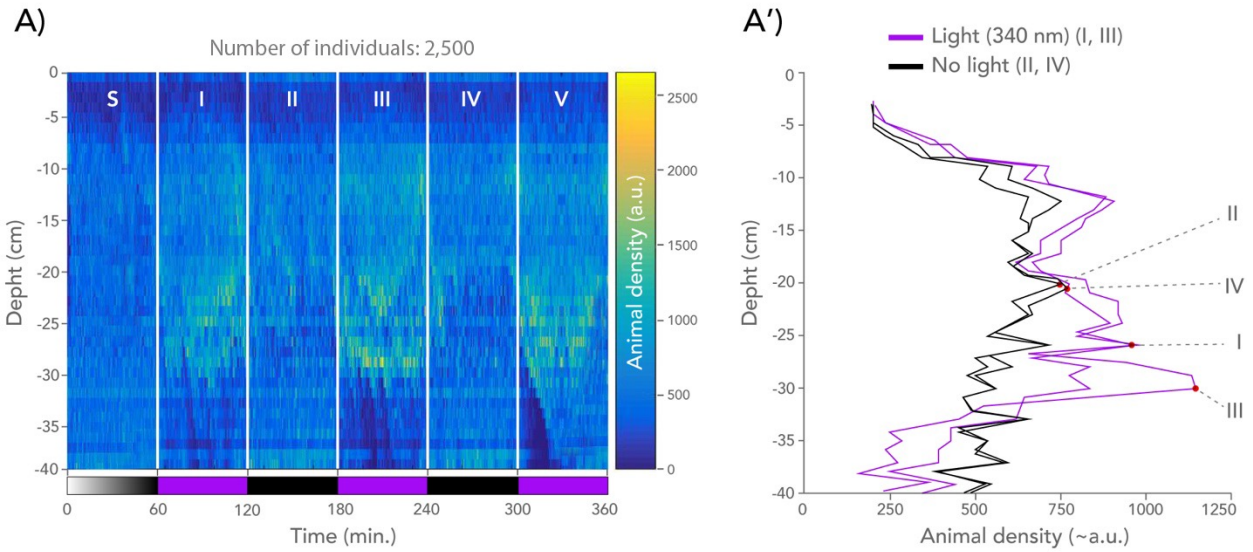

Fig 28. A) Heat maps showing the relative animal density along the height of the water column during UV 340 nm light experiment. Downwelling UV light in an intensity of 6,2x10^{7} photons d^{-1} sr^{-1} cm^{-2} was applied in phases I, III,

and IV. No light stimulus was applied in phases S, II, and V. S represents the stabilization phase. Warmer colours represent greater abundance of animals in the monitored area. A') Graphical representation of the mean animal density for each central phase (I to IV) along the height of the water column. The maximum animal density peak for each of these phases has been highlighted. There is a spatial coincidence of the light phases I and III peaks, and of the no light phases II and IV peaks.

When observing the graph that shows the animal vertical distribution over the water column in each phase (Fig. 28A'), a proximity correspondence within the picks of each kind of phase occurs. Thus, thanks to these data it is possible to state that four armed echinopluteus larvae tend to avoid 340 nm downwelling UV light in an average radiance of $6{,}2x10^{7}$ photons d^{-1} sr^{-1} cm^{-2}; and that the animal population prefers to be at 25-32 cm from the water surface while illuminating with this light source.

B) The behaviour of plutei under violet (420 nm) light

In this and following experiments, the light stimulus was always applied in an average radiance of $7{,}7x10^{7}$ photons d^{-1} sr^{-1} cm^{-2}. In the heat map that results this experiment (Fig. 28B) we can observe that animals repeat the previous distribution of animals during central no light phases (II and IV). On the contrary to no light phases, when a 420 nm violet light stimulus is applied, animals tend to aggregate themselves. Such aggregation can be better noticed while analysing Fig. 28B'. On this image (Fig. 28B'), the 420 nm light phases maximum peaks cluster in the -10 to -20 cm area of the water column, while the no light phases maximum peaks cluster in the -20/-25 region of the water column. This insight indicates that plutei may have a subtle light-driven gravitaxis behaviour for such a wavelength. This tendency is contrary to the one observed while applying UV light. In this experiment the larvae clearly aggregate during light stimulation avoiding both the top and the bottom of the column.

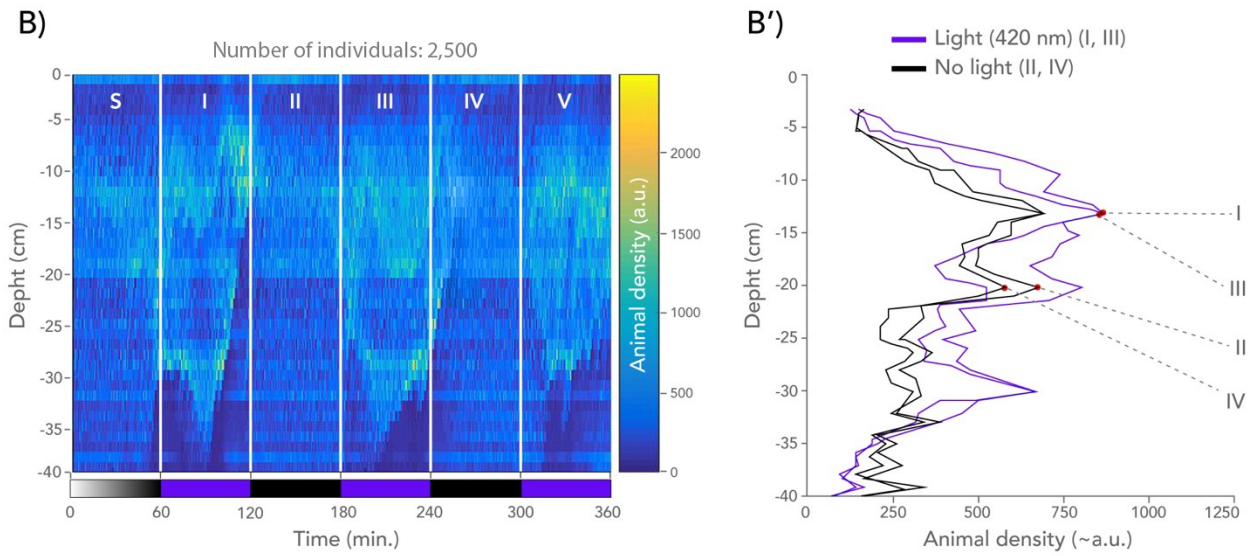

Fig 28. B) Heat maps showing the relative animal density along the height of the water column during violet 420 nm light experiment. Downwelling violet light in an average radiance of $7{,}7x10^{7}$ photons d^{-1} sr^{-1} cm^{-2} was applied in phases I, III, and V. No light stimulus was applied in phases S, II, and IV. S represents the stabilization phase. Warmer colours represent greater abundance of animals in the monitored area. B') Graphical representation of the mean animal density for each central phase (I to IV) along the height of the water column. The maximum animal density peak for each of these phases has been highlighted. There is a spatial coincidence of the light phases I and III peaks, and of the no light phases II and IV peaks.

C) The behaviour of plutei under blue (490 nm) light

In the heat map of this experiment (Fig. 28C) it is possible to observe that animals maintain a homogeneous distribution all over the column when no-light stimulus is applied, just as in previous cases. While observing the phases in which 490 nm blue light is applied, animals tend to aggregate themselves in the second fourth-section more closely located to the bottom of the water column, at 20 to 30 cm from the water surface (Fig. 28C'). The localisation of the animal population in this region while applying blue 490 nm light its similar to the one observed while applying UV 340 nm light, thus indicating that this light stimulus induces a light-driven gravitaxis behaviour in four armed echinoplutei. This condition, however, is less accused in this case with respect to the one observed while applying UV (maximum average peak of animal density under blue 490 nm for phases I and II: 800 a.u.; maximum average peak of animal density under UV for phases I and II: 950 a.u.).

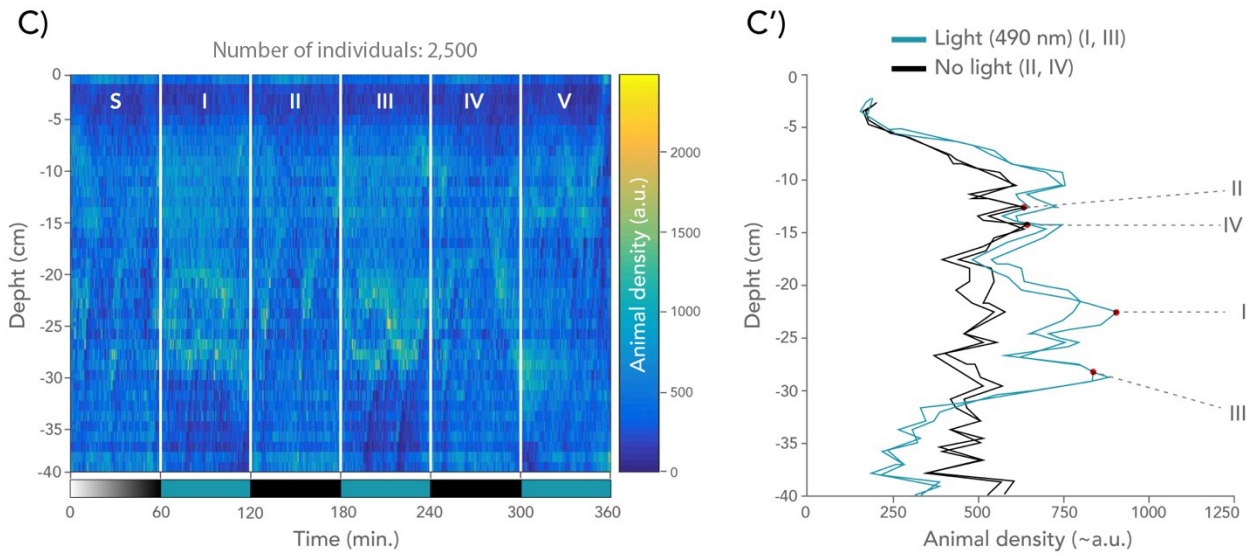

Fig 28. C) Heat maps showing the relative animal density along the height of the water column during blue 490 nm light experiment. Downwelling blue light in an average radiance of $7{,}7x10^{7}$ photons d^{-1} sr^{-1} cm^{-2} was applied in phases I, III and V. No light stimulus was applied in phases S, II and IV. S represents the stabilization phase. Warmer colours represent greater abundance of animals in the monitored area. C') Graphical representation of the mean animal density along the height of the water column during the central light (I, III) and no light (II, IV) phases of the experiment. The maximum animal density peak for each of these phases has been highlighted. There is spatial coincidence of the light phases I and III peaks, and of the no light phases II and IV peaks.

D) The behaviour of plutei under turquoise (505 nm) light

In the heat map of this experiment (Fig. 28D) animals also have a general homogeneous distribution when no-light stimulus is applied; still it is possible to see that the animal population is way more concentrated in the last five centimetres of the plankton cell. This animal concentration may be real or may be related to a misalignment of one of the IR LEDs. Moreover, when 505 nm light are tuned on (phases I and III), animals tend to distribute themselves in a similar pattern between the two phases, but in two clusters instead of one (Fig. 28D'). Such a 'two-cluster' disposition contrasts with the behavioural pattern found in previous experiments, were animals clustered in a single group. This 'division' of the population can be difficulty interpreted. Still, it is interesting to see that for the maximum animal density peak of light phase I (circa 1,100 animals; depth: -26 cm),

a second maximum animal density peak of phase III follows (circa 1,050 animals; depth: -29 cm); and that for the maximum animal density peak of light phase III (circa 1,120 animals; depth: -12 cm), a second maximum animal density peak of phase I follows (circa 1,100 animals; depth: -14 cm). Whether the 505 nm light cue or other cofounding factors induce the decision of this division must be further studied in future experiments. Maybe the larvae do not have any photosensible protein related to this wavelength, thus some of the larvae interpret this light in a different way respect to another's.

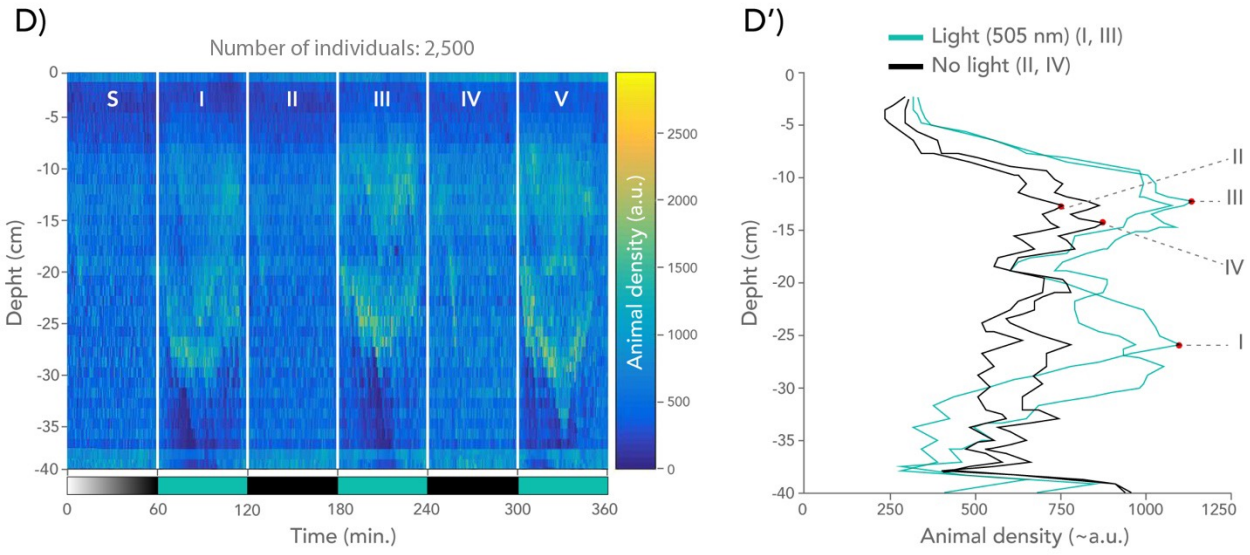

Fig 28. D) Heat maps showing the relative animal density along the height of the water column during turquoise 505 nm light experiment. Downwelling turquoise light in an average radiance of $7{,}7 \times 10^{7}$ photons d^{-1} sr^{-1} cm^{-2} was applied in phases I, III, and V. No light stimulus was applied in phases S, II, and IV. S represents the stabilization phase. Warmer colours represent greater abundance of animals in the monitored area. D') Graphical representation of the mean animal density along the height of the water column during the central light (I, III) and no light (II, IV) phases of the experiment. The maximum animal density peak for each of these phases has been highlighted. There is neither spatial coincidence of the light phases I and III peaks, nor of the no light phases II and IV peaks. Animals distribute themselves in two groups located at different depths when the light stimulus was applied.

E) The behaviour of plutei under green (535 nm) light

Bearing in mind the heat map of this experiment (Fig. 28E) we can observe that animals keep a homogeneous distribution all over the plankton cell when no-light stimulus is applied.

Furthermore, when 535 nm light is turned on (phases I and III) animals tend to distribute themselves in a 'two-cluster' disposition that resembles the one found in the experiment done by using turquoise 505 nm light as stimulus (Fig. 28E'). These similarities make sense considering that both light sources have a difference of 30 nm between each other, thus being possibly quite subtle for the larvae. During this experiment, the highest peak of animal density of phase I (circa 745 a.u.) is located at approximately 6.5 cm from the water surface. This peak almost overlaps with the second peak of animal density of phase III (circa 760 a.u.; depth: -6.5 cm). The highest peak of animal density of phase III (circa 900 a.u.; depth: -26 cm) is though not related to the second highest peak of animal density of phase I (circa 760 a.u.; depth: -7.5 cm). Since for this light experiment there is neither spatial coincidence of the light phases I and III peaks, nor of the no light phases II and IV peaks, this experiment has been considered as not conclusive.

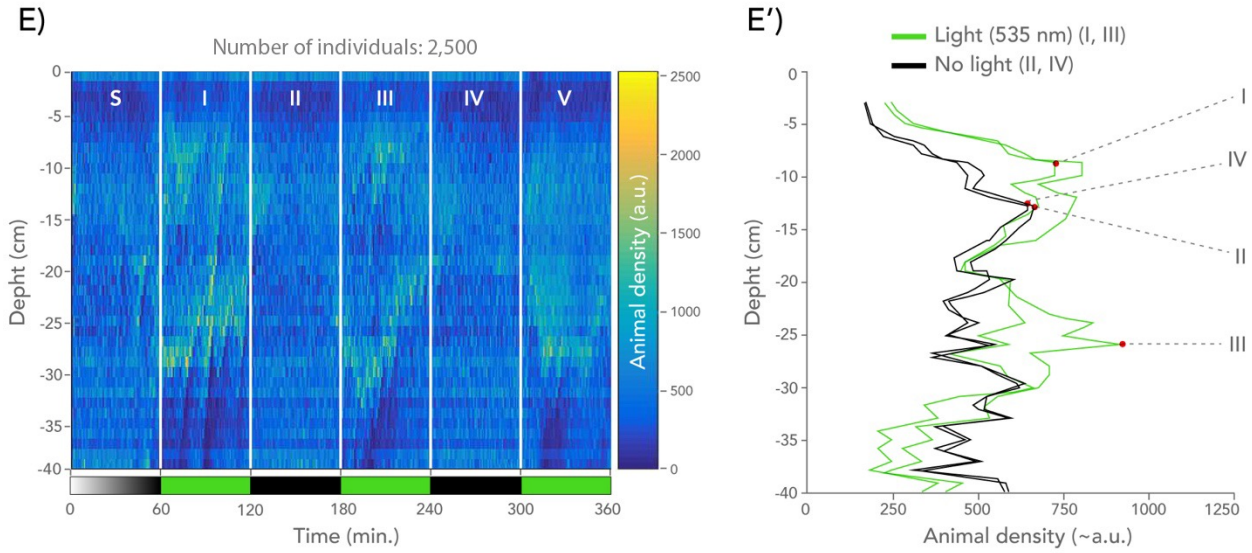

Fig 28. E) Heat maps showing the relative animal density along the height of the water column during green 535 nm light experiment. Downwelling green light in an average radiance of $7{,}7\times10^{7}$ photons d^{-1} sr^{-1} cm^{-2} was applied in phases I, III, and V. No light stimulus was applied in phases S, II, and IV. S represents the stabilization phase. Warmer colours represent greater abundance of animals in the monitored area. E') Graphical representation of the mean animal density along the height of the water column during the central light (I, III) and no light (II, IV) phases of the experiment. The maximum animal density peak for each of these phases has been highlighted. There is neither spatial coincidence of the light phases I and III peaks; nor of the no light phases II and IV peaks. Animals seems to distribute themselves in two groups located at different depths when the light stimulus was applied.

F) The behaviour of plutei under amber (590 nm) light

In the heat map of this experiment (Fig. 28F), animals show a homogeneous distribution over the plankton cell under no-light stimulus (phases II and IV); however, when having a look at Fig. 28F' it is possible to see that a notable part of the animals tend to be in the last 5 cm of the water column, like in the experiment D (505 nm turquoise light). When 590 nm 'amber' light is applied, and while looking the heat map, it is difficult to see if animals react with the same speed in comparison with previous experiments. However, from Fig. 28F' it is still possible to distinguish that while lights are on (phases I and III), animals group themselves between the section of the column located at a distance of 27 to 34 cm from the surface. This information suggests that when 590 nm amber light is applied in an average radiance of 7,7x10^7 photons d^{-1} sr^{-1} cm-2, echinoplutei go towards depths of -27 to -34 cm.

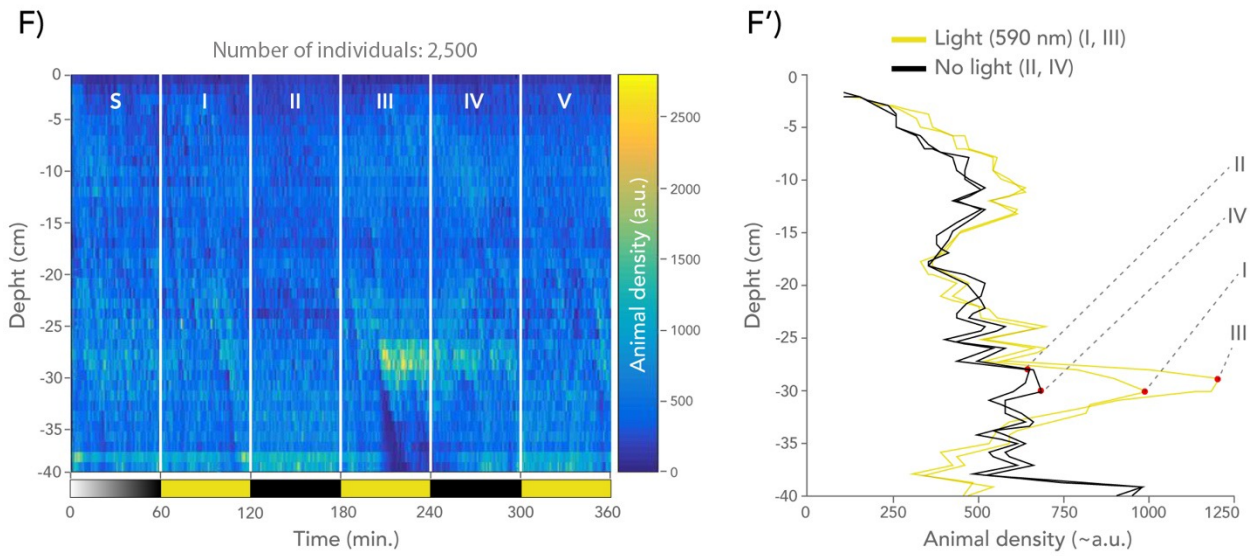

Fig 28. F) Heat maps showing the relative animal density along the height of the water column during amber 590 nm light experiment. Downwelling amber light in an average radiance of 7,7x10^7 photons d^{-1} sr^{-1} cm^{-2} was applied in phases I, III, and V. No light stimulus was applied in phases S, II, and IV. S represents the stabilization phase. Warmer colours represent greater abundance of animals in the monitored area. F') Graphical representation of the mean animal density along the height of the water column during the central light (I, III) and no light (II, IV) phases of the experiment. The maximum animal density peak for each of these phases has been highlighted. There is spatial coincidence of the light phases I and III peaks; and of the no light phases II and IV peaks.

G) The behaviour of plutei under orange (617 nm) light

Taking into consideration the heat map of this experiment (Fig. 28G), animals exhibit a homogeneous distribution over the plankton cell under no-light stimulus (phases II and IV). Conversely, when 617 nm orange light is applied (phases I and III), animals seem to have a quite strong pattern of distribution towards the upper half of the water column. Such a concentration is not just observed in the heat map (bear in mind that the heat map colour scale is adjusted depending on the average concentration of animals all over the cell), but also from Fig. 28G'. This information suggests that when 617 nm orange light is applied in an average radiance of $7{,}7x10^{7}$ photons d^{-1} sr^{-1} $cm^{-}2$, plutei tend to be in the 2 to 20 cm region from the water surface. This is a peculiar and unexpected response (larvae very suddenly appear in the upper part of the column without decreasing in density in any other part). A possible explanation of that is that the cameras of the set up are able to perceive some amounts of the 617 nm stimulus light.

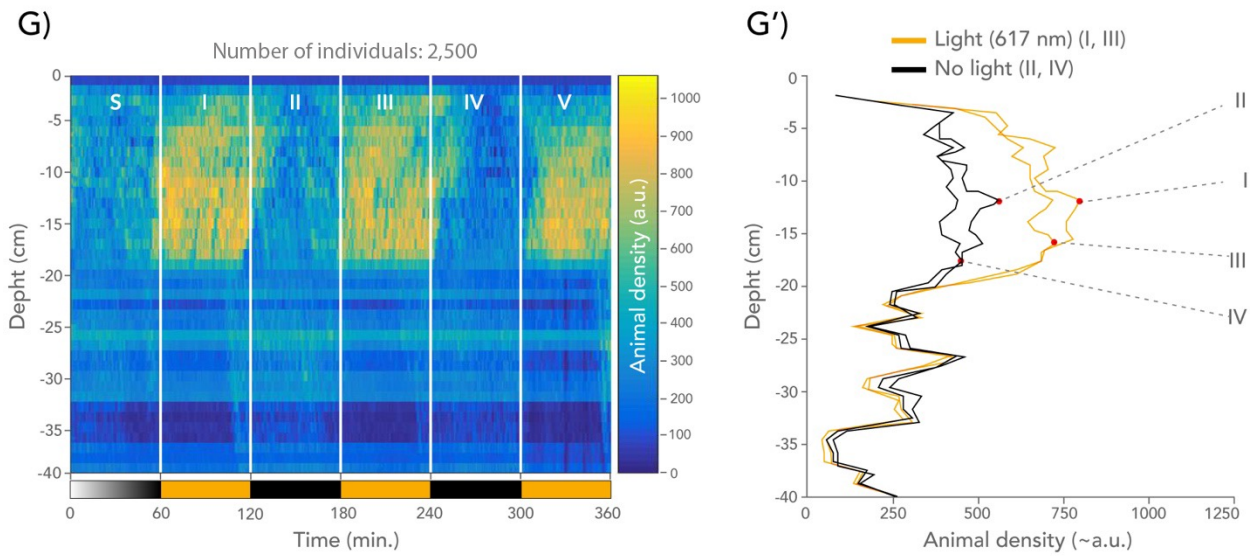

Fig 28. G) Heat maps showing the relative animal density along the height of the water column during the orange 617 nm light experiment. Downwelling orange light in an average radiance of $7{,}7x10^{7}$ photons d^{-1} sr^{-1} cm^{-2} was applied in phases I, III, and V. No light stimulus was applied in phases S, II, and IV. S represents the stabilization phase. Warmer colours represent greater abundance of animals in the monitored area. G') Graphical representation of the mean animal density along the height of the water column during the central light (I, III) and

no light (II, IV) phases of the experiment. The maximum animal density peak for each of these phases has been highlighted. There is spatial coincidence of the light phases I and III peaks; and of the no light phases II and IV peaks.

All together, these data suggest that, while keeping temperature, salinity, oxygen, and animal concentration in similar ranges, light is a cue factor involved in the vertical migration movements of four armed *Paracentrotus lividus* larvae in absence of predators.

3.4 Discussion and future directions

Quantitative studies of plankton biology in the natural setting are fraught with difficulties. The open ocean represents a complex environment with many changing variables such as light, salinity, temperature, density of the populations, or diversity of animals encountered. Thus, it is useful to combine field and controlled laboratory experiments. To facilitate current studies on the vertical migration of small planktonic transparent larvae, a portable custom-built set up was designed and used. This device allows not only the fine tuning of light intensity, but also the wavelength of stimuli provided in a single assay. Other variables (e.g. salinity, temperature, oxygen level, lack of predators, or density of the population) can be kept constant to reduce confounding factors.

Thanks to this set up and by studying the echinopluteus larvae of *Paracentrotus lividus* at four armed stage (seven days' post fertilization), it is possible to state that small animals equipped with non-directional photoreceptors, the simplest photoreceptors possible, are still capable of perceiving light stimuli as well as undergoing vertical migrations. This has been demonstrated by the behavioural pattern exhibited by these Ambulacraria larvae under different light conditions. More in detail, out of the seven light sources provided as stimulus, five (UV 340 nm, violet 420 nm, blue 490 nm, amber 590 nm, and orange 617 nm) are the ones showing a clearer differential behaviour in comparison with the no-light phases of their respective experiments. The light stimuli situated in the 'green' range of visible light (turquoise 505 nm and green 535 nm) instead

did not give consistent results. This may indicate that: (i) the larvae do not care much about lights in this range of wavelengths; and (ii) since this light may not be of ecological relevance for the larvae, there is a possible lack of photosensible proteins associated with this range of lights. Even if the lack of time and resources do not allow me to compare day and night behaviours of larvae both well fed or hungry, neither to do more rounds of experiments for each of the wavelengths at different intensities, taking these insights as starting point, some relevant ideas can be discussed.

3.4.1 Correlations found between the genomic and transcriptomic data of this species and its behavioural pattern

Nine opsin genes have been found in the genome of *Paracentrotus lividus*: one *r-opsin*, two *c-opsin*, three *Go-opsins*, one *echinopsin*, one *peropsin*, and one *RGR-opsin* (D'Aniello et al., 2015 and herein, Chapter 1). As it is widely known, genomic data cannot tell us if all these genes are expressed during the life cycle of the animal or not, so more remotely can inform us about its expression during a specific larval stage. However, the encoding of more than one opsin sequence in the genome of *P. lividus* already indicates that this animal has, in principle, the capacity to express an important number of opsin proteins and thus, the potentially to respond to a number of different light stimuli all over its life cycle (Table 4). Indeed, such a genomic information is consistent with the variety of behaviours exhibited by the larvae used during our experiments. When investigating the transcriptomic data available for such an echinoderm species (data generated by the Genome Sequencing Consortium Génoscope, Corbel project infrastructure: www.corbel-project.eu), we found that six opsin genes are activated at four armed larval stages (Fig. 29). Of those, just one, the *Pl-opsin3.1.2*, have a higher expression with respect to other opsins found (26.00 read counts). This number of opsin-encoding genes allows us to better estimate the availability of photosensible proteins of this group at the developmental stage where we perform the behavioural assays.

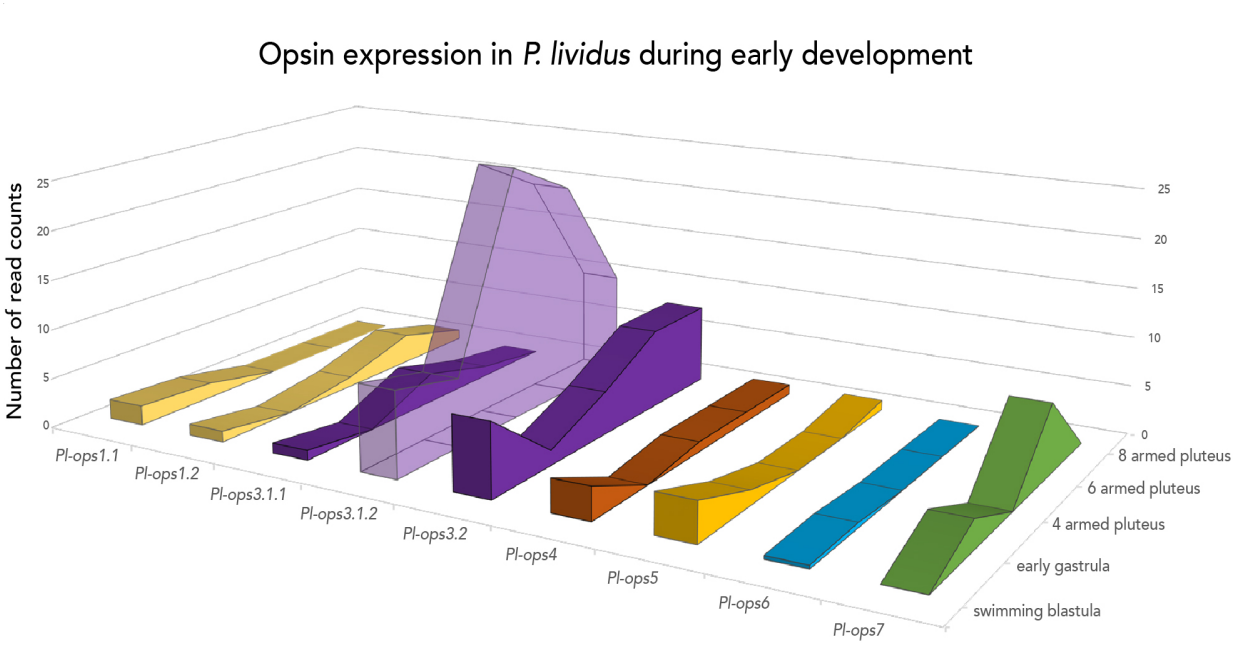

Fig 29. Gene expression profile of the opsins found in *Paracentrotus lividus* during early development. Of the nine opsins found in *P. lividus*, the *Pl-opsin3.1.2* is the highly expressed one at four armed pluteus stage. Opsin counts were quantified by Dr. Elijah Lowe (Stazione Zoologica Anton Dohrn, Italy) by using the Salmon 8.2 quasi-mapping-based mode (Patro et al., 2017). Data source: Genome Sequencing Consortium Génoscope, Corbel project infrastructure (www.corbel-project.eu).

Table 4 – OPSIN EXPRESSION IN *P. LIVIDUS* DURING EARLY DEVELOPMENT

OPSIN GROUP	GENE NAME	SWIMMING BLAS-TULA	EARLY GASTRULA	4 ARMED PLUTEUS	6 ARMED PLUTEUS	8 ARMED PLUTEUS
C-opsins	*Pl-opsin1.1*	1.99	1.53	0.00	0.00	0.00
	Pl-opsin1.2	1.13	0.00	1.00	3.00	1.00
Go-opsins	*Pl-opsin3.1.1*	1.00	0.00	3.00	1.00	0.00
	Pl-opsin3.1.2	8.73	7.00	26.00	22.00	10.00
	Pl-opsin3.2	7.50	1.50	4.40	8.00	8.00
R-opsin	*Pl-opsin4*	3.32	0.00	1.00	1.00	1.00
Echinopsins	*Pl-opsin5*	4.00	1.50	0.00	0.00	1.00
Peropsins	*Pl-opsin6*	0.33	0.50	0.00	0.00	0.00
RGR-opsins	*Pl-opsin7*	0.01	2.92	0.01	7.16	0.00

Table 4. Gene expression profile of the opsins found in *Paracentrotus lividus* during early development. Of the nine opsins found in *P. lividus*, the *Pl-opsin3.1.2* is the highly expressed one at four armed pluteus stage. Opsin counts were quantified by Dr. Elijah Lowe (Stazione Zoologica Anton Dohrn, Italy) by using the Salmon 8.2 quasi-mapping-based mode (Patro et al., 2017). Data source: Genome Sequencing Consortium Génoscope, Corbel project infrastructure (www.corbel-project.eu).

3.4.2 An energetically trade-off: Having various opsins expressed during early development could 'compensate' the lack of cell specializations founded in the class I photoreceptor cells of the echinopluteus

While comparing the relatively high number of opsin putatively expressed in this echinoderm larva with the morphological simplicity found in the cells that populate the apical organ of other plutei (Valero-Gracia et al., 2016 and herein, Chapter 2), it is interesting to observe that these larvae seem to lack of highly-modified sensory cells. None of the cells found in our electron microscopy works seem to be neither rhabdomeric nor ciliary, and apparently the lack of cell-specialization of this kind also occurs in other plutei (Thurston Lacalli, University of Saskatchewan, Canada; and Robert Burke, University of Victoria, Canada, personal communication). Maybe the photoreceptor system of the larva is adapted to provide differential photic responses in situations where light is not very limited. Therefore, the development of further specializations of the cell membrane in form of cilia or rhabdoms is not needed for packing more opsin proteins in a limited space. This lack of complex cellular morphologies could be ascribed to a save-of-energy strategy. Indeed, the quoted energy saved could be dedicated instead to other vital functions such as the functioning of the ciliary band (the main purpose of the larva is to facilitate the dispersion of the animal population), or to the development of the adult rudiment. This 'saving-energy by means on keeping cellular simplicity' strategy match well when taking into the ecological context of the animal (adult sea urchin populations of this species are usually located at sub littoral areas to about 30 metres' depth, thus regions where almost all lights of the visible range arrive in good quantities). But, if there is a real lack of membrane specializations in this photoreceptor cells, the question is: does this morphology reflect an ancestral character, or rather a secondary loss from more

complex cellular specialisations? Unfortunately, this is a question that most probably will remain open for a while. For having a proper answer in this matter it will be necessary to collect morphological data of the photoreceptor cell structure of a number of echinoderm species outside of this echinoid clade, as well as to compare it with the available fossil record.

3.4.3 Echinoplutei exhibit a variety of light-driven behavioural gravitaxis patterns depending on the light stimuli provided

While the morphology of the studied cells in the vicinity of the apical organ is relatively simple, a notable number of opsin proteins may 'compensate' this situation by adding sensitivity to the photoreceptor system in a discretional way. This information results quite interesting because, while some classical studies assessed that "there is no evidence that there are photoreceptors in the pluteus larvae" (Hyman, 1955) or that "there is no evidence that plutei undergo an ontogenetic vertical migration" (Thorson, 1964; Forward, 1976), our current data (both behavioural and of gene expression) indicates the contrary; thus, that echinoids of this clade have opsin positive cells flanking the apical organ during larval stages (Valero-Gracia et al., 2016); and that plutei have a differential light-driven gravitaxis that seems to depend on the light stimulus provided. In other words, the echinopluteus photoreceptor system might be potentially able to 'discriminate' between different colours even if its photoreceptor system is very crude in regards to resolution.

Perhaps this variety on the light-driven behaviours exhibited explains the discrepancies of previous studies done with sea urchin larvae, investigations in which the light stimuli provided were not as controlled as in here due to technical

limitations that can be ascribed to such historic moment (Lyon, 1906; Runnström, 1918; Mortensen, 1921; Fox, 1925). If the animal has maintained or developed such a variety of opsins during evolution, there must be an ecological advantage associated to this condition. So, the next question to be done must be: is this animal larva able to discriminate between different light wavelengths? For answering such a mystery, response/intensity curves at different wavelengths have to be made. Even if the experimental results here shown are not totally conclusive it is that the larval population have a different light-driven gravitaxis behaviour that may depend on the light stimuli provided (Fig. 30).

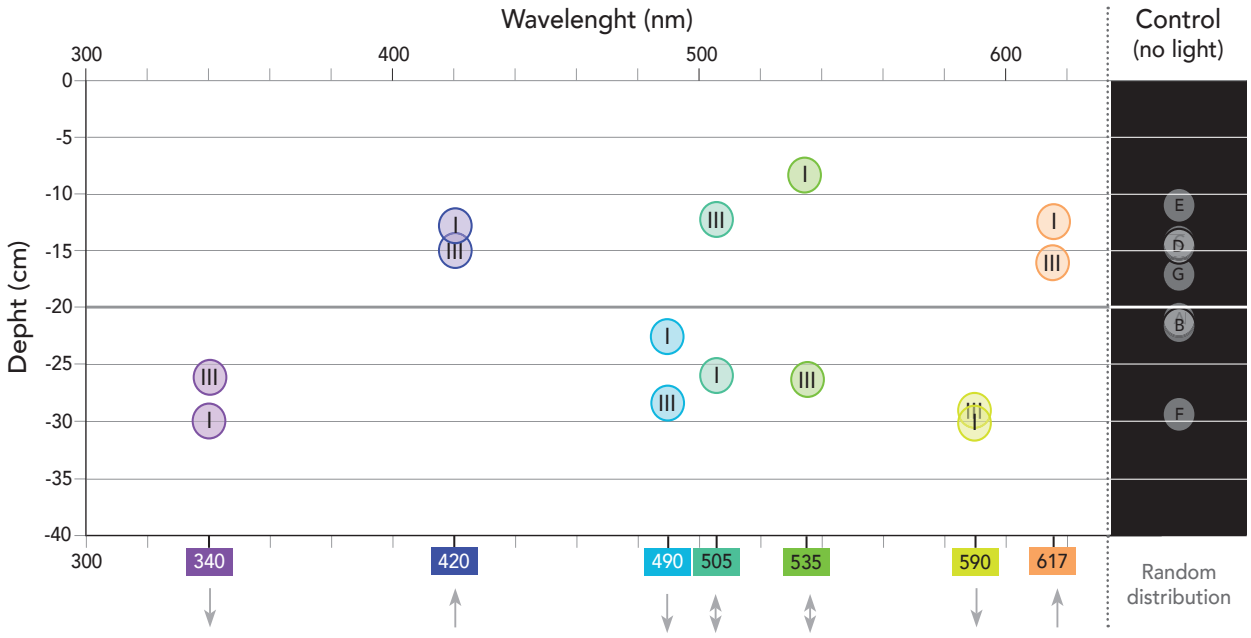

Fig 30. Larval distribution over the water column while applying different light/no-light stimuli. Left side: the seven pair of circles indicate the maximum concentration of larvae during a certain light phase of the experiments done. Roman numerals indicate which light phase of each experiment represents such data point. The colour of the circle is indicative of the wavelength used during such experiment. Arrows indicate the mean movement of the animal population with respect to the centre of the water column (-20 cm). Right side: larval distribution over the water column in phase II (no-light) for each of the seven experiments reported above. Each grey circle represents the maximum peak of distribution of animals during no light conditions. Letters (A to F) indicate to which of the seven experiment each circle belong.

While illuminating our water column with 340 nm UV light we can observe a net movement of the larval population towards the second lower half of the water column. UV light of this wavelength can be found roughly till depths of 15 to 20 meters depending on water clearance (Holm-Hansen et al., 1993). Taking into account that UV light induces DNA mutations and that the larvae carried all the genetic material necessary not only for itself, but also for the adult that will later on develop, the selection of a photoprotein that senses this wavelength is a great adaptive character. These data are in agreement with previous studies (Mortensen, 1921; Fox, 1924; Pennington and Elmet, 1956).

While illuminating out the plankton cell with 420 nm violet light, the situation is the contrary one. Animals tend to go upper in the water column. Violet lights in this range are present almost all over the first section of the water column until 130 to 150 meters in depth. Since in this second experiment just one wavelength has been provided, it seems logic that animals behave actively swimming towards the upper half of the water column (other lights commonly associated with surface oceanic layers were not present, therefore in this situation we are mimicking the photic situation available in regions below 130 meters from the water surface). In this region not only algae are less abundant, but also such niche may be too in depth for settling (remember that adult urchins of this species use to be at less than 50 metres in depth).

It is trickier to comment the situation observed while illuminating larvae with 'blue-green' lights. In the first of this experiments (490 nm 'blue' light) animals situated themselves in the second lower half of the water column. In the second (505 nm 'turquoise' light) the animal population divides itself in two groups, one going below the centre of the water column, and another going above. This situation is similar to the one present while applying 535 nm 'green' light, but in this case the differences between both phases is even larger. Given these data into account, it seems

that larvae move themselves freely both upper and lower in the water column while these lights are applied to the plankton cell. This may indicate that larvae are ok under these light conditions; thus, no particular movement of the population is observed.

While examining the behaviour found while applying 590 nm 'amber' light, it is interesting to see that larvae tend to go towards the lower half of the column, just as while applying UV light. Both of these lights (UV 340 nm and amber 590 nm) are founded in the first 10 metres from the ocean surface. Maybe larvae prefer to stay under this shallower area of the water column to avoid DNA damaging and predators. It is interesting to observe that larvae illuminated with 617 nm 'orange' light tend to go to the second upper half. While interpreting this data point was difficult at first (a very close light source situated at 590 nm in the spectra gave us the opposite pattern of movement), then we realize that some of the algae that these animals fed (e.g. *Rhodomonas* sp.) have this colour (690-710 nm) in their chlorophyll (Kaňa et al., 2012). All together, these insights indicate that larvae might have two sets of photoproteins: one set used as a depth-gauge mechanism, and another set dedicated to perceive their algal food source in great concentrations.

3.4.4 A mechanistic model for understanding simple photodetection

The data presented in this chapter provide information about how an animal equipped with non-directional photoreceptors is able to vertically orient itself in the water column depending on light stimuli. To further discuss the observations done herein I propose a speculative, simple depth-gauge model that could explain the disparities reported in previous studies done with pluteus larvae of this and other species.

To regulate vertical position, a zooplankter must orient vertically, and move either up or down in response to environmental cues indicative of depth (Creutzberg, 1975; Mileikovsky,

1973). Orientation can be controlled by active sensory structures such as statocysts, or by passive mechanisms such as differential drag on body regions, spiral swimming, or non-uniform body density (Chia et al., 1984; Pennington and Emlet, 1986). In the case of the sea urchin larva, the body mass distribution is asymmetrical, and it orients the animal apex-down (Pennington and Emlet, 1986), as represented in Fig. 31. Given this morphology and mass distribution, in the absence of ciliary beating, the animal tends to fall.

Taking this into account, and in conjunction with the photobehavioural data presented here, I propose that 340 nm UV-avoidance behaviour is mediated by the ciliary-arrest of the ciliary band that rims the aboral side of the animal. This mechanism could explain a putative non-directional UV light sensitivity mediated by one of the opsin expressed in the transcriptome of the larva at this stage (most probably the Go-opsin *Pl-opsin3.1.1* for being the most expressed one at the studied larval stage; the ortholog of this Go opsin *Pl-opsin3.1.1* is the opsin *Sp-opsin3.2*, a molecule localized in two cells that flanks the apical organ of the larva, for more details see Chapter 2). If this pair of cells are mediating UV light responses, the light information may be integrated by the apical organ, resulting in the arrest of motile cilia that compound the ciliary band (Fig. 31A). Given the shape and mass-distribution of the larva, it is a logical conclusion that the animal, in the absence of moto-ciliary movement, falls. Once the larva reaches an area with less UV radiation a second opsin or opsins, that are yet undiscovered, could re-activate the ciliary beating (Fig. 31B). This double-feedback loop could allow the larva to maintain its position in the water column in a depth-gauge system. This system would allow the animal to guide itself in the water column towards a photic area where algae can be found, but still below the region where intense UV radiation can damage it. This behavioural model partially unites the metabolic hypotheses (the 'why'), with the light dependent hypotheses (the 'how'), thus demonstrating once more that complex biological systems are intimately coordinated.

Another interesting observation made during our experiments that support this depth-gauge system hypothesis is the slow sinking speed of the sea urchin larva (average mean speed of sinking of 0.6 cm per minute). Because sea urchin larvae seem to migrate very small distances vertically, could be that none of the standard diel vertical hypotheses can be apply to this study case. One possibility is that sea urchin larvae stay very high up all the time. This would place them constantly in the upper layers where their phytoplankton food stays all the time. Note that phytoplankton are also very restricted in how far up and down they can move. Phytoplankton need to be high up to get much light for photosynthesis, but they may also want to avoid the high UV levels just under the surface. The same may then apply to sea urchin larvae: stay high up in the water column where the phytoplankton is, but avoid getting very close to the surface because there is too much harmful UV-light.

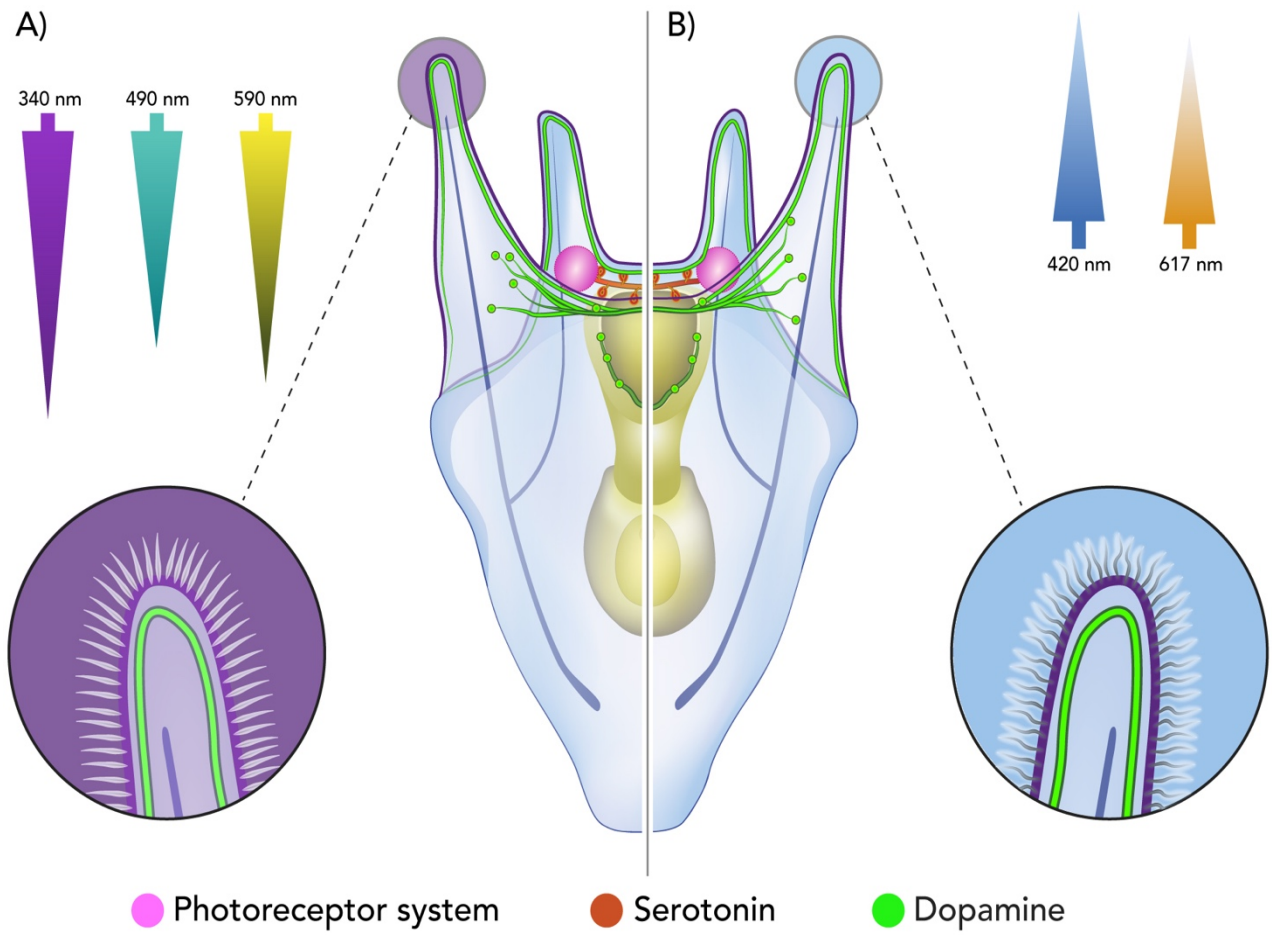

Fig 31. Depth-gauge system-model that explains the vertical migration movement of ciliated larvae in the water column in response to light cues. Light information is integrated by the larval nervous system: A) In presence of 340, 490, and 590nm light stimuli, ciliary beating ceases and the animal falls to avoid UV damage. B) In presence of 420 and 617 nm light stimuli, the ciliary beating is activated and the larva may move upwards to reach the photic area where oxygen and nutrients are found.

3.4.5 Future directions

Through these experiments we were able to establish that (i) plutei perceive light cues; (ii) that plutei can control their vertical position in the water column; and (iii) that plutei may potentially discriminate between different light stimuli. However, these experiments were a repeat of one (i.e., these experiments are a n=1). More repetitions of each of these experiments are needed to disentangle how light affects the behaviour of these animals are needed. Since time and resources for this research are limited, coming up next I would like to provide some guidelines to be follow. Further complementary directions related to this chapter and to other chapters are also described in 'Conclusions and future perspectives'.

As stated, the echinopluteus larva is potentially able to discriminate between several light wavelengths. An indication of it is the behavioural data obtained during our experiments. Still, to better understand the light-driven gravitaxis behaviour of this larva, it is necessary to create response/intensity curves at various wavelengths. Such experiments can be easily done by following the protocol here established for the main data collection, and by applying a number of neutral density filters to decrease the transmittance intensity of the light stimuli provided by different log orders of magnitude. For better mimicking the gradient of light available at different depths of the ocean, an IR transmitting dye absorbing in the same wavelength as the stimulus light can be used. Furthermore, it would be interesting to compare the modulation of

the vertical position of the animals while mixing different light wavelengths. Moreover, a number of assays in which nutritional stage and circadian clock differs may help to accept or confute the depth-gauge model that I have propose. All experiments have to be done over the early development of the animal, thus starting from swimming blastula and till eight armed pluteus stage. It would be interesting then to compare the different behaviours observed over the development with the available transcriptomic data of this and other close related species.

Our experiments have been done 'assuming' that these *Paracentrotus lividus* larvae are equipped only with non-directional photoreceptors. Still, to confirm this idea, another behavioural set up in which it is possible to change not just the light stimulus provided, but also the direction of the light source, would be needed. This machine will enable to rule out the possible use of any of the internal structures of the animal as shedding pigment to undergo directional photoreception (Fig. 32). Such a set up will follow the design and optical principles that apply for our Dial Vertical Migration set up II, but changing the shape of the water column and adding a number of identical modules side by side located. Thanks to this new set up it would be possible to provide to the larvae a bigger environment where they can move more freely too, thus decreasing the Reynolds number created by the walls of the water column. The availability of having five modules repeated will enable a better comparison of the same biological replica behaviour under the same or different light regimes even while light is coming from different angles. Overall, this study has provided a rich and interesting experimental framework to be continued by future investigations.

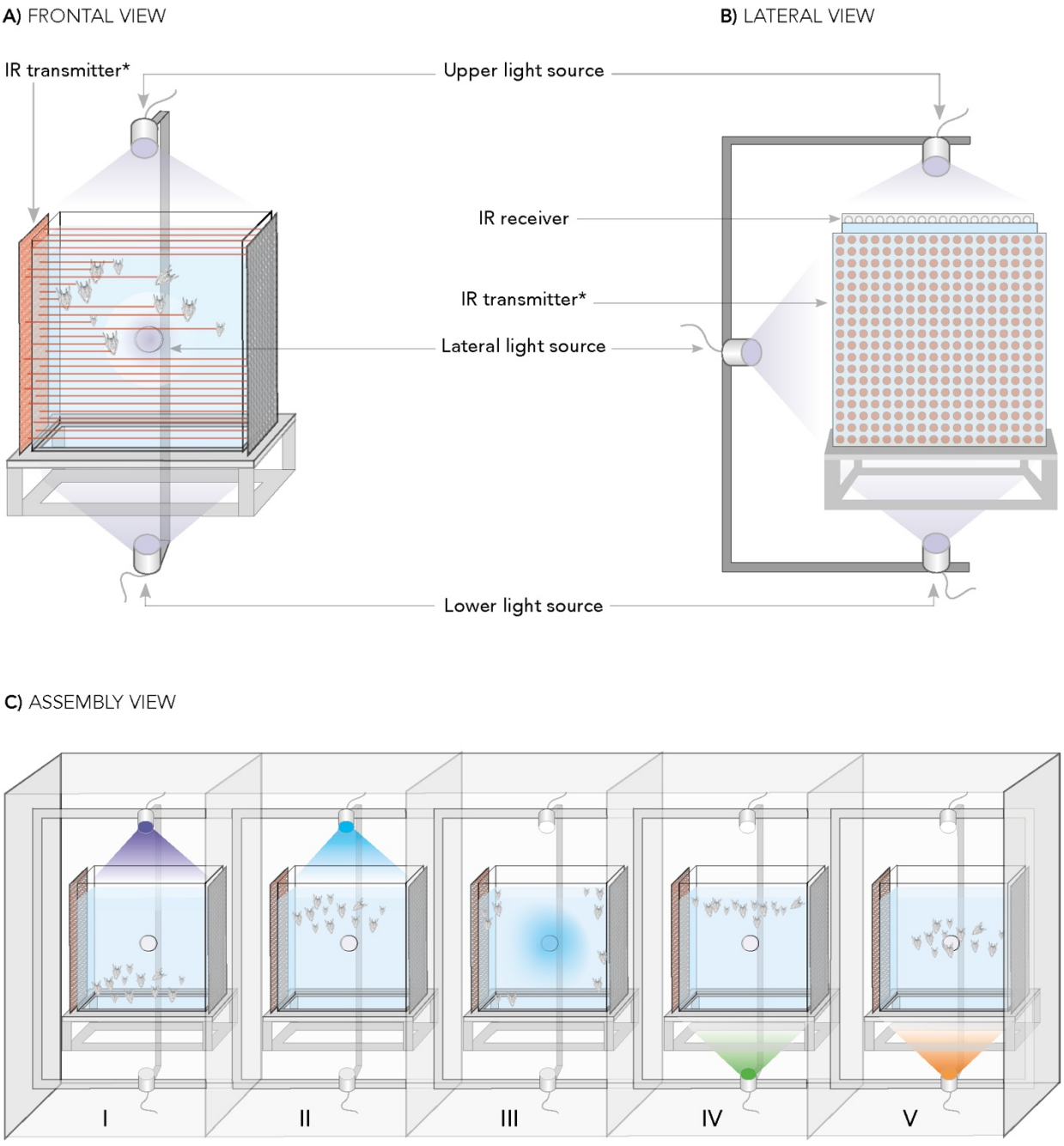

Fig 32. The 'Plankton Cube', a new behavioural set up to be build, do allow to direct the light source from different sides to rule out 3D phototaxis by decreasing the possibility of distraction of the larvae by the walls of the water cell. A) Each of the cubes is based on the same IR scattering principle of the larvae with respect to the water to trace the movement of the larvae. B) The whole set up consists in five cubic modules that allow the researcher to perform various experiments at the same time.

3.5 Material and methods

3.5.1 Vertical migration (VM) set up I: A prototype for doing the pilot experiments

First pilot experiments devoted to test if echinoplutei were able to undergo light-driven gravitaxis were done with a prototypic home-made set up prepared at the Stazione Zoologica Anton Dohrn (Naples, Italy). Such a set up consisted of five 50 mL laboratory cylinders (internal diameter: 2.2 cm; total height: 18 cm), a black box, a 'white' fluorescent light source, and a timer that turns on and off the light source (Fig. 33). Having five cylinders allowed to do five technical replicas for each round of experiments while using the same batch of animals. The laboratory cylinders were covered all over their walls but in two longitudinal parallel sides with black tape to exclude lateral light penetrance. The uncovered areas were used as 'windows' to assess the approximate vertical position of the animals inside the prototype plankton cell (Fig. 33).

The movement of the larvae was assessed by comparing the position of the larval population in the water column at different time points. For observing the position of the larval population in the water column at a given time point, a flashlight equipped with a red filter was used. To reduce the influence of lateral light during experiments, windows were covered with black cardboard all over the time except when controlling the position of the larvae. Such cylinders were located inside the quoted black box equipped with an upper fluorescent lamp Philips Master TL-D Super 80 (approximate range of wavelengths: 380-700 nm; luminous flux according to the manufacturer: 1,300 lm).

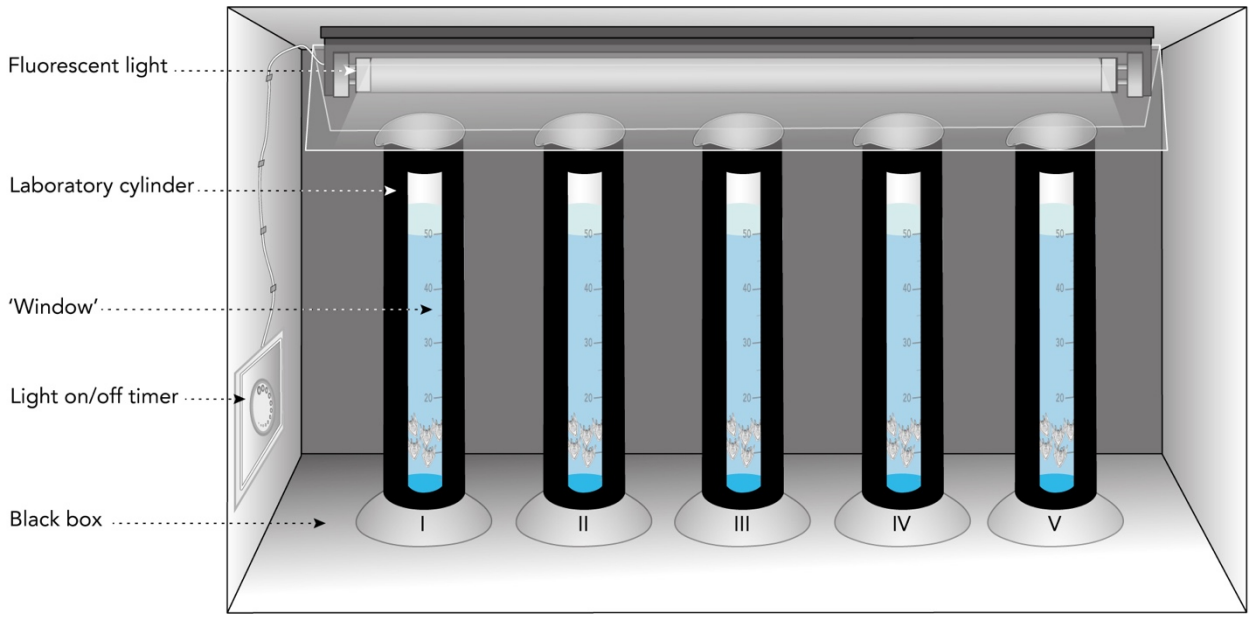

Fig 33. Vertical migration set up I. This simple set up consist a box that contains five 50 mL laboratory cylinders (I to V) covered with black tape to exclude lateral light penetrance, a fluorescent white light source, and a timer to regulate the turning on and of of the white-light fluorescent bulb.

3.5.2 Vertical migration (VM) set up II: Hardware design and optical principles

A more sophisticated set up (VM set up II) was later created in Lund University (Lund, Sweden) for better controlling the light stimuli provided to the animals as well as the vertical animal migration during the experiments. This second set up created consists of a 410 x 20 x 20 mm cell (from this point onwards, the 'plankton column' or 'cell') that aims to mimic the first section of the oceanic water column in a scaled way, plus a number of IR LEDs that creates a light sheet (Fig. 34A). Such IR light source interacts with the transparent larvae, thus allowing to record the position of single individuals of the animal population by the IR cameras in absence of visible light (the larvae are detected by the scattering of IR light that they cause; direct IR does not reach the cameras). As light stimuli, seven different light sources (340, 420, 490, 505, 535, 590, and 617 nm) selected for its biological relevance and different penetration rate in the water column were used. Such light sources can be

fully controlled in terms of radiance thanks to an electronic LED controller. The construction is completed with two IR cameras (1.3-megapixel mono GigE PoE infrared cameras; Blackfly, Richmond, BC, Canada), a 50/50% broad band beam splitter, a control panel, and some other optical components (Fig. 34A-F). The contraption has a portable size of 440 x 520 x 300 mm. The drew up of this device was done by Prof. Dan Eric Nilsson (Lund University, Sweden) and built by Dr. A. Darudi (Light Guide in Lund AB, Lund, Sweden) with some help of John Kirwan (Lund University, Sweden) and me.

The plankton column is illuminated by two parallel rows of IR LEDs from the right side (Fig. 35A). Each row has an array of LEDs that overlaps its illumination with the parallel one to avoid any dark area over the plankton column (Fig. 35B). On the left side of the plankton column, a mirror reflects the IR light scattered by the animals swimming on the cell, thus allowing to decrease the distance between the camera and the IR arrays (Figs. 34D; 35B). The light scattered then reaches the two IR cameras that are beside the column (Figs. 34E; 35B; 36A). Each camera faces an area of 210 mm of the plankton cell: one used for the upper half, and the other one for the bottom half. Both cameras record an overlapping area of 10 mm that corresponds to the middle point of the plankton column. This overlapping area is necessary to combine the data from both cameras. Above the column, an adjustable LED provides a light source (Figs. 34C; 36B). A second LED holder ready to be used is positioned at 90º with respect to the LED located above the column (Figs. 34C; 36B). A 50/50% beam splitter is positioned at 45º at the intersection of both light sources. This beam splitter can be used to blend light from both light sources, if necessary (Fig. 36B). Different LEDs can be mounted and interchanged by adjusting the LED chip host.

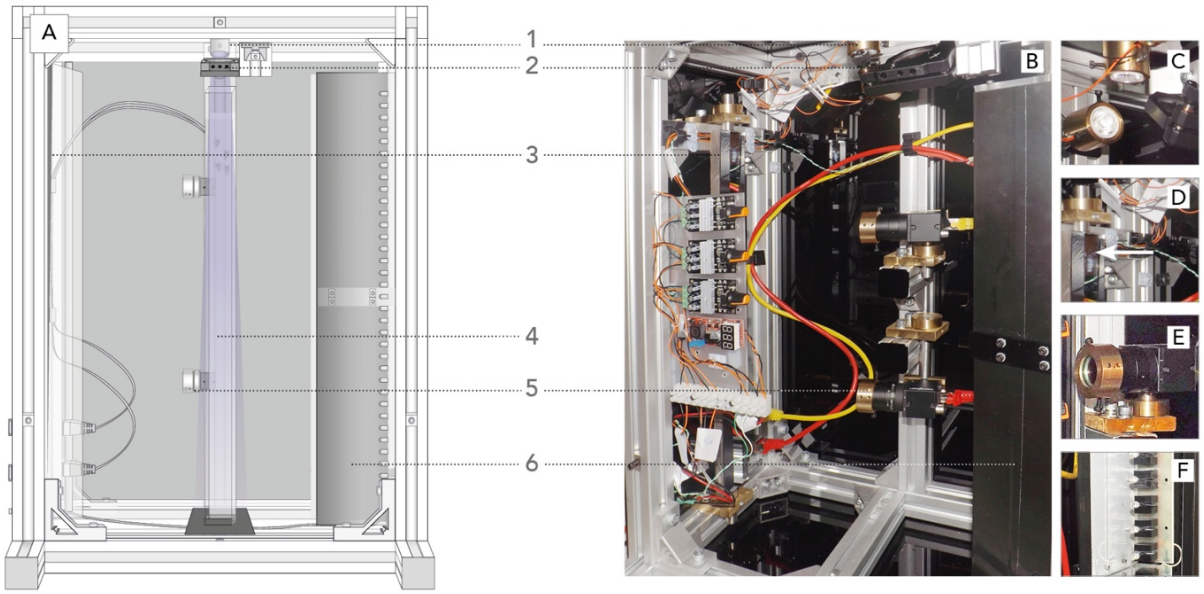

Fig 34. Vertical migration set up II. A) Schematic drawing of the device; illustration made by Santiago Valero-Medranda. B) Photograph of the device, frontal view. C) Light stimuli LEDs. D) Mirror (arrow head). E) One of the IR cameras. F) Array of square IR LEDs used as a light source for recording the animals. Numbers indicate: 1) light-stimuli LEDs; 2) beam splitter; 3) mirror; 4) plankton column; 5) IR camera II; 6) IR light sheet bulkhead.

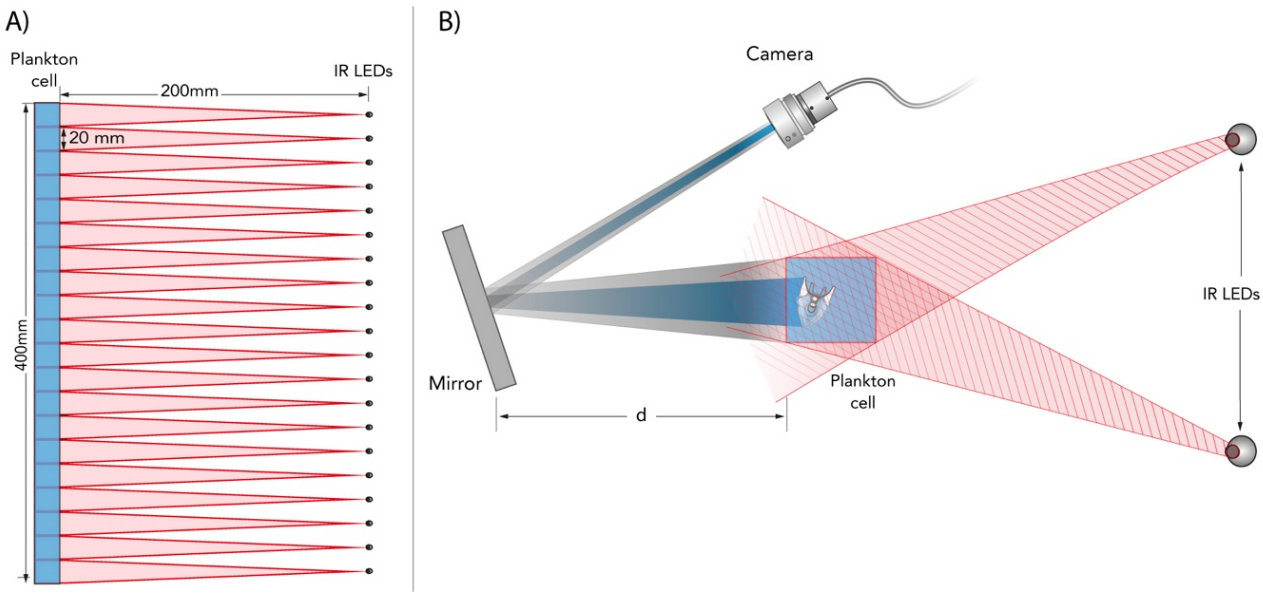

Fig 35. A) Diagram of the disposition of the IR LEDs with respect to the plankton column, lateral view. B) Diagram indicating the ray paths of the two parallel IR LEDs arrays with respect to the plankton column, top view. The overlapping light of each parallel couple of LEDs illuminates the whole sagittal plane of the column. As a consequence of the mirror, the distance between the IRs LEDs is halved, making the device more portable for field works. Illustrations made by Santiago Valero-Medranda.

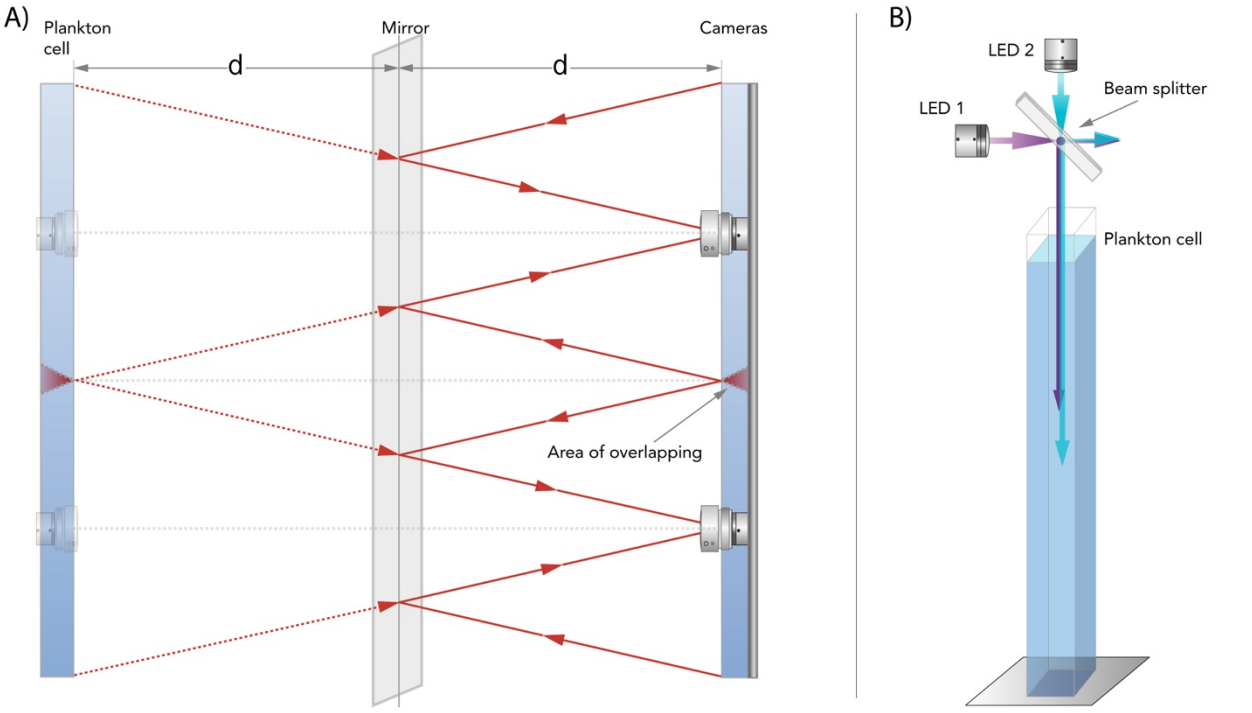

Fig 36. A) Optical drawing of the pathway followed by the IR light, side view. B) Representation of how the beam splitter operates in order to mix two light sources. Illustrations made by Santiago Valero-Medranda.

3.5.3 VM set up II: Available light stimuli

With this VM set up II in its current configuration, small planktonic animals can be tested against seven light stimuli: 'UV' (normalised intensity peak at 340 nm), 'violet' (420 nm), 'blue' (490 nm), 'turquoise' (505 nm), 'green' (535 nm), 'amber' (590 nm), and 'orange' (617 nm); both either alone or in combination of two. These lights have different penetration properties on the ocean column, thus potentially allowing us to test the behaviour of the studied animals in a scenario that mimics different ocean depths (for more information, see General Introduction). However, since most vertical migrations occur over at least 20 to 40 metres, a 40 centimetres column cannot simulate the intensity gradient over such depth ranges. As a possible solution to this technical problem, Prof. Dan Eric Nilsson (Lund University, Sweden) suggested to use an IR transmitting dye

absorbing in the same wavelengths as the stimulus light to simulate a larger depth range. This idea was not pursued in this study due to the lack of funding and time; future investigations will follow this experimental strategy though. In sake of precision, the illumination radiance of each of the light stimulus available was measured with an optic fibber immersed inside the plankton cell directly connected to a calibrated spectro-radiometer (RSP900-R, International Light, Peabody, MA, USA). The plankton cell was filled with sea water prior to light measurements and the water level was maintained constantly all over the light measurements. All measurements were done in a set of different intensities directly modulated by the LED controller software programmed for the set up (for scripts see Appendix I). As control of these measurements, the 100% light point of each wavelength was repeated twice: one at the beginning, and another at the end of all other measurements for such a wavelength. A full slot of light measurements of the first source to be measured (490 nm) was also done at the end of all other light source calculations for controlling possible disarrangements in the calibration of the spectro-radiometer. The resulting average differences between these two sets of radiance measurements was less than 4%, thus indicating that the spectro-radiometer was calibrated all over the results. The measurements made for each wavelength at different intensities can be found in Fig. 37.

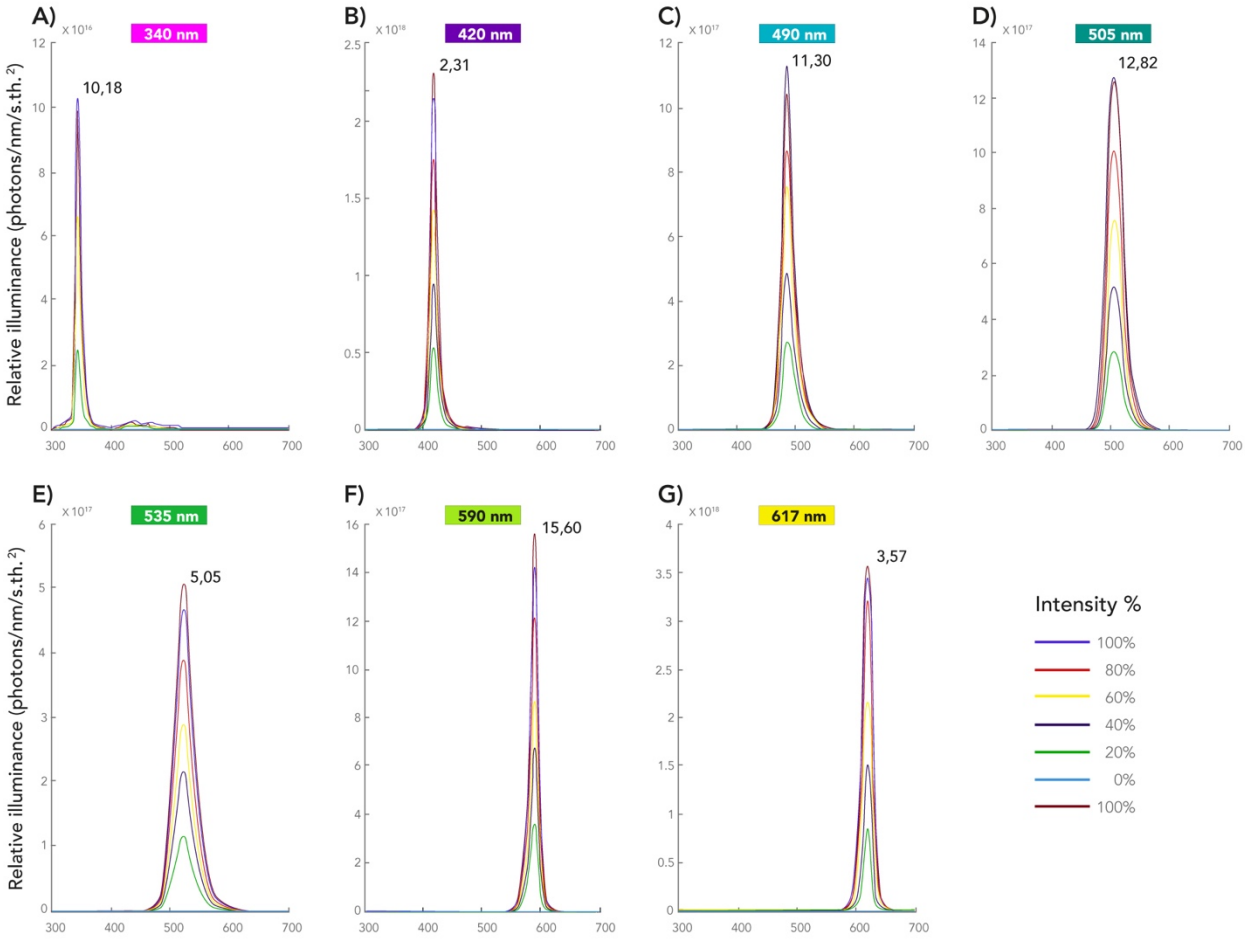

Fig 37. Light stimuli available in the VM set up II. Seven LEDs, with emission peaks of 340 nm ('UV'), 420 nm ('violet'), 490 nm ('blue'), 505 nm ('turquoise'), 535 nm ('green'), 590 nm ('amber') and 617 nm ('orange') can be used alone or in pairs in any possible combination. The radiance of each LED was measured at six different intensities modulated with the program 'LED controller'.

After light measurements, calculations were made to standardize the radiance of all light sources when possible. All light stimuli employed in the reported experiments but UV 340 nm have an average radiance of $7{,}7x10^{7}$ photons d^{-1} sr^{-1} cm^{-2}; this average radiance was chosen to reach regular daylight intensities for a receptor with matching lambda maximum. Unfortunately, it was not possible to regulate the 340 nm UV LED at the same radiance of the other light sources due to limitations on the available LED chips of this wavelength on the market. UV light working at 100% has a final power of $6{,}2x10^{7}$ photons d^{-1} sr^{-1} cm^{-2}. A graph on the distribution of the seven available light

sources with respect to the spectrum as well as the normalize intensities values used for each of them can be consulted in Fig. 38.

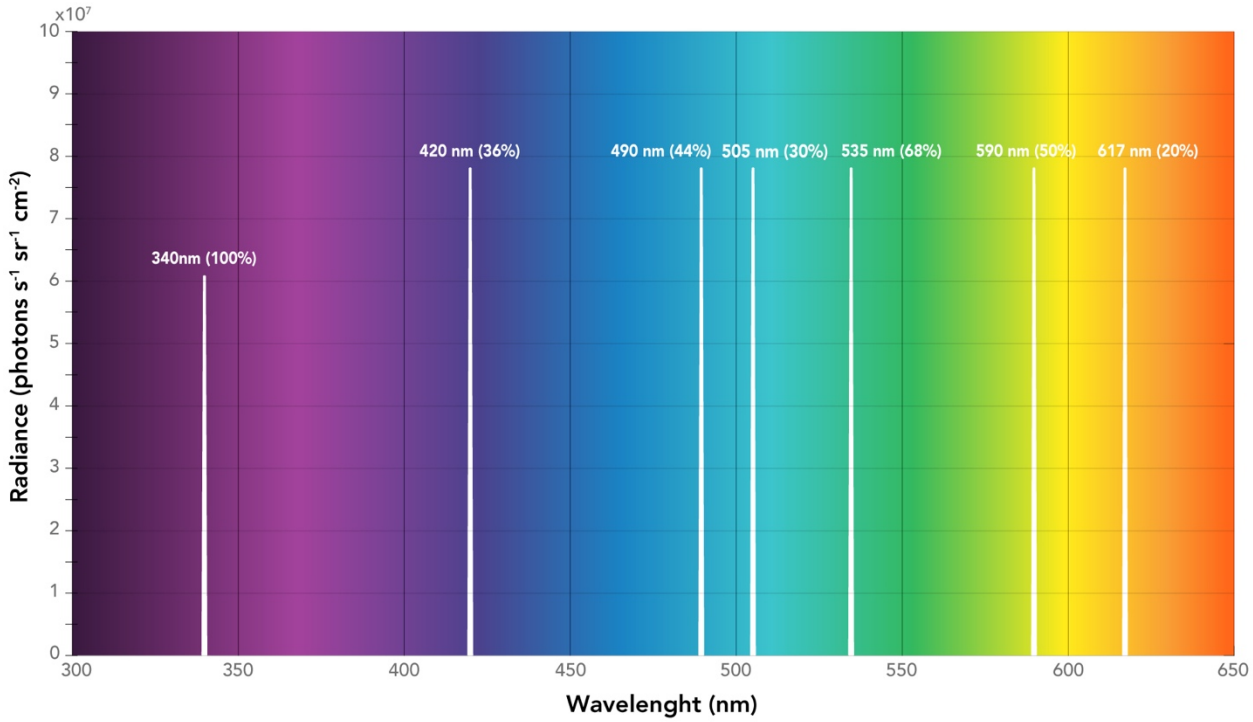

Fig 38. Light stimuli distribution over the spectrum. Each light stimulus has been regulated to standardise it with other light sources in terms of radiance. The final intensities settled with 'LED controller' program for each light source is presented as percentage within brackets. All light stimuli employed in the reported experiments but UV 340nm have an average radiance of $7{,}7\times10^{7}$ photons d^{-1} sr^{-1} cm^{-2}. UV light working at 100% has a final power of $6{,}2\times10^{7}$ photons d^{-1} sr^{-1} cm^{-2}.

3.5.4 VM set up II: Programming and data recording

All programs used for running the device VM II were created using MatLab version R2015b (MathWorks, Natick, MA, USA) by Dr. A. Darudi (Light Guide in Lund AB, Lund, Sweden) and Jochen Smolka (Lund University, Sweden). To control the light stimuli and IR LEDs, a program called 'LED controller' was developed (Appendix I). This program provides a user-friendly interface for setting different intensities for the LED light sources.

The main program ('Graphic User Interface', see Appendix I) is used to record the behavioural data, and divides the plankton cell image capture by the two IR cameras in 20 bins of 20 x 20 x 20mm. Each IR camera receives the information from 10 of these bins. The resulting image is then mathematically corrected to adjust geometric aberrations by means of a script contained in the program. The 10 mm overlap between images, from the upper and lower cameras, is used to reconstruct the IR image of the whole plankton cell. The IR light that arrives to each camera corresponds to the light scattered by the larvae. Because of this system, it is possible to record the larval response in the absence of visible light. Image sequences were analysed by using a program denominated 'Plankton column analysis' (Appendix I) wrote by Jochen Smolka (Lund University, Sweden). This program identifies the presence of three bright pixels interconnected from the IR image. With this information, the program produces a graph that shows the distribution of bright pixels (corresponding to a planktonic organism) as a function of density per unit of space per time. Examples of these graphs can be found all over the section 'Results' of this chapter.

3.5.5 Animals

For experiments done in the Stazione Zologica Anton Dohrn (Naples, Italy), ripe *Paracentrotus lividus* were collected by diving in the Gulf of Naples (Naples, Italy), and housed in 12ºC circulating aquaria. Spawning was induced by shaking the animals vigorously. Prior to fertilisation, eggs were checked for shape and integrity and sperm were checked for motility. The eggs of each female were fertilised by sperm from three males to increase genetic diversity. Fertilised eggs were then rinsed several times with filtered sea water to avoid polyspermy. For all the experiments done, embryos and larvae were cultured in 5 L beakers filled with filtered natural sea water (mesh pore size: 0.2 mm) collected in the

surroundings of Marechiaro (Naples, Italy). Animal cultures were stirred with Plexiglas rotating paddles driven by electric clock motors. Larvae were maintained at a temperature of 14°C and a salinity of 34‰ at a maximum concentration of five putei per mL. Plutei were fed as described in Chapter 2.

For experiments done in the Vision Group (Lund, Sweden), larval cultures ready to be used were sent from Stazione Zoologica Anton Dohrn (Naples, Italy) to Lund University (Lund, Sweden). These larvae came from adult sea urchins bred and cultivated at the Stazione Zoologica Anton Dohrn. Embryos and larvae were cultured in 5 L Erlenmeyer flaks filled with filtered natural sea water (mesh pore size: 0.2 mm) collected at Gullmarfjorden (Svén Loven Centre for Marine Sciences, Kristineberg, Sweden) following the protocol described by Cirino et al., 2017. Water salinity was corrected to 34‰ by adding Sigma Sea Salts (S9883). Larval cultures pH, salinity, oxygen level, and ion concentration was controlled by using a pH-meter Metler Toledo SG78 SevenGo Duo Pro. Also in this case plutei were fed as described in Chapter 2.

For Chapter 3 we decided to use *Paracentrotus lividus* instead of *Strongylocentrotus purpuratus* (used in Chapter 2 for molecular and morphological characterisation) larvae for three reasons: (i) there is an easier access to this European species; (ii) the Stazione Zoologica keeps these sea urchins in conditions allowing to get gametes at any time of the year; and (iii) for these behavioural experiments several batches of synchronously developing larvae are needed, and *P. lividus* grows faster and at a more convenient temperature (for comparing the developmental timings of these two species, see Fenaux et al., 1985; Smith et al., 2008). Still, these two species, *Paracentrotus lividus* and *Strongylocentrotus purpuratus*, are relatively close related (both belongs to the Echinidea) thus, they are

suitable for comparing the basic features of their photoreceptor system. The adult sea urchins used for the experiments here reported have been maintained at the animal facility of the Stazione Zoologica Anton Dohrn by Paola Cirino (Stazione Zoologica Anton Dohrn, Italy).

3.5.6 Experimental design: Generalities

In the following paragraphs I describe the general methods used prior to commencement of all experiments done. For each set of experiments, a description on the results obtained can be found in a heading with the same name in the Results section.

Paracentrotus lividus larvae were kept in starving conditions 48 hours prior to the behavioural experiments. All experiments were carried out with seven days' postfertilisation larvae (four armed pluteus stage). Plutei were concentrated immediately prior to the experiment by inverted filtration. After filling the plankton cell with live larvae and sea water, the column was inverted four times to ensure an initial homogeneous distribution of animals all over the column. Temperature was maintained constantly within the range of 14°C ± 1°C. Salinity was kept at 34‰ for all assays. Oxygen level was maintained at circa 10.1 mg/L.

3.5.7 Experimental protocol I: Pilot experiments for testing the light-driven gravitaxis capability of *P. lividus* plutei

First pilot experiments done were devoted to testing if echinoplutei were able to undergo light-driven gravitaxis. Animals were exposed to downwelling 'white' light in a very simple set up situated in the Stazione Zoologica Anton Dohrn (Naples, Italy). Prior to the experiments, larvae were kept in an incubator chamber with a light regime of 12/12

hours' light/no light conditions for mimicking natural day/night conditions. An approximate number of 1,000 four armed stage larvae were pippeted into each 50 mL lab cylinder (final density of circa 20 larvae/mL). Next, laboratory cylinders were brought to a final volume of 50 mL with filtered natural sea water. Following, all cylinders were rotated upside down four times to ensure homogeneous distribution of larvae all over the tubes. These experiments were repeated with larvae collected both during day and night phases over five times.

3.5.8 Experimental protocol II: Preliminary observations of the larval sinking speed

After ascertaining that a consistent negative gravitaxis behaviour occurred while exposing four armed plutei to a 380-700 nm 'white' light, preliminary observations to study the swimming speed of sinking were done. For so, and by using the VM set up located in the Stazione Zoologica Anton Dohrn, the horizontal distribution of the plutei was assessed following various periods of illumination. More in detail, plutei behaviours were observed after 10 (cylinder I), 30 (cylinder II), 60 (cylinder III), and 90 (cylinder IV) minutes of 'white' light exposition. The fifth cylinder containing water and plutei (cylinder V) was kept in dark as control. For testing the disposition of the larvae on cylinder V, a red-light source was used. This set of experiments were done at 12 am and 12 pm on the first day, and at 12 am on the second day of the experiment to rule out the possible influence of circadian rhythmicity. In these experiments, cylinders were rotated upside down four times to ensure homogeneous distribution of animals as in the previous section before commencement, and an initial stabilisation ('S') phase of 60 minutes of no light was settled prior to light exposure. Visu observations of the different experiments then followed.

3.5.9 Experimental protocol III: First experiments with the VM set up II, calculating the effect size to inform the experimental design

In these and in following experiments the set up used was the VM II situated in Lund University (Lund, Sweden). Pilot experiments for determining the quantity of animals to set in the plankton cell were done at two different concentrations: 250 animals (Fig. 27A, A'; B, B') and 2,500 animals (Fig. 27C, C'; D, D') respectively. For each of the concentrations, measurements were done twice: one time collecting larvae in the middle of the light half of the day (Fig. 27A, A'; C, C'), and another time collecting the animals in the middle of the dark half of the day (Fig. 27B, B'; D, D'). When animals were collected during the light half of the day (Fig. 27A, A'; C, C'), the first condition was always 60 minutes of 'light stimulus off'; following, the light stimulus was turned on during another 60 minutes. On the contrary, when the animals were collected during the dark half of the day (Fig. 27B, B'; D, D'), the first condition was always 60 minutes of 'light stimulus on', and a 60 minutes 'light off' stimulus followed. Such a 'two phases' regime was repeated three times. Since various of the bibliographical sources consulted indicated a negative phototaxis of UV light by other sea urchin larval species (e.g., Pennington and Emlet, 1986), all the experiments of this section were done using UV at $6{,}2x10^{7}$ photons d^{-1} sr^{-1} cm^{-2} as light stimulus.

3.5.10 Experimental protocol IV: Main data collection, testing the vertical migration of four armed plutei under illumination of seven different wavelengths

In each of these experiments, the larval response was recorded during 360 minutes in a time series of circa 1 second per frame. All experiments started with 60 minutes of no-light. Following, a given light was provided during another 60 minutes. Such a regime

(60 minutes' no-light plus 60 minutes' light) was repeated three times for having internal experimental replicas. The first 60 minutes recorded under no-light conditions (phase 'S') were not considered in our analysis to allow water and animals to stabilize themselves. Phase V was considered as an internal experimental control.

3.6 References

Brierley, A. S. (2014). Diel vertical migration. *Current Biology*, *24*(22), R1074-R1076.

Byron, E. R. (1982). The adaptive significance of calanoid copepod pigmentation: a comparative and experimental analysis. *Ecology*.

Chia, F. S., Buckland-Nicks, J., & Young, C. M. (1984). Locomotion of marine invertebrate larvae: a review. *Canadian Journal of Zoology*, *62*(7), 1205-1222. Creutzberg, F. (1975). *Orientation in space: animals. Invertebrates*. Marine ecology.

Creutzberg, F. (1975). Orientation in space: animals: invertebrates. *Marine ecology*, *2*(Part 2), 555-655.

D'Aniello, S., Delroisse, J., Valero-Gracia, A., Lowe, E. K., Byrne, M., Cannon, J. T., ... & Lowe, C. J. (2015). Opsin evolution in the Ambulacraria. *Marine Genomics*, *24*, 177-183.

Eastwood, J. (1972). *The development and photic behavior of Lytechinus variegatus echinoplutei larvae*.

Enright, J. T. (1977). Diurnal vertical migration: adaptive significance and timing. Part 1. Selective advantage: a metabolic model. *Limnology and Oceanography*, *22*(5), 856-872.

Enright, J. T., & Honegger, H. W. (1977). Diurnal vertical migration: Adaptive significance and timing. Part 2. Test of the model: Details of timing. *Limnology and Oceanography*, *22*(5), 873-886.

Hyman, L. H. (1955). The Invertebrates. Volume IV. Echinodermata. *McGraw-Hill*, *763*, 408.

Fenaux, L., Cellario, C., & Etienne, M. (1985). Variations in the ingestion rate of algal cells with morphological development of larvae of Paracentrotus lividus (Echinodermata: Echinoidea). *Marine Ecology Progress Series*, 161-165.

Forward Jr, R. B. (1976). Light and diurnal vertical migration: photobehavior and photophysiology of plankton. In *Photochemical and photobiological reviews* (pp. 157-209). Springer US.

Fox, H. M. (1925). The effect of light on the vertical movement of aquatic organisms. *Biological Reviews*, *1*(4), 219-224.

Geller, W. (1986). Diurnal vertical migration of Zooplankton in a temperate great lake (Lake Constance): a starvation avoidance mechanism? *Archiv für Hydrobiologie. Supplementband. Monographische Beiträge*, *74*(1), 1-60.

Holm-Hansen, O., Lubin, D., & Helbling, E. W. (1993). Ultraviolet radiation and its effects on organisms in aquatic environments. In *Environmental UV photobiology* (pp. 379-425). Springer US.

Kaňa, R., Kotabová, E., Sobotka, R., & Prášil, O. (2012). Non-photochemical quenching in cryptophyte alga Rhodomonas salina is located in chlorophyll a/c antennae. *PLoS One*, *7*(1), e29700.

Kerfoot, W. C. (1985). Adaptive value of vertical migration: Comments on the predation hypothesis and some alternatives. *Contributions in Marine Science*, *68*.

Kremer, P., & Kremer, J. N. (1988). Energetic and behavioral implications of pulsed food availability for zooplankton. *Bulletin of Marine Science*, *43*(3), 797-809.

Lampert, W. (1989). The adaptive significance of diel vertical migration of zooplankton. *Functional Ecology*, *3*(1), 21-27.

Lock, A. R., & McLaren, I. A. (1970). The effect of varying and constant temperatures on the size of a marine copepod. *Limnology and Oceanography*, *15*(4), 638-640.

Lyon, E. P. (1906). Note on the geotropism of Arbacia larvae. *The Biological Bulletin*, *12*(1), 21-22.

McLaren, I. A. (1963). Effects of temperature on growth of zooplankton, and the adaptive value of vertical migration. *Journal of the Fisheries Board of Canada*, *20*(3), 685-727.

McLaren, I. A. (1974). Demographic strategy of vertical migration by a marine copepod. *The American Naturalist*, *108*(959), 91-102.

Mileikovsky, S. A. (1973). Speed of active movement of pelagic larvae of marine bottom invertebrates and their ability to regulate their vertical position. *Marine Biology*, *23*(1), 11-17.

Mortensen, T. (1921). *Studies of the Development and Larval Forms of Echinoderms*. Danske Vidensk. Selsk. Skrifter.

Neya, T. (1965). Photic behavior of sea urchin larvae, Hemicentrotus pulcherrimus. *Zoological Magazine (Tokyo)*, *74*, 11-16.

Orcutt, J. D., & Porter, K. G. (1983). Diel vertical migration by zooplankton: constant and fluctuating temperature effects on life history parameters of Daphnia. *Limnology and Oceanography*, *28*(4), 720-730.

Patro, R., Duggal, G., Love, M. I., Irizarry, R. A., & Kingsford, C. (2016). Salmon provides accurate, fast, and bias-aware transcript expression estimates using dual-phase inference. *BioRxiv*, 021592.

Pearre, S. (1979). On the adaptive significance of vertical migration. *Limnology and Oceanography*, *24*(4), 781-782.

Pennington, J. T., & Emlet, R. B. (1986). Ontogenetic and diel vertical migration of a planktonic echinoid larva, Dendraster excentricus (Eschscholtz): occurrence, causes, and probable consequences. *Journal of Experimental Marine Biology and Ecology*, *104*(1-3), 69-95.

Reese, E. S. (1966). The complex behavior of echinoderms. *Physiology of Echinodermata*, *157*, 218.

Runnström, J. (1918). *Zur Biologie und Physiologie der Seeigellarve*. Nilssen.

Siebeck, O. (1978). UV-Toleranz und Photoreaktivierung bei Daphnien aus Biotopen verschiedener Höhenregion. *Naturwissenschaften*, *65*(7), 390-391.

Smith, M. M., Cruz Smith, L., Cameron, R. A., & Urry, L. A. (2008). The larval stages of the sea urchin, Strongylocentrotus purpuratus. *Journal of Morphology*, *269*(6), 713-733.

Stich, H. B., & Lampert, W. (1984). Growth and reproduction of migrating and non-migrating Daphnia species under simulated food and temperature conditions of diurnal vertical migration. *Oecologia*, *61*(2), 192-196.

Swift, M. C. (1976). Energetics of vertical migration in Chaoborus trivittatus larvae. *Ecology*, *57*(5), 900-914.

Théel, H. (1892). *On the development of Echinocyamus pusillus (O. F. Müller)* (Vol. 3). Edv. Berling, Upsala.

Thorson, G. (1964). Light as an ecological factor in the dispersal and settlement of larvae of marine bottom invertebrates. *Ophelia*, *1*(1), 167-208.

Valero-Gracia, A., Petrone, L., Oliveri, P., Nilsson, D. E., & Arnone, M. I. (2016). Non-directional Photoreceptors in the Pluteus of Strongylocentrotus purpuratus. *Frontiers in Ecology and Evolution*, *4*, 127.

Zaret, T. M., & Suffern, J. S. (1976). Vertical migration in zooplankton as a predator avoidance mechanism. *Limnology and oceanography*, *21*(6), 804-813.

CONCLUSIONS AND FUTURE DIRECTIONS

CONCLUSIONS AND FUTURE DIRECTIONS

This study has investigated the photoreceptor mechanisms of the Ambulacraria clade. The main conclusions obtained are:

1) A comprehensive phylogeny of Ambulacraria opsins was created to assess orthologies and to identify gene novelties and modifications (Chapter 1). The opsin toolkit of Ambulacraria possesses all the main classical opsin groups (c-opsins, r-opsins and Go-opsins). This supports the proposition that Urbilateria, the last bilaterian common ancestor, had a photoreceptor system with ciliary, Go, and rhabdomeric opsins. Furthermore, a protein motif of each opsin group was provided to facilitate future investigations on the photoreception of the clade.

2) Two Go-opsin positive cells were localized in *Strongylocentrotus purpuratus* larvae (Chapter 2). These putative photoreceptors appear to be non-directional; the presence of shading pigments on these cells and its surroundings has been ruled out by means of transmission electron microscopy. Since the simplest class of photoreceptors is non-directional (class I), the photoreceptor system found in the echinoplutei could resemble the photoreceptor system present in the first larvae that appeared early during evolution.

3) A novel, quantitative methodology to investigate the vertical migration of small planktonic larvae under different light conditions has been created (Chapter 3). This

prototypic set up allows to trace the vertical movement of small transparent larvae even under no-visible light conditions. This set up mimics the different light conditions present at different depths of the ocean water column. Our data suggest that the four armed pluteus of *Paracentrotus lividus* is capable to drive its vertical migration, and that this light-driven gravitaxis change depending on the kind of light provided.

Altogether, this study represents one of the first steps to better understand the photoreception mechanisms of Ambulacraria. Keeping in mind that this subject is still fairly unexplored, I have here outlined some of the key areas in which this fruitful research field can be developed, and how this can be achieved.

In future, the availability of more genomic and transcriptomic data will allow us to better appraise the opsin toolkit present in the Ambulacraria clade both between species and the various life stages. For instance, in the larval visual system of the Hemichordata, rhabdomeric photoreceptor cells are present, but accompanying r-opsins have not been identified in the opsin toolkit of this clade. Consequently, a detailed investigation of the opsin-type present in these larval ocelli would be intriguing. Moreover, as novel groups of opsins have been identified in the echinoderms, it will be interesting to assay how widespread these opsin types are and what their evolutionary history and function is. In future, a comparative assessment of the photoreceptor apparatus of the different Ambulacraria larvae across diverse clades could provide a powerful means of assessing the homology between these systems in dipleurula-like larvae.

Specifically, amongst the larval stages of *Strongylocentrotus purpuratus*, it would be useful to evaluate whether any other opsin expression can be identified. The presence of such opsin,

in combination with the *Sp-opsin3.2* here located, could mediate a depth-gauge photic mechanism that will potentially allow the larva to guide itself in the water column towards a photic area where algae can be found, but still below the region where intense UV radiations can damage it; or be involved in other roles at later developmental stages. Moreover, co-expression has been identified between the neuropeptide *SpTRH* and the Go opsin *Sp-opsin3.2* in four armed pluteus stage. It would be interesting to identify what the biological meaning of this co-expression is and how these two proteins are interrelated. In addition, knock out techniques could be applied to determine the specific role of *Sp-opsin3.2*. Thanks to the behavioural protocol here described, the spectral sensitivity of the photoreceptor system of wild type animals and knock out animals can be compared.

Supplementary co-expression studies would be helpful for identifying other contributors to the gene regulatory network involved in the photodetection of this species. Tables 5 and 6 indicate a number of genes and proteins which may play an important role in the photoreceptor system of this species and which expression patterns can be assessed for. A list of primers of known components of the ciliary and rhabdomeric phototransduction cascade found for this species are also provided to facilitate future molecular investigations.

Further experiments are required to evaluate the behavioural data here presented and discussed. A more robust statistical framework must be applied to systematically quantify the movement of animals and provide measurements of variance and precision. In addition, many further experiments are possible to investigate the properties of the light detection system in this species. For instance, other spectral ranges can be investigated to determine if the animal has sensitivities in that range, as well as combinations of wavelengths and light intensities. With this set up, animals with knock out modifications or animals to whom drug

treatments have been applied can be used to test the theoretical depth-gauge mechanism here proposed. Instructions for creating a new behavioural set up to gain further insights into the photo behaviour of these larvae are also provided.

Table 5 – *S. purputatus* orthologs of transcription factors playing crucial role during photoreceptor cell development in vertebrates and their reciprocal best blast hit

Gene name (GeneBank accession number of query protein)	GeneBank accession number of top *Strongylocentrotus purpuratus* result/RNA-seq evidence	E-value	Reciprocal best BLAST query result Protein name (Species; GeneBank accession number)	E-value	Transcriptional targets in vertebrates
Ath5 (NP_989999.1)	SPU_003681/ND	3e-07	TRIADDRAFT_9478 (*Trichoplax adhaerens*; EDV25594.1)	9e-18	–
Brn3a/Brn3c (AAU13951.1)	SPU_025632/ WHL22.738139	9e-75	BRN3 transcription factor (*Saccoglossus kowalevskii*; NP_001161509.1)	1e-125	ND
Brn3b (NP_997972.1)	SPU_025632/ WHL22.738139	2e-74	BRN3 transcription factor (*Saccoglossus kowalevskii*; NP_001161509.1)	1e-125	Brn3a(+), Brn3c(–) Dlx1/Dlx2 (–), Otx2(–), Crx(–)
Crx (AAH53672.1)	SPU_010424/ WHL22.532435	1e-23	Orthodenticle-related protein (*Hemicentrotus pulcherrimus*; BAA28675.1)	0.0	Crx(+), Cone Opsin (+), rhodopsin(+), Nr3e(+), Otx2(–)
Dlx1/Dlx2 (AAC60025.1)	SPU_002815/ WHL22.107309	1e-29	Dlx (*Paracentrotus lividus*; ADW95343.1)	3e-154	Brn3b(+), Crx(–) TrkB(+), Dlx56ie(+), Nrp-2(–) (forebrain)
Dlx5/Dlx6 (AAC52843.1)	SPU_002815/ WHL22.107309	4e-28	Dlx (*Paracentrotus lividus*; ADW95343.1)	3e-154	ND
Irx5 (NP_001165398.1)	SPU_010351/ WHL22.651130	1e-35	IrxA (*Paracentrotus lividus*; ADW95342.1)	0.0	CaBP5(+), PMCA1(+), Recoverin(+)
Irx6 (ABM92083.1)	SPU_010351/ WHL22.651130	5e-44	IrxA (*Paracentrotus lividus*; ADW95342.1)	0.0	Vsx1(–)
Isl1 (EDM10395.1)	SPU_023730/ WHL22.143854	e-105	Insulin gene enhancer protein ISL-1 isoform X2 (*Callorhinchus mili*; XP_007890396.1)	2e-161	Brn3a(+), Brn3b(+)
Isl2 (EAW99220.1)	SPU_023730/ WHL22.143854	2e-93	Insulin gene enhancer protein ISL-1 isoform X2 (*Callorhinchus mili*; XP_007890396.1)	2e-161	Zic2(–), EphB1(–)
Lhx1 (NP_005559.2)	SPU_006991/ WHL22.720614	e-113	Transcription factor HpLim1 (*Hemicentrotus pulcherrimus*; BAB13725.1)	0.0	ND
Lhx2 (ABO93218.1)	SPU_004021/ WHL22.91758	7e-49	Lim homeobox 2/9 protein (*Saccoglossus kowalevskii*; NP_001158443.1)	7e-111	Rax(+), Pax6(+), Six3(+), Six6(+)
Meis1/Meis2 (NP_002389.1)	SPU_011202/ WHL22.2236	e-120	Homeobox protein Meis2 isoform X7 (*Saccoglossus kowalevskii*; XP_006811521.1)	2e-179	smad1(+), tbx5(+), vax2(–), Cyclin D1(+), C-myc(+)
Oc1 (AAH24053.1)	SPU_016449/ WHL22.288683	9e-74	Onecut/Hnf6 (*Paracentrotus lividus*; ADW95349.1)	0.0	Lhx1(+), Prox1 (+)
Oc2 (NP_004843.2)	SPU_016449/ WHL22.288683	2e-74	Onecut/Hnf6 (*Paracentrotus lividus*; ADW95349.1)	0.0	ND
Otx2 (BAC53612.1)	SPU_010424/ WHL22.532435	5e-29	Orthodenticle-related protein (*Hemicentrotus pulcherrimus*; BAA28675.1)	0.0	Crx(+), Rax(+), Blimp1(+)

Gene name (GeneBank accession number of query protein)	GeneBank accession number of top *Strongylocentrotus purpuratus* result/RNA-seq evidence	E-value	Reciprocal best BLAST query result Protein name (Species; GeneBank accession number)	E-value	Transcriptional targets in vertebrates
Pax2 (CAA39302.1)	SPU_014539/ WHL22.619292	1e-64	Paired box protein (*Paracentrotus lividus*; AAB70245.1)	5e-109	Pax6(–)
Pax6 (ABO70134.1)	SPU_006786/ WHL22.585629	1e-54	Pax-6 (*Paracentrotus lividus*; AAA75363.1)	2e-77	Pax2(–), Atoh7(+), Ngn2(+), Crx(–)
Vax2 (CAB56166.1)	SPU_002592/ WHL22.113468	6e-16	Homeobox protein EMX1 isoform X2 (*Ovis aries*; XP_011978947.1)	7e-55	Pax6(–)
Vsx1 (NP_001090191.1)	SPU_000485/ WHL22.249523	1e-52	Homeobox protein EMX1 isoform X2 (*Ovis aries*; XP_011978947.1)	7e-55	Recoverin(+), Neto1(+), NK3R (+), CaB5(+), Vsx2(–), Cabp5 (–), Irx6 (–)
Prox1 (AAI64571.1)	SPU_015984/ WHL22.531966	4e-59	Prospero homeobox protein 1 isoform X2 (*Callorhinchus mili*; XP_007903216.1)	6e-88	$p27^{KIP1}$(+), $p57^{KIP2}$(+)
Rax (O97039.1)	SPU_014289/ WHL22.523971	4e-35	Retina and anterior neural fold homeobox (*Saccoglossus kowalevskii*; NP_001158375.1)	4e-50	Pax6(+) Otx2(+), β-arrestin(+), rhodopsin(+)
Rx (NP_038463.2)	SPU_014289/ WHL22.523971	8e-37	Retina and anterior neural fold homeobox (*Saccoglossus kowalevskii*; NP_001158375.1)	4e-50	–
Six1/2 (NP_005973.1)	SPU_017379/ WHL22.121485	e-103	SIX homeobox 1 (*Saccoglossus kowalevskii*; NP_001277017.1)	5e-137	–
Vsx2 (NP_878314.1)	SPU_000485/ WHL22.249523	1e-60	Visual system homeobox 2-like (*Saccoglossus kowalevskii*; XP_002736712.1)	1e-76	P27KIP1(–), Crx(–), Vsx1(–)

For each query protein, the corresponding *Strongylocentrotus purpuratus* protein model is listed with the E-value of the top BLAST results. The *Strongylocentrotus purpuratus* protein model was then used as a query in a reciprocal best BLAST search of the non-redundant protein datababase (NCBI) and the top result is listed along with the E-value of the BLAST result. RNA-se data supports the developmental mRNAgene expression of each of these protein models. ND, not determined; (+) indicates positively regulated transcription targets; (–) indicates negative regulation of transcriptional target; Pax2+* does not contain a full homeobox.

Table 6 – A) *S. purputatus* orthologs of known components of the ciliary and rhabdomeric phototransduction cascade in other animal systems and their reciprocal best blast hit

Protein name (GeneBank accession number of query protein)	GeneBank accession number of top *Strongylocentrotus purpuratus* result	E-value	Reciprocal best BLAST query result Protein name (Species; GeneBank accession number)	E-value	RNA-seq evidence
Ciliary components					
G-alpha-s subunit (BAA81697)	SPU_007485	e-106	Guanine nucleotide-binding protein G(s) alpha subunit (*Lytechinus variegatus*; AAS38583.1)	0.0	WHL22.735798
G-alpha-i subunit (ACB05685.1)	SPU_013414	e-167	Guanine nucleotide-binding protein G(i) alpha subunit (*Patiria pectinifera*; P30676.3)	0.0	WHL22.762062
Transducin G-alpha-t1 (AAB01735.1)	SPU_013414	3e-82	Guanine nucleotide-binding protein G(i)_alpha subunit (*Patiria pectinifera*; P30676.3)	0.0	WHL22.762062
Transducin G-gamma-t1 (AAH25929.1)	SPU_030086	1e-07	Guanine nucleotide-binding protein G(I)/G(S)/G(O) subunit gamma-10 (*Danio rerio*; NP_001191955.1)	2e-17	WHL22.253891
GRK1 G protein-coupled receptor kinase (AAH96611.1)	SPU_005149	1e-86	G protein-coupled receptor kinase 5 (*Saccoglossus kowalevskii*; XP_002742089.2)	3e-173	WHL22.421157
GMP-PDE alpha rod (NP_666198.1)	SPU_017533	e-128	cGMP-specific 3',5'-cyclic phosphodiesterase-like (*Saccoglossus kowalevskii*; XP_002733933.2)	0.0	WHL22.554631
GMP-PDE beta rod (P23440.3)	SPU_017533	e-135	cGMP-specific 3',5'-cyclic phosphodiesterase-like (*Saccoglossus kowalevskii*; XP_002733933.2)	0.0	WHL22.554631
GMP-PDE delta (O55057.1)	SPU_017612	2e-47	Carbohydrate sulfotransferase 15-like isoform X2 (*Scleropages formosus*; KKX11357.1)	5e-57	WHL22.621157
Phospodiesterase (ACB05690)	SPU_028720	e-135	High affinity cGMP-specific 3',5'-cyclic phosphodiesterase 9A-like (*Saccoglossus kowalevskii*; XP_006818123.1)	0.0	WHL22.281736
Cyclid nucleotide gated ion channel (CAB42891.1)	SPU_000314	e-174	Cyclic nucleotide-gated olfactory channel-like (*Saccoglossus kowalevskii*; XP_006813621.1)	0.0	WHL22.92304
RGS9-1 regulator of G-protein signalling 9 isoform 1 (NP_035398_2)	SPU_002521	7e-84	Regulator of G-protein signaling 7-like (*Saccoglossus kowalevskii*; XP_006813719.1)	0.0	WHL22.319117
GC1 guanylyl cyclase GC-E precursor (NP_032218.2)	SPU_024339	e-126	Guanyl cyclase (*Hemicentrotus pulcherrimus*; BAA04660.1)	0.0	WHL22.210138
Recoverin (NP_033064.1)	SPU_026993	1e-42	Hippocalcin-like protein (*Saccoglossus kowalevskii*; NP_001161566.1)	2e-128	WHL22.599379
GCAP1 guanylyl cyclase-activating protein 1 (NP_032215.2)	SPU_026993	4e-30	Hippocalcin-like protein (*Saccoglossus kowalevskii*; NP_001161566.1)	2e-128	WHL22.599379
GCAP2 guanylyl cyclase-activating protein 2	SPU_026993	4e-33	Hippocalcin-like protein (*Saccoglossus kowalevskii*; NP_001161566.1)	2e-128	WHL22.599379

Protein name (GeneBank accession number of query protein)	GeneBank accession number of top Strongylocentrotus purpuratus result	E-value	Reciprocal best BLAST query result Protein name (Species; GeneBank accession number)	E-value	RNA-seq evidence
Rhabdomeric components					
G-alpha-q subunit (ACB05683)	SPU_003898	e-177	Guanine nucleotide-binding protein G(q) alpha subunit (*Lytechinus variegatus*; AAS38584.1)	0.0	_
Phospholipase C (ACB05675)	SPU_009929	e-101	1-phosphatidylinositol 4,5-bisphosphate phosphodiesterase classes I and II isoform X2 (Orussus abietinus; XP_012270478.1)	0.0	WHL22.169178
Trp-C protein (ACB05689)	SPU_017326	1e-41	Short transient receptor potential channel 4-like (*Saccoglossus kowalevskii*; XP_006820265.1)	0.0	WHL22.316252
Shared components					
Visual G beta (ACB05681)	SPU_000508	3e-99	Guanine nucleotide-binding protein G(I)/G(S)/G(T) subunit beta-1 (*Zootermopsis nevadensis*; KDR23891.1)	0.0	WHL22.101602
Rhodopsin kinase (ACB05677)	SPU_001621	0.0	Beta-adrenergic receptor kinase 2 (*Haliaeetus leucocephalus*; XP_010580351.1)	0.0	WHL22.64904
Arrestin (ACB05679)	SPU_023889	7e-26	Beta-arrestin (*Saccoglossus kowalevskii*; NP_001171767.1)	0.0	WHL22.709217
Retinal-binding protein (ACB05687)	SPU_004473	1e-52	SEC14-like protein 2 isoform X1 (*Larimichthys crocea*; XP_010749651.1)	8e-119	WHL22.664046

For each query protein, the corresponding *Strongylocentrotus purpuratus* protein model is listed with the E-value of the top BLAST results. The *Strongylocentrotus purpuratus* protein model was then used as a query in a reciprocal best BLAST search of the non-redundant protein datababase (NCBI) and the top result is listed along with the E-value of the BLAST result. RNA-se data supports the developmental mRNAgene expression of each of these protein models. Blast: Basic Local Alignment Search Tool; PDE: phospodiesterase; TRP: transient receptor potential.

Table 6 – B) *S. purpuratus* homologs to ciliary and rhabdomeric phototransduction cascade components

Ciliary components

A) G-alpha-s subunit (SPU_007485/ WHL22.735798)

```
>SPU_007485.1 CDS Sequence
ATGGGTTGCTTCGGGAACGGCCTGTCAAGCGAAGAGAAAGATGAAGAAAAGAAGCGAAAGGAGGCTAACAAGAAGATTGAAAAGCAACTCCAGAAGG
ACAAGCAAATATACAGAGCAACGCATCGGCTATTATTGCTTGGTGCTGGTGAATCAGGAAAAAGTACCATCGTGAAACAAATGAGAATTCTTCATGT
AGATGGATTCTCACCAGATGAAAGAAAGAAGAAAATAGAAGATATAAGAAGGAATATTCGAGATGCAATTATTACAATAACAGGGGCCATGAGCACA
TTGTCACCGCCTATTCAACTAGCAGAACCTCAGAACCAATTTCGGTTGGATTATATTCAAGATGTCTCCAGTTCACCAGACTTCGACTACCCAGAAG
AATTCTGGGACCACACAAAACATTTATGGATAGATGCTGGAGTTCAAGGCTGCTACGACAGGTCGCACGAATATCAACTTATAGATAGCGCACAATA
TTTTTTAGATAGAGTTGATACAATAAGAAGACCAGACTATGCTCCCGACCTACAGGACATTCTCCGGTGTCGTGTCTTGACGTCTGGAATCTTTGAA
ACAAAATTCCAAGTGGACAAAGTCAACTTTCACATGTTCGATGTAGGAGGACAGAGAGACGAAAGGAGAAAATGGATCCAATGTTTCAATGATGTGA
CGGCCATCATCTTTGTAGTAGCCTGCAGTAGTTACAACCTGGTGTTGAGAGAAGACCCAAACCAGAACAGACTGAGGGAGTCACTAGAACTGTTCAG
GAGCATCTGGAATAACAGGTGGTTGCGGACAATTTCAGTGATCCTCTTCCTCAACAAACAGGACTTACTGGCTGAGAAGGTCCAAGCAGGAAGGTCT
AAGATCGAGGACTACTTTAGCGAGTATGCAATGTACACAATCCCACCCGATGCCGCTACAGACACTGGTGAACCAGAGGATGTCTTGCGAGCCAAGT
ACTTCATCAGAGATGAATTCCTGCGAATCAGCACGGCGAGCGGCGACGGCCGACATTACTGCTACCCCCACTTCACCTGTGCCGTGGATACAGAGAA
CATCCGACGAGTCTTTGACGATTGTCGGGACATCATCCAAAGGATGCATCTTCGGCAATATGAGTTGCTGTGA
```

OLIGO	start	len	tm	gc%	any_th	3'_th	hairpin	seq
A1 LEFT PRIMER	420	20	59.01	50.00	0.00	0.00	0.00	AGATGCTGGAGTTCAAGGCT
A2 RIGHT PRIMER	1067	20	58.74	50.00	0.00	0.00	0.00	TTCTCTGTATCCACGGCACA

SEQUENCE SIZE: 1140

PRODUCT SIZE: 648, PAIR ANY_TH COMPL: 0.00, PAIR 3'_TH COMPL: 0.00

B) G-alpha-i subunit or Transducin G-alpha-t1 (SPU_013414/ WHL22.762062)

```
>SPU_013414.1 CDS Sequence
ATGGGGTGCGCTACGAGCGCAGAAGATAAAGCGGCCGCTGAGCGGTCGAAAATGATTGATAGAAATCTACGGTTAGAAGGAGAAAAAGCAGCAAGAG
AAGTAAAATTATTGCTCTTAGGGGCTGGTGAATCAGGGAAAAGTACAATTGTAAAACAAATGAAGATTATACATGAAGAAGGGTACTCTGAAGAAGA
TTGTAGGCAGTATAAACCCGTGGTATACAGTAACACAATTCAATCCATGATAGCCATCATCAGAGCTATGGGTTCACTCAAGATTGACTTCGGAGAC
ACAGAAAGAGCAGATGATGCAAGGCAATTATTTGCCCTGGCTGGGCAGGCAGAAGAAGGTGAACTCAGCACTGAACTAGCAGCGGTTATGAAGCGGT
TATGGGCAGACTCAGGTGTCCAAGCATGCTTTAGCCGGTCCAGGGAGTATCAACTCAACGATTCTGCATCATATTACCTGAATGCCTTGGATCGGTT
GTCAGCGCCTGGTTACATCCCTACACAACAAGATGTTCTTAGGACAAGAGTCAAGACCACTGGTATCGTAGAGACGCATTTCACCTTCAAGGAACTT
CACTTCAAAATGTTTGATGTTGGAGGTCAGAGGTCAGAGAGAAAGAAGTGGATACACTGTTTTGAGGGTGTGACTGCAATCATCTTCTGTGTGGCTC
TCAGTGCCTATGATTTGGTTCTGGCAGAAGATGAGGAAATGGTAAGATTTGTGTTTTGTTCTTTTTGTTTCCTGTATATGTACATGCTTGTGGCCGT
GGTGTCTGTATTCCTCAATTGTTGTTTTTCTTTAAAAGTAACTATTCCCCCCCCCAAAAAAAATAAAAAATAA
```

OLIGO	start	len	tm	gc%	any_th	3'_th	hairpin	seq
B1 LEFT PRIMER	37	20	58.99	50.00	10.17	0.00	0.00	GCTGAGCGGTCGAAAATGAT
B2 RIGHT PRIMER	664	20	59.24	50.00	13.14	0.00	0.00	TGATTGCAGTCACACCCTCA

SEQUENCE SIZE: 849

PRODUCT SIZE: 586, PAIR ANY_TH COMPL: 0.00, PAIR 3'_TH COMPL: 0.00

C) Transducin G-gamma-t1 (SPU_030086/ WHL22.253891)

```
>SPU_030086.1 CDS Sequence
ATGTCACAAGTAACGGCGCTGAAGAAGACCGTAGAGCAGCTACGATCGGAGGCAAAGATCGAACGGATCACCGTATCTCAGGCTTGTAACCAGCTCCA
GGAATACTGCTTACAACACGAGGCGGATGACTGTCTACTAAAAGGAATCGCTGCACATGCCAACCCGTTCAAGGAAAAGCAAAAGTGCACTATTTTG
```

D) GRK1 G protein-coupled receptor kinase (SPU_005149/ WHL22.421157)

```
>SPU_005149.1 CDS Sequence
GTTAGTCTTGCCTATGCCTTTGAGATGAAAGAAGCACTGTGTCTGGTCCTGACCATCATGAATGGTGGTGACCTCAAGTTCCACATACATAACATGG
GTAGTCCAGGGTTTGAGGAGGAGAGGGCTAGGTTCTACGCAGCAGAGATCCTCTGTGGTTTGGAGGACCTTCACCGATTGAGGATCGTCTACCGGGA
TATGAAGCCAGAGAATATCCTCCTAGATGATCATGGTCATGTACGTATCTCTGACCTGGGTCTAGCAGTGGAGATACCTGAGAATGACACCATCAGG
GGCAGAGTAGGAACGGTGGGCTACATGGCTCCTGAGGTGGTGAAGAACGAGAGGTATACATTCAGTCCAGACTACTGGGGTCTCGGATGTCTTATCT
ATGAGATGATAGAAGGAAGGGCTCCATTCCGAGCGAGGAAGGAGAAGGTCAAGAGGGAAGAGGTCGACCGGAGAGTCAAAGAAGACGACGAGAAGTA
CAGCCAGAAGTTCAGCACCGAAGCACAGGACATCTGTAAAAAGTTGTTGCAGAAGGACCCAGCGTTAAGAATGGGGTTTGAGAACGGCACCGCACAG
ACTGTCAAGGATCATTCATTCTTCAACTCCATCAGCTTCAGCCGGCTTGAAGCTGGAAAGCTCGATCCACCCTTTGAACCTGATAAGAGGGCCGTGT
ATGCAAAAGACGTGCTGGACATAGAACAGTTCTCAACCGTCAAAGGAGTAAACTTGGACCAAAACGATGACAGATTCTACACCAAATTCAACTCGGG
GAGTGTAGCAATTCCATGGCAAATGGAGATGATTGAGACGCAAGTATTTCTTGAGCTGAATGTGTTTGGGCCCAACGGCACTCTAACAGCTGACTTG
ATGCCTGATCTACCGCCACCACCCCCAAAGCAAGGTTTCTTCAGGAGGATATTTAGGATTAAGGCAGCGATGATCGACAATGACACCTTGCCAAACA
ACCCTCCTGACCAAGAGAGGGCGCTCTAA
```

OLIGO	start	len	tm	gc%	any_th	3'_th	hairpin	seq
D1 LEFT PRIMER	159	20	59.10	55.00	0.00	0.00	0.00	GGAGGACCTTCACCGATTGA
D2 RIGHT PRIMER	847	20	59.04	50.00	0.00	0.00	0.00	GCCCAAACACATTCAGCTCA

SEQUENCE SIZE: 999

PRODUCT SIZE: 689, PAIR ANY_TH COMPL: 0.00, PAIR 3'_TH COMPL: 0.00

E) GMP-PDE alpha rod or GMP-PDE beta rod (SPU_017533/ WHL22.554631)

>SPU_017533.1 CDS Sequence
ATGGCTACTGCTCTAAATCATGTTTCAAGGGAGGAGGTTGAAAAATATCTGGAAGCTAACCATGATGTTGCAACAGACATTTTTGTAACAAAAGCCA
CTCCAGATATGATTGATCAATGGCTATCCAAGCATGCCAACTCCCTTCACAAGCATGGAGAAGGCAGTCCACAGGATGTCAGTTCCTGGCCAGATGT
ATCAATGAAATTAACTGAGAAAGGAGTGTTCCAGTCCATACGAAAATCCTTCAACATATCTGGAACCAAGAGCTTGCGGAATCTGCTCTCACCCCGT
CGCAGAAAGTCAACGCTGAAAAGGAATAAATCTGCTTTGAGGCAACTTGACGAGAAAGAACTTTTCATGGAACTCATCAGAGATATAGCTGATGAAC
TGGATCTGAATACACTTTGCCACAAAATTTTGATGAATGTCAGCATTCTTACAAATGGTGACAGATGCAGCCTCTTTCTTGCCCGAGGCACCAAGGA
TAGACGCTTTCTTGTTTCCAAGCTCTTTGATGTGAACGAGAACTCTACCGTGGAAGATTCATTGCACTCTGAAGAGGAGGAGATCCACATCCCATTT
GGGCAAGGCATTGCTGGCCATGTTGCTCAGACCAAGGAAACAGTCAACATCAAGAATGCCTATGAGGACAAGCGTTTCAACCCCGAGGTAGACAAGA
TCACTGGATACAAGACCCACAGCATCATGTGTATGCCAATCTGTAACCATGATGGTGAGGTGGTGGGCGTGGCTCAGGTCATCAACAAGATCACTGG
TTCTCATGAGTTTGCCGCCAAGGATGAAGAGGCACAGGTTGAACTGAGAAGAATAGTGTCACATGAGTTCAACCCTGCAGATGAAGAGGTGTTCAAA
AACTACTTGACCTTTTGCGGCATCGGGATAATGAATGCTCAGCTTTTCGAGATGTCCGTCAACGAGTACAAGAGGAATCAGATGCTACTTCAACTGG
CTCGAGGTATCTTTGAAGAGCAGACTTCCTTGGACAATGTGGTTCACAAGATAATGAGGCAAGCAGTTAGTCTGCTGAAGTGCCAGCGATGCATGGT
TTTCATCTTAGAGACAACAGAAGAATCGTACTTGCCCGCTCAGCTGAGAATGGCAGAAGGGAAACGACATTCAATAGCTTACCAGTCCAGTTTTGAT
GCTCCATTGAATGACGTCAAGAACATCAGCTTCCTGAAGGGTTTCGAACTTACAGATGAGGATACAGAGAAACTCAAGACAATCCCTCATGAGATGC
TGAAAAACTCAATCAATGCTACTATAGCCCGTCATGTTGCTGATTCAGGAGAGACAACCAATATCGCTGACTTCACTGTGCAGAAACAGTTCAAGGA
AATAAGTGACGTGGACCCAGAATTCAGGATTCGATCCGTCCTCTGCCAACCCATCTACAACAGTGAGCAGAAGATTATTGGTGTAGCTCAGATGATC
AACAAGGCTTGCAAACAGACCTTCACAGACCAGGATGAACATCTCTTTGAGGCTTTTGCTATCTTCTGTGGACTGGGTATCCACAACACTCAGATGT
TTGAGAATGCTATGAGGCTGATGGCCAAGCAACAGGTTGCCCTTGATGTGCTCTCGTACCACGCAACTGCACAACCAGACGAGGTTTCAAAACTCAA
GAAAAGTTGTGTGCCTTCAGCGCGGGAGTTGAAGCTGTATGAGTTCAGCTTCAGTGACTTTGACTTGACAGAAGATCAGACACTTCAAGGCACACTG
AGGATGTTCATCGAGTGTAACCTCATCGAGAAGTACCACATCCCATATGACGTACTCTGTAGATGGACGCTGAGTGTACGTAAGAACTACAGACCAG
TGATCTACCACAATTGGCGGCATGCTTTCAATGTGGCCCAAACAATGTTCTCCATTGTAATGACTGGAAAGCTGAGGAAGCTTCTGACAGACCTGGA
AATTTTTGCTCTCATCGTTGCCTGTCTCTGCCATGACCTGGATCATAGGGGGACCAACAACACTTTCCAAGTCAAGACTTCTTCCCCACTGTCTCTG
CTGTATGGTACCTCTACCATGGAACATCATCACTTTGATCACTGCATTATGATACTCAACAGTGAGGGAAACAACATCTTTGAGTTCATGTCTCCTG
ACGATTACCGTGAGGCTATAAGGATGTTGGAAAGTGCCATTCTGTCAACCGATTTGGCTATCTACTTCAAGAAGAGGGCTGATTTCTTCAAGCTGGT
AGAAAAAGGAGAGCACACATGGGACAATGAGGAAAAGAAGGGGCTGCTCAGGGGTATGCTGATGACAGCCTGTGATGTGTCAGCTATTGCCAAGCCA
TGGCTAGTCCAGCAGAAAGTGGCTGAGTTGGTCTTCAGTGAGTTCTTTCAGCAAGGCGATTTGGAGAGAGAAAAGCTCAAAGAAGAACCAATGGCGA
TGATGGACCGCAAGAAGAAGGATGAACTCCCTAAGATGCAAGTGGGTTTCATCGATGGCATCTGTATGCCTGTCTACAAGATGTTCGCTGAGCTGTG
GCCAGACCTAAAACCGCTCGAATCGGGAACCCAGCTCAACCGTGATAACTGGCAAGCATTGTCTGAAGGGAAAGAGCCAAATGATTGGGGATCTTCC
CCTCCCTCCCTCCAAACAAGCAAACAAATGGAGAGCACGATCCTCCAGAACGACAGGACCCAACTGGATACCCTTGATGAGAAACCTTCGTTGGAAT
GCATACAGAAGCAGGAAGGTAGTAGGAGTACTGGGGGCGGTGAACCCAAGAAACGGGGCTCACAGATGAGCCAACAATGCAAGGAAGCCCTGGCAGC
AAAGAAAAACAAGAGCTCCCTTTGTTCAGTAATT

OLIGO	start	len	tm	gc%	any_th	3'_th	hairpin	seq
E1 LEFT PRIMER	1461	20	58.97	50.00	0.00	0.00	0.00	GGCTTGCAAACAGACCTTCA
E2 RIGHT PRIMER	2008	20	58.96	55.00	0.00	0.00	0.00	GGAAAGTGTTGTTGGTCCCC

PRODUCT SIZE: 548, PAIR ANY_TH COMPL: 0.00, PAIR 3'_TH COMPL: 0.00

F) GMP-PDE delta (SPU_017612/ WHL22.621157)

>SPU_017612.1 CDS Sequence
ATGACACTGGAAGATTGGCATATCAATTGCACGGGACTCCTTCCAGAAGTATTCGATTTTCTTAATCTGGAAAAGAAGTCCGGTAAGACGATAGCGC
AATTTTGCGAGAAGAAATTGCAGAACGGTAACAAGTTCAGTGAGAAAGTGCTGCTACCTGTAGGTAACGTCGACAAGGTTGAAACGGATGCGATACA
GCATAGCAAGGCGGATGTGAAGGCGTCTGCATATTCCACCACTGGTCGGACGTACATGTATTTGAAGTACGTGGCCTGCTTGATCCGCCGTCTACAG
TGCTTGAAGTTCCGTCGCAAGCAGGCGGTCACAGAATTAGTCTTCTTGACTGATGAGCTTATGATCGATTTCAGTGAGAAAGTGCTGCTACCTGTAG
GTAACGTCGACAAGGTTGAAACGGATGCGATGCAGCATAGCAAGGCGGGTGTGAAGGCGTCTGGTGACCGATCTTCTCACAGAAACTGGATGAATCT
CAGAGATGCAGATTCAGGCAAAATCATGTGGCAAGGTCATGATGATTTATCGGCCCCGGATGGTGAGCATGAAGCCAGGGTGCCCAAGAAGATCCTC
AAATGCAAAGCCATCTCACGTGAAGTCAACTTCTCTTCCTTGGAGCCCATGCATCAATTCCGTCTTGAACAGAGGGTACTATTCAAAGGACGCTGCT
TAGAAGAATGGTTTTTTGAATTTGGCTTTGTAATACCGAACTCAACCAACACGTGGCAGTCAACGATAGAAGCAGCTGCAGAGGGACAAATGATGCC
CGCATCAGTACTCAGGTAA

OLIGO	start	len	tm	gc%	any_th	3'_th	hairpin	seq
F1 LEFT PRIMER	16	20	58.97	50.00	0.00	0.00	0.00	TGGCATATCAATTGCACGGG
F2 RIGHT PRIMER	610	20	59.03	50.00	11.31	0.00	0.00	TGACTTCACGTGAGATGGCT

SEQUENCE SIZE: 795

PRODUCT SIZE: 595, PAIR ANY_TH COMPL: 9.62, PAIR 3'_TH COMPL: 6.18

G) Phospodiesterase (SPU_028720/ WHL22.281736)

>SPU_028720.1 CDS Sequence
ATGCCTGATGTCAAGTGTGTCTGCTGCAAGGCTCACGATGAAGTCCTTCATGGTGTTCTCACGCACGTTTCGGAGCAAATGACAAAGGCCTTCCGAA
TAAACGAGATGAAAGATGAGATGCTTAACCGGCTTAACGTCATGCAGCAAAGAATCGAAATGGAAGGCATGAAGGCGATAGAGATTGAAAAATGTAA
AATGGAGATACGAGCCATCAAGGATGAACTACTTGCGGCAAAGAGCCGCCATGCGAACTTCTGCAAGTGCACCATACCGGCAGCCCAGGGGAACGAT

ACACGGATCGTCGCGAAGCGTGATGTCCCGAAATACCCCAAGTACACACTGTCACGCGAGACAAAGGAGTACCTCAAGAAGCCGACGTTCGACATTT
GGCATTGGGAATCGAATGAGATGCTCTGTCTTTTGGAACACATGTACCATGAGCTGGGCTTAGTAAACGAGTTTCACATGAATCCGATTGTTCTTCG
GCGATTTCTGGAGAACTACCGCAACAACCCGTTCCACAACTTTCGCCACTGCTTCTGCGTGACGCAGATGATGTACGGGATGATCTACCTGTGCGAC
CTGCAGTCTAAGGTGTGCCTCTCAGATCTGGGCATCCTACTCACGGCGGCAGTGTGCCATGATTTGGATCACCCAGGGTTCAACAACACCGCCCGGA
AAACTATCGCAATTATTCTGCAAAATTGCAAGATTTACTGTGAATTGGATCGCGACGCAAATCGCGAAGGTGTGAACGTCCCTATTGTCACAGAGCA
TTCGATAGGAATGTTACGTATTTTGTATTCTTACATTCCTTATTCTGGATACAGATATCAGATCAATGCTCGAACCGACCTGGCTATCCGATACAAC
GACATATCACCTCTAGAGAATCATCATTGTGCAGTGGCCTTCAAGATCATCAGCAACCCAGAATGCAACATCTTCAGGAACGTGCCGGAAGAACAGT
TCAAGGATATTCGGCAGGGTATCATCATGCTGATCATGGCGACCGATATGGCCCGTCATTCGGAGATCCTGGACCAGTTCAAAGCCCAGGTCGAAAG
TGGATTCGACTTCTCGAACCAGGAACATCTCAACTACCTTCGAATGGTATTGATCAAGTGCTGTGATATCTCTAACGAGGTTAGACCGTCTGATGTT
TCGGAGCCCTGGGTGGATTGCTTACTGGAGGAATATTTTATGCAGAGTGATCGGGAGAAGATAGAGGGTCTACCTGTAGCATCATTCATGGACCGTG
ACAAGGTGACAAAGCCCACAGCTCAAGTCGGATTCATCAAGTTCGTCCTCATCCCAATGTTTGAGGTGGTGGCGAAGCTCTTCACTCAGCTGAATGA
TTCAGTTGTAGAGCCGCTGCGATCCGCCCTCTACCGGTATGAAGAACAGAAGTTGAAGGAAGATCAGATCAAAGAGAAGCTGAGAGAGACGGCAAGA
ATTCGAGCGGAACAGGAGGGCGTGGACTAA

OLIGO	start	len	tm	gc%	any_th	3'_th	hairpin	seq
G1 LEFT PRIMER	10	20	58.98	50.00	0.00	0.00	0.00	GTCAAGTGTGTCTGCTGCAA
G2 RIGHT PRIMER	536	20	58.98	50.00	0.00	0.00	0.00	CAGTGGCGAAAGTTGTGGAA

SEQUENCE SIZE: 1485

PRODUCT SIZE: 527, PAIR ANY_TH COMPL: 0.00, PAIR 3'_TH COMPL: 0.00

H) Cyclid nucleotide gated ion channel (SPU_000314/ WHL22.92304)

>SPU_000314.1 CDS Sequence
ATGTACAGAAAATTGAGTCCAGTGACCATAGTGATCAGAAACTCCCAGCGCAAGAAACCCAAGATAATCGTTTTTGATCGTTCATCGGGGACCTATT
CATCCTGGCTGTTCATCATCACTGTGGCAGTCCTATACAATTTGTACCTCATCATAGCTCGGGCATCTTTTGTTCAGCTCCAGACGAACTATCGAAA
TATTTGGTTTGCTCTGGATTACATCTGTGATTTCATTTACATCCTAGATATCTGCGTGCAGTTCAGAACAGGTTATTTGGAGCAGGGTTTGTTGGTG
GTGGATTCAACGAAACTGAGAATAAACTACATGCGAGCCCGTAAAGTGACCTTCTACCTAGATGTACTATCCATGCTCCCTCTTGATTTCCTCTACT
TCAAAATCACCACAGTCTATGCCATTGTCAGGCTACCCAGACTATTAAGGTTTCATAGAGCATTAGAGTTCTTCGAACGTACAGAGACCATCACCAA
CTACCCCAACATCGTCCGCGTCGTCAACCTCATCATCTACATCATCGTCATCATCCATTGGAATGCTTGTATCTACTTCTCAATATCCAAAGAAATT
GGACTGGGCGAGGATGAATGGGTTTATGATAATAAATTTATGATGGAGTTACCAAACGGAACAAAGATATCTACTGATTCACTAACCAGAAGGTATA
TCTACAGTCTGTATTGGTCAACATTAACACTGACTACCATTGGAGAGACACCGAAACCAGTGACGAACGCAGAGCATCTTTTCGTTGTAATTGATTT
CCTTGTTGGGGTGCTTATCTTCGCCACCATTGTCGGTAATGTAGGCTCTATGATAAGCCACATGAATGCGAGTAAAGCAGACTTTCAGAACCGTATT
GATGGTGTGAAGCACTACATGAGCCTGCGTAAGGTCAGCAAAGAACTCGAACAAAGAATCATCAAATGGTTTGACTATATATGGTCCAATAAAAAGA
CCCTCGACGAAGAAGCAATACTCAACACTTTACCCGAGAAACTGCGGGCTGAAATTGCAATCCACGTTCACATGGACACTTTAAGACGAGTTACAAT
CTTTTCTGATTGCGAACCAGGACTGCTGGTGGAACTGGTCCTGAAACTGAAACCTCAGGTGTTTAGTCCGGGAGATTTCGTTTGTCGGAAGGGTGAC
ATCGGACGAGAGATGTACATCGTGAAGCAGGGTAAACTTCAGGTGGTCGGTGAGGATGGTAAGACTGTTTATGCTACTTTAAGTGACGGCAGTTACT
TCGGTGAGATCAGCATTCTTAACGTACCTGGTAGCTTATCAGGTAACCGTCGAACTGCCAACGTACGAAGTGTTGGCTATTCGGACGTGTTCTGTCT
ATCAAAGGACGATCTTCTAGATGCCCTCAAGGAGTATCCTGAAGCGAGGGTTATTCTAGAGGAGAGAGGGCGTACTATCTTAATGAAAGATGGTTTG
ATCGATGAGGAAGCCGCTAAGCGAGGTGGACGCACCGCAGAGCAAGTCGAACAGCTTGAGAAACTGGATCGCTTGGATGGGAATTTGAACCATTTGC
AAACTCGCTTCTCACGCCTTCTGCAGGAGTATAGCAATTCTCAGATGAAACTGAAACAGAGATTGACGAGGTTGGAGAAGAAGATGAAATCAGTGAG
AAGCTCTCAGTCAAACAATGAAGCGACACCAAGGTCTGGTCTGGACACTGAAATAGACACGAACAGAGGTTACGTGTCATGA

OLIGO	start	len	tm	gc%	any_th	3'_th	hairpin	seq
H1 LEFT PRIMER	503	20	59.08	55.00	0.00	0.00	0.00	GCGTCGTCAACCTCATCATC
H2 RIGHT PRIMER	1091	20	59.02	50.00	0.00	0.00	0.00	AGTCCTGGTTCGCAATCAGA

PRODUCT SIZE: 589, PAIR ANY_TH COMPL: 0.00, PAIR 3'_TH COMPL: 0.00

I) RGS9-1 regulator of G-protein signalling 9 isoform 1 (SPU_002521/ WHL22.319117)

>SPU_002521.1 CDS Sequence
ATGGCACACTGGCGGCGGGTCAACGGTGCTGGTGATGAGGAATGCTCACACCCGAATCTTATCGTCTATCGAAAGATCGAAAGATTGATTCAGCGAA
TGCAAGATGAAAGGAACGGTGTACCTGTCCGGACTGTCAAAAGTTTCATGTCAAAAGTTCCTAGTGTTTTTACAGGAGCTGATCTGGTTCAATGGTT
GATGAAGACATTAGATATTGATCAAGGTAATGACACTAGATCGTCAGCGAATTCAATACATTTAGGGTCATTGCTAGCAGCACATGGCTATTTCTTC
CCCATAACGGATCACGTACTAACACTGAAGGATGACAACACATTCTATAGGTTTCAAACACCTTACTTCTGGCCCTCAAATTGTTGGGAACCGGAAA
ACACAGATTATGCGGTATACTTGTGCAAACGAACTATGCAAAACAAATCAAGGCTAGAACTGGCAGATTATGAAGCAGAAAATCTGGCCAAATTGCA
GCGGATGTTTTCTCGAAAATGGGAGTTCATCTTCATGCAAGCAGAGGCACAAGCAAAGGTGGATAAGAAGAGAGATAAGATGGAGAGGAAAGTGTTG
GATAGTCAAGAAAGAGCGTTCTGGGACGTCCATCGGCCTGTACCAGGCTGCGTCAACACTACTGAAATGGACATCAAGAAACTCAGCAGAATCAACA
GAACATTCAAGAAGAAAAAGATCAACTCACCTGAAGATGGTGATAGATGTCCGTCAGATTCAGACATACAATCAGCTTCAGAAGAAAGCAAGAGACA
GGTGGAGATGCTGAAAGCAAGATTAGAAAAGAGGCAGTACAAGACGTCTAAGGTGGCAGAACTATTAATAGCATACTGTCAGCAGTATCGAGACTAC
GACTCGTTTCTCTCGACGGAGCTGGGTCCAAATCCTTGGATAACGGACGACACAGCATTGTGGGAAGCTGCCTCAACTATGAGTTTGAAGGAGGTAC
CAGTGTACAGGGTCAAAAAATGGGGTTTCTCCTTCGATGATCTCCTGAAGGACTCCCTAGGGAGAGATCAGCTCTCAAAGTTCCTGGCTAAGGAGTT
CAGTGATGAAAACCTGAGGTTTTGGATTGCATGTCAAGACCTCAAAAAGATGACTTTCAGTCAAGTACCAGCAAAAGTGCAGCAAATATACAGTGAA
TTCTTGTCAGACAGTTCACACAGTCCCATCAACGTGGATTCAAAGATCCTGGACACTACACGCAAAAACATGAAGAACCCCAACCGCTACACCTTTG
ATGCCGCCCAGGAACATATATACACGCTAATGCGCAGCGATAGTTACCCCCGTTTTCTCAGGTCGGAACAGTACAAGGAGCTGCTTAACCCAAAGAA
AAAGACCAAGTCTCTGATCCCTAAATTGCCCAGTCTGGCAACCAAGGCCGAAGTCTTGGATAAATGA

OLIGO	start	len	tm	gc%	any_th	3'_th	hairpin	seq
I1 LEFT PRIMER	815	20	58.95	50.00	19.32	0.00	0.00	ACAAGACGTCTAAGGTGGCA
I2 RIGHT PRIMER	1330	20	58.85	55.00	1.66	1.66	0.00	GTTCCGACCTGAGAAAACGG

SEQUENCE SIZE: 1425

PRODUCT SIZE: 516, PAIR ANY_TH COMPL: 5.34, PAIR 3'_TH COMPL: 0.00

J) GC1 guanylyl cyclase GC-E precursor (SPU_024339/ WHL22.210138)

```
>SPU_024339.1 CDS Sequence
ATGGCGCATGCACGACACCTGTTCCTATTGTTGGTCGCCTTTACGATCACGATGGTGATTGCGAGATTGGACTTCAATCCAACCATCATCAACGAAG
ATCGTGGAAGAACCAAAATTCACGTTGGATTACTGGCAGAATGGACGACCGCAGACGGAGACCAAGGAACACTGGGCTTTCCCGCTCTTGGTGCTTT
ACCATTAGCAATATCATTGGCCAACCAAGATTCTAACATTCTTAATGGATTCGACGTTCAGTTTGAATGGGTTGACACCCACTGTGATATTAACATC
GGAATGCATGCTGTAAGCGATTGGTGGAAACGAGGCTTTGTTGGTGTTATTGGACCGGGTTGTGGTTGTACCTATGAGGGTCGTCTTGCCTCTGCTC
TCAACATCCCCATGATCGACTATGTTTGTGATGAAAACCCAGTATCGGACAAATCCATCTATCCAACTTTCCTTCGTACCATTCCACCAAGCATCCA
AGTTGTCGAAGCCATGATCCTTACACTACAAAGATACGACTGGGATCAGGTGTCAGTAGTTGTTGAAAATATCACAAAGTACCGGAACATCTTTAAC
ACAATGAAGGACAAATTTGATGAGCGAGATTATGAGATTCTGCACGAGGAGTATTATGCAGGATTCGATCCATGGGACTACGAAATGGATGATCCTT
TCTCTGAAATTATCCAACGGACTAAAGAAACAACGAGAATTTATGTATTCTTTGGTGATGCTAGCGACCTTCGTCAGTTTGCTATGACAGCCTTAGA
TGAGGGAATCTTAGACTCGGGTGATTATGTGATTCTTGGAGCCGTCGTTGATTTAGAAGTCAGAGACAGTCAAGATTATCATAGTCTCGATTATATC
CTGGACACATCTGAATACTTGAATCAGATAAATCCTGATTATGCACGACTCTTTAAGAATCGAGAATATACTAGAAGTGACAATGACCGTGCGCTTG
AAGCTTTGAAGAGTGTTATCATTGTTACTGGAGCACCAGTACTAAAAACAAGAAACTGGGATCGATTTTCAACCTTTGTGATCGACAACGCACTTGA
TGCGCCTTTCAATGGTGAACTAGAATTAAGAGCTGAAATTGACTTTGCATCGGTGTATATGTTTGATGCCACGATGCAGCTTTTGGAAGCATTGGAT
CGCACACACGCGGCCGGGGGTGATATATATGATGGAGAAGAAGTGGTTTCGACCCTCTTAAACTCGACGTATCGAAGTAAGACCGACACCTTCTATC
AGTTTGATGAGAATGGAGACGGTGTAAAGCCTTATGTTCTACTGCATCTTATACCTATACCTAAAGGAGATGGAGGAGCGACTAAAGATTCACTTGG
CATGTATCCTATCGGAACATTTAATAGAGAAAACGGCCAATGGGGTTTTGAAGAGGCTTTGGATGAGGATGCAAACGTTTTGAGACCTGTTTGGCAT
AACAGAGATGAACCTCCTCTGGACATGCCTCCTTGTGGATTCCATGGCGAACTTTGCACAAATTGGGCACTTTATCTTGGAGCTTCTATACCGACCT
TCCTCATCATCTTTGGAGGACTAATTGGTTTCTTTATTTACAGGAAGCGGGCGTACGAAGCAGCACTTGATAGCTTGGTGTGGAAGGTTGACTGGAG
TGAAGTACAAACTAAAGCAACGGATACAAATTCTCAGGGATTCTCCATGAAGAACATGGTTATGAGTGCCATCTCGGTCATATCGAATGCTGAAAAA
CAACAGATATTTGCTACCATTGGTACATACAGGGGTACAGTGTGTGCTCTTCATGCAGTTCATAAGAACCACATTGATCTGACAAGGGCTGTAAGAA
CTGAGCTGAAAATAATGCGTGACATGAGACATGATAACATTTGTCCTTTCATCGGAGCTTGTATTGATCGTCCTCATATCAGTATCCTGATGCACTA
CTGCGCTAAGGGAAGCTTGCAGGATATTCTTGAGAATGATGACATCAAGCTGGACAGTATGTTCTTGTCATCACTGATTGCTGACCTGGTCAAAGGC
ATCGTCTATCTGCATAGTTCGGAGATCAAATCGCATGGGCATCTGAAATCAAGCAACTGTGTGGTCGATAACCGTTGGGTACTTCAGATCACTGATT
ATGGCCTGAATGAATTCAAGAAGGGACAGAAACAAGATGTCGACCTCGGTGACCATGCAAAACTAGCCCGTCAATTGTGGACATCACCAGAGCATCT
CCGACAAGAAGGGAGCATGCCTACAGCAGGCTCCCCTCAAGGAGATATATACTCGTTTGCTATCATCTTGACTGAACTTTACTCAAGACAAGAGCCC
TTCCATGAGAACGAAATGGATCTAGCAGATATCATTGCACGAGTGAAGATTGGTGAAGTGCCGCCCTATCGTCCGATCCTGAATGCAGTAAATGCTG
CTGCTCCAGACTGTGTACTCAGTGCGATACGTGCATGCTGGCCTGAAGATCCTGATGACCGACCCAATATCATGGCAGTACGCACCATGTTAGCTCC
ATTGCAGAAAGGATTGAAACCTAACATTCTGGACAACATGATTGCCATCATGGAACGCTATACCAATAACTTGGAAGAACTAGTAGATGAACGAACA
CAGGAACTGCAGAAGGAGAAGACTAAGACAGAACAACTACTTCATCGTATGCTTCCACCATCCATTGCATCTCAGCTGATCAAGGGTATTGCTGTCT
TACCCGAAACCTTTGAAATGGTATCCATCTTCTTCTCTGACATTGTTGGTTTTACTGCCCTCTCTGCGGCTAGTACACCAATTCAGGTCGTGAACCT
GCTGAATGATTTGTACACTCTTTTCGATGCCATTATTTCCAACTATGACGTGTACAAGGTCGAAACCATTGGAGATGCATACATGCTTGTATCCGGT
TTACCTCTCCGTAATGGAGATCGTCATGCTGGTCAGATCGCATCTACTGCTCATCATCTCTTAGAATCTGTCAAAGGATTCATTGTACCTCATAAAC
CCGAGGTCTTCCTTAAACTCCGTATTGGTATCCATTCGGGTTCATGTGTCGCTGGCGTAGTTGGTCTAACGATGCCTCGTTATTGTCTCTTTGGAGA
TACCGTCAACACAGCATCCCGTATGGAATCAAATGGACTTGCTCTGCGAATCCACGTTAGTCCATGGTGCAAACAGGTTCTGGATAAGCTTGGTGGT
TATGAACTTGAAGATCGAGGCCTTGTTCCAATGAAGGGTAAAGGAGAAATCCATACCTTCTGGTTGCTAGGACAAGATCCAAGCTACAAGATCACCA
AGGTCAAACCACCACCACAGAAGCTCACTCAAGAGGCCATAGAGATCGCTGCTAATCGTGTCATACCTGATGACGTCTAA

OLIGO            start  len      tm     gc%  any_th  3'_th hairpin seq
J1 LEFT PRIMER      2196   20   59.02   50.00   17.47   1.62    0.00 ACTAGCCCGTCAATTGTGGA
J2 RIGHT PRIMER     2687   20   58.88   50.00    0.00   0.00    0.00 GCAATGGATGGTGGAAGCAT

PRODUCT SIZE: 492, PAIR ANY_TH COMPL: 0.00, PAIR 3'_TH COMPL: 0.00
```

K) Recoverin or GCAP1 guanylyl cyclase-activating protein 1 or GCAP2 guanylyl cyclase-activating protein 2 (SPU_026993/ WHL22.599379)

```
>SPU_026993.1 CDS Sequence
ATGATCAACACCATACTTAAAGCTGGAGACTTCCACAAGACTGGGGAGTGCTTCAGATTTTTTAATTGTTTTCACCCAGTTAAAGATGAAGTTAAGT
TATGGTCACGCGATAGCATTGTGAAAGAAACAGTGTGGAAGCGATCAGAAAAGGTTGATCATCTAGCATATTGTCCTAGTGGACACCTAACCGTGGA
AGAATTCAAGAAGATATATGGCAACTTTTTCCCTTACGGCGATGCGTCAAAGTTTGCAGAGCATGTATTCCGCACATTTGACTCCAACAGCGACGGC
ACAATCGACTTCCGTGAATTCATCTGCGCCCTGAGCGTCACGTCGCGAGGGAAGCTGGAGGAGAAACTGAAATGGGCCTTCAGTATGTACGACTTGG
ACGGCAACGGATATATATCAAGACAAGAAATGCTAGAAATTGTACAGGCGATCTACAAGATGGTCGGCACAGTGATGAAGATGCCCGAGGACGAGTC
GACGCCCGAGAAGAGGACAGACAAGATCTTCCGACAGATGGACGAGAACCTGGACGGCAAACTTTCCCTGGCTGAATTCATCAAGGGGGCGAAACAG
GACCCCTCGATAGTCAGGCTTCTCCAATGCGACCCTAGCGGGAGCGCTGTGACGAAGTGA

OLIGO               start  len      tm     gc%  any_th  3'_th hairpin seq
K1 LEFT PRIMER         39   20   59.09   55.00   11.09   0.00    0.00 GACTGGGGAGTGCTTCAGAT
K2 RIGHT PRIMER       561   20   58.96   50.00    0.00   0.00    0.00 TTCAGCCAGGGAAAGTTTGC
SEQUENCE SIZE: 642

PRODUCT SIZE: 523, PAIR ANY_TH COMPL: 0.00, PAIR 3'_TH COMPL: 0.00
```

Rhabdomeric components

L) G-alpha-q subunit (SPU_003898/ -)

```
>SPU_003898.1 CDS Sequence
ATGGCTTGTTGTCTCAGCGAAGAAGCGAAAGAACAGAAGAGAATCAACCAAGAAATAGAGAAACAGCTACGAAAAGACAAACGAGATGCACGAAGGG
AGCTCAAGTTACTGTTGTTGGGCACGGGAGAGAGTGGTAAAAGTACATTCATCAAGCAGATGAGAATTATTCATGGGGCAGGTTACACGGAAGAAGA
TAGGAAGACATTCACCAAGCTTGTATACCAAAATATTTTCATGGCCATCAATGCAATGATCAGAGCCATGGACACACTCAAGATAGCCTACGGCGAC
```

```
CCTACAAATGAGAAAAAAGCTCAGGAGGTCAGATTAATAGACCACGAAACAGTAACGGTATTTCATGAGCCATACATAGGTTATGTAGATTGTATAT
GGAATGATTCAGGAATTCAAGAATGTTATGACAGAAGGAGAGAATACCAGCTCACAGATTCAGCAAAATACTACCTTAGTGATTTAAAGAGAATTTC
AGATTCAAACTATATACCTACGGAACAAGATGTACTCAGAGTACGAGTACCCACAACAGGAATCATTGAATATCCGTTTGATCTAGATTCAATTATT
TTCAGGATGGTCGATGTTGGAGGGCAGAGGTCAGAACGACGAAAGTGGATTCACTGTTTTGAGAATGTCACATCTATAATGTTTCTAGTCGCCTTAA
GTGAATATGACCAATTGCTTGTCGAGTCAGATAGTGAGGTGATATTAAAAGTGCGAGTGCGATTTGATCCTGACCAGTACCGACGCTACAAGTGGCG
CCTTCGACTGGCCATCATCATCCTGCCCCTGCTCTTCACTGTGATCAACCTGGTCTCAGGGATCTTGATCCGTGTGTTAGACGGCGAGCATGCCAAA
CACGACACACTCACCACTAGAGTTATCCTCAATGAAGGTCTCTTCCTCCTTGCAGCAGTCTGGCTTTCCATCTGTATCTGGAAGATAACACACATGA
CGTCAGCCAACGTGCTCCTTGAGGCAAGGGGAACCACAGTAGGTCAAGCCTGTGTTGCATGTGTAGTCATCATCCTCCTGTATGTGACC

OLIGO            start  len      tm     gc%  any_th  3'_th hairpin seq
L1 LEFT PRIMER       258   20   58.94   50.00   12.51    0.00    0.00 AGCCATGGACACACTCAAGA
L2 RIGHT PRIMER      821   20   59.38   55.00    0.00    0.00    0.00 ATCACAGTGAAGAGCAGGGG
SEQUENCE SIZE: 1059

PRODUCT SIZE: 564, PAIR ANY_TH COMPL: 0.00, PAIR 3'_TH COMPL: 0.00
```

M) Phospholipase C (SPU_009929/ WHL22.169178)

```
>SPU_009929.1 CDS Sequence
GATGACACAATCGACCCTAAGAAGTTCACATATGATGTTTTCTTCACATTCTACCTTCGCTTAGTCAACCAAAAAGAAGTGGACAGATTATTCCAAG
AGATGGGAGCGAGGAACAAGCCCTATTTGCAGACAGCCCAACTGGTAAAGTTCCTGAACAATGAACAGCGTGACCCTCGTCTTAATGAGATCCTTTA
TCCATTCTATGATGCCAAGACAGCTATAAGTATCCTGGAGAGGTTTGAGAAGAACAAACAGTTTGCCAAGAAAGGTAACATGTCAATAGAGGGATTG
ATTCGTTATCTAATCAGTGATGATAACCAGGTGGATGGTCTGGAGTCTTATCTTATTGCTCAAGATATGGAGCAACCATTGGCTCATTACTTCATCA
AATCATCTCACAACACATACCTCACAGGTCATCAGTTGACAGGGAAGTCGACCGTTGAGATCTATCGTCAGGTGTTACTATCAGGATGTCGCTGTGT
AGAGCTGGATTGCTGGGATGGTAAAGGTGATACAGACCCTGAACCGGATGTGATAGAAGCCATTAATGAAACAGCCTTCAAGACGTCGGAGTACCCT
GTTATCCTTTCCTTTGAGAATCACTGCAATCAAAAGCAGCAGGCCAAGATGGCTCATTATTGCAGAACAATCTTTGGAGACAAGCTTCTCATTGATC
CACTCCCAGAGTTTCCTTTGGAAGCGGGGAAGCCGCAGCCCTGTCCGGCAGCTCTCAAGAATAAGATCCTGGTGAAGAACAAGAAACGCAAGCACAC
AGATGCAAGCAAGAAACGAGCAGCCTCTCGAAGAGGTAGCAAGCGTAAAATGCTCCTACAGATCTCAGAAGTGACTTATGATGAGACTATTATCCCA
GACGACTCAGGAAAGGGAGTGAAGACAATTGAGGAGACGGCTGAGACACCAGAACAAAATGGAGAAGTCACAGTGAAAAGTGATGATGTAAAGCAGA
GAAGAAAATTATCTCGACAGGAGGCACAAGAGAAAAGTGGAGATGTTGAAATGAACGGTGAAAATGGAGATGCAGGCAATGATTCCAAACTGACTGA
TGTCCAAGAGGACGACGATGAGGAGAGTGATGAAAGCGATGATGAGGAAGCTCTCAGTAAGGAAGAAGCGCTCAAAAAGCTGCAGGAAAAGAAAGAC
AGGGGTACAGCTGGTCAAGAAGCAGAGGCCGGAGCTGAGATGTCAGCCTTGGTCAATTACGTCCAGCCGGTCCATTTCTCAACTTTTGAAGGGTCAG
ACAAGAGAAACCACAGCTATGAGATCTCATCATTTGTGGAAACTTCAGCCATGAACAGAGTCAAGGAAAATCCTGTGGAATTCGTCAACTACAACAA
GAGACAATTGTCTAGGATCTACCCTAAAGGAACCAGAGTAGACTCAAGTAACTTCATGCCTCAGATCTTTTGGAATGTTGGTTGCCAGTTGGTTGCT
CTCAACTACCAAAATCTTGATCTACCAATGCAACTGAATCTTGGTCTGTTCAATCTGAATGGTAGAACAGGATATATCCTTAAACCTGACTTCATGC
GAAGAAAGGACCGCCATTTTGATCCCTTCGCTGAATCCACCATGGATGGCATTGTAGCTGCTACCGTAGAGGTCAAGGTGCTATCTGGCCAGTTCTT
GAAGAAGGTTGGAACATACATTGAGGTGGACATGTTTGGTCTACCAGCAGACACAGTAAGGAAGAAGTATAAGACTAAGACTATCAACAATACTGGT
ATCAACCCTCAGTATGAAGATGATGGCTTCATCTTTCCCAAGGTTATCATGCCTAAACTAGCTATGTTAAGAATCACTGCATATGACGATAACAACA
AACAGATTGGACATCGTATTCTACCAGTAGAATCACTCAGACCAGGGTATCGTCACATCCCTCTGCGCAATGAGCTCTACCAGCCTCTCCTCATGCC
ATCAGTCTTTGTCCACATCAAGGTCAAAGACTACGTGCCCGTTGGTCTGGCAAACTTTGCAGATGCTCTGGTCAATCCTATCCAGCATCAGCTCAAG
ATGGATGAACAGGTCAAGATCAGGACAGAAGCTCTCTCAATTCTCTTGGAAGAAGCCAAATTGATGGAGGAATCGAAAGAAGCTGCAGTAGAGGACA
GTCCCGATGATATGGCTAACACCTCCACACCGGAGCCTCAAAAAGAAGAGACCGGTGAGGGATCAAGTTCACCTGAGCAGGAGAGTAAACCTCCAAT
AGATAATGCTGCCATAACTGAGGGGATGCCTAGTAACAAACCACTGGAACATACTAGGCTGGAAATGCTAGAGAAGAGGGACAGCGTTGATGCGTTG
CCCCCGACGATGAAGAAAGTATCCAGGCCATCCAGACAGTCAGAGGAGATAGTTGCTGCCACCATTGATGAGATTAAAGTAGAGAAGAAATATGTGA
AGGTGAAGACACGGCTGGACAATGAGCTCAATAAGCTGGTGAAGAAACAAGAGAAAAAACAGAGTAAACTCAAGAAGGGTCAGTCCAAGGACATCAC
TAAATTCAAGATGTCTCAAGAGAAAGCGAGGAGGAATAAAGAGAAGAAGCTGGTTTCCATGGAGAAGAAGATGCTCAAGAACACAACTCCTGAAGAA
GCCAAACAGCAAAGTGCCAAAACTATGGAGCAGTTAGAGCAAGAACAAGAAAAAGAGATGCTGAAGAAGCAAGTGAGCCAGGAGGATGCGTTGATAG
GTCTGTACAGACGTCACTACCTGGAGGAGAAGGAGCTGAAGGTGGAGCATGCAGAGATGCTCTTTGAGCTTCAGATGGATCTCATGGCAGCTATACA
TGAAAAACAACTCAAGAAACTAGATGGTCAGCACAAGAAGTAA

OLIGO              start  len      tm     gc%  any_th  3'_th hairpin seq
M1 LEFT PRIMER      1075   20   59.06   60.00    0.00    0.00    0.00 GAGGACGACGATGAGGAGAG
M2 RIGHT PRIMER     1571   20   58.83   50.00    0.00    0.00    0.00 AAATGGCGGTCCTTTCTTCG

PRODUCT SIZE: 497, PAIR ANY_TH COMPL: 2.80, PAIR 3'_TH COMPL: 2.25
```

N) Trp-C protein (SPU_017326/ WHL22.316252)

```
>SPU_017326.1 CDS Sequence
ATGCCCAAGTTCTACCATGTCGATTCGCTCAGTGACCGCATCCCCCTCCAGATCGTCCGGAAAGAAGTGCCCCTATCACCGGCCGAGAAGCAGTACC
TGTTGGCGGTAGAGCGCGGAGACTTCGCCAGTGTCCGCCATGCACTCGAAGAGGCGGAGATCTACTTTAACATCAACATCAACTGCAGGGATCCCCT
TGGTAGAACTGCGCTCCAGATCGCCATCCAGAATGAGAATATCGAGATCATTGAGCTCCTACTTCGTTACCATGTACACGTGGGCGACGCTCTCCTT
CACGCCATCGATGAGGAGGTGGTTGAGGCCGTCGAACTCCTCCTCAACTATAAACCTCCAAAGAAGGATCTCCATGTTCGGATACTGCAAGAGACCC
AAGAATCCGACTACGATTCCGACATCTCCCCGGTTATCATGGCGGCTCATCGGAACAACTACGAGATCCTCAAAGTGCTGTTAGAACGCGGGGCATC
GATCCCTAAACCTCACGATGTCAAGTGCGGCTGCGACGACTGCAAGGCCAGCATACGTCACGATGGCTTGCGACATTCGCGGTCAAGGCTAAATATC
TACCGTGCCCTCGCTAGCTCTTCGCTGATCGCCCTGTCCAGCGATGATCCCGTACTCACTGCCTTTGAGTTGAGTTGGGAGCTGCGAAAACTCAGTC
ATAAAGAAAACGAGTTCAAAGAGGAGTACGAGAAGCTAGCTGAGAACTGTCGAGTGTTTGCGACACAGCTGTTAGACCAGACGAGGGGATCTCATGA
ACTTTCAACAATCCTTAACCGCGATGAAGATGCTCCATCGAGTGAGGAACCCCTCAGCAGATTAAGACTTGCCATCAAGTACAAGCAAAAAGCGTTT
ACGGCCCATCCGAATTGCCAGCAGCTGCTCGCAGAGGAGTGGTACCAGGGCCTACCGGGCTGGCGGAGGCAGCATTGGACCCTCAAGGTGGTCATCA
GCTTCTTTGTGGGCATGTCCTTTCCTCTGCTCTCCTTCATGTACCTCCTGGCGCCCAAGACTAAGCTTGGTCGGATACTTCGTCTTCCATTCATCCA
GTTCATTTGTCATAGTGCCTCCTATTTGATTTTTGTCGTCTTACTTCTCATGGCTTCGCTCGAATTCACCAACAAGTCAACGTCCACTCGCGTCGAC
ATGCGTGGTCCCCCGCCCACGGATGTCGAGCTCCTTATCGCCTGGTGGATCGCAGGGTTTGTGTGGGCAGAAATCAAACAACTCTGGGACGCGGGAA
TAATCGAGTATCTTCATGACTGGTGGAATTTACTCGATTTCATAACCAACTCGCTTTATATAACAGTCATAGGTCTAAGGGTCACGGCATACGTAAA
TATACACATAATCCTTAACGAGTCTTACGGCGATAAGGACCTGTTACGAGCGGAGTGGGACATGTGGGATCCGACGCTCTTAGCTGAAGCAGCCTTC
```

GCCGTCGCAAATGTATTGAGCATGCTTCGTCTGGTATACCTCTTCACCGCAAACTCTCACCTGGGACCTCTCCAGATCTCCTTAGGACGCATGGTCG
AGGACATCATCAAGTTCGCTTTTCTAGCCATCCTCGTCCTCTTCTCCTTCGCAGCCGGTCTCAATCAGCTCTACTGGGTGTATAGCAGCCCCCCTCC
TGACGGTAGTGGGTGCACCGGGGTGACCTGTGAAAATCAGGACCATAATGTATTCTCAAATATGCTGACGTCGCTGGAGGCGTTGATGTGGGCCATC
TTTGGCCAGCTGCAGGTATCCGTAGTCAACCTCCCAACAAGTCATGACGTCACCGTGTTCATCGGCGCCGTCATGCTCTGCACATACAGCGTCATCA
CCATTGTCATCCTTCTCAATCTCCTCATCGCCATGATGAACACCTCGTTCCAGAAAATTCAGACCCGAGCCGACATGGAGTGGAAGTTCGCCCGAGC
CAAGCTGTGGATGAGTTACTTCGAAGAAGGCAACACCCTTCCTTCCCCCTTCAACACCATTCCAAGCCCAAAGTCATTCTACTATTTATTCCGATAT
TTATGGAAAAATATATGCTGTTGCCAATGGAAGCTAAAGAAACAAGCCAGTGTCAACAGAGTGCGAGATCAGACCCAAAAGAAGAAGGAGAAAGACG
ATGACTATCAGAGGGTCGTGAAAAACTTGGTCAAGCGTTACCTGAAGTACTCTAAGCGTGGTGAGCAAGAGAAGGGCGTCACCGAGGATGATCTCAA
CGAGATCAAACAGGACATCTCTGCATTCCGTTACGAGATGCTGGAAATCCTCAAGAACAAGGACCCAGTTATCGCTCCCAAAAGCGTCAAGTTCCAA
AACGGAACCGGTGGCAATGGCCCCGATCCTAGCCGAAAGACCACGAACTCATCCGATGACGAGAATAAGCTTCACCGAGTCCCGTCTTACCTCTTTC
GGAAGGGTAAGAAGGGTAAGAAGAGTCCGTCACATGACCAGCCCGCCATTAAGCCAATCAAGAGCGCCCCCATCCGGGATGAGGATTACGCCATGCC
CGATTTTTTAAAAGTGAAAAACGTGAAGAACGTGATGGTGGCAGTCAACGAACTCCAGAAGAAATCTATGAGGAGAAGGTTATCACAGGCCGCGGTG
ATTGAGGCGAGAGCTCAAGAGGAGAGACGGTTGTCTGCAGCGTCTCTATCACCTGATGCCATACAGGAGGTGGCTCCGCCATGGAAAAAGCCAACTT
TGAGTGATTCGGGCATATCCGAATCGGTGGAAGACCCACCCGTTCCCAGGAAGTTAGACACGGTCAACGAGTATTCGACGGAGGAGGAAGGAGTAAG
TCAGAGTGGTGGTAGTCAGGAGAGGAAAGACAGGGATGTTGATGATGTGGACGATTCATCGCGAAGATCATCGCTTACTGGGAGAGCCCCTCTGAGG
AGAGAAAAGGCTTTTGCGTCAAGAATGGAGGAAGAGGGCAATCCGCCGGTGATTCCTCCAGCAGATCCAAACGCACCCTCTCCGGACGCCAGTGCCG
ATTCGCAGAGCACCTCAGGGATAGCCTCGACAAACAATAGCTTCCAATCGCAGGACTCAAGAGAGGACGACCTTGACGATGAGAACGACGATGGTGA
CGATGACGATGACGACGACGACGAAGACGATGATCTACATATCACTGAGGCCAACGCTACTAACAGCAGCGAGGAGATCGACGAAGACGCCTCG
GTCGATCGAGTAAATTTATCGCCGCTGCTTGGTAGTAGTGGGGGCGTTGGAGATCAACCTTTGACAGAAATTCCGCAGCTTAATTGGCAATCCAAAA
GGCCTTCAAACCCATGGACGGACAATAATCCCCCAAAAGATGGCATCGAAATGAAGAGATATGTCTACAATGGTTTCAACAACTCATCACAATGA

OLIGO	start	len	tm	gc%	any_th	3'_th	hairpin	seq
N1 LEFT PRIMER	1765	20	59.03	55.00	0.00	0.00	0.00	TCCGTAGTCAACCTCCCAAC
N2 RIGHT PRIMER	2204	20	59.03	50.00	0.00	0.00	0.00	TCTTGCTCACCACGCTTAGA

PRODUCT SIZE: 440, PAIR ANY_TH COMPL: 0.00, PAIR 3'_TH COMPL: 0.00

Shared components

O) Visual G beta (SPU_000508/ WHL22.101602)

>SPU_000508.1 CDS Sequence
ATGGCGACTGAATTAGAACATCTACGGCATGAAGGGGAGACCTTAAAAAACCAAATCAGGGATGCCAGGAAGGCTGTACAAGATACCACATTGATGC
AAGTCACACAGAATATGGATCCAGTTGGAAGAATTCAAATGAGAACTCGTCGCACACTTCGGGGTCATTTGGCAAAAATATACGCCATGCATTGGGG
TACAGATTCAAGCAGAAACCTAGTGAGTGCGTCACAGGATGGCAAATTGATAGTCTGGGATTCATACACAACTAATAAGGTGCATGCAATTCCATTG
CGGTCCAGCTGGGTGATGACCTGTGCCTATGCTCCTACCGGTAGTTTTGTGGCCTGTGGAGGTCTCGACAACATATGTTCAATCTATAGCCTCAAGA
CCAGAGAAGGCAATGTTCGTGTAAGCAGAGAACTCCCAGGACATACCGGTTACCTATCATGCTGCCGATTTATCGATGACAATCAAATAGTAACTAG
TTCAGGAGATATGTCATGGTAA

OLIGO	start	len	tm	gc%	any_th	3'_th	hairpin	seq
O1 LEFT PRIMER	20	20	58.95	55.00	0.00	0.00	0.00	ATCTACGGCATGAAGGGGAG
O2 RIGHT PRIMER	432	20	59.09	55.00	0.00	0.00	0.00	ATGTCCTGGGAGTTCTCTGC

SEQUENCE SIZE: 507

PRODUCT SIZE: 413, PAIR ANY_TH COMPL: 0.00, PAIR 3'_TH COMPL: 0.00

P) Rhodopsin kinase (SPU_001621/ WHL22.64904)

>SPU_001621.1 CDS Sequence
ATGGCGGATCTAGAAGCCGTTTTGGCGGATGTGAGCTACCTTATGGCGATGGAGAAGAGTAAATCTACTCCGGCTGCCAGGGCAAGCAAGAAGCTGG
TTCTTCCTGACCCGAGTGTAAGAACAGTGATGTACAAATACTTGGAGGAAAGGAAAGAAATCACATTTGAAAAGATCTTTGGACAAAAGCTTGGATA
TCTTCTGTTCAAAGACTACTGTGAGAATTGCGCAGATGTGCAAGTCCAGCAACTGCAATTCTATGAAGCGATCAAAGATTACGAAAAACTTGACACC
CTTGATGAAAGGCTAGAAGAAGCCAGAAGAATCTTTGATAACTACATCATGAAGGAAGTCTTATCATGTACACATCAATTCTCAAAGTCAGCAGTAG
AAAACGTGAGACAAAGACTGACCAACCAAGAAGCCAAACCAGACCTCTTTAGTGACTACATAACTGAAATCCTCAATTCACTGAAAGGAGAAATATT
TCAGAAATTTTTAGAAAGTGATAAGTTTACTAGGTTTTGCCAGTGGAAAAATGTAGAACTAAATATAAATGGCATGTTGTCAATGAATGACTTCAGT
GTACACAGAATAATTGGCAGGGGTGGCTTTGGAGAAGTTTACGGGTGCCGCAAGGCTGACACCGGCAAAATGTATGCAATGAAATGCCTGGATAAGA
AGCGGATAAAGATGAAGTCTGGAGAAACACTTGCCCTCAACGAAAGAATAATGCTTTCTCTAGTCAGTGAGACTGATTGTCCGTTCATCGTGTGCAT
GACGTATGCATTCCAAACACCAGATAAACTCTGTTTTATTCTAGATCTTATGAATGGTGGAGACCTCCACTACCACTTGTCACAGCACGGTGTATTC
TCAGAGGAAGAGGTTGGCTTCTACGCAGCAGAGATCATCTTGGGTCTAGAGCACATGCATGTCCGTAACGTGGTCTACCGTGACCTCAAGCCTGCTA
ACATCCTACTCGATGAGAATGGTCATGTCCGTATCTCGGATCTCGGTCTGGCCTGCGACTTCTCGTCGAAGAAACCACACGCCAGTGTAGGTACCCA
TGGTTACATGGCCCCTGAAGTACTGTCCAAAGGAACTGCCTACGACTCCAGCGCTGACTGGTTCTCATTAGGATGTATGTTGTTCAAGCTACTCCAT
GGGCACAGTCCGTTCAGGCAGCACAAGACGAAAGACAAGCATGAGATTGATCGGATGACATTGACCATGGATGTTGAGTTCCCAGACAAGATGAGTG
ATGAGATGCGAGCATTACTAGCAGGTCTACTACAGAGAGAGGTAGCAAGCAGGTTAGGCTGTGAAGGCAGAGGGGCAACAGAAGTGAGAGAGCACCC
CTTCTTCAAGACTACAGACTGGAACCAAGTATACTATCAAAAGGTACAACCTCCCCTCATACCACCCAGAGGTGAAGTCAACGCTGCGGATGCCTTC
GATATCGGATCCTTTGATGAGGACGACGTTAAGGGGATCAAGGTAAGAAACCTTCCTTTTCTCACTTTTCTGAACCTTAAAACCTAA

OLIGO	start	len	tm	gc%	any_th	3'_th	hairpin	seq
P1 LEFT PRIMER	414	20	59.04	55.00	0.00	0.00	0.00	CCAAGAAGCCAAACCAGACC
P2 RIGHT PRIMER	973	20	58.94	50.00	0.00	0.00	0.00	TGTTAGCAGGCTTGAGGTCA

SEQUENCE SIZE: 1542

PRODUCT SIZE: 560, PAIR ANY_TH COMPL: 4.55, PAIR 3'_TH COMPL: 9.24

Q) Arrestin (SPU_023889/ WHL22.709217)

```
>SPU_023889.1 CDS Sequence
ATGGATGTTAGATCTGTGGTTACACTGATCCACAGACTGCTTGGGGTTGTTGCACAATCTGATTTAGGGTGTTATCAGTTTTCATCGCTGGCGCTAC
AGCTTAGAAAAGTGTTGGAGGGCTACAGGGCTGGAGCAGTATTCAAGAAATCAAGCCCTAATGGCAAGATCACAACATATCTTGGCAAAAGAGATTT
TGTCGATCATCAAACGCACATCGATCCAATTGATGGAGTTGTGTTAGTAGACCCAGACTACCTGAAGGAGAGGAAGGTCTTCGCTCATGTCCTAGCA
GCATTCCGCTATGGTCGGGAGGATCTGGATGTCCTGGGTCTGACCTTCAGGAAGGACCTGTACTTAGCTTCAGTCCAGGTCTACCCTAAGCCATCCG
ATGAGCAGAGACCACTTACCAGACTTCAAGAGAGACTCATCAAGAAGCTAGGCCCTAATGCGTATCCCTTCTACTTTGAACTGCCGATCAATTCTCC
TTCATCGGTCACGCTGCAGCCTGCACCAGGTGATACAGGCAAACCATGCGGTGTAGATTACGAACTCAAAACTTACGTTGCAGAAACGATGGATGAG
AAACCCCACAAGAGGAACTCTGTTCGGCTTGCCATCAGGAAGGTCACCTATGCCCCTGACGTCCCAGGCCCACAACCCACAGCTGAAGCACAGAAAG
ACTTTGTAGTTAGCCCAGGAGCTCTTCATCTAGAGGCAACACTTGACAAAGAGATGTACTACCATGGAGAAAGCATTGAGGTTAACGTCACCATAGC
CAACAATTCAAACCGAACGGTGAAGAAGATACGGGTGTCGGTCCGGCAGTACGCGGACATCTGCCTCTTCTCAACCGCACAGTACAAATGCCCAGTA
GCTGTAATGGAAACAGAAGATCCTGGATACGGTCTGCCTCTCAAACCTAGCCAGAAGCTGACCAAGGTATTCTGTGTCACGCCGTTACTTGACAACA
ATCGAGACAAGCGAGGGCTGGCGCTAGATGGCAAGCTTAAACATGAGGATACAAACCTGGCTTCATCCACACTGTTAAGTGCAAAAACAGAGAAGGA
ACGTGAGAGCCTGGGAATCATTGTACAGTACAAGGTCAAAGTGAAGCTAATCATCGGCTACGGAGGGGACTTATCGGTGGAGCTACCATTCACTATG
ACCCATCCTAAACCCGTTGAAGAAGAACCAGCACCTGTTCCTGCCCCTAGCCCCAACACTAACAAAGAGACAAATGAGGTTCCAGTTGACACAAATC
TTATCAATTTTGATGCAAATGGTAGTGACAACCAGCAGAAGCTTGAGGACGAGGATGATGATTTGATATTTGAGGATTTCGCCAGACTCCGACTCAA
AGGCACAGAGGGTGAAGGAACAGAGGCTTGA
OLIGO               start  len      tm     gc%  any_th  3'_th hairpin seq
Q1 LEFT PRIMER        688   20   59.09   55.00    4.08   0.00    0.00 GTTAGCCCAGGAGCTCTTCA
Q2 RIGHT PRIMER      1228   20   59.01   55.00    0.00   0.00    0.00 TGTTAGTGTTGGGGCTAGGG
SEQUENCE SIZE: 1389

PRODUCT SIZE: 541, PAIR ANY_TH COMPL: 0.00, PAIR 3'_TH COMPL: 0.82
```

R) Retinal-binding protein (SPU_004473/ WHL22.664046)

```
>SPU_004473.1 CDS Sequence
ATGAGTGGTTTTGTCGGAGATTTAAGTGAGAAGCAATCGAAAGCACTGAATGAGCTAAAATCTAGATTAGATGGAGTTGATCTTCCCGAACCAGATG
ATGTTAATATTGATTCCTACCTCTTAAAATGGCTCAGGGCTCGTCAATTTAATGTTGAACAAGCAGAACATATGCTAAGAAATCATTTATCATTCAG
GGAAAAGTGGAACGTGCAATCGCTGCTAGACAATTGGCATCCACCCGAGGTGCTGGACAAATACATGGTCGGAGGCTTGTGCGGGTTCGACAAAGGA
GGCTCACCTGTTTGGTACGAGCCGTTTGGTTACTTTGACCCGAGGGGTGTGGTTCTGTCGAGTACGGGAAATGACCTGACGAAAATGAAGATCCAGA
TATGTGAAGAAATCCTCTCTCAGCTCAGGTCACAGACAAAGAAGCTAGGGAAGCCGATAGACAGGATGGTCATTGTGTTTGACTTGGAGAAAGCGGG
TCTCTCTCACATCTGGAAGCCATTCATCGATCGATACAACCTCATCCTGCAAATATTCGAAGCCCACTACCCAGAAATGCTCAAAAAGTGCTTTGTG
ATTAATGCTCCAGCTTTCTTCTCGATCGGTTTCAACTTGATCAAGAAATTCCTGAGTGAGGCTACCAAGAATAAAGTCGTTGTTCTTGGAGGGAATT
ACCAGGATGTATTAAAAGAAGCGATAGGTGAAGACTTGCCTGCTCATTTTGGTGGTACAGTATGTGACCCAGATGGTGACCCCCGCTGCGTGTCAAA
GATCCGATTTGGTGGAAAGGTGCCTGAGTCATTCTACCTGAAGGATAATTTCATGCATGAAGGCAGACTGACTGAGGTCAATATAGGTCATGGGTCA
AACTTAGAGCTTACGTACGAGGTCAAGGAGGAAGGCCATGTACTCAAGTGGGAGTTTATGACAAGACATAACAACATTGGTTTTGGAGTGTTCTACC
AGCCATCCCCAGATACCAAGAGAGCACAGTGGGAGGAGGTGGTGGAGAGAACAAGATGCTCATGTCATCTGGTACCGGAGATTGGAGGATATTCTTG
TGAGAAGCTGGGAACGTACATTGTCCAGTTTGACAATAGCTTCAGCTGGATGAGAGGCTCTCTACAGGGTCCGGCTGATTCACGCAGACAATGGGTG
AACCAGTATAATATTGCTCCAATCATCCTGAAGCAATCCCCTGGTACTCTGCAAGACCACTGTCACTCAATCAGGACCGAGGCTAAACACAGTCCTG
CGGAGAAGCCTTAG

OLIGO               start  len      tm     gc%  any_th  3'_th hairpin seq
R1 LEFT PRIMER        215   20   58.98   50.00   11.22   0.08    0.00 CGCTGCTAGACAATTGGCAT
R2 RIGHT PRIMER       808   20   58.93   50.00    0.00   0.00    0.00 ATGACTCAGGCACCTTTCCA
SEQUENCE SIZE: 1275

PRODUCT SIZE: 594, PAIR ANY_TH COMPL: 0.00, PAIR 3'_TH COMPL: 0.00
```

APPENDIX I:

MAIN PROGRAMS DEVELOPED TO RUN

THE VERTICAL MIGRATION SET UP II

APPENDIX I: MAIN PROGRAMS DEVELOPED TO RUN THE VERTICAL MIGRATION SET UP II

Plankton column: graphic user interface

```
FUNCTION VARARGOUT = PLANKTON_COLUMN(VARARGIN)
% PLANKTON_COLUMN MATLAB CODE FOR PLANKTON_COLUMN.FIG
%      PLANKTON_COLUMN, BY ITSELF, CREATES A NEW PLANKTON_COLUMN OR RAISES
THE EXISTING
%      SINGLETON*.
%
%      H = PLANKTON_COLUMN RETURNS THE HANDLE TO A NEW PLANKTON_COLUMN OR THE
HANDLE TO
%      THE EXISTING SINGLETON*.
%
%      PLANKTON_COLUMN('CALLBACK',HOBJECT,EVENTDATA,HANDLES,...) CALLS THE
LOCAL
%      FUNCTION NAMED CALLBACK IN PLANKTON_COLUMN.M WITH THE GIVEN INPUT
ARGUMENTS.
%
%      PLANKTON_COLUMN('PROPERTY','VALUE',...) CREATES A NEW PLANKTON_COLUMN
OR RAISES THE
%      EXISTING SINGLETON*.  STARTING FROM THE LEFT, PROPERTY VALUE PAIRS ARE
%      APPLIED TO THE GUI BEFORE PLANKTON_COLUMN_OPENINGFCN GETS CALLED.  AN
%      UNRECOGNIZED PROPERTY NAME OR INVALID VALUE MAKES PROPERTY APPLICATION
%      STOP.  ALL INPUTS ARE PASSED TO PLANKTON_COLUMN_OPENINGFCN VIA
VARARGIN.
%
%      *SEE GUI OPTIONS ON GUIDE'S TOOLS MENU.  CHOOSE "GUI ALLOWS ONLY ONE
%      INSTANCE TO RUN (SINGLETON)".
%
% SEE ALSO: GUIDE, GUIDATA, GUIHANDLES

% EDIT THE ABOVE TEXT TO MODIFY THE RESPONSE TO HELP PLANKTON_COLUMN

% BEGIN INITIALIZATION CODE - DO NOT EDIT
GUI_SINGLETON = 1;
GUI_STATE = STRUCT('GUI_NAME',       MFILENAME, ...
                   'GUI_SINGLETON',  GUI_SINGLETON, ...
                   'GUI_OPENINGFCN', @PLANKTON_COLUMN_OPENINGFCN, ...
                   'GUI_OUTPUTFCN',  @PLANKTON_COLUMN_OUTPUTFCN, ...
                   'GUI_LAYOUTFCN',  [] , ...
                   'GUI_CALLBACK',   []);
IF NARGIN && ISCHAR(VARARGIN{1})
    GUI_STATE.GUI_CALLBACK = STR2FUNC(VARARGIN{1});
END

IF NARGOUT
    [VARARGOUT{1:NARGOUT}] = GUI_MAINFCN(GUI_STATE, VARARGIN{:});
ELSE
    GUI_MAINFCN(GUI_STATE, VARARGIN{:});
```

```
END
% END INITIALIZATION CODE - DO NOT EDIT

% --- EXECUTES JUST BEFORE PLANKTON_COLUMN IS MADE VISIBLE.
FUNCTION PLANKTON_COLUMN_OPENINGFCN(HOBJECT, EVENTDATA, HANDLES, VARARGIN)
% THIS FUNCTION HAS NO OUTPUT ARGS, SEE OUTPUTFCN.
% HOBJECT    HANDLE TO FIGURE
% EVENTDATA  RESERVED - TO BE DEFINED IN A FUTURE VERSION OF MATLAB
% HANDLES    STRUCTURE WITH HANDLES AND USER DATA (SEE GUIDATA)
% VARARGIN   COMMAND LINE ARGUMENTS TO PLANKTON_COLUMN (SEE VARARGIN)
% CHOOSE DEFAULT COMMAND LINE OUTPUT FOR PLANKTON_COLUMN
HANDLES.OUTPUT = HOBJECT;

% UPDATE HANDLES STRUCTURE
GUIDATA(HOBJECT, HANDLES);

% UIWAIT MAKES PLANKTON_COLUMN WAIT FOR USER RESPONSE (SEE UIRESUME)
% UIWAIT(HANDLES.FIGURE1);
%
TR=0;
WHILE TR==0
    TRY
        %LOAD PARAMETERES
        PARAMETERES=LOAD('PARAMETERES.MAT');
        TR=1;
    CATCH
        WARNDLG('CAN NOT LOAD PARAMETERS')
        RETURN
    END
END

SET(HANDLES.THRESHOLD,'STRING', NUM2STR(PARAMETERES.THRE));
SET(HANDLES.BIAS,'STRING', NUM2STR(PARAMETERES.BIAS));
SET(HANDLES.X1_CAM1,'STRING', NUM2STR(PARAMETERES.X1_CAM1));
SET(HANDLES.X1_CAM2,'STRING', NUM2STR(PARAMETERES.X1_CAM2));
SET(HANDLES.WIDTH,'STRING', NUM2STR(PARAMETERES.WIDTH));
SET(HANDLES.H1_COLUMN,'STRING',NUM2STR(PARAMETERES.H1));
SET(HANDLES.H2_COLUMN,'STRING', NUM2STR(PARAMETERES.H2));
SET(HANDLES.SHOW_PROCESS,'VALUE', 0);
%
SET(HANDLES.FF_CAM1,'STRING', PARAMETERES.FF_CAM1);
SET(HANDLES.FF_CAM2,'STRING', PARAMETERES.FF_CAM2);

% UPDATE HANDLES STRUCTURE
%GUIDATA(HOBJECT, HANDLES);

% --- OUTPUTS FROM THIS FUNCTION ARE RETURNED TO THE COMMAND LINE.
FUNCTION VARARGOUT = PLANKTON_COLUMN_OUTPUTFCN(HOBJECT, EVENTDATA, HANDLES)
% VARARGOUT  CELL ARRAY FOR RETURNING OUTPUT ARGS (SEE VARARGOUT);
% HOBJECT    HANDLE TO FIGURE
% EVENTDATA  RESERVED - TO BE DEFINED IN A FUTURE VERSION OF MATLAB
% HANDLES    STRUCTURE WITH HANDLES AND USER DATA (SEE GUIDATA)

% GET DEFAULT COMMAND LINE OUTPUT FROM HANDLES STRUCTURE
VARARGOUT{1} = HANDLES.OUTPUT;

FUNCTION THRESHOLD_CALLBACK(HOBJECT, EVENTDATA, HANDLES)
% HOBJECT    HANDLE TO THRESHOLD (SEE GCBO)
% EVENTDATA  RESERVED - TO BE DEFINED IN A FUTURE VERSION OF MATLAB
% HANDLES    STRUCTURE WITH HANDLES AND USER DATA (SEE GUIDATA)
```

```
% HINTS: GET(HOBJECT,'STRING') RETURNS CONTENTS OF THRESHOLD AS TEXT
%        STR2DOUBLE(GET(HOBJECT,'STRING')) RETURNS CONTENTS OF THRESHOLD AS A
DOUBLE
THRE = STR2DOUBLE(GET(HOBJECT,'STRING'));
SET(HANDLES.THRESHOLD,'STRING', NUM2STR(THRE));
GUIDATA(HOBJECT, HANDLES);

% --- EXECUTES DURING OBJECT CREATION, AFTER SETTING ALL PROPERTIES.
FUNCTION THRESHOLD_CREATEFCN(HOBJECT, EVENTDATA, HANDLES)
% HOBJECT    HANDLE TO THRESHOLD (SEE GCBO)
% EVENTDATA  RESERVED - TO BE DEFINED IN A FUTURE VERSION OF MATLAB
% HANDLES    EMPTY - HANDLES NOT CREATED UNTIL AFTER ALL CREATEFCNS CALLED

% HINT: EDIT CONTROLS USUALLY HAVE A WHITE BACKGROUND ON WINDOWS.
%       SEE ISPC AND COMPUTER.
IF ISPC && ISEQUAL(GET(HOBJECT,'BACKGROUNDCOLOR'),
GET(0,'DEFAULTUICONTROLBACKGROUNDCOLOR'))
    SET(HOBJECT,'BACKGROUNDCOLOR','WHITE');
END

FUNCTION BIAS_CALLBACK(HOBJECT, EVENTDATA, HANDLES)
% HOBJECT    HANDLE TO BIAS (SEE GCBO)
% EVENTDATA  RESERVED - TO BE DEFINED IN A FUTURE VERSION OF MATLAB
% HANDLES    STRUCTURE WITH HANDLES AND USER DATA (SEE GUIDATA)

% HINTS: GET(HOBJECT,'STRING') RETURNS CONTENTS OF BIAS AS TEXT
%        STR2DOUBLE(GET(HOBJECT,'STRING')) RETURNS CONTENTS OF BIAS AS A
DOUBLE

% --- EXECUTES DURING OBJECT CREATION, AFTER SETTING ALL PROPERTIES.
BIAS = STR2DOUBLE(GET(HOBJECT,'STRING'));
SET(HANDLES.BIAS,'STRING', NUM2STR(BIAS));

GUIDATA(HOBJECT, HANDLES);

FUNCTION BIAS_CREATEFCN(HOBJECT, EVENTDATA, HANDLES)
% HOBJECT    HANDLE TO BIAS (SEE GCBO)
% EVENTDATA  RESERVED - TO BE DEFINED IN A FUTURE VERSION OF MATLAB
% HANDLES    EMPTY - HANDLES NOT CREATED UNTIL AFTER ALL CREATEFCNS CALLED
% HINT: EDIT CONTROLS USUALLY HAVE A WHITE BACKGROUND ON WINDOWS.
%       SEE ISPC AND COMPUTER.
IF ISPC && ISEQUAL(GET(HOBJECT,'BACKGROUNDCOLOR'),
GET(0,'DEFAULTUICONTROLBACKGROUNDCOLOR'))
    SET(HOBJECT,'BACKGROUNDCOLOR','WHITE');
END

FUNCTION X1_CAM1_CALLBACK(HOBJECT, EVENTDATA, HANDLES)
% HOBJECT    HANDLE TO X1_CAM1 (SEE GCBO)
% EVENTDATA  RESERVED - TO BE DEFINED IN A FUTURE VERSION OF MATLAB
% HANDLES    STRUCTURE WITH HANDLES AND USER DATA (SEE GUIDATA)

% HINTS: GET(HOBJECT,'STRING') RETURNS CONTENTS OF X1_CAM1 AS TEXT
%        STR2DOUBLE(GET(HOBJECT,'STRING')) RETURNS CONTENTS OF X1_CAM1 AS A
DOUBLE
X1_CAM1 = STR2DOUBLE(GET(HOBJECT,'STRING'));
SET(HANDLES.X1_CAM1,'STRING', NUM2STR(X1_CAM1));
GUIDATA(HOBJECT, HANDLES);
% --- EXECUTES DURING OBJECT CREATION, AFTER SETTING ALL PROPERTIES.
FUNCTION X1_CAM1_CREATEFCN(HOBJECT, EVENTDATA, HANDLES)
% HOBJECT    HANDLE TO X1_CAM1 (SEE GCBO)
```

```
% EVENTDATA  RESERVED - TO BE DEFINED IN A FUTURE VERSION OF MATLAB
% HANDLES    EMPTY - HANDLES NOT CREATED UNTIL AFTER ALL CREATEFCNS CALLED

% HINT: EDIT CONTROLS USUALLY HAVE A WHITE BACKGROUND ON WINDOWS.
%       SEE ISPC AND COMPUTER.
IF ISPC && ISEQUAL(GET(HOBJECT,'BACKGROUNDCOLOR'),
GET(0,'DEFAULTUICONTROLBACKGROUNDCOLOR'))
    SET(HOBJECT,'BACKGROUNDCOLOR','WHITE');
END

FUNCTION X1_CAM2_CALLBACK(HOBJECT, EVENTDATA, HANDLES)
% HOBJECT    HANDLE TO X1_CAM2 (SEE GCBO)
% EVENTDATA  RESERVED - TO BE DEFINED IN A FUTURE VERSION OF MATLAB
% HANDLES    STRUCTURE WITH HANDLES AND USER DATA (SEE GUIDATA)

% HINTS: GET(HOBJECT,'STRING') RETURNS CONTENTS OF X1_CAM2 AS TEXT
%        STR2DOUBLE(GET(HOBJECT,'STRING')) RETURNS CONTENTS OF X1_CAM2 AS A
DOUBLE
X1_CAM2 = STR2DOUBLE(GET(HOBJECT,'STRING'));
SET(HANDLES.X1_CAM2,'STRING', NUM2STR(X1_CAM2));
GUIDATA(HOBJECT, HANDLES);

% --- EXECUTES DURING OBJECT CREATION, AFTER SETTING ALL PROPERTIES.
FUNCTION X1_CAM2_CREATEFCN(HOBJECT, EVENTDATA, HANDLES)
% HOBJECT    HANDLE TO X1_CAM2 (SEE GCBO)
% EVENTDATA  RESERVED - TO BE DEFINED IN A FUTURE VERSION OF MATLAB
% HANDLES    EMPTY - HANDLES NOT CREATED UNTIL AFTER ALL CREATEFCNS CALLED

% HINT: EDIT CONTROLS USUALLY HAVE A WHITE BACKGROUND ON WINDOWS.
%       SEE ISPC AND COMPUTER.
IF ISPC && ISEQUAL(GET(HOBJECT,'BACKGROUNDCOLOR'),
GET(0,'DEFAULTUICONTROLBACKGROUNDCOLOR'))
    SET(HOBJECT,'BACKGROUNDCOLOR','WHITE');
END

FUNCTION WIDTH_CALLBACK(HOBJECT, EVENTDATA, HANDLES)
% HOBJECT    HANDLE TO WIDTH (SEE GCBO)
% EVENTDATA  RESERVED - TO BE DEFINED IN A FUTURE VERSION OF MATLAB
% HANDLES    STRUCTURE WITH HANDLES AND USER DATA (SEE GUIDATA)

% HINTS: GET(HOBJECT,'STRING') RETURNS CONTENTS OF WIDTH AS TEXT
%        STR2DOUBLE(GET(HOBJECT,'STRING')) RETURNS CONTENTS OF WIDTH AS A
DOUBLE
WIDTH = STR2DOUBLE(GET(HOBJECT,'STRING'));
SET(HANDLES.WIDTH,'STRING', NUM2STR(WIDTH));
GUIDATA(HOBJECT, HANDLES);

% --- EXECUTES DURING OBJECT CREATION, AFTER SETTING ALL PROPERTIES.
FUNCTION WIDTH_CREATEFCN(HOBJECT, EVENTDATA, HANDLES)
% HOBJECT    HANDLE TO WIDTH (SEE GCBO)
% EVENTDATA  RESERVED - TO BE DEFINED IN A FUTURE VERSION OF MATLAB
% HANDLES    EMPTY - HANDLES NOT CREATED UNTIL AFTER ALL CREATEFCNS CALLED

% HINT: EDIT CONTROLS USUALLY HAVE A WHITE BACKGROUND ON WINDOWS.
%       SEE ISPC AND COMPUTER.
IF ISPC && ISEQUAL(GET(HOBJECT,'BACKGROUNDCOLOR'),
GET(0,'DEFAULTUICONTROLBACKGROUNDCOLOR'))
    SET(HOBJECT,'BACKGROUNDCOLOR','WHITE');
END
```

```
FUNCTION H1_COLUMN_CALLBACK(HOBJECT, EVENTDATA, HANDLES)
% HOBJECT    HANDLE TO H1_COLUMN (SEE GCBO)
% EVENTDATA  RESERVED - TO BE DEFINED IN A FUTURE VERSION OF MATLAB
% HANDLES    STRUCTURE WITH HANDLES AND USER DATA (SEE GUIDATA)

% HINTS: GET(HOBJECT,'STRING') RETURNS CONTENTS OF H1_COLUMN AS TEXT
%        STR2DOUBLE(GET(HOBJECT,'STRING')) RETURNS CONTENTS OF H1_COLUMN AS A
DOUBLE
H1 = STR2DOUBLE(GET(HOBJECT,'STRING'));
SET(HANDLES.H1_COLUMN,'STRING', NUM2STR(H1));
GUIDATA(HOBJECT, HANDLES);

% --- EXECUTES DURING OBJECT CREATION, AFTER SETTING ALL PROPERTIES.
FUNCTION H1_COLUMN_CREATEFCN(HOBJECT, EVENTDATA, HANDLES)
% HOBJECT    HANDLE TO H1_COLUMN (SEE GCBO)
% EVENTDATA  RESERVED - TO BE DEFINED IN A FUTURE VERSION OF MATLAB
% HANDLES    EMPTY - HANDLES NOT CREATED UNTIL AFTER ALL CREATEFCNS CALLED

% HINT: EDIT CONTROLS USUALLY HAVE A WHITE BACKGROUND ON WINDOWS.
%       SEE ISPC AND COMPUTER.
IF ISPC && ISEQUAL(GET(HOBJECT,'BACKGROUNDCOLOR'),
GET(0,'DEFAULTUICONTROLBACKGROUNDCOLOR'))
    SET(HOBJECT,'BACKGROUNDCOLOR','WHITE');
END

FUNCTION H2_COLUMN_CALLBACK(HOBJECT, EVENTDATA, HANDLES)
% HOBJECT    HANDLE TO H2_COLUMN (SEE GCBO)
% EVENTDATA  RESERVED - TO BE DEFINED IN A FUTURE VERSION OF MATLAB
% HANDLES    STRUCTURE WITH HANDLES AND USER DATA (SEE GUIDATA)

% HINTS: GET(HOBJECT,'STRING') RETURNS CONTENTS OF H2_COLUMN AS TEXT
%        STR2DOUBLE(GET(HOBJECT,'STRING')) RETURNS CONTENTS OF H2_COLUMN AS A
DOUBLE
H2 = STR2DOUBLE(GET(HOBJECT,'STRING'));
SET(HANDLES.H2_COLUMN,'STRING', NUM2STR(H2));
GUIDATA(HOBJECT, HANDLES);

% --- EXECUTES DURING OBJECT CREATION, AFTER SETTING ALL PROPERTIES.
FUNCTION H2_COLUMN_CREATEFCN(HOBJECT, EVENTDATA, HANDLES)
% HOBJECT    HANDLE TO H2_COLUMN (SEE GCBO)
% EVENTDATA  RESERVED - TO BE DEFINED IN A FUTURE VERSION OF MATLAB
% HANDLES    EMPTY - HANDLES NOT CREATED UNTIL AFTER ALL CREATEFCNS CALLED

% HINT: EDIT CONTROLS USUALLY HAVE A WHITE BACKGROUND ON WINDOWS.
%       SEE ISPC AND COMPUTER.
IF ISPC && ISEQUAL(GET(HOBJECT,'BACKGROUNDCOLOR'),
GET(0,'DEFAULTUICONTROLBACKGROUNDCOLOR'))
    SET(HOBJECT,'BACKGROUNDCOLOR','WHITE');
END

FUNCTION FF_CAM1_CALLBACK(HOBJECT, EVENTDATA, HANDLES)
% HOBJECT    HANDLE TO FF_CAM1 (SEE GCBO)
% EVENTDATA  RESERVED - TO BE DEFINED IN A FUTURE VERSION OF MATLAB
% HANDLES    STRUCTURE WITH HANDLES AND USER DATA (SEE GUIDATA)

% HINTS: GET(HOBJECT,'STRING') RETURNS CONTENTS OF FF_CAM1 AS TEXT
%        STR2DOUBLE(GET(HOBJECT,'STRING')) RETURNS CONTENTS OF FF_CAM1 AS A
DOUBLE
HANDLES.FF_CAM1 = GET(HOBJECT,'STRING');
```

```
GUIDATA(HOBJECT, HANDLES);

% --- EXECUTES DURING OBJECT CREATION, AFTER SETTING ALL PROPERTIES.
FUNCTION FF_CAM1_CREATEFCN(HOBJECT, EVENTDATA, HANDLES)
% HOBJECT    HANDLE TO FF_CAM1 (SEE GCBO)
% EVENTDATA  RESERVED - TO BE DEFINED IN A FUTURE VERSION OF MATLAB
% HANDLES    EMPTY - HANDLES NOT CREATED UNTIL AFTER ALL CREATEFCNS CALLED
% HINT: EDIT CONTROLS USUALLY HAVE A WHITE BACKGROUND ON WINDOWS.
%       SEE ISPC AND COMPUTER.
IF ISPC && ISEQUAL(GET(HOBJECT,'BACKGROUNDCOLOR'),
GET(0,'DEFAULTUICONTROLBACKGROUNDCOLOR'))
    SET(HOBJECT,'BACKGROUNDCOLOR','WHITE');
END

% --- EXECUTES ON BUTTON PRESS IN FLAT_FIELD.
FUNCTION FLAT_FIELD_CALLBACK(HOBJECT, EVENTDATA, HANDLES)
% HOBJECT    HANDLE TO FLAT_FIELD (SEE GCBO)
% EVENTDATA  RESERVED - TO BE DEFINED IN A FUTURE VERSION OF MATLAB
% HANDLES    STRUCTURE WITH HANDLES AND USER DATA (SEE GUIDATA)
X1_CAM1 = STR2DOUBLE(GET(HANDLES.X1_CAM1,'STRING'));
X1_CAM2 = STR2DOUBLE(GET(HANDLES.X1_CAM2,'STRING'));
WIDTH = STR2DOUBLE(GET(HANDLES.WIDTH,'STRING'));

MAKE_FLATFIELD_V6_GUI  %MAKE FLAT FIELD FILES

FN1_N = [FILENAME(1:END-11) '_FF_CAM1.DAT'];
FN2_N = [FILENAME(1:END-11) '_FF_CAM2.DAT'];
FN_BORDERS = [FILENAME(1:END-11) '_BORDERS.MAT'];

BORDERS.X1_CAM1 = A1_X1;
BORDERS.X1_CAM2 = A2_X1;
BORDERS.WIDTH = WIDTH;

SAVE(FN1_N,'A1_AV_NORM','-ASCII');
SAVE(FN2_N,'A2_AV_NORM','-ASCII');

SAVE(FN_BORDERS, '-STRUCT', 'BORDERS')

SET(HANDLES.FF_CAM1,'STRING', FN1_N);
SET(HANDLES.FF_CAM2,'STRING', FN2_N);

SAVE_PARAMETERES_GUI

FIGURE(11);IMAGESC(A1_AV_NORM)
FIGURE(12);IMAGESC(A2_AV_NORM)

% --- EXECUTES ON BUTTON PRESS IN SELECT_COLUMN_BORDERS.
FUNCTION SELECT_COLUMN_BORDERS_CALLBACK(HOBJECT, EVENTDATA, HANDLES)
% HOBJECT    HANDLE TO SELECT_COLUMN_BORDERS (SEE GCBO)
% EVENTDATA  RESERVED - TO BE DEFINED IN A FUTURE VERSION OF MATLAB
% HANDLES    STRUCTURE WITH HANDLES AND USER DATA (SEE GUIDATA)
[FILENAME, PATHNAME, FILTERINDEX] = UIGETFILE('*.*', 'SELECT AN IMAGE');

K1 = STRFIND(FILENAME,'CAM1');
K2 = STRFIND(FILENAME,'CAM2');

IF ISEMPTY(K1) ~= 1
    FNS = FILENAME(1:K1-1);
    WARN = [' '];
```

```
    SET(HANDLES.WARNINGS,'STRING', WARN);

ELSEIF ISEMPTY(K2) ~= 1
    FNS = FILENAME(1:K2-1);
    WARN = [' '];
    SET(HANDLES.WARNINGS,'STRING', WARN);

ELSE
    WARN = ['INPUT FILE NAME IS NOT VALID'];
    SET(HANDLES.WARNINGS,'STRING', WARN);
    RETURN

END

JJ = 1;
FN1 = [PATHNAME FNS 'CAM1_' NUM2STR(JJ) '.PNG'];
FN2 = [PATHNAME FNS 'CAM2_' NUM2STR(JJ) '.PNG'];

AP1 = IMREAD(FN1);
A1_S = MEAN(AP1');
FIGURE(11);PLOT(A1_S);TITLE('SELECT THE BORDERS OF COLUMN IN CAMERA #1')
[X1 Y1] = GINPUT(2);
IF X1(1)<X1(2)
    X1_CAM1 = FIX(X1(1));
    DIS_1 = FIX(X1(2))-FIX(X1(1));
ELSE
    X1_CAM1 = FIX(X1(2));
    DIS_1 = FIX(X1(1))-FIX(X1(2));
END
CLOSE
AP2 = IMREAD(FN2);
A2_S = MEAN(AP2');
FIGURE(11);PLOT(A2_S);TITLE('SELECT THE BORDERS OF COLUMN IN CAMERA #2')
[X1 Y1] = GINPUT(2);
IF X1(1)<X1(2)
    X1_CAM2 = FIX(X1(1));
    DIS_2 = FIX(X1(2))-FIX(X1(1));
ELSE
    X1_CAM2 = FIX(X1(2));
    DIS_2 = FIX(X1(1))-FIX(X1(2));
END
CLOSE
WIDTH = FIX((DIS_1+DIS_2)/2);
X2_CAM1 = X1_CAM1 + WIDTH;
X2_CAM2 = X1_CAM2 + WIDTH;

SET(HANDLES.X1_CAM1,'STRING', NUM2STR(X1_CAM1));
SET(HANDLES.X1_CAM2,'STRING', NUM2STR(X1_CAM2));
SET(HANDLES.WIDTH,'STRING', NUM2STR(WIDTH));

FIGURE(12);
SUBPLOT(1,8,[1 2 3 4]);IMAGESC(AP1(X1_CAM1:X2_CAM1,:)')
SUBPLOT(1,8,[5 6 7 8]);IMAGESC(AP2(X1_CAM2:X2_CAM2,:)')

% --- EXECUTES ON BUTTON PRESS IN ANALYSE.
FUNCTION ANALYSE_CALLBACK(HOBJECT, EVENTDATA, HANDLES)
% HOBJECT    HANDLE TO ANALYSE (SEE GCBO)
% EVENTDATA  RESERVED - TO BE DEFINED IN A FUTURE VERSION OF MATLAB
% HANDLES    STRUCTURE WITH HANDLES AND USER DATA (SEE GUIDATA)
```

```
BIAS = STR2DOUBLE(GET(HANDLES.BIAS,'STRING'));
THRE_C = STR2DOUBLE(GET(HANDLES.THRESHOLD,'STRING'));
X1_CAM1 = STR2DOUBLE(GET(HANDLES.X1_CAM1,'STRING'));
X1_CAM2 = STR2DOUBLE(GET(HANDLES.X1_CAM2,'STRING'));
WIDTH = STR2DOUBLE(GET(HANDLES.WIDTH,'STRING'));
H1 = STR2DOUBLE(GET(HANDLES.H1_COLUMN,'STRING'));
H2 = STR2DOUBLE(GET(HANDLES.H2_COLUMN,'STRING'));
FN1_N = (GET(HANDLES.FF_CAM1,'STRING'));
FN2_N = (GET(HANDLES.FF_CAM2,'STRING'));

H1 = 1;
H2 = 39;
SET(HANDLES.H1_COLUMN,'STRING', NUM2STR(H1))
SET(HANDLES.H2_COLUMN,'STRING', NUM2STR(H2))

IF EXIST(FN1_N) == 2 && EXIST(FN2_N) == 2
    WARN = [' '];
    SET(HANDLES.WARNINGS,'STRING', WARN);
ELSE
    WARN = ['FLAT FIELD FILES ARE NOT VALID OR NOT EXIST'];
    SET(HANDLES.WARNINGS,'STRING', WARN);
    RETURN
END

SH = GET(HANDLES.SHOW_PROCESS,'VALUE');

FN1_N = GET(HANDLES.FF_CAM1,'STRING');
FN_BORDERS = [FN1_N(1:END-12) '_BORDERS.MAT'];

DATA=LOAD(FN_BORDERS);
VARIABLES=FIELDS(DATA);
X1_CAM1 = DATA.(VARIABLES{1});
X1_CAM2 = DATA.(VARIABLES{2});
WIDTH = DATA.(VARIABLES{3});

SET(HANDLES.X1_CAM1,'STRING', NUM2STR(X1_CAM1));
SET(HANDLES.X1_CAM2,'STRING', NUM2STR(X1_CAM2));
SET(HANDLES.WIDTH,'STRING', NUM2STR(WIDTH));

PLANKTON_COLUMN_ANALYSIS_V5_GUI  %ANALYSE THE DATA

PLOT_SAVE_RESULTS

TIME_T = LINSPACE(0,DT,LENGTH(A_TOTAL(1,:)));
A_TOTAL_T(1:39,:) = A_TOTAL;
A_TOTAL_T(40,:) = TIME_T;

FN1 = [PATHNAME FNS 'DISTR_TIME-BIAS_' NUM2STR(BIAS) '_THRE_' NUM2STR(THRE_C)
'_DISTR.DAT'];
FN2 = [PATHNAME FNS 'DISTR_TIME-BIAS_' NUM2STR(BIAS) '_THRE_' NUM2STR(THRE_C)
'_TOTALNUMBER.DAT'];
SAVE(FN1, '-ASCII' ,'A_TOTAL_T')
SAVE(FN2, '-ASCII' ,'A_TOTAL_SUM')

% --- EXECUTES ON BUTTON PRESS IN SHOW_PROCESS.
FUNCTION SHOW_PROCESS_CALLBACK(HOBJECT, EVENTDATA, HANDLES)
% HOBJECT    HANDLE TO SHOW_PROCESS (SEE GCBO)
% EVENTDATA  RESERVED - TO BE DEFINED IN A FUTURE VERSION OF MATLAB
% HANDLES    STRUCTURE WITH HANDLES AND USER DATA (SEE GUIDATA)
```

```
% HINT: GET(HOBJECT,'VALUE') RETURNS TOGGLE STATE OF SHOW_PROCESS

% --- EXECUTES ON BUTTON PRESS IN PLOT_RESULTS.
FUNCTION PLOT_RESULTS_CALLBACK(HOBJECT, EVENTDATA, HANDLES)
% HOBJECT    HANDLE TO PLOT_RESULTS (SEE GCBO)
% EVENTDATA  RESERVED - TO BE DEFINED IN A FUTURE VERSION OF MATLAB
% HANDLES    STRUCTURE WITH HANDLES AND USER DATA (SEE GUIDATA)

H1 = STR2DOUBLE(GET(HANDLES.H1_COLUMN,'STRING'));
H2 = STR2DOUBLE(GET(HANDLES.H2_COLUMN,'STRING'));

[FILENAME, PATHNAME, FILTERINDEX] = UIGETFILE('*.DAT', 'SELECT THE DATA FILE
OF DISTRIBUTION');
FN1 = [PATHNAME FILENAME];

K1 = STRFIND(FILENAME,'DISTR');

IF ~ISEMPTY(K1)
    A_TOTAL_T = LOAD(FN1);
    PLOT_SAVE_RESULTS_GUI

END

FUNCTION FF_CAM2_CALLBACK(HOBJECT, EVENTDATA, HANDLES)
% HOBJECT    HANDLE TO FF_CAM2 (SEE GCBO)
% EVENTDATA RESERVED - TO BE DEFINED IN A FUTURE VERSION OF MATLAB
% HANDLES    STRUCTURE WITH HANDLES AND USER DATA (SEE GUIDATA)

% HINTS: GET(HOBJECT,'STRING') RETURNS CONTENTS OF FF_CAM2 AS TEXT
%        STR2DOUBLE(GET(HOBJECT,'STRING')) RETURNS CONTENTS OF FF_CAM2 AS A
DOUBLE
HANDLES.FF_CAM2 = GET(HOBJECT,'STRING');

GUIDATA(HOBJECT, HANDLES);

% --- EXECUTES DURING OBJECT CREATION, AFTER SETTING ALL PROPERTIES.
FUNCTION FF_CAM2_CREATEFCN(HOBJECT, EVENTDATA, HANDLES)
% HOBJECT    HANDLE TO FF_CAM2 (SEE GCBO)
% EVENTDATA  RESERVED - TO BE DEFINED IN A FUTURE VERSION OF MATLAB
% HANDLES    EMPTY - HANDLES NOT CREATED UNTIL AFTER ALL CREATEFCNS CALLED

% HINT: EDIT CONTROLS USUALLY HAVE A WHITE BACKGROUND ON WINDOWS.
%       SEE ISPC AND COMPUTER.
IF ISPC && ISEQUAL(GET(HOBJECT,'BACKGROUNDCOLOR'),
GET(0,'DEFAULTUICONTROLBACKGROUNDCOLOR'))
    SET(HOBJECT,'BACKGROUNDCOLOR','WHITE');
END
% --- EXECUTES ON BUTTON PRESS IN CHANGE_FF1.
FUNCTION CHANGE_FF1_CALLBACK(HOBJECT, EVENTDATA, HANDLES)
% HOBJECT    HANDLE TO CHANGE_FF1 (SEE GCBO)
% EVENTDATA  RESERVED - TO BE DEFINED IN A FUTURE VERSION OF MATLAB
% HANDLES    STRUCTURE WITH HANDLES AND USER DATA (SEE GUIDATA)
ANS = 0;
WHILE ANS == 0;
    [FILENAME, PATHNAME, FILTERINDEX] = UIGETFILE('*.*', 'LOAD THE FLAT FIELD
OF CAM1');
    FN1_N=[PATHNAME FILENAME];
    K1 = STRFIND(FILENAME,'CAM1');
    IF ISEMPTY(K1)
```

```
        WARN = ['INPUT FILE NAME IS NOT A VALID FLAT FIELD OF CAM1'];
        SET(HANDLES.WARNINGS,'STRING', WARN);

        SELECTION = QUESTDLG('DO YOU WANT TO STOP FILE SELECTION?',...
            'CLOSE REQUEST FUNCTION',...
            'YES','NO','YES');
        SWITCH SELECTION,
            CASE 'YES',
                %DELETE(GCF)
                %CLOSE
                RETURN
            CASE 'NO'
        END

    ELSE
        ANS = 1;
        SET(HANDLES.FF_CAM1,'STRING', FILENAME);
        WARN = [''];
        SET(HANDLES.WARNINGS,'STRING', WARN);

    END
END

% --- EXECUTES ON BUTTON PRESS IN CHAMGE_FF2.
FUNCTION CHAMGE_FF2_CALLBACK(HOBJECT, EVENTDATA, HANDLES)
% HOBJECT    HANDLE TO CHAMGE_FF2 (SEE GCBO)
% EVENTDATA  RESERVED - TO BE DEFINED IN A FUTURE VERSION OF MATLAB
% HANDLES    STRUCTURE WITH HANDLES AND USER DATA (SEE GUIDATA)
ANS = 0;
WHILE ANS == 0;
    [FILENAME, PATHNAME, FILTERINDEX] = UIGETFILE('*.*', 'LOAD THE FLAT FIELD
OF CAM1');
    FN1_N=[PATHNAME FILENAME];
    K1 = STRFIND(FILENAME,'CAM2');
    IF ISEMPTY(K1)
        WARN = ['INPUT FILE NAME IS NOT A VALID FLAT FIELD OF CAM1'];
        SET(HANDLES.WARNINGS,'STRING', WARN);

        SELECTION = QUESTDLG('DO YOU WANT TO STOP FILE SELECTION?',...
            'CLOSE REQUEST FUNCTION',...
            'YES','NO','YES');
        SWITCH SELECTION,
            CASE 'YES',
                %DELETE(GCF)
                %CLOSE
                RETURN
            CASE 'NO'
        END

    ELSE
        ANS = 1;
        SET(HANDLES.FF_CAM2,'STRING', FILENAME);
        WARN = [''];
        SET(HANDLES.WARNINGS,'STRING', WARN);

    END
END

% --- EXECUTES ON BUTTON PRESS IN SAVE_PARAMETERS.
FUNCTION SAVE_PARAMETERS_CALLBACK(HOBJECT, EVENTDATA, HANDLES)
```

```
% HOBJECT    HANDLE TO SAVE_PARAMETERS (SEE GCBO)
% EVENTDATA  RESERVED - TO BE DEFINED IN A FUTURE VERSION OF MATLAB
% HANDLES    STRUCTURE WITH HANDLES AND USER DATA (SEE GUIDATA)

PARAMETERES.BIAS = STR2DOUBLE(GET(HANDLES.BIAS,'STRING'));
PARAMETERES.THRE = STR2DOUBLE(GET(HANDLES.THRESHOLD,'STRING'));
PARAMETERES.X1_CAM1 = STR2DOUBLE(GET(HANDLES.X1_CAM1,'STRING'));
PARAMETERES.X1_CAM2 = STR2DOUBLE(GET(HANDLES.X1_CAM2,'STRING'));
PARAMETERES.WIDTH = STR2DOUBLE(GET(HANDLES.WIDTH,'STRING'));
PARAMETERES.H1 = STR2DOUBLE(GET(HANDLES.H1_COLUMN,'STRING'));
PARAMETERES.H2 = STR2DOUBLE(GET(HANDLES.H2_COLUMN,'STRING'));
PARAMETERES.FF_CAM1 = (GET(HANDLES.FF_CAM1,'STRING'));
PARAMETERES.FF_CAM2 = (GET(HANDLES.FF_CAM2,'STRING'));

SAVE('PARAMETERES.MAT', '-STRUCT', 'PARAMETERES')

FUNCTION WARNINGS_CALLBACK(HOBJECT, EVENTDATA, HANDLES)
% HOBJECT    HANDLE TO WARNINGS (SEE GCBO)
% EVENTDATA  RESERVED - TO BE DEFINED IN A FUTURE VERSION OF MATLAB
% HANDLES    STRUCTURE WITH HANDLES AND USER DATA (SEE GUIDATA)

% HINTS: GET(HOBJECT,'STRING') RETURNS CONTENTS OF WARNINGS AS TEXT
%        STR2DOUBLE(GET(HOBJECT,'STRING')) RETURNS CONTENTS OF WARNINGS AS A
DOUBLE

% --- EXECUTES DURING OBJECT CREATION, AFTER SETTING ALL PROPERTIES.
FUNCTION WARNINGS_CREATEFCN(HOBJECT, EVENTDATA, HANDLES)
% HOBJECT    HANDLE TO WARNINGS (SEE GCBO)
% EVENTDATA  RESERVED - TO BE DEFINED IN A FUTURE VERSION OF MATLAB
% HANDLES    EMPTY - HANDLES NOT CREATED UNTIL AFTER ALL CREATEFCNS CALLED

% HINT: EDIT CONTROLS USUALLY HAVE A WHITE BACKGROUND ON WINDOWS.
%       SEE ISPC AND COMPUTER.
IF ISPC && ISEQUAL(GET(HOBJECT,'BACKGROUNDCOLOR'),
GET(0,'DEFAULTUICONTROLBACKGROUNDCOLOR'))
    SET(HOBJECT,'BACKGROUNDCOLOR','WHITE');
END
% --- EXECUTES DURING OBJECT CREATION, AFTER SETTING ALL PROPERTIES.
FUNCTION CUNTER_CREATEFCN(HOBJECT, EVENTDATA, HANDLES)
% HOBJECT    HANDLE TO CUNTER (SEE GCBO)
% EVENTDATA  RESERVED - TO BE DEFINED IN A FUTURE VERSION OF MATLAB
% HANDLES    EMPTY - HANDLES NOT CREATED UNTIL AFTER ALL CREATEFCNS CALLED

% --- EXECUTES ON BUTTON PRESS IN STOP.
FUNCTION STOP_CALLBACK(HOBJECT, EVENTDATA, HANDLES)
% HOBJECT    HANDLE TO STOP (SEE GCBO)
% EVENTDATA  RESERVED - TO BE DEFINED IN A FUTURE VERSION OF MATLAB
% HANDLES    STRUCTURE WITH HANDLES AND USER DATA (SEE GUIDATA)

STOP = 1;
GLOBAL STOP
```

Plankton column: data analysis

```
%% LOAD FLAT FIELD
A1_AV_NORM_P=LOAD(FN1_N);
A2_AV_NORM_P=LOAD(FN2_N);
```

```
A1_AV_NORM = A1_AV_NORM_P/MAX(MAX(A1_AV_NORM_P));
A2_AV_NORM = A2_AV_NORM_P/MAX(MAX(A2_AV_NORM_P));

%% PARAMETERES
RGB = 1;  %SELECT RIGHT COLOR FOR COLOR CAMERA
BIN = 40;   %DIVISIONS OF THE CELL
STOP = 0;

A1_X1 = X1_CAM1;
A1_X2 = X1_CAM1 + WIDTH;

A2_X1 = X1_CAM2;
A2_X2 = X1_CAM2 + WIDTH;

CX1=1;
CX2=(A1_X2-A1_X1)+1;

CY1=1;
CY2=(A1_X2-A1_X1)+1;

%% LOAD DATA
[FILENAME, PATHNAME, FILTERINDEX] = UIGETFILE('*.*', 'SELECT AN IMAGE');

K1 = STRFIND(FILENAME,'CAM1');
K2 = STRFIND(FILENAME,'CAM2');

IF ISEMPTY(K1) ~= 1
    FNS = FILENAME(1:K1-1);
    WARN = [' '];
    SET(HANDLES.WARNINGS,'STRING', WARN);

ELSEIF ISEMPTY(K2) ~= 1
    FNS = FILENAME(1:K2-1);
    WARN = [' '];
    SET(HANDLES.WARNINGS,'STRING', WARN);

ELSE
    WARN = ['INPUT FILE NAME IS NOT VALID'];
    SET(HANDLES.WARNINGS,'STRING', WARN);
    RETURN
END

JJ = 1;
FN1 = [PATHNAME FNS 'CAM1_' NUM2STR(JJ) '.PNG'];
FN2 = [PATHNAME FNS 'CAM2_' NUM2STR(JJ) '.PNG'];
EP1 = 0.0;
EP2 = 0.0;

    AP = IMREAD(FN1);
    A1_S = SUM(SUM(DOUBLE(AP(A1_X1:A1_X2,:,RGB))-BIAS));
    AP = IMREAD(FN2);
    A2_S = SUM(SUM(DOUBLE(AP(A2_X1:A2_X2,:,RGB))-BIAS));

WHILE EXIST(FN1) == 2 && EXIST(FN2) == 2
    %DISP(NUM2STR(JJ))
    SET(HANDLES.CUNTER,'STRING', NUM2STR(JJ));
%     IF GET(HANDLES.STOP,'VALUE')
%         RETURN
%     END
```

```
    DRAWNOW
    %PAUSE(1)
    AP = IMREAD(FN1);
    A1P = DOUBLE(AP(A1_X1:A1_X2,:,RGB));

    AP = IMREAD(FN2);
    A2P = DOUBLE(AP(A2_X1:A2_X2,:,RGB));

    A1 = (A1P-BIAS) ./(SUM(SUM(A1P+BIAS)));
    A1_C = ((A1) ./ (A1_AV_NORM - EP1 ));

    A2 = (A2P-BIAS) ./(SUM(SUM(A2P+BIAS)));
    A2_C = ((A2) ./ (A2_AV_NORM - EP1));

    A1_C = A1_C; %./ SUM(SUM(A1_C+A2_C));
    A2_C = A2_C; %./ SUM(SUM(A1_C+A2_C));

    IF JJ==1
        THRE = THRE_C * (STD2(A1_C)+STD2(A2_C))/2 +
(MEAN(MEAN(A1_C))+MEAN(MEAN(A2_C)))/2;
    END

    ID=FIND(A1_C < THRE);
    A1_C(ID) = 0;
    ID=FIND(A1_C >= THRE);
    A1_C(ID) = 1;

    ID=FIND(A2_C < THRE);
    A2_C(ID) = 0;
    ID=FIND(A2_C >= THRE);
    A2_C(ID) = 1;

    A1_CUT = A1_C(CX1:CX2,:);
    A2_CUT = A2_C(CX1:CX2,:);

    A1_CUT_M = SUM(A1_CUT);
    A2_CUT_M = SUM(A2_CUT);
FOR II = 1:20
        A1_M(II) = SUM(A1_CUT_M((1:64)+(II-1)*64));
        A2_M(II) = SUM(A2_CUT_M((1:64)+(II-1)*64));
    END

    A_TOTAL(1:20,JJ) = A2_M;
    A_TOTAL(20,JJ) = (A2_M(20)+A1_M(1))/2;
    A_TOTAL(21:39,JJ) = A1_M(2:20);
    A_TOTAL_SUM(JJ) = SUM(A_TOTAL(:,JJ));

    IF SH == 1
        PS = GET(0,'SCREENSIZE');
        H0 = FIGURE(1);
        SET(H0, 'POSITION', [1,100,PS(3)/2,PS(4)/2])
        SUBPLOT(3,8,[1 4]);IMAGESC(A2_CUT); AXIS OFF; COLORMAP GRAY
        SUBPLOT(3,8,[5 8]);IMAGESC(A1_CUT); AXIS OFF; COLORMAP GRAY
        SUBPLOT(3,8,[9 16]);PLOT(A_TOTAL(:,JJ));
        SUBPLOT(3,8,[17 24]);PLOT(A_TOTAL_SUM);
        H3 =
FIGURE(3);IMAGESC(A_TOTAL);SET(GCA,'YDIR','NORMAL');YLABEL('HIGHT (CM)')
        SET(H3, 'POSITION', [PS(3)/2,100,PS(3)/2,PS(4)/2])
```

```
        DRAWNOW
    END

    JJ=JJ+1;
    FN1 = [PATHNAME FNS 'CAM1_' NUM2STR(JJ) '.PNG'];
    FN2 = [PATHNAME FNS 'CAM2_' NUM2STR(JJ) '.PNG'];
    %PAUSE(1)
END

IF SH ==1
    CLOSE(H0)
    CLOSE(H3)
END
```

Calibration program

```
WARNING OFF
%% PARAMETERES
RGB = 1;  %SELECT RIGHT COLOR FOR COLOR CAMERA
% PN=4;
% BIAS = 2;   %BIAS LEVEL OF THE CAMERS

A1_X1 = X1_CAM1;
A1_X2 = X1_CAM1 + WIDTH;

A2_X1 = X1_CAM2;
A2_X2 = X1_CAM2 + WIDTH;
%
%% LOAD DATA
[FILENAME, PATHNAME, FILTERINDEX] = UIGETFILE('*.*', 'PICK AN IMAGE');

K1 = STRFIND(FILENAME,'CAM1');
K2 = STRFIND(FILENAME,'CAM2');

IF ISEMPTY(K1) ~= 1
    FNS = FILENAME(1:K1-1);

ELSEIF ISEMPTY(K2) ~= 1
    FNS = FILENAME(1:K2-1);

ELSE
    WARNDLG('INPUT FILE NAME IS NOT VALID')
    RETURN

END

II = 1;
FN1 = [PATHNAME FNS 'CAM1_' NUM2STR(II) '.PNG'];
FN2 = [PATHNAME FNS 'CAM2_' NUM2STR(II) '.PNG'];
AP = IMREAD(FN1);
AP1 = AP(A1_X1:A1_X2,:,RGB);
A1 = ZEROS(SIZE(AP1));
A2 = ZEROS(SIZE(AP1));

WHILE EXIST(FN1) == 2 && EXIST(FN2) == 2
     SET(HANDLES.CUNTER,'STRING', NUM2STR(II))
%     IF GET(HANDLES.STOP,'VALUE')
%         RETURN
```

```
%     END
    DRAWNOW

    AP = IMREAD(FN1);
    APP1 = DOUBLE(AP(A1_X1:A1_X2,:,RGB));

    AP = IMREAD(FN2);
    APP2 = DOUBLE(AP(A2_X1:A2_X2,:,RGB));


    AP1 = APP1 ./ SUM(SUM(APP1));
    A1 = MAX([STD(AP1) ; A1]);

    %FIGURE(11);PLOT(A1)
    %DRAWNOW

    AP2 = APP2 ./ SUM(SUM(APP2));
    A2 = MAX([STD(AP2) ; A2]);
    %FIGURE(111);PLOT(A2)
    %DRAWNOW

    II=II+1;
    FN1 = [PATHNAME FNS 'CAM1_' NUM2STR(II) '.PNG'];
    FN2 = [PATHNAME FNS 'CAM2_' NUM2STR(II) '.PNG'];

END

A1_PV = A1;
A2_PV = A2;

FOR IH = 1:LENGTH(AP1(:,1))
    A1_AV_N2(IH,:) = A1_PV;
    A2_AV_N2(IH,:) = A2_PV;
END

A1_AV_NORM = A1_AV_N2; % ./ SUM(SUM(A1_AV_N2));
A2_AV_NORM = A2_AV_N2; % ./ SUM(SUM(A2_AV_N2));
```

LED CONTROLLER

```
FUNCTION VARARGOUT = LED_CONTROLER(VARARGIN)
%
%LED_CONTROLER MATLAB CODE FOR LED_CONTROLER.FIG
%      LED_CONTROLER, BY ITSELF, CREATES A NEW LED_CONTROLER OR RAISES THE
EXISTING
%      SINGLETON*.
%
%      H = LED_CONTROLER RETURNS THE HANDLE TO A NEW LED_CONTROLER OR THE
HANDLE TO
%      THE EXISTING SINGLETON*.
%
%      LED_CONTROLER('CALLBACK',HOBJECT,EVENTDATA,HANDLES,...) CALLS THE
LOCAL
%      FUNCTION NAMED CALLBACK IN LED_CONTROLER.M WITH THE GIVEN INPUT
ARGUMENTS.
%
%      LED_CONTROLER('PROPERTY','VALUE',...) CREATES A NEW LED_CONTROLER OR
```

```
RAISES THE
%      EXISTING SINGLETON*.  STARTING FROM THE LEFT, PROPERTY VALUE PAIRS ARE
%      APPLIED TO THE GUI BEFORE LED_CONTROLER_OPENINGFCN GETS CALLED.  AN
%      UNRECOGNIZED PROPERTY NAME OR INVALID VALUE MAKES PROPERTY APPLICATION
%      STOP.  ALL INPUTS ARE PASSED TO LED_CONTROLER_OPENINGFCN VIA VARARGIN.
%      *SEE GUI OPTIONS ON GUIDE'S TOOLS MENU.  CHOOSE "GUI ALLOWS ONLY ONE
%      INSTANCE TO RUN (SINGLETON)".
%
% SEE ALSO: GUIDE, GUIDATA, GUIHANDLES

% EDIT THE ABOVE TEXT TO MODIFY THE RESPONSE TO HELP LED_CONTROLER

% BEGIN INITIALIZATION CODE - DO NOT EDIT
GUI_SINGLETON = 1;
GUI_STATE = STRUCT('GUI_NAME',       MFILENAME, ...
                   'GUI_SINGLETON',  GUI_SINGLETON, ...
                   'GUI_OPENINGFCN', @LED_CONTROLER_OPENINGFCN, ...
                   'GUI_OUTPUTFCN',  @LED_CONTROLER_OUTPUTFCN, ...
                   'GUI_LAYOUTFCN',  [] , ...
                   'GUI_CALLBACK',   []);
IF NARGIN && ISCHAR(VARARGIN{1})
    GUI_STATE.GUI_CALLBACK = STR2FUNC(VARARGIN{1});
END

IF NARGOUT
    [VARARGOUT{1:NARGOUT}] = GUI_MAINFCN(GUI_STATE, VARARGIN{:});
ELSE
    GUI_MAINFCN(GUI_STATE, VARARGIN{:});
END

% END INITIALIZATION CODE - DO NOT EDIT

% --- EXECUTES JUST BEFORE LED_CONTROLER IS MADE VISIBLE.
FUNCTION LED_CONTROLER_OPENINGFCN(HOBJECT, EVENTDATA, HANDLES, VARARGIN)
% THIS FUNCTION HAS NO OUTPUT ARGS, SEE OUTPUTFCN.
% HOBJECT    HANDLE TO FIGURE
% EVENTDATA RESERVED - TO BE DEFINED IN A FUTURE VERSION OF MATLAB
% HANDLES    STRUCTURE WITH HANDLES AND USER DATA (SEE GUIDATA)
% VARARGIN   COMMAND LINE ARGUMENTS TO LED_CONTROLER (SEE VARARGIN)

% CHOOSE DEFAULT COMMAND LINE OUTPUT FOR LED_CONTROLER
HANDLES.OUTPUT = HOBJECT;

% UPDATE HANDLES STRUCTURE
GUIDATA(HOBJECT, HANDLES);

% UIWAIT MAKES LED_CONTROLER WAIT FOR USER RESPONSE (SEE UIRESUME)
% UIWAIT(HANDLES.FIGURE1);

% --- OUTPUTS FROM THIS FUNCTION ARE RETURNED TO THE COMMAND LINE.
FUNCTION VARARGOUT = LED_CONTROLER_OUTPUTFCN(HOBJECT, EVENTDATA, HANDLES)
% VARARGOUT  CELL ARRAY FOR RETURNING OUTPUT ARGS (SEE VARARGOUT);
% HOBJECT    HANDLE TO FIGURE
% EVENTDATA  RESERVED - TO BE DEFINED IN A FUTURE VERSION OF MATLAB
% HANDLES    STRUCTURE WITH HANDLES AND USER DATA (SEE GUIDATA)

% GET DEFAULT COMMAND LINE OUTPUT FROM HANDLES STRUCTURE
VARARGOUT{1} = HANDLES.OUTPUT;

% --- EXECUTES ON SLIDER MOVEMENT.
```

```
FUNCTION SLIDER1_CALLBACK(HOBJECT, EVENTDATA, HANDLES)
% HOBJECT    HANDLE TO SLIDER1 (SEE GCBO)
% EVENTDATA  RESERVED - TO BE DEFINED IN A FUTURE VERSION OF MATLAB
% HANDLES    STRUCTURE WITH HANDLES AND USER DATA (SEE GUIDATA)

% HINTS: GET(HOBJECT,'VALUE') RETURNS POSITION OF SLIDER
%        GET(HOBJECT,'MIN') AND GET(HOBJECT,'MAX') TO DETERMINE RANGE OF
SLIDER
VAL=ROUND(GET(HOBJECT,'VALUE')*100);
SET(HANDLES.EDIT1,'STRING',NUM2STR(VAL));

% --- EXECUTES DURING OBJECT CREATION, AFTER SETTING ALL PROPERTIES.
FUNCTION SLIDER1_CREATEFCN(HOBJECT, EVENTDATA, HANDLES)
% HOBJECT    HANDLE TO SLIDER1 (SEE GCBO)
% EVENTDATA  RESERVED - TO BE DEFINED IN A FUTURE VERSION OF MATLAB
% HANDLES    EMPTY - HANDLES NOT CREATED UNTIL AFTER ALL CREATEFCNS CALLED

% HINT: SLIDER CONTROLS USUALLY HAVE A LIGHT GRAY BACKGROUND.
IF ISEQUAL(GET(HOBJECT,'BACKGROUNDCOLOR'),
GET(0,'DEFAULTUICONTROLBACKGROUNDCOLOR'))
    SET(HOBJECT,'BACKGROUNDCOLOR',[.9 .9 .9]);
END

% --- EXECUTES ON BUTTON PRESS IN PUSHBUTTON1.
FUNCTION PUSHBUTTON1_CALLBACK(HOBJECT, EVENTDATA, HANDLES)
% HOBJECT    HANDLE TO PUSHBUTTON1 (SEE GCBO)
% EVENTDATA  RESERVED - TO BE DEFINED IN A FUTURE VERSION OF MATLAB
% HANDLES    STRUCTURE WITH HANDLES AND USER DATA (SEE GUIDATA)
GLOBAL ST
VAL=GET(HANDLES.SLIDER1,'VALUE')
LEDPORT(ST,1,VAL*100);

% --- EXECUTES ON SLIDER MOVEMENT.
FUNCTION SLIDER2_CALLBACK(HOBJECT, EVENTDATA, HANDLES)
% HOBJECT    HANDLE TO SLIDER2 (SEE GCBO)
% EVENTDATA  RESERVED - TO BE DEFINED IN A FUTURE VERSION OF MATLAB
% HANDLES    STRUCTURE WITH HANDLES AND USER DATA (SEE GUIDATA)

% HINTS: GET(HOBJECT,'VALUE') RETURNS POSITION OF SLIDER
%        GET(HOBJECT,'MIN') AND GET(HOBJECT,'MAX') TO DETERMINE RANGE OF
SLIDER
VAL=ROUND(GET(HOBJECT,'VALUE')*100);
SET(HANDLES.EDIT2,'STRING',NUM2STR(VAL));

% --- EXECUTES DURING OBJECT CREATION, AFTER SETTING ALL PROPERTIES.
FUNCTION SLIDER2_CREATEFCN(HOBJECT, EVENTDATA, HANDLES)
% HOBJECT    HANDLE TO SLIDER2 (SEE GCBO)
% EVENTDATA  RESERVED - TO BE DEFINED IN A FUTURE VERSION OF MATLAB
% HANDLES    EMPTY - HANDLES NOT CREATED UNTIL AFTER ALL CREATEFCNS CALLED

% HINT: SLIDER CONTROLS USUALLY HAVE A LIGHT GRAY BACKGROUND.
IF ISEQUAL(GET(HOBJECT,'BACKGROUNDCOLOR'),
GET(0,'DEFAULTUICONTROLBACKGROUNDCOLOR'))
    SET(HOBJECT,'BACKGROUNDCOLOR',[.9 .9 .9]);
END

% --- EXECUTES ON BUTTON PRESS IN PUSHBUTTON2.
FUNCTION PUSHBUTTON2_CALLBACK(HOBJECT, EVENTDATA, HANDLES)
% HOBJECT    HANDLE TO PUSHBUTTON2 (SEE GCBO)
% EVENTDATA  RESERVED - TO BE DEFINED IN A FUTURE VERSION OF MATLAB
```

```
% HANDLES    STRUCTURE WITH HANDLES AND USER DATA (SEE GUIDATA)
GLOBAL ST
VAL=GET(HANDLES.SLIDER2,'VALUE')
LEDPORT(ST,2,VAL*100);
% --- EXECUTES ON SLIDER MOVEMENT.
FUNCTION SLIDER3_CALLBACK(HOBJECT, EVENTDATA, HANDLES)
% HOBJECT    HANDLE TO SLIDER3 (SEE GCBO)
% EVENTDATA  RESERVED - TO BE DEFINED IN A FUTURE VERSION OF MATLAB
% HANDLES    STRUCTURE WITH HANDLES AND USER DATA (SEE GUIDATA)

% HINTS: GET(HOBJECT,'VALUE') RETURNS POSITION OF SLIDER
%        GET(HOBJECT,'MIN') AND GET(HOBJECT,'MAX') TO DETERMINE RANGE OF
SLIDER
VAL=ROUND(GET(HOBJECT,'VALUE')*100);
SET(HANDLES.EDIT3,'STRING',NUM2STR(VAL));

% --- EXECUTES DURING OBJECT CREATION, AFTER SETTING ALL PROPERTIES.
FUNCTION SLIDER3_CREATEFCN(HOBJECT, EVENTDATA, HANDLES)
% HOBJECT    HANDLE TO SLIDER3 (SEE GCBO)
% EVENTDATA  RESERVED - TO BE DEFINED IN A FUTURE VERSION OF MATLAB
% HANDLES    EMPTY - HANDLES NOT CREATED UNTIL AFTER ALL CREATEFCNS CALLED

% HINT: SLIDER CONTROLS USUALLY HAVE A LIGHT GRAY BACKGROUND.
IF ISEQUAL(GET(HOBJECT,'BACKGROUNDCOLOR'),
GET(0,'DEFAULTUICONTROLBACKGROUNDCOLOR'))
    SET(HOBJECT,'BACKGROUNDCOLOR',[.9 .9 .9]);
END

% --- EXECUTES ON BUTTON PRESS IN PUSHBUTTON3.
FUNCTION PUSHBUTTON3_CALLBACK(HOBJECT, EVENTDATA, HANDLES)
% HOBJECT    HANDLE TO PUSHBUTTON3 (SEE GCBO)
% EVENTDATA  RESERVED - TO BE DEFINED IN A FUTURE VERSION OF MATLAB
% HANDLES    STRUCTURE WITH HANDLES AND USER DATA (SEE GUIDATA)
GLOBAL ST
VAL=GET(HANDLES.SLIDER3,'VALUE')
LEDPORT(ST,3,VAL*100);

% --- EXECUTES ON SLIDER MOVEMENT.
FUNCTION SLIDER4_CALLBACK(HOBJECT, EVENTDATA, HANDLES)
% HOBJECT    HANDLE TO SLIDER4 (SEE GCBO)
% EVENTDATA  RESERVED - TO BE DEFINED IN A FUTURE VERSION OF MATLAB
% HANDLES    STRUCTURE WITH HANDLES AND USER DATA (SEE GUIDATA)

% HINTS: GET(HOBJECT,'VALUE') RETURNS POSITION OF SLIDER
%        GET(HOBJECT,'MIN') AND GET(HOBJECT,'MAX') TO DETERMINE RANGE OF
SLIDER
VAL=ROUND(GET(HOBJECT,'VALUE')*100);
SET(HANDLES.EDIT4,'STRING',NUM2STR(VAL));

% --- EXECUTES DURING OBJECT CREATION, AFTER SETTING ALL PROPERTIES.
FUNCTION SLIDER4_CREATEFCN(HOBJECT, EVENTDATA, HANDLES)
% HOBJECT    HANDLE TO SLIDER4 (SEE GCBO)
% EVENTDATA  RESERVED - TO BE DEFINED IN A FUTURE VERSION OF MATLAB
% HANDLES    EMPTY - HANDLES NOT CREATED UNTIL AFTER ALL CREATEFCNS CALLED

% HINT: SLIDER CONTROLS USUALLY HAVE A LIGHT GRAY BACKGROUND.
IF ISEQUAL(GET(HOBJECT,'BACKGROUNDCOLOR'),
GET(0,'DEFAULTUICONTROLBACKGROUNDCOLOR'))
    SET(HOBJECT,'BACKGROUNDCOLOR',[.9 .9 .9]);
END
```

```
% --- EXECUTES ON BUTTON PRESS IN PUSHBUTTON4.
FUNCTION PUSHBUTTON4_CALLBACK(HOBJECT, EVENTDATA, HANDLES)
% HOBJECT    HANDLE TO PUSHBUTTON4 (SEE GCBO)
% EVENTDATA  RESERVED - TO BE DEFINED IN A FUTURE VERSION OF MATLAB
% HANDLES    STRUCTURE WITH HANDLES AND USER DATA (SEE GUIDATA)
GLOBAL ST
VAL=GET(HANDLES.SLIDER4,'VALUE')
LEDPORT(ST,4,VAL*100);

% --- EXECUTES ON BUTTON PRESS IN PUSHBUTTON5.
FUNCTION PUSHBUTTON5_CALLBACK(HOBJECT, EVENTDATA, HANDLES)
% HOBJECT    HANDLE TO PUSHBUTTON5 (SEE GCBO)
% EVENTDATA  RESERVED - TO BE DEFINED IN A FUTURE VERSION OF MATLAB
% HANDLES    STRUCTURE WITH HANDLES AND USER DATA (SEE GUIDATA)
GLOBAL ST
FIND_PROT;
SET(HANDLES.TEXT1,'STRING',ST);
%LEDPORT(ST,0,50);  % SET VALUE TO COM PORT 8 INSTEAD OF USING FIND_PROT
%GET(HANDLES.TEXT1)

% --- EXECUTES DURING OBJECT CREATION, AFTER SETTING ALL PROPERTIES.
FUNCTION TEXT1_CREATEFCN(HOBJECT, EVENTDATA, HANDLES)
% HOBJECT    HANDLE TO TEXT1 (SEE GCBO)
% EVENTDATA  RESERVED - TO BE DEFINED IN A FUTURE VERSION OF MATLAB
% HANDLES    EMPTY - HANDLES NOT CREATED UNTIL AFTER ALL CREATEFCNS CALLED

FUNCTION EDIT1_CALLBACK(HOBJECT, EVENTDATA, HANDLES)
% HOBJECT    HANDLE TO EDIT1 (SEE GCBO)
% EVENTDATA  RESERVED - TO BE DEFINED IN A FUTURE VERSION OF MATLAB
% HANDLES    STRUCTURE WITH HANDLES AND USER DATA (SEE GUIDATA)

% HINTS: GET(HOBJECT,'STRING') RETURNS CONTENTS OF EDIT1 AS TEXT
%        STR2DOUBLE(GET(HOBJECT,'STRING')) RETURNS CONTENTS OF EDIT1 AS A
DOUBLE

% IF SI==1
%     VAL=(STR2NUM(ST(1)))/100
% ELSEIF SI==2
%     VAL=(STR2NUM(ST(1))*10+STR2NUM(ST(2)))/100
% ELSE
%     VAL=(STR2NUM(ST(1))*100+STR2NUM(ST(2))*10+STR2NUM(ST(3)))/100
% END
VAL=STR2NUM(GET(HOBJECT,'STRING'))/100;
SET(HANDLES.SLIDER1,'VALUE',VAL);

% --- EXECUTES DURING OBJECT CREATION, AFTER SETTING ALL PROPERTIES.
FUNCTION EDIT1_CREATEFCN(HOBJECT, EVENTDATA, HANDLES)
% HOBJECT    HANDLE TO EDIT1 (SEE GCBO)
% EVENTDATA  RESERVED - TO BE DEFINED IN A FUTURE VERSION OF MATLAB
% HANDLES    EMPTY - HANDLES NOT CREATED UNTIL AFTER ALL CREATEFCNS CALLED

% HINT: EDIT CONTROLS USUALLY HAVE A WHITE BACKGROUND ON WINDOWS.
%       SEE ISPC AND COMPUTER.
IF ISPC && ISEQUAL(GET(HOBJECT,'BACKGROUNDCOLOR'),
GET(0,'DEFAULTUICONTROLBACKGROUNDCOLOR'))
    SET(HOBJECT,'BACKGROUNDCOLOR','WHITE');
END

FUNCTION EDIT2_CALLBACK(HOBJECT, EVENTDATA, HANDLES)
% HOBJECT    HANDLE TO EDIT2 (SEE GCBO)
```

```
% EVENTDATA  RESERVED - TO BE DEFINED IN A FUTURE VERSION OF MATLAB
% HANDLES    STRUCTURE WITH HANDLES AND USER DATA (SEE GUIDATA)

% HINTS: GET(HOBJECT,'STRING') RETURNS CONTENTS OF EDIT2 AS TEXT
%        STR2DOUBLE(GET(HOBJECT,'STRING')) RETURNS CONTENTS OF EDIT2 AS A
DOUBLE
VAL=STR2NUM(GET(HOBJECT,'STRING'))/100;
SET(HANDLES.SLIDER2,'VALUE',VAL);

% --- EXECUTES DURING OBJECT CREATION, AFTER SETTING ALL PROPERTIES.
FUNCTION EDIT2_CREATEFCN(HOBJECT, EVENTDATA, HANDLES)
% HOBJECT    HANDLE TO EDIT2 (SEE GCBO)
% EVENTDATA  RESERVED - TO BE DEFINED IN A FUTURE VERSION OF MATLAB
% HANDLES    EMPTY - HANDLES NOT CREATED UNTIL AFTER ALL CREATEFCNS CALLED

% HINT: EDIT CONTROLS USUALLY HAVE A WHITE BACKGROUND ON WINDOWS.
%       SEE ISPC AND COMPUTER.
IF ISPC && ISEQUAL(GET(HOBJECT,'BACKGROUNDCOLOR'),
GET(0,'DEFAULTUICONTROLBACKGROUNDCOLOR'))
    SET(HOBJECT,'BACKGROUNDCOLOR','WHITE');
END

FUNCTION EDIT3_CALLBACK(HOBJECT, EVENTDATA, HANDLES)
% HOBJECT    HANDLE TO EDIT3 (SEE GCBO)
% EVENTDATA  RESERVED - TO BE DEFINED IN A FUTURE VERSION OF MATLAB
% HANDLES    STRUCTURE WITH HANDLES AND USER DATA (SEE GUIDATA)

% HINTS: GET(HOBJECT,'STRING') RETURNS CONTENTS OF EDIT3 AS TEXT
%        STR2DOUBLE(GET(HOBJECT,'STRING')) RETURNS CONTENTS OF EDIT3 AS A
DOUBLE
VAL=STR2NUM(GET(HOBJECT,'STRING'))/100;
SET(HANDLES.SLIDER3,'VALUE',VAL);

% --- EXECUTES DURING OBJECT CREATION, AFTER SETTING ALL PROPERTIES.
FUNCTION EDIT3_CREATEFCN(HOBJECT, EVENTDATA, HANDLES)
% HOBJECT    HANDLE TO EDIT3 (SEE GCBO)
% EVENTDATA  RESERVED - TO BE DEFINED IN A FUTURE VERSION OF MATLAB
% HANDLES    EMPTY - HANDLES NOT CREATED UNTIL AFTER ALL CREATEFCNS CALLED

% HINT: EDIT CONTROLS USUALLY HAVE A WHITE BACKGROUND ON WINDOWS.
%       SEE ISPC AND COMPUTER.
IF ISPC && ISEQUAL(GET(HOBJECT,'BACKGROUNDCOLOR'),
GET(0,'DEFAULTUICONTROLBACKGROUNDCOLOR'))
    SET(HOBJECT,'BACKGROUNDCOLOR','WHITE');
END

FUNCTION EDIT4_CALLBACK(HOBJECT, EVENTDATA, HANDLES)
% HOBJECT    HANDLE TO EDIT4 (SEE GCBO)
% EVENTDATA  RESERVED - TO BE DEFINED IN A FUTURE VERSION OF MATLAB
% HANDLES    STRUCTURE WITH HANDLES AND USER DATA (SEE GUIDATA)

% HINTS: GET(HOBJECT,'STRING') RETURNS CONTENTS OF EDIT4 AS TEXT
%        STR2DOUBLE(GET(HOBJECT,'STRING')) RETURNS CONTENTS OF EDIT4 AS A
DOUBLE
VAL=STR2NUM(GET(HOBJECT,'STRING'))/100;
SET(HANDLES.SLIDER4,'VALUE',VAL);
% --- EXECUTES DURING OBJECT CREATION, AFTER SETTING ALL PROPERTIES.
FUNCTION EDIT4_CREATEFCN(HOBJECT, EVENTDATA, HANDLES)
% HOBJECT    HANDLE TO EDIT4 (SEE GCBO)
% EVENTDATA  RESERVED - TO BE DEFINED IN A FUTURE VERSION OF MATLAB
```

```
% HANDLES    EMPTY - HANDLES NOT CREATED UNTIL AFTER ALL CREATEFCNS CALLED

% HINT: EDIT CONTROLS USUALLY HAVE A WHITE BACKGROUND.
%       SEE ISPC AND COMPUTER.
IF ISPC && ISEQUAL(GET(HOBJECT,'BACKGROUNDCOLOR'),
GET(0,'DEFAULTUICONTROLBACKGROUNDCOLOR'))
    SET(HOBJECT,'BACKGROUNDCOLOR','WHITE');
END

% --- EXECUTES ON BUTTON PRESS IN PUSHBUTTON6.
FUNCTION PUSHBUTTON6_CALLBACK(HOBJECT, EVENTDATA, HANDLES)
% HOBJECT    HANDLE TO PUSHBUTTON6 (SEE GCBO)
% EVENTDATA  RESERVED - TO BE DEFINED IN A FUTURE VERSION OF MATLAB
% HANDLES    STRUCTURE WITH HANDLES AND USER DATA (SEE GUIDATA)
GLOBAL ST
LEDPORT(ST,1,0);

% --- EXECUTES ON BUTTON PRESS IN PUSHBUTTON7.
FUNCTION PUSHBUTTON7_CALLBACK(HOBJECT, EVENTDATA, HANDLES)
% HOBJECT    HANDLE TO PUSHBUTTON7 (SEE GCBO)
% EVENTDATA  RESERVED - TO BE DEFINED IN A FUTURE VERSION OF MATLAB
% HANDLES    STRUCTURE WITH HANDLES AND USER DATA (SEE GUIDATA)
GLOBAL ST
LEDPORT(ST,2,0);

% --- EXECUTES ON BUTTON PRESS IN PUSHBUTTON8.
FUNCTION PUSHBUTTON8_CALLBACK(HOBJECT, EVENTDATA, HANDLES)
% HOBJECT    HANDLE TO PUSHBUTTON8 (SEE GCBO)
% EVENTDATA  RESERVED - TO BE DEFINED IN A FUTURE VERSION OF MATLAB
% HANDLES    STRUCTURE WITH HANDLES AND USER DATA (SEE GUIDATA)
GLOBAL ST
LEDPORT(ST,3,0);
% --- EXECUTES ON BUTTON PRESS IN PUSHBUTTON9.
FUNCTION PUSHBUTTON9_CALLBACK(HOBJECT, EVENTDATA, HANDLES)
% HOBJECT    HANDLE TO PUSHBUTTON9 (SEE GCBO)
% EVENTDATA  RESERVED - TO BE DEFINED IN A FUTURE VERSION OF MATLAB
% HANDLES    STRUCTURE WITH HANDLES AND USER DATA (SEE GUIDATA)
GLOBAL ST
LEDPORT(ST,4,0);

% --- IF ENABLE == 'ON', EXECUTES ON MOUSE PRESS IN 5 PIXEL BORDER.
% --- OTHERWISE, EXECUTES ON MOUSE PRESS IN 5 PIXEL BORDER OR OVER
PUSHBUTTON2.
FUNCTION PUSHBUTTON2_BUTTONDOWNFCN(HOBJECT, EVENTDATA, HANDLES)
% HOBJECT    HANDLE TO PUSHBUTTON2 (SEE GCBO)
% EVENTDATA  RESERVED - TO BE DEFINED IN A FUTURE VERSION OF MATLAB
% HANDLES    STRUCTURE WITH HANDLES AND USER DATA (SEE GUIDATA)
```

APPENDIX II: PUBLICATIONS

Marine Genomics 24 (2015) 177–183

Contents lists available at ScienceDirect

Marine Genomics

Marine genomics for evolution and development

Opsin evolution in the Ambulacraria

S. D'Aniello [a,*,1], J. Delroisse [b,c,1], A. Valero-Gracia [a], E.K. Lowe [a,d], M. Byrne [e], J.T. Cannon [f,g,h], K.M. Halanych [f], M.R. Elphick [c], J. Mallefet [i], S. Kaul-Strehlow [j], C.J. Lowe [k], P. Flammang [b], E. Ullrich-Lüter [l], A. Wanninger [m], M.I. Arnone [a]

[a] Department of Biology and Evolution of Marine Organisms, Stazione Zoologica Anton Dohrn, Villa Comunale, 80121 Napoli, Italy
[b] Biology of Marine Organisms and Biomimetics, Research Institute for Biosciences, University of Mons, Avenue du Champs de Mars 6, 7000 Mons, Belgium
[c] School of Biological & Chemical Sciences, Queen Mary University of London, London E1 4NS, UK
[d] BEACON Center for the Study of Evolution in Action, Michigan State University, East Lansing, MI, USA
[e] Schools of Medical and Biological Sciences, The University of Sydney, Sydney, NSW, Australia
[f] Department of Biological Sciences and Molette Biology Laboratory for Environmental and Climate Change Studies, Auburn University, Auburn, USA
[g] Department of Zoology, Naturhistoriska Riksmuseet, Stockholm, Sweden
[h] Friday Harbor Laboratories, University of Washington, Friday Harbor, WA 98250, USA
[i] Laboratory of Marine Biology, Earth and Life Institute, Université Catholique de Louvain, Louvain-La-Neuve, Place Croix du Sud 3, bt L7.06.04, 1348 Louvain-la-Neuve, Belgium
[j] Department of Molecular Evolution and Development, University of Vienna, Althanstrasse 14, 1090 Vienna, Austria
[k] Hopkins Marine Station of Stanford University, Pacific Grove, CA 93950, USA
[l] Museum fuer Naturkunde Berlin, Invalidenstr 43, 10115 Berlin, Germany
[m] Department of Integrative Zoology, University of Vienna, Althanstrasse 14, 1090 Vienna, Austria

ARTICLE INFO

Article history:
Received 22 July 2015
Received in revised form 2 October 2015
Accepted 2 October 2015
Available online 23 October 2015

Keywords:
Opsin
Photoreceptor cell evolution
Ambulacraria
Echinoderm
Hemichordate
Phylogeny
Echinopsin

ABSTRACT

Opsins — G-protein coupled receptors involved in photoreception — have been extensively studied in the animal kingdom. The present work provides new insights into opsin-based photoreception and photoreceptor cell evolution with a first analysis of opsin sequence data for a major deuterostome clade, the Ambulacraria. Systematic data analysis, including for the first time hemichordate opsin sequences and an expanded echinoderm dataset, led to a robust opsin phylogeny for this cornerstone superphylum. Multiple genomic and transcriptomic resources were surveyed to cover each class of Hemichordata and Echinodermata. In total, 119 ambulacrarian opsin sequences were found, 22 new sequences in hemichordates and 97 in echinoderms (including 67 new sequences). We framed the ambulacrarian opsin repertoire within eumetazoan diversity by including selected reference opsins from non-ambulacrarians. Our findings corroborate the presence of all major ancestral bilaterian opsin groups in Ambulacraria. Furthermore, we identified two opsin groups specific to echinoderms. In conclusion, a molecular phylogenetic framework for investigating light-perception and photobiological behaviors in marine deuterostomes has been obtained.

1. Introduction

In animals, the prototypical molecules involved in photoreception and vision are opsin proteins (Terakita, 2005). Opsins are G-protein coupled receptors (GPCR) that consist of an apoprotein covalently bound to a chromophore (11-retinal) (Terakita, 2005). The nitrogen atom of the amino group of residue K296, situated in helix VII, binds to the retinal molecule through a Schiff-base linkage, forming a double bond with the carbon atom at the end of this molecule (Hargrave et al., 1983). Residue K296 is, therefore, crucial for light absorption, and its presence or absence can be used as a molecular fingerprint to judge whether or not a GPCR is a bona fide opsin.

Recent investigations on opsin phylogeny resolved six distinct groups present in metazoans: ciliary opsins, rhabdomeric opsins, Go-opsins, neuropsins, peropsins, and RGR (RPE-retinal G protein-coupled receptor) opsins (Porter et al., 2012; Feuda et al. 2012; Terakita et al., 2012). A vast number of opsins are also expressed in non-ocular tissues (Porter et al., 2012; Koyanagi et al., 2005; Terakita et al., 2012).

With regard to opsin evolution in the deuterostomes, genomic and transcriptomic data of a number of chordates have been used to identify and characterize their opsins (e.g. Holland et al., 2008; Kusakabe et al., 2001). However, little attention has been paid to Ambulacraria, the sister group to all extant chordates, (i.e. cephalochordates, urochordates,

* Corresponding author.
E-mail address: salvatore.daniello@szn.it (S. D'Aniello).
[1] These authors contributed equally to this work.

http://dx.doi.org/10.1016/j.margen.2015.10.001

and vertebrates, Edgecombe et al., 2011), a key clade to reconstruct the opsin set of the common ancestor of extant deuterostomes.

The present study integrates opsin sequences from two ambulacrarian sub-lineages: enteropneust Hemichordata (Harrimaniidae, Spengelidae, Ptychoderidae and Torquaratoridae), and the pentameral Echinodermata comprising five classes (Crinoidea, Ophiuroidea, Asteroidea, Holoturoidea and Echinoidea).

The phylogenetic relationship of echinoderms and hemichordates as sister groups within Ambulacraria, as shown in Fig. 1, was already suggested by Metschnikoff (1881), and supported by Nielsen (2012). The monophyly of Ambulacraria is also well supported by molecular phylogenetic analyses (Cannon et al., 2014; Telford et al., 2014). Moreover, Cannon and colleagues showed that the six hemichordate subgroups cluster into two monophyletic taxa, Enteropneusta and Pterobranchia (Rhabdopleuridae and Cephalodiscidae). Finally, Fig. 1 conforms to the Asterozoa hypothesis separating the Echinozoa (Echinoidea + Holothuroidea) and the Asterozoa (Asteroidea + Ophiuroidea), which is now well supported by recent molecular phylogenies (Cannon et al., 2014; Telford et al., 2014; O'Hara et al., 2014).

Other than a few structural investigations of eye-like structures in some asteroid species (e.g. the starfish optic cushion) and in enteropneust larvae (Brandenburger et al., 1973; Nezlin and Yushin, 2004; Braun et al., 2015), the molecular mechanisms of echinoderm and hemichordate photoreception remained enigmatic until recently. Immunohistochemical studies indicated the presence of a putative rhodopsin in the asteroid *Asterias forbesi* and in the ophiuroid *Ophioderma brevispinum* (Johnsen, 1997). Subsequently, Raible et al. (2006) analyzed the 'rhodopsin-type' G-protein-coupled receptors family in an echinoid genome (*Strongylocentrotus purpuratus*). They predicted six bona fide opsin sequences, four of which were reported independently by Burke et al. (2006). Later, Ooka et al. (2010) cloned an "encephalopsin" orthologue in the sea urchin *Hemicentrotus pulcherrimus*. Recently, more opsin sequences have been found in sea urchins (*S. purpuratus*; *Paracentrotus lividus*), starfish (*Asterias rubens*), and brittle stars (*Ophiocomina nigra*, *Amphiura filiformis*) (Delroisse et al., 2013, 2014, 2015; Ullrich-Lüter et al., 2011, 2013). These studies highlighted the expression of ciliary and rhabdomeric opsins in various echinoderm tissues. Also, a large opsin gene repertoire was identified in the brittle star *A. filiformis*, pinpointing notable differences with findings from the previously published sea urchin genome (Delroisse et al., 2014). However, a comprehensive description of opsin diversity in echinoderms is still lacking and almost nothing is known about hemichordate opsins.

Therefore, to characterize and describe the diversity of the opsin family in the Ambulacraria, we conducted a detailed analysis of 6 genomic and 24 transcriptomic sequence databases. This work represents the first attempt to describe and characterize the evolution of the opsin "toolkit" in the ambulacrarian lineage. We performed a phylogenetic study using the largest dataset of ambulacrarian opsin sequences to date, including representatives of a previously neglected group, Hemichordata.

2. Materials and methods

2.1. Data mining

Strongylocentrotus purpuratus opsins belonging to all the paralogous classes (Supp. File 1) were used as starting query sequences for tBLASTx against transcriptomic and genomic databases including public databases (NCBI, JGI, Ensemble, Echinobase (www.echinobase.org/), BioInformatique CNRS-UPMC (http://octopus.obs-vlfr.fr/) and Genoscope (http://www.genoscope.cns.fr/spip/Generation-de-ressources.html). The parameters used across all our tBLASTx searches were the following: Matrix: Blosum62; gap penalties: existence: 11; extension: 1; neighboring words threshold: 13; window for multiple hits: 40. Additionally, our dataset was further enriched using various unpublished genomic and transcriptomic databases obtained from several independent research projects (Suppl. Files 1 and 2). This includes transcriptomes from adult specimens' tissues, such as cuverian tubules and integument from *Holothuria forskali*, muscle of *Parastichopus californicus*, radial nerve from *A. rubens*, arms from *Labidiaster annulatus*, *Ophiopsila aranea*, *Astrotomma agassizii* and *Antedon mediterranea*, proboscis from *Saccoglossus mereschkowskii* and *Torquaratorid* sp., whole adult body of *Leptosynapta clarki* and anterior part of the body from *Harrimaniidae* sp. and *Schizocardium braziliense*. Several other transcriptomes obtained from embryos or larvae from *P. lividus*, *Heliocidaris erythrogramma*, *Eucidaris*

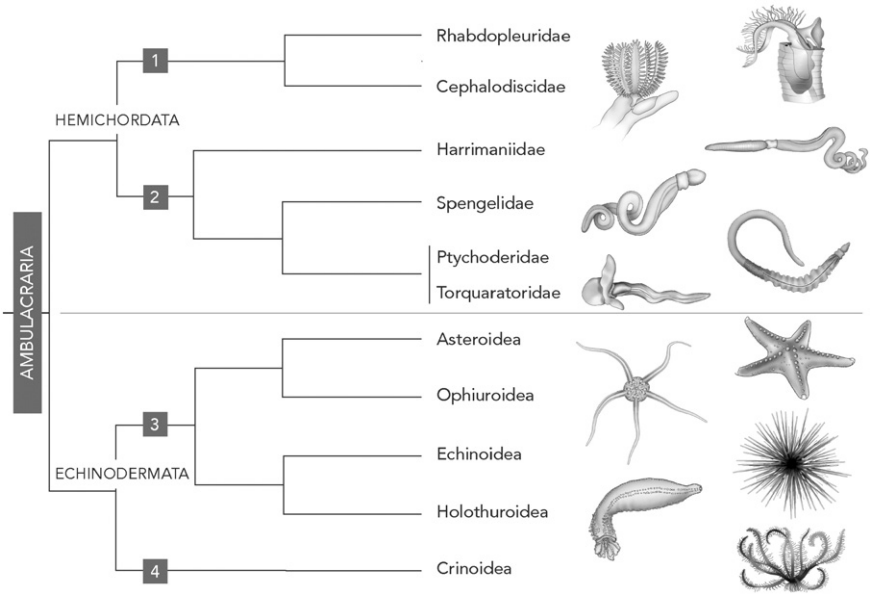

Fig. 1. Ambulacrarian phylogenetic relationships and their adult forms. The Ambulacraria consist of two groups: Hemichordata, bilateral animals subdivided in six clades: Cephalodiscidae, Rhabdopleuridae, Harrimaniidae, Spengelidae, Ptychoderidae and Torquaratoridae, and the pentameral Echinodermata, comprising: Crinoidea, Ophiuroidea, Asteroidea, Holoturoidea and Echinoidea. For each class there is a representation of the adult body plan. The numbers represented on the figure correspond to the two hemichordate subgroups: 1. Pterobranchia and 2. Enteropneusta, and the two echinoderm subgroups 3. Eleutherozoa and 4. Crinozoa.

tribuloides, *Parasticopus parvimensis*, *Saccoglossus kowalevskii* and *Ptychodera flava* (Suppl. Files 1 and 2) were also screened. The absence of echinopsin-like sequences in other metazoans was checked using blast search analysis. The raw predicted opsin sequences used in this study are listed in the Suppl. File 3 in fasta format.

2.2. Alignment and phylogenetic analyses

Predicted protein alignments were performed with SeaView v4.2.12 (Galtier et al., 1996; Gouy et al., 2010) using the MUSCLE algorithm (Edgar, 2004). To improve phylogenetic reconstruction, N-terminal and C-terminal ends were trimmed and the alignment was manually corrected in order to minimize gaps and eliminate ambiguous and misaligned regions. Sequences that were shorter than 60 amino acids were removed to avoid bias. However, these could potentially correspond to true opsins and merit further study.

Maximum likelihood analyses (ML) of our dataset were conducted on Michigan State University's High Performance Computing Cluster using PhyML v3.0 (Guindon and Gascuel, 2003), and nodal support assessed with 1000 bootstrap replicates is indicated. The alignment is shown in Suppl. File 4 (phylip format) and Suppl. File 5 (image). A best-fit model analysis was performed using MEGA6 (following the AIC criteria) (Tamura et al., 2013; Kumar et al., 2008) and WAG+G+F amino acid substitution model was found to be the best suited (Whelan and Goldman, 2001). Three melatonin receptor sequences from *S. purpuratus* (Echinodermata) and three from *S. kowalevskii*

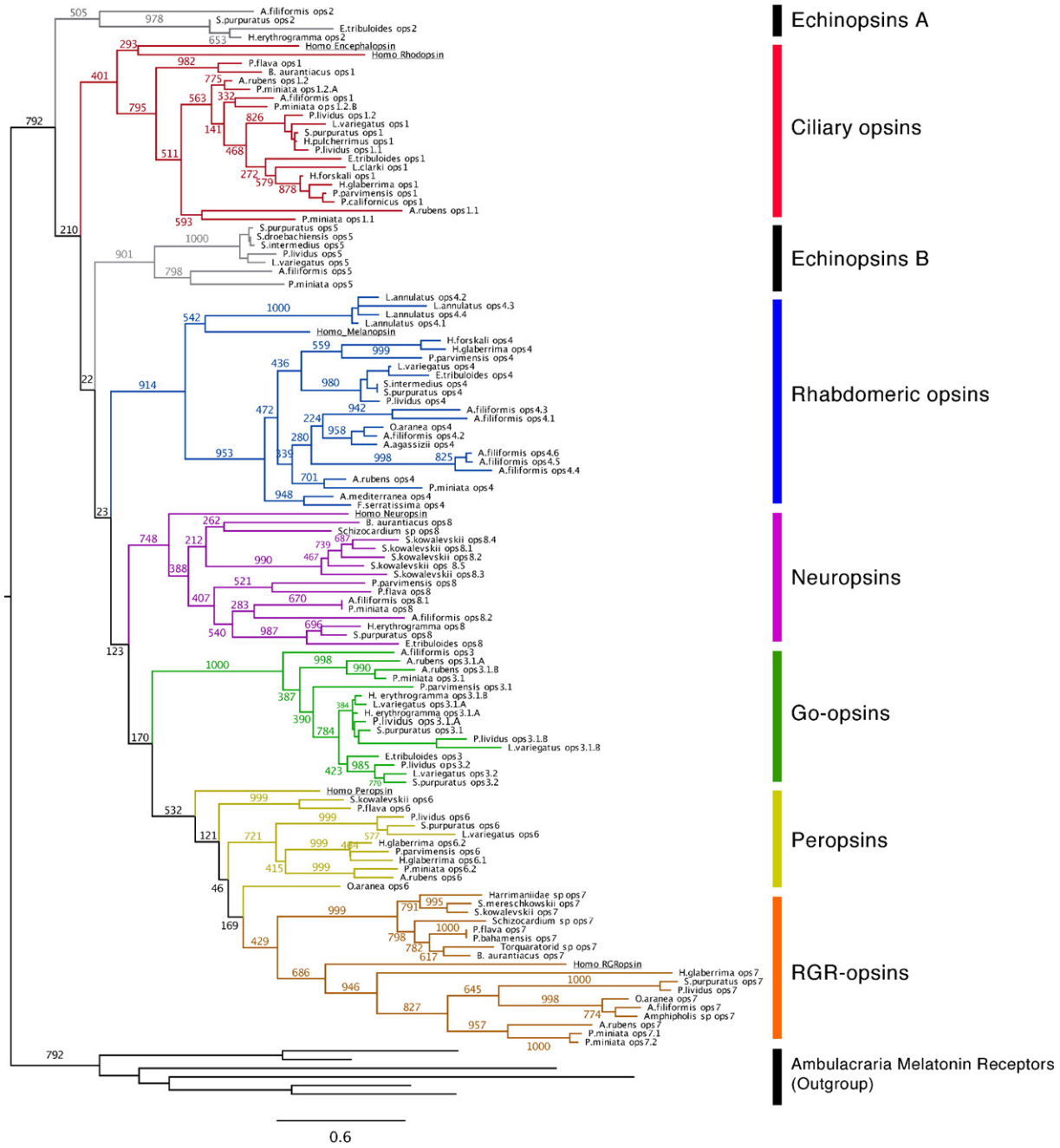

Fig. 2. Phylogenetic reconstruction of ambulacrarian opsins. 119 opsins from 31 different ambulacrarian species cluster in eight highly supported groups in this maximum likelihood (ML) based analysis. R-opsins in blue, c-opsins in red, Go-opsins in green, neuropsins in purple, peropsins in yellow and RGR-opsin in orange. Visualization was generated with fig tree.

(Hemichordata) were chosen as the best outgroup for the opsin phylogeny, as previously proposed by Plachetzki et al. (2010) and Feuda et al. (2014).

2.3. Consensus fingerprint of ambulacrarian opsin groups

Ambulacraria opsins were clustered according to their estimated position within opsin subfamilies and a multiple alignment of a 35 amino-acid long peptide region, including the 7th transmembrane domain with the opsin-specific lysine (K296), was performed with SeaView v4.2.12 for each opsin group supported in our phylogenetic tree. The selected region spanned residues 286 to 320 of the *Rattus norvegicus* rhodopsin sequence used as a reference (Palczewski et al., 2000). The consensus sequence was generated on the basis of the alignment for each class of ambulacrarian opsin using Geneious®8.1.5.

3. Results

3.1. Phylogeny and opsin distribution within ambulacrarian groups

Using a collection of both genomic and transcriptomic data (see Materials and methods and Suppl. File 2 for details), a final set of 119 protein sequences, representing 31 ambulacrarian species, was generated for our phylogenetic reconstruction, which included 6 outgroup sequences and 6 human reference opsin sequences (Suppl. Files 1 and 3 for raw predicted protein sequences). The trimmed opsin alignment is shown in the Suppl. File 5 (see Suppl. File 4 for the alignment phylip file). We employed maximum likelihood using the WAG+G+F model with melatonin receptors as an outgroup. Canonical opsin groups are well supported in our analysis (Fig. 2), demonstrating the presence of a complex opsin toolkit in Ambulacraria.

Interestingly, according to our data, two novel groups of opsins were found, which we have named echinopsin-A and echinopsin-B groups. Ad hoc BLAST searches against metazoan online database (NR, NCBI) clearly indicated the absence of these two opsin types outside the echinoderm lineage (Suppl. Fig. 6). The previously identified Sp-opsin2 and Sp-opsin5 belong to echinopsins-A and echinopsins-B, respectively (Raible et al., 2006).

A complete opsin profile including at least one representative of each prototypical opsin group (opsin 1-8) was detected in the sea urchin *S. purpuratus*, but not in *Lytechinus variegatus* or *P. lividus*. The genomes of the latter two species have not yet been comprehensively sequenced and annotated, and therefore some opsin genes may be missing due to incomplete sequence coverage. With the exception of echinopsin-B, a complete opsin profile was found in the genome sequence data of the starfish *Patiria miniata*. The starfish *A. rubens* radial nerve transcriptome also contained several opsins, including ciliary, Go-, RGR-opsins.

Surprisingly, rhabdomeric and Go-opsins do not seem to be present in hemichordates in our dataset. However, this requires confirmation through more extensive taxonomic sampling of hemichordate sequence data because, at present, only one hemichordate genome has been fully sequenced (*S. kowalevskii*). In several opsin groups we observed lineage-specific duplications: two c-opsins in *P. miniata* and *A. rubens*; five neuropsins in *S. kowalevskii*; four r-opsins in *L. annulatus* and six r-opsins in *A. filiformis*; two Go-opsins in the echinoids *L. variegatus*, *S. purpuratus* and *H. erythrogramma*. Nevertheless, some of these

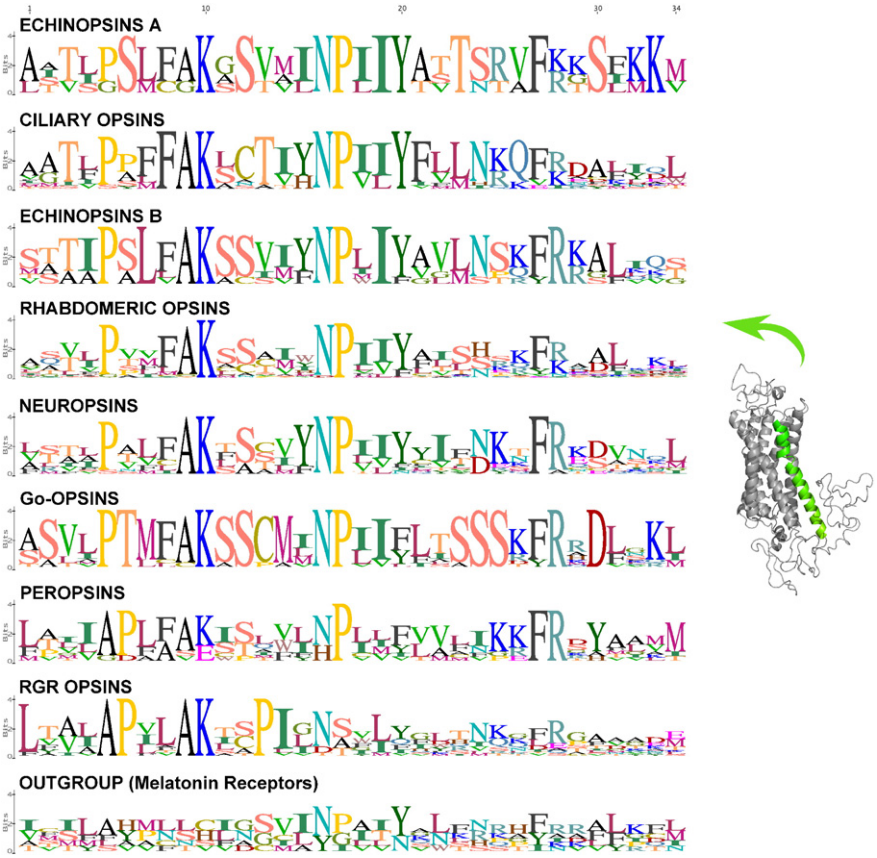

Fig. 3. Consensus sequences of different opsin groups. Graphical representations of opsin amino acid patterns within the multiple alignments of the 7th transmembrane domain and the protein G linkage site. The 7th transmembrane domain is highlighted in green in the tridimensional representation of a typical opsin receptor. Alignment is limited to the highly conserved regions including the opsin-specific lysine residue and the "NPxxY$(x)_6$F" pattern. The lysine residue involved in the Schiff base formation - equivalent to K296 of the *R. norvegicus* rhodopsin — is present in position 10. The pattern "NPxxY$(x)_6$F" (position 302–313 of the *R. norvegicus* rhodopsin sequence) is present in position 17–28. The size of each amino acid indicates the probability to find this specific amino acid for the considered position. Amino acid patterns of Melatonin receptors used as an outgroup in the phylogenetic analysis is also presented.

molecules present a short overlapping sequence, and therefore we cannot exclude that they could be part of unique genes. In this case, the number of genes would have been overestimated.

3.2. Alignment of the transmembrane domain and opsin fingerprint

In order to build a consensus fingerprint to distinguish the various ambulacrarian opsin groups, the 7th transmembrane domain and C-terminal tail region of our sequence dataset were aligned and a graphical representation was generated (Fig. 3). All sequences were characterized by the general structure of G protein-coupled receptors (GPCRs) comprising seven transmembrane (TM) domains. Numerous residues characteristic of opsins are present in the opsin sequences of Ambulacraria. However, as several sequences are partial, not all characteristic residues could be detected in all sequences. Most of the opsin sequences also contained the highly conserved lysine residue (equivalent to K296 of the *R. norvegicus* rhodopsin) critical for Schiff base linkage formed with retinal, except three sea-urchin peropsins (Sp-opsin 6, Pl-opsin 6, Lv-opsin 6) in which it is substituted by a glutamate (E). The dipeptide NP (position 302-303 of the *R. norvegicus* rhodopsin sequence) is also highly conserved among all the subfamilies except in peropsins (N/HP) and RGR-opsins, which show divergence in these residues (also rhabdomeric opsins to a lesser extent). Amino-acid conservation for each opsin group from our phylogenetic analysis is shown in Fig. 3. Ambulacrarian c-opsins, r-opsins and echinopsins-A displayed a highly conserved tyrosine (Y306). Conversely, the histidine (H310) appears distinctive of the ambulacrarian r-opsins (Fig. 3) and r-opsins in general (human melanopsin, octopus rhodopsin and *Drosophila* Rh1-opsin). In our dataset the tripeptide SSS, positioned at residues 309-402 of the reference protein, is a distinctive feature of ambulacrarian Go-opsins.

These representations will be particularly useful in future studies in support of phylogenetic analysis to assign novel, unknown sequences to lineage-specific opsin groups.

4. Discussion

Our phylogenetic analyses showed ambulacrarian opsin sequences to be represented in all six prototypical bilaterian opsin groups: ciliary opsins, rhabdomeric opsins, neuropsins, Go-opsins, peropsins and RGR-opsins (Fig. 4). Even though ciliary opsins, peropsins and RGR-opsins are in general well supported in the literature, a relatively poor nodal support was obtained for these groups using our ambulacraria opsin data set. In addition we confirmed the presence of two novel echinoderm-specific opsin groups, which we have named echinopsins (echinopsin-A and echinopsin-B). These novel groups of opsins, which were found only in Echinoidea, Ophiuroidea and Asteroidea, respectively cluster as a sister group of all other opsins and as a sister group of all

Phylum	Class	Species	TOTAL	R-opsins / opsins 4	C-opsins / opsins 1	Go opsins / opsins 3	Neuropsins / opsins 8	Peropsins / opsins 6	RGR-opsins / opsins 7	Echinopsins A / opsins 2	Echinopsins B / opsins 5
Echinodermata	Echinoidea	***Strongylocentrotus purpuratus***	**8**	**1**	**1**	**2**	**1**	**1**	**1**	**1**	**1**
		Strongylocentrotus droebachiensis	1								1
		Strongylocentrotus intermedius	2	1							1
		Lytechinus variegatus	**6**	**1**	**1**	**2**		**1**			**1**
		Paracentrotus lividus	**7**	**1**	**1**	**2**		**1**	**1**		**1**
		Hemicentrotus pulcherrimus	1		1						
		Eucidaris tribuloides	5	1	1	1	1			1	
		Heliocidaris erythrogramma	3			1	1			1	
	Holothuroidea	*Parastichopus californicus*	1		1						
		Parastichopus parvamensis	5	1	1	1	1	1			
		Leptosynapta clarki	1		1						
		Holothuria forskali	2	1	1						
		Holothuria glaberrima	4	1	1			1	1		
	Ophiuroidea	***Amphiura filiformis***	**13**	**6**	**1**	**1**	**2**		**1**	**1**	**1**
		Ophiopsila aranea	3	1				1	1		
		Astrotomma agassizii	1	1							
		Amphipholis sp	1						1		
	Asteroidea	*Asterias rubens*	6	1	2	1		1	1		
		Patiria miniata	**10**	**1**	**2**	**1**	**1**	**2**	**2**		**1**
		Labidiaster annulatus	4	4							
	Crinoidea	*Antedon mediterranea*	1	1							
		Florometra serratissima	1	1							
Hemichorda	Harrimaniidae	***Saccoglossus kowalevskii***	7				5	1	1		
		Saccoglossus mereschkowskii	1						1		
		Harrimaniidae sp. (Iceland)	1						1		
	Spengelidae	*Schizocardium c.f. braziliense*	2				1		1		
	Ptychoderidae	*Ptychodera flava*	4		1		1	1	1		
		Ptychodera bahamensis	1						1		
		Balanoglossus c.f. aurantiacus	3		1		1		1		
	Torquaratoridae	*Torquaratoid sp. (iceland)*	1						1		

Fig. 4. Opsin distribution within the investigated ambulacraria species. For each species the number of opsin belonging to classical groups were reported. Those species for which no opsins were found are not reported in the table (for additional informations see Suppl. File 1). Species for which the genome data are available are in bold.

opsins except echinopsins-A and ciliary opsins (Fig. 4). A deeper analysis of these groups of proteins, including more hemichordate opsin sequences, is needed in order to determine if they represent an echinoderm or ambulacrarian novelty. Clear orthologs of echinopsin-A and echinopsin-B where not encountered in any metazoan genome (exept echinoderms), as shown in Suppl. Fig. 6. Nevertheless, we cannot state conclusively that these represent lineage-specific clades because new genomes could reveal that echinopsin-A and echinopsin-B are indeed not restricted to echinoderms or ambulacrarians.

Our analysis failed to reveal a rhabdomeric opsin (r-opsin) in hemichordates. The absence of such an opsin type is surprising because many enteropneust tornaria larvae possess eyespots that bear photoreceptors with clear microvillar surface enlargement (Brandenburger et al., 1973; Nezlin and Yushin, 2004; Braun et al., 2015). So far, photoreception in microvillar photoreceptor cell types has been demonstrated to generally deploy opsins of the so-called rhabdomeric type (r-opsins), although co-expression of other opsin types in microvillar/rhabdomeric photoreceptors has been shown in recent studies (Randel et al., 2013). However, although our analysis reveals no such opsin in any of the examined enteropneust species, it should be noted that genomic information is only available from the direct developer *S. kowalevskii*, which does not have a larval (tornarian) stage in its life cycle. Moreover, most of hemichordate transcriptomes in our study were generated using adult tissues; it is therefore possible that the absence of r-opsin in this group of animals is due to a limitation of data availability from this understudied group of animals.

In contrast to the lack of r-opsins in enteropneusts, our analyses showed several cases of opsin gene duplication. Obviously in some instances the locus of duplication prompted a large expansion of the gene family, as is the case of the five neuropsins found in *S. kowalevskii*, and the six rhabdomeric opsins in *A. filiformis*, with the latter previously described by Delroisse et al. (2014). However, the fragmentary information about these duplicates makes it difficult to predict the exact number of functional opsin proteins in Ambulacraria. Whether or not these duplicated genes have subfunctionalized roles should be experimentally investigated by knock-out or silencing experiments.

Until recently, under-representation of many taxonomic groups in comparative studies of photoreceptor evolution has hidden the real extent of opsin diversity (Porter et al., 2012; Feuda et al., 2014). As more opsins have been characterized, these sequences have been classified into narrow pre-defined groups (e.g. Group 4 opsins), implying theoretical functional similarities that might not always be correct (Shichida and Matsuyama, 2009). At present, however, the rapidly increasing availability of entire genomes and transcriptomes provides a large number of sequences for investigating the evolution and functional diversity of the opsin family in greater detail. Likewise, our phylogenetic analysis of ambulacrarian opsins provides a better understanding of opsin evolution, nevertheless future metazoan genomes could certainly help to draw a more definitive evolutionary scenario.

Supplementary data to this article can be found online at http://dx.doi.org/10.1016/j.margen.2015.10.001.

Acknowledgments

The authors would like to thank Santiago Valero-Medranda for the illustrations in Fig. 1; Prof. Andy Cameron, Dr. Joel Smith, the staff of Echinobase for giving access to various echinoderm sequences, and Thierry Lepage and Genoscope *P. lividus* Project No. 17. Paola Oliveri, UCL (UK) and Yi-Hsien Su, Academia Sinica of Taipei (Taiwan) for their suggestions in the early phase of the project. The authors would like to thank Elise Hennebert, Mélanie Demeuldre, Akihito Omori, Atsushi Ogura and Masa-aki Yoshida for providing access to the *A. rubens* tube foot transcriptome, the *H. forskali* cuverian tubule transcriptome and the *Oxycomanthus japonicus* embryo transcriptome respectively. S. D'Aniello is supported by a Marie Curie Career Integration Grant, FP7-PEOPLE-2011-CIG (grant no. PCIG09-GA-2011-293871). J. Delroisse is currently supported by BBSRC grant no. BB/M001644/1 awarded to M.R. Elphick (QMUL). A. Valero-Gracia is supported by the Marie Curie ITN 'Neptune' (grant no. 317172, PI: M.I. Arnone). This work is supported in part by the "National funds for research" (FNRS) of Belgium (FRFC grant no. 2.4590.11). K.M. Halanych and J.T Cannon hemichordate's transcriptomes were funded by the USA National Science Foundation (grant no. DEB-0816892). E. Ullrich-Lüter is supported by a grant of the German Research foundation (DFG) grant no: UL 428/2-1. M. Byrne is supported by that Australian Research Council (DP120102849). S. Kaul-Strehlow is supported by a grant of the Austrian Science Fund (FWF, M-1485).

References

Brandenburger, J.L., Woollacott, R.M., Eakin, R.M., 1973. Fine structure of eyespots in tornarian larvae (phylum: Hemichordata). Z. Zellforsch. Mikrosk. Anat. 142, 89–102.
Braun, K., Kaul-Strehlow, S., Ullrich-Lüter, E., Stach, T., 2015. Structure and ultrastructure of eyes of tornaria larvae of *Glossobalanus marginatus*. Org. Divers. Evol. 15, 423–428.
Burke, R.D., Angerer, L.M., Elphick, M.R., Humphrey, G.W., Yaguchi, S., Kiyama, T., et al., 2006. A genomic view of the sea urchin nervous system. Dev. Biol. 300, 434–460.
Cannon, J.T., Kocot, K.M., Waits, D.S., Weese, D.A., Swalla, B.J., Santos, S.R., et al., 2014. Phylogenomic resolution of the hemichordate and echinoderm clade. Curr. Biol. 24, 2827–2832.
Delroisse, J., Lanterbecq, D., Eeckhaut, I., Mallefet, J., Flammang, P., 2013. Opsin detection in the sea urchin *Paracentrotus lividus* and the sea star *Asterias rubens*. Cah. Biol. Mar. 54, 721–727.
Delroisse, J., Ortega-Martinez, O., Dupont, S., Mallefet, J., Flammang, P., 2015. *De novo* transcriptome of the European brittle star *Amphiura filiformis* pluteus larvae. Mar. Genomics 23, 109–121.
Delroisse, J., Ullrich-Lüter, E., Ortega-Martinez, O., Dupont, S., Arnone, M.I., Mallefet, J., et al., 2014. High opsin diversity in a non-visual infaunal brittle star. BMC Genomics 15, 1035.
Edgar, R.C., 2004. MUSCLE: multiple sequence alignment with high accuracy and high throughput. Nucleic Acids Res. 32, 1792–1797.
Edgecombe, G.D., Giribet, G., Dunn, C.W., Hejnol, A., Kristensen, R.M., Neves, R.C., et al., 2011. Higher-level metazoan relationships: recent progress and remaining questions. Organ. Divers. Evol. 11, 151–172.
Feuda, R., Hamilton, S.C., McInerney, J.O., Pisani, D., 2012. Metazoan opsin evolution reveals a simple route to animal vision. Proc. Natl. Acad. Sci. 109, 18868–18872.
Feuda, R., Rota-Stabelli, O., Oakley, T.H., Pisani, D., 2014. The comb jelly opsins and the origins of animal phototransduction. Genome Biol. Evol. 6, 1964–1971.
Galtier, N., Gouy, M., Gautier, C., 1996. SEAVIEW and PHYLO_WIN: two graphic tools for sequence alignment and molecular phylogeny. Comput. Appl. Biosci. 12, 543–548.
Gouy, M., Guindon, S., Gascuel, O., 2010. SeaView version 4: a multiplatform graphical user interface for sequence alignment and phylogenetic tree building. Mol. Biol. Evol. 27, 221–224.
Guindon, S., Gascuel, O., 2003. A simple, fast, and accurate algorithm to estimate large phylogenies by maximum likelihood. Syst. Biol. 52, 696–704.
Hargrave, P.A., McDowell, J.H., Curtis, D.R., Wang, J.K., Juszczak, E., Fong, S.L., et al., 1983. The structure of bovine rhodopsin. Biophys. Struct. Mech. 9, 235–244.
Holland, L., et al., 2008. The amphioxus genome illuminates vertebrate origins and cephalochordate biology. Genome Res. 18, 1100–1111.
Johnsen, S., 1997. Identification and localization of a possible rhodopsin in the echinoderms *Asterias forbesi* (Asteroidea) and *Ophioderma brevispinum* (Ophiuroidea). Biol. Bull. 193, 97–105.
Koyanagi, M., Kubokawa, K., Tsukamoto, H., Shichida, Y., Terakita, A., 2005. Cephalochordate melanopsin: evolutionary linkage between invertebrate visual cells and vertebrate photosensitive retinal ganglion cells. Curr. Biol. 15, 1065–1069.
Kumar, S., Nei, M., Dudley, J., Tamura, K., 2008. MEGA: a biologist-centric software for evolutionary analysis of DNA and protein sequences. Brief. Bioinform. 9, 299–306.
Kusakabe, T., Kusakabe, R., Kawakami, I., Satou, Y., Satoh, N., Tsuda, M., 2001. Ci-opsin1, a vertebrate-type opsin gene, expressed in the larval ocellus of the ascidian *Ciona intestinalis*. FEBS Lett. 506, 69–72.
Metschnikoff, V.E., 1881. Über die systematische Stellung von Balanoglossus. Zool. Anz. 4, 139–157.
Nezlin, L.P., Yushin, V.V., 2004. Structure of the nervous system in the tornaria larva of Balanoglossus proterogonius (Hemichordata: Enteropneusta) and its physiogenetic implications. Zoomorphology 123, 1–13.
Nielsen, C., 2012. Animal evolution. Oxford University Press.
O'Hara, T.D., Hugall, A.f., Thuy, B., Moussalli, A., 2014. Phylogenomic resolution of the class Ophiuroidea unlocks a global microfossil record. Curr. Biol. 24, 1874–1879.
Ooka, S., Katow, T., Yaguchi, S., Yaguchi, J., Katow, H., 2010. Spatiotemporal expression pattern of an encephalopsin orthologue of the sea urchin *Hemicentrotus pulcherrimus* during early development, and its potential role in larval vertical migration. Develop. Growth Differ. 52, 195–207.
Palczewski, K., Kumasaka, T., Hori, T., Behnke, C.A., Motoshima, H., Fox, B.A., et al., 2000. Crystal structure of rhodopsin: a G protein-coupled receptor. Science 289, 739–745.
Plachetzki, D.C., Fong, C.R., Oakley, T.H., 2010. The evolution of phototransduction from an ancestral cyclic nucleotide gated pathway. Proc. Biol. Sci. 277, 1963–1969.

Porter, M.L., Blasic, J.R., Bok, M.J., Cameron, E.G., Pringle, T., Cronin, T.W., Robinson, P.R., 2012. Shedding new light on opsin evolution. Proc. R. Soc. B Biol. Sci. 279, 3–14.
Raible, F., Tessmar-Raible, K., Arboleda, E., Kaller, T., Bork, P., Arendt, D., et al., 2006. Opsins and clusters of sensory G protein-coupled receptors in the sea urchin genome. Dev. Biol. 300, 461–475.
Randel, N., Bezares-Calderón, L.A., Gühmann, M., Shahidi, R., Jékely, G., 2013. Expression dynamics and protein localization of rhabdomeric opsins in *Platynereis* larvae. Integr. Comp. Biol. 53, 7–16.
Shichida, Y., Matsuyama, T., 2009. Evolution of opsins and phototransduction. Philos. Trans. R. Soc. Lond. Ser. B Biol. Sci. 364, 2881–2895.
Tamura, K., Stecher, G., Peterson, D., Filipski, A., Kumar, S., 2013. MEGA6: molecular evolutionary genetics analysis version 6.0. Mol. Biol. Evol. 30, 2725–2729.
Telford, M.J., Lowe, C.J., Cameron, C.B., Ortega-Martinez, O., Aronowicz, J., Oliveri, P., Copley, R.R., 2014. Phylogenomic analysis of echinoderm class relationships supports Asterozoa. Proc. R. Soc. Lond. Ser. B 281, 20140479.
Terakita, A., 2005. The opsins. Genome Biol. 6, 213.
Terakita, A., Kawano-Yamashita, E., Koyanagi, M., 2012. Evolution and diversity of opsins. Wiley Interdiscip. Rev. Nanomed. Nanobiotechnol. 1, 104–111.
Ullrich-Lüter, E.M., D'Aniello, S., Arnone, M.I., 2013. C-opsin expressing photoreceptors in echinoderms. Integr. Comp. Biol. 53, 27–38.
Ullrich-Lüter, E.M., Dupont, S., Arboleda, E., Hausen, H., Arnone, M.I., 2011. Unique system of photoreceptors in sea urchin tube feet. PNAS 108, 8367–8372.
Whelan, S., Goldman, N., 2001. A general empirical model of protein evolution derived from multiple protein families using a maximum-likelihood approach. Mol. Biol. Evol. 18, 691–699.

frontiers in Ecology and Evolution

ORIGINAL RESEARCH
published: 14 November 2016
doi: 10.3389/fevo.2016.00127

Non-directional Photoreceptors in the Pluteus of *Strongylocentrotus purpuratus*

Alberto Valero-Gracia[1], *Libero Petrone*[2], *Paola Oliveri*[2], *Dan-Eric Nilsson*[3] and *Maria I. Arnone*[1]*

[1] Biology and Evolution of Marine Organisms, Stazione Zoologica Anton Dohrn, Naples, Italy, [2] Research Department of Genetics, Evolution and Environment, University College London, London, UK, [3] Lund Vision Group, Department of Biology, Lund University, Lund, Sweden

In comparison to complex visual systems, non-directional photoreception—the most primitive form of biological photodetection—has been poorly investigated, although it is essential to many biological processes such as circadian and seasonal rhythms. Here we describe the spatiotemporal expression pattern of the major molecular actors mediating light reception—opsins—localized in the *Strongylocentrotus purpuratus* larva. In contrast to other zooplanktonic larvae, the echinopluteus lacks photoreceptor cells with observable shading pigments involved in directional visual tasks. Nonetheless, the echinopluteus expresses two distinct classes of opsins: a Go-opsin and a rhabdomeric opsin. The Go-opsin, *Sp-opsin3.2,* is detectable at early (3 days post fertilization) and four armed pluteus stages (4 days post fertilization) in two cells that flank the apical organ. To rule out the presence of shading pigments involved in directional photoreception, we used electron microscopy to explore the expression domain of Go-opsin *Sp-opsin3.2* positive cells. The rhabdomeric opsin Sp-Opsin4 expression is detectable in clusters of cells located around the primary podia at the five-fold ectoderm pentagonal disc stage (day 18–21) and thereafter, thus indicating that Sp-Opsin4 may not be involved in the photoreception mechanism of the larva, but only of the juvenile. We discuss the putative function of the relevant cells in their neural context, and propose a model for understanding simple photodetection in marine larvae.

Keywords: eye evolution, Go-opsin, invertebrate larvae, r-opsin, sea urchin, zooplankton

OPEN ACCESS

Edited by:
Wayne Iwan Lee Davies, University of Western Australia, Australia

Reviewed by:
Karen Carleton, University of Maryland, College Park, USA
Mitsumasa Koyanagi, Osaka City University, Japan

***Correspondence:**
Maria I. Arnone
miarnone@szn.it

Specialty section:
This article was submitted to Behavioral and Evolutionary Ecology, a section of the journal Frontiers in Ecology and Evolution

Received: *07 August 2016*
Accepted: *18 October 2016*
Published: *14 November 2016*

Citation:
Valero-Gracia A, Petrone L, Oliveri P, Nilsson D-E and Arnone MI (2016) Non-directional Photoreceptors in the Pluteus of Strongylocentrotus purpuratus. Front. Ecol. Evol. 4:127. doi: 10.3389/fevo.2016.00127

INTRODUCTION

While the vast majority of studies on animal photoreception have so far focused on directional photoreceptors—systems comprising at least one cell with a photosensitive opsin together with shading pigments that enable it to discriminate the directionality of light—, less is known about non-directional photoreception, the simplest and earliest evolving type of photoreception. Non-directional photoreceptors, which can be difficult to detect due to a lack of visible screening pigments, allow the monitoring of absolute light intensities of the environment. Consequently, they are widely used as an input to the circadian clock system and also for a wide variety of other tasks. For instance, non-directional photoreceptors can be used as a depth gauge, as a warning for harmful levels of UV radiation, for shadow detection, or be involved in the regulation of feeding, movement and reproduction rhythms (Bennett, 1979; Paul and Gwynn-Jones, 2003; Leech et al., 2005; Nilsson, 2009, 2013).

Opsins are G-protein coupled receptors involved in light-perception. Based on their amino acid sequence, they can be divided into four groups: tetraopsin, xenopsin, Gq-opsin, and c-opsin (Ramirez et al., 2016; for other classifications see: Plachetzki et al., 2007; Arendt, 2008; Koyanagi et al., 2008; Porter et al., 2011; Feuda et al., 2012). The presence of opsins provides a clear landmark for localizing putative photoreceptor cells even in the absence of shading pigments and, as a consequence, the localization of opsin-expressing cells is important for finding directional and non-directional photoreceptors.

In echinoderms, efforts to describe photoreceptors have primarily focussed on adult specimens. The phototactic behavior commonly observed in adult sea urchins, in addition to their photosensitive ectoderm associated with an endoskeleton (which could act as shading structure, lens or filter) make them a useful model for studying diffuse photoreception (Raup, 1966; Hendler and Byrne, 1987; Johnsen, 1997; Johnsen and Kier, 1999; Aizenberg et al., 2001). Before the advent of molecular genetics, studies of photoreception in echinoids concentrated on cell morphology and physiology, as well as understanding behavioral responses such as spine movements, tube foot reaction, covering, color change, and more recently visual navigation (Holmes, 1912; Millott, 1953, 1954, 1976; Thornton, 1956; Millot and Yoshida, 1958; Millott and Manly, 1961; Yoshida, 1966; Yoshida et al., 1984; Johnsen, 1994; Blevins and Johnsen, 2004; Yerramilli and Johnsen, 2010). Later, the publication of the sea urchin *Strongylocentrotus purpuratus* genome lead to the discovery of nine opsins, a number of transcription factors involved in photoreceptor cell differentiation (*e.g.*, *irx5*, *irx6*, *dlx1/dlx2*, *rx*, *ath*) and several orthologous genes putatively involved in the phototransduction cascade (e.g., visual G-beta subunit, rhodopsin kinase, arrestin, retinal-binding protein, G-alpha-s subunit, transducin G-gamma-t1, recoverin, G-alpha-q subunit) in this species (Sodergren et al., 2006; D'Aniello et al., 2015). This information has made it possible to use molecular tools to investigate photoreception in echinoids (Burke et al., 2006; Raible et al., 2006). The first biochemical efforts to investigate the mechanisms of photoreception in *S. purpuratus* have resulted in the localization of the rhabdomeric opsin Sp-Opsin4 in basal (i.e., in the stalk area proximal to the compound plates) and disk (i.e., in the tube feet most apical part) microvillar cells of the adult tube feet (Ullrich-Lüter et al., 2011). Furthermore, a ciliary opsin, Sp-Opsin1 has been immunodetected in cells located in locomotory and buccal tube feet, as well as in the proximal stalk region of tridentate pedicellaria (Ullrich-Lüter et al., 2013), the latter being jawed appendages used against parasites (Coppard et al., 2010). These findings have allowed Ullrich-Lüter et al. (2011) to describe a unique system of photoreception in which the entire sea urchin, using its skeleton as photoreceptor screening device, functions as a "giant eye." This is also in agreement with previous observations on the photobehaviour of a *Diadema* species that lead to the suggestion that the shadow produced by the spines on the animal body surface is used for inferring the visual landscape (Woodley, 1982). However, in comparison with the light detection systems of adult echinoids, the photoreception mechanisms of their planktonic larvae have been so far poorly investigated.

While ancestral adult metazoans were likely benthic, it is probable that a pelagic larval stage evolved very early in animal evolution (Jägersten, 1972; Nielsen, 2008). This idea has led many scientists to investigate the directional simple eyespots of marine larvae in search of something resembling a "proto-eye" (Smith, 1935; Thorson, 1964; Brandenburger et al., 1973; Marsden, 1984; Pires and Woollacott, 1997; Leys and Degnan, 2001; Nordstrom et al., 2003; Jékely et al., 2008; Gühmann et al., 2015). Such simple eyespots or ocelli constitute class II photoreceptors (photoreceptor cells associated with shading pigments) in accordance with the classification of Nilsson (2013). To our knowledge, only few cases of non-directional (class I) photoreceptors have been documented in marine zooplanktonic larvae (Arendt et al., 2004; Passamaneck, 2011; Vöcking et al., 2015). In these cases, and in contrast to what we can observe in the echinopluteus, the larvae studied possess eyespots, thus making it more difficult to study class I photoreception in an independent way.

To better elucidate the origins of animal vision, an event that most probably happened in the Precambrian marine environment, the study of larvae with class I photoreception is essential. In this paper we identify a Go based photoreceptor system in a zooplanktonic larva of the deuterostome lineage that potentially lacks directional photoreceptors. To localize the putative photoreceptor cells of the larva at early and late developmental stages, we analyzed the expression of the opsins *Sp-opsin3.2* (Go) and Sp-Opsin4 (rhabdomeric) using whole mount *in situ* hybridization and immunohistochemistry, respectively. Further, the presence of shading pigments in the vicinity of the encountered Go-opsin based photoreceptor cells was ruled out by exploring both the apical organ as well as the basal area of the anterolateral arms by using a transmission electron microscopy (TEM) approach. The putative role of these photoreceptor cells in non-directional photoreception of the pluteus is discussed.

RESULTS

The Go Opsin *Sp-opsin3.2* Is Detected in Two Cells That Flank the Apical Organ of the Larva

In order to characterize the presence of putative photoreceptor cells in the sea urchin larva we first consulted the transcriptomic expression of *S. purpuratus* opsins. After analyzing the publicly available RNAseq data coming from a survey of 10 embryonic stages (Tu et al., 2014) we concluded that, of the nine genes encoding opsins found in the genome, the Go opsin *Sp-opsin3.2* (SPU027633) and the echinopsin *Sp-opsin2* (SPU003451) are the only opsin genes expressed at significant levels. Starting from the late gastrula stage (48 h), these two genes show expression levels reaching the value of about 100 transcripts per embryo at the early pluteus stage (72 h), when neurons start to differentiate (for gene expression profiling see **Supplementary Figure 1**). Next, successful amplification of the Go opsin *Sp-opsin3.2* was carried out, and the corresponding antisense riboprobe was used to localize the cells of interest. Unfortunately, various attempts in

the amplification with different set of primers of the "echinopsin" *Sp-opsin2* did not give any result.

Here, both RNA fluorescence (**Figures 1A–C**; 3 days post fertilization: dpf larvae, early four armed larvae) and chromogenic (**Figures 1D–F**; 4dpf, four armed larvae) whole mount *in situ* hybridization (WMISH) revealed that the Go opsin *Sp-opsin3.2* is expressed in two cells arranged bilaterally adjacent the apical organ—i.e., a portion of the epithelium that form the oral hood that is considered to act as central nervous system of the larva (Byrne et al., 2007)—and at the base of the left and right anterolateral arms (for a schematic view of the 4 armed pluteus in which we included the terminology used in this work, see **Figure 2**). The expression of this gene in such a small number of cells is consistent with the above mentioned low levels of expression observed from the transcriptomic data. In order to identify the position of these *Sp-opsin3.2* positive cells with respect to the ciliary band (the distinct thickening of ciliated epidermis that outlines the oral field and traces the edges of the four larval arms), cilia were labeled by immunohistochemistry with anti-acetylated α-tubulin after *Sp-opsin3.2* WMISH. As shown by both *in situ* techniques (**Figure 1**), the main body of these cells appear to be located just orally to the thick epidermal band of the ciliated cells (see **Figure 2** for schematic representation). The *Sp-opsin3.2* positive cells are suggestive of the presence of a photoreception system in the sea urchin larvae.

TEM Analysis Reveals Absence of Shading Pigments in the Larva Apical Region

A key difference between visual and non-visual photoreception system is the presence of shading structures, generally in the form of pigment cells, in proximity of light perceiving cells. Therefore, *S. purpuratus* larvae were observed under the light microscope at 4, 6, and 8 arm stages to detect for the presence of observable pigments that can be organized to act as shading for the described *Sp-opsin3.2* positive cells. The only pigmented cells found in the vicinity of these cells were the granulated pigment cells, a particular population of red colored cells of dendritic morphology and immune role that are distributed all over the body (Ho et al., 2016). We therefore decided to explore the presence of screening pigments in the vicinities of the Go *Sp-opsin3.2* opsin-positive cells by means of TEM.

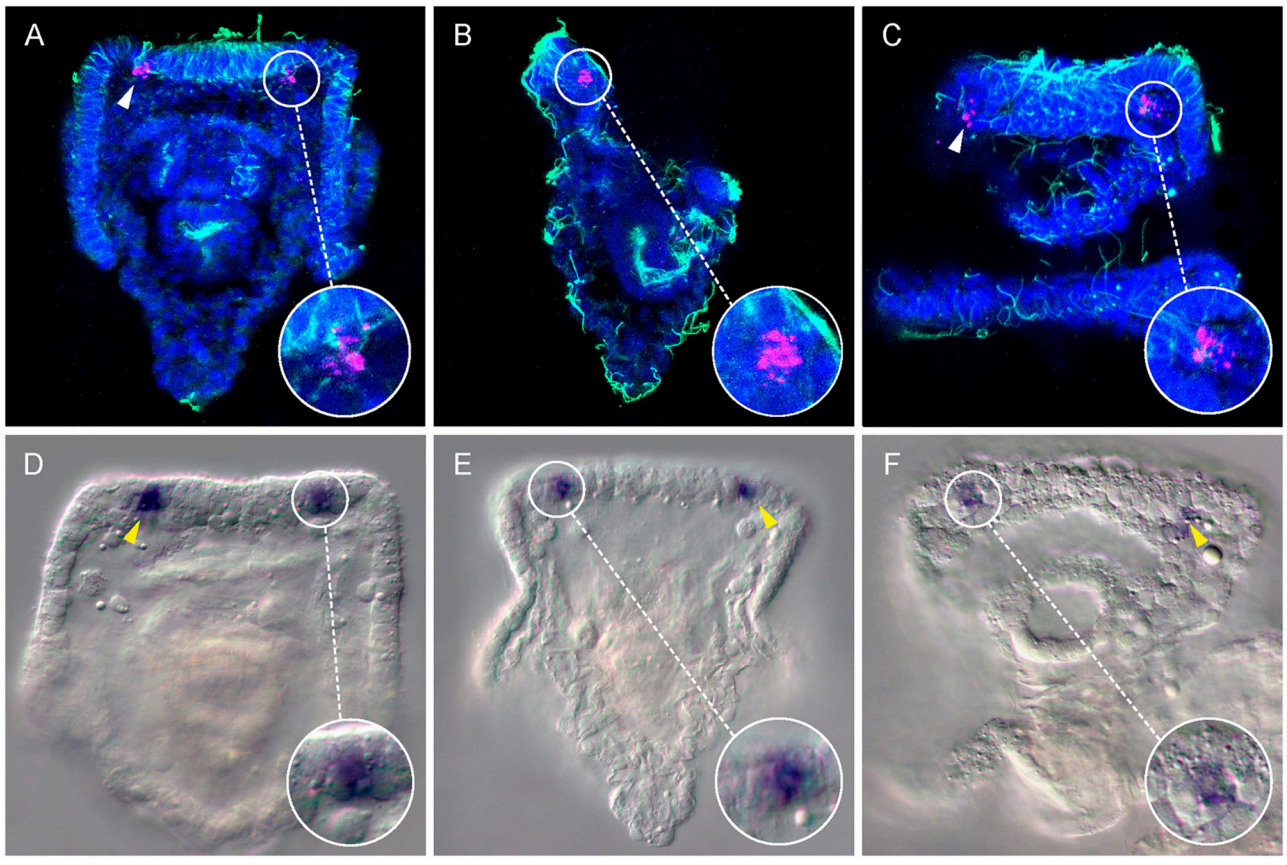

FIGURE 1 | Expression of the Go-opsin *Sp-opsin 3.2* in early plutei. A couple of *Sp-opsin 3.2* bilateral symmetrical cells were detected at cellular resolution between the base of the anterolateral arms and the apical organ of echinopluteus by means of fluorescent (**A–C**, 3dpf) and chromogenic (**D–F**, 4dpf) *in situ* hybridizations. **(A–C)** Confocal-micrographs; *Sp-opsin3.2 in situ* hybridization (magenta) was coupled with acetylated α-tubulin immunohistochemistry (green); nuclei were counterstained with DAPI (blue). **(A)** Abanal view; **(B)** right-lateral view; **(C)** mouth view. **(D–F)** Light-micrographs. **(D,E)** abanal view; **(F)** mouth view. Arrow heads indicate *Sp-opsin3.2* positive cells.

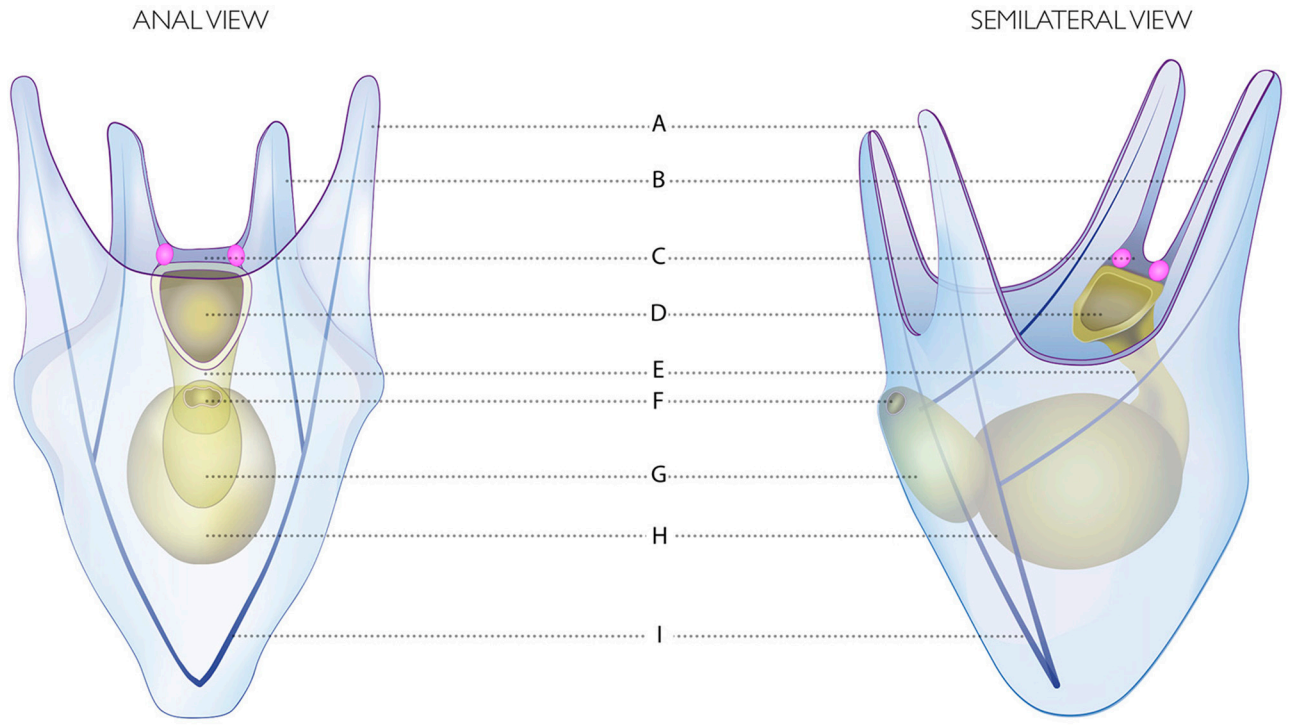

FIGURE 2 | Drawing of the four-armed pluteus of *S. purpuratus*. (A) Postoral arms. **(B)** Anterolateral arms. **(C)** Apical organ. **(D)** Mouth. **(E)** Esophagus. **(F)** Anus. **(G)** Intestine. **(H)** Stomach. **(I)** Skeletal rods. The Go *Sp-opsin3.2* opsin positive cells are represented in pink.

Shading pigments involved in directional photoreception, which can be located both in the opsin positive cells or adjacently, are easily recognized in TEM as a group of black-solid dots in the cytoplasm (e.g., Marshall and Hodgson, 1990; Leys and Degnan, 2001). For our TEM analysis, three larvae were fixed, and transversal sections of 50–70 nm were made in the apical region in search of shading pigments (**Figure 3A**). Of them, micrographs corresponding to different sections of the apical organ (**Figures 3D,E**) and the bases of the left (**Figures 3B,C**) and right (**Figures 3F,G**) anterolateral arms were selected. Interestingly, none of the cells embedded in the apical organ nor in the area of the ciliary band exhibited observable shading pigments. In particular, the regions of the ectoderm in between the apical organ and either left or right anterolateral arms (encircled in **Figures 3A,C,F**) where the *Sp-opsin3.2* positive cells are located (see also schematics of **Figure 2**) are void of shading pigment granules. These findings suggest that the *Sp-opsin3.2* positive cells are not involved in directional photoreception. Serial multiplex immunogold labeling experiments are needed to better characterize the morphology of the encountered *Sp-opsin3.2* positive cells.

Sp-opsin4, the Rhabdomeric Opsin, Was Detected in the Adult Rudiment at Pentagonal Disc Stages and Thereafter

Due to limitations of WMISH efficiency on late developmental stages and the availability of a specific antibody against the sea urchin rhabdomeric opsin Sp-Opsin4 (Ullrich-Lüter et al., 2011), we decided to use an immunohistochemical approach to explore the opsin toolkit of the premetamorphic larva. During late larval development (second week of development and thereafter), a portion of the coelom and the overlying ectoderm get in contact and form the imaginal adult rudiment (Smith et al., 2008; Heyland and Hodin, 2014; for a schematic view see drawings in **Figure 4**). This rudiment represents the presumptive juvenile that grows from the left side of the larva (for a schematic, see **Figure 4A**). In order to analyze the spatiotemporal expression of the rhabdomeric opsin Sp-Opsin4, we tested its presence in time series of 3, 4, 5, 6, and 7 days (4 armed pluteus), 16d (6 armed pluteus, contact flattened stage), 17d (6 armed pluteus, 5-fold mesoderm stage), 18d (8 armed pluteus, 5-fold ectoderm stage), 19d (8 armed pluteus, primary podia stage), 21d (8 armed pluteus, primary podia-folded stage), and 23d (8 armed pluteus, primary podia-touching stage) post fertilization (for staging of the echinopluteus see also Smith et al., 2008; Heyland and Hodin, 2014). These experiments suggested the absence of expression of the rhabdomeric opsin Sp-Opsin4 prior to the tube feet formation in any part of the larva. No protein expression was found either in *sensu stricto* larval structures until the 5-fold mesoderm stages (17dpf; **Figures 4B,B′**) with our method. Larvae started to exhibit Sp-Opsin4 positivity in conspicuous clusters of cells on the vestibular floor at pentagonal disc stage that would give rise to the tube feet disc during 5-fold ectoderm stage, a stage in which the ectoderm and the primordia of the five podia begin to push through the floor of the vestibular ectoderm (day 18;

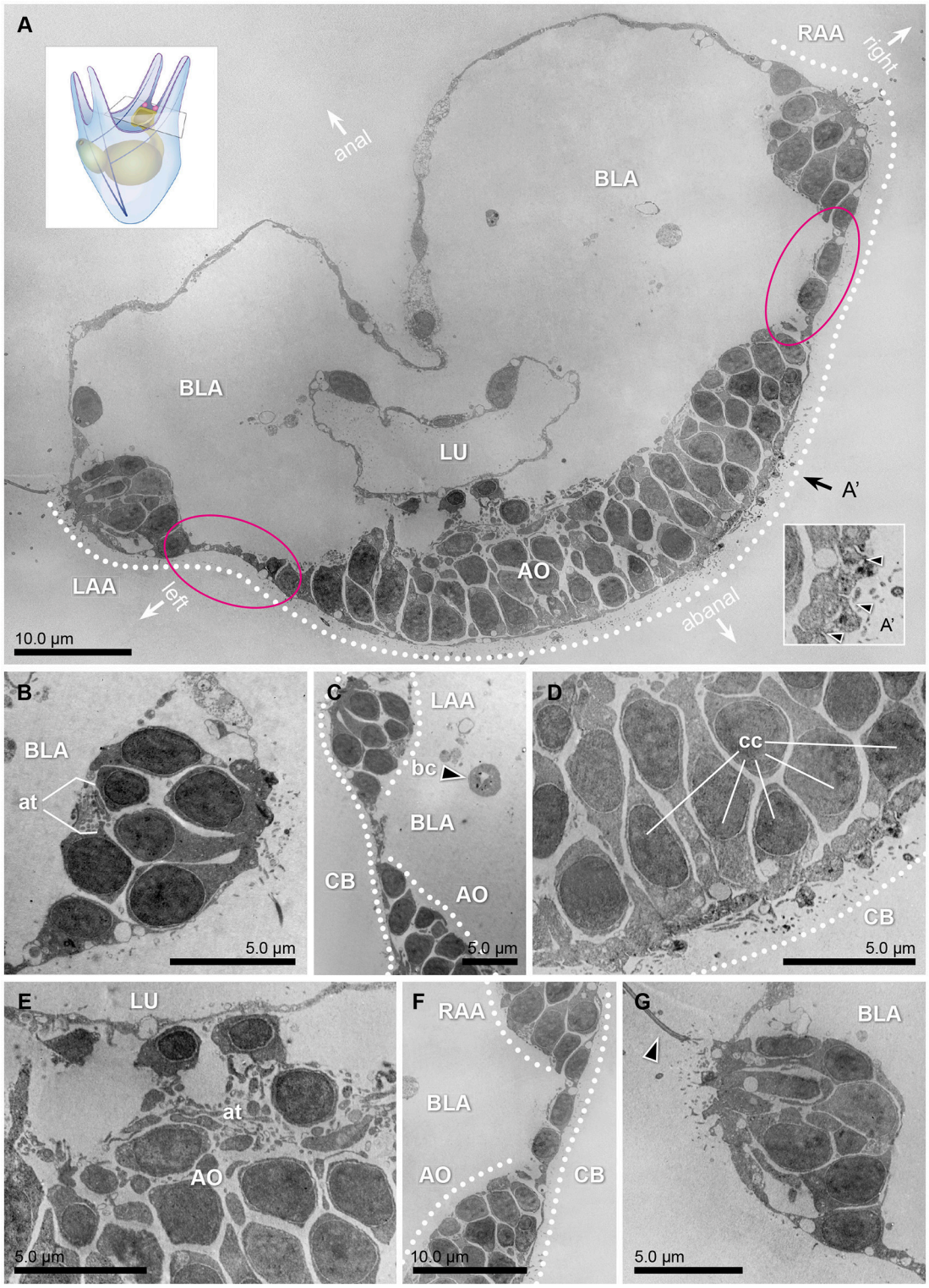

FIGURE 3 | Transmission electron micrographs of a 3dpf (early 4 armed) pluteus, different sections of three specimens at the level of the apical region. **(A)** Collage of 324 transversal micrographs showing a panoramic view of the abanal half of the larvae (apical region). On it, the bases of the left and right anterolateral arms (LAA and RAA, respectively), as well as the lumen (LU) of the gut, surrounded by the blastocoel (BLA), the ciliary band (CB, dotted line), and the apical organ (AO) are shown. The stippled line corresponds to the ectodermal region in which the ciliary band is located. A representation of the whole 4 armed pluteus larva and

(Continued)

FIGURE 3 | Continued
cutting area can be seen in the lower right corner. (A') Detail of the cross sectional profile of the motile cilia (arrow heads) that compose the ciliary band. The orientation of the animal is defined by the axes: anal, abanal, left and right. **(B)** Transversal section of the base of the anterolateral arm, left side. On it, the axon tract (at) that connects this area with the nervous system can be distinguished. **(C)** Transversal section of the region that connects the left anterolateral arm (LAA) with the apical organ (AO). Pigmented cells cannot be detected in any of the cells flanking the apical organ, where the Go-opsin *Sp-opsin3.2* was detected. The black arrow head points to a blastocoelar cell (bc). **(D,E)** Detail micrographs of the apical organ, an area considered as the central system of the animal, rich on ciliated cells (cc) and axon tracts (at). **(F)** Transversal section of the region that connects the right anterolateral arm (RAA), with the apical organ (AO). **(G)** Transversal section of the base of the anterolateral arm, right side. The arrow head points one of the cilia of the region.

Figures 4C,C′). At this point, the interior of the 5 incipient podia are spherical in shape or shorter than wide. We also detected Sp-Opsin4 positive cells later on, in the tube feet disc during advanced rudiment stage, when the primary podia are taller than they are wide, but the podia are not yet folding in toward one another (day 20–21; **Figures 4D,D′**). At tube-foot protrusion stage (day 21–45), Sp-Opsin4 positive cells were detected both in disc (**Figure 4E**) and basal (**Figure 4F**) photoreceptors of the tube feet. These data indicate that the rhabdomeric opsin Sp-opsin4 may not regulate the photoreception mechanism of the larva, but only of the juvenile, where it appears to be involved in negative phototaxis (Ullrich-Lüter et al., 2011). For a schematic view on the different rudimental stages, see **Figures 4B′–F′**.

DISCUSSION

Our findings show that, at least, two opsin classes are expressed in *Strongylocentrotus purpuratus* prior to metamorphosis: first the Go opsin *Sp-opsin3.2* in the apical region of the larva at 3 and 4 dpf (4 armed pluteus), and then the rhabdomeric opsin Sp-Opsin4 in the tube feet of the presumptive juvenile (day 29 and thereafter, 8 armed pluteus). The different opsin classes in the sea urchin may serve different needs to integrate light information depending on the life stage, where the pelagic larva and the benthic adult face very different challenges.

Of the opsin-positive cells encountered, just the two *Sp-opsin3.2* positive-cells localized in the flanks of the apical organ can be considered part of the *sensu-stricto* larval tissues. In our study, no rhabdomeric opsins have been found in larval structures. Because the aim of this study is to improve our understanding of photoreception in marine larvae, the rhabdomeric opsin Sp-opsin4, which is expressed in presumptive juvenile tissues, will not be further discussed. For an account on the possible role of Sp-opsin4 positive photoreceptor cells in mediating negative phototaxis of sea urchin juveniles (see Ullrich-Lüter et al., 2011).

Ancientness of Go-Opsins

Phylogenetic analyses indicate the presence of at least seven opsins in the last common ancestor of Bilateria (Ramirez et al., 2016), thus suggesting that light reception had many roles very early in animal evolution. These opsins, together with present-day animal opsins, have been classified into four groups: (i) tetraopsins (Go-opsins, RGR/retinochrome opsins and neuropsins), (ii) xenopsins, (iii) Gq-opsins (including canonical and non-canonical r-opsins as well as "chaopsins"), and (iv) c-opsins, i.e., canonical c-opsins and bathyopsins (Ramirez et al., 2016). While the canonical c- and r-opsin groups have been extensively studied, little is known about the Go opsin group included in the tetraopsin clade (Gühmann et al., 2015).

In support of the ancient origin of the Go opsins, cells expressing this class of opsins have been localized in diverse animal clades, thereby suggesting the presence of this opsin group before the protostome-deuterostome split. Examples of Go-opsins are found in the ciliary cells of the eyes of the adult scallop *Patinopecten yesooensis* (Kojima et al., 1997), in the gastrula of the brachiopod *Terebratalia transversa* (Passamaneck and Martindale, 2013), in the rhabdomeric adult eye of the polychaete *Platynereis dumerilii* (Gühmann et al., 2015) as well as in the photoreceptor system here described. In the amphioxus *Branchiostoma belcheri,* a Go-opsin has been demonstrated by an *in vitro* analysis (Koyanagi et al., 2002) but, to our best knowledge, this is the first report in which the spatial expression of a Go-opsin has been described in a deuterostome larva.

Non-directional Photoreceptors

In marine invertebrates, the expression of opsins in non-visual photoreceptors has been documented in the apical organ of planktonic larvae of protostome and deuterostome lineages (e.g., Arendt et al., 2004 and herein). A shared feature of these apical organs—regions specified by conserved developmental patterning mechanisms (Marlow et al., 2014)—is the presence of multiple sensory cells connected to the nervous system, which regulates ciliary beating and the vertical position of the animal in the water column (Tosches et al., 2014). In vertebrates, a population of non-directional retinal ganglion cells (the intrinsically photosensitive photoreceptive retinal ganglion cells: ipRGCs), are critical in relaying light information to the brain in order to control circadian photo-entrainment, pupillary light reflex, and sleep (Provencio et al., 1998; Schmidt et al., 2011).

Our discovery of non-directional photoreceptors in the pluteus of *S. purpuratus* suggests that these cells may also have a role in controlling the vertical position of the larva in the water column, which may be used for monitoring the time of day or the depth (Nilsson, 2013). This adjustment is likely to be achieved by modulating the length and frequency of ciliary arrests, as proposed for this and other marine larvae (e.g., Wada et al., 1997; Maldonado et al., 2003; Braubach et al., 2006; Jékely et al., 2008). The use of non-directional photoreceptors in vertebrates for tasks such as the regulation of nocturnal-diurnal behaviors (Provencio et al., 1998; Schmidt et al., 2011) could represent the retention of such chronobiological role.

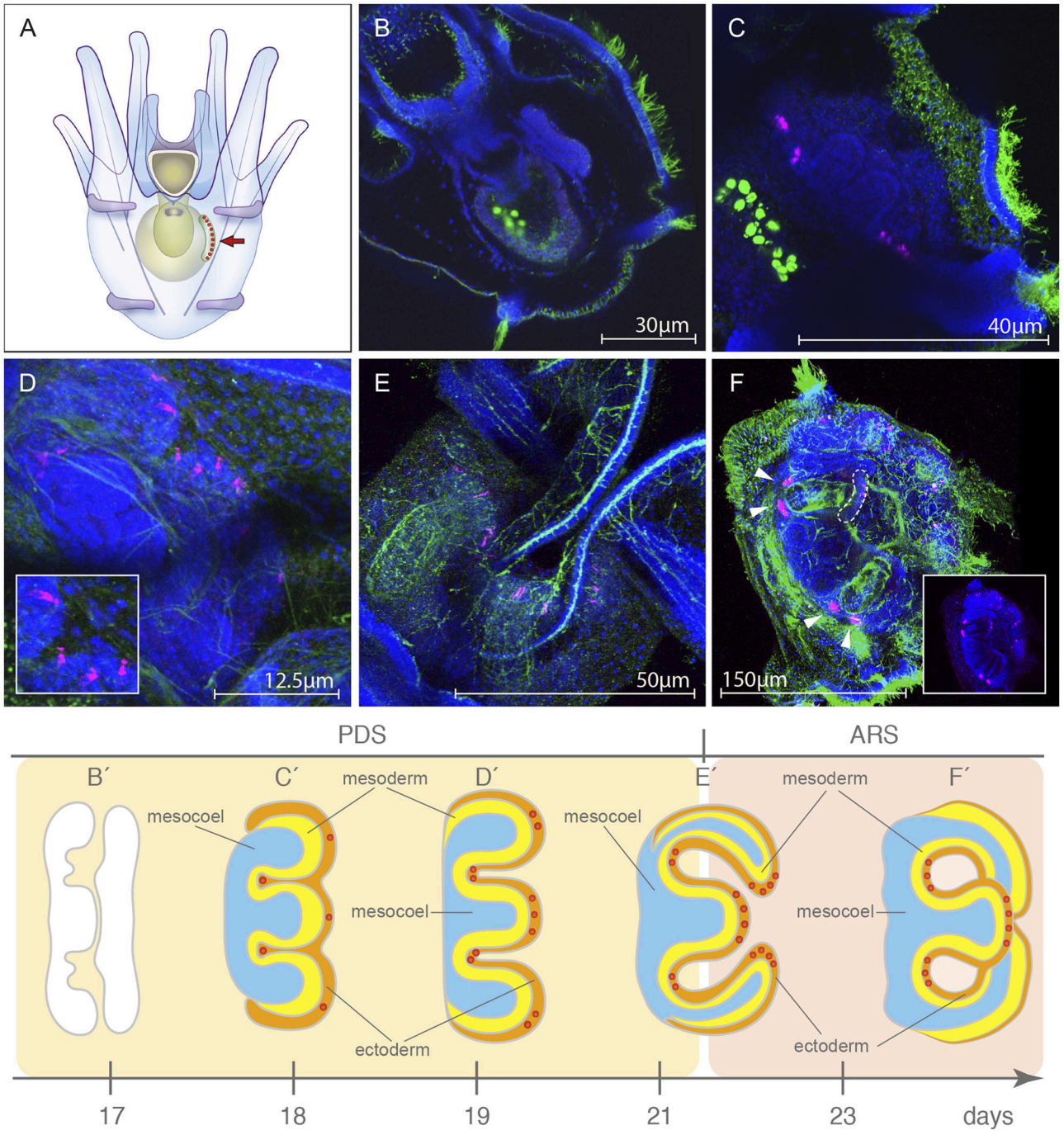

FIGURE 4 | Localization of the rhabdomeric opsin Sp-opsin4 in the developing tube feet of the presumptive juvenile. (A) Schematic of the 8 armed pluteus stage, anal view, in which the area of growing of the rudiment (arrow) is shown. **(B,B′)** Sp-opsin4 was not detected in adult plate at 5-fold ectoderm stage (day 17; pentagonal disc stage, PDS). **(C,C′)** During the 5-folding of the ectoderm (day 18, PDS), the rudiment of the larva starts to exhibit Sp-opsin4 positivity in clusters of conspicuous cells at the presumptive basal tube feet. **(D,D′)** At primary podia stage (day 19, PDS), the presumptive disc tube feet of the vestibular floor are positive for Sp-opsin4. **(E,E′)** Sp-opsin4 photoreceptor cells are visible in the tube feet disc of the folded primary podia (day 21; transition between the PDS and the advanced rudiment stage, ARS), both in disc and basal photoreceptor cells of the tube feet. **(F,F′)** Sp-opsin4 positive cells were detected at tube-foot protrusion stage (day 23-45, ARS). Stages redrawn from Heyland and Hodin (2014). PDS and ARS stages are named following the nomenclature proposed by Smith et al. (2008). The red dots in **(C′-F′)** represent the Sp-opsin4 positive cells and can be used as a landmark to locate and orient rudiment in **(C–F)**. Confocal micrographs color code: Sp-opsin4 in magenta; acetylated α-tubulin **(B–E)** and 1E11 **(F)** in green; DAPI in blue. The bright green staining in the stomach of the larvae shown in **(B,C)** is due to autofluorescence of the ingested microalgae.

Bilateral Disposition and Lack of Shading Pigments

The absence of shading pigments in the region where the *Sp-Opsin3.2* is expressed strongly suggests that these opsin-positive cells lack directional sensitivity, but whether this represents a plesiomorphic character or a secondary loss is not immediately clear. Directional photoreception for phototaxis, with shading pigment near the site of opsin expression, is believed to have evolved from non-directional photoreception where screening pigment is not needed (Nilsson, 2009, 2013). Directional photoreceptors are typically bilaterally paired organs (Brandenburger et al., 1973; Arendt and Wittbrodt, 2001; Braun et al., 2015), whereas non-directional photoreceptors are often un-paired median structures (Mano and Fukada, 2007; Van Gelder, 2008). Our finding of paired non-directional photoreceptors represents an interesting intermediate.

The bilateral arrangement of photoreceptor cells is typically associated with helical swimming behaviors in the pluteus and other marine invertebrate larvae (Lacalli et al., 1990; reviewed in Jékely, 2009). Bilaterally paired photoreceptors may seem redundant for non-directional photoreception, and without shading pigment they do not have the directionality required for phototaxis.

It is possible that the shading pigment associated with these opsin-positive cells might have been lost during evolution to increase transparency or reduce energy expenditure. The lack of shading pigments may have been favored by selection to allow a better camouflage against predators (Nilsson, 1996). Consequently, the bilateral arrangement of these opsin positive cells may be primitive, and the lack of screening pigment a consequence of an adaptive transition from a directional to a non-directional role. Alternatively, it is possible that the pluteus have retained the non-directional photoreceptors of "Urbilateria," an ancestor that may have had both directional and non-directional photoreceptors (Arendt and Wittbrodt, 2001). The bilateral arrangement of these non-directional photoreceptors would have been the result of developmental constrains associated with the bilateral symmetry, or maybe profitable for increasing the robustness and sensitivity of the photoreceptor system.

To better understand when a possible switch occurred (i.e., whether Go-opsins originally mediated a non-directional task in the dipleurula larvae of the Ambulacraria stem group, or if an association with screening pigments was lost secondarily in the Echinodermata crown group) a further comparison of the photoreceptor systems of different dipleurula-type larvae is required.

The fact that the two bilateral photoreceptors connected to the apical organ of the pluteus larva use a Go-opsin, while r-opsins are present in similar structures of nearly all other larvae, results remarkable. One possible explanation to why putative homologous paired photoreceptors express distinct opsins in different Bilateria clades could be that Urbilateria had bilaterally paired photoreceptors with r-opsin, c-opsins and Go-opsins serving different functions (Feuda et al., 2012; Ramirez et al., 2016). This variety of functions can be ascribed to the need of different spectral or temporal properties, as well as to different roles in the transducing the light signal. Losses would then account for the fact that echinoid larvae seem to have only a Go-opsin, most other protostomes only a r-opsin, and vertebrates c- and r-opsins. Cell duplication and subsequent specialization must also be assumed for vertebrates.

Putative Role of Go-Opsin Positive Cells in Sea Urchin Larvae

The most plausible role of the Go photoreceptors described in this study is the regulation of vertical movement of the larva during photoperiodic transitions (Jékely et al., 2008; Mason and Cohen, 2012). Such a unimodal system could resemble the earliest photoreceptor mechanism in the first marine larvae. If this is the case, study of this system could provide clues as how the first planktonic animals perceived light cues. It remains possible that other opsins are present at the same larval stage that have not been identified.

Because the main locomotory organ of the pluteus is the ciliary band, it would be informative to know whether the *Sp-Opsin3.2* positive cells are connected to the ciliary band via the nervous system, which has been described as "a network of cells that span the blastocoel and connect nearly all parts of the larva" (Ryberg and Lundgren, 1977). Previous studies of the nervous system of the pluteus of *Strongylocentrotus droebrachiensis* (Burke, 1978), a closely related species, report the presence of serotonergic neurons in the area of the apical organ, located between the cells homologous to the Go-opsin expressing cells of *S. purpuratus*. This serotonergic system is suggested to be involved in the regulation of the ciliary band activity in the pluteus (Gustafson et al., 1972; Burke, 1978; Yaguchi and Katow, 2003) and also in many other marine larvae (*e.g.*, Mackie et al., 1969; Beiras and Widdows, 1995; Pires and Woollacott, 1997; Kuang and Goldberg, 2001). The topology of the *SpOpsin3.2* expressing cells in the proximity of serotonergic neurons lead us to hypothesize that Go expressing cells may be involved in locomotory control, probably in the activation or excitation of the ciliary band to position the animal in the upper photic zone. Knockout experiments of this opsin coupled with behavioral experiments could be used to test this hypothesis.

METHODS

Strongylocentrotus purpuratus, Adult Care and Larval Culture

Adult *S. purpuratus* were obtained from San Diego Bay at 25–30 m in depth (San Diego, CA, USA) and housed in 12°C circulating seawater aquaria at the Stazione Zoologica Anton Dohrn, Italy. Spawning was induced by intracoelomic injection of 0.5M KCl. Embryos/larvae were cultured in Mediterranean filtered seawater (mesh pore size: 0.2 mm) diluted in de-ionized water (final salinity: 32.5‰) and kept at 15°C on a 12/12 h light/dark cycle. From 3 days onwards, larvae were fed with a mixed diet of *Isochrysis galbana* [∼2,000 cells mL^{-1}] and *Rhodomonas sp.* [∼2,000 cells mL^{-1}]. All larval cultures were maintained at a decreasing with age concentration from 5 to 1

pluteus mL^{-1}, mixed by gentle rotary stirring and washed every other day. Larval washes were made by inverted filtration (mesh size: 100 μM).

Gene Cloning and RNA Probe Preparation

Contig sequence for *Sp-opsin3.2* was identified in the genome (ref. code: SPU027633) and transcriptome (ref. code: WHL22.338995) data sets. A 1,175 bp transcript was amplified by PCR with the cloning primers *Sp-opsin3.2*-F (5′-CCACTCATTTCGTGCGGATT-3′) and *Sp-opsin3.2*-R (5′-CTCTAGTGATGACGGGCGAT-3′) from cDNA prepared with a Bio-Rad iScript synthesis kit, ligated into pGEMT-easy vector (Promega), and transformed into Top10 chemically competent *E. coli* (Invitrogen). Clone fragments were verified by Sanger sequencing prior to riboprobe generation. DIG-labeled antisense and sense (negative control) RNA probes were generated from plasmid DNA with T7- and SP6-RNA polymerases (Roche) respectively, and purify with mini Quick Spim Columns (Roche).

Fluorescent *In situ* Hybridization Coupled with Immunohistochemistry

Strongylocentrotus purpuratus larvae were collected at early pluteus stage (3dpf), fixed overnight at 4°C in 4% paraformaldehyde/0.1M MOPS pH 7, 0.5M NaCl, washed thoroughly in MOPS buffer, and stored in 70% ethanol until use. Whole mount fluorescent *in situ* hybridization (FISH) was performed as described in Andrikou et al. (2013). Immunohistochemistry coupled to WMISH was performed by incubating the larvae with anti-acetylated α-tubulin antibody (Sigma-Aldrich T6793, St Louis, MO, USA) in a dilution 1:250 together with the anti-DIG antibody; the secondary antibody was a goat anti-mouse IgG-Alexa 488 (Invitrogen, CA, USA) diluted 1: 1000.

Chromogenic *In situ* Hybridization

Four-armed *S. purpuratus* larvae were fixed at 4dpf as explained above. Single probe chromogenic in situ hybridization on whole mount fixed embryos was performed as previously described by Ransick (2004) with the following changes: (i) all washes were carried out in TBST (0.2M Tris pH 7.5, 0.15M NaCl, 0.1% Tween-20); (ii) hybridization was performed over-night at 60°C; (iii) 1X SSC and 0.1X SSC washes were performed at 60°C; (iv) Anti-Digoxigenin-AP, Fab fragments (Roche) were diluted 1: 2000.

Immunohistochemistry

Larvae were fixed in 4% paraformaldehyde in PBS pH 7.4 containing 0.5M NaCl for 30 min at room temperature. Late 6 and 8 armed larvae (days 14–23) were post-treated 2 min with pure cold MetOH in order to partially remove membrane lipids and facilitate antibody penetration. After five 5 min rinses in phosphate buffered saline (PBS), samples were washed thoroughly in PBS/0.1% Tween-20 (PBST). Following incubations were carried out on an orbital shaker. The first blocking step was performed with 4% heat-inactivated Normal Goat Serum (NGS) in PBST for 1 h, prior to incubating specimens with primary antibodies anti-Sp-opsin4 1:50 [1.21 mg mL^{-1}] (Ullrich-Lüter et al., 2011), anti-1E11 1:100 [∼10.00 mg mL^{-1}] (monoclonal antibody that recognize S. purpuratus synaptotagmin B and is used as "pan-neural" marker; Nakajima et al., 2004), and anti-acetylated α-tubulin (Sigma T6793) 1:250—in PBST overnight at 4°C. After five washes in PBST, a second blocking step was performed as described above prior to incubating specimens with secondary antibodies—goat anti-rabbit IgG-Alexa 488 and goat anti-mouse IgG-Alexa 647—diluted 1: 1,000 in blocking buffer (4% NGS in PBST) at 4°C overnight. All specimens were washed thoroughly in PBS and then counterstained with DAPI (1 μg/mL in PBS) for nuclear labeling. For Sp-opsin4 antibodies, controls were carried out using their respective rabbit pre-immune sera. For commercial antibodies, control experiments were run in parallel by omitting primary antibodies.

Transmission Electron Microscopy

Strongylocentrotus purpuratus plutei were first fixed in modified Karnovsky solution (2.5% glutaraldehyde, 2% paraformaldehyde, and 3% sucrose in 0.1 M phosphate buffer pH 7.4 containing 0.5M NaCl) for 1 h at room temperature. After several rinses in PBS, samples were post fixed in 1% osmium tetraoxide in distilled water 1 h at 7°C, and dehydrated in a series of ethanol (30/50/70/96/100) and infiltrated and embedded in EPON (Agar 100). Samples were kept at 60°C for 48 h to allow polymerization. Thin sections (50–70 nm) were cut with a diamond knife with a Leica EM UC7 ultramicrotome and mounted on pioloform coated copper grids.

Imaging

Light microscopic images were taken using a Zeiss M1 Axio Imager microscope. Confocal acquisition was performed on a Zeiss LSM 510 Meta confocal microscope. TEM acquisitions were performed on a 120 kV JEOL 1400 plus microscope with a bottom mounted CMOS camera. Figure plates were made with Illustrator CS6 (Adobe). Brightness/contrast and color balance adjustments were always applied to the whole image and not to parts.

AUTHOR CONTRIBUTIONS

AVG and MIA conceptualized and designed the study. AVG grew the larvae, did the fluorescence *in situ* hybridization of *Sp-opsin3.2* coupled with immunohistochemistry, performed the immunohistochemistry assays of Sp-opsin4, supervised the transmission electron microscopy assays done with the assistance of the EM personnel from the Microscopy Facility (Department of Biology, Lund University), and wrote the manuscript with the assistance of DN, MIA, and PO. LP did the molecular cloning and chromogenic *in situ* hybridization of *Sp-opsin3.2*. All authors approved the final text.

FUNDING

AVG is supported by the Marie Curie ITN "Neptune" (grant number: 317172, FP7 PEOPLE Work Programme of the

European Commission, PI: MIA). LP was supported by HFSP research grant RGY0082/2010 to PO.

ACKNOWLEDGMENTS

We are grateful to Santiago Valero-Medranda (Spain) for the scientific illustrations presented all over the article. The authors would also thank John Kirwan and Emily Baird (Lund University, Sweden) for critical reading and commenting the manuscript. We acknowledge Ola Gustafsson and Carina Rasmussen, from the Microscopy Facility at the Department of Biology (Lund University, Sweden) for their help in preparing and processing the electron microscopy samples, Patrick Leahy (Kerchoff Marine Station, Caltech, Corona del Mar, CA, USA) for collecting *S. purpuratus* adults, and Davide Caramiello (Stazione Zoologica Anton Dohrn, Italy) for caring of adult urchins and culturing of microalgae.

SUPPLEMENTARY MATERIAL

The Supplementary Material for this article can be found online at: http://journal.frontiersin.org/article/10.3389/fevo.2016.00127/full#supplementary-material

Supplementary Figure 1 | Graph of the quantitative transcriptome data for *Sp-opsin 3.2* and *Sp-opsin 2* (http://www.echinobase.org:3838/quantdev/).

REFERENCES

Aizenberg, J., Tkachenko, A., Weiner, S., Addadi, L., and Hendler, G. (2001). Calcitic microlenses as part of the photoreceptor system in brittlestars. *Nature* 412, 819–822. doi: 10.1038/35090573

Andrikou, C., Iovene, E., Rizzo, F., Oliveri, P., and Arnone, M. I. (2013). Myogenesis in the sea urchin embryo: the molecular fingerprint of the myoblast precursors. *EvoDevo* 4:33. doi: 10.1186/2041-9139-4-33

Arendt, D. (2008). The evolution of cell types in animals: emerging principles from molecular studies. *Nat. Rev. Genet.* 9, 868–882. doi: 10.1038/nrg2416

Arendt, D., Tessmar-Raible, K., Snyman, H., Dorresteijn, A. W., and Wittbrodt, J. (2004). Ciliary photoreceptors with a vertebrate-type opsin in an invertebrate brain. *Science* 306, 869–871. doi: 10.1126/science.1099955

Arendt, D., and Wittbrodt, J. (2001). Reconstructing the eyes of Urbilateria. *Philos. Trans. R. Soc. B Biol. Sci.* 356, 1545–1563. doi: 10.1098/rstb.2001.0971

Beiras, R., and Widdows, J. (1995). Effect of the neurotransmitters dopamine, serotonin and norepinephrine on the ciliary activity of mussel (*Mytilus edulis*) larvae. *Mar. Biol.* 122, 597–603. doi: 10.1007/BF00350681

Bennett, M. F. (1979). "Extraocular Light Receptors and Circadian Rhythms," in *Comparative Physiology and Evolution of Vision in Invertebrates Handbook of Sensory Physiology*. (Berlin, Heidelberg: Springer Berlin Heidelberg), 641–663.

Blevins, E., and Johnsen, S. (2004). Spatial vision in the echinoid genus *Echinometra*. *J. Exp. Biol.* 207, 4249–4253. doi: 10.1242/jeb.01286

Brandenburger, J. L., Woolacott, R. M., and Eakin, R. M. (1973). Fine structure of eyespots in tornarian larvae (Phylum: *Hemichordata*). *Z. Zellforsch. Mikrosk. Anat.* 142, 89–102. doi: 10.1007/BF00306706

Braubach, O. R., Dickinson, A. J. G., Evans, C. C. E., and Croll, R. P. (2006). Neural control of the velum in larvae of the gastropod, *Ilyanassa obsoleta*. *J. Exp. Biol.* 209, 4676–4689. doi: 10.1242/jeb.02556

Braun, K., Kaul-Strehlow, S., Ullrich-Lüter, E., and Stach, T. (2015). Structure and ultrastructure of eyes of tornaria larvae of *Glossobalanus marginatus*. *Organ. Divers. Evol.* 15, 423–428. doi: 10.1007/s13127-015-0206-x

Burke, R. D. (1978). Structure of nervous-system of pluteus larva of *Strongylocentrotus-Purpuratus*. *Cell Tissue Res.* 191, 233–247. doi: 10.1007/BF00222422

Burke, R. D., Angerer, L. M., Elphick, M. R., Humphrey, G. W., Yaguchi, S., Kiyama, T., et al. (2006). A genomic view of the sea urchin nervous system. *Dev. Biol.* 300, 434–460. doi: 10.1016/j.ydbio.2006.08.007

Byrne, M., Nakajima, Y., Chee, F. C., and Burke, R. D. (2007). Apical organs in echinoderm larvae: insights into larval evolution in the *Ambulacraria*. *Evol. Dev.* 9, 432–445. doi: 10.1111/j.1525-142X.2007.00189.x

Coppard, S. E., Kroh, A., and Smith, A. B. (2010). The evolution of pedicellariae in echinoids: an arms race against pests and parasites. *Acta Zool.* 93, 125–148. doi: 10.1111/j.1463-6395.2010.00487.x

D'Aniello, S., Delroisse, J., Valero-Gracia, A., Lowe, E. K., Byrne, M., Cannon, J. T., et al. (2015). Opsin evolution in the *Ambulacraria*. *Mar. Genomics* 24(Pt 2), 177–183. doi: 10.1016/j.margen.2015.10.001

Feuda, R., Hamilton, S. C., McInerney, J. O., and Pisani, D. (2012). Metazoan opsin evolution reveals a simple route to animal vision. *Proc. Natl. Acad. Sci. U.S.A.* 109, 18868–18872. doi: 10.1073/pnas.1204609109

Gühmann, M., Jia, H., Randel, N., Verasztó, C., Bezares-Calderón, L. A., Michiels, N. K., et al. (2015). Spectral tuning of phototaxis by a Go-opsin in the rhabdomeric eyes of platynereis. *Curr. Biol.* 25, 2265–2271. doi: 10.1016/j.cub.2015.07.017

Gustafson, T., Lundgren, B., and Treufeldt, R. (1972). Serotonin and contractile activity in the echinopluteus. A study of the cellular basis of larval behaviour. *Exp. Cell Res.* 72, 115–139. doi: 10.1016/0014-4827(72)90573-3

Hendler, G., and Byrne, M. (1987). Fine structure of the dorsal arm plate of *Ophiocoma wendti*: evidence for a photoreceptor system (*Echinodermata*, *Ophiuroidea*). *Zoomorphology* 107, 261–272. doi: 10.1007/BF00312172

Heyland, A., and Hodin, J. (2014). A detailed staging scheme for late larval development in *Strongylocentrotus purpuratus* focused on readily-visible juvenile structures within the rudiment. *BMC Dev. Biol.* 14:22. doi: 10.1186/1471-213X-14-22

Ho, E. C., Buckley, K. M., Schrankel, C. S., Schuh, N. W., Hibino, T., Solek, C. M., et al. (2016). Perturbation of gut bacteria induces a coordinated cellular immune response in the purple sea urchin larva. *Immunol. Cell Biol.* 94, 861–874. doi: 10.1038/icb.2016.51

Holmes, S. J. (1912). Phototaxis in the sea urchin *Arbacia punctulata*. *J. Anim. Behav.* 2, 126–136. doi: 10.1037/h0076037

Jägersten, G. (1972). Evolution of the Metazoan life cycle. *BMC Evol. Biol.* 13:171.

Jékely, G. (2009). Evolution of phototaxis. *Philos. Trans. R. Soc. B Biol. Sci.* 364, 2795–2808. doi: 10.1098/rstb.2009.0072

Jékely, G., Colombelli, J., Hausen, H., Guy, K., Stelzer, E., Nédélec, F., et al. (2008). Mechanism of phototaxis in marine zooplankton. *Nature* 456, 395–399. doi: 10.1038/nature07590

Johnsen, S. (1994). Extraocular sensitivity to polarized light in an echinoderm. *J. Exp. Biol.* 195, 281–291.

Johnsen, S. (1997). Identification and localization of a possible rhodopsin in the echinoderms *Asterias forbesi* (*Asteroidea*) and *Ophioderma brevispinum* (*Ophiuroidea*). *Biol. Bull.* 193, 97–105. doi: 10.2307/1542739

Johnsen, S., and Kier, W. M. (1999). Shade-seeking behaviour under polarized light by the brittlestar *Ophioderma Brevispinum* (*Echinodermata: Ophiuroidea*). *J. Mar. Biol. Assoc.* 79, 761–763. doi: 10.1017/S0025315498000940

Kojima, D., Terakita, A., Ishikawa, T., Tsukahara, Y., Maeda, A., and Shichida, Y. (1997). A novel Go-mediated phototransduction cascade in scallop visual cells. *J. Biol. Chem.* 272, 22979–22982. doi: 10.1074/jbc.272.37.22979

Koyanagi, M., Takano, K., Tsukamoto, H., Ohtsu, K., Tokunaga, F., and Terakita, A. (2008). Jellyfish vision starts with cAMP signaling mediated by opsin-G(s) cascade. *Proc. Natl. Acad. Sci. U.S.A.* 105, 15576–15580. doi: 10.1073/pnas.0806215105

Koyanagi, M., Terakita, A., Kubokawa, K., and Shichida, Y. (2002). Amphioxus homologs of Go-coupled rhodopsin and peropsin having 11-cis- and all-trans-retinals as their chromophores. *FEBS Lett.* 531, 525–528. doi: 10.1016/S0014-5793(02)03616-5

Kuang, S. H., and Goldberg, J. I. (2001). Laser ablation reveals regulation of ciliary activity by serotonergic neurons in molluscan embryos. *J. Neurobiol.* 47, 1–15. doi: 10.1002/neu.1011

Lacalli, T. C., Gilmour, T., and West, J. E. (1990). Ciliary band innervation in the bipinnaria larva of *Piaster ochraceus*. *Philos. Trans. R. Soc. B Biol. Sci.* 371–390. doi: 10.1098/rstb.1990.0206

Leech, D. M., Padeletti, A., and Williamson, C. E. (2005). Zooplankton behavioral responses to solar UV radiation vary within and among lakes. *J. Plankton Res.* 27, 461–471. doi: 10.1093/plankt/fbi020

Leys, S. P., and Degnan, B. M. (2001). Cytological basis of photoresponsive behavior in a sponge larva. *Biol. Bull.* 201, 323–338. doi: 10.2307/1543611

Mackie, G. O., Spencer, A. N., and Strathmann, R. (1969). Electrical activity associated with ciliary reversal in an echinoderm larva. *Nature* 223, 1384–1385. doi: 10.1038/2231384a0

Maldonado, M., Durfort, M., McCarthy, D. A., and Young, C. M. (2003). The cellular basis of photobehavior in the tufted parenchymella larva of demosponges. *Mar. Biol.* 143, 427–441. doi: 10.1007/s00227-003-1100-1

Mano, H., and Fukada, Y. (2007). A median third eye: pineal gland retraces evolution of vertebrate photoreceptive organs. *Photochem. Photobiol.* 83, 11–18. doi: 10.1562/2006-02-24-IR-813

Marlow, H., Tosches, M. A., Tomer, R., Steinmetz, P. R., Lauri, A., Larsson, T., et al. (2014). Larval body patterning and apical organs are conserved in animal *Evolution* 12, 1–17. doi: 10.1186/1741-7007-12-7

Marsden, J. R. (1984). Swimming in response to light by larvae of the tropical serpulid *Spirobranchus giganteus*. *Mar. Biol.* 83, 13–16. doi: 10.1007/BF00393081

Marshall, D. J., and Hodgson, A. N. (1990). Structure of the cephalic tentacles of some species of prosobranch limpet (Patellidae and Fissurellidae). *J. Molluscan Stud.* 56, 415–424. doi: 10.1093/mollus/56.3.415

Mason, B. M., and Cohen, J. H. (2012). Long-Wavelength photosensitivity in coral planula larvae. *Biol. Bull.* 222, 88–92. doi: 10.1086/BBLv222n2p88

Millott, N. (1953). Light emission and light perception in species of *Diadema*. *Nature* 171, 973–974.

Millott, N. (1954). Sensitivity to light and the reactions to changes in light intensity of the echinoid *Diadema antillarum* Philippi. *Philos. Trans. R. Soc. B Biol. Sci.* 238, 187–220. doi: 10.1098/rstb.1954.0009

Millott, N. (1976). The photosensitivity of Echinoids. *Adv. Mar. Biol.* 13, 1–52.

Millott, N., and Manly, B. M. (1961). The iridophores of the echinoid *Diadema antillarum*. *J. Cell Sci.* s3–102, 181–194.

Millot, N., and Yoshida, M. (1958). The Photosensitivity of the sea echinoid *Diadema antillarum* Phillipi: responses to increases in light intensity. *Proc. Zool. Soc. Lond.* 133, 67–71.

Nakajima, Y., Kaneko, H., Murray, G., and Burke, R. D. (2004). Divergent patterns of neural development in larval echinoids and asteroids. *Evol. Dev.* 6, 95–104. doi: 10.1111/j.1525-142X.2004.04011.x

Nielsen, C. (2008). Six major steps in animal evolution: are we derived sponge larvae? *Evol. Dev.* 10, 241–257. doi: 10.1111/j.1525-142X.2008.00231.x

Nilsson, D. E. (1996). Eye ancestry: old genes for new eyes. *Curr. Biol.* 6, 39–42. doi: 10.1016/S0960-9822(02)00417-7

Nilsson, D. E. (2009). The evolution of eyes and visually guided behaviour. *Philos. Trans. R. Soc. B Biol. Sci.* 364, 2833–2847. doi: 10.1098/rstb.2009.0083

Nilsson, D. E. (2013). Eye evolution and its functional basis. *Vis. Neurosci.* 30, 5–20. doi: 10.1017/S0952523813000035

Nordström, K., Wallén, R., Seymour, J., and Nilsson, D. (2003). A simple visual system without neurons in jellyfish larvae. *Proc. R. Soc. B Biol. Sci.* 270, 2349–2354. doi: 10.1098/rspb.2003.2504

Passamaneck, Y. J. (2011). Ciliary photoreceptors in the cerebral eyes of a protostome larva. *Evodevo* 2:6. doi: 10.1186/2041-9139-2-6

Passamaneck, Y. J., and Martindale, M. Q. (2013). Evidence for a phototransduction cascade in an early brachiopod embryo. *Integr. Comp. Biol.* 53, 17–26. doi: 10.1093/icb/ict037

Paul, N. D., and Gwynn-Jones, D. (2003). Ecological roles of solar UV radiation: towards an integrated approach. *Trends Ecol. Evol.* 18, 48–55. doi: 10.1016/S0169-5347(02)00014-9

Pires, A., and Woollacott, R. M. (1997). Serotonin and dopamine have opposite effects on phototaxis in larvae of the bryozoan *Bugula neritina*. *Biol. Bull.* 192, 399–409. doi: 10.2307/1542749

Plachetzki, D. C., Degnan, B. M., and Oakley, T. H. (2007). The origins of novel protein interactions during animal opsin evolution. *PLoS ONE* 2:e1054. doi: 10.1371/journal.pone.0001054

Porter, M. L., Blasic, J. R., Bok, M. J., Cameron, E. G., Pringle, T., Cronin, T. W., et al. (2011). Shedding new light on opsin evolution. *Proc. R. Soc. B Biol. Sci.* 279, 3–14. doi: 10.1098/rspb.2011.1819

Provencio, I., Jiang, G., De Grip, W. J., Hayes, W. P., and Rollag, M. D. (1998). Melanopsin: An opsin in melanophores, brain, and eye. *Proc. Natl. Acad. Sci. U.S.A.* 95, 340–345. doi: 10.1073/pnas.95.1.340

Raible, F., Tessmar-Raible, K., Arboleda, E., Kaller, T., Bork, P., Arendt, D., et al. (2006). Opsins and clusters of sensory G-protein-coupled receptors in the sea urchin genome. *Dev. Biol.* 300, 461–475. doi: 10.1016/j.ydbio.2006.08.070

Ramirez, M. D., Pairett, A. N., Pankey, M. S., Serb, J. M., Speiser, D. I., Swafford, A. J., et al. (2016). The last common ancestor of bilaterian animals possessed at least 7 opsins. *bioRxiv* 052902. doi: 10.1101/052902

Ransick, A. (2004). Detection of mRNA by in situ hybridization and RT-PCR. *Methods Cell Biol.* 74, 601–620. doi: 10.1016/S0091-679X(04)74024-8

Raup, D. M. (1966). "The endoskeleton," in *Physiology of Echinodermata*, ed R. A. Boolootian (New York, NY: Interscience), 379–395.

Ryberg, E., and Lundgren, B. O. (1977). Extra-ectodermal strands in the ciliated bands of the echinopluteus. *Dev. Growth Differ.* 19, 299–308. doi: 10.1111/j.1440-169X.1977.00299.x

Schmidt, T. M., Chen, S.-K., and Hattar, S. (2011). Intrinsically photosensitive retinal ganglion cells: many subtypes, diverse functions. *Trends Neurosci.* 34, 572–580. doi: 10.1016/j.tins.2011.07.001

Smith, F. (1935). The development of *Patella vulgata*. *Philos. Trans. R. Soc. B Biol. Sci.* 225, 95–125. doi: 10.1098/rstb.1935.0008

Smith, M. M., Cruz Smith, L., Cameron, R. A., and Urry, L. A. (2008). The larval stages of the sea urchin, *Strongylocentrotus purpuratus*. *J. Morphol.* 269, 713–733. doi: 10.1002/jmor.10618

Sodergren, E., Weinstock, G. M., Davidson, E. H., Cameron, R. A., Gibbs, R. A., Angerer, R. C., et al. (2006). The Genome of the Sea Urchin *Strongylocentrotus purpuratus*. *Science* 314, 941–952. doi: 10.1126/science.1133609

Thornton, I. W. B. (1956). Diurnal migrations of the echinoid *Diadema setosum* (Leske). *Br. J. Anim. Behav.* 4, 143–146. doi: 10.1016/S0950-5601(56)80108-1

Thorson, G. (1964). Light as an ecological factor in the dispersal and settlement of larvae of marine bottom invertebrates. *Ophelia.* 1, 167–208. doi: 10.1080/00785326.1964.10416277

Tosches, M. A., Bucher, D., Vopalensky, P., and Arendt, D. (2014). Melatonin signaling controls circadian swimming behavior in marine zooplankton. *Cell* 159, 46–57. doi: 10.1016/j.cell.2014.07.042

Tu, Q., Cameron, R. A., and Davidson, E. H. (2014). Quantitative developmental transcriptomes of the sea urchin *Strongylocentrotus purpuratus*. *Dev. Biol.* 385, 160–167. doi: 10.1016/j.ydbio.2013.11.019

Ullrich-Lüter, E. M., D'Aniello, S., and Arnone, M. I. (2013). C-opsin expressing photoreceptors in echinoderms. *Integr. Comp. Biol.* 53, 27–38. doi: 10.1093/icb/ict050

Ullrich-Lüter, E. M., Dupont, S., Arboleda, E., Hausen, H., and Arnone, M. I. (2011). Unique system of photoreceptors in sea urchin tube feet. *Proc. Natl. Acad. Sci. U.S.A.* 108, 8367–8372. doi: 10.1073/pnas.1018495108

Van Gelder, R. N. (2008). Non-visual photoreception: sensing light without sight. *Curr. Biol.* 18, R38–R39. doi: 10.1016/j.cub.2007.11.027

Vöcking, O., Kourtesis, I., and Hausen, H. (2015). Posterior eyespots in larval chitons have a molecular identity similar to anterior cerebral eyes in other bilaterians. *Evodevo* 6, 1. doi: 10.1186/s13227-015-0036-0

Wada, Y., Mogami, Y., and Baba, S. (1997). Modification of ciliary beating in sea urchin larvae induced by neurotransmitters: beat-plane rotation and control of frequency fluctuation. *J. Exp. Biol.* 200, 9–18.

Woodley, J. D. (1982). "Photosensitivity in *Diadema antillarum*: Does it show scototaxis?" in *The International Echinoderm Conference, Tampa Bay September 14–17, 1981*, ed J. M. Lawrence (Rotterdam: AA Balkema), 61.

Yaguchi, S., and Katow, H. (2003). Expression oftryptophan 5-hydroxylase gene during sea urchin neurogenesis and role of serotonergic nervous system in larval behavior. *J. Comp. Neurol.* 466, 219–229. doi: 10.1002/cne.10865

Yerramilli, D., and Johnsen, S. (2010). Spatial vision in the purple sea urchin *Strongylocentrotus purpuratus* (*Echinoidea*). *J. Exp. Biol.* 213, 249–255. doi: 10.1242/jeb.033159

Yoshida, M. (1966). "Photosensitivity, Chapter 18," in *Physiology of Echinodermata*, ed R. A. Boolootian (New York, NY: John Wiley), 435–464.

Yoshida, M., Takasu, N., and Tamotsu, S. (1984). "Photoreception in Echinoderms," in *Photoreception and Vision in Invertebrates*, ed M. A. Ali (Boston, MA: Springer US), 743–771.

Conflict of Interest Statement: The authors declare that the research was conducted in the absence of any commercial or financial relationships that could be construed as a potential conflict of interest.

Valero-Gracia et al. Frontiers in Zoology (2016) 13:45
DOI 10.1186/s12983-016-0177-6

Frontiers in Zoology

RESEARCH Open Access

Comparative localization of serotonin-like immunoreactive cells in Thaliacea informs tunicate phylogeny

Alberto Valero-Gracia[1†], Rita Marino[1†], Fabio Crocetta[1,2], Valeria Nittoli[1], Stefano Tiozzo[3] and Paolo Sordino[1*]

Abstract

Background: Thaliaceans is one of the understudied classes of the phylum Tunicata. In particular, their phylogenetic relationships remain an issue of debate. The overall pattern of serotonin (5-HT) distribution is an excellent biochemical trait to interpret internal relationships at order level. In the experiments reported here we compared serotonin-like immunoreactivity at different life cycle stages of two salpid, one doliolid, and one pyrosomatid species. This multi-species comparison provides new neuroanatomical data for better resolving the phylogeny of the class Thaliacea.

Results: Adults of all four examined thaliacean species exhibited serotonin-like immunoreactivity in neuronal and non-neuronal cell types, whose anatomical position with respect to the nervous system is consistently identifiable due to α-tubulin immunoreactivity. The results indicate an extensive pattern that is consistent with the presence of serotonin in cell bodies of variable morphology and position, with some variation within and among orders. Serotonin-like immunoreactivity was not found in immature forms such as blastozooids (Salpida), tadpole larvae (Doliolida) and young zooids (Pyrosomatida).

Conclusions: Comparative anatomy of serotonin-like immunoreactivity in all three thaliacean clades has not been reported previously. These results are discussed with regard to studies of serotonin-like immunoreactivity in adult ascidians. Lack of serotonin-like immunoreactivity in the endostyle of Salpida and Doliolida compared to *Pyrosomella verticillata* might be the result of secondary loss of serotonin control over ciliary beating and mucus secretion. These data, when combined with other plesiomorphic characters, support the hypothesis that Pyrosomatida is basal to these clades within Phlebobranchiata and that Salpida and Doliolida constitute sister-groups.

Keywords: Comparative neuroanatomy, Evolution, Immunohistochemistry, Thaliaceans, Tunicata, Zooplankton

Background

Thaliacea is a class of pelagic tunicates that undergo alternation of generations between the sexual blastozooid stage and the asexual oozooid stage (reviewed in [1]). This clade comprises three orders: Pyrosomatida, Salpida, and Doliolida [2]. Despite a rich literature describing the anatomical characters of thaliaceans, the phylogenetic position within orders is still disputed. Most authors proposed a nested position of Thaliacea within the class 'Ascidiacea', thus recognized as a paraphyletic group formed by the Stolidobranchiata, Aplousobranchiata and Phlebobranchiata clades [3–6]. This view suggests that the thaliaceans, with their planktonic life style, diverged from a benthic ancestor. However, there is no consensus on the relationships among Thaliacean orders. Some authors proposed that Pyrosomatida and Salpida group independently from Doliolida [7–9], while more recent works suggested that Pyrosomatida branched off first, and that Salpida and Doliolida are sister groups [10–12]. To date, molecular phylogenetic analyses based on ribosomal markers have been hindered by long-branch attraction [6]. Analyses based on morphological characters have not overcome such error, mainly because of the lack of a more

* Correspondence: paolo.sordino@szn.it
†Equal contributors
[1]Biology and Evolution of Marine Organisms, Stazione Zoologica Anton Dohrn, Villa Comunale, 80121 Naples, Italy
Full list of author information is available at the end of the article

comprehensive taxon sampling, particularly covering all three thaliacean orders [11, 12].

When molecular and morphological phylogenies conflict, neuroarchitectural traits offer a wealth of hitherto largely-unexploited characters which can make valuable contributions to phylogenetic inference even among distantly related groups (e.g., tardigrades, onychophorans, kinorhynchs and priapulids) [13–17]. However, when adopting neural characters, extensive sampling of crown-group representatives is required to assess the origin of evolutionary traits. In thaliaceans, comparative anatomy is particularly problematic due to the complexity of their life cycles and the difficulty of comparing homologous structures. As a consequence, it is essential to sample taxa across all orders.

To better understand thaliacean phylogenetic relationships, we analysed the distribution of serotonin-like immunoreactivity in specimens from the three orders and at different stages of their life cycle. Monoamine serotonin is an ancient and conserved neurotransmitter found throughout Opisthokonta [18]. Serotonin can trigger several physiological functions that range from regulation of ciliary band activity [19], to feeding circadian patterns [20], and influencing emotional state [21]. In addition to neurotransmitter functions, serotonin has also non-neurogenic roles. For instance, it affects cardiac morphogenesis and neural crest cell migration during early mammalian and chicken embryonic development [22–24], modulates gastrulation in echinoderms and insects [25–27], and plays a role in the determination of left-right asymmetry in amphibians and birds [28, 29]. Cellular distribution of serotonin is a reliable biochemical trait to infer phylogenetic hypotheses due to the ancestral nature of this amine, its diffuse role in nervous transmission, and its metabolic and developmental functions [13, 17, 30, 31]. Moreover, the precise classification and description of serotonin-like immunoreactive cells is needed to improve taxonomic comparability [31]. Serotonin-like immunoreactivity in thaliaceans has been described in oozooids of *Doliolum nationalis* (Borgert, 1893) (Doliolida) and *Thalia democratica* (Forsskål in Niebuhr, 1775) (Salpida) [32–34]. Immunoreactivity to serotonin was observed in both species in different organs such as cerebral ganglion, intestine, pericoronal bands, and in a structure termed the 'placenta', a single layer of flattened follicle cells that covers the embryo during development [9, 35]. Recently, Braun and Stach classified serotonin-like immunoreactive cells of Ascidiacea, Appendicularia and Thaliacea in three types: one neuronal and two non-neuronal, spherical and elongated respectively. Each of these cell types has a conserved tissue type-specific distribution [34]. However, cell lineage studies are needed to elucidate the origin of serotonin-like immunoreactive cells.

To understand the evolution of the serotonergic system in Thaliacea, three additional species were examined at different successive life cycle stages, including a member of the order Pyrosomatida. Immunohistochemistry against acetylated and tyrosinated α-tubulins was combined with nuclear staining in order to provide overall anatomical landmarks of the nervous system and an antibody against 5HT serotonin was used to describe the distribution of serotonin-like immunoreactive cells. Our study provides a more complete description of thaliacean serotonergic nervous system, with the aim of better understanding the course of neurotransmitter system evolution in this group of invertebrate chordates.

Results

Organization of the serotonergic nervous system in the pyrosomatid *Pyrosomella verticillata* (Péron, 1804)

Pyrosomes form tubular colonies consisting of barrel-shaped individual animals (oozooid) that bud off near the posterior closed end of the colony [36]. The nervous system of the pyrosomatid oozooid is an ovoid mass which comprises two regions with contrasting development and function, the neural gland connected to the ciliated funnel, and a voluminous cerebral ganglion [37]. Mature zooids of the tetrazooid colony showed serotonin-like immunoreactivity in neuronal cells of the cerebral ganglion and in the visceral nerve (medial posterior nerve, mpn) running antero-posteriorly and encircling the cerebral ganglion (Fig. 1a–e). The peribranchial tube exhibits two lateral tufts of α-tubulin-positive cilia crossed by the serotonin-like immunoreactive mpn fibres (Fig. 1f). Serotonin-like immunoreactivity was also detected in spherical cell bodies on the pericoronal bands around the oral siphon (Fig. 1c), in two bilaterally symmetrical antero-posterior rows within the endostyle (Fig. 1g), and in a single row in a structure identified as the pyloric gland (Fig. 1h). Early forming and young primary blastozooids growing in the *P. verticillata* tetrazooid colony exhibited axons labelled with the anti-α-tubulin antibody, but no serotonin-like immunosignals were observed (data not shown).

Organization of serotonergic nervous system in the salpids *Thalia democratica* and *Ihlea punctata* (Forsskål in Niebuhr, 1775)

Thalia democratica

A thorough description of the structure of *T. democratica* cerebral ganglion has been provided by Lacalli and Holland [38]. Serotonin-like immunoreactive neurons were found in the posterior half of the cerebral ganglion (Fig. 2a, b, c). A central cluster of serotonin-like immunopositive perikarya was localized near the posterior margin of the neuropil (Fig. 2b). In addition, the cerebral ganglion of *T. democratica* exhibited two paired

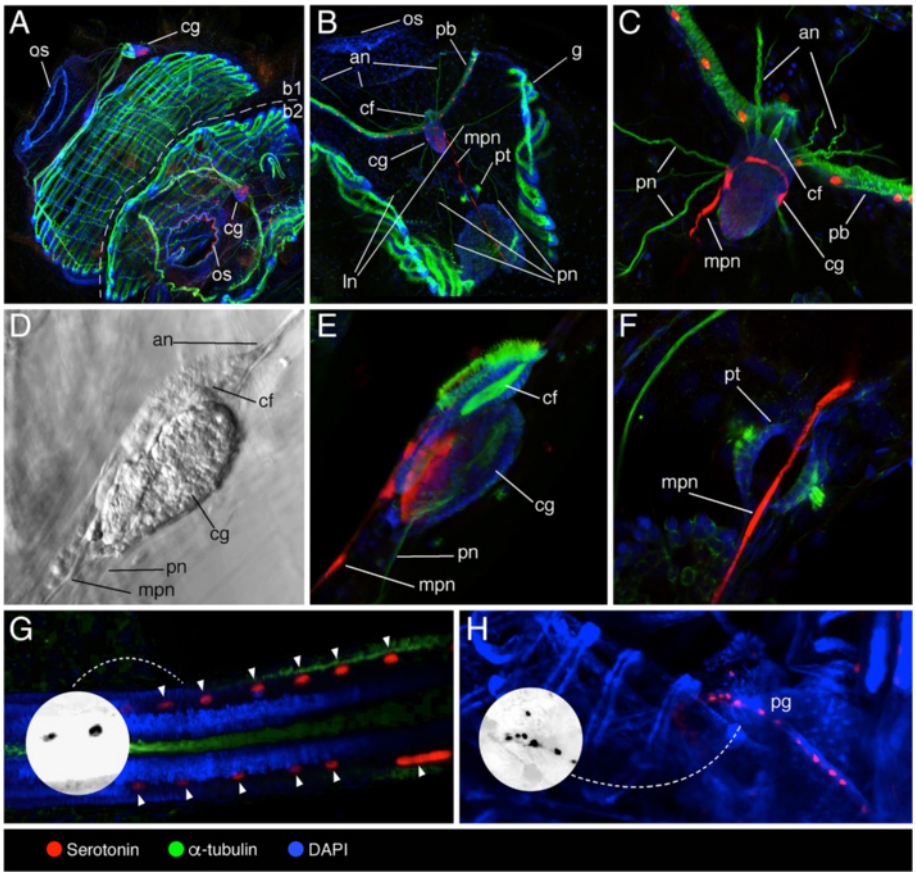

Fig. 1 Localization of serotonin-like immunoreactivity, acetylated α-tubulin, and DAPI in *Pyrosomella verticillata* tetrazooid colony. **a** Adult blastozooids (b1 and b2), overview. Oral siphons (os) and cerebral ganglia (cg) highlighted. **b** Mature blastozooid highlighting oral siphon (os), pericoronal bands (pb), ciliated funnel (cf), gills (g), peribranchial tube (pt) and with motor nerves (anterior (an), lateral (ln), posterior (pn) and medial posterior (mpn) nerves) extending from the cerebral ganglion (cg). **c** Detail of the ciliated funnel (cf) and cerebral ganglion (cg) in dorsal view. **d**, **e** Light (**d**) and confocal (**e**) magnification of the cerebral ganglion (cg) (lateral view) in connection with the ciliated funnel (cf). **f** Detail of mpn crossing a peribranchial tube (pt). **g** Detail of the endostyle (serotonin-like immunopositive cells marked with arrowheads), with grayscale invert editing to highlight serotonin-like immunoreactive cell shape (inset). **h** Detail of the posterior part of one adult zooid, highlighting the pyloric gland (pg), with grayscale invert editing to highlight serotonin-like immunoreactive cell shape (inset)

clusters of serotonin-like immunoreactive neurons laterally (Fig. 2b). Depth color-code analysis of serotonin-like immunoreactivity suggests that a loose bundle of nervous fibres extends ventrally through the neuropil from the central core (Additional file 1). Nervous fibres projecting from the ventral margin of the cerebral ganglion were found to adjoin anteriorly to the optic bundles of the eye (Fig. 2c). Double labelling for serotonin and acetylated α-tubulin suggested that some of the lateral serotonin-like immunoreactive neurons extend fibres as would be expected in case of motor neurons (Fig. 2c). As reported by Pennati et al. [33], serotonin-like immunoreactivity was detected on the pericoronal bands (Fig. 3a), in the digestive system (oesophagus and intestine) (Fig. 2d, e) and on the posterior end of the branchial septum (Fig. 2d). In the first organ, immunoreactive cell bodies have an elongated morphology and are organized in a single row (Fig. 2a), in the second one they are both spherical and elongated and are organized in single and multiple rows (Fig. 2d, e), while in the third one serotonin-like immunoreactive cells are both spherical and elongated, and form two bilateral rows (Fig. 2d). Serotonin-like immunopositive cells were not seen in ciliated funnel (data not shown) and endostyle (Fig. 2f).

Although the anatomy of oozooids and blastozooids of *T. democratica* is similar in many respects, serotonin-like immunoreactivity was not detected in the early aggregate blastozooids derived by strobilation from a posterior stolon of the oozooid (Fig. 2g–i). In blastozooids at developmental stage II sensu Brien [39], labelling of α-tubulins highlighted neural fibres running along the pericoronal bands and in a visceral longitudinal nerve extending to the

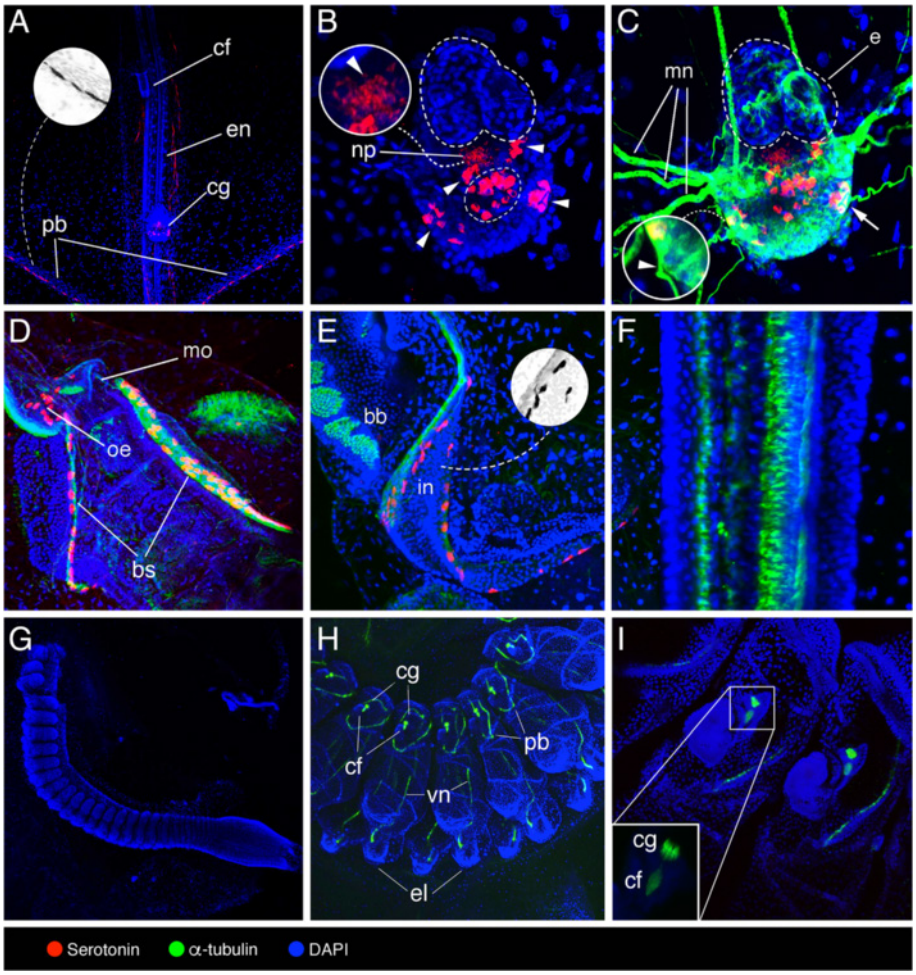

Fig. 2 Localization of serotonin-like immunoreactivity, acetylated α-tubulin, and DAPI in *Thalia democratica*. **a**–**f** Adult oozooids. **g**–**i** Aggregate blastozooids. **a** General view of the anterior region that contains the ciliated funnel (cf), endostyle (en), cerebral ganglion (cg), and pericoronal bands (pb), with grayscale invert editing to highlight serotonin-like immunoreactive cell shape in the pericoronal bands (inset). **b** Detail of the cerebral ganglion highlighting peripheral (arrowheads) and central (encircled) serotonin-like immunoreactive cells, and fibres projecting ventrally through the neuropil (arrowhead in the inset). **c** Detail of the cerebral ganglion highlighting eye (e), neuropil (np) (arrow indicates α-tubulin and serotonin co-labelled neuron), and motor nerves (mn) extending from peripheral serotonergic neurons (arrowhead indicates α-tubulin immunoreactive nerve). **d** Detail of mouth (mo), oesophagus (oe) and branchial septum (bs). **e** Magnification of intestine (in) and branchial barrier (bb), with grayscale invert editing to highlight serotonin-like immunoreactive cell shape (inset). **f** Detail of the endostyle. **g** General view of early aggregate blastozooids at developmental stage I sensu Brien [39]. **h**, **i** Details of aggregate blastozooids at developmental stage II sensu Brien [39] highlighting ciliated funnel (cf), cerebral ganglion (cg), pericoronal bands (pb), visceral nerve (vn), and eleoblast (el)

eleoblast (i.e., a specialized epithelial organ of some thaliaceans) [38] (Fig. 2g–i).

Ihlea punctata

In the *I. punctata* oozooids, serotonin-like immunopositive neurons were scattered at the ventral posterior margin of the cerebral ganglion, near the exit of axonal projections extending from it (Fig. 3a). Serotonin-like immunoreactivity was also encountered in spherical cell bodies along the pericoronal bands (Fig. 3b) and in regularly arranged rows in the oesophagus (Fig. 3c). No endostyle was observed in any of the *I. punctata* oozooids examined.

Organization of the serotonergic nervous system in the doliolid *Doliolina muelleri* (Krohn, 1852)

In comparison with salps and pyrosomes, doliolids have a long generation time and their life cycle encompasses different zooids [40]. Their typical body plan is barrel-shaped with two wide siphons and 8–9 circular muscle bands. The neural complex of Doliolida groups the cerebral ganglion (the central nervous system, composed by neurons and the neuropil), the neural gland (an ectodermal structure of unclear function), and the ciliated funnel, sometimes called "vibratile organ" [36]. The cerebral ganglion of *D. muelleri* phorozooids is localized dorsally in the middle of the body, and long nerves

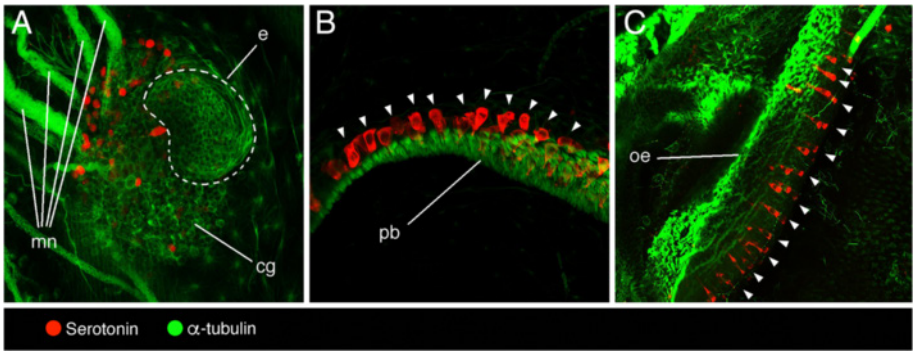

Fig. 3 Localization of serotonin-like immunoreactivity and tyrosinated α-tubulin in *Ihlea punctata* oozooids. **a** Cerebral ganglion (cg) with eye (e) and motor nerves (mn) extending from it. **b** Pericoronal bands (pb), serotonin-like immunopositive cells marked with arrowheads. **c** Oesophagus (oe), serotonin-like immunopositive cells marked with arrowheads

emerge from it elongating anteriorly and posteriorly (Fig. 4a). Two clusters of 3–4 serotonin-like immunoreactive neurons are seen laterally in the cerebral ganglion (Fig. 4b), in close proximity to neurons projecting motor nerves (Fig. 4c). A continuous row of serotonin-like immunoreactive spherical cells was seen at the junction of the pericoronal bands (Fig. 4d, e). This region has been previously described as the ciliated funnel in Doliolida [32, 41] but it is probably not homologous to the funnel that links the neural complex (neural gland) to the branchial chamber [42]. Few and sparse spherical and elongated serotonin-like immunoreactive cells were found in the initial tract of the digestive system (mouth and oesophagus) (Fig. 4f). Serotonin-like immunoreactivity was not detected in pericoronal bands and endostyle (Fig. 4g, h).

The barrel-shaped zooid growing in one side of the head of *D. muelleri* tadpole larvae gradually takes on the adult form while the larval tail degenerates (Fig. 5a–c). No serotonin-like immunoreactivity was overall detected in cell bodies or nerves from larvae and young zooids. In young zooids, α-tubulin marked major nerves that appeared to connect a fibre plexus within the neural ganglion to the entire body (Fig. 5a', b) and a bundle of fibres running through the ciliated funnel (Fig. 5c). No α-tubulin immunoreactivity was observed in tadpole larvae attached to the young zooids (Fig. 5d, d').

Discussion

Serotonin-like immunoreactivity in the nervous system, implications for brain evolution

Based on the localization of serotonin-like immunoreactive neuronal cells with descending projections through the neuropil, Hay-Schmidt [13, 43–47] suggested that an orthogonal organisation of the nervous system was likely present in the last common ancestor of chordates, an idea previously proposed by Garstang [48]. This ancestral condition should be observed also in thaliaceans due to the phylogenetic placement of this clade within 'ascidians'. We found that serotonin-like immunopositive neurons are symmetrically distributed in the cerebral ganglion of the examined Doliolida and Salpida species and that, at least in *T. democratica*, serotonin-like immunoreactive tracts project transversally through the neuropil (Additional file 1) [34]. Recent works based on the gene expression study of orthologous transcription factors during development suggests that the ascidian CNS holds molecular evidence of brain compartment homology with vertebrate fore-, mid-and hindbrain [3, 49]. In thaliaceans, it will be of great interest to compare gene expression pattern of transcription factors involved in the differentiation of the three organizing centres in the vertebrate brain: the anterior neural ridge, the zona limitans intrathalamica and the isthmic organizer (e.g. *Fgf8*, *Fgf17*, *Fgf18*, *Sfrp1/5*, *Hh*, *Wnt1*) [50]. This would help in understanding to which degree the homologous neuroectodermal signalling centers that pattern deuterostome bodies were conserved or diverged in Thaliacea. However, evidence of chordate features in ascidians does appear before metamorphosis, while thaliaceans examined in the present study are all post-metamorphic stages. This suggests that caution is needed when interpreting gene or protein expression patterns in mature forms of thaliaceans.

Based on the expression of several pituitary markers (e.g., *Pitx*, *Pax2/5/8*, *Six1/2*), the ciliated funnel of ascidians has been suggested to be homologous to the adenohypophysis, a major organ of the vertebrate endocrine system that regulates various physiological processes such as stress, growth, and reproduction (reviewed in [51]). In thaliaceans, the ciliated funnel could be responsive to the detection of olfactory information from the environment thus eliciting specific behavioural responses [33]. The evidence presented here concerning the absence of serotonin-like immunoreactive cells in the ciliated funnel of the examined specimens is in agreement with similar reports in appendicularians, 'ascidians' and

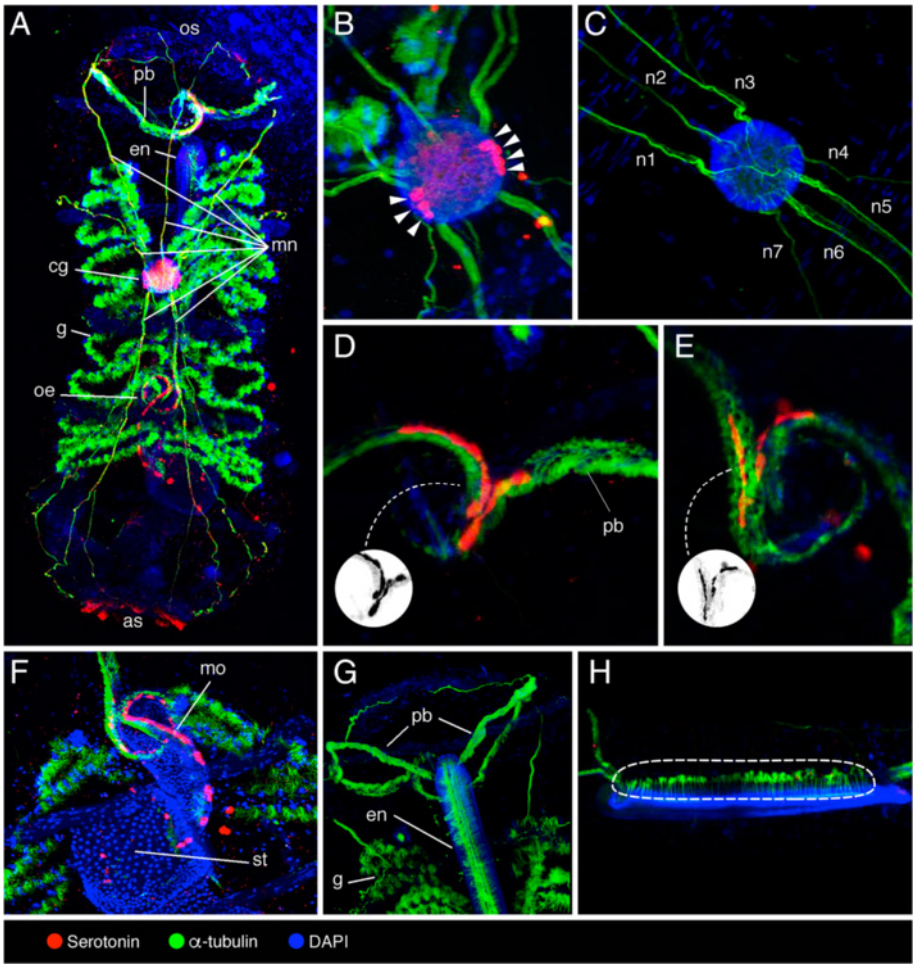

Fig. 4 Localization of serotonin-like immunoreactivity, acetylated α-tubulin, and DAPI in *Doliolina muelleri* phorozooid. **a** Dorsal view of the whole mount phorozooid, highlighting oral siphon (os), pericoronal bands (pb), endostyle (en), motor nerves (mn), cerebral ganglion (cg), gills (g), oesophagus (oe), and atrial siphon (as). **b**, **c** Cerebral ganglion with lateral clusters of serotonergic neurons (arrowheads), and motor nerves protruding from it (mn 1–7) at different magnifications. **d**, **e** Pericoronal bands (pb), with grayscale invert editing to highlight serotonin-like immunoreactive cell shape (inset). **f** Initial tract of the digestive system highlighting stomach (st) and serotonergic cells in the mouth (mo). **g** Anterior part of the specimen highlighting pericoronal bands (pb), endostyle (en), and gills (g). **h** Lateral view of the endostyle highlighting the long cilia protruding from it (encircled)

salpids [32, 34, 52–55]. While discounting the use of the serotonergic system in the ciliated funnel of tunicates, this finding suggests that the prominent role played by the local production of serotonin in the pituitary gland is an acquired feature of vertebrates.

Serotonin-like immunoreactivity in non-neural tissues

The tunicate endostyle, a structure homologous of the vertebrate thyroid, is a ventral U-shaped organ made by folds of the pharyngeal epithelium that secretes mucus for filter feeding [56]. Each mirror-image side of the tunicate endostyle displays between five and nine zones of distinctive cells, including supporting and glandular zones as well as zones with iodinating capacity [57, 58]. In stolidobranch, aplousobranch and phlebobranch ascidians, serotonergic cells were exclusively found in the lateral portion of the endostyle, between zone seven (known to have iodinating capacity), and eight (which consists of ciliated cells) [34, 54, 55, 59–61]. Based on our analysis, serotonin-like immunoreactivity in the endostyle of thaliaceans was detected only in *P. verticillata*, in a lateral zone near a band of ciliated cells, just as in ascidians. The observation that salpids and doliolids lack serotonin-like immunoreactivity in the endostyle provides support for an evolutionary scenario in which Pyrosomatida is the first group branching from the class Thaliacea [11]. However, the absence of serotonin-like immunoreactivity in the endostyle of salpids and doliolids could be a character associated with independent changes in the control of thyroid hormone production rather than an ancestral state; however, this has not yet been verified.

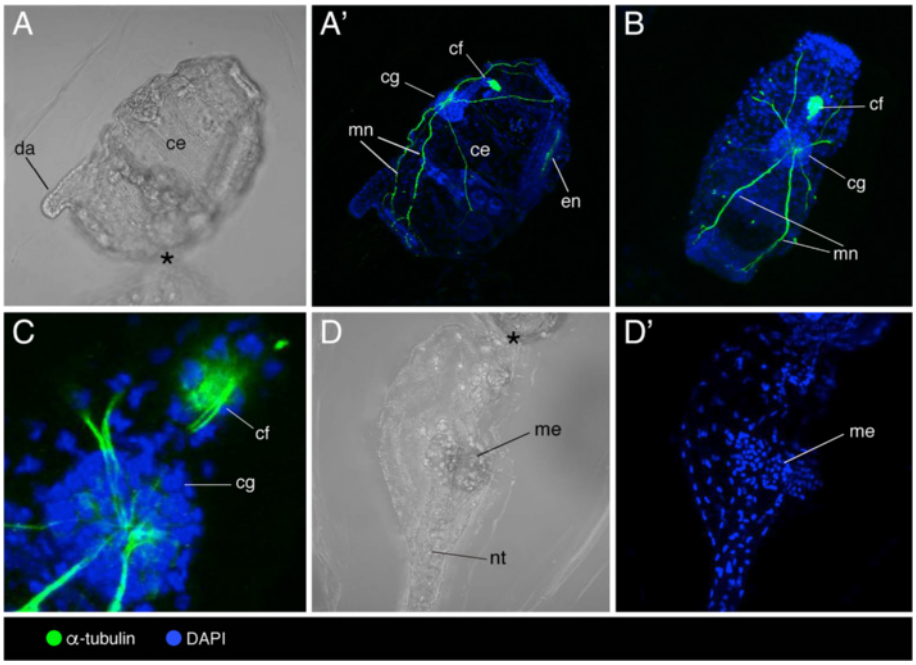

Fig. 5 Localization of acetylated α-tubulin and DAPI in tadpole larvae and young zooids of *Doliolina muelleri*. **a**–**d'** Light (**a**, **d**) and confocal (**a**', **b**, **c**, **d**') images of a single tadpole larva (**d**, **d**') connected with a young zooid (**a**, **a**', **b**, **c**) highlighting cerebral ganglion (cg), ciliated funnel (cf), dorsal appendix (da), endostyle (en), mesoblast (me), major nerves (mn) and notochord (nt); area of contact between zooid and tadpole larvae marked with asterisk (*). **b**, **c** Dorsal view of the young zooid. **d**, **d**' Detail of the tadpole larva

The peripharyngeal (pericoronal) bands of pyrosomatids, salpids and doliolids are rich in ciliated cells and could have a role in mechanoreception [62]. The presence of serotonin-like immunoreactive spherical cells in the pericoronal bands, of ascidians as are in thaliaceans suggests a phylogenetic link between these two tunicate classes [34, 54, 55, 59–61].

The post-pharyngeal digestive tract of tunicates consists of mouth, oesophagus, stomach, intestine, and anus [63, 64]. Digestive functions are also ascribed to the pyloric gland, an organ that begins at the globular gland that encrusts and opens to the intestine. The tunicate pyloric gland is composed of tubules and ampullae that grow from the outer wall of the stomach and is considered to be one of the major synapomorphies of the group [65, 66]. In ascidians, the occurrence of spherical and elongated cell bodies that are serotonin-like immunoreactive is reported in distinct tracts of the digestive system, including oesophagus, stomach and intestine [32, 34, 52, 54, 55]. In our work, serotonin-like immunoreactive cell bodies in the oesophagus of Salpida and Doliolida species, as seen in ascidians, likely reflect a plesiomorphic condition. Conversely, serotonin-like immunoreactivity in the pyloric gland of *P. verticillata* seems to be an independently derived character.

The serotonergic system is not required in immature forms

We did not detect serotonin-like immunoreactivity in *Thalia democratica* juveniles (blastozooids), in larvae and young asexual zooids of doliolid or in sexual hermaphrodite blastozooid stages of the pyrosomatid examined. The lack of expression of 5HT suggests that serotonin acquires its functionality only in mature thaliacean zooids, thus not having a role in early development. However, serotonin expression may be still present but not detectable with our methods due to low levels or poor permeabilization, prompting for transcriptional activity studies of genes belonging to the serotonin biosynthetic pathway.

Phylogenetic relationships within Thaliacea

Due to their classification as chordates, the subphylum Tunicata has been central to discussions on the evolution of deuterostomes and craniates [66–76]. Nonetheless, the internal phylogenetic relationships of the tunicate class Thaliacea remain uncertain. Thaliacea is recovered as monophyletic regardless of the number of taxa analysed, the molecular data type used, or the phylogenetic method applied, with the exception of one study which used partial 28S rDNA sequences [10]. Almost all studies agree in grouping Thaliacea as sister

group of Phlebobranchiata, one of the classical 'Ascidiacea' groups (where 'Ascidiacea' = Phlebobranchiata + Stolidobranchiata + Aplousobranchiata). We assume Phlebobranchiata as out-group for our phylogenetic comparison, due to the placement of this clade as adelphotaxon of Thaliacea in many studies [4, 7, 66, 77].

A scheme summarizing the differential spatial distribution of serotonin-like immunoreactivity among organs in Thaliacea is shown in Fig. 6.

Character comparisons suggesting that pyrosomatids originated early in the evolutionary history of thaliaceans include the presence of serotonergic cells in the endostyle and pyloric gland as in the phlebobranch *Phallusia mammillata* [54]. This condition is not present in the Salpida or Doliolida species examined, as discussed above. Since the presence of serotonin-like immunoreactivity alone cannot be considered as an uncontroverted character of phylogenetic value, we supplemented our molecular data with ten morphological and life cycle characters extracted from the literature [32]. Apomorphies such as the existence of inner longitudinal vessels in branchial basket and the presence of ontogenetic rudiment of atrial opening are common features shared just between Pyrosomatida and Phlebobranchiata [66]. The ciliated funnel is a very variable organ both with respect to its anatomy and its topology. It is associated with the cerebral ganglion in appendicularians, pyrosomatids and 'ascidians', but not in salpids nor in doliolids [37, 78–80]. Otherwise, the topology of the ciliated funnel in salpids is distinct from that of pyrosomatids and 'ascidians' in that it is not continuous to the pericoronal bands [37, 42]. Further, the presence of dorsal lamina, branchial tentacles and distinct muscle bands used in jet propulsion in Salpida and Doliolida [66] supports a sister group relationship between these two thaliacean orders. By applying a principle of parsimony, these characters (Fig. 7) seem to favour the phylogenetic hypothesis in which Pyrosomatida, an order often classified within the 'ascidians' [11, 80, 81], and not Doliolida [6], is the first branching group from Thaliacea.

Conclusion

Here we present a study of serotonergic immunoreactivity in the three thaliacean orders, and provide a first description of the pyrosomatid serotonergic system. The analysis of the distribution of serotonin-like immunopositive cells in adult thaliacean oozooids appear to depict shared characters with ascidians. Remarkably, serotonin-like immunoreactivity is not present in immature thaliacean zooids, suggesting that this amine is not crucial for the morphogenesis of the species examined. Differences in serotonin-like immunoreactive arrangement in endostyle, initial tract of the digestive system and pyloric gland, plus a review of life cycle and morphological data, prompt us to support the phylogenetic hypothesis in which Pyrosomatida is the first Thaliacean order that diverged from the Ascidiacea clade, thus positioning Salpida and Doliolida as sister groups. Data from more species and the support of

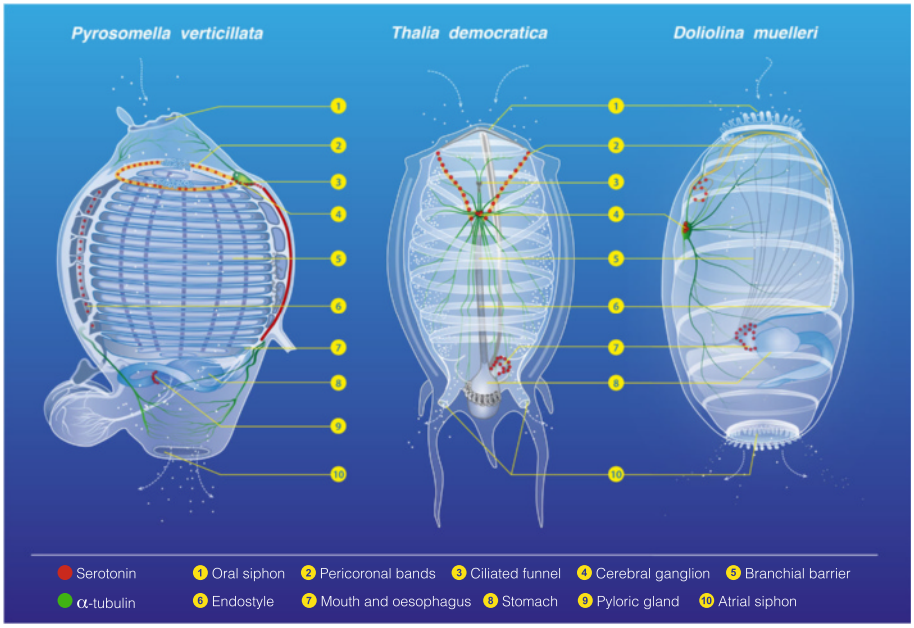

Fig. 6 The serotonin-like immunoreactive nervous system in Thaliacea. serotonin-like immunopositive cells in adult *Pyrosomella verticillata*, *Thalia democratica* and *Doliolina muelleri*

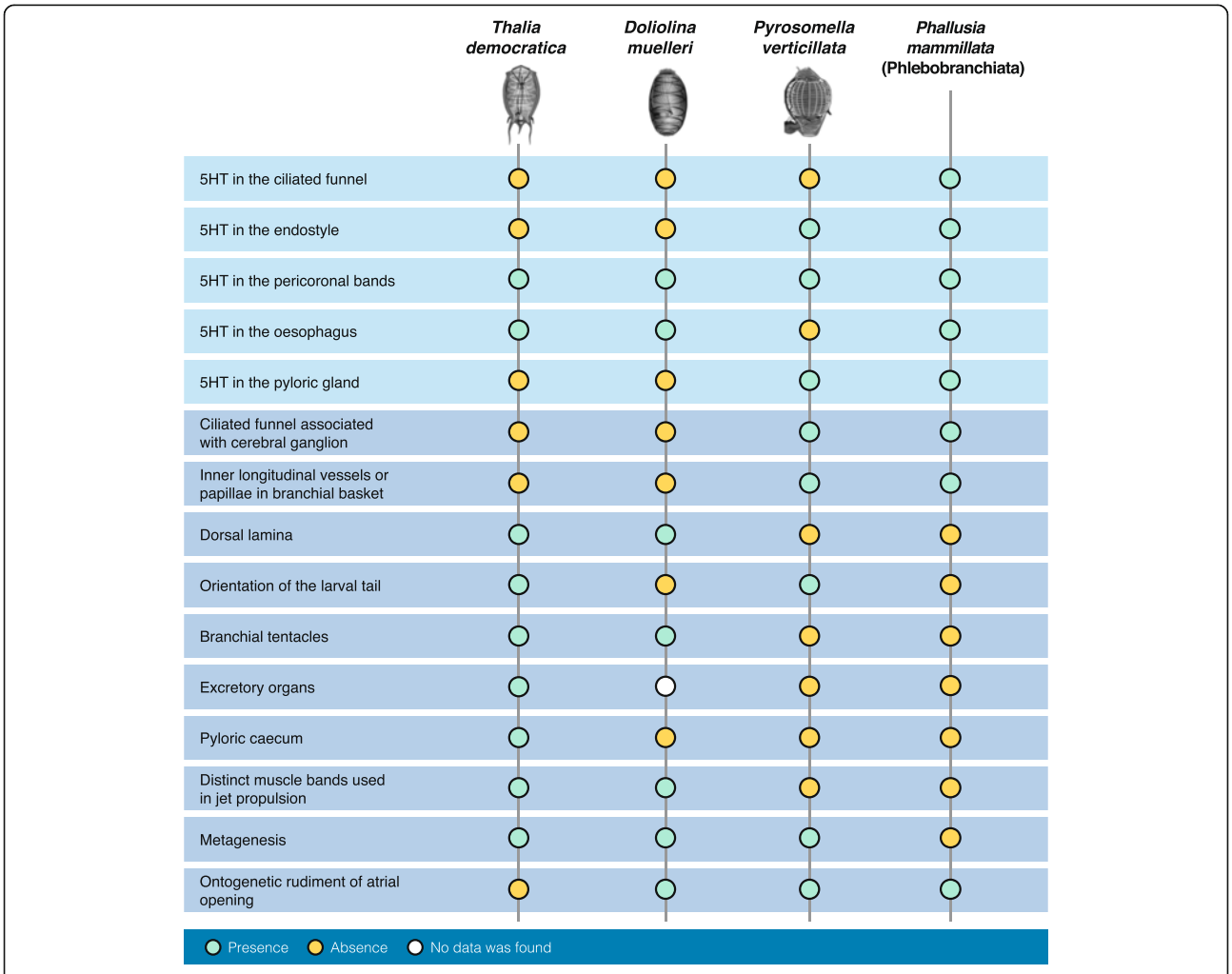

Fig. 7 Phylogenetic characters. Comparison of serotonin-like immunoreactivity distribution and selected plesiomorphies in thaliacean orders and in the phlebobranch species, *Phallusia mammillata*. Non-neural data from [35, 52, 61, 76, 77]

molecular based phylogenetic and/or phylogenomic analyses will be crucial to make more robust the relationships among different clade of Thaliaceans.

Methods

Animal collection and identification

Samples were collected in the Western Mediterranean using vertical plankton tows-200 μm mesh size-in the localities of Rade de Villefranche-sur-Mer (France) (43° 42′18″N 7°18′45″E) (*Pyrosomella verticillata* and *Ihlea punctata*) and Gulf of Naples (Italy) (40°48′5″N 14°15′ E) (*Thalia democratica* and *Doliolina muelleri*). Specimens were identified under stereomicroscope following taxonomic keys in [82] and [83].

Whole mount immunocytochemistry and imaging

Specimens were fixed in 4 % paraformaldehyde/0.1 M MOPS pH 7.4 containing 0.5 M NaCl, overnight at 4 °C. After several washes in phosphate buffered saline (PBS), samples were treated with 0.5 mg/ml cellulase (Sigma C1184) in PBS pH 5.5 for 10 min at 37 °C in order to partially digest the tunic and facilitate antibody penetration. Following this, incubations were carried out on a rotating shaker. Specimens were permeabilized for 20 min in PBS/0.25 % Triton X-100 (PBTr). A blocking step was performed with 30 % heat-inactivated Normal Goat Serum (NGS) in PBTr for 2 h, prior to incubating specimens with primary antibodies-anti-5HT (serotonin) (Immunostar 20080), anti-tyrosinated α-tubulin (Sigma T9028), and anti-acetylated α-tubulin (Sigma T6793)-diluted 1:300 in PBS containing 0.1 % Tween-20 (PBST) and 30 % NGS, for 60 h at 4 °C. After extensive washes in PBST, samples were incubated at 4 °C overnight with secondary antibodies-goat anti-rabbit IgG-Alexa 488 and goat anti-mouse IgG-Alexa 647-diluted 1:400 in blocking buffer (1 % BSA in PBST). All samples were washed thoroughly in PBS. All specimens except *Ihlea punctata* were counterstained with DAPI (1 μg/ml in PBS) for

nuclear labelling. Control experiments were run in parallel by omitting primary antibodies.

Image acquisition was performed on Zeiss LSM 510 Meta and Leica SP5 confocal microscopes. Z-stack images were analyzed and processed with Fiji and Photoshop CS6 (Adobe). Figure plates were made with Illustrator CS6 (Adobe). Brightness/contrast, inversion and colour balance adjustments where applied, were applied to the entirety of the image and not to parts thereof.

Additional file

Additional file 1: Visual assessment of serotonin-like immunoreactivity in *Thalia democratica* cerebral ganglion. (A–E) Five consecutive frontal sections ranging dorsal to ventral from Z = 14 to Z = 18 every 4.54 μm, showing elongating serotonin-like immunoreactive bundle (squared line). (F) Color-coded 2D image from hyperstacks Z = 14–18, showing different depth distribution of lateral clusters of serotonin-like immunoreactive neurons (arrows), central cluster of serotonin-like immunoreactive neurons (dashed line) and serotonin-like immunoreactive nervous fibre bundle (squared line). (JPG 1000 kb)

Acknowledgments
We are grateful to Alessandro Minelli (University of Padova, Italy) and John Kirwan (Lund University, Sweden) for critical reading and commenting the manuscript. The authors would also thank Santiago Valero-Medranda (Spain) for illustrating Figs. 6 and 7, and the fishery services at MEDA-Stazione Zoologica Anton Dohrn (Italy). Sampling at the Observatoire Océanologique de Villefranche-sur-mer (France) have been done with the support of EMBRC-France.

Funding
AVG is supported by the Marie Curie ITN 'Neptune' program (grant no. 317172), and was supported by an Erasmus-Leonardo fellow (Universidad Autónoma de Madrid and Spanish National Government), and a Réseau d'Activité Scientifique André Picard mobility grant (Pierre et Marie Curie University and French Italian Government) during the early stage of this study. FC and VN have been supported by a SZN PhD fellowship and a MIUR PON Grant (PONa3_00239), respectively.

Authors' contributions
AVG, FC, ST, VN and PS participated in the collection of specimens. AVG, RM, and ST carried out immunocytochemical experiments and confocal laser-scanning microscopy. AVG, ST and PS conceived the paper and drafted a first version. All other authors assisted in drafting the manuscript. All authors read and approved the final manuscript.

Competing interests
The authors declare that they have no competing interests.

Declarations
Experiments were performed in accordance with the European Union animal welfare guidelines [European Communities Council Directive of September 22, 2010 (2010/63/UE)]. Data sharing not applicable to this article as no datasets were generated or analysed during the current study.

Author details
[1]Biology and Evolution of Marine Organisms, Stazione Zoologica Anton Dohrn, Villa Comunale, 80121 Naples, Italy. [2]Institute of Marine Biological Resources and Inland Waters, Hellenic Centre for Marine Research, GR-19013 Anavyssos, Greece. [3]Observatoire Océanographique, CNRS, Sorbonne Universités, UPMC Univ Paris 06, Laboratoire de Biologie du Développement de Villefranche-sur-mer, 06230 Villefranche-sur-Mer, France.

Received: 3 May 2016 Accepted: 16 September 2016
Published online: 29 September 2016

References
1. Deibel D, Lowen B. A review of life cycles and life-history adaptations of pelagic tunicates to environmental conditions. ICES J Mar Sci. 2012; 69(3):358–69.
2. Piette J, Lemaire P. Thaliaceans, the neglected pelagic relatives of ascidians: a developmental and evolutionary enigma. The Q Rev Biol. 2015;90(2):117–45.
3. Wada H, Saiga H, Satoh N, Holland PW. Tripartite organization of the ancestral chordate brain and the antiquity of placodes: insights from ascidian Pax-2/5/8. Hox and Otx genes Development. 1998;125:1113–22.
4. Swalla BJ, Cameron CB, Corley LS, Garey JR. Urochordates are monophyletic within the deuterostomes. Syst Biol. 2000;49:52–64.
5. Zeng L, Swalla BJ. Molecular phylogeny of the protochordates: chordate evolution. Can J Zool. 2005;83:24–33.
6. Tsagkogeorga G, Turon X, Hopcroft RR, Tilak MK, Feldstein T, Shenkar N, et al. An updated 18S rRNA phylogeny of tunicates based on mixture and secondary structure models. BMC Evol Biol. 2009;9:187.
7. Holland LZ. Fine structure of spermatids and sperm of *Dolioletta gegenbauri* and *Doliolum nationalis* (Tunicata: Thaliacea): implications for tunicate phylogeny. Mar Biol. 1989;101:83–95.
8. Godeaux J. Systematics of Doliolida. Workshop "Progress in Belgian Oceanographic Research". Bull Soc R Sci Liège. 1996;65:83–5.
9. Compère P, Godeaux JEA. On endostyle ultrastructure in two new species of doliolid-like tunicates. Mar Biol. 1997;128:447–53.
10. Christen R, Braconnot JC. Molecular phylogeny of tunicates. A preliminary study using 28S ribosomal RNA partial sequences: implications in terms of evolution and ecology. In: Bone Q, editor. The biology of pelagic tunicates. Oxford: Oxford University Press; 1998. p. 265–73.
11. Govindarjan AF, Bucklin A, Madin LP. A molecular phylogeny of the Thaliacea. J Plankton Res. 2011;33:843–53.
12. Tsagkogeorga G, Cahais V, Galtier N. The population genomics of a fast evolver: high levels of diversity, functional constraint, and molecular adaptation in the tunicate *Ciona intestinalis*. Genome Biol Evol. 2012;4(8):740–9.
13. Hay-Schmidt A. The evolution of the serotonergic nervous system. P Roy Soc Lond B Bio. 2000;267:1071–9.
14. Temereva E, Wanninger A. Development of the nervous system in *Phoronopsis harmeri* (Lophotrochozoa, Phoronida) reveals both deuterostome-and trochozoan-like features. BMC Evol Biol. 2012;12:121.
15. Herranz M, Pardos F, Boyle MJ. Comparative morphology of serotonergic-like immunoreactive elements in the central nervous system of kinorhynchs (Kinorhyncha, Cyclorhagida). J Morphol. 2013;274:258–74.
16. Mayer G, Martin C, Rüdiger J, Kauschke S, Stevenson PA, Poprawa I, et al. Selective neuronal staining in tardigrades and onychophorans provides insights into the evolution of segmental ganglia in panarthropods. BMC Evol Biol. 2013;13:230.
17. Martín-Durán JM, Wolff GH, Strausfeld NJ, Hejnol A. The larval nervous system of the penis worm *Priapulus caudatus* (Ecdysozoa). Phil Trans R Soc B. 2016;371:20150050.
18. Azmitia EC. Serotonin and brain: evolution, neuroplasticity, and homeostasis. Int Rev Neurobiol. 2007;77:31–56.
19. Doran SA, Koss R, Tran CH, Christopher KJ, Gallin WJ, Goldberg JI. Effect of serotonin on ciliary beating and intracellular calcium concentration in identified populations of embryonic ciliary cells. J Exp Biol. 2004;207:1415–29.
20. Nichols CD. 5-HT2 receptors in *Drosophila* are expressed in the brain and modulate aspects of circadian behaviors. Dev Neurobiol. 2007;67:752–63.
21. Wilkinson LO, Dourish CT. Serotonin and animal behavior. In: Peroutka SJ, editor. Serotonin receptor subtypes: Basic and clinical aspects. New York: Wiley-Liss; 1991. p. 147–210.
22. Yavarone MS, Shuey DL, Tamir H, Sadler TW, Lauder JM. Serotonin and cardiac morphogenesis in the mouse embryo. Teratology. 1993;47:573–84.
23. Moiseiwitsch JR, Lauder JM. Serotonin regulates mouse cranial neural crest migration. Proc Natl Acad Sci U S A. 1995;92:7182–6.
24. Choi DS, Ward SJ, Messaddeq N, Launay JM, Maroteaux L. 5-HT2B receptor-mediated serotonin morphogenetic functions in mouse cranial neural crest and myocardiac cells. Development. 1997;124:1745–55.
25. Cameron RA, Smith LC, Britten RJ, Davidson EH. Ligand-dependent stimulation of introduced mammalian brain receptors alters spicule symmetry and other morphogenetic events in sea urchin embryos. Mech Dev. 1994;45:31–47.
26. Colas JF, Launay JM, Vonesch JL, Hickel P, Maroteaux L. Serotonin synchronises convergent extension of ectoderm with morphogenetic gastrulation movements in *Drosophila*. Mech Dev. 1999;87:77–91.

27. Buznikov GA, Peterson RE, Nikitina LA, Bezuglov VV, Lauder JM. The pre-nervous serotonergic system of developing sea urchin embryos and larvae: pharmacologic and immunocytochemical evidence. Neurochem Res. 2005;30:825–37.
28. Fukumoto T, Kema IP, Levin M. Serotonin signaling is a very early step in patterning of the left-right axis in chick and frog embryos. Curr Biol. 2005;15:794–803.
29. Fukumoto T, Blakely R, Levin M. Serotonin transporter function is an early step in left-right patterning in chick and frog embryos. Dev Neurosci. 2005; 27:349–63.
30. Buznikov GA, Lambert HW, Lauder JM. Serotonin and serotonin-like substances as regulators of early embryogenesis and morphogenesis. Cell Tissue Res. 2001;305:177–86.
31. Richter S, Loesel R, Purschke G, Schmidt-Rhaesa A, Scholtz G, Stach T, et al. Invertebrate neurophylogeny-suggested terms and definitions for a neuroanatomical glossary. Front Zool. 2010;7:29.
32. Stach T. Comparison of the serotonergic nervous system among Tunicata: implications for its evolution within Chordata. Org Divers Evol. 2005;5:15–24.
33. Pennati R, Dell'Anna A, Zega G, De Bernardi F. Immunohistochemical study of the nervous system of the tunicate *Thalia democratica* (Forsskal, 1775). Eur J Histochem. 2012;56, e16.
34. Braun K, Stach T. Comparative study of serotonin-like immunoreactivity in the branchial basket, digestive tract, and nervous system in tunicates. Zoomorphology. Pubished online 02 June 2016. DOI 10.1007/s00435-016-0317-8.
35. Bone Q, Pulsford AL, Amoroso EC. The placenta of the salp (Tunicata: Thaliacea). Placenta. 1985;6:53–63.
36. Godeaux JEA, Bone Q, Braconnot JC. Anatomy of Thaliacea. In: Bone Q, editor. The biology of pelagic tunicates. Oxford: Oxford University Press; 1998. p. 1–24.
37. Godeaux J. Contribution à la connaissance des thaliacés (pyrosome et doliolum): embryogénèse et blastogénèse du complexe neural, constitution et développement du stolon prolifère. Faculté des sciences: Université de Liège; 1957.
38. Lacalli TC, Holland LZ. The developing dorsal ganglion of the salp *Thalia democratica*, and the nature of the ancestral chordate brain. Philos Trans R Soc Lond B Biol Sci. 1998;353:1943–67.
39. Brien P. Embranchement des Tuniciers. In: Grasse PP, editor. Morphologie et reproduction. Paris: Traité de Zoologie; 1948. p. 545–930.
40. Paffenhöfer GA, Köster M. From one to many: on the life cycle of *Dolioletta gegenbauri* Uljanin (Tunicata, Thaliacea). J Plankton Res. 2011;33:1139–45.
41. Deibel D, Paffenhöfer GA. Cinematographic analysis of the feeding mechanism of the pelagic tunicate *Doliolum nationalis*. Bull Mar Sci. 1988;43:404–12.
42. Uljanin VN. Die Arten der Gattung *Doliolum* im Golfe von Neapel und den angrenzenden Meeresabschnitten. Leipzig: W. Engelmann; 1884. p. 1–140.
43. Holland ND, Holland LZ. Serotonin-containing cells in the nervous system and other tissues during ontogeny of a lancelet. Branchiostoma floridae Acta Zool. 1993;74:195–204.
44. Ekström P, Nyberg L, Van Veen T. Ontogenetic development of serotoninergic neurons in the brain of a teleost, the three-spined stickleback. An immunohistochemical analysis. Dev Brain Res. 1985;17:209–24.
45. Van Mier P, Joosten HWJ, Van Rheden R, Ten Donkelaar HJ. The development of serotonergic raphespinal projections in *Xenopus laevis*. Int J Dev Neurosci. 1986;4:465471–5.
46. Wallace JA. An immunocytochemical study of the development of central serotonergic neurons in the chick embryo. J Comp Neurol. 1985;236:443–53.
47. Wallace JA, Lauder JM. Development of the serotonergic system in the rat embryo: an immunocytochemical study. Brain Res Bull. 1983;10:459–79.
48. Garstang W. Preliminary note on a new theory of the phylogeny of the Chordata. Zool Anz. 1894;17:122–5.
49. Manni L, Lane NJ, Sorrentino M, Zaniolo G, Burighel P. Mechanism of neurogenesis during the embryonic development of a tunicate. J Comp Neurol. 1999;412:527–41.
50. Pani AM, Mullarkey EE, Aronowicz J, Assimacopoulos S, Grove EA, Lowe CJ. Ancient deuterostome origins of vertebrate brain signalling centres. Nature. 2012;483:289–94.
51. Kano S. Genomics and developmental approaches to an ascidian adenohypophysis primordium. Integr Comp Biol. 2010;50:35–52.
52. Fritsch HAR, Van Noorden S, Pearse AGE. Gastro-intestinal and neurohormonal peptides in the alimentary tract and cerebral complex of *Ciona intestinalis* (Ascidiaceae). Cell Tissue Res. 1982;223:369–402.
53. Pestarino M. Occurrence of different secretin-like cells in the digestive tract of the ascidian *Styela plicata* (Urochordata, Ascidiacea). Cell Tissue Res. 1982;226:231–5.
54. Pennati R, Groppelli S, Sotgia C, Candiani S, Pestarino M, De Bernardi F. Serotonin localization in *Phallusia mammillata* larvae and effects of serotonin antagonists during larval development. Dev Growth Differ. 2001;43:647–56.
55. Tiozzo S, Murray M, Degnan BM, De Tomaso AW, Croll RP. Development of the neuromuscular system during asexual propagation in an invertebrate chordate. Dev Dyn. 2009;238:2081–94.
56. Godeaux J. Functions of the endostyle in the tunicates. Bull Mar Sci. 1989; 45:228–42.
57. Barrington EJW, Franchi L. Organic binding of iodine in the endostyle of *Ciona intestinalis*. Nature. 1956;177:432.
58. Thorpe A, Thorndyke MC. The endostyle in relation to iodine binding. Symp Zool Soc Lond. 1975;36:159–77.
59. Sakharov DA, Salimova N. Serotonin-containing cells in the ascidian endostyle. Experientia. 1982;38:802–3.
60. Georges D. Presence of cells resembling serotonergic elements in four species of tunicates. Cell Tissue Res. 1985;242:341–8.
61. Nilsson O, Fredriksson G, Öfverholm T, Ericson LE. Electron-microscopic immunocytochemistry of 5-hydroxytryptamine in the ascidian endostyle. Cell Tissue Res. 1988;253:137–43.
62. Caicci F, Gasparini F, Rigon F, Burighel P, Manni L. The oral sensory structures of Thaliacea (Tunicata) and consideration of the evolution of hair cells in Chordata. J Comp Neurol. 2013;521:2756–71.
63. Fedele M. Sulla nutrizione degli animali pelagici III. Ricerche sui Salpidae. Boll Soc Nat Napoli. 1933;45:49–117.
64. Fedele M. Sul complesso delle funzioni che intervengono nel meccanismo ingestivo dei Salpidae. Atti Accad Naz Lincei Rc. 1933;17:241–5.
65. Burighel P, Cloney R. Urochordata: Ascidiacea. In: Harrison FW, Ruppert EE, editors. Microscopic Anatomy in Invertebrates, Vol. 15, Hemichordata, Chaetognatha, and the invertebrate chordates. New York: Wiley-Liss; 1997. p. 221–347.
66. Stach T, Turbeville JM. Phylogeny of Tunicata inferred from molecular and morphological characters. Mol Phylogenet Evol. 2002;25:408–28.
67. Kowalevsky A. Zum Verhalten des Rückengefässes und des guirlandenförmigen Zellstranges der Musciden während der Metamorphose. Biol Centralbl. 1886;6:74–9.
68. Romer AS. Major steps in vertebrate evolution. In: Greenstein JS, editor. Contemporary Readings in Biology. New York: MSS Information Corporation; 1972. p. 107–22.
69. Maisey JG. Heads and tails: a chordate phylogeny. Cladistics. 1986;2:201–56.
70. Schaeffer B. Deuterostome monophyly and phylogeny. In: Hecht MK et al., editors. Evolutionary Biology. New York: Plenum Press; 1987. p. 179–235.
71. Cameron CB, Garey JR, Swalla BJ. Evolution of the chordate body plan: new insights from phylogenetic analyses of deuterostome phyla. Proc Natl Acad Sci U S A. 2000;97:4469–74.
72. Holland LZ. Body-plan evolution in the Bilateria: early antero-posterior patterning and the deuterostome-protostome dichotomy. Curr Opin Genet Dev. 2000;10:434–42.
73. Nielsen C. Animal Evolution. Oxford: Oxford University Press; 2012.
74. Delsuc F, Brinkmann H, Chourrout D, Philippe H. Tunicates and not cephalochordates are the closest living relatives of vertebrates. Nature. 2006; 439:965–8.
75. Delsuc F, Tsagkogeorga G, Lartillot N, Philippe H. Additional molecular support for the new chordate phylogeny. Genesis. 2008;46:592–604.
76. Nielsen C. Larval and adult brains. Evol Dev. 2005;7:483–9.
77. Wada H, Satoh N. Details of the evolutionary history from invertebrates to vertebrates, as deduced from the sequences of 18S rDNA. Proc Natl Acad Sci U S A. 1994;91:1801–04.
78. Ruppert EE. Structure, ultrastructure, and function of the neural gland complex of *Ascidia interrupta* (Chordata, Ascidiacea): clarification of hypotheses regarding the evolution of the vertebrate anterior pituitary. Acta Zool. 1990;71:135–49.
79. Søviknes AM, Glover JC. Spatiotemporal patterns of neurogenesis in the appendicularian *Oikopleura dioica*. Dev Biol. 2007;311:264–75.
80. Herdman WA. A phylogenetic classification of animals: (for the use of students). London: Macmillan and Co; 1885.
81. Lahille F. Recherches sur les tuniciers des côtes de France. Tulouse: Imprimerie Lagarde et Sebille; 1890.
82. Van Soest RWM. A monograph of the order Pyrosomatida (Tunicata, Thaliacea). J Plankton Res. 1981;3:603–31.
83. Godeaux J. The relationships and systematics of the Thaliacea, with keys for identification. In: Bone Q, editor. The biology of pelagic tunicates. Oxford: Oxford University Press; 1998. p. 273–94.

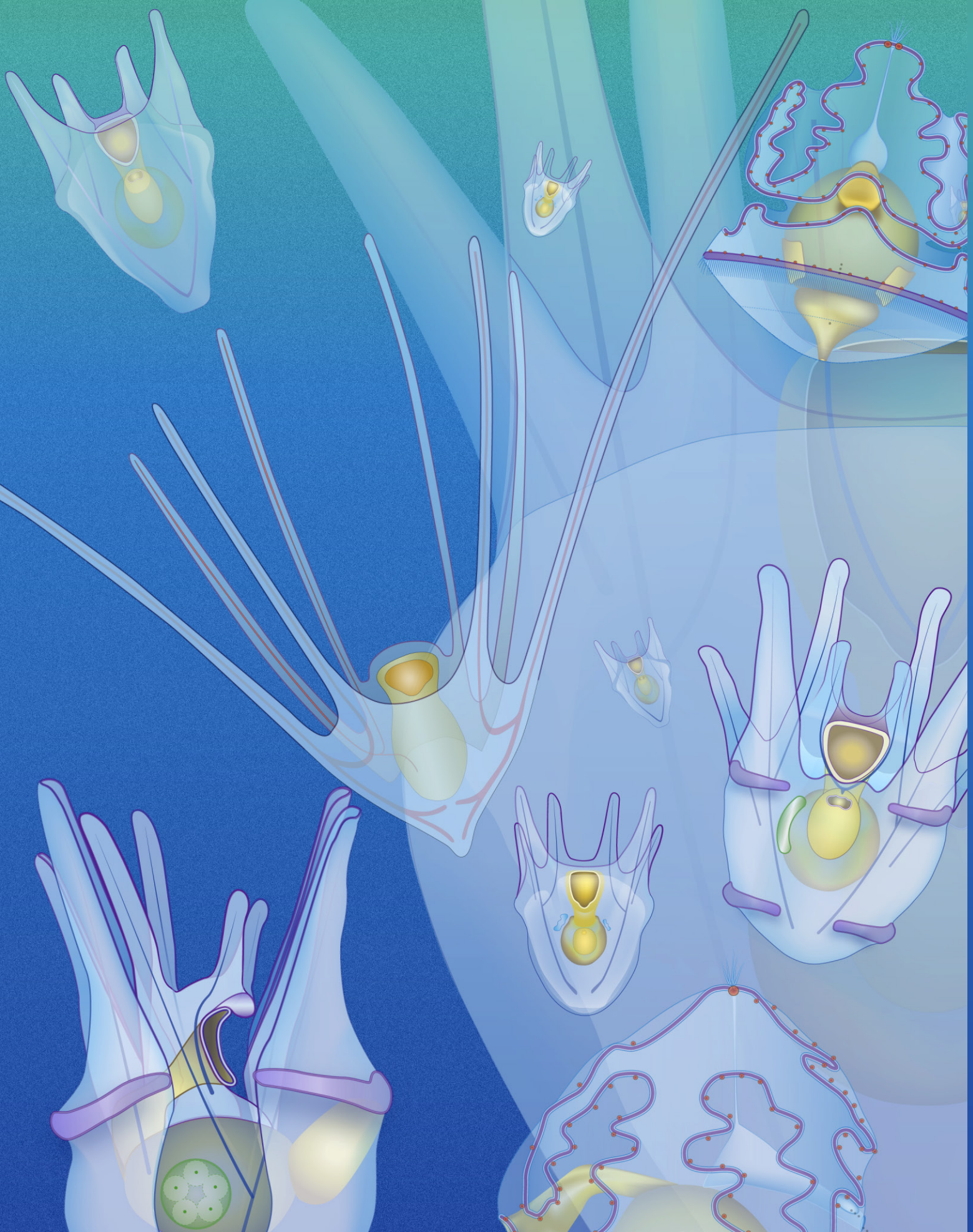

The Open University

Stazione Zoologica Anton Dohrn Napoli

LUND UNIVERSITY

MARIE CURIE ACTIONS

neptune

Marie Curie Initial Training Network

KUNGL. VETENSKAPS-AKADEMIEN

THE ROYAL SWEDISH ACADEMY OF SCIENCES